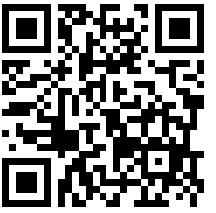

SRPSKO HEMIJSKO DRUŠTVO (BEOGRAD)

BULLETIN OF THE CHEMICAL SOCIETY Belgrade

(Glasnik Hemijskog društva — Beograd)
Vol. 34, No. 1, 1969

Published by
SRPSKO HEMIJSKO DRUŠTVO (BEOGRAD)
1969

Translated and published for U.S. Department of Commerce and
the National Science Foundation, Washington, D.C., by
the NOLIT Publishing House, Terazije 27/II, Belgrade, Yugoslavia
1969

Edited by
PAUL PIGNON

Printed in "Prosveta", Belgrade

14th MEETING OF THE CHEMISTS OF THE SOCIALIST REPUBLIC OF SERBIA AND SYMPOSIUM ON METALLURGY

and

ANNUAL CONVENTION OF THE SERBIAN CHEMICAL SOCIETY

January 27—29, 1969

HELD AT THE SCHOOL OF TECHNOLOGY AND METALLURGY
UNIVERSITY OF BEOGRAD

CONTENTS

Page

EXTRACTION AND PROCESSING OF IRON AND STEEL

A. Zorina, S. Milivojević, Đ. Žumberković and V. Žumberkovic
Testing of Reductivity of Indigenous Iron Ores and Sinters . 1

T. Grgurač, S. Kovačić and I. Kovačić
Replacing Limestone by Dolomite in Making Self-Fluxed Sinter . 2

S. Ivaniš and S. Kovačić
Magnetizing Roasting of Brand from Tomašica 2

T. Grgurač, S. Ivaniš, S. Kovačič and I. Kovačić
The Possibilities of Replacing Coke Breeze in Iron Ore Sintering 2

A. Čavić
Influence of Magnesia Content on Slag Properties and Blast Furnace Practice 3

A. Markotić
The Influence of $BaSO_4$ on the Viscosity of Blast-Furnace Dross 3

S. Kovačić and V. Kovačić
Iron Ore Reduction Without a Blast Furnace — Present State and Prospects of Various Procedures 4

N. Gaković, Lj. Nedeljković and A. Čavić
Kinetics of Removal of Sulphur from Blast Furnace Slag . . . 4

P. Vuksanović
Process of Disoxidation of Low Alloy Steel Alloyed with Chrome 5

I. Stojšić
Electron-Beam Melting of Metals-Our Facilities and Recent Work 6

V. G. Logomerac and I. M. Cvitan
Separation of Steel Scrap from Open-Hearth Slag and its Fine Grinding 6

N. Gaković, T. Raić, Z. Luketić, I. Bokšan and S. Ubiparip
Processing of Mechanically Capped Steel 7

N. Gaković, Lj. Nedeljković and M. Todorović
Statistical Analysis of Some Parameter Relations in the Pouring of Mechanically Capped Steel 7

D. Cvetanović
Possibilities of Using Domestic White Bauxite as Raw Material for Electrofused Refractories 8

Page

D. Cvetković
Durability of the Refractory Lining of Forging Furnaces in Dependence on Size of Refractory Briks and the Method of Lining 8

M. Jovanović, E. Krotin and Z. Popović
The Influence of Excess Air on the Flame Temperature in the Combustion of Propane-Butane Mixture 9

F. Havliček
A Theory of the Filtration of Melts in the Biphasic Zone during Solidification 9

J. Pribyl
A Contribution to the Theory of Pipe Formation 10

C. Mirković
Non-Equilibrium Thermodynamics in Processes of Treatment of Metals by Casting 11

N. Obradović and M. Popović
Recent Methods of Investment Casting Shell Production 12

I. Stojšić N. Obradović, M. Popović and M. Tufegdžić
Effect of Vacuum Remelting of Steel 12

Đ. Milosavljević
Characteristics of Metal Solidified in Presence of Chill 13

B. Đurković, D. Sinadinović and I. Ilić
Vacuum and Zonal Refining of Indium 13

Đ. Cvetanović and Lj. Rikalović
An Arc Furnace Reducibility Test on the Stogovo Manganese Sinter for Production of "Carbure" Feromanganese and of Silicomanganese 14

EXTRACTION OF NONFERROUS METALS

V. Živanović
Application of Ion-Exchange and Solvent Extraction Processes in Hydrometallurgy. Possibilities and Our Experience 15

M. Spasić, D. Vučurović and I. Ilić
Chlorination of Nickel Oxide 15

M. Spasić, D. Vučurović and R. Vračar
Oxidation of Pyrite by Gaseous Oxygen from Aqueous Suspension at High Temperatures in an Autoclave 16

D. Đurković and R. Ćosović
High Purity Metals — Our Possibilities and Experience 16

Č. Kostić
Partial Desulphurization of Copper Concentrates in a Fluosolid Reactor 17

Č. Kostić and Lj. Rikalović
Sulphate Roasting of Lead-Copper Matte in a Fluosolids Reactor 17

Lj. Rikalović and Č. Kostić
Evaporation Roasting of Low-Grade Antimony Ore in a Fluosolids Reactor 18

Lj. Rikalović and Č. Kostić
A Study of the Roasting Parameters of Domestic Pyrites for Producing Elementary Sulphur 18

Page

J. Krišto and D. Šurbatović
Alkaline Process for Dressing Copper (Dust from Lead Refining) 19

F. Nišić, J. Krišto and S. Vuksanović
Electrolytic Zinc Slurry Treated by Leaching in Sulphuric Acid 20

S. Vuksanović and J. Krišto
Lead-Calcium Alloy Recovery by a Carbide Process with the Addition of Metallic Aluminum 20

B. Savić
The Influence of Thermodynamic Parameters on Matte Converting at the Copper Smelting Works, Bor 21

V. G. Logomerac
Smelting Low Grade Bauxite 21

I. Kovačić and S. Kovačić
Agglomeration of Manganic Flotation Concentrate by Sintering 22

B. Bunji, N. Pacović and V. Živanović
Technology of Low-Grade Domestic Uranium Ores 22

Z. Đukić, J. Milosavljević, M. Lazarević, D. Pejčić, D. Krstić and M. Stanojević
Results in Production of "Ceramic Grade" Uranium Dioxide . . 23

D. Đurković and R. Ćosović
Thermal Decomposition of Tungsten Hexachloride 23

R. Ćosović and D. Đurković
A New Method for Separating Zirconium from Technical-Purity Chloride Solutions 24

N. Pacović
Contribution to the Technology of Vanadium Pentoxide Recovery from „White Mud" — A Byproduct in Alumina Production . . 24

B. Đurković
Current Problems of Rare Metal Metallurgy 25

B. Đurković, G. Jovanović and S. Bogić
Problems of Winning Germanium from Reverbatory Furnace Dust in Bor 25

B. Đurković, D. Sinadinović and R. Vračar
Treatment of Germanium-Containing Concentrate for Obtaining Germanium 26

G. Jovanović and S. Bogić
Regeneration of Germanium from Waste Materials of El Niš Electronics Enterprise 26

PHYSICAL METALLURGY AND CONTROL

B. Koroušić
The Application of Solid Electrolytes in Research on Metallurgical Reactions 27

D. Mihajlović
The Relation N = f(ε) in Low-Cycle Metal Fatigue 27

Page

K. Bela and Lj. Matović
Method of Express Quantitative Spectroscopic Analysis of Iron and Steel Casts on Glass Spectroscope 28

A. Todorović, M. Karakašević and S. Lisinac
Direct Spectroscopic Determination of Ag, Cu, Bi and Sb in Samples Taken from Lead Refining 29

B. Bošković-Vasiljević
Radiography of Light Metals 30

M. Horgas, Z. Horgas, Lj. Božić, and V. Žumberković
Determination of Oxides in Steel 30

M. Dujmić
Determination of the Specific Surface Area of Powders 31

M. Branković
Measurement of Linear Shrinkage of Metal 31

V. M. Stefanović and M. Rogulić
A Transmission Electron-Microscopic Study of the Deffects of Neutron-Irradiated Low-Carbon Steel 32

M. Juvan and S. Đorđević
Development of a New Steel for Rails With Higher Resistance to Wear 32

S. Đorđević
Effect of Hydrogen on the Expansion of Rail Steel 33

Đ. Milosavljević
Structure of Metallic Welds Obtained by the Electron Beam Welding Technique 34

D. D. Mitkov
The Influence of Iron on the Properties of Al-Si Alloys With Regard to the Structure 34

N. Novović-Simović and M. M. Rogulić
The Effect of Ultrasonic Vibrations on the Solidification of Cd—Zn Alloy 35

S. Stojadinović
Some Observations and New Approaches Concerning the Action of Sea-Water on the System Steell/Al Zn Mg 35

P. Vuksanović
Changes in Tempering and Release of Low Alloy Steel for Rearings of Quality Č. 4146 35

Č. Dostanić
Partial (Differentiated) Hardening of Forging Tools 36

J. Žvokelj
Applicability of Dilatometric Method for the Study of Retained Austenite of Some Tool Steels 37

S. B. Đorđević
X-Ray Analysis of Thermal Treatment of Carbonic Steels of Different Carbon Content 37

N. Vidojević and N. Novović-Simović
Dilatometric Investigation of the Tempering of Steel in Which Secondary Hardening Occurs 38

Page

S. Malčić, A. Mihajlović, A. Mance and P. Tepavac
X-Ray Investigation of the Monoclinization of Alpha-Uranium Lattice in the U-Nb System 39

M. Jovanović
Kinetics of Isothermal Growth of Second Phase Particles in Dilute Uranium 39

A. Mihajlović, A. Mance, S. Malčić and P. Tepavac
Kinetics of $\beta \rightarrow \alpha'$ Transformation in Low Molybdenum-Uranium Alloys 40

B. Đurić, N. Janković and M. Marjanović
Kinetics of the Eutectoid Decomposition of the Gamma Phase in Uranium-Niobium Alloy 40

Đ. Lazarević
Influence of Radiation on the Phase Composition of Low Alloyed Uranium 41

M. Gligić and Đ. Lazarević
Influence of Alloying Addition on the Resistance of Low-Alloyed Uranium 41

D. Mihajlović and M. Kostić
Metallographic Investigation of Dilute Cu—Zr Alloys 42

GENERAL CHEMISTRY

B. Živanović and Lj. Trbojević
Study on Metal Powder Pressing 43

R. Stiglić and M. Stevanović
The Electrical Conductivity of Sintered UO_2 43

B. Živanović, D. Uskoković and M. M. Ristić
A Study on the First Stage Sintering Kinetics of Molybdenum Powder 44

J. Petković, M. Vlajić and I. Stamenković
Changes in Characteristics Properties of UO_2 Powders in Oxido-Reduction Cycles 44

P. Pavlović, I. Stamenković and D. Radovanović
An Isothermal Calorimeter for Measuring Thermodynamic Parameters of the Solid State 44

Č. Petrović, D. Đorđević and V. Alimpić
Electroless Nickel Plating of Copper at Temperatures Above 100°C 45

D. Đorđević, Č. Petrović and V. Alimpić
Electroless Nickel Plating of Metal Casings at Temperatures Higher Than 100°C 45

D. Đorđević, Č. Petrović and V. Alimpić
Electroless Nickel Plating of Silicon in Nonaqueous Solutions 46

D. Đorđević, Č. Petrović and V. Alimpić
Physical and Chemical Characteristics of Nickel Plating on Silicon Obtained by Electroless Plating in Nonaqueous Solutions . . . 46

Page

I. Krstanović, M. Jančić, S. Đurić and Lj. Radonjić
Crystallographic Investigations in the Systems Mn—Si and Cr—Si 46

Z. Stavrić and H. Kočica
Effect of Calcined Alumina on Mechanical and Electrical Characteristics of Electrical Porcelain Bodies 47

R. Nikolić
Effect of Some Properties of Pre-Synthesized Magnesium Silicate on the Plastic Behavior of Steatite Bodies 47

V. G. Logomerac
Granulation of the New Phosphoric Fertilizer "Pelofos" by Granulating and Compacting 48

PHYSICAL CHEMISTRY

P. S. Putanov, B. Aleksić and B. Đukanović
Differential Thermal Analysis of Chromium Hydroxides Precipitated at Various Temperatures 49

P. S. Putanov, Ž. D. Jovanović and B. D. Aleksić
The Influence of Changes in the Chemical Composition on the Low-Temperature Water-Gas Shift Catalyst on its Behavior During Thermal Treatment 49

P. S. Putanov, Ž. Jovanović and A. Terlecki-Baričević
Influence of Composition of the ZnO—Cr_2O_3—CuO Catalyst on the Electrical Conductivity and Catalytic Activity in the Water-Gas Shift Reaction 50

P. S. Putanov and B. Aleksić
Investigation of the Properties of Heterogeneous Catalysts by Magnetic Methods 50

P. S. Putanov and M. Jovanović
The Electron Work Function as a Characteristic of Solid Catalysts 51

D. Jovanović and J. Veličković
The Determination of the Constant of Initiation (k_i) in Thermal Polymerization from Distribution Moments and the Polymerization Rate 51

S. Mladenović and V. Mitrović
Relation Between Cadmium Corrosion and Current Efficiency in Cadmium Sulfate Solutions Containing Sulfuric Acid 52

R. Despotović
Distribution of Radionuclides in a Polycomponent System . . . 52

D. M. Dražić, S. Đorđević, M. Vojnović and B. Paštrović
pH Change at the Electrode Surface in Hydrogen Evolution Reaction 53

A. R. Despić and D. B. Šepa
Study of Mechanisms of Complex Reactions. Electrochemical Oxygen Reduction in Acid Solutions 53

A. R. Despić, D. M. Dražić and R. T. Atanasoski
Properties of the Electrochemical Double Layer on Pyrolytic Graphite (II) 54

Page

R. R. Adžić and D. M. Dražić
Influence of the Structure of the Active Carbon on the Acitivity of the Supported Catalyst 54

M. Vojnović and D. Šepa
Electron Charge Transfer in the System Sb(III)/Sb(V) at Platinum Electrode 55

S. Đorđević, D. M. Dražić, M. Vojnović, V. Pandurović and B. Paštrović
Electrodeposition and Dissolution of Cobalt in Sulphamate Electrolytes 55

T. J. Janjić, L. B. Pfendt and M. B. Ćelap
A Study of D,L-Threonine Copper Complexes in Solution . . . 56

M. B. Ćelap, T. J. Janjić and P. N. Radivojša
Study of the Reactions of Hexanitrocobaltates(III) with Amino Acids. VI. Substitution Kinetics and Mechanism of Reaction with Glycine, Alanine, β-Alanine and α-Aminobutyric Acid and Synthesis of Corresponding Tetranitroaminoacidato-Cobaltates(III) . . . 56

O. Tatić—Janjić
Potentiometric Study of Liquid Amalgams in Nonaqueous Solvents at Higher Temperatures 57

M. Đ. Jančić and Lj. M. Radonjić
Reactive Diffusion in Germanium-Transitions Metal Systems . 57

M. Đ. Jančić and Lj. M. Radonjić
Kinetics of Formation of New Phases in the Silicon-Calcium Systems 58

K. F. Zmbov
Mass Spectrometry Studies of Vapors Over Mixed Oxides at High Temperatures 58

J. Janjić, D. Pešić and D. Janković
The Emission Electronic Spectrum of the $C^{12}O^{18}$ Molecule . . . 58

M. V. Šušić, D. R. Vučelić, D. B. Karaulić, and S. V. Paušek
N.M.R. Investigation of Propylene Sorption on Zeolites 4A, 5A, and 13× 59

M. V. Šušić, D. R. Vučelić, S. V. Mentus and D. B. Karaulić
Sorption of Hydrogen and Deuterium on the Zeolite Linde 5A 59

M. V. Šušić, D. R. Vučelić, D. B. Karaulić, S. V. Paušek and V. J. Milaković
Contribution of Some N.M.R. Effects to the Elucidation of Sorption Mechanisms of Gases on Solid Surfaces 60

ORGANIC CHEMISTRY

R. Jovanović
The Influence of the Texturising Conditions on the Macroscopic and Fine Structure of Frizzled Yarns 61

R. Jovanović and V. Miletić
On The Reliability of Various Methods for Determining the Low Molecular Weight Components in Polycaprolactam Fibers .. . 61

R. Jovanović, J. Jakševac and S. Levkova
Effects of Microorganisms on Acrylic Fibers 62

Page

J. Vanđel
Sorption of Streptomycin on Amberlite Irc-50 Ion Exchange Resin 63

J. Vanđel
Decationization of Streptomycin Solution on Ion Exchange Resins 63

S. N. Rašajski and D. M. Petrović
Solubility of Ergosterol Esters in Mixtures of Some Organic Solvents 64

I. Vavra and N. Đokić
Determination of the Degree of Swelling of Crosslinked Dextran (Dextran Gel) 64

S. Jovanović
Size and Structure of the Elementary Fibers of Cotton Cellulose 65

S. N. Rašajski and Lj. P. Vrhovac
Coagulation of Cellulose in the Form of Fibers from Cadoxen Solution and Some Properties of the Regenerated Cellulose . . 65

S. E. Petrović, J. A. Šenborn and S. M. Petrović
Separation of Nucleosides and Their Bases on Starch Thin Layers 65

S. M. Petrović and V. D. Canić
Separation of Carbohydrates by Thin-Layer Chromatography . 66

V. D. Canić and N. U. Perišić-Janjić
Circular Thin-Layer Chromatography on Starch of Cations and Anions 66

Lj. Đaković, P. Dokić and M. Kovačev-Dolai
The Influence of Some Factors on Particle Size Distribution of Oil/Water Type Emulsions 67

K. Petrović
Gas Chromatographic Determination of C_6-C_8 Aromatics and Some Other Hydrocarbons in Gasoline on Open Tubular Columns 67

S. M. Jovanović and M. Stanković
The Influence of the Surface Properties of the Filler-Carrier on the Fractionating Efficiency of a Baker-Williams Column . . . 68

J. Veličković, D. Jovanović and N. Valent
A Study of the Composition Distribution of Styrene Methylmethacrylate Copolymers 68

R. Borisavljević, S. Jovanović and Đ. Kosanović
Bulk Polymerization of Cetylmethacrylate 69

J. Veličković and S. Vasović
Synthesis and Polymerization of Dialkylitaconates 69

J. Veličković and S. Vasović
Relationship Between Intrinsic Viscosity and Molecular Weight of Polydialkylitaconates 70

ANALYTICAL CHEMISTRY

T. Kiss, I. Zsigrai and R. Krizsán
Determination of Various Metals by Complexometric Titration in Non-Aqueous Solutions 71

Page

H. Weisz and T. Kiss
Application of Catalysis in the Ring Oven Method 71

H. Weisz and T. Kiss
Precipitation Titration With Potassium Iodide by Catalytic Thermometric End-Point Detection and by Using Arsenic(III) Cerium(IV) as Indicator Reaction 72

V. Vajgand, F. Gaál, S. Brusin and Lj. Zrnić
Catalytic Thermometric Titrations of Bases and Acids in Non-Aqueous Media 72

V. Vajgand and M. Jaredić
Determination of Palladium by Thioglycolic Acid and Investigation of the Composition of the Palladoglycolate Complex . . . 73

V. Vajgand and T. Pastor
Determination of Mixtures of Primary, Secondary and Tertiary Amines 74

M. S. Jovanović and L. J. Bjelica
Biamperometric Titrations of Organic Acids in a Mixture of Solvents Using a Bismuth Electrode Pair 75

V. Vajgand, D. Galović and Ž. Miljković
Electrogravimetric Determination of Mercury in Metallic Mercury and Amalgams 76

S. Mladenović and M. M. Isaković
Polarographic Determination of Zinc in Cadmium 76

S. Mladenović and J. Lutz
Polarographic Determination of Tin in the Presence of Lead . . 77

M. Jovanović and V. Rekalić
Polarographic Behavior of Oxalyl Dihydrazide 77

M. Klisak and M. Marinković
Emission Spectrometric Determination of Beryllium in Copper-Base Alloys with Stabilized Arc 78

M. Pravica and A. Muk
The Influence of Substituents on the Dissociation Constants of Picramic Reagents 78

TESTING OF REDUCTIVITY OF INDIGENOUS IRON ORES AND SINTERS

A. ZORINA, S. MILIVOJEVIĆ, Đ. ŽUMBERKOVIĆ and V. ŽUMBERKOVIĆ

Hasan Brkić Institute of Metallurgy, Zenica

For determination of the reductive properties of iron yielding raw materials, a laboratory process has been developed for reduction of samples in the current of carbon monoxide, with continual analysis of the gas after contact with the sample.

The samples subjected were sinter produced by the Ironworks Zenica and ores from the Vareš and Ljubija deposits, of different mineralogical composition. Examinations under isothermic conditions of heating, the influence of the size of the grain on reductivity was tested. Reductivity is characterised by the speed of the process in time, when the sample was reduced 40%, according to L.v Bogdandy. Testing under increasing temperature, the development of thermochemical reactions was observed, which depend on decomposition of the mineralogical components of the samples. Classification of the tested samples according to reductivity was carried out. Stamples of sinter showed to be markedly poor in reductivity. In a series of iron ore tests, poorest reductivity was shown by samples of limonite from Ljubija and blue hematite from Vareš. The poor reductivity of Ljubija limonite is explained by the low temperature at the beginning of sinterisation, and that of the blue hematite from Vareš by the compactness, as the structure of the lumps of ore is not penetrable by gases.

REPLACING LIMESTONE BY DOLOMITE IN MAKING SELF-FLUXED SINTER

T. GRGURAČ, S. KOVAČIĆ and I. KOVAČIĆ

Institute of Metallurgy, Sisak

In semi-industrial tests on a Greenawalt-type sintering device with sintering surface of 0.366 m^2 limestone was replaced by dolomite from 0 to 100% at constant CaO/SiO_2 (about 1.2) and $(CaO+MgO)/SiO_2$ (about 1.2) ratios.

The effect on some sinter parameters (strength, yield degree of desulphuration, degree of oxidation, and reductibility) is shown graphically.

MAGNETIZING ROASTING OF BRAND FROM TOMAŠICA

S. IVANIŠ and S. KOVAČIĆ

Institute of Metallurgy, Sisak

Roasting tests in an 82 mm diameter laboratory fluidizing reactor on samples of low-grade brand from Tomašica (Fe — 27.52%) have been done.

Blast-furnace gas with different concentrations of CO_2+H_2(33.16 and 5%) was used for reduction and fluidization. The roasting temperature and time were varied, and the quality of the product estimated by reducing oxide roasting and determining the magnetic fraction, or in case of reduction roasting by chemical analysis too.

THE POSSIBILITIES OF REPLACING COKE BREEZE IN IRON ORE SINTERING

T. GRGURAČ, S. IVANIŠ, S. KOVAČIĆ and I. KOVAČIĆ

Institute of Metallurgy, Sisak

From data in the literature and considering existing possibilities in Yugoslavia, coal from Vrška Čuka was tested first, and then petrol-coke. Pilot plant and industrial experiments proved that both could be used as fuel for iron ore sintering.

INFLUENCE OF MAGNESIA CONTENT ON SLAG PROPERTIES AND BLAST FURNACE PRACTICE

A. ČAVIĆ

Hasan Brkić Institute of Metallurgy, Zenica

The blast furnace slags of the Zenica Iron and Steel Works which have a very specific composition have been studied.

The viscosity of industrial and semisynthetic slags was measured and it was found that baria up to 15 percent did not change the viscosity, while the addition of magnesia decreased it.

The temperatures of slags and metals were measured during tapping. The temperatures were about 100°C lower than is usual in normal practice.

In order to improve the properties of the slag and check laboratory results a trial was carried on in which some of the limestone in the charge was replaced by dolomite. The content of magnesia in the slag was increased by about 30% and the generally improved blast furnace operation has been achieved. Slag with an increased magnesia content has a higher desulfurizing power.

The beneficial influence of magnesia is due to its effect on slag viscosity, but in order to get the full advantage it has to be added to the mixture for sintering, the general standard of blast furnace operation has to be improved and the temperatures of slag and metal have to be higher.

THE INFLUENCE OF $BaSO_4$ ON THE VISCOSITY OF BLAST-FURNACE DROSS

A. MARKOTIĆ

Faculty of Technology, University of Zagreb, Metallurgical Department, Sisak

The paper reviews the experience of some foreign and Yugoslav authors who have dealt with the influence of barium compounds (primarily BaO) on the viscosity of blast-furnace slag, illustrated with graphs.

The present theory of the formation of blast-furnace slag is based on the assumption that its viscosity depends on the range of lattice polimerisation by means of SiO_2. Basic oxides destroy the lattice and so reduce slag viscosity, which reaches its minium value (the most convenient one) when it consists of orthosilicate type compounds in the form $2\ MeO \times SiO_2$ where MeO is a basic oxide, e.g. CaO, MnO, MgO or BaO.

Study of slag obtained from ores high in $BaSO_4$ (from Vareš) has shown that $BaSO_4$ (found as BaO in slag) has a certain influence on the distribution of components, changing their ratios.

IRON ORE REDUCTION WITHOUT A BLAST FURNACE — PRESENT STATE AND PROSPECTS OF VARIOUS PROCEDURES

S. KOVAČIĆ and V. KOVAČIĆ

Institute of Metallurgy, Sisak

Various procedures for reducing iron ore without a blast furnace are arousing great interest. Data from the literature and congress reports have been compiled to get an overall view of procedures which seem promising for application, whether they have been applied on a laboratory, pilot or industrial scale.

KINETICS OF REMOVAL OF SULPHUR FROM BLAST FURNACE SLAG

N. GAKOVIĆ, LJ. NEDELJKOVIĆ and **A. ČAVIĆ**

Institute of Chemistry, Technology and Metallurgy, Beograd

In order to determine the mechanism by which blast furnace slag gives off sulphur in to an oxidizing atmosphere as SO_2 the Zenica blast furnace slag was studied.

Trials were made in the temperature range 1300 to 1600°C with gases of various oxidizing potentials. A mixture of nitrogen with a controlled proportion of oxygen was used.

A possible mechanism of removal of sulphur has been derived on the basis of the overall activation energy.

PROCESS OF DISOXIDATION OF LOW ALLOY STEEL ALLOYED WITH CHROME

P. VUKSANOVIĆ

Ironworks — Nikšić

The task of this paper is to describe the contemporary method of disoxidation for the production of low alloy steel, based on results of a large number of industrial experiments.

During the disoxidation period in the production of the charge, very soon in the circular furnace slag with a low content of FeO is formed, so that the oxygen content of the steel decreases comparatively fast and reaches a concentration which conforms to conditions of balance with carbon.

The disoxidation media Si, Si-Mn and Ca-Si during casting provide a relatively small decrease of the oxygen content, but their use in the vessel before casting leads to a considerable improvement with regard to impurities. It is different with disoxidatives which directly after dissolution in the steel, bind the major part of the oxygen in the form of primary oxides and are quickly segregated and eliminated from the molten steel. When kept longer in the vessel than prescribed, in such case it does not lead to any results. Under this group of disoxidatives fall aluminum and titan and disoxidative alloys which contain aluminum, such as ferro-aluminum and calcium--aluminum.

The problem of diffused disoxidation is all the more complex in that it must reach a much lower content of oxygen than the one which is required to balance with carbon. The inadequate part of this disoxidation is that it is not possible to add larger quantities of disoxidatives (Si, Al) at the beginning of the refining period. The process of diffused disoxidation demands a much longer time to reach concentration of the oxygen, which ensures quality of the steel.

The testing of diffused-sedimented disoxidation carried out in electric furnaces shows results on the basis of which it can be concluded that a suitable selection of disoxidatives and composition of the slag, can provide steel of quality.

ELECTRON-BEAM MELTING OF METALS—OUR FACILITIES AND RECENT WORK

I. STOJŠIĆ

Institute for Technology of Nuclear and other Mineral Raw Materials, Beograd

The first part of the report describes the electron-beam technique of melting metals and alloys and compares it with the other controlled-atmosphere melting techniques. Characteristics of the Institute's EMO60 are given.

Recent research included the electron-beam melting of zirconium and copper. The results are given, and some comparisons are made with results of arc and induction-and-arc melting of these metals. In the case of zirconium better refinement is obtained with electron-beam than with arc melting. Recent results also indicate that vacuum induction melting of electrolytic copper in a graphite crucible gives better refinement than electron-beam melting.

SEPARATION OF STEEL SCRAP FROM OPEN-HEARTH SLAG AND ITS FINE GRINDING

V. G. LOGOMERAC and I. M. CVITAN

Faculty of Technology, University of Zagreb, Metallurgy Department Sisak, and Engineering Bureau of the Building Industry, Zagreb

The economic value of the steel scrap always present in open-hearth slag is reviewed. Data are given on the efficiency of removing this scrap during crushing of the slag in jaw crushers. A mill plant for the purified slag is further described. Parameter of fine grinding in the ball mill and indicators obtained are given.

Finely ground slag is used for the production of the Pelofos phosphorous fertilizer.

PROCESSING OF MECHANICALLY CAPPED STEEL

N. GAKOVIĆ, T. RAIĆ, **Z. LUKETIĆ**, I. BOKŠAN and S. UBIPARIP
Institute of Chemistry, Technology and Metallurgy, Beograd

Steel poured into bottle moulds was compared with rimmed steel poured into open moulds. Processing of steel in open-hearth furnaces and pouring of mechanically capped steel in 2-ton bottle moulds was studied. Steelmaking procedure and pouring practice are discussed on the basis of recorded data for selected heats under given conditions. The optimum conditions for processing and pouring were determined from the results for ingot quality, positions on blowholes, surface quality of ingots, yield of rolling, etc.

STATISTICAL ANALYSIS OF SOME PARAMETER RELATIONS IN THE POURING OF MECHANICALLY CAPPED STEEL

N. GAKOVIĆ, **LJ. NEDELJKOVIĆ** and M. TODOROVIĆ
Institute of Chemistry, Technology and Metallurgy, Beograd

Parameters recorded for 50 heats of a tube steel processed in a 45-ton open-hearth furnace and poured into bottle-top moulds are grouped into steelmaking factors and pouring factors. Each parameter has been correlated with the thickness of blowhole-free skin, which is taken as a basic index of steel quality. The regressions were calculated on an Elliott 803 computer. Using these results the most important parameters were selected and in the next step of the calculation mutually correlated. The relations obtained are discussed in the light of existing views on the solidification mechanism of mechanically capped ingots.

POSSIBILITIES OF USING DOMESTIC WHITE BAUXITE AS RAW MATERIAL FOR ELECTROFUSED REFRACTORIES

D. CVETANOVIĆ

Institute for Technology of Nuclear and other Mineral Raw Materials, Beograd

Thanks to its low Fe_2O_3 content and a convenient Al_2O_3 to SiO_2 ratio, Montenegrin white bauxite represents an interesting raw material for the production of electrofused alumosilicate refractories. We tested this in experiments, melting calcined white bauxite in a 220 kVA three-phase arc furnace. The melts were cast in sand molds.

Using a suitable melting and casting technique and a corresponding charge composition it was to get simple-shaped castings of desired sizes having a satisfactory surface. The Fe_2O_3 content of the melt may be reduced by using charcoal. In a similar way it is also possible to remove any SiO_2 surplus, the ferrosilicon formed settling at the furnace bottom.

DURABILITY OF THE REFRACTORY LINING OF FORGING FURNACES IN DEPENDENCE ON SIZE OF REFRACTORY BRICKS AND THE METHOD OF LINING

D. CVETKOVIĆ

Faculty of Mining and Metallurgy and Institute for Copper, Bor

Forging furnaces for big ingots at the Zenica Iron and Steel Works work under very severe temperature conditions — with very frequent and relatively large temperature changes. This causes strong thermal stresses in the refractory bricks and in walls and some constructional parts of the refractory lining. Fundamental problems are: cracking of bricks and big pieces falling down, so that the life of the lining is only 8—10 months; deformation of parts of the lining which must be replaced during furnace campaign which requires shutdown. Since October, 1966 we have been carrying out research on these furnaces with a view to increase the lining endurance by using smaller bricks of a different cross section shape and a new method of lining construction allowing room for expansion of each brick on all sides. It has been shown that the lining life can be prolonged to at least 4—5 years.

THE INFLUENCE OF EXCESS AIR ON THE FLAME TEMPERATURE IN THE COMBUSTION OF PROPANE-BUTANE MIXTURE

M. JOVANOVIĆ, E KROTIN and Z. POPOVIĆ

Faculty of Technology and Metallurgy, University of Beograd

The combustion of propane-butane mixture has been investigated. The temperature of combustion was calculated whenever combustion was possible i.e. when the combustion temperature was greater than the ignition temperature. The calculations show that combustion is possible when the excess air coefficient lies between 0.6 (range of incomplete combustion) and 4.9 (range of complete combustion). These results are compared with the experimental data obtained with laboratory equipment for ranges where measurements were possible. There are significant discrepancies in some ranges: the coefficient of heat loss is greater than 1 for some ranges of incomplete combustion. Some of the discrepancies could be explained.

A THEORY OF THE FILTRATION OF MELTS IN THE BIPHASIC ZONE DURING SOLIDIFICATION

F. HAVLIČEK

Higher School of Mining, Ostrava, Czechoslovakia

According to current opinions the internal quality of castings depends on the thickness of the biphasic zone during solidification. The thermal axial porosity is also related to this.

The zone of filtration can be established via many other factors: viscosity, thermal conductivity, specific weight of the melt, rate of castings, etc. It has been thought so far that the movement of the melt in the biphisic zone stops by the time 30% of solid phase has formed. According to the recent opinion the contraction of the melt lasts much longer — until the formation of about 80% solid phase. Between the formation of 30% and 80% of solid phase, the solution filters through the solid crystal lattice.

Filtration reduces axial porosity. Suitable filtration is advantageous because it reduces the rate of solidification near the walls of the casting. The data presented indicate the direction for future work.

A CONTRIBUTION TO THE THEORY OF PIPE FORMATION

J. PRIBYL

Higher School of Mining, Ostrava, Czechoslovakia

In the formation of PIPES the volume changes

1. during cooling of the melt
2. during change of state
3. due to volume change of the compact solid phase.

With the graphitizing allyos there is also

4. an increase in the volume due to graphitization.

The resulting shrinkage can be written algebraically as the sum of volume changes 1—4.

Due to graphitization in the melt and in the loosesolid phase the volume of graphite increases by ΣV_{grt}. This reduces the growth of PIPES. Graphitization in the compact solid phase increases the volume of graphite by ΣV_{grs}. The preshrinkage expansion depends on this.

A large number of tests were conducted on a nodular cast with $S = \frac{C_{gr}}{C_{tot}} \geqslant 0.7$ and a mould shape hardness $\delta_f \geqslant 75$ *GF*. The volume of PIPES also depends on the graphitization factor $\zeta = \frac{\Sigma V_{grt}}{\Sigma V_{grs}}$ and on the shape factor $\Psi = \frac{F_{conc} + F_q}{F_{conv} + F_q}$ (F_{conc} – concave surface area of casting, F_{conv} = convex area, F_q flat surface). The volume of PIPES $V_{st} = \Theta$. Under this condition we also have $S_{gr} \geqslant 0.7$, $\delta_f \geqslant 75$ GF, $\zeta \geqslant 0.4$, $\varphi \geqslant 0.7$. In this case funnels are not needed.

NON-EQUILIBRIUM THERMODYNAMICS IN PROCESSES OF TREATMENT OF METALS BY CASTING

C. MIRKOVIĆ

Non-equilibrium thermodynamics is a relatively new branch of macroscopic physics which within a short period has earned many recognitions, and has found considerable practical application and discovered new possibilities for theoretic and practical solutions of a number of production problems.

Processes of treatment of metals by casting belong to the group of problems which are theoretically advanced considerably, although not sufficiently developed and treated by methods of classic thermodynamics, but not by the application of non-equilibrium thermodynamics. In casting processes special attention is attached to the phase of solidification of the molten metal poured in various casting moulds, as at this juncture the main characteristics of the casting are formed and which define its quality and suitablity in exploiting. Molten metal, as a defined thermodynamic system, enters into a number of mutual actions with the mould which are divided in three basic forms: thermic, mechanic and physico-chemical mutual actions. These mutual actions are characterised by difference in value of the factors for intensity and extensity, which represent parameteres of the conditions of the system and which are numerous. The general picture of such mutual actions is rather well known today as has been advanced by methods of classic thermodynamics. However, many details of this complex require further study wherein non-equilibrium thermodynamics represent a turing point and which should lead to a general and quantitative theoretical solution adaptable to practical use. Taking into consideration the phenomenological relations, non-equilibrium thermodynamics enable us to perceive the substance of complexity and simultaneous action of numerous factors during the process of solidification of molten metals in moulds, and at the same time leads to a quantitative enlightement of prevailing laws and innovations for further exacting developpment of the theory of casting processes.

RECENT METHODS OF INVESTMENT CASTING SHELL PRODUCTION

N. OBRADOVIĆ and **M. POPOVIĆ**

Institute for Technology of Nuclear and other Mineral Raw Materials, Beograd

Preparation of molds for melting refractory reactor metals calls for new materials for refractory shells.

Our research has shown that dimension changes of the materials due to thermal stresses are minimal. Bending strength is increased, while the quality of the mold and casting surfaces is the same as obtained with ground silica powder.

EFFECTS OF VACUUM REMELTING OF STEEL

I. STOJŠIĆ, **N. OBRADOVIĆ**, M. POPOVIĆ and M. TUFEGDŽIĆ

Institute for Technology of Nuclear and other Mineral Raw Materials, Beograd

To get optimum qualities of some special steels they are vacuum remelted. The parameters of vacuum, retention time, temperature etc., and the characteristics of the starting material determine the final effect of remelting. Results we got with vacuum-induction, arc and electron-beam remelting of 100Cr6 ball-bearing steel are in accordance with those previously obtained by others. On a very limited scale we also remelted UTOP-1 steel.

These results are the first from our program of vacuum steel remelting.

CHARACTERISTICS OF METAL SOLIDIFIED IN PRESENCE OF CHILL

Đ. MILOSAVLJEVIĆ

Boris Kidrič Institute of Nuclear Sciences, Vinča

The microstructure of decanted specimens solidified on a water cooled chill immersed in a tin bath was examined. The temperature of the melt and the time the chill was kept in the melt were varied. The results are discussed in the light of recent literature data concerning the theory of metal solidification.

VACUUM AND ZONAL REFINING OF INDIUM

B. ĐURKOVIĆ, **D. SINADINOVIĆ** and I. ILIĆ

Institute of Chemistry, Technology and Metallurgy, Beograd

The results of laboratory test on purifying technical indium to high purity by vacuum and zonal refining are reported. They were obtained by studying the behavior of the metals appearing as the main impurities in technical indium (Zn, Cd and Pb). The effect of temperature, of vacuum — in the case of vacuum refining, and the number of passes — in the case of zonal refining, were also studied. By vacuum refining more than 90% of zinc, cadmium and lead could be eliminated. Zonal refining gave a much poorer refining effect.

AN ARC FURNACE REDUCIBILITY TEST OF THE STOGOVO MANGANESE SINTER FOR PRODUCTION OF "CARBURE" FEROMANGANESE AND OF SILICOMANGANESE

Đ. CVETANOVIĆ and LJ. RIKALOVIĆ

Institute for Technology of Nuclear and other Mineral Raw Materials, Beograd

We examined the possibility of reducing domestic "Stogovo" manganese sinter in a 220 kVA three-phase arc furnace. Reduction tests for production of "carbure" ferromanganese were done with and without flux, according to whether rich or a poor slag was desired. The rich slag was used for the production of silicomanganese.

The results indicate that the "Stogovo" sinter can be used as a raw material and the products are of a quality corresponding to current standards. Both processes are convenient for an industrial-scale application.

APPLICATION OF ION-EXCHANGE AND SOLVENT EXTRACTION PROCESSES IN HYDROMETALLURGY. POSSIBILITIES AND OUR EXPERIENCE

V. ŽIVANOVIĆ

Institute for Technology of Nuclear and other Mineral Raw Materials, Beograd

Ion exchange and solvent extraction in treatment of ores are frequently very effective for concentrating and separating metals, both from leach and from waste solutions.

A very wide application of both processes has followed the rapid development of synthetic resins and organic solvents, this application being especially marked in the extractive metallurgy of rare and noble metals, isotope separation etc.

In this report possibilities of practical application of solid and liquid ion exchangers are reviewed and process methods are described.

Our research so far has included problems of concentration and separation of uranium, copper, gold, silver, nickel, cobalt, zinc, iron, manganese and other metals, and the introduction of these processes in various flowsheets.

CHLORINATION OF NICKEL OXIDE

M. SPASIĆ, D. VUČUROVIĆ and I. ILIĆ

Faculty of Technology and Metallurgy, University of Beograd

Thermodynamics and kinetics of the chlorination of nickel oxide with gaseous chlorine at high temperatures are given. By thermodynamic analysis the free enthalpies are determined and equilibrium constants for given conditions are calculated. Cl_2 chlorina-

tion of NiO was investigated. The possibilities of stepping up both the reaction rate and the degree of chlorination were also examined. On the basis of these investigations the mechanism of chlorination is analysed.

OXIDATION OF PYRITE BY GASEOUS OXYGEN FROM AQUEOUS SUSPENSION AT HIGH TEMPERATURES IN AN AUTOCLAVE

M. SPASIĆ, D. VUČUROVIĆ and **R. VRAČAR**

Faculty of Technology and Metallurgy, University of Beograd

This work covers the chemistry, kinetics and thermodynamics of heterogeneous oxidation of pyrite by gaseous oxygen under autoclave conditions.

In studying the effect of working parameters, particular attention was paid to the distribution of oxidation products, and the conditions which give the biggest yield of sulphuric acid were defined.

HIGH PURITY METALS — OUR POSSIBILITIES AND EXPERIENCE

D. ĐURKOVIĆ and R. ĆOSOVIĆ

Institute for Technology of Nuclear and other Mineral Raw Materials, Beograd

The first part of the report is a short review of methods used at the Institute for Technology of Nuclear Raw Materials for production of high purity metals: zone melting, vacuum distillation, thermal decomposition of halides and amalgam electrolysis.

Our work so far has included the refining of the following metals by the zone melting method: germanium, zirconium, copper, aluminum, antimony, the refining of tin and lead being in the course of study.

We use the method of thermal decomposition of iodides for purifying zirconium and titanium. Tungsten and molybdenum are purified by thermal decomposition of chlorides.

By vacuum distillation industrial-grade magnesium is refined to nuclear-grade purity; antimony regulus is purified to the high-purity grade metal.

We purify cadmium and indium by amalgam electrolysis.

PARTIAL DESULPHURIZATION OF COPPER CONCENTRATES IN A FLUOSOLID REACTOR

Č. KOSTIĆ

Institute for Technology of Nuclear and other Mineral Raw Materials, Beograd

We have studied the possibility of partial desulphurization of the Bor smelting plant feed by fluosolids roasting. The aim was to get a copper matte containing 40% copper in a reverberatory furnace.

Changing the feed to air ratio the desulphurization degree was followed. For a given ratio all other parameters of roasting were determined: specific capacity of the reactor, ratio of roasting fractions, magnetite content of the calcine, flue gases composition, etc.

The results indicate that it is feasible to use fluosolids reactors for roasting the feed of the new Bor smelting plant.

SULPHATE ROASTING OF LEAD-COPPER MATTE IN A FLUOSOLIDS REACTOR

Č. KOSTIĆ and LJ. RIKALOVIĆ

Institute for Technology of Nuclear and other Mineral Raw Materials, Beograd

The possibility of copper-extraction by oxide-sulphate roasting lead-copper matte in a fluosolids reactor was examined. Tests were carried out using a mixture with a Pb-Cu matte to pyrite ratio of 3 : 1 to 4.7 : 1 in the temperature range 550—600° C.

The degree of copper sulphatization was determined by water leaching the calcine. 48—57% Cu was leached; with an addition of sulphuric acid 80—90% was leached, depending on the mixture composition and roasting conditions. The Cu : Fe ratio in the leach

liquor was 9—26 : 1 and the SO_2 content of the flue gases 4.8—6.5%. The procedure is convenient for industrial-scale treatment of lead--copper matte.

EVAPORATION ROASTING OF LOW-GRADE ANTIMONY ORE IN A FLUOSOLIDS REACTOR

LJ. RIKALOVIĆ and Č. KOSTIĆ

Institute for Technology of Nuclear and other Mineral Raw Materials, Beograd

In tests of evaporation roasting of low-grade antimony ore the following roasting parameters were determined:

— Bed temperature,
— α, i.e. atmosphere
— Total antimony evaporation
— Direct recovery of antimony

It was shown that fluosolids reduction-evaporation roasting may be successfully used for low-grade antimony ores, on an industrial scale.

A STUDY OF THE ROASTING PARAMETERS OF DOMESTIC PYRITES FOR PRODUCING ELEMENTARY SULPHUR

LJ. RIKALOVIĆ and Č. KOSTIĆ

Institute for Technology of Nuclear and other Mineral Raw Materials, Beograd

The production of elementary sulphur by thermal decomposition of domestic pyrites in a fluosolids reactor was studied. In the second phase of study divalent iron sulphide (FeS) was oxide roasted to get pyrite cinder with an as low content of sulphur as possible.

Optimum conditions for the thermal decomposition of pyrite and oxide roasting of FeS were established:

— Temperature
— Degree of sulphur evaporation
— Degree of sulphur elimination in pyrite cinder

The results obtained will be usful for solving this problem on an industrial scale.

ALKALINE PROCESS FOR DRESSING COPPER (DUST FROM LEAD REFINING)

J. KRIŠTO and D. ŠURBATOVIĆ
Trepča Lead and Zinc Institute, Kosovska Mitrovica

Some tests were done on laboratory and industrial scales on copper dust by an alkaline process. This was done by the addition of (expressed as wt. % of copper duct) NaOH 6—8%; coke 1—2%; enamel 7%, and if necessary 6% of pyrite, depending on sulphur content in the dust. Working temperature 1100° C.

Recovery:

Copper matte (composition Cu 55%, Pb 7%)
Pig Lead (composition Cu 0.4—0.8%)
Slag (composition Cu 2.80%, Pb 2.70%)
Speiss (composition Cu 59%, Pb 8%, Sb 10%, As 10—20%, Ni 2—5%)

The advantages of this process are: the increased copper and lead recovery in the form of separate products, less metal losses and more efficient operation of the furnaces.

ELECTROLYTIC ZINC SLURRY TREATED BY LEACHING IN SULPHURIC ACID

F. NIŠIĆ, J. KRIŠTO and S. VUKSANOVIĆ

Trepča Lead and Zinc Institute, Kosovska Mitrovica

Slurry of the composition Zn 24.1—27.0%, Fe 30—32%; Cu 0.51—0.75%; Cd 0.132—0.150%; Pb 1.8—4.5% was leached by returned electrolyte of the composition: H_2SO_4 150—174 g/lit, Zn 56.7—70.1 g/lit, with the addition of iron filings in order to decompose zinc ferrite.

The removal of iron from the leaching was accomplished in two steps, together with neutralization by zinc calcine.

The slurry from leaching had the composition: Zn 10.0—14.3%; Cd 0.05—0.075%; Cu 0.245—0.310%; Pb 5.4—8.1%; Fe 21.9—28.3%.

Slurry from purification: Zn 11.8—14.0%; Cd 0.042—0.067%; Pb 1.7—1.9%; Fe 31.7—43.8%; Cu 0.420—0.510%.

The metal recovery from the slurry in leaching was: Zn 79.2——85.8%; Cd 77.6—88.0%; Cu 74.9—83.2%.

The metal recovery from zinc calcine in purification was: Zn 73.7—84.4%; Cd 64.9—85.8%.

LEAD-CALCIUM ALLOY RECOVERY BY A CARBIDE PROCESS WITH THE ADDITION OF METALLIC ALUMINUM

S. VUKSANOVIĆ and J. KRIŠTO

Trepča Lead and Zinc Institute, Kosovska Mitrovica

The process of de-bismuthation refining pig lead is based on the effect of metallic calcium and magnesium which form intermetal compounds with the bismuth from the lead. The calcium is added in the form of lead-calcium alloy. Up to now this alloy has been obtained at Trepča by a carbide process without the addition of aluminum.

Some laboratory, pilot plant and industrial tests have been done on obtaining lead-calcium alloy by the addition of metallic aluminum under a cover of calcium and sodium chloride. The calcium content in the alloy obtained ranged from 2.80—3.50%,

while by the old process the alloy had 2.21% of calcium. This of course increased the recovery of metallic calcium and lead, and hence the productive capacities of the existing plant.

THE INFLUENCE OF THERMODYNAMIC PARAMETERS ON MATTE CONVERTING AT THE COPPER SMELTING WORKS, BOR

B. SAVIĆ

Institute for Copper, Bor

Recent results in the field of matte convertion and some questions concerning the thermodynamics of the chemical reactions are dealt with.

Particular reference is made to the reactions of formation and dissociation of magnetite and to making use of this phenomenon for producing a magnetite protective layer on the refractory lining of the converter. Experimental results parameters which optimized convertion conditions and produce a magnetite protective layer are given.

SMELTING LOW GRADE BAUXITE

V. G. LOGOMERAC

Faculty of Technology, University of Zagreb, Metallurgy Department, Sisak

The process, conditions and results of smelting ferruginous bauxite from Istria in a pilot blast furnace are described. The purpose of these trials was to obtain three types of slag: with 10—20, 10 and below 10 percent of SiO_2, to be used for obtaining alumina by leaching.

It was shown that it is possible to smelt ferruginous bauxite for obtaining quality pig iron and slag with a definite chemical composition. By keeping the CaO: Al_2O_3 ratio at a certain value, normal operation of the furnace and fluidity of the slag can be maintained. As regards the SiO_2 content, it seems that it is practically impossible to get less than 10 percent under these pilot conditions,

while 10—20 percent is convenient. The addition of about 50 percent scrap iron to the charge ensures economic production of pig iron along with slag which can be used for the production of cement. The slag obtained showed pronounced hydraulic properties.

AGGLOMERATION OF MANGANIC FLOTATION CONCENTRATE BY SINTERING

I. KOVAČIĆ and S. KOVAČIĆ

Institute of Metallurgy, Sisak

The experiments were performed on the conventional Greenawalt type semi-industrial sintering device. Owing to specific circumstances, the only component of the basic mixture was manganic floatation concentrate from manganese ore of the "Rudnici boksita" mines (Bos. Krupa).

The concentrate was first granulated in a pelletizing disk 1 m in diametar. The rew pellets with suitable physical, chemical and mechanical properties were partially dried, so that the sintering mixture, after the returend fines and fuel were added, had the desired humidity. The sinter obtained was completely satisfactory with regard to its mechanical properties.

TECHNOLOGY OF LOW-GRADE DOMESTIC URANIUM ORES

B. BUNJI, N. PACOVIĆ and V. ŽIVANOVIĆ

Institute for Technology of Nuclear and other Mineral Raw Materials, Beograd

Uranium represents an energy source of the near future. This is the reason for very persistent effort in prospecting and evaluating Yugoslav deposits of uraniferous ores.

Our activity has been directed towards processes which are technically and economically feasible with regard to our raw materials and local conditions.

The report reviews technological results with ores of different characteristics. Current trends of progress in this field are also outlined.

RESULTS IN PRODUCTION OF "CERAMIC GRADE" URANIUM DIOXIDE

Z. ĐUKIĆ, J. MILOSAVLJEVIĆ, M. LAZAREVIĆ, D. PEJČIĆ, D. KRSTIĆ and M. STANOJEVIĆ

Institute for Technology of Nuclear and other Mineral Raw Materials, Beograd

On the base of previous lab-scale research a pilot plant was erected for the production of ceramic grade uranium dioxide. During its operation optimal parameters were determined. They ensure production of sinterable uranium dioxide whose chemical and physical properties correspond to "ceramic grade" standards.

Parameters for dissolution of technical purity concentrate, solvent extraction, ammonium diuranate precipitation, calcination and UO_3—UO_2 reduction, and characteristics of the final product are given.

THERMAL DECOMPOSITION OF TUNGSTEN HEXACHLORIDE

D. ĐURKOVIĆ and R. ĆOSOVIĆ

Institute for Technology of Nuclear and other Mineral Raw Materials, Beograd

The rate of thermal decomposition of tungsten hexachloride on a hot filament was studied by a dynamic method, i.e. by continuous elimination of chlorine by degassing. The filament was mounted in an evacuated laboratory glass apparatus.

The rate of decomposition was investigated in dependence on:

— temperature of the filament, i.e. decomposition temperature;
— temperature of the reaction vessel, i.e. the vapor pressure of tungsten chloride.

The rate of decomposition lay within the limits 25—170 mg/h/cm and increased with the temperature of decomposition and with the vapor pressure of the chloride.

A NEW METHOD FOR SEPARATING ZIRCONIUM FROM TECHNICAL-PURITY CHLORIDE SOLUTIONS

R. ĆOSOVIĆ and D. ĐURKOVIĆ

Institute for Technology of Nuclear and other Mineral Raw Materials, Beograd

The method is based on the hydrolysis of zirconyl chloride to the dioxyhydrate at a temperature above 160°C and a pressure corresponding to the vapor pressure of the solution.

We examined parameters influencing the rate of the process and the degree of hydrolysis — temperature, time, and concentration of zirconium and of free acid in the starting solution and established optimum conditions.

The characteristics of the process are: high selectivity (exept for hafnium which behaves similarly), high purity of the final product (99.9% + 2% HfO_2), high yield (96—99%), and possibility of getting fine-grained powder (up to 80% minus 6 microns).

CONTRIBUTION TO THE TECHNOLOGY OF VANADIUM PENTOXIDE RECOVERY FROM "WHITE MUD" — A BYPRODUCT IN ALUMINA PRODUCTION

N. PACOVIĆ

Institute for Technology of Nuclear and other Mineral Raw Materials, Beograd

"White Mud" may represent an important raw material for production of vanadium pentoxide. Activity in this field of technology is considerable.

The report gives results of our research on the hydrogen reduction of alkaline water solutions obtained by leaching "white mud" in order to separate vanadium pentoxide. The rate of reduction is given as a function of parameters such as:

— vanadium concentration in solution,
— hydrogen partial pressure,
— catalyst type and surface, etc.

The possibility of using this process on an industrial scale is indicated.

CURRENT PROBLEMS OF RARE METAL METALLURGY

B. ĐURKOVIĆ

Faculty of Technology and Metallurgy, University of Beograd

The development of new branches of technology and industry, particularly electronics and rocket and nuclear technology, are closely linked with the development of rare metal metallurgy. This communication points out some specific features of rare metal metalurgy, with particular reference to current problems. The forms in which rare metals are found in nature and their specific properties which determine their applications are special factors influencing the complexity of their production. Beside a general survey, this communication gives a short summary of the research situation in rare metal metallurgy in Yugoslavia.

PROBLEMS OF WINNING GERMANIUM FROM REVERBATORY FURNACE DUST IN BOR

B. ĐURKOVIĆ, G. JOVANOVIĆ and S. BOGIĆ

Institute of Chemistry, Technology and Metallurgy, Beograd and Institute for Copper, Bor

This paper gives the results of laboratory and pilot plant trials of winning germanium from reverbatory furnace dust. Conditions for leaching germanium from raw material are given and problems arising are discussed. Detailed research results concerning the treatment of solutions up to the technical germanium dioxide stage are presented. For obtaining germanium from very poor solutions an ion-exchange procedure using Wofatite E adapted by tannin solution and so-called sorbent SG has been examined and very interesting results have been obtained. The hydrochloric acid formed as the germanium eluate is submitted to continual distillation and germanium tetrachloride vapor is hydrolized and converted to hydrated oxide as the final product. The economic aspects of the method are also considered.

TREATMENT OF GERMANIUM-CONTAINING CONCENTRATE FOR OBTAINING GERMANIUM

B. ĐURKOVIĆ, **D. SINADINOVIĆ** and R. VRAČAR

Institute of Chemistry, Technology and Metallurgy, Beograd

The results of tests on obtaining germanium concentrate from copper refloating concentrate are reported. Germanium was separated from the main concentrate by sublimation roasting in a neutral or reducing atmosphere. Sulphide sublimate in which more than 95% of the germanium had been converted was obtained.

The sulphide sublimate was then treated in two ways:

— in an oxidizing atmosphere at high temperature;

— with organic solvents, where free sulphur was eliminated from metal sulphides.

Metallurgical germanium concentrate containing more than 5% germanium was obtained.

On the basis of the results a flow sheet for treating copper refloating concentrate (Bor) to obtain metallurgical germanium has been worked out.

REGENERATION OF GERMANIUM FROM WASTE MATERIALS OF EI NIŠ ELECTRONICS ENTERPRISE

G. JOVANOVIĆ and S. BOGIĆ

Institute for Copper, Bor

Procedure for regeneration of germanium from waste materials has been worked out. It is based on application of sodium peroxide, and can be used for low grade (abrasion) and or high grade (cutting) waste. The prepared material is treated with aqueous solution of sodium peroxide under definite conditions. Elementary germanium is thereby transformed into soluble sodium metagermanate. Hydrochloric acid is added to a definite pH. Sodium metagermanate turns into hardly insoluble heptagermanate, which is turned into germanium tetrachloride by distillation and rectification.

With further application of standard operations polycrystalline germanium is obtained whose quality corresponds to the requirements of the electronics industry.

The procedure is economical and practical.

PHYSICAL METALLURGY AND CONTROL

THE APPLICATION OF SOLID ELECTROLYTES IN RESEARCH ON METALLURGICAL REACTIONS

B. KOROUŠIĆ

Metallurgy Institute, Ljubljana, and Metallurgy Institute University of Zürich

The properties of solid electrolytes are briefly reviewed. The relation between electrode potential and the equlibrium oxygen partial pressure (activity) in oxygen concentration cells incorporating solid electrolytes possessing a predominantly anionic conductivity was studied.

Technological application of galvanic cells designed to provide high-temperature thermodynamic data, including cells functioning as oxygen meters or electrolysis cells is discussed. The possibility of transfering oxygen inos by an externally applied potential is discussed, with special reference to the possibility of electrolytic--desoxidation of metals and slags.

THE RELATION N = f(ε) IN LOW-CYCLE METAL FATIGUE

D. MIHAJLOVIĆ

Faculty of Technology and Metallurgy, University of Beograd

In metal fatigue under low-cycle strain the relation between the number of cycles to failure *(N)* and the strain amplitude *(ε)* is given by Coffin's empirical equation $N^k \triangle \varepsilon = C$. The reasons for the known divergences from this relation in the behavior of some metals and alloys are different.

The parallel examination of high purity copper, Cu-90% Zn alloy and low-carbon steel with 0.04% C by the single plane alter-

nate bending method showed to what extent defect accumulation in the crystal lattice influences the correspondence with Coffin's equation.

To help explain the results a parallel study of work hardening as a function of strain amplitude was made.

METHOD OF EXPRESS QUANTITATIVE SPECTROSCOPIC ANALYSIS OF IRON AND STEEL CASTS ON GLASS SPECTROSCOPE

K. BELA and LJ. MATOVIĆ

Ironworks — Nikšić

The method falls under the group of visual quantitative spectroscopic methodics which employs the nine-degree reducer and in literature is known as "Method of visual photographic photomeasuring". The spectrum region used is between 3750—4050 Å on the glass spectroscope ISP-51. A short description of the principle of the methodics is given and the basic equation is deduced on which the method is based.

Detailed descriptions are given of the working conditions and the mode of preparing work diagrams. The mode of checking the work diagrams is described and three tables are included showing calculations of "the relative midarithmetic deviation in percentages" between chemical and spectroscopic methods with Si, Mn and Cr in cast iron. A separate table gives the basic characteristics of 7 work diagrams for cast iron and 4 work diagrams for steel cast.

From the inclination of the work diagrams the aberrance has been calculated in percentage of the analysed content, which can be expected from an aberrance of the relative visual estimate of the intensity of darkening of plus or minus 0.1 and plus or minus 0.2 units.

The shortest time for a single determination of Si, Mn, Cr and Mo of cast iron is 8 minutes. This includes the time required from receipt of the prepared sample for analysis up to delivery of the results for these elements.

At the end of the paper a conclusion is given with a critical review of this strictly subjective and empirical method, during an era of existence of highly perfected and various devises for spectroscopic analysis.

DIRECT SPECTROSCOPIC DETERMINATION OF Ag, Cu, Bi AND Sb IN SAMPLES TAKEN FROM LEAD REFINING

A. TODOROVIĆ, M. KARAKAŠEVIĆ and S. LISINAC

Trepča Lead and Zinc Institute, Kos. Mitrovica

Our laboratory spectroscopically determines these elements directly in samples from the lead refining plant on the French Cameca apparatus.

Ag	0.12 — 0.25 %	Bi	0.02 — 0.25 %
	0.0003 — 0.01 %		0.002 — 0.015%
Cu	0.05 — 0.13 %	Sb	0.05 — 0.5 %
	0.0003 — 0.004%		
	0.0025 — 0.04 %		

The spectral lines used are:

Ag — 3382.9 Å
Cu — 3247.5 Å
Bi — 3067.7 Å
Sb — 2598.1 Å

The comparison line used is Pb — 4057.82 Å on which a fixed photomultiplier is set during analysis.

Excitation is by high voltage spark; 3000 Cm, 320 μH.

The entrance slit of the spectrograph is 25 μ, the exit slit to the analyzing photomultiplier 100 μ and to the photomultiplier on the standard line 200 μ.

One electrode is a round plate of lead of diameter 3.5 cm and 1.0 to 1.3 cm thick. The other is of graphite with a hemispherical tip. The distance between the electrodes is 3.5 mm.

Recording time per element is 12 seconds.

RADIOGRAPHY OF LIGHT METALS

B. BOŠKOVIĆ-VASILJEVIĆ

Institute of Serbia for Testing Materials

The success of industrial radiography in the past few years has stimulated an intensive search for an isotope suitable for the radiography of light metals. The utilization of "bremsstrahlung"--induced X-rays makes it possible to extend the range of portable radiographic sources in the low energy range. The application of such a source in the radiographic inspection and examination of light metals and alloys is described.

DETERMINATION OF OXIDES IN STEEL

M. HORGAS, Z. HORGAS, LJ. BOŽIĆ, and V. ŽUMBERKOVIĆ

Hasan Brkić Institute of Metallurgy, Zenica

Isolation of the oxide phase by direct chlorination of killed carbon steel samples in a chlorine vacuum apparatus has been attempted. Due to the reaction of non-oxide phases (largely silicium from the steel) with oxygen and moisture from the chlorine and the apparatus, the amount of oxide isolated was many times greater than the actual oxide content of the steel. Silica dioxide generated during chlorination of the steel was in greater part soluble in warm 1% NaOH.

To avoid reaction with oxygen, a new continuous-flow apparatus has been developed for the chlorination of steel in a stream of chlorine. The chlorine is passed over glowing carbon (900 °C) whereby oxygen is removed by binding into CO. Oxygen and moisture are driven out of the apparatus with pure argon.

Oxide isolate obtained in the continuous-flow apparatus was chemically and mineralogically analyzed. The results were compared with the results for oxide obtained by electrolysis and chlorination of the isolate. The quantity of isolate was checked by the determination of oxygen in the steel.

The results showed that this relatively fast and low-cost method of direct chlorination can be successfully applied for the determination and investigation of the oxide phase in this kind of steel.

DETERMINATION OF THE SPECIFIC SURFACE AREA OF POWDERS

M. DUJMIĆ

Institute of Metallurgy, Sisak

Various methods for determining the specific surface area of powders were examined: Olevsky's separation method, the separation method using Kiesekalte and Mate's equation together with the RRS diagram; the direct method using Blaine's apparatus; the direct method using Svensson's apparatus. The principles of each method are given and the procedure and apparatus are described. Measurements were made on various materials. The results are tabulated together with an explanation.

MEASUREMENT OF LINEAR SHRINKAGE OF METAL

M. BRANKOVIĆ

Faculty of Technology and Metallurgy, University of Beograd

Linear shrinkage of metal is being more and more used for the control of the process of melting. It is measured on specially constructed apparatus. The mode of operation of apparatus constructed at the Faculty and measurements of linear shrinkage made with it are presented. They are in the main consisten with the established lines of cooling for the corresponding kind of cast.

A TRANSMISSION ELECTRON-MICROSCOPIC STUDY OF THE DEFFECTS OF NEUTRON-IRRADIATED LOW-CARBON STEEL

V. M. STEFANOVIĆ and M. ROGULIĆ

Boris Kidrič Institute of Nuclear Sciences, Vinča and Faculty of Technology and Metallurgy, University of Beograd

The effect of irradiation temperature and grain size on the dislocation density of low-carbon steel has been investigated by transmission electron microscopy. Thin foil specimens, suitable for direct microscopic observation — were prepared from the material (mean grain diameter 0.17 and 0.07 mm) after neutron irradiation: 2.5×10^{18} n.cm^{-2}, E $>$ 1 MeV, at 320 and 450°C. The dislocation density of the material irradiated at 320°C was considerably greater than that of the nonirradiated material. The dislocation density of the material irradiated at 450°C was unchanged. A number of small Frank sessile dislocation loops were observed near grain boundaries of the coarse-grained material irradiated at 450°C. It is believed that they could not have been due to defect condensation, but to shrinkage of long dislocation lines by one of the cross-slip mechanisms.

Based on the hypothesis that the defects observed are in part responsible for irradiation hardening, an attempt has been made to correlate the transmission electron microscopic results with the mechanical property changes obtained earlier. Using certain known expressions and a derived relation, increments of the yield stress were calculated and compared with the experimentally predicted values.

DEVELOPMENT OF A NEW STEEL FOR RAILS WITH HIGHER RESISTANCE TO WEAR

M. JUVAN and S. ĐORĐEVIĆ

"Hasan Brkić" Institute of Metallurgy, Zenica

Operating conditions becoming more severe from day to day demand rails from steel with better characteristics. Already several decades research abroad has been devoted to this problem, but solutions of a universal character have not yet been found.

This study, which is the first of its kind in Yugoslavia, represents an attempt to improve rail quality by using low-alloyed Mn steel. The most important thing was to eliminate the possibility of flakes formation and ways of cooling were tried. Testings of low alloyed Mn steel rails have shown better results than carbon steel rails.

EFFECT OF HYDROGEN ON THE EXPANSION OF RAIL STEEL

S. ĐORĐEVIĆ

Hasan Brkić Institute of Metallurgy, Zenica

Tests have been conducted on rail steel (rolled steel rails) to find relationship between its plastic properties (expansion and contraction) and the amount of hydrogen it contains.

A large number of expansion specimens were aged at room and higher temperatures, in air, water or oil, for different times. After tensile tests their content of hydrogen and expansion and contraction were measured. The results showed the following:

— Hydrogen reduces the plastic properties of rail steel. The higher its concentration the lower the expansion and contraction of the steel.

— Effusion of hydrogen from the steel takes place during ageing, both at room and higher temperatures. The effusion is greater the longer the ageing and the higher the temperature.

STRUCTURE OF METALLIC WELDS OBTAINED BY THE ELECTRON BEAM WELDING TECHNIQUE

Đ. MILOSAVLJEVIĆ

Boris Kidrič Institute of Nuclear Sciences, Vinča

The advantage of electron beam over other welding techniques is discussed. The structures of copper, stainless steel and Zircalloy-2 welds obtained by electron beam and TIG welding are compared. The solute and impurity redistribution and structural characteristics of electron-beam welded seams are analyzed.

THE INFLUENCE OF IRON ON THE PROPERTIES OF Al—Si ALLOYS WITH REGARD TO THE STRUCTURE

D. D. MITKOV

Motor and Tractor Factory, Novi Beograd

The influence of iron in given concentrations in Al-Si alloys on their casting and mechanical properties has been studied. A moderate effect of this element on the alloy fluidity, and a strongly negative influence on the mechanical properties because of segregation of undesirable microconstituents in the basic structure were established. If for any reason it is impossible to get a low iron content, some compensation is possible by adding neutral neutralizers like Mn or Co, or by modified heat treatment, depending on the iron content.

THE EFFECT OF ULTRASONIC VIBRATIONS ON THE SOLIDIFICATION OF Cd—Zn ALLOY

N. NOVOVIĆ-SIMOVIĆ and M. M. ROGULIĆ

Faculty of Technology and Metallurgy, University of Beograd

The influence of ultrasonic vibrations on the solidification of Cd-Zn alloy near eutectic composition has been investigated. The change in the structure was followed by optical microscope. The results indicate that ultrasonic vibrations produce a certain change in the structure under the horn.

SOME OBSERVATIONS AND NEW APPROACHES CONCERNING THE ACTION OF SEA-WATER ON THE SYSTEM STEEL/Al Zn Mg

S. STOJADINOVIĆ

Faculty of Civil Engineering, University of Sarajevo

Comprehensive studies of the steel/Al Zn Mg alloy system were carried out in order to determine the mechanism of corrosion. The investigated systems included 6 environments.

The following methods were applied to define the systems: chemical, electrochemical and metallographical, and examination of surface appearance. The characteristic changes of these properties as a function of the stage of corrosion were determined for system.

CHANGES IN TEMPERING AND RELEASE OF LOW ALLOY STEEL FOR REARINGS OF QUALITY Č. 4146

P. VUKSANOVIĆ

Ironworks, Nikšić

This paper covers an explanation of changes in structure which take place when tempering and releasing steel for production of roller bearings quality Č.4146 (DIN 9100Cr6, Gost ŠH 15). Tests

were made out of charges of regular production and charges under separate conditions in laboratory furnaces. Testing consisted of tempering conditions (temperature of austenisation 840°C), temperature region of release to 350°C. Tests of the microstructure on optical and electronic microscopes were conducted, a good part consisted of tensity and hardness. Increase of the tensity and partial decrease of the volume when releasing to 180°C, under normal conditions, can be considered as a result of decreases of inner tensity of strain and an increase of the carbide segregations. The later fall of tensity indicates disappearance of the remaining austenite and increase of volume.

Structural tests on the electronic microscope relate movement of the remaining austenite and segregated carbide in the tempered state, and the release region to 350°C.

With growth of the releasing temperature of over 150°C, the remaining austenite disappears more intensively, dissolving fully at a temperature of about 260°C. Simultaneoulsy on releasing this steel, at a temperature of over 150°C, segregation sets in of small needleshaped carbides of sub-microscopic size. At a temperature of over 300°C, cubical carbides of cementitic type are formed. These carbides increase, and at a higher temperature round off the edges, so that with further growth of temperature (over 600°C) they coagulate in oval round forms.

PARTIAL (DIFFERENTIATED) HARDENING OF FORGING TOOLS

Č. DOSTANIĆ

Enterprise "14. Oktobar", Kruševac

A new process of hardening of forging tools is presented, consisting of tempering only the layer of the tool (gravure) to the desired hardness, the other parts of the remaining unhardened. The advantage of this process is that the connecting parts of the tool remain "soft" so that the usual cracks and breakage do not occur, with a decrease of the deformation of the connections to the tools of the machine. The time required for the thermic treatment is reduced to more than a half.

Further, the equipment needed for the thermic treatment is described, and at the end a comparative table is given showing the classic method and the new one with regard to time required for tempering, hardness, resistance of the tools, regeneration of the tools, repair of the tools etc.

APPLICABILITY OF DILATOMETRIC METHOD FOR THE STUDY OF RETAINED AUSTENITE OF SOME TOOL STEELS

J. ŽVOKELJ

Institute of Metallurgy, Ljubljana

In steel research the dilatometric method is applied mainly for transformation points and thermal expansion coefficients. However its applicability can be extended for instance the study of the retained austenite which is present in considerable amounts in some tool-steels after quenching. By means of dilatometric analysis it is possible to determine under which tempering conditions the retained austenite undergoes transformation or becomes fully stabilized.

In this work a dilatometric method for quantitative determination of the amount of retained austenite is described and some results are given. The method is based on changes of thermal expansion coefficients due to different amounts of austenite.

X-RAY ANALYSIS OF THERMAL TREATMENT OF CARBONIC STEELS OF DIFFERENT CARBON CONTENT

S. B. ĐORĐEVIĆ

Hasan Brkić Institute of Metallurgy, Zenica

The crystal lattice of the martensite of welded steels is a centered tetragonal and can be considered as a partial deformation of the iron lattice. The relation of the axis of the lattice c/a determinates the degree of tetragonality. Such a martensite lattice shown

on the x-ray picture gives separated deflexed lines — Fe, (doublets). The space between the lines of the doublet depends on the relation of the axis c/a to the tetragonal lattice. Such a lattice can be established in steel with a carbon content of 0.6%.

Steels containing 0.2, 0.38, 0.6 and 1.08% have been examined. Samples were tempered in water of room temperature. On the basis of the doublety of the lines of the welded steel of 1.08% C, it was calculated that the martensite contains 0.9% C. Steels with a carbon content of 0.38 and 0.60% showed the carbon content of the martensite to be 0.23 and 0.75% respectively, established on the basis of the width of the deflexed lines.

When releasing the welded steel, the doublets unite and give a wide line the width of which decreases when increasing the temperature of the release. The lines of steel of 0.6% C when released also become narrower with an increase of the temperature of the release.

DILATOMETRIC INVESTIGATION OF THE TEMPERING OF STEEL IN WHICH SECONDARY HARDENING OCCURS

N. VIDOJEVIĆ and N. NOVOVIĆ-SIMOVIĆ

Faculty of Technology and Metallurgy, University of Beograd

The influence of the heating rate on the tempering of steel in which secondary hardening appeared has been investigated. The tests were carried out after the usual quenching of specimens and after quenching, low-temperature tempering and cold plastic deformation. Dilatometry and hardness measurements were used to investigate the kinetics of the isothermal tempering process. We found that the rate of tempering and the previous cold working had a certain effect on the tempering of the given steel and on the hardness that could be obtained.

X-RAY INVESTIGATION OF THE MONOCLINIZATION OF ALPHA-URANIUM LATTICE IN THE U-Nb SYSTEM

S. MALČIĆ, A. MIHAJLOVIĆ, A. MANCE and P. TEPAVAC

Boris Kidrič, Institute of Nuclear Sciences, Beograd

The monoclinization of the crystal lattice of alpha-uranium versus Nb-concentration was investigated on samples quenched in salt water and oil from the region of gamma solid solution. Monoclinization was followed by the Laue-breadth ratios for diffraction peaks 112 and 131 of alpha-uranium. Measurements were carried out on an X-ray diffractometar with a GM-counter and recorder. The results suggest that the so-called α'_b -phase actually represents the period from the begining of lattice monoclinization up to the moment when splitting of the lines becomes visible on X-ray photographs. Therefore it does not seem justified to consider the α'_b as a separate phase. The boundary between the orthorhombic (α'_a) and monoclinic (α''_b) phase is found at a concentration of about 3 w/o Nb for both quenching rates.

KINETICS OF ISOTHERMAL GROWTH OF SECOND PHASE PARTICLES IN DILUTE URANIUM

M. JOVANOVIĆ

Boris Kidrič Institute of Nuclear Sciences, Vinča

Transmission electron-metallography was used to study the growth of second phase particles as a function of annealing time and temperature in a multicomponent uranium alloy containing small amounts of molybdenum, silicon, aluminium and iron. Specimens were annealed in the alpha range at 600, 625 and 640°C. On annealing, larger particles were able to grow at the expense of smaller ones so the number of particles diminished. The variation of average particle radius with time was of the form $r = kt^n$. From the value of the coefficient n_A in the modified Avrami equation it was concluded that the particle growth rate changes on annealing. The activation energy for the growth process was 1.97 eV.

KINETICS OF $\beta \rightarrow \alpha'$ TRANSFORMATION IN LOW MOLYBDENUM-URANIUM ALLOYS

A. MIHAJLOVIĆ, A. MANCE, S. MALČIĆ and P. TEPAVAC

Boris Kidrič Institute of Nuclear Sciences, Vinča

The effect of overheating degree in the γ and β temperature regions on the kinetics of the isothermal $\beta \rightarrow \alpha'$ transformation was investigated in 0.45 and 0.6% (weight) molybdenum alloys by means of metallography and X-ray diffraction. It was found that at room temperature the $\beta \rightarrow \alpha'$ transformation depends on time, which indicates that thermal activation affects the kinetics of the process. The general kinetic equation $x = k\tau^n$ was applied, and k and n parameters were calculated. The applicability of the modified Avrami equation $z = 1 - \exp(-k\tau^{n_1})$ was also verified by determining k_1 and n_1, parameters, and a correlation was found between the calculated value of $n_1 = 2 - 3$ and the experimentaly established mode of growth of the martensitic phase. There are indications that the transformation kinetics changes during the transition from the upper to the lower β-solid-solution region.

KINETICS OF THE EUTECTOID DECOMPOSITION OF THE GAMMA PHASE IN URANIUM-NIOBIUM ALLOY

B. ĐURIĆ, N. JANKOVIĆ and M. MARJANOVIĆ

Boris Kidrič Institute of Nuclear Sciences, Vinča

The isothermal eutectoid decomposition of the gamma phase in uranium alloys with 5 and 10 wt.% Nb was followed. On the basis of metallographic examination the TTT diagrams were constructed and the kinetic parameters of the process determined. Increasing niobium content decreases the rate of eutectoid decomposition.

INFLUENCE OF RADIATION ON THE PHASE COMPOSITION OF LOW ALLOYED URANIUM

Đ. LAZAREVIĆ

Boris Kidrič Institute of Nuclear Sciences, Vinča

The effects of neutron radiation on the resistance of binary uranium alloys are reported. At a radiation temperature of 450°C two concurent processes occur-secondary phase precipitation enhanced by a non-equilibrium concentration of vacancies, and redissolution due to the action of fission fragments. The kinetics of these processes depends on the neutron flux, the type of alloying additions and on the initial state of the alloys.

INFLUENCE OF ALLOYING ADDITION ON THE RESISTANCE OF LOW-ALLOYED URANIUM

M. GLIGIĆ and Đ. LAZAREVIĆ

Boris Kidrič Institute of Nuclear Sciences, Vinča

The kinetics of resistance changes caused by annealing of quenched alloys has been studied. A difference in the diffusion rate of different alloying additions in the uranium lattice was established. From the temperature coefficient of resistivity it is concluded that the contribution of alloying additions to the resistivity of uranium depends on their ionic radius. The larger the difference between the ionic radii of uranium and the addition, the larger its contribution to the resistivity, which is in agreement with theoretical results.

METALLOGRAPHIC INVESTIGATION OF DILUTE Cu—Zr ALLOYS

D. MIHAJLOVIĆ and **M. KOSTIĆ**

Faculty of Technology and Metallurgy, University of Beograd

Copper-zirconium alloys are very suitable for application in electrical engineering because of their convenient combination of electrical conductivity and strength, so that they have recently been studied intensively.

Cast, solution heat treated and quenched, and artificially aged specimens of Cu alloys with 0.05—1.0 wt.% Zr were investigated by optical metallography. Cast specimens showed dendritic segregation, shifting the $\alpha/(\alpha+Cu_3Zr)$ phase boundary. The morphology of the Cu_3Zr intermetallic phase separated in eutectic and after artificial ageing at 350, 400 and 500°C precipitated in the α matrix was studied. The metallography was supplemented by hardness measurements. Special attention was paid to specimen preparation for metallography, viz., mechanical and electrolytic polishing and etching.

GENERAL CHEMISTRY

STUDY ON METAL POWDER PRESSING

B. ŽIVANOVIĆ and LJ. TRBOJEVIĆ

Boris Kidrič Institute of Nuclear Science, Vinča

The pressing of iron, chromium, molybdenum and copper powders over a wide range of pressing pressures (0.25—10.0 t cm^{-2}) was investigated. From the experimental data it was possible to derive a semi-empirical equation which represents the relation between green density and pressing pressure. By phenomenological analysis of the pressing process, the physical meanings of the parameters in this equation were interpreted. This gives the practical possibility of determining the compressibility of metal powders.

THE ELECTRICAL CONDUCTIVITY OF SINTERED UO_2

R. ŠTIGLIĆ and M. STEVANOVIĆ

Boris Kidrič Institute of Nuclear Science, Vinča

The room temperature conductivity of sintered UO_2 specimens of different densities and grain sizes has been measured. The specimens were obtained by sintering in the temperature range 1100—1560°C in an H_2 atmosphere. The conductivity of the same specimens was also measured after thermal treatment at 1750°C and 1800°C in an He atmosphere. The data have been analysed with regard to the influence of porosity, grain size and oxygen content.

A STUDY ON THE FIRST STAGE SINTERING KINETICS OF MOLYBDENUM POWDER

B. ŽIVANOVIĆ, **D. USKOKOVIĆ** and M. M. RISTIĆ
Boris Kidrič Institute of Nuclear Science, Vinča

The first stage sintering of molybdenum powder in the temperature range 1100—1400°C was investigated. The experiments were carried out by dilatometric technique in an argon atmosphere. Grain boundary diffusion was found to be the most probable material transport mechanism in sintering in this temperature range.

CHANGES IN CHARACTERISTICS PROPERTIES OF UO_2 POWDERS IN OXIDO-REDUCTION CYCLES

J. PETKOVIĆ, M. VLAJIĆ and I. STAMENKOVIĆ
Boris Kidrič Institute of Nuclear Science, Vinča

Cycled oxydation and reduction causes pulverization of UO_2 powder. The reason is the difference between the molar volumes of UO_2 and U_3O_8. This phenomena was applied to activate non-sinterable UO_2 powders and to pulverize sintered UO_2 pellets. Changes in powder characteristics with the number of oxidation-reduction cycles were studied. The initial oxidation stage of sintered UO_2 was investigated on an optical microscope.

AN ISOTHERMAL CALORIMETER FOR MEASURING THERMODYNAMIC PARAMETERS OF THE SOLID STATE

P. PAVLOVIĆ, I. STAMENKOVIĆ and D. RADOVANOVIĆ
Boris Kidrič Institute of Nuclear Science, Vinča

Literature data concerning calorimetric methods for solids were critically analyzed. An isothermal calorimeter for determining heats of solution of solids in neutral alkaline and slightly acid solvents in

the temperature range 20—90°C was designed and constructed. Its calibration, and preliminary experiments with materials having an enlarged surface area have been carried out. With this calorimeter quantitative analysis of surface thermodynamic parameters is possible.

ELECTROLESS NICKEL PLATING OF COPPER AT TEMPERATURES ABOVE 100 °C

Č. PETROVIĆ, D. ĐORĐEVIĆ and V. ALIMPIĆ

Institute of Chemistry, Technology and Metallurgy, Beograd

The possibility of electroless nickel plating of copper using nickel sulphate or nickel chloride baths at temperatures higher than 100°C has been investigated. As solvents organic substances boiling appreciably above 100°C were used instead of water. The rate of deposition was determined over a large range of temperature and time.

ELECTROLESS NICKEL PLATING OF METAL CASINGS AT TEMPERATURES HIGHER THAN 100°C

D. ĐORĐEVIĆ, Č. PETROVIĆ and V. ALIMPIĆ

Institute of Chemistry, Technology and Metallurgy, Beograd

The nickel plating of the metal casings by chemical reduction at temperatures above 100°C has been investigated. Operating conditions are given for depositing Ni from sulphate and chloride baths. The adherence and hardness of the plating and its resistance to various chemical agents were studied.

ELECTROLESS NICKEL PLATING OF SILICON IN NONAQUEOUS SOLUTIONS

D. ĐORĐEVIĆ, Č. PETROVIĆ and V. ALIMPIĆ

Institute of Chemistry, Technology and Metallurgy, Beograd

Electroless nickel plating of silicon using a sulphate or chloride bath at temperatures higher than 100°C has been studied. As solvents organic substances boiling appreciably above 100°C were used instead of water. The dependence of the rate of deposition on the temperature and plating time was investigated.

PHYSICAL AND CHEMICAL CHARACTERISTICS OF NICKEL PLATING ON SILICON OBTAINED BY ELECTROLESS PLATING IN NONAQUEOUS SOLUTIONS

D. ĐORĐEVIĆ, Č. PETROVIĆ and **V. ALIMPIĆ**

Institute of Chemistry, Technology and Metallurgy, Beograd

From nonaqueous solutions at temperatures higher than 100°C adherent, homogeneous and smooth coatings were obtained. The strength of the bond between plating and silicon, the micro hardness of coatings and their resistance to high temperatures and thermal stresses were studied. Their resistance to various chemical agents was also investigated.

CRYSTALLOGRAPHIC INVESTIGATIONS IN THE SYSTEMS Mn--Si AND Cr—Si

I. KRSTANOVIĆ, M. JANČIĆ, S. ĐURIĆ and LJ. RADONJIĆ

Institute of Chemistry, Technology and Metallurgy, Beograd

Unit cell dimensions of $CrSi_3$ $CrSi_2$, Cr_3Si and Cr_5Si_3 were improved by fitting by the least-square method. For this purpose a program was set up for an Elliot 803 B computer. In the system Mn-Si the components $MnSi_{1.5}$, $MnSi_{1.7}$ and $MnSi_{2.0}$ were investi-

gated in more detail. Three-dimensional intensity data were recorded on the Weissenberg goniometer from a single crystal of $MnSi_{1,7}$. Positions of the interatomic vectors confirmed a previous model for this structure, but slight revision is needed in orded to accommodate a variable amount of silicium in the investigated region of the system.

EFFECT OF CALCINED ALUMINA ON MECHANICAL AND ELECTRICAL CHARACTERISTICS OF ELECTRICAL PORCELAIN BODIES

Z. STAVRIĆ and H. KOČICA

Electroporcelain Enterprise, Aranđelovac

The mechanical and electrical characteristics depend on the structure, composition and the ratio of crystalline to glassy phase.

The properties of electrical porcelain bodies were found to be strongly affected by variation of the $SiO_2 : Al_2O_3$ ratio.

Tests were made to identify the effect of Al_2O_3 crystal and grain size.

The effect of different coefficients of thermal expansion of the glaze and body was also investigated.

Optimal firing conditions were also determined.

EFFECT OF SOME PROPERTIES OF PRE-SYNTHESIZED MAGNESIUM SILICATE ON THE PLASTIC BEHAVIOR OF STEATITE BODIES

R. NIKOLIĆ

Electroporcelain Enterprise, Aranđelovac

In manufacturing steatite two types of magnesium silicate can be used as a body component: natural magnesium silicate (talc) and synthetic magnesium silcate of various compositions.

The effects of some properties of pre-synthesized magnesium silicate with a molar ratio of metasilicate to orthosilicate of 1 : 1 on

the plastic behavior of a steatite body were studied. The various possibilities for plastification of synthetic steatite are discussed and some quality monitoring methods are suggested.

GRANULATION OF THE NEW PHOSPHORIC FERTILIZER "PELOFOS" BY GRANULATING AND COMPACTING

V. G. LOGOMERAC

Faculty of Technology, University of Zagreb, Metallurgical Department, Sisak

A thermal method for producting Pelofos fertilizer from steel mill wastes and raw phosphate and the main data on this fertilizer which now occupies an important place in Yugoslav agriculture after 10 years of systematic lab and field trials was described earlier. Here methods of granulation are described.

Granulation is done using a balling disc, adding water and some waste acids. Pelofos proved to be a very suitable material for granulation. Conditions of granulation and all the relevant data are given.

A new method of granulation called compacting is further described, and the results obtained in tests on Pelofos caried out in Germany are given.

The two methods are compared and the author give his estimation of their practical application for the granulation of fertilizer.

DIFFERENTIAL THERMAL ANALYSIS OF CHROMIUM HYDROXIDES PRECIPITATED AT VARIOUS TEMPERATURES

P. S. PUTANOV, **B. ALEKSIĆ** and B. ĐUKANOVIĆ

Institute of Chemistry, Technology and Metallurgy, Beograd

The ifluence of temperature during the precipitation of chromium hydroxides was investigated as part of a systematic study of the influence of precipitation conditions on the further genesis of chromium oxide.

Hydroxides were precipitated with 0.5 N solution of NH_4OH from an 0.5 N solution of chromium nitrate at a temperature of 20—80°C.

DTA with various heating rates in hydrogen, nirogen, air and vacuum indicated a different behaviour of the hydroxides precipitated at different temperatures.

THE INFLUENCE OF CHANGES IN THE CHEMICAL COMPOSITION OF THE LOW-TEMPERATURE WATER-GAS SHIFT CATALYST ON ITS BEHAVIOR DURING THERMAL TREATMENT

P. S. PUTANOV, **Ž. D. JOVANOVIĆ** and B. D. ALEKSIĆ

Institute of Chemistry, Technology and Metallurgy, Beograd

Differential thermal analysis and thermogravimetry of catalyst samples with promotors added by coprecipitation were carried out in the temperature range from room temperature to 600°C, in vacuum, air, a stream of nitrogen, of hydrogen, of mixtures of these gases, and of the reaction mixture nitrogen-hydrogen-carbon monoxide-steam.

The results gave more detailed information about the behaviour of low-temperature water-gas shift catalyst with a various amounts of promotor during thermal treatment.

INFLUENCE OF COMPOSITION OF THE $ZnO—Cr_2O_3—CuO$ CATALYST ON THE ELECTRICAL CONDUCTIVITY AND CATALYTIC ACTIVITY IN THE WATER-GAS SHIFT REACTION

P. S. PUTANOV, Ž. JOVANOVIĆ and **A. TERLECKI-BARIČEVIĆ**

Institute of Chemistry, Technology and Metallurgy, Beograd

The variation of conductivity with temperature in vacuum and in the air was investigated on pellets of the catalyst preheated and stabilized at 340°C.

The results show a definite correlation between conductivity, catalytic activity and composition in the range of the component ratio optimal for the water-gas shift reaction.

INVESTIGATION OF THE PROPERTIES OF HETEROGENEOUS CATALYSTS BY MAGNETIC METHODS

P. S. PUTANOV and **B. ALEKSIĆ**

Institute of Chemistry, Technology and Metallurgy, Beograd

Magnetic methods are not widely used for the determination of properties of heterogeneous catalysts, and there exist conflicting opinions about their applicability.

On various examples the usefulness of developing and applying magnetic methods in conjunction with other methoods is demonstrated.

THE ELECTRON WORK FUNCTION AS A CHARACTERISTIC OF SOLID CATALYSTS

P. S. PUTANOV and **M. JOVANOVIĆ**

Institute of Chemistry, Technology and Metallurgy, Beograd

Determination of the electron work function represents an experimental method for obtaining information about the electronic state of the catalyst surface and the adsorbed layer.

Methods of direct determination (thermionic saturation current method, photoelectric method and field-emission microscope) and an indirect method for determining relative changes of the work function (by measurement of contact potential difference) are presented.

Examples of the application of these methods are given. A comparison of the methods is made, including their applicability and nature of the information they yield.

THE DETERMINATION OF THE CONSTANT OF INITIATION (k_i) IN THERMAL POLYMERIZATION FROM DISTRIBUTION MOMENTS AND THE POLYMERIZATION RATE

D. JOVANOVIĆ and J. VELIČKOVIĆ

Faculty of Technology and Metallurgy, University of Beograd

From data on molecular weights distribution and the rate of polymerization an expression for the direct determination of the constant of initiation (k_i) is derived. The calculation is based on expressions relating the moments of distribution and the grouped rate constants of the polymerization reactions,

$$\mu_r = 1/2\,(r+1)!\;M_0^r\,[k_p/(k_t/k_t)^{1/2}]^{r-1}\,(1-[M]/[M_0])$$

and the overall rate for the same mechanism in thermal polymerization,

$$-d[M]/dt = (k_i/k_t)^{1/2} \cdot k_p\,[M]^2.$$

It was noted that differentiating these equations all constants except k_i can be eliminated:

$$\frac{\left(\frac{d}{d[M]}\right)(-d[M]/dt)^{1/2}}{1/M_0\left\{exp\left(\frac{d}{d_2}\right)[\log \mu_r/(r+1)\,!]\right\}} = k_i$$

allowing the direct calculation of the constant of initiation.

The method was used to calculate k_i from data on vinyl polymerizations taken from the literature.

RELATION BETWEEN CADMIUM CORROSION AND CURRENT EFFICIENCY IN CADMIUM SULFATE SOLUTIONS CONTAINING SULFURIC ACID

S. MLADENOVIĆ and V. MITROVIĆ

Faculty of Technology and Metallurgy, University of Beograd

Cadmium corrosion in a cadmium sulfate solution depends both on the sulfuric acid concentration and, especially, on the content of antimony, copper, iron and cobalt.

The dependence of current efficiency for cadmium on the concentration of sulfuric acid, cadmium, zinc, antimony, iron, copper and cobalt in the electrolyte for cadmium electro-winning has been experimentally confirmed.

By comparing cadmium corrosion and current efficiency for cadmium in cadmium sulfate solution containing sulfuric acid, it has been shown that the former is higer in electrolyte solutions where the latter is lower.

DISTRIBUTION OF RADIONUCLIDES IN A POLYCOMPONENT SYSTEM

R. DESPOTOVIĆ

"Ruđer Bošković" Institute, Zagreb

A heterogeneous system is formed from a homogeneous one; the radionuclide present is homogeneously distributed between the phases formed. The radioactivity of the solid phases Σn^S and of the

liquid phase Σn^L analyzed as $[\Sigma n^S]\ [\Sigma n^L]^{-1}$ in dependence on the molar fractions of the components give data for a determination of the mode of interaction between the constituents. Several typical examples are described.

pH CHANGE AT THE ELECTRODE SURFACE IN HYDROGEN EVOLUTION REACTION

D. M. DRAŽIĆ, S. ĐORĐEVIĆ, **M. VOJNOVIĆ** and B. PAŠTROVIĆ

Institute of Chemistry, Technology and Metallurgy, Beograd and Faculty of Technology and Metallurgy, University of Beograd

A new method of measuring pre-electrode layer pH has been developed. The basic innovation is the electrode, at the same time working and pH-indicating. It was prepared by deposition of a porous film of a suitable metal on a commercial glass electrode. The film of metal acts as the working electrode while at the glass electrode the pH of the pre-electrode layer was measured at the same time. The behavior of this electrode in the rest and during hydrogen evolution was studied. η-log i and pH-log i curves were registered simultaneously.

STUDY OF MECHANISMS OF COMPLEX REACTIONS. ELECTROCHEMICAL OXYGEN REDUCTION IN ACID SOLUTIONS

A. R. DESPIĆ and **D. B. ŠEPA**

Institute of Chemistry, Technology and Metallurgy, Beograd and Faculty of Technology and Metallurgy, University of Beograd

Possible intermediate species plausible as reaction participants in electrochemical oxygen reduction in solutions of pH = O have been considered. Unit steps were generated by digital computer. Using an experimental value for the activation energy and termodynamic-kinetic criteria, all plausible unit steps were chosen. Possible mechanisms are presented in matrix form and discussed.

PROPERTIES OF THE ELECTROCHEMICAL DOUBLE LAYER ON PYROLYTIC GRAPHITE (II)

A. R. DESPIĆ, D. M. DRAŽIĆ and **R. T. ATANASOSKI**

Institute of Chemistry, Technology and Metallurgy, Beograd and Faculty of Technology and Metallurgy, University of Beograd

The differential capacity of the electrochemical double layer on pyrolytic graphite has been determined as a function of electrode potential and the anisotropy of the graphite. An AC brigde method was used. The measurements were performed in Na_2SO_4 solutions of different concentrations, and the potential of zero charge of the graphite was estimated. The measured double layer capacities are compared with the values calculated for an approximate model of the double layer at the corresponding graphite surface.

INFLUENCE OF THE STRUCTURE OF THE ACTIVE CARBON ON THE ACTIVITY OF THE SUPPORTED CATALYST

R. R. ADŽIĆ and D. M. DRAŽIĆ

Institute of Chemistry, Technology and Metallurgy, Beograd and Faculty of Technology and Metallurgy, University of Beograd

Platinum or silver was deposited from the corresponding salt by chemical reduction in situ on active carbons with different surface areas and with different types of oxide on the surface as the catalyst support. The activity of the carbons for some electrochemical reactions (O_2 reduction, H_2 ionization) was examined. It was found that the activity of the electrode increased with increasing real surface area of the carbon, and that it depended to certain extent on the kind of surface compound.

ELECTRON CHARGE TRANSFER IN THE SYSTEM Sb(III)/Sb(V) AT PLATINUM ELECTRODE

M. VOJNOVIĆ and D. ŠEPA

Institute of Chemistry, Technology and Metallurgy, Beograd and Faculty of Technology and Metallurgy, University of Beograd

The process of the electrochemical oxidation Sb (III)→Sb(V) at platinum electrode in acid solutions has been studied: i) at constant solution pH and various concentration ratois of Sb(V) and Sb(III); ii) at constant concentration ratio of Sb(V) and Sb(III) and different pH values of the solution. On the basis of the contemporary theory of heterogeneous charge transfer the kinetics and mechanism of the process are discussed.

ELECTRODEPOSITION AND DISSOLUTION OF COBALT IN SULPHAMATE ELECTROLYTES

S. ĐORĐEVIĆ, D. M. DRAŽIĆ, **M. VOJNOVIĆ**, V. PANDUROVIĆ and B. PAŠTROVIĆ

Institute of Chemistry, Technology and Metallurgy, Beograd and Faculty of Technology and Metallurgy, University of Beograd

Electrodeposition and dissolution of cobalt in sulphamate electrolytes has been studied: i) at constant electrolyte pH and various concentrations of cobalt; ii) at constant concentration of cobalt and different electrolyte pH's; iii) at different temperatures. In some experiments the change of pH of the electrolyte in the preelectrode layer was registered simultaneously. The kinetics and mechanism of the process are discussed.

A STUDY OF D,L-THREONINE COPPER COMPLEXES IN SOLUTION

T. J. JANJIĆ, L. B. PFENDT and M. B. ĆELAP

Faculty of Sciences, University of Beograd

In a previous communication it was shown that copper (II)-ion and D,L-threonine for two complexes, in the ratio 1 : 1 and 1 : 2. Continuing our investigations we determined stability constants and the number of protons generated in the reactions. The determinations were carried out by a combination of electrochemical and spectrophotometric methods. In addition, it was found that the 1 : 2 complex is a dibasic weak Brönsted acid whose dissociation constants were determined. From the experimental data concentrations of all components in solutions and their absorption spectra were determined.

STUDY OF THE REACTIONS OF HEXANITROCOBALTATES(III) WITH AMINO ACIDS. VI. SUBSTITUTION KINETICS AND MECHANISM OF REACTION WITH GLYCINE, ALANINE, β-ALANINE AND α-AMINOBUTYRIC ACID AND SYNTHESIS OF CORRESPONDING TETRANITROAMINOACIDATOCOBALTATES(III)

M. B. ĆELAP, T. J. JANJIĆ and P. N. RADIVOJŠA

Faculty of Sciences, University of Beograd, and Institute of Chemistry, Technology and Metallurgy, Beograd

The reactions of sodium hexanitrocobaltates (III) with glycine, alanine, β-alanine and α-aminobutyric acid (2—20° C, pH 6.94 and 9.33) have been investigated. Two of the six nitro-groups in the complex ions were replaced by one amino acid ligand giving rise to the corresponding tetranitroaminoacidatocobaltates (III).

The reactions are first-order in hexanitrocobaltate (III) ion and zero order in amino acid ligands. On the basis of the kinetic data a probable substitution mechanism is proposed.

In addition, the corresponding procedures were worked out for the synthesis of the following four new classes of coordination compounds of tervalent cobalt with amino acids: tetranitroglyci-

natocobaltates (III), tetranitroalaninatocobaltates (III), tetranitro-(β-alaninato) -cobaltates (III), and tetranitro (α-aminobutyrato) cobaltates (III).

POTENTIOMETRIC STUDY OF LIQUID AMALGAMS IN NONAQUEOUS SOLVENTS AT HIGHER TEMPERATURES

O. TATIĆ—JANJIĆ

Faculty of Technology and Metallurgy, University of Beograd

Electromotive forces for the cells without liquid junction, of the type Me /Me^{z+}, nonaqueous solvent/MeHg, were measured, using cadmium, tin or bizmuth as metals and glycerol or diethylen glycol as solvents. The measurements were carried out in the temperature range from 130° to 170°, for various amalgam concentrations in the liquid state. The measured electromotive force values are compared with corresponding data from other sources.

REACTIVE DIFFUSION IN GERMANIUM-TRANSITIONS METAL SYSTEMS

M. Đ. JANČIĆ and LJ. M. RADONJIĆ

Institute of Chemistry, Technology and Metallurgy, Beograd

Kinetics of formation of new phases at contacts between germanium and transitions metals (Cr, Mn, Fe, Ni) has been investigated. The kinetic curves with the corresponding rate equation and rate constant have been determined. The rate constant was calculated using the temperature dependence of the kinetic constant. The change of the mechanism and kinetics of the process with temperatures is discussed.

KINETICS OF FORMATION OF NEW PHASES IN THE SILICON-CALCIUM SYSTEM

M. Đ. JANČIĆ and **LJ. M. RADONJIĆ**

Institute of Chemistry, Technology and Metallurgy, Beograd

Kinetics of diffusion in the single-crystal silicon-calcium system has been studied. The influence of the orientation and perfection of the crystal structure of the silicon on the kinetics of formation of new phases was investigated. The kinetic equation is given and the activation energy calculated using the temperature dependence of the kinetic constant.

MASS SPECTROMETRY STUDIES OF VAPORS OVER MIXED OXIDES AT HIGH TEMPERATURES

K. F. ZMBOV

Boris Kidrič Institute of Nuclear Sciences, Beograd

A mass spectrometer coupled with a Knudsen effusion cell was used to study gaseous molecules above ternary oxides at high temperatures. The composition of vapors and the heats of vaporization have been determined for several mixed oxides containing lithium and transition metals. The heats of reaction involving gaseous LiMO (M Ga, In) molecules were measured and used to evaluate the heats of atomization of these molecules.

THE EMISSION ELECTRONIC SPECTRUM OF THE $C^{12}O^{18}$ MOLECULE

J. JANJIĆ, **D. PEŠIĆ** and D. JANKOVIĆ

Faculty of Technology, University of Novi Sad and Boris Kidrič Institute of Nuclear Science, Vinča

The Ångström band system of the $C^{12}O^{18}$ molecule in the region between 6100 and 4100 Å was obtained in a carbon hollow cathode discharge tube in the presence of oxygen 18 and excess of helium.

The spectrum was taken in the first order of a 3 m Eagle spectrograph. A vibrationl analysis was carried out. The measured isotope shifts confirm that the CO molecule emits the observed spectrum.

N.M.R. INVESTIGATION OF PROPYLENE SORPTION ON ZEOLITES 4A, 5A, AND 13X

M. V. ŠUŠIĆ, D. R. VUČELIĆ, **D. B. KARAULIĆ**, and S. V. PAUŠEK
Faculty of Sciences, University of Beograd

The mechanism of sorption and the state of propylene on the zeolites 4A, 5A, and 13X was investigated. In all cases it was established that physical sorption takes place on the surfaces. On the zeolite 4A, besides the physical sorption, chemisorption plays a dominant role followed by polypropylene formation. It can be assummed that the polymerization is effected by the cations which are in a close contact with the propylene molecules.

The mobility of the propylene molecules at a degree of surface coverage of $k = 0.8$ does not depend on the nature of the cations and the crystal structure of the lattice, a fact pointing to the oxygen ions as sorption centers. At small surface coverages $k = 0.04$, the mobility depends on the nature of the cations. The zeolites 4A and 13X with Na^+ cations show mobilites of the same order of magnitude, which is about twice less than the mobility on the 5A zeolite. This is in accord with the double charge of the Ca^{++} ion in the lattice. Therefore, it can be concluded that the first molecules of propylene are sorbed on the cations of the zeolites.

SORPTION OF HYDROGEN AND DEUTERIUM ON THE ZEOLITE LINDE 5A

M. V. ŠUŠIĆ, D. R. VUČELIĆ, **S. V. MENTUS** and D. B. KARAULIĆ
Faculty of Sciences, University of Beograd

The sorption of hydrogen and deuterium on the zeolite 5A was followed by gas chromatography. It was established that the zeolite shows a catalytic effect similar to the one known on aluminium

trioxide. However, this effect takes place only in the presence of light hydrogen in the gas phase thus eliminating hypotheses dealing with predominant chemisoprtion of the catalytic mechanism. It can be assumed that the action of the surface is reflected in the appropriate rates of equilibration on the zeolite.

CONTRIBUTION OF SOME N.M.R. EFFECTS TO THE ELUCIDATION OF SORPTION MECHANISMS OF GASES ON SOLID SURFACES

M. V. ŠUŠIĆ, **D. R. VUČELIĆ**, D. B. KARAULIĆ, S. V. PAUŠEK and V. J. MILAKOVIĆ

Faculty of Sciences, University of Beograd

Relaxation times were determined of the following sorbed molecules: water, methyl alcohol, ethyl alcohol, and propylene on zeolites 4A, 5A, and 13X.

The theory of the irregular build-up of the mono- and polylayers was checked as well as the corresponding Pfeifer equation. The results of the spin-echo and broad-line techniques agree well with one another and show that this mechanism cannot be generalized for all sorption processes. Among the investigated molecules, only molecules of the methyl and ethyl alcohols are sorbed according to the above mechanism in cases when the degree of surface coverage exceeds $k = 0.1$. The water molecules show some deviations from the sorption mechanism according to this theory in the entire range of the monolayer build-up; in case of propylene this mechanism becomes unacceptable in the whole sorption range.

In the range of surface coverage with $k < 0.1$ a peculiar coordination bonding of the adsorbate molecules to the zeolite takes place.

ORGANIC CHEMISTRY

THE INFLUENCE OF THE TEXTURISING CONDITIONS ON THE MACROSCOPIC AND FINE STRUCTURE OF FRIZZLED YARNS

R. JOVANOVIĆ

Faculty of Technology and Metallurgy, University of Beograd

The effects of temperature, the number of turns and the tightness of filaments on the macroscopic and fine structure of poliamide frizzled yarns has been investigated. The domestic poliamide multifilament type 6 fiber "Yulon", fineness 70/42 den, and the type 66 multifilament fiber of 70/23 den produced by the Italian firm Rodiatoce were investigated. Texturising was performed on an ARST type FT-1 machine.

The following indices for the macroscopic structure were used: the number of frizzles per unit length, the width and height of the frizzles, degree of frizzling and the stability of the frizzles.

Changes in the fine structure with different texturising conditions were examined by X-rays.

ON THE RELIABILITY OF VARIOUS METHODS FOR DETERMINING THE LOW MOLECULAR WEIGHT COMPONENTS IN POLYCAPROLACTAM FIBERS

R. JOVANOVIĆ and V. MILETIĆ

Faculty of Technology and Metallurgy, University of Beograd

The influence of method and time of extraction on the efficiency of analytical methods for polycaprolactam extracts and on the mean values of the results obtained with fibers from which softening agents have been removed were investigated.

Caprolactam monomer and oligomers were removed from nylon 6 yarn by water boiling under reflux, or by Soxlet extraction in

which condensed water is recycled over the sample in TGL 142-2033 Soxlet extractor.

Low molecular weight components were determined by gravimetry and by chemical and optical methods for determining them in solution.

EFFECTS OF MICROORGANISMS ON ACRYLIC FIBERS

R. JOVANOVIĆ, J. JAKŠEVAC and S. LEVKOVA

Faculty of Technology and Metallurgy, University of Beograd

The effects of microorganisms on Yugoslav-produced acrylic fibers have been studied. Eight test-microorganisms from the collection of the Microbiological Laboratory of the Faculty of Technology and some molds isolated from acrylic fibers contaminated during warehousing were used. Two of these latter were indentified as Aspergillus sp., two as Penicillium sp., one as Stachybotrys sp., and one strain was not identified.

Growth of the microorganisms was estimated visually and the damage to fibers determined microscopicaly by following changes in the fiber's morphology and by measuring its strength. Samples were examined for a period of 240 days. The results show:

— that molds and bacteria can grow on acrylic yarn;

— acrylic fibers were most attacked by Chaetomium globosum, Trichoderma viride and Bacillus mycoides, bacteria having a greater effect than molds;

— microscopic examination and affinity for dyes showed that local deterioration of fibres and the phenomena of fibrilation occur;

— the maximum loss in fiber strength varied from 8 to 15 percent depending on the microorganism and time of exposure of the sample.

SORPTION OF STREPTOMYCIN ON AMBERLITE IRC-50 ION EXCHANGE RESIN

J. VANĐEL

Department of Technical Microbiology of the Galenika Research Institute, Zemun

The sorption and elution of streptomycin from aqueous solutions in the presence of earth alkali metals was studied. Calcium and magnesium ions are sorbed and eluted together with the streptomycin on Amberlite IRC-50. The salts of these constitute the main ballast in the eluates in streptomycin production. Sorption and elution curves for ion exchange of all three ions from filtered broth and aqueous solution are given. The regeneration curves of Amberlite IRC—50 are also given.

DECATIONIZATION OF STREPTOMYCIN SOLUTION ON ION EXCHANGE RESINS

J. VANĐEL

Department of Technical Microbiology of the Galenika Research Institute, Zemun

Decationization of streptomycin solution on various cation exchange resins in hydrogen form was studied. The antibiotic solution was passed through beds of Amberlite IR—120, Amberlite IR—124 and Wofatite KPS and the degree of decationization investigated. The best resin for this part of streptomycin recovery was found.

In the production of streptomycin the inorganic salts are eliminated from the eluate on cation exchange resins.

SOLUBILITY OF ERGOSTEROL ESTERS IN MIXTURES OF SOME ORGANIC SOLVENTS

S. N. RAŠAJSKI and D. M. PETROVIĆ

Faculty of Technology and Metallurgy, University of Beograd

The solubility of ergosterol esters — acetate, butyrate, caprylate and kalmitate — in polar solvents (ethyl-, n-butyl, n-octylalcohol), in nonpolar slovents (benzene, cyclohexane) and in slovent mixtures has been determined in the temperature range 15—65° C. The solubilities of all the substances were highest in cyslohexane: benzene mixtures. As the number of carbon atoms in the acid part of the molecule increases the solubility maximum shifts towards solvent mixtures with a greater cyclohexane content. The solubility of ergosterol esters and benzoic and substituted benzoic acids (p-NO_2, p-NH_2, p-$N(CH_3)_2$ was also investigated, and the effect of the substituent polarity on the composition of the maximum-solubility solvent mixture is determined.

DETERMINATION OF THE DEGREE OF SWELLING OF CROSSLINKED DEXTRAN (DEXTRAN GEL)

I. VAVRA and N. ĐOKIĆ

Faculty of Technology, University of Novi Sad and Institute of Food Technology, Novi Sad

It has been established experimentally that the centrifugation method does not give reliable enough data about the degree of swelling of dextran gel preparations. The results depend on the time of centrifugation and the particle size of the sample as well as the centrifuging force. Free water which remains on the surface of the minced sample and which fictively raise the amount of bound water.

A very simple method has been developed which eliminates the above deficiency by using filter-paper which takes up the surface water from the swollen big pieces of block polymerized sample.

Parallel obtained by this method and by centrifugation allowed determination of a correction for surface water and of the degree of swelling of bead polymerized preparations.

SIZE AND STRUCTURE OF THE ELEMENTARY FIBERS OF COTTON CELLULOSE

S. JOVANOVIĆ

Institute of Chemistry, Technology and Metallurgy, Beograd

Up to now data about the size and structure of the elementary fibers of cotton cellulose have been obtained by X-ray analysis and electron microscopy. In this work the kinetics of depolymerization of alkali cellulose by oxygen were studied and distribution curves of molecular weights plotted. From this data the dimensions of the elementary fibers were determined. The results agree to within the experimental error with those obtained by other methods.

COAGULATION OF CELLULOSE IN THE FORM OF FIBERS FROM CADOXEN SOLUTION AND SOME PROPERTIES OF THE REGENERATED CELLULOSE

S. N. RAŠAJSKI and **LJ. P. VRHOVAC**

Faculty of Technology and Metallurgy, University of Beograd

Cadoxen solution of cellulose was extruded through a nozzle into a coagulation bath. By energetic mixing, cellulose was obtained in the form of fine fibers. Fibers of the regenerated cellulose were investigated in order to determine: average dimensions, water sorption and average degree of polymerisation. Electron micrographs and X-ray diffraction patterns of a sheet of fiber were recorded.

SEPARATION OF NUCLEOSIDES AND THEIR BASES ON STARCH THIN LAYERS

S. E. PETROVIĆ, J. A. ŠENBORN and S. M. PETROVIĆ

Department of Chemistry, University of Novi Sad

The separation of nucleosides and their bases by two-dimensional chromatography on rice starch layers is described. The solvents, water and water — 25% ammonia (60 : 40) were used for sepa-

ration in the two dimensions, respectively. Spots were identified under UV light of 254 mμ. The method was applied for separation of substances isolated from natural materials.

SEPARATION OF CARBOHYDRATES BY THIN-LAYER CHROMATOGRAPHY

S. M. PETROVIĆ and V. D. CANIĆ

Faculty of Technology, University of Novi Sad

The separation of 13 sugars by means of 8 solvents and one- and two-dimensional chromatography on cellulose and starch layers is described. Good results were obtained on cellulose. Two-dimensional chromatography proved to be a satisfactory and widely applicable method in research of carbohydrates.

CIRCULAR THIN-LAYER CHROMATOGRAPHY ON STARCH OF CATIONS AND ANIONS

V. D. CANIĆ and **N. U. PERIŠIĆ-JANJIĆ**

Faculty of Technology, University of Novi Sad

The cations of five analytical groups and seventeen anions, divided to four groups, were separated by circular thin-layer chromatography on maize starch. Twelve solvents were used for separation and eight reagents for identification.

THE INFLUENCE OF SOME FACTORS ON PARTICLE SIZE DISTRIBUTION OF OIL/WATER TYPE EMULSIONS

LJ. ĐAKOVIĆ, P. DOKIĆ and **M. KOVAČEV-DOLAI**

Faculty of Technology, University of Novi Sad

O/W type emulsions at concentrations of 30%, 50% and 70% oil phase, stabilized by addition of 1% of Na-dodecylbenzenesulfonate, gelatin and casein, have been investigated.

The particle size distribution of emulsions stabilized by Na-dodecylbenzenesulfonate was determined in dependence on the agitation time (8, 12, 20, 60 and 120 min.). Changes in distribution were observed in aged emulsions. The experimental results were used to check distribution curves.

GAS CHROMATOGRAPHIC DETERMINATION OF C_6-C_8 AROMATICS AND SOME OTHER HYDROCARBONS IN GASOLINE ON OPEN TUBULAR COLUMNS

K. PETROVIĆ

Petroleum Refinery, Pančevo

Determination of aromatics in petroleum fractions by gas chromatography is very important for various extraction processes and in processes for improving the motor gasoline quality. Using the earlier experience from this area of gas chromatography a method for determining C_6—C_8 aromatics and some of the more important hydrocarbon components in synthetic and natural hydrocarbon compounds has been worked out.,

Results were obtained on support coated open tubular columns under isothermal conditions and with the programmed temperature operation as well.

THE INFLUENCE OF THE SURFACE PROPERTIES OF THE FILLER-CARRIER ON THE FRACTIONATING EFFICIENCY OF A BAKER-WILLIAMS COLUMN

S. M. JOVANOVIĆ and M. STANKOVIĆ

Institute of Chemistry, Technology and Metallurgy, Beograd

Between the column filler and the polymer to be fractionated and the solvent-nonsolvent mixture there are adsorption forces whose ratio determines which polymers and solvent-nonsolvent mixtures can be fractionated on a Baker--Williams column.

To examine the influence of the surface properties of the carrier on the fractionating efficiency of the column, fractionation of PMMA prepared by suspension- and bulk-polimerization was studied. The column was filled with teflon particles in one experiment and glass beads in an other. The results are compared and discussed.

A STUDY OF THE COMPOSITION DISTRIBUTION OF STYRENE METHYLMETHACRYLATE COPOLYMERS

J. VELIČKOVIĆ, D. JOVANOVIĆ and N. VALENT

Faculty of Technology and Metallurgy, University of Beograd and Institute of Chemistry, Technology and Metallurgy, Beograd

Six samples of styrene methylmethacrylate copolymers of different chemical composition, polymerized to conversions of 15 or 25%, were fractionated according to composition and molecular weight with benzene-methanol on a column with a temperature and concentration gradient, and the composition and intrinsic viscosities of the fractions were determined. The composition distribution curves indicate the existence of low molecular weight fractions with an unexpectedly high styrene content at the beginning of the fractionation, while the following 80 to 90% of the material is of uniform composition. The statistically calculated criteria of chemical inhomogeneity according to Fuchs indicate an increase of overall uniformity at higher conversions within the region investigated. An explanation for this behavior based on termination by disproportionation is proposed.

BULK POLYMERIZATION OF CETYLMETHACRYLATE

R. BORISAVLJEVIĆ, S. JOVANOVIĆ and Đ. KOSANOVIĆ

Galenika Chemicals, Zemun and Institute of Chemistry, Technology and Metallurgy, Beograd

Kinetics of radical bulk polymerization of cetylmethacrilate at various temperatures (50, 60, 70 and 80°C) and concentrations of the initiator was investigated. The initiator was α, α' -azoizobutyronitrile in concentrations of 0.05—1%. From the results the rate and rate constants of polymerization, the activation energy and $(E_p—1/2\ E_o)$ were calculated.

The rate constants obtained and corresponding literature data for methyl-, ethyl- propyl- and n-butylmethacrylate are compared and discussed.

SYNTHESIS AND POLYMERIZATION OF DIALKYLITACONATES

J. VELIČKOVIĆ and **S. VASOVIĆ**

Faculty of Technology and Metallurgy, University of Beograd and Institute of Chemistry, Technology and Metallurgy, Beograd

The homologous monomer series of n-dialkylesters from dimethyl- to diundecylitaconate and several iso-dialkylesters were prepared by esterification. The monomers do not polymerise thermally, however with azobisiso-butyronitrile as an initiator tacky to brittle polymers can be obtained. The relative rate of polymer formation was studied by continuously measuring the increase of relative viscosity in bulk polymerization at 70°C and lower temperatures. Observations indicate that the relative viscosity increase is proportional to the initiator concentration. However, the effect on the intrinsic viscosity of the polymer is negligible: polymer intrinsic viscosities from polydimethyl- to polydioctylitaconate did not exceed 25 cc/g in toluene at 25°C. In attempts to obtain higher molecular weights, polymerising at lower temperatures, values as high as 75 cc/g (for polydimethylitaconate prepared at 35.5°C) were observed, practically independent of the initiator concentration. With monomers of higher molecular weights intrinsic viscosity

values above 100 cc/g can be obtained, the influence of the initiator concentration being more pronounced. The anomalous behavior is ascribed to chain transfer with the monomer, its intensity decreasing with decreasing temperatures and with increase of the alkyl group of the monomer.

RELATIONSHIP BETWEEN INTRINSIC VISCOSITY AND MOLECULAR WEIGHT OF POLYDIALKYLITACONATES

J. VELIČKOVIĆ and S. VASOVIĆ

Faculty of Technology and Metallurgy, University of Beograd, and Institute of Chemistry, Technology and Metallurgy, Beograd

Several synthesized samples of polydimethyl-, polydibutyl- and higher polydialkylitaconates were fractionated with benzene-methanol on a Baker-Williams column with quartz sand as the support and with a temperature gradient from 50 to 20°C. From molecular weight measurements by light scattering on unfractionated samples and the fractions obtained, using the Zimm extrapolation, and from intrinsic viscosity measurements in benzene, toluene and other solvents, Mark-Houvink type relations were established. The relation for polydimethylitaconate, $[\eta] = 1.72.10^{-2}.M_w^{0.58}$, in benzene at 25°C, indicates unexpectedly high molecular weights at relatively low intrinsic viscosities. From fractionation data the type of distribution was determined, and from K_Θ, obtained by extrapolation, the dimensions of the unperturbed polymer coil were calculated.

DETERMINATION OF VARIOUS METALS BY COMPLEXOMETRIC TITRATION IN NON-AQUEOUS SOLUTIONS

T. KISS, **I. ZSIGRAI** and R. KRIZSÁN

Institute of Chemistry, University of Novi Sad

A method for the determination of zinc and cadmium by direct titration with EDTA in dimethylsulphoxide as solvent using PAN as indicator and a method for the determination of magnesium by direct titration with EDTA in formamide using Eriochrome Black T have been developed. A procedure for the determination of cadmium, barium and magnesium by direct potentiometric titration with EDTA in formamide using a mercury indicator electrode has been developed. Alternatively cadmium can be determined by a potentiometric back titration of the excess EDTA with iron(III)-chloride in formamide using a platinum indicator electrode. Semimicro, micro and submicro amounts of metals were determined with 0.05 M, 0.001 M and 0.0002 M EDTA solutions.

APPLICATION OF CATALYSIS IN THE RING OVEN METHOD

H. WEISZ and **T. KISS**

Institute of Chemistry, University of Freiburg in Breisgau, Federal German Republic, and Institute of Chemistry, University of Novi Sad

A procedure for detecting catalyzing substances by the ring oven technique has been developed and the detection limit determined. The catalyst is washed into the ring and then treated with concentrated solution of substances which react only in the presence of the catalyst with a colour change. In this way bismuth(III) was

detected as a catalyst of the reaction between lead(II) and tin(II) sulphide, thiosulphate, thiocyanate, diethyldithiocarbamate and cysteine as catalysts of the reaction between iodine and azide, copper(II) as a catalyst of the reduction of iron(III) thiocyanate by thiosulphate, and phosphate as a catalyst of the reaction between molybdate and ascorbic acid. The detection limit varies from 1 ng to 10^{-6}ng of the catalyst in 1 μl of the sample washed into the ring.

PRECIPITATION TITRATION WITH POTASSIUM IODIDE BY CATALYTIC THERMOMETRIC END-POINT DETECTION AND BY USING ARSENIC(III)-CERIUM(IV) AS INDICATOR REACTION

H. WEISZ and **T. KISS**

Institute of Chemistry, University of Freiburg in Breisgau, Federal German Republic, and Institute of Chemistry, University of Novi Sad

A method for the determination of silver, mercury(II) or palladium(II) by direct titration with potassium iodide has been developed. Bromide or thyocyanate were determined by back titrating an excess of silver with potassium iodide; chloride, bromide, thyocyanite, ferrocyanate or sulphide by back titrating an excess of mercury(II) with potassium iodide. The end-point was determined by the heat generated in the indicator reaction between arsenic(III) and cerium(IV) which is catalyzed by iodide ions.

CATALYTIC THERMOMETRIC TITRATIONS OF BASES AND ACIDS IN NON-AQUEOUS MEDIA

V. VAJGAND, F. GAÁL, **S. BRUSIN** and LJ. ZRNIĆ

Faculty of Sciences, University of Beograd and Institute of Chemistry, University of Novi Sad

Coulometric catalytic thermometric titrations of tertiary amines and salts of organic acids in mixtures of acetic anhydride, acetic acid (7 : 1) and sodium perchlorate have been developed, using the

generation of hydrogen ions at a mercury, or if hydroquinone is added to the solution titrated, a platinum anode.

Weak bases, such as caffeine, were succesfully determined when acetic acid was replaced by acetic anhydride as the solvent, with hydrogen ions being generated at a platinum electrode in the presence of hydroquinone. The results obtained are compared with those of coulometric titration with photometric or potentiometric end-point detection.

Coulometric titrations of tertiary amines and salts of organic acids in a mixture of propionic anhydride, propionic acid (7 : 1) and sodium perchlorate by the above mentioned methods are described. The technique of differential thermometric titration in catalytic titrations with coulometric generation of the titrant was applied here for the first time. The base samples taken were 0.8 to 3.0 mg, and the average deviation between samples was less than $\pm 1\%$.

Catalytic thermometric titration was successfully applied in the coulometric determination of acids in a mixture of acetone, diacetone alcohol and sodium perchlorate as supporting electrolyte, by generating the titrant at a platinum cathode. The results are in good agreement with those obtained by other instrumental methods.

DETERMINATION OF PALLADIUM BY THIOGLYCOLIC ACID AND INVESTIGATION OF THE COMPOSITION OF THE PALLADOGLYCOLATE COMPLEX

V. VAJGAND and **M. JAREDIĆ**

Faculty of Sciences, University of Beograd and Faculty of Liberal Arts, Priština

The complex of palladium with thioglycolic acid has so far not been investigated in detail. We have studied its composition and the possibility of determining palladium via this complex by various instrumental methods.

The complex was isolated from ethanol by neutralizing the acid solution with ammonium hydroxide to pH 5. By paper electrophoresis in an ammonia buffer solution at pH 10 it was established that the complex was anionic in character. The stoichiometric ratio between the metal and ligands in the complex determined spectrophotometrically by the molar ratio method was 1 : 2. From IR

spectra it was established that there was no bonding between the metal and the carboxyl group. Considering the percentage composition we consider the most likely formula to be $NH_4OOC—CH_2—$ $—S—Pd—S—CH_2—COOH$.

By reaction with hydrogen sulfide, ammonium hydroxide and potassium cyanide it was established that the stability constant of the complex ion lies between those for the ammonia and cyanide complexes of palladium. By measuring the electrode potential of the palladium electrode the value of 10^{45} was obtained for this constant.

The fact that the complex is coloured was utilized for the determination of microgram amounts of palladium on the basis of the Beer law.

The redox properties of thioglycolic acid made it possible to determine palladium by amperometric and potentiometric titration, the latter being applicable for macro amounts of palladium as well.

Errors of determination of palladium by these method are below 1%, and the precision is quite satisfactory.

DETERMINATION OF MIXTURES OF PRIMARY, SECONDARY AND TERTIARY AMINES

V. VAJGAND and **T. PASTOR**

Faculty of Sciences, University of Beograd

Components of ternary mixtures of primary, secondary and tertiary amines were determined. Two or three titrations with perchloric acid in glacial acetic acid were necessary for each determination. In the first sample the total amount of amines was determined. To the second sample acetic anhydride was added and tertiary amine was titrated. In the third sample the sum of secondary and tertiary amine was obtained after removing the primary amine with phthalic anhydride or salicylaldehyde. The first two titrations were carried out in glacial acetic acid, and the third either in the same solvent, when primary amine was removed with phthalic anhydride, or in a mixture of acetic acid and methylethylketone when it was removed with salicylaldehyde. Salicylaldehyde can be used to block primary amines in analyses both of aliphatic and of aro-

matic amines, whereas phthalic anhydride yields good results only when the secondary and tertiary amines in the mixture are aliphatic. For analyses of mixtures containing a tertiary aromatic amine, phthalic anhydride cannot be used because autooxidative dealkylation of N, N-dialkylanilines occurs when samples are treated with the reagent in acetic acid.

BIAMPEROMETRIC TITRATIONS OF ORGANIC ACIDS IN A MIXTURE OF SOLVENTS USING A BISMUTH ELECTRODE PAIR

M. S. JOVANOVIĆ and L. J. BJELICA

Faculty of Technology and Metallurgy, University of Beograd and Institute of Chemistry, University of Novi Sad

The results of biamperometric titrations of mixtures of some strong (inorganic) and weak (organic) acids by means of a strong base, using a bismuth — bismuth electrode pair, have already been reported. In aqueous solution the titration curve was V-shaped when determining an acid alone and had two minimums of the indicator current when determining acids in a mixture. This time mixtures of only organic acids sufficiently different in pK values in an ethanol-water solvent mixture were investigated.

Standardisation of approx. 0.05 N picric, benzoic and acetic acid against sodium hydroxide, were made by the potentiometric pH/V method. Biamperometric determinations of these acids using bismuth electrodes in ethanol-water mixture also gave V-shaped curves and were in excellent agreement with the potentiometric method. Mixtures of picric and benzoic and picric and acetic acid in mol-ratios 1 : 10 to 10 : 1 in 50% ethanol were also determined. The titration curves showed two sharp inflections, and the errors made were under 1% for the more concentrated component of the mixture.

ELECTROGRAVIMETRIC DETERMINATION OF MERCURY IN METALLIC MERCURY AND AMALGAMS

V. VAJGAND, **D. GALOVIĆ** and Ž. MILJKOVIĆ

Faculty of Sciences, University of Beograd, Institute for Nuclear Raw Materials, Beograd, and Research Laboratory of Elektronska Industrija, Niš

A procedure for rapid determination of macroamounts of mercury at a silver-plated platinum gauze electrode (after Fischer) is described. The electrolyte contains 200 ml of 0.1 M perchloric acid and it is possible, at an applied voltage of 2.2 V and current of 0.5 A, monitoring the cathode potential, to determine 0.1—0.5 g of mercury to an accuracy of 0.2 mg. By this method it is possible to determine mercury in the presence of copper, iron, bismuth, cadmium, zinc and alkaline and alkaline earth metals, which makes it possible to analyse dental alloys, amalgams and ores containing mercury.

POLAROGRAPHIC DETERMINATION OF ZINC IN CADMIUM

S. MLADENOVIĆ and M. ISAKOVIĆ

Faculty of Technology and Metallurgy, University of Beograd

In a supporting electrolyte consisting of ammonium hydroxide and ammonium chloride the cadmium wave appears before the zinc wave, and can interfere in the polarographic determination of zinc.

The polarographic determination of zinc in the presence of cadmium in ammonium carbonate supporting electrolyte is not always reliable due to the instability of the later.

If the cadmium is complexed by means of sodiumdiethyldithiocarbamate (cupral), zinc can be determined polarographically in its presence in ammonium hydroxide-ammonium chloride supporting electrolyte.

POLAROGRAPHIC DETERMINATION OF TIN IN THE PRESENCE OF LEAD

S. MLADENOVIĆ and J. LUTZ

Faculty of Technology and Metallurgy, University of Beograd

The half-wave potentials of lead and tin for the reduction of their ions at the dropping mercury electrode from the usual supporting electrolytes are very close, and direct polarographic determination of tin in the presence of lead is not possible in this case.

In a supporting electrolyte consisting of ammonium acetate and sodium salt of EDTA the determination of tin is possible in the presence of lead, which complexes with EDTA. In this supporting electrolyte considerable amounts of zinc do not interfere. From the anodic waves of tin in this supporting electrolyte the polarographic determination of tin in the presence of lead, cadmium and zinc is also possible.

POLAROGRAPHIC BEHAVIOR OF OXALYL DIHYDRAZIDE

M. JOVANOVIĆ and V. REKALIĆ

Faculty of Technology and Metallurgy, University of Beograd

The polarographic behavior of oxalyl dihydrazide (ODH) in dependence on pH has been studied. Above pH 4, ODH produces a well-defind wave, the half-wave potential being —1.78V v.s.S.C.E. The height of this wave is proportional to the concentration of ODH. At pH below 4 another wave appears at —1.41V v.s. S.C.E. With increasing acidity of the solution the height of this wave increases. However, the height of the wave at —1.78V decreases, and the wave disappears in stronger acidic solution. In the presence of some metal ions (Al^{+++}) a third wave appears at —1.2 to —1.3V v.s. S.C.E, the height of which is proportional to the concentration of the metal for concentrations from 0.5 to 5mM.

EMISSION SPECTROMETRIC DETERMINATION OF BERYLLIUM IN COPPER-BASE ALLOYS WITH STABILIZED ARC

M. KLISKA and **M. MARINKOVIĆ**

Boris Kidrič Institute of Nuclear Sciences, Vinča

Alloys are dissolved in a mixture of nitric and sulfuric acid and the solution obtained is sprayed with pneumatic nebulizer. The aerosol obtained is then introduced into the discharge zone of the disc stabilized arc. The monochromator from the Hilger Uvispek spectrophotometer was used and intensities of beryllium spectrum lines measured with nonintegrating photoelectric detectors. Influences of different cations and anions on the emission of beryllium lines were investigated. Precision of the procedure is comparable with those in flame photometry.

THE INFLUENCE OF SUBSTITUENTS ON THE DISSOCIATION CONSTANTS OF PICRAMIC REAGENTS

M. PRAVICA and **A. MUK**

Boris Kidrič Institute of Nuclear Sciences, Vinča

Some reagents derived from bis-azo-chromotropic acid have been investigated. The dissociation constants of the first and second -OH group of naphthalene were determined. The influence of substituents on the dissociation constants are discussed. This effect is compared with the influence of the same substituents on the protonation constants.

Izdavač:

IZDAVAČKO PREDUZEĆE "NOLIT", BEOGRAD TERAZIJE 27/II

*

Štampa:

GRAFIČKO PREDUZEĆE "PROSVETA", BEOGRAD,
ĐURE ĐAKOVIĆA 21

SRPSKO HEMIJSKO DRUŠTVO (BEOGRAD)

BULLETIN OF THE CHEMICAL SOCIETY Belgrade

(Glasnik Hemijskog društva — Beograd)
Vol. 34, No. 2-3-4, 1969

Published by
SRPSKO HEMIJSKO DRUŠTVO (BEOGRAD)
1969

Translated and published for U.S. Department of Commerce and
the National Science Foundation, Washington, D.C., by
the NOLIT Publishing House, Terazije 27/II, Belgrade, Yugoslavia
1970

Translated by
LAZAR STANOJEVIĆ

Edited by
PAUL PIGNON

Printed in "Prosveta", Belgrade

CONTENTS

Page

Ankica M. Antić-Jovanović and *Dimitrije S. Pešić:*
Emission Spectra of CuOH and CuOD in the Regions 5100—5600 Å and 6150—6300 Å 5

Darinka J. Stojković, Milan M. Jakšić, and *Branislav Ž. Nikolić:*
Determination of Hypochlorous Acid Dissociation Constant by Straight Line Method 13

Miodrag Đ. Jančić, Ljiljana M. Radonjić, and *Ildiko M. Klejn:*
Superstructure in the System Bismuth-Tellurium-Selenium 23

Branko I. Božić and *Nada P. Vidojević:*
Austenite Breakdown in High-Manganese Hadfield Steel 29

Slobodan K. Končar-Đurdević and *Ivanka P. Petković:*
Dynamic Adsorption of Organic Vapors on "Blocked" Silica Gel. I. Adsorption of Benzene, Toluene and Xylene Vapors 37

Dragutin M. Dražić and *Radoslav R. Adžić:*
Influence of Surface Treatment af Active Carbon on Its Activity in Fuel Cell Electrodes 43

Darinka J. Stojković, Milan M. Jakšić and *Branislav Ž. Nikolić:*
Polarization Characteristics of Lead Dioxide Slectrode in Electrolytic Chlorate and Perchlorate Production 51

Slobodan D. Radosavljević, Vera Č. Šćepanović, and *Milena M. Jovanović:*
Investigation of the Solution of Aluminum-III-Fluoride 57

Vilim J. Vajgand and *Mileta D. Jaredić:*
Study of the Composition of the Palladous Thioglycolate Complex and the Determination of Palladium with Thioglycolic Acid by Potentiometric and Amperometric Titration 61

Kosta I. Nikolić, Ksenija R. Velašević, and *Anđelija B. Đukanović:*
Manganese Chloride Compounds with Alkylpyridine Hydrochlorides . . 71

Ksenija D. Sirotanović and *Zorica Ž. Nikić:*
Synthesis of 2-N- and 2-S-Substituted Propanoic Acids (α-Amino Thiolactic Acids) and Their Esters 77

Mirjana Hranisavljević-Jakovljević, Radmila Dimitrijević, and *Gordana Marković:*
Monosaccharide Sulphates. I. Preparation and Purification of D-Glucose-3-Sulphate and D-Glucose -6-Sulphate 83

Ubavka B. Mioč:
Conditions for the Application of Arc-excited Swan's Bands in Quantitative Spectrochemical Analysis 89

Vilim J. Vajgand and *Todor J. Todorovski:*
Interferometric Precipitation Titration 97

Page

Vilim J. Vajgand and *Tibor Pastor:*
The Use of Phthalic Anhydride in the Determination of Various Mixtures of Primary, Secondary and Tertiary Amines in Acetic Acid 103

Vilim J. Vajgand and Tibor J. Pastor:
Determination of Primary, Secondary and Tertiary Amines Mixtures Blocking Primary Amines with Salicylaldehyde in a Methylethylketone-Acetic Acid Mixture 117

Milica Dragojević and *Momir S. Jovanović*
Argentometric Determination of Some Systems Using Depolarization End Point 127

GLASNIK HEMIJSKOG DRUŠTVA, Vol. 34, No. 2-3-4, 1969, pp. 163—169

GHDB-46

535.333:546.56

Original Scientific Paper

EMISSION SPECTRA OF CuOH AND CuOD IN THE REGIONS 5100—5600 Å AND 6150—6300 Å*

by

ANKICA M. ANTIĆ-JOVANOVIĆ and DIMITRIJE S. PEŠIĆ

Copper salts in flame emit molecular as well as line spectra. The molecular spectrum falls within the 4100—6600 Å region and contains two band groups considerably different in intensity and structure[1]. The bands in one group, lying mainly in the red and blue portions of the spectrum, have a well-defined structure and belong to the diatomic oxide, hydride or halogen radical if haloids are introduced into the flame. The other group contains diffuse bands which are not dependent on the nature of the copper salt. The most prominent among them lie in the green spectral region, between 5350 and 5500 Å, while those of much lower intensity in the red region, between 6150 and 6250 Å, have not yet been identified with certainty.

These bands were first recorded by Eder and Valenta[2] who attributed the red portion to the diatomic oxide molecule of copper, while the green portion was left unidentified. Much later, Singh[3] tried to analyze this system more closely and attributed the bands to the Cu_2 molecule. However, the emission spectrum obtained by Kleman and Lindkvist[4] from copper in a King's furnace, where it was proved by the isotope effect that the emitter was the Cu_2 molecule, does not conform to Singh's data[3]. Considerable headway in explaining this group of bands was made by Bulewicz and Sugden[5]. From the results of quantitative flame photometry, which shows that the band intensity depends on the composition of the gaseous mixture in flames of the same temperature, and by analogy with similar spectra emitted by alkaline-earth metal oxyhydride radicals, Bulewicz and Sugden[5] concluded that the emitter was the CuOH radical.

The object of this study was to obtain spectroscopic confirmation for the nature of the emitter of this group of bands using the isotope shift technique which proved to be highly convenient for the determination of the oxyhydride spectrum of alkaline-earth metals[6, 7, 8].

* Communicated in part at the 13th Symposium of Chemists of the SR of Serbia, Belgrade, January 1968.

EXPERIMENTAL

Two excitation sources were used: flame (butane-air, acetylene-air, oxy-hydrogen, oxy-acetylene) and vacuum arc. Copper salts (sulfates, nitrates, chlorides) were introduced into the flame by means of standard dispersers. The arc was excited between copper electrodes in an atmosphere of water vapor or heavy water vapor (98%), or in pure oxygen in a chamber previously evacuated to about 10^{-3} *mm* Hg. The pressure of vapor or gas was 15—30 *mm* Hg. Since the arc between pure copper electrodes was very unstably, we used a hollow anode filled with the copper salt (most often chloride). The arc between these electrodes was considerably more stable. At 7 Å and 220 V DC, satisfactory exposures were obtained in 12—15 min on a Zeiss PGS-2 diffraction spectrograph with 7 Å/*mm* dispersion in the first order. Exposure for the corresponding flame spectra was at least 1 h for the oxy-acetylene flame, and slightly longer for the others. Wavelengths were measured by comparison with iron lines to an accuracy of ± 0.5 Å for a large number of bands. Most of the measurements are mean values from 2—3 recordings on one or more plates.

RESULTS AND DISCUSSION

Appearance of Spectra

(a) *Green System* — The general appearance of the spectrum in the 5200—5550 Å region is seen in Fig. 1 (spectra b-d), and the corresponding microphotometer tracings in Fig. 2.

In this region, 43 bands emitted in the flame and vacuum arc in water vapor atmosphere and 25 bands in the vacuum arc in heavy water were indentified. The general appearance of the spectra is too complex for them to be ascribed to a diatomic emitter. The bands are of approximately the same intensity. They are not degraded in any defined way, while their rotational structure at medium-high dispersion is very complex. The arc spectrum in water vapor and the flame spectrum are identical (Fig. 1, spectra *b* and *c*). The differences originate from the presence of strong oxide bands between 5228—5237 and 5274—5313 Å (Fig. 1, spectrum *a*) [9] in the copper + water vapor spectrum, which do not appear in the flame, especially not in the butane flame. Differences also arise from the dissimilar intensity distribution because of the differing temperatures of the arc and the flame. The presence of copper atomic lines (λ 5218.2 and 5292.5 Å) and the intensive blackening around them also make the arc spectrum appear somewhat different to the flame spectrum, which is the same for all flames and independent of the copper salt. Going toward longer wavelengths, both arc and flame spectra become increasingly diffuse and weaker, which restricts the possibility of measuring the wave lengths beyond 5530 Å. From 5350 Å up to the violet range, the continuum masking most of these bands gets weaker, but the general decline in intensity and blurring render impossible any higher accuracy of wavelength measurement than that mentioned above. Table 1 gives the head positions of bands identified in the flame and in vacuum arc in water vapor.

The spectrum emitted in heavy water vapor resembles that in water vapor, only it is still more complex and diffuse (Fig. 1, spectrum *d*). With

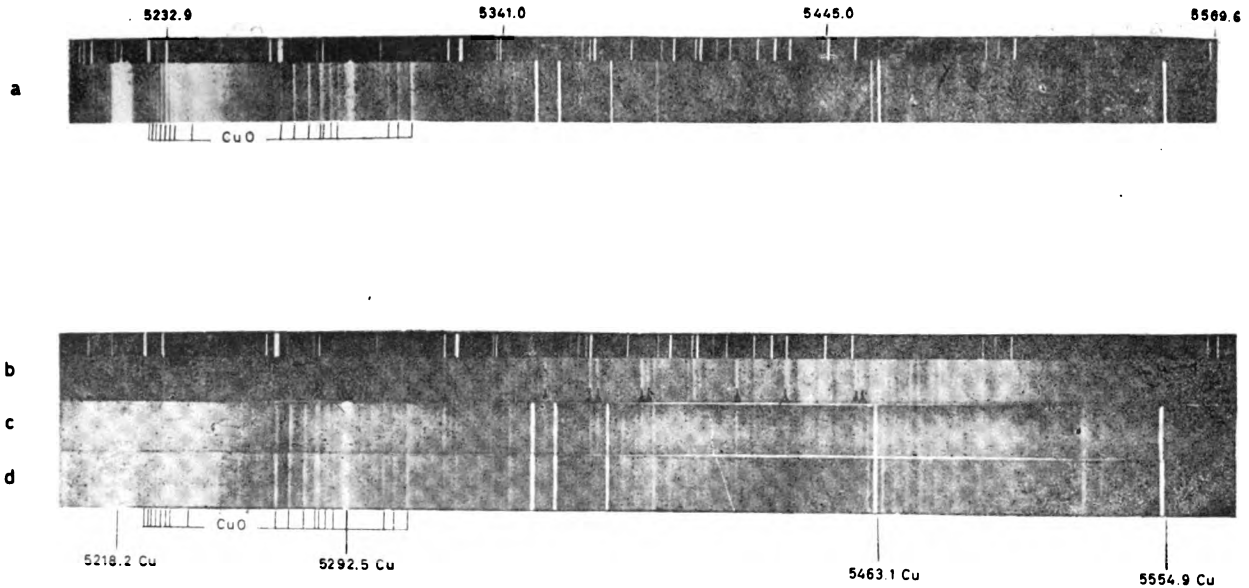

Figure 1.

Parts of the CuO, CuOH and CuOD spectra

a — metalic copper in the vacuum arc in oxygen atmosphere;
b — copper chloride in butane-air flame;
c — copper chloride in the vacuum arc in water vapor;
d — copper chloride in the vacuum arc in heavy water vapor.

most of the bands (Table 2) isotope shift was registered relative to the ordinary water atmosphere bands. These displacements are of the order of 1—25 cm^{-1}. They are very complex, which makes it difficult to establish any correlation between the corresponding bands of isotope molecules.

(b) *Red System* — In the flame spectrum, in the 6150—6300 Å region, 16 bands were identified (Table 1). Owing to their very low intensity and the still broader diffusion than in the green bands measurements could not be made to any higher accuracy than ±1--2 Å. Bands were not noted in the vacuum arc spectra in water vapor or heavy water vapor. The region in which these bands might be expected is occupied by the rotational structure of strong oxide bands around 6150 Å which appear in the flame only

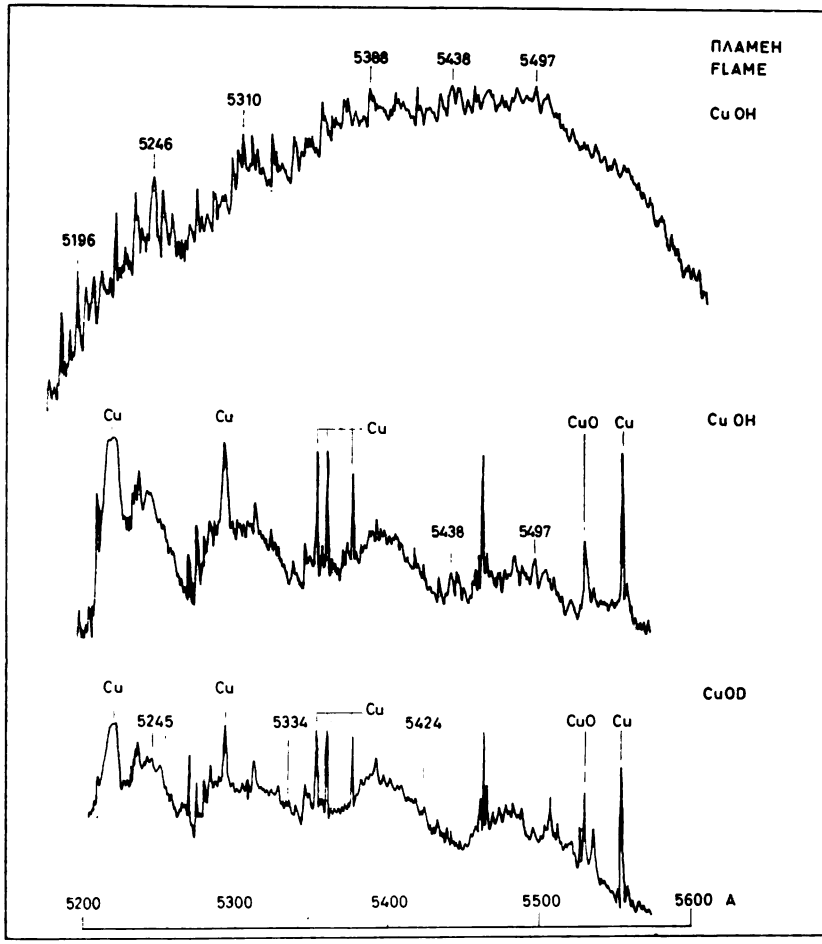

Figure 2

Microphotometer tracings of flame and vacuum arc spectra of CuOH and CuOD.

TABLE 1

Wavelengths of Outstanding Bands of CuOH

λ, Å	I	Deg.	λ, Å	I	Deg.	λ, Å	I	Deg.
6301	2	M	5483.4	6	M	5338	4	M
6277	3	M	5476.7	6	M	5326.4	6	R?
6264	3	M	5474	7	M	5324	8	M
6261	1	M	5468.4	6	M	5313.5	5	M
6259	1	M	5466.5	6	M	5310	7	M
6250	3	M	5458.7	8	M	5301	6	R
6237	1	M	5457	9	M	5297.8	6	M
6235	1	M	5451	4	R	5288	2	R
6233	1	M	5446.5	6	R	5277.7	3	M
6225	1	M	5445.3	7	R	5274.4	3	M
6220	2	M	5438	4	R	5258	2	M
6210	3	M	5435	6	M	5252	4	R
6206	2	M	5434.3	8	M	5246	8	M
6204	2	M	5424	5	R	5233	4	M
6191	2	M	5418.6	10	R?	5230	1	M
6187	2	M	5404.7	7	R?	5227	2	M
			5402.8	5	M	5221	5	M
5530.5	2	M	5401	4	M	5210	2	R?
5528.7	2	M	5390	8	M	5206.8	3	M
5523.5	2	M	5388	9	M	5202	3	M
5521	1	M	5374.6	9	M	5196	3	M
5515	1	M	5371	99	M	5186	2	M
5512	1	M	5362.6	4	R	5178	2	M
5510	1	M	5358	3	R	5164	1	M
5503	3	M	5356.5	8	R?	5157	1	M
5497	6	M	5339.3	4	M	5151	1	M
5485.5	5	M						

The bands occur only in the flame.

TABLE 2

Wavelengths of Outstanding Bands of CuOD

λ, Å	I	Deg.	λ, Å	I	Deg.	λ, Å	I	Deg.
5457	2	M	5408	3	M	5343.8	3	M
5455.8	2	M	5405.8	2	M	5339.8	3	M
5451.8	2	M	5404	2	M	5335	2	M
5447.6	2	M	5402	4	M	5333	3	M
5443.4	2	M	5397	4	M	5328.2	4	M
5439	2	M	5375.4	3	M	5251	3	M
5432	3	M	5370	2	M	5245.5	3	M
5424	2	M	5355	2	M			

as band heads. However, the manner in which these bands originate and their independence of the nature of the copper salt indicates that the emitter is the same as that of the green bands.

Identification of Emitters

The nature of the emitters was identified by comparing the spectra.

Twenty-one of the 43 bands identified showed good agreement with the band positions given by Singh[3] for the Cu_2 spectrum. However, the Cu_2 molecule could have been immediately ruled out as an emitter on account of the data presented by Kleman and Lindkvist[4]. The conditions in the arc and the fact that the spectrum flame does not depend on the copper salt suggest that the emitter is a molecule made up of Cu, O and H atoms. This is borne out by the measured isotope shift resulting from replacing water by heavy water which unequivocally proves the presence of hydrogen in the emitter. A comparison between the resulting spectrum and the spectrum in hydrogen atmosphere rules out the hydride band which would be in part resolved at the given dispersion. An analysis of the spectra obtained in pure oxygen 16 and oxygen 18 also rules out an oxide spectrum.

To determine the kind of molecule, i.e. the number of atoms which make up the emitter-molecule, spectrographs were run in a mixed atmosphere of water and heavy water in an approximately equal ratio. The recordings thus obtained do not show any new bands but only the overlapping of the bands previously detected in water and heavy water. This proves the presence of only one H atom, or only one hydroxyl radical. That one copper atom is present in the emitter was established by Bulewicz and Sugden[5] in a study on the stability of this molecule in flame. From these data, it was concluded that the emitter is the CuOH radical. This is supported by the rotational structure which is not resolved in any way, and by the irregular shift — characteristics of nonlinear polyatomic molecules such as CuOH. Also supporting the hypothesis of an oxyhydride emitter is the fact that the bands investigated fall within the same spectral region as the spectrum of the isoelectronic CuF molecule.

School of Sciences
Department of Physical Chemistry
Belgrade University
and
Boris Kidrič Institute of Nuclear
Sciences, Belgrade

Received 19 December, 1968

REFERENCES

1. Pearse, R. W. B. and A. G. Gaydon. *The Identification of Molecular Spectra.* 3rd Ed. — London: Chapman and Hall, 1963.
2. Eder, J. M. and E. Valenta. *Atlas Typischer Spektren* — Wien: A. Holder, 1911.
3. Singh, N. L. "Flame Spectra of Copper Salts" — *Proceedings of the Indian Academy of Sciences* (Bangalore) 231 A: 1—21, 1946.
4. Kleman, B. and S. Lindkvist. "The Band-Spectrum of the Cu_2-Molecule" — *Arkiv for Fysik* (Stockholm) 8: 333—339, 1954.
5. Bulewicz, E. M. and T. M. Sugden. "Determination of the Dissociation Constants and Heats of Formation of Molecules by Flame Photometry" — *Transactions of the Faraday Society* (London) 52: 1481—1488, 1956.
6. Gaydon, A. G. "Green and Orange Band Spectra of CaOH, CaOD and Calcium Oxide" — *Proceedings of the Royal Society* (London) 231 A: 437—445, 1955.
7. Charton, M. and A. G. Gaydon. "Band Spectra Emitted by Strontium and Barium in Arcs and Flames" — *Proceedings of the Physical Society* (London) 69: 520—526, 1956.
8. Pešić, D. and A. G. Gaydon. "Band Spectra of Magnesium Oxide and Hydroxide between 4000 and 3600 Å" — *Proceedings of the Physical Society* (London) 72: 244—249, 1959.
9. Antić-Jovanović, A., D. Pešić, and A. G. Gaydon. "The Spectrum of CuO; Study of the Orange-Red System Using O^{18}: — *Proceedings of the Royal Society* (London) 307 A: 399—406, 1968.

GLASNIK HEMIJSKOG DRUŠTVA, Vol. 34, No. 2-3-4, 1969, pp. 171—180

GHDB-47

546.133.1-36:541.132.081.7

Original Scientific Paper

DETERMINATION OF HYPOCHLOROUS ACID DISSOCIATION CONSTANT BY STRAIGHT LINE METHOD

by

DARINKA J. STOJKOVIĆ, MILAN M. JAKŠIĆ, and BRANISLAV Ž. NIKOLIĆ

According to Foerster[1, 2], the conversion of hypochlorous acid and hypochlorite ions, or total active chlorine, into chlorate is given by the equation

$$2\,HOCl + OCl^- \longrightarrow ClO_3^- + 2\,H^+ + 2\,Cl^- \qquad (1)$$

and represents the basic chemical reaction in the industrial electrolytic production of chlorates which achieves maximum current efficiency. Since the simultaneous determination of the reacting components (HOCl and OCl^-) in the inevitable presence of hydrochromic acid is inaccessible as yet, at least in simple industrial practice, production and the kinetics of active chlorine conversion can be monitored through the formal dissociation constant of HOCl and the concentration of hydrogen and active chlorine ions, which are easily accessible to determination[3]. Hence the knowledge and determination of the formal dissociation constant of HOCl is of practical significance for defining and checking industrial production of chlorates.

The dissociation constant of hypochlorous acid has long attracted attention (Table 1) and a number of studies deal with its determination[4-22]. Because HOCl is a very weak acid, and also very unstable and reactive, the determination is difficult. The conversion of active chlorine (1), particularly at higher temperatures makes impossible the maintenance of constant amounts of HOCl and OCl^- during the determination. Not only do the amounts of HOCl and OCl^- vary during measurement, but the changes are themselves functions of *pH*.

The sensitiveness of the determination is best proved by literature values[4-22] for the thermodynamic dissociation constant of HOCl which differ one from another by factors of up to 10^4 (Table 1).

The formal dissociation constant in concentrated sodium chloride solutions is highly significant for the monitoring of a large number of industrial processes, such as electrolytic chlorine production, chemical and electrolytic production of hypochlorites, and for the chlorination and bleaching

of cellulose. However, dissociation constants of hypochlorous acid for as high ionic strengths as this (5-6 M NaCl) have not been determined to date.

TABLE I

Dissociation Constant of HOCl According to Literature Data

Author	t°C	$10^8 \cdot K_a$	Reference
1. J. Sand	17	3.7	4
2. W. A. Nayes and T. A. Wilson	25	0.067	5
3. F. G. Soper	25	1.0	6
4. F. Giordani	30	1.3	7
5. F. H. Yorston	room	4.0	8
6. H. T. S. Britton and E. N. Dodd	15	3.2	9
7. G. F. Davidson	18—20	3.7	10
8. J. W. Ingham and J. Morrison	18	3.5	11
9. G. M. Gallart	25	10.5	12
10. A. Rius and V. Arnal	25	14.6	13
11. A. Skrabal and A. Berger	25	5.6	14
12. A. Skrabal and R. Skrabal	25	6.4	15
13. G. Holst	25	6.8	16
14. H. Hagisawa	25	3.0	17
15. M. Kiese and A. B. Hastings	5	2.8	18
16. J. Hoye	20	104.0	19
17. M. W. Lister	27	3.8	20
18. R. Caramazza	25	2.95	21
19. J. C. Morris	20	2.905	22
	30	3.18	
	35	3.44	

THEORETICAL FOUNDATIONS OF THE STRAIGHT LINE METHOD

The *pH*-metric, or straight line method for the determination of constants of weak acids or bases was recently developed by Despić[3]. The dissociation constant is determined by titrating the weak acid with a strong base, or the weak base with a strong acid, monitoring the change of *pH* during one titration, but without requiring a knowledge of the concentrations of the tittrated acid or base. The only stipulation is that titration should begin outside the *pH* range in which the given acid or base is found in the fully associated state.

The method likewise allows the determination of dissociation constants by titration from the *pH* range in which all the acid or base is completely dissociated, but then the initial concentration must be known.

The other two conditions imposed by this method are: the absence of additional weak acids or bases with similar dissociation constants, and constancy of the concentration of the acid or base during its titration.

Throughout the titration the weak acid (HA) is present partly in dissociated [A^-] and partly in associated [HA] state, relative to the initial concentration $[HA]_0$ we have

$$[HA] = [HA]_0 - [A^-] \qquad (2)$$

so that the formal dissociation constant (K_f) of the acid may be written

$$K_f = \frac{[H^+] \cdot [A^-]}{[HA]_0 -]A^-]} \tag{3}$$

Solving this equation for the hydrogen ion concentration

$$[H^+] = K_f \cdot [HA]_0 \cdot \frac{1}{[A^-]} - K_f \tag{4}$$

we obtain the convenient expression for the function $[H^+] = f\frac{1}{[A^-]}$, which enables us, by the determination of the instantaneous concentrations of hydrogen ion and dissociated acid at every moment of titration, to plot a straight line whose intersection with the ordinate immediately gives the dissociation constant. Apart from this, when the initial acid concentration is known, the constant can also be determined from the slope of the straight line.

The sum of the initial amount of OH^- ions and that introducted by titration up to a given time, minus the concentration at that time gives the amount of OH^- ions expended neutralizing the weak acid. It exactly equals the increment of the dissociated state i.e. of anions (A^-).

Potentiometric titration of a known amount of a strong base with a strong acid whose titer is known, or vice versa, yields a relationship between concentration of hydrogen ions in solution and the corresponding *pH* value. From this a conversion factor (γ) is obtained which for the given solution of a given ionic strength defines the relationship between the activity and the hydrogen ion concentration:

$$a_{H^+} = \gamma \cdot [H^+] \tag{5}$$

Thus in the titration of a weak acid in a solution of the same ionic strength the concentration of hydrogen ions can be determined at every moment of titration if γ is known by following the pH and conversion using γ.

Accordingly, knowing the conversion factor γ, which in the limiting case approaches or coincides with the hydrogen ion activity factor, it is also possible to determine changes in the concentration of anions of a weak acid during titration.

ACTIVITY FACTORS AS FUNCTION OF IONIC STRENGTH

Critchfield and Johnson[24, 25] demonstrated that the *pH* value of an electrolyte at constant hydrogen-ion concentration is a linear function of ionic strength, i.e. of the neutral salt concentration and its heat of hydration:

$$p\mathrm{H} = -\log [H^+] - \mathrm{J}(0{,}18 + 6 \cdot 10^{-3} \Delta Hs), \tag{6}$$

where $J = \frac{n}{2} M$, (M = molarity, n = number of ions building the neutral

salt, and Hs = heat of hydration of the neutral salt. Thus NaCl and $NaClO_3$ mixtures in concentrations typical for the electrolytic production of chlorates would have pH's reduced by 1 or more compared with a solution of the same hydrogen-ion concentration in the absence of the neutral salt. In other words, the introduction of 5—6 mols of NaCl or $NaClO_3$ into a pure solution of the given hydrogen-ion concentration changes the hydrogen ion activity factor by about one order of magnitude or more.

According to other authors[26, 27, 28], the presence of the above concentrations of kitchen salt and chlorates does not appreciably change the activity factors of other components (HOCl, OCl^-), which appear in the expression which defines the dissociation constant of hypochlorous acid, while the activity of water is also approximately unity[26].

Since the ratio of all the other activity factors (HOCl and OCl^-) and the activity of water appearing in the expression for the dissociation constant of hypochlorous acid at ionic strengths used in electrolytic production of chlorine and chlorates is about 1, whereas the activity factor of hydrogen ions is ten times higher, the introduction of neutral salts could be expected to apparently raise the thermodynamic dissociation constant in accordance with the change of the hydrogen-ion acrivity factor.

Schwabe[25] demonstrated that the antilog of the pH measured in NaCl solutions of high ionic strengths sufficiently accurately gives the hydrogen-ion activity, so that the conversion factors also sufficiently accurately represent the hydrogen ion activity factors.

EXPERIMENTAL

In 5 M NaCl solutions, which are of practical importance for the electrolytic production of chlorine and chlorates, a known amount of 0.01 N NaOH with 0.1 N HCl was potentiometrically titrated with a glass electrode at constant temperatures of 25.40 and 60°C, which are also of practical interest. To prevent changes in ionic strength, the 0.1 N HCl also contained 5 M NaCl. By plotting the negative pH values (ordinate) against hydrogen-ion concentration (abscissa), straight lines were obtained (Fig. 1) which pass through the origin and whose slopes give the desired conversion factors (Table 2).

In the 50 *ml* alkaline solution of 5 M NaCl some hypochlorite was always generated electrolytically, always under the same conditions, using platinum electrodes. The pH-metric titration for determination of the dissociation constant was also conducted from the alkaline range because of the stability of active chlorine, which required a knowledge of the initial hypochlorite concentration $[HA]$. The total active chlorine was determined by potentiometry using platinum and SCE electrodes with an arsenite solution. Buffering was achieved by saturating the solution with sodium hydrocarbonate according to the method recently described by Ibl[29].

The sum of the introduced $[H^+]$ and initial $[H^+]_0$ minus the measured concentration $[H^+]_a$ was subtracted from the initial concentration $[HA]_0$ to obtain the concentration of dissociated hypochlorous acid $[A^-]$ at the given point of titration:

$$[A^-] = [HA]_o - \{[H^+]_o + [H^+]_a - [H^+]_a\}. \qquad (7)$$

TABLE 2

Conversion Factors and Dissociation Constant of HOCl

Experimental and calculated values	Temperature		
	25°C	40°C	60°C
1. Conversion factor	10.0	9.30	6.58
2. Formal dissociation constant of HOCl obtained by extrapolation	$6.0 \cdot 10^{-8}$	$1.10 \cdot 10^{-8}$	$3.45 \cdot 10^{-8}$
3. Formal dissociation constant of HOCl obtained from the slope	$4.54 \cdot 10^{-9}$	$8.04 \cdot 10^{-9}$	$2.30 \cdot 10^{-9}$
4. Approximative thermodynamic dissociation constant of HOCl (combination 1 and 3)	$4.54 \cdot 10^{-8}$	$7.46 \cdot 10^{-8}$	$1.505 \cdot 10^{-7}$

All concentrations were always reduced to the instantaneous volume. They were obtained by means of the conversion factor previously determined in solutions of the same ionic strength without the presence of the weak acid and the *pH* reading during titration i.e. the microburette readings of the amount of acid introduced.

Plotting the reciprocal values of Eq. (7) on the abscissa against the hydrogen-ion concentration obtained by *pH*-metry using the conversion factor γ, straight lines were obtained whose intersection with the ordinate (Figs. 2, 3, 4) directly yielded the desired HOCl dissociation constants for the given temperatures (Table 2).

Since the initial concentrations (AC) were known, the constants could also be calculated from the slope of the straight line (Table 2).

For all measurements a special *pH*-meter with an expanded scale was used, permitting an accuracy of reading to greater than two decimal places (*pH-m*V-meter, Radiometer pHM 25).

DISCUSSION AND CONCLUSION

The values obtained for conversion factors conform with the theoretical functional relationship given by Critchfield and Johnson[24]. It is hypothesized that the salts having sufficiently positive hydration heat values, taking away water molecules from the hydration envelope of hydrogen ions will intensify its activity in proportion to the amount of neutral salt introduced.

The obtained formal dissociation constants differ by an order of magnitude from the most reliable values for the thermodynamic constant determined in dilute solutions[21, 22]. However, multiplied by the hydrogen-ion conversion factor γ the give approximately the same values.

As a matter of fact, according to Weiss[28] the activity factor of hypochlorous acid (f_{HOCl}) ranges between 1,3 and 1.4 in 5 M solutions of kitchen salt and sodium chlorate. Imagawa[27] has recently given a value for the

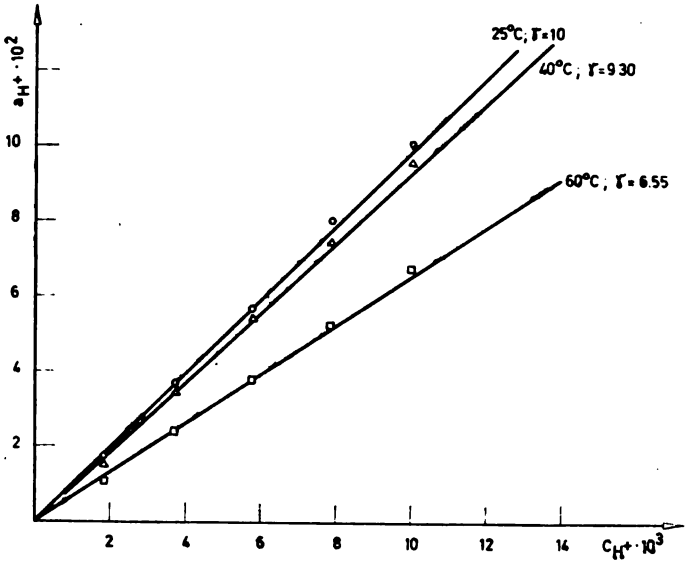

Figure 1.

Ratio of a_{H^+} to C_{H^+} in 5 M NaCl solution at 25, 40 and 60°C

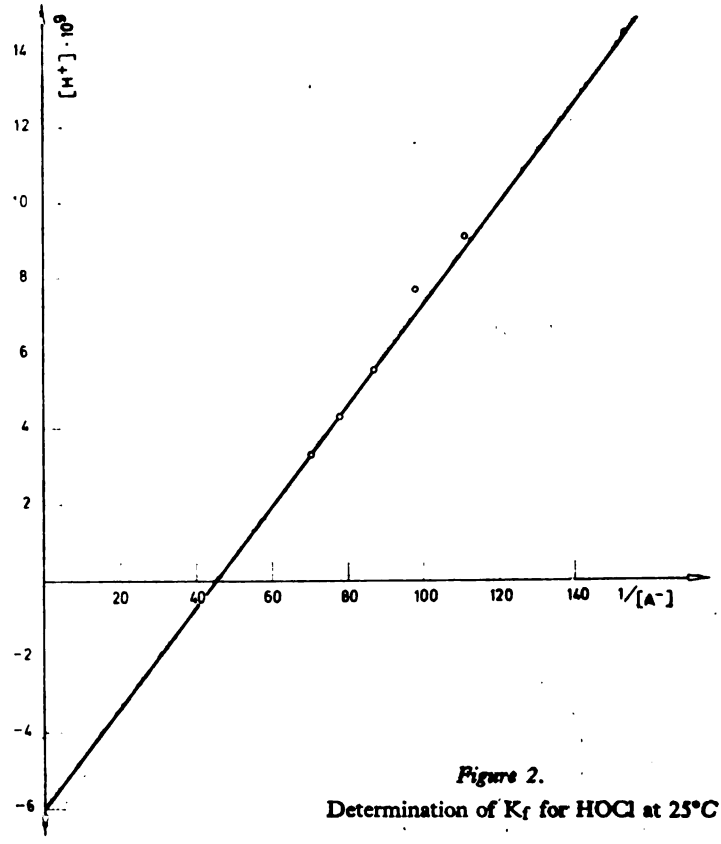

Figure 2.

Determination of K_f for HOCl at 25°C

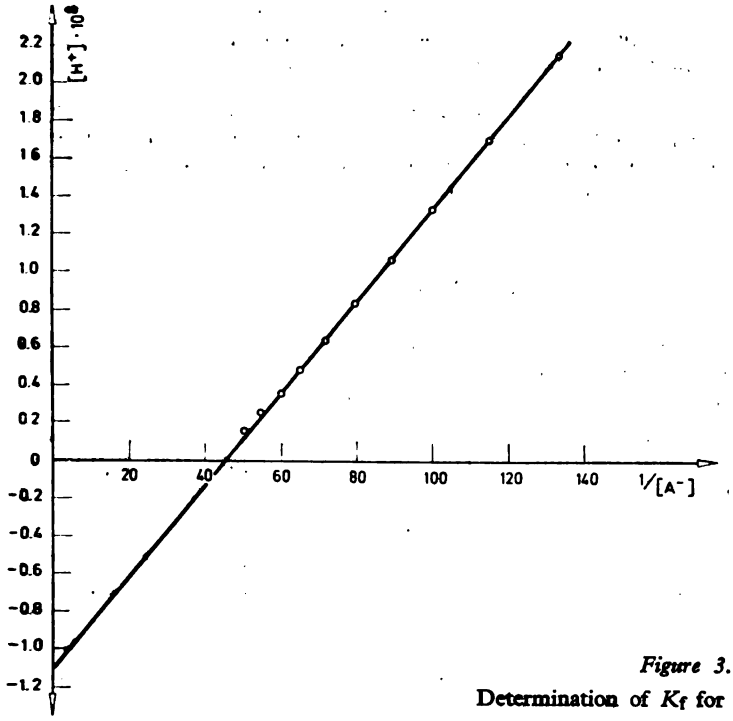

Figure 3.
Determination of K_f for HOCl at 40°C

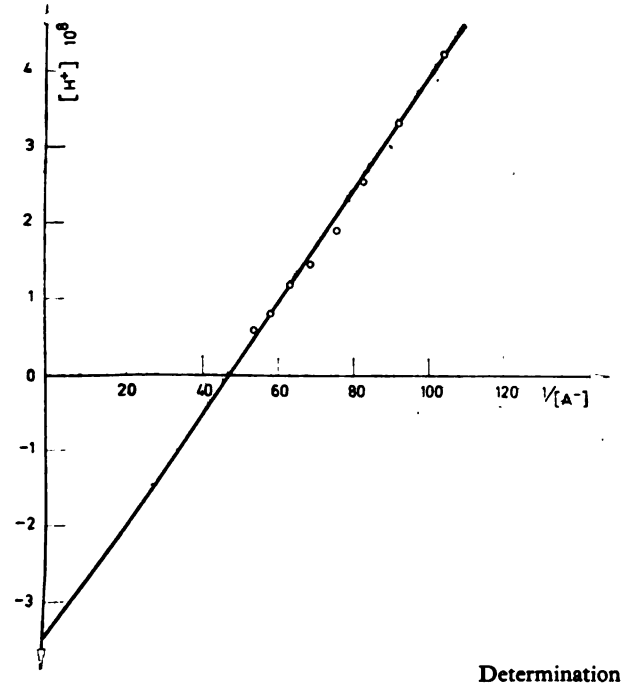

Figure 4.
Determination of K_f for HOCl at 60°C

hypochlorite-ion activity factor (f_{OCl^-}) in 5 M solution of kitchen salt and chlorate of $f_{OCl^-} = 1.064$. This value agrees well with the hypochlorite-ion activity factor given by De Valera[26] for solutions of the same ionic strength.

Accroding to De Valera[26] the activity of water, which for concentrated solutions is expressed by the ratio between the vapor pressure of higher than 5 M solutions of kitchen salt (p) and the vapor pressure pure water (p_0), $a_{H_2O} = p/p_0$, for our case is 0.8[26], or

$$\frac{f_{OCl^-}}{a_{H_2O} \cdot f_{HOCl}} \approx 1.$$

The resulting conclusion, assuming that $f_{OCl^-}/a_{H_2O} \cdot f_{HOCl} \approx 1$ is valid, is that the thermodynamic dissociation constant of hypochlorous acid remains unchanged in 5 M kitchen salt solutions.

Accordingly, the approximate thermodynamic dissociation constants of hypochlorous acid obtained as the products of conversion factors and the formal dissociation constants by the method described (Table 2) are consistent with the thermodynamic data[21, 22].

In the theoretical considerations it was however noted that a difference of one order of magnitude could be expected. Since under these conditions the hydrogen-ion activity factor is increased ten times while the thermodynamic dissociation constant remains unchanged, this would require an order of magnitude of 0.1 for f_{OCl^-}, or a ten times greater f_{HOCl}, which was beyond the scope of our study.

The formal dissociation constant expressed as a function of absolute temperature (values obtained from the slope of the straight line) is

$$-\log K_f = \frac{1.94 \cdot 10^3}{T} + 1.72, \tag{8}$$

while the temperature dependence of the approximate thermodynamic constant, by multiplying by γ, may be written

$$pK_a = -\log K_a = \frac{1.39 \cdot 10^3}{T} + 2.48. \tag{9}$$

Since the hydrogen-ion activity factor is increased by one order of magnitude in the solutions for electrolytic production of chloirine and chlorates, the pH-metric or straight line method proved to be higly suitable because it takes this fact into consideration.

Institute of Chemistry, Technology and Metallurgy,
Department of Electrochemistry
Belgrade
and
School of Technology and Metallurgy
Department of Physical Chemistry
and Electrochemistry
Belgrade

Received 18 July, 1968

REFERENCES

1. Foerster, F. and E. Müller. "Beiträge zur Theorie der Elektrolyse von Alkalichloridlösungen" — *Zeitschrift für Elektrochemie* 9: 171—185, 195—208, 1903.
2. Foerster, F. "The Electrolysis of Hypochlorite Solutions" — *Trans. Am. Electrochemical Society* 46: 23, 1924.
3. Jakšić, M. M., A. R. Despić, I. M. Csonka, and B. Ž. Nikolić. "Theory and Practice of a Modified Technology for the Electrolytic Chlorate Production", in: *Symposium of the Electrochemical Society, Boston, 5—9 May, 1968.*
4. Sand, J. "Die Stärke der unterchlorigen Säure II" — *Zeitschrift für physikalische Chemie* 48: 610—614, 1904.
5. Noyes, W. A. and T.A. Wilson. "The Ionization Constant of Hypochlorous Acid. Evidence for Amphoteric Ionization" — *Journal of the American Chemical Society* (Washington) 44: 1630—1637, 1922.
6. Soper, F. G. "The Ionization Constant of Hypochlorous Acid" — *Journal of the Chemical Society* 125: 2227—2231, 1924.
7. Giordani, F. "Kinetics of the Decomposition of Solutions of Sodium Hypochlorite" — *Gazzetta* 54: 844—860, 1924.
8. Yorston, F. H. "Measurement of Hydrogen-Ion Concentration of Bleach Liquors with the Glass Electrode" — *Pulp and Paper Magazine* (Canada) 31: 374—375, 1931.
9. Britton, H. T. S. and E. N. Dodd. "Glass Electrode Determination of the Dissociation Constant of Hypochlorous Acid" — *Trans. Faraday Society* 29: 537—538, 1933.
10. Davidson, G. F. "The Determination of the Hydrogen-Ion Concentration, Concentration of Hypochlorite Solutions with the Glass Electrode. (a) The Dissociation Constant of Hypochlorous Acid. (b) The *p*H Variations of Hypochlorite Solutions during the Bleaching of Cotton" — *J. Textile Indust., Shirley Institute Mem.* 24: 185—206, 1933.
11. Ingham, J. W. and J. Morrison. "The Dissociation Constant of Hypochlorous Acid: Glass-Electrode Potential Determinations" — *Journal of the Chemical Society* 1200—1205, 1933.
12. Gallart, J. M. "The Dissociation Constant of Hypochlorous Acid" — *Ann. Soc. Espan. Fis. y Quim.* 31: 422—426, 1933.
13. Rius, A. and V. Arnal. "The Dissociation Constant of Hypochlorous Acid, as Determined from the Potentiometric Curve of Neutralization" — *Ann. Soc. Espan. Fis. y Quim.* 31: 497—509, 1933.
14. Skrabal, A. and A. Berger. "Zur Bestimmung der Dissoziations-konstante der unterchlorigen Säure auf kinetischem Wege" — *Monatsh.* 70: 168—192, 1937.
15. Skrabal, A. and R. Skrabal. "Zur Kinetik der Hypochlorit- und Hypobromitreaktion" — *Monatsh.* 71: 251—274, 1938.
16. Holst, G. "The Dissociation Constant of Hypochlorous Acid" — *Svensk Kem. Tid.* 52: 258—261, 1940.
17. Hagisawa, H. "Dissociation Constant of Hypochlorous Acid" — *Bulletin of the Institute for Physical and Chemical Research* (Tokyo) 19: 1220—1228, 1940.
18. Kiese, M. and A. B. Hastings. "Die katalytische Hydration von Kohlendioxyd" — *Journal of Biological Chemistry* 132: 267—280, 1940.
19. Hoye, J. — *Forhandlinger Kong. Norske Videnskabere* 14: 1, 1942.

20. Lister, M. W. "Decomposition of Hypochlorous Acid" — *Canadian Journal of Chemistry* 30: 879—889, 1952.
21. Caramazza, R. "Measurement of Dissociation Constant of Unstable Weak Acids. I. Hypochlorous Acid" — *Gazz. chim. Ital. Gazzetta* 87: 1507—1521, 1957.
22. Morris, J. C. "The Acid Ionization Constant of HOCl from 5 to 35°" — *Journal of Physical Chemistry* 70: 3798—3805, 1966.
23. Despić, A. R. and Lj. Vujisić. (MS., 1966).
24. Critchfield, F. E. and J. B. Johnson. "Effect of Neutral Salts on the pH of Acid Solutions" — *Analytical Chemistry* 31: 570—572, 1959.
25. Schwabe, K. "Acidity Concentrated Electrolytic Solutions" — *Electrochimica Acta* 12: 67—93, 1967.
26. Valera, V. de. "On the Theory of Electrochemical Chlorate Formation" — *Trans. Faraday Society* 49: 1338—1351, 1953.
27. Imagawa, H. "Chemical Reactions in the Electrolytic Cell for Manufacturing Chlorate. I. Vapor Pressure of Hypochlorous Acid on Its Aqueous Solutions" — *Journal of the Japanese Electrochemical Society* 18: 382: 385, 1950; "The Vapor Pressure of Hypochlorous Acid in Sodium Chlorate Solution" — *ibid* 19: 271: 274, 1951; "Chemical Reactions in the Electrolytic Cell for Manufacturing Chlorate. III." — *ibid* 20-25—28, 1952; "Chemical Reactions in the Electrolytic Cell for Manufacturing of Chlorate. IV." — *ibid* 20: 571: 574, 1952; "Chemical Reactions of the Chlorate Cell" — *ibid* 21: 520—525, 1953.
28. Weiss, J. J. "Bemerkungen zur Kinetik der Chlorbleichlaugen" — *Zeitschrift für Anorganische Chemie* 192: 97—104, 1930.
29. Ibl, N. "On the Mechanisms of Anodic Chlorate Formation in Dilute NaCl Solution" — *Journal of the Electrochemical Society* (to be published).

GLASNIK HEMIJSKOG DRUŠTVA, Vol. 34, No. 2-3-4, 1969, pp. 181—186

GHDB-48 541.123.3:546.87:546.24:546.23:548.7

Original Scientific Paper

SUPERSTRUCTURE IN THE SYSTEM BISMUTH-TELLURIUM-SELENIUM

by

MIODRAG Đ. JANČIĆ, LJILJANA M. RADONJIĆ, and ILDIKO M. KLEJN

INTRODUCTION

In recent years the V—VI compounds, including Bi_2Te_3, have been studied fairly comprehensively with a view to obtaining materials with thermoelectric properties.

Lange[1] was the first to study the crystal structure of Bi_2Te_3. The crystal belongs to the spatial group D^5_{3d} -R_{3m}. It was found that Bi_2Te_3 and Bi_2Se_3 form unlimited solid solutions ($Bi_2Te_{3-x}Se_x$) whose crystal structure is the same as that of Bi_2Te_3. The atomic parametres of $Bi_2Tr_{3-x}Se_x$ were determined for $x = 0$, $x = 1$, and $x = 3$[2].

Atoms of the electropositive (Bi) and electronegative (Te, Se) components occur in layers. Designating the latter with Y, the distribution of atoms along the C_6 axis may be expressed

$$-Y(2)-\mathrm{Bi}-Y(1)-\mathrm{Bi}-Y(2)-Y(2)-\mathrm{Bi}-Y(1)-\mathrm{Bi}-Y(2)-$$

The layer of Y-atoms in the center of this unit, denoted $Y(1)$, lies between two layers of bismuth atoms. Each of the unit's outer layers, designated $Y(2)$, neighbors on bismuth atoms on one side and on a $Y(2)$ atomic layer on the other.

Most studies published deal with the physical and transport features of the systems Bi_2Te_3 — Bi_2Se_3[2, 4, 5, 6]. In the alloy Bi_2Te_2 Se the ratio between Te and Se atoms allows the $Y(2)$ layers to be entirely filled with Te atoms, and the $Y(1)$ layers with Se atoms. This enables the structural ordering of Bi_2Te_2Se[2]. On the other hand, in a disordered alloy, Se and Te atoms may occupy the $Y(1)$ and $Y(2)$ layers in a disorderly way.

Bland and Basinski[3] found by X-ray diffraction analysis that the structure of Bi_2Te_3Se is isomorphous with tetradymite Bi_2Te_2S whose Y (1) layers are occupied by sulfur atoms. The structure of tetradymite corresponds to the ordered structure of Bi_2Te_2Se as determined by Birkholtz and Drabble[4].

The purpose of this study was to find out whether an ordered structure can occur in the solid solution of 90% Bi_2Te_3 + 10% Bi_2Se_3, which

has proved to be an excellent *n*-branch thermoelectric material. The quenched specimen (90% Bi_2Te_3 + 10% Bi_2Se_3) was heat treated and analyzed by X-ray diffraction. The transition from the disordered to the ordered state was confirmed by measuring the integral intensity of reflection. Parallel measurement of changes in thermoelectric properties (α, $\varkappa$, ρ) with structural ordering were made to investigate the effect of the ordering on thermoelectric properties.

EXPERIMENTAL

Preparation of Specimens — Bi, Te and Se (5N purity) in stoichiometric ratio were melted in Ø 15 *mm* evacuated (3×10^{-3} *mm* Hg) guaritz ampoules. The melt was kept at 780°C for 4—6 h with constant mixing. After slow cooling, test specimens were made from the obtained crystal by melting (in Ø 6 *mm* evacuated quartz ampoules) and rapid cooling in dry ice and in air. The specimens were homogenized in the ampoules by heat treatment at different temperatures (400°, 320°, 260° and 450°C) for times of 5 h to 20 days. Three-stage heat treatment was also used: at 450°C for 1 h, at 320°C for 5 h and at 240°C from 10 h to 20 days, or the inverse sequence of temperatures.

Metallography of heat treated specimens confirmed their monophasic structure. All specimens were X-ray analyzed.

X-Ray Diffraction — The transformation from the ordered into the disordered state in specimens of the same composition was investigated by diffractometry and radiography in a Ø 56 chamber with Cu K radiation and an Ni-filter. Radiography lasted 6—8 h at an anode voltage of 35 *kV* and 15 *mA* current.

The change in intensity of the (322), (332) and (444) reflections was studied.

Measurement of Electrical Properties — For the measurement of thermoelectric properties of the specimens, a slight modification of Kherman's method[7] was used. Thermal capacity was determined by current impulses, measuring thermal diffusion by Ångström's method. All measurements were made at room temperature.

RESULTS

Electrical Conductivity — The specific electrical resistivity of Bi_2Te_3 and of the heat treated solid solution Bi-Te-Se is shown in Table 1. These are mean values of five measurements at room temperature. The values for the resistivity of Bi_2Te_3 are taken from the literature for comparison[8].

X-Ray Diffraction — Diffraction patterns for Bragg angles of 20° to 140° were indexed according to the hexagonal system by trial and error. Reflections (002) and (hkO) were first indexed making use of the published values for the lattice parameters *a* and *c*. Then the whole X-ray diffraction pattern was indexed by comparing these with the published debyegrams for Bi_2Te_3 and Bi_2Te_2Se.

The debyegram shows symmetrical extinction for $/-h, +k+1/ \neq 3n$ (n = whole number) which indicates rhombohedral form of the primitive cell. The indexed reflections were reduced to the basic reflections for a rhombohedral unit cell.

TABLE 1

Change in Specific Electrical Resistivity with Heat Treatmant of Solid Solution Bi Te Se ($\Omega\ cm^{-1}$)

Composition	90% Bi_2Te_3 + 10% Bi_2Se_3						Bi_2Te_3
Time (h) / temp. (°C)	5	15	20	30	40	70	
400	$6.3 \cdot 10^{-3}$	$1.3 \cdot 10^{-3}$	$1.28 \cdot 10^{-3}$	$1.25 \cdot 10^{-3}$	$1.2 \cdot 10^{-3}$	$1.15 \cdot 10^{-3}$	$2 \cdot 10^{-3}$
320	$6.7 \cdot 10^{-3}$	$6.7 \cdot 10^{-3}$	$7.4 \cdot 10^{-3}$	$7.1 \cdot 10^{-3}$	$7.6 \cdot 10^{-3}$	$7.8 \cdot 10^{-3}$	
260	$7.3 \cdot 10^{-3}$	$8.0 \cdot 10^{-3}$	$7.9 \cdot 10^{-3}$	$7.6 \cdot 10^{-3}$	$7.3 \cdot 10^{-3}$	$8.0 \cdot 10^{-3}$	

The debyegrams for the heat treated and quenched specimens are similar and have the same reflections for the same value of the angle 2θ. They have the same lattice parameters

$$c = 30.04 \pm 0.02\ \text{Å} \quad \text{and} \quad a = 4.308 \pm 0.003\ \text{Å}$$

These values do not agree fully with those established by other researchers.

Many reflections overlap. Also reflection intensities at high angles are too low to be measured precisely. According to the established model of structural ordering, the debyegrams for heat treated specimens do not show superstructure reflections, but the integral intensity of certain reflections differs considerably from that of the reflections of quenched specimens.

Reflections (322), (332) and (444) are strong and suitable for the measurement of integral intensity. The ratios of integral intensities of the corresponding reflections of heat treated and quenched specimens are presented in Table 2.

TABLE 2

Ratio between Integral Intensities of Corresponding Reflexions of Heat Treated and Quenched Specimens

Reflection (hkl)	$I_{hkl\ heat.}/I_{hkl\ quen.}$
(322)	1.8
(332)	0.9
(444)	1.6

DISCUSSION

According to the literature [2], the exothermic heat of formation of slowly cooled specimens exceeds that of quenched specimens, which shows that there is a transition from an ordered to a disordered state. The heat treated (ordered) phase approximates the tetradymite structure, since Se atoms mostly occupy the *Y* (1) layer, while the quenched (disordered) phases represent random distributions of Se and Te atoms in the *Y* (1) and *Y* (2)

layers of the C_{33} structure. The difference between the energy of formation of heat treated and quenched specimens is equal to the energy of ordering. The maximum ordering which can occur in the solid solution Bi_2Te_3 — Bi_2Se_3 corresponds to the Bi_2Te_2Se structure and complies with the suggested crystallographic model of ordering[5].

The theory of closest neighbors can be approximatively applied to an alloy of Bi_2Te_3—$_xSe_x$. The increase in heat of formation of ordered Bi_2Te_3—$_xSe_x$ from Bi_2Te_3 to Bi_2Te_2Se is due to the formation of additional Bi—Se (1) bonds. In the Bi_2Te_2Se to Bi_2Se range the formation of an ordered structure is associated with a gradual decrease in the number of new Bi—Se (1) bonds, so that the heat of formation decreases from the maximum value for Bi_2Te_2Se to zero for Bi_2Se_3.

Bismuth has greater affinity for selenium than for tellurium, as is demonstrated by the electronegative character of these elements: Se (2.4) and Te (2.1)[6]. This greater affinity shows itself in stronger isothermic heat of formation and in higher melting temperature of Bi_2Se_3 than Bi_2Te_3, and also in greater isothermic heat of solution of selenium in bismuth than that of tellurium in bismuth. When selenium atoms are introduced into Bi_2Te_3 they replace Te (1) atoms (where they can bind with six adjacent bismuth atoms) rather than Te (2) atoms (where they would bind only with the three closest out of the adjacent bismuth atoms). Analyses of the bond length show that Bi—$Y(1)$ is more of an ionic bond than would be the case with the Bi—$Y(2)$ bond which is more covalent. The $Y(2)$—$Y(2)$ bond is approximately of the van der Waals' type. The share of ionic bonding in the mixed covalent-ionic bond between Bi—$Y(1)$ and Bi—$Y(2)$ can as yet be expressed only qualitatively. Since the share of ionic bonding in the Bi—$Y(1)$ bond is greater, selenium, being more electronegative than tellurium, will first start to replace Te atoms at position $Y(1)$.

The occurrence of superstructural reflections on the powder diffraction pattern is convincing evidence of structural ordering. Since the powder patterns of the heat treated specimens do not contain any reflection not observed with the quenched specimens, the transition from the ordered to the disordered state was considered in terms of structural factors.

For a given reflection (hkl), the structural factor $F(hkl)$ is defined by

$$F(hkl) = \sum_n f_n \, e^{2\pi i(hx_n + ky_n + lz_n)}.$$

The summation is over all atoms in the unit cell; f_n = atomic dispersion factor; $(x_n\ y_n\ z_n)$ = position coordinates of the nth-atom of the unit cell.

Ordering of the selenium and tellurium atoms in the $Y(1)$ and $Y(2)$ layers does not affect the bismuth layers, so that the lattice parameters do not change.

The structural factors of the disordered and ordered alloys are

$$F(hkl)_{ord.} = {}^1/_3 f_{Se} + 2 f_{Bi} \cdot \cos 2\pi u (h+k+l) + {}^2/_3 f_{Te} \cos 2\pi v (h+k+l)$$

and

$$F(hkl)_{disord.} = ({}^1/_3 f_{Se} + {}^2/_3 f_{Te}) [1 + 2 \cos 2\pi v (h+k+l)] + 2 f_{Bi} \cdot \cos 2\pi u (h+k+l).$$

Since the occupation of the $Y(1)$ layers by Se atoms retains on the whole C_{3i} crystal structure, ordering does not diminish the symmetry of the disordered solid solution and superstructural reflections do not appear.

Ordering of the structure is manifested by a change in the integral intensity of reflection because the structural factors of the ordered and disordered alloys are not equal. Calculations for $u = 0.3961$ and $v = 0.7883$ with a temperature factor $B = 1.5 \times 10^{16}/cm^2$ show that only the intensity of low-order reflections changes during ordering.

Since the atomic dispersion factor of Bi is much greater than those of Te and Se, and since bismuth atoms take the same positions in the ordered as in the disordered structure, the reflections of high intensity which originate mainly from the strong dispersion of bismuth atoms contribute little to the change in reflection intensity during ordering. On the other hand, the reflections of low intensity are little affected by bismuth atoms (because in that case $\cos 2\pi u\,|h+k+l| \approx 0$), so that the ordering of the Te and Se atoms causes considerable change in the intensity of reflections. According to predictions from the equation for integral intensity, heat treatment of the specimen should strengthen reflections (322) and (444) and weaken reflection (332), which confirms the predicted transition from the ordered into the disordered state. Experimental values obtained for the change of intensity of these reflections agree with the findings of Bland and Basinski[3] concerning solid solutions of similar composition.

Measurements of electrical and thermal conductivity conform with the observed occurrence of structural ordering. The greatest change in the integral intensity of reflection coincides with the electrical conductivity maximum and the thermal conductivity minimum. Ordering reduces resistivity more electrical than thermal conductivity. This may probably be interpreted by a more rapid change in mobility of particles induced by structural ordering than in phonon, scattering responsible for thermal resistivity.

ACKNOWLEDGEMENT

Measurements of electrical resistivity were made by Ferenc Kermendi, to whom the authors' thanks are due.

Institute of Chemistry, Technology and Metallurgy
Belgrade

Received 25 January, 1968

REFERENCES

1. Lange, P. W. "Ein Vergleich zwischen Bi_2Te_3 und Bi_2Te_2S" — *Naturwissenschaft* (Berlin) 27: 133—135, 1939.
2. Misra, S. B. "On the Solid Solutions of Bismuth Telluride and Bismuth Selenide" — *Journal of the Physics Chemistry* (sic) (London) 25: 1233—1241, 1964.
3. Bland, J. A. and S. J. Basinski. "Investigation of the Structure of Solid Solution Bi Te Se" — *Journal of Canada Physics* (sic) (Ottawa) 39: 1040—1058, 1961.
4. Birkholtz, U. Z. "Strukturantersuchungen am System Bi_2Te_2" — *Zeitschrift für Naturforschung* (Tübingen) 13a: 780—789, 1958.
5. Nakajima, S. M. "The Crystal Structure of Bi_2Te_{3-x} Se_x" — *Journal of the Physics Chemistry Solids* (sic) (London) 24: 479—485, 1963.
6. Greenway, D. L. "Band Structure of Bi Te Se" — *Journal of the Physics Chemistry Solids* (sic) (London) 26: 1585—1604, 1965.
7. Kherman, I. T. "Metody izmereniia termoelektricheskikh parametrov" (Methods for Measurement of Thermoelectric Parameters) — *Pribory i tekhnika eksperimentov* (Moskva) 4: 381—398, 1963.
8. Gordiakova, G. N. "Izuchenie termoelektricheskikh svoistv Bi Te Se" (Study of the Thermoelectric Properties of Bi Te Se) — *Zhurnal tekhnicheskoy fiziki* (Moskav) 28: 3—17, 1958.

GLASNIK HEMIJSKOG DRUŠTVA, Vol. 34, No. 2-3-4, 1969, pp. 187—195

GHDB-49 669.112.227.1:669.15'74.017.1

Original Scientijic Paper

AUSTENITE BREAKDOWN IN HIGH-MANGANESE HADFIELD STEEL

by

BRANKO I. BOŽIĆ and NADA P. VIDOJEVIĆ

Manganese steel with 1.0—1.4% C and 10—14% Mn, known as Hadfield steel, has special mechanical and technological properties. Under equilibrium conditions its structure is supereutectoid, with α and $(Fe, Mn)_3$ C phases as the basic constituents. Owing to high carbon and manganese contents, the M_s temperature of this steel is very low so that austenitic structure is retained after rapid quenching from 950—1050°C. Carbides are not observed in this structure because of increased carbon solubility at high manganese content.

Hadfield steel treated in this way possesses high plasticity and toughness with a tensile strength of 80—110 kg/mm^2, an elongation limit less than 40—50% of the tensile strength, and a hardness of 200—250 HB. It has a high resistance to wear under pressure. This is due to the fact that cold deformation induces such strengthening, which may be explained by the high carbon atom concentration in the solid solution, hindering the movement of dislocations, and by easier generation of packing defects in the face-centered cubic of lattice austenite[1, 2].

High toughness in combination with great resistance to wear give Hadfield steel manifold practical uses. Since the austenitic strucure which gives the steel these properties, is unstable at higher temperatures, observations of austenite decomposition depending on temperature are of practical importance. (For example, it has been found that austenite breakdown, although increasing hardness, reduces resistance to wear[3].) Here the direct isothermal decomposition of austenite provides a suitable method for investigating the kinetics of the decomposition in the steel and the nature of the transformation products — which is the subject of this study. It was also of interest to find out how previous quenching affects the kinetics of the isothermal austenite reaction, since quenching changes the state of the austenite.

MATERIAL AND METHOD

The steel was of the following composition: C 1.16%, Mn 13.36%, Si 0.39%, Cr 1.47%, S 0.035%.

Specimens of Ø 10 × 2 *mm* were cut out from a forged bar of 13 *mm* diameter. Since the initial structure of the steel showed a small amount of undissolved carbides, the temperature of their complete dissolution was determined experimentally. This temperature was 1 000 ± 10°, and the dissolving time was 30 min.

In the first test series the specimens were transferred from the furnace for carbide dissolution into one containing molten lead where isothermal treatment was conducted at temperatures of 400, 450, 500, 550, 600, 650 and 700° for 15 min to 48 h, or 144 h at 400°, To supplement and check the results a small number of specimens were isothermally treated at 475, 525 and 575°.

In the second series the specimens, after austenitization at 1 000° for 30 min, were quenched in water and then kept at temperatures within the range 400—700° for 10 min to 48 h, or up to 96 h at 400°.

The isothermal austenite reaction was studied via microstrusctural examination and Vickers hardness measurements (30 kg/cm^2).

Standard methods were used to prepare specimens for microstructural investigation, always with grinding off 0.3—0.4 *mm* layers in which decarburization might have occurred. The specimens were etched according to the following procedure: 15 *sec* in 3% HNO_3 in alcohol, washing in alcohol, 15 *sec* in 10% HCl in alcohol, briefly submersion in 2% NH_4OH in alcohol, washing in alcohol and drying. If necessary, the whole etching procedure was repeated. Microscopic observations and photographing were at a magnification of 450 x, or in a few cases at 1 000 x.

For specimens directly isothermally treated for 48 h at all the temperatures the amounts of transformation products were determined by planimetry of the micrographs, from which the approximate percentages of transformed austenite at different temperatures were calculated.

For hardness measurement, as a rule 10 impressions were made in each specimen and the mean hardness value calculated.

RESULTS AND DISCUSSION

Microscopy of the products of isothermal austenite decomposition showed that at all temperatures within the range 450—700° the austenite transformation began with carbide precipitation both in direct isothermal treatment or after quenching. Concerning the nature of the precipitated carbide phase there is considerable evidence that this is a cementite-type carbide $(Fe, Mn)_3C$[4, 5]. After some time in the temperature region of 450 to 650°, finely lamellar perlite precipitates. In case of the direct isothermal treatment at 400°, austenite breakdown was not observed even after 144 h, while with previously quenched specimens a certain minimal precipitation of carbide could be observed on grain boundaries after 96 h. (If carbide did not precipitate, the etching was not able to reveal grain boundaries.)

In direct isothermal decomposition carbide precipitated in a reticular pattern on austenite grain boundaries in that temperature region in which it is only product of austenite breakdown (Fig. 1), or in a reticular and platelet pattern at temperatures where carbide precipitation is succeeded by perlite (Fig. 2). The amount of carbide precipitated depended on the tem-

perature and duration of isothermal decomposition. It increases with decreasing temperature down to 550°, and then falls off below this temperature. With increasing time of treatment the amount of carbide precipitated rises at first, but at all temperatures the precipitation of carbide stops relatively soon and the austenite either remains stable or continues to precipitate perlite.

At temperatures of 650 and 700° it was observed that carbide precipitated in some places as a lamellar product with austenite which resembles perlite (Fig. 3 and 4). Sufficient magnification reveals that the carbide lamellae are continuous with the carbide precipitated on grain boundaries. Since such precipitation of carbide takes place on only few grains, its cause is presumably the local segregation of carbon and manganese.

At all temperatures in the perlite region (450—650°) it was noted that in the places where the first carbide lamellae precipitated, after some time perlite nodules appeared in which carbide coagulated at higher temperatures, while the structure of the perlite occurring at lower temperatures was very fine (Figs. 5—8).

Apart from carbide, perlite and austenite, specimens of advanced transformation also contained a needle-like constituent which might be ε-martensite, as available data suggest ready occurrence of non-magnetic ε-martensite in carbon-impoverished sites[6, 7].

From the microscopy results for directly isothermally treated specimens a graph was drawn showing the isothermal reaction of austenite in the steel (Fig. 9). Curve I in this graph displays the beginnings of carbide formation at different temperatures of isothermal treatment, Curve II the times at which perlite began to form. The graph shows that the austenite-carbide transformation starts most rapidly at 575°, while the incubation period of perlite precipitation is shortest at 550°. At every test temperature, even after long treatment, considerable amounts of austenite remained unprecipitated. Planimetry of transformation products on the micrographs of specimens isothermally treated at different temperatures for 48 h indicates that the highest austenite transformation percentage (50%) occured at 500°.

Austenite also decomposed in the same way after quenching. However, on comparing the decomposition kinetics for the two methods of specimen treatment it is noted that after quenching the transformation began earlier than in case of direct isothermal treatment. Also, at temperatures above 450° the incubation period of austenite breakdown in the former case did not depend on temperature. For long decomposition times the transformation percentage was virtually the same in both cases,

The graph in Fig. 10 presents the dependence of hardness on the time of isothermal decomposition at different temperatures (the case of direct isothermal treatment). Hardness increases with decomposition time at all temperatures, except 400°. The increase is particularly marked with the specimens treated at 500, 550 and 600°. Correlating changes in structure with those in hardness, it is readily seen that the hardness increase resulted from the precipitation of carbide and perlite, the effect of the latter on the hardness being far the greater[8]. The value for the hardness depends on the amount of transformation products. It is higher the higher the percentage of transformation. Thus the highest hardness value was shown by

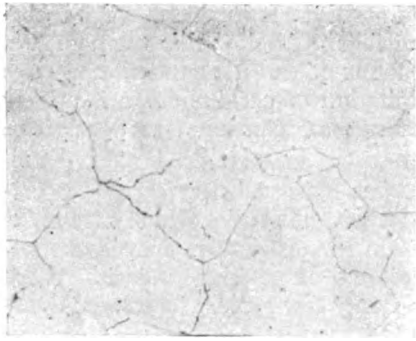

Figure 1

1000°/650°, 4 h: carbide lattice on austenite grain boundaries

Figure 2

1000°/550°, 1 h: carbide platelets in austenite

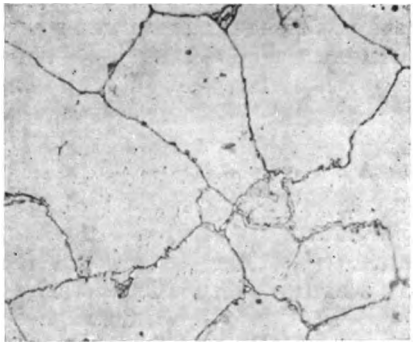

Figure 3

1000°/700°, 16 h: carbide lattice on austenite grain boundaries, with local extensions

Figure 4

1000° (water) 650°, 48 h: carbide lattice on grain boundaries with lamellar carbide aggregate

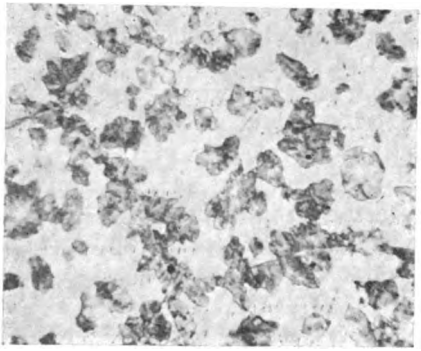

Figure 5

1000°/600°, 4 h: carbide and perlite in austenite

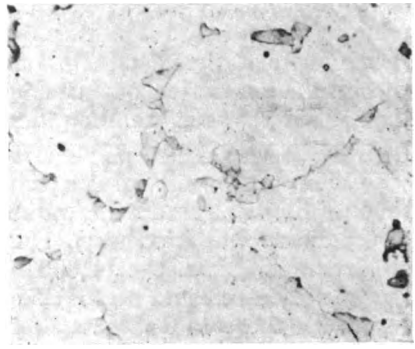

Figure 6

1000°/500°, 48 h: maximum amount of perlite in austenite

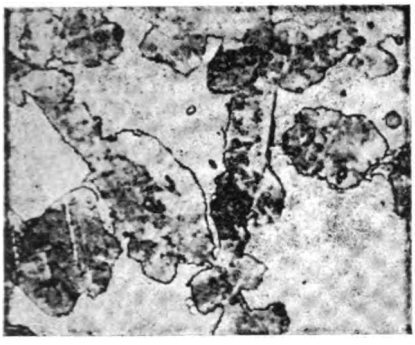

Figure 7
1000°/500°, 48 h: perleit, austenite and *e*-martensite

Figure 8
1000° (water) 600°, 48 h: coagulation of carbide in perlite; austenite, *e*-martensite

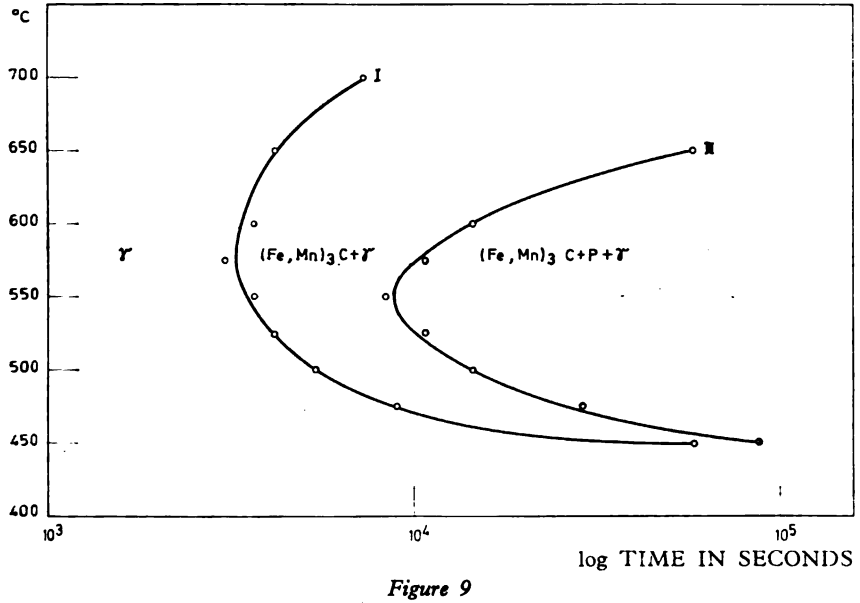

Figure 9

the specimen treated at 500° for 48 h. The same changes in hardness with time of isothermal treatment at different temperatures are displayed by the previously quenched specimens, apart from some minor differences in the hardness value.

The conclusion that may be drawn from the results obtained are as follows:

(1) Isothermal decomposition of austenite in the Hadfield steel investigated, isothermally treated with or without previous quenching, begins by carbide precipitation in the temperature region 450° to 700°. At temperatures of 450° to 650° carbide precipitation is followed by perlite precipitation. Under direct isothermal treatment at 400°, there was no transfor-

mation even after 144 h, while in case of isothermal treatment after quenching a minimal precipitation of carbide on grain boundarisies could be detected after 96 h.

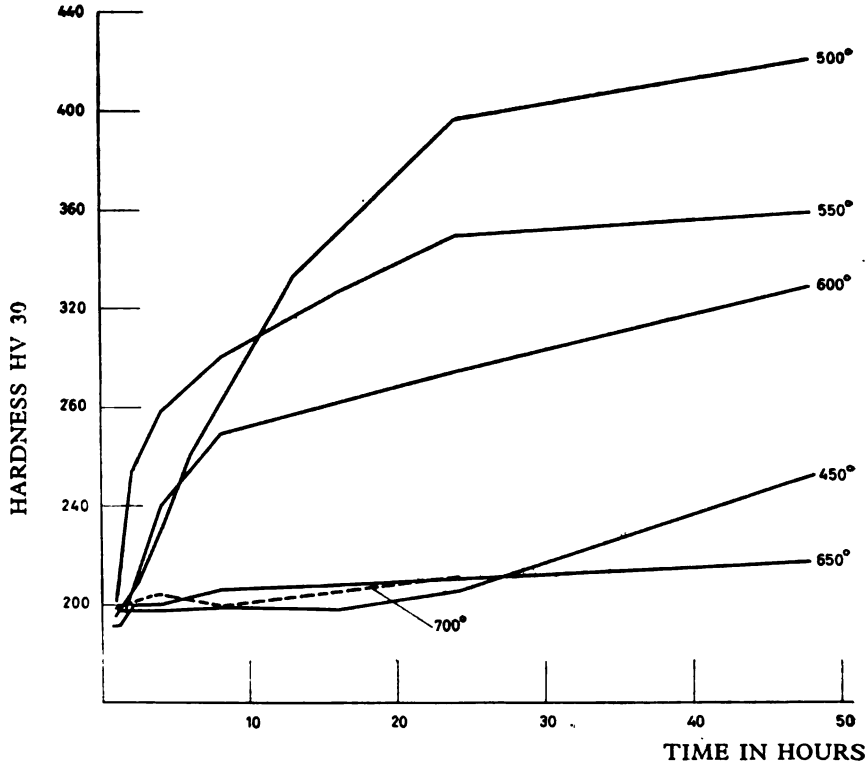

Figure 10

(2) Austenite transformation remained incomplete at every test temperature. The maximum transformation percentage after 48 h treatment was observed at a temperature of 500°.

(3) Advanced austenite transformation is accompanied by rising hardness in which the effect of precipitated perlite hardness by far exceeds that of carbide. The maximum hardness was achieved by isothermal austenite decomposition at 500° for 48 h.

The mode of isothermal decomposition of austenite was consistent with the modes established for other steels of similar composition[5, 6, 7, 8].

(4) A comparison of decomposition kinetics for the two methods of thermal treatment reveals that austenite transformation after quenching began earlier than in the case of direct isothermal treatment, and that the incubation period of austenite breakdown at temperatures higher than 450° in the former case did not depend on temperature. Obviously, by rapid

quenching in water from the austenitization temperature a larger number of defects vacancies form in the austenite crystal structure which then step up the formation of centers of crystallization of carbide. However, since the further increase in the number of centers of crystallization of carbide and the occurrence of perlite are thermally activated processes the percentage of isothermal transformation after long decomposition is virtually the same with both treatments applied.

ACKNOWLEDGEMENT

Our thanks are due to S. Trivić and M. Cvišić for assistance in the experimental work.

School of Technology and Metallurgy
Institute of Physics and Metallurgy
Belgrade University

Received 19 February, 1969

REFERENCES

1. White, C. H. and R. W. K. Honeycombe. "Structural Changes during the Deformation of High-Purity Iron-Manganese-Carbon Alloys" — *Journal of the Iron and Steel Institute* 200: 457, 1962.
2. Roberts, W. N. "Deformation Twinning in Hadfield Steel" — *Trans. of Met. Soc. of AIME* 230: 372, 1964.
3. Shchulepnikova, A. G. "Iznosostoikost' vysokomargantsovistykh stalei v razlichnom strukturnom sostoianii" (Resistance to Wear of High-Manganese Steels of Different Structural Composition) — *Metallovedenie i termicheskaia obrabotka metallov* (10): 61, 1968.
4. Petsch, W. "Die kristallographischen Eigenschaften der Zementitausscheidung im Austenit" — *Archiv für das Eisenhüttenwesen* 34: 381, 1963.
5. Zakharova, M. I. and Van-Khua-Fou. "Issledovanie raspada presyshchennogo rastvora v margantsovistoi stali" (Decomposition of Supersaturated Solid Solution in Manganese Steel) — *Fizika metallov i metallovedenie* 9: 236, 1960.
6. Castro, R., and P. Garnier. "Ouelques structures de decomposition des aciers austénitiques au manganèse" — *Revue de Métallurgie* 55: 17, 1958.
7. Grigorkin, V. I., Iu. V. Grdina, *et al.* "Issledovanie fazovogo sostava austenitno margantsovistoi stali pri termicheskoi obrabotke" (I Phase Composition of Austenitic Manganese Steel after Thermal Treatment) — *Izvestiia vysshikh uchebnykh zavedeniia, Chernaia Metallurgiia* (12): 112, 1967.
8. Irvine, K. J. and F. B. Pickering. "Austenitic Manganese Steel" — *Iron and Steel* 29: 135, 1956.

GLASNIK HEMIJSKOG DRUŠTVA, Vol. 34, No. 2-3-4, 1969, pp. 197—202

GHDB-50

541.183:661.183.7:547.53

Original Scientific Paper

DYNAMIC ADSORPTION OF ORGANIC VAPORS ON "BLOCKED" SILICA GEL. I.

ADSORPTION OF BENZENE, TOLUENE AND XYLENE VAPORS

by

SLOBODAN K. KONČAR-ĐURĐEVIĆ and IVANKA P. PETKOVIĆ

Our previous study[1] dealt with the adsorption of benzene, toluene and xylene vapors on "blocked" active carbon. The term "blocked" was used to designated active carbon on which methylene blue had previously been adsorbed from different concentrations of aqueous solution up to saturation. In this way different degrees of blocking of the active positions were obtained. The adsorbent blocked in this manner was exposed to the air current saturated with vapors of benzene, toluene and xylene. A linear inversely proportional (sic) dependence was found between the amount of methylene blue blocking the adsorbent and the amount of vapor adsorbed.

The objective of this study was to investigate the behavior of silica gel under similar conditions of dynamic adsorption.

The procedures applied were the same as in the previous study[1], but the apparatus in which adsorption was conducted was elaborated to some extent. A vessel for maintaining the incoming air at a definite constant temperature (15°C) was added. The air was passed through a copper spiral joined to a test tube containing thermometer. All this was put into a thermostat cooled by iced water because of the specific conditions of work.

Another addition was a test tube with inlet and outlet tubes and a thermometer. It was placed behind the U-tube for adsorption to check the temperature of the outgoing gas mixture.

To prevent any condensation during adsorption the air was saturated with the organic solvent vapors at 15°C, while adsorption itself took place at 25°C ± 0.5°C.

The flow of air was kept constant at 2.30 lit/min. Adsorption was interrupted for weighing the U-tube every 5 min at first and every 15 min later until constant weight.

RESULTS

Figure 1 shows the dynamic adsorption on unblocked silica gel of the vapors of benzene, toluene and xylene from air saturated at 15°C. It is evident that the amount adsorbed increases with increasing molecular

weight of the adsorbate and that the equilibrium is reached quicker the lower the molecular weight. This is explained by the size and shape of the molecules[2, 3].

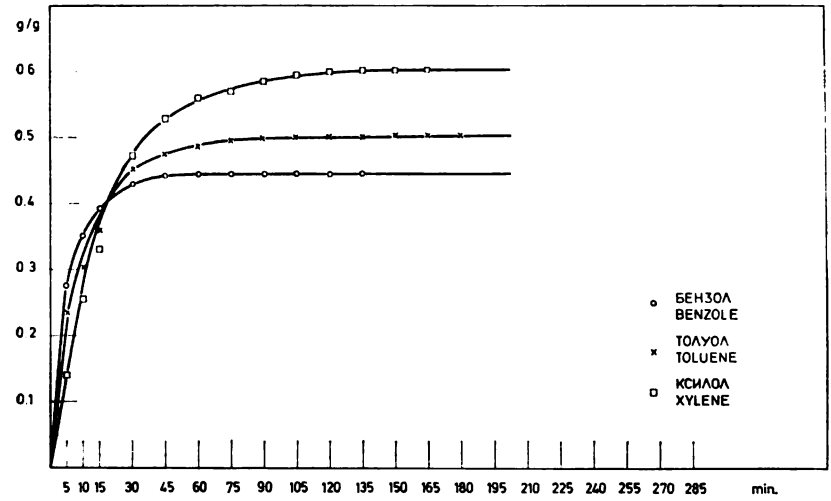

Figure 1

Dynamic adsorption of saturated vapors of benzene, toluene and xylene from air on unblocked silica gel

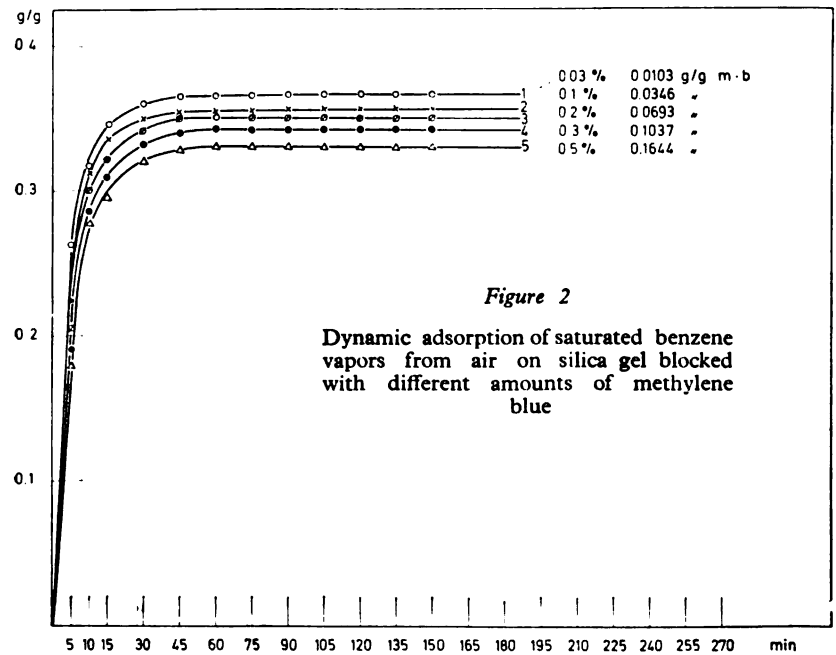

Figure 2

Dynamic adsorption of saturated benzene vapors from air on silica gel blocked with different amounts of methylene blue

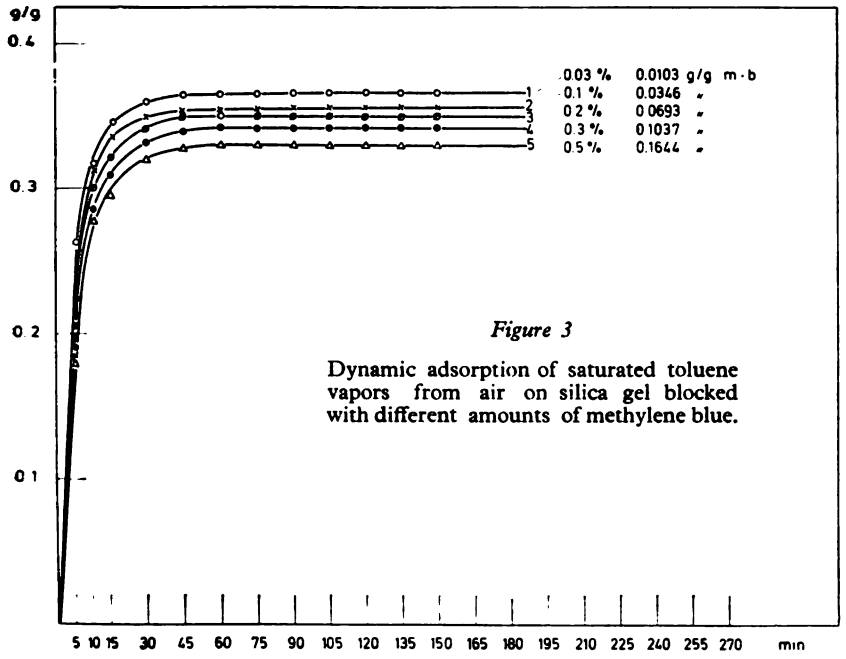

Figure 3

Dynamic adsorption of saturated toluene vapors from air on silica gel blocked with different amounts of methylene blue.

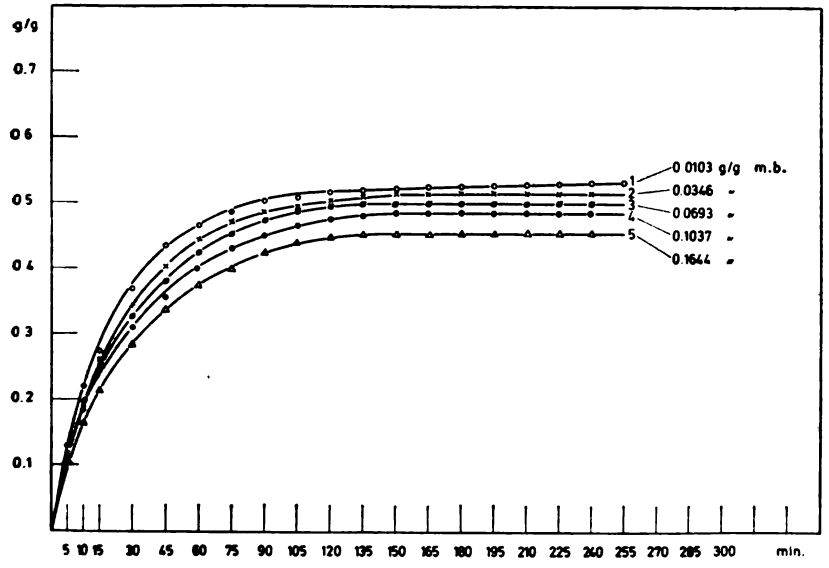

Figure 4

Dynamic adsorption of saturated xylene vapor from air on silica gel blocked with different amounts of methylene blue

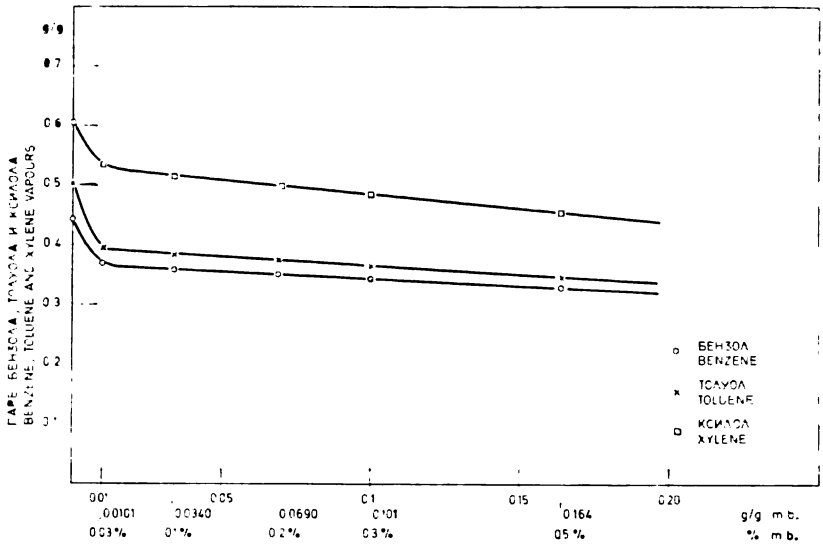

Figure 5

The relation between the amount of saturated vapor adsorbed in the equilibrium state and the quantity of methylene blue used to block the silica gel

The figures show the dynamic adsorption of vapors of benzene (Fig. 2), toluene (Fig. 3) and xylene (Fig. 4) on silica gel blocked with different amounts of methylene blue (abbreviated to m.b. in the graphs). It is seen that the greater the amount of methylene blue adsorbed the smaller the equilibrium amount of adsorbed vapor. The radii of the dynamic adsorption curves show that equilibrium is reached the sonner the more methylene blue is adsorbed. We believe that this results from the gradual blocking of the minute pores for the vapor molecules as well as from the blocking of adsorption centers on the gel itself[4, 5, 6, 7].

Figure 5 shows the relation between the quantities of vapor of benzene, toluene and xylene adsorbed in the equilibrium state on silica gel previously blocked with different amounts of methylene blue. It may be noted that the amount adsorbed is much reduced compared with the unblocked adsorbent even when a very small quantity of methylene blue is adsorbed (see the first two points). Later this dependence can be represented by a straight line of negative slope, as is unequivocally inferred from the three straight lines.

A comparison of these three curves and the three obtained after the same procedure using active carbon (1) reveals great similarities.

School of Technology
Dept. of Chemical Engineering
and
Experimental Demonstration Laboratory
Belgrade University

Received 30 January, 1969

REFERENCES

1. Končar-Đurđević, S. and I. Petković. "Dinamička adsorpcija organskih para na blokiranim adsorbensima" (Dynamic Adsorption of Organic Vapors on "Blocked" Adsorbents) — *Glasnik memijskog društva* (Beograd) 30* 245—260, 1965.
2. Cassidy Gomes, H. *Adsorption and Chromatography* — New York, London: Interscience Publishers, Inc., 1951.
3. Brunauer, S. *The Adsorption of Gasses and Vapors, Volume I, Physica' Adsorption* — Princeton: University Press, 1945.
4. Elston, J. A. "Rates of Water Vapor Adsorption from Air by Silica Gel" — *Industrial and Engineering Chemistry* 31: 988—992, 1939.
5. Figueras, F. R., L. de Mourgues, and P. Renard. "Adsorption physique et chimique d'etanol sur un catalyser silice-alumine synthetique par une methode dynamique" — *Journal de Chimie Physique* 65: 1393—1398, 1968.
6. Van den Hul, H. J. and J. Lyklema. "Determination of Specific Surface Areas of Dispersed Materials. Comparison of the Negative Adsorption Method with Some Other Methods" — *Journal of the American Chemical Society* 90: 3010—3015, 1968.
7. Hirscher, E. A. and S. Amon. "A Tool in the Preparation of High-Purity Saturated Hydrocarbons" — *Industrial and Engineering Chemistry* 39: 1585—1596, 1947.

* Available in English translation from Clearinghouse for Federal Scientific and Technical Information, Springfield, Virginia, 22151.

GLASNIK HEMIJSKOG DRUŠTVA, Vol. 34, No. 2-3-4, 1969, pp. 203—210

GHDB-51

661.183.2:539.211:621.352

Original Scientific Paper

INFLUENCE OF SURFACE TREATMENT OF ACTIVE CARBON ON ITS ACTIVITY IN FUEL CELL ELECTRODES

by

DRAGUTIN M. DRAŽIĆ and RADOSLAV R. ADŽIĆ

It was shown recently[1, 2] that good carbon fuel cell electrodes impregnated with a small quantity of catalyst (e.g. Pt, Ag, etc.) can only be made when high surface area active carbon is used. Also, for obtaining high electrode activity the proper carbon surface treatment is of no less importance. However, it is very difficult to quantitatively resolve the true effects of these factors from the experimental measurements, since all known methods for increasing surface area simultaneously affect the surface state and vice versa.

In this paper conclusions from the investigation of carbon treatment for hydrogen electrode[1] are further developed, and an attempt is made to resolve the two effects mentioned above on the basis of additional experimental results of different active carbon treatments for hydrogen and oxygen electrode reactions.

EXPERIMENTAL

a) *Active carbon treatment* — Commercial active carbon in pellet form (type R-52, product of the Miloje Zakić factory, Kruševac, real surface area cca 700 m^2/g) was pretreated in a Soxlet apparatus with HCl as described in ref. (1). After grinding and sieving the 80—120 micron fraction was heated in a quartz furnace in CO_2 at 950°C for 2 hours, and subsequently in NH_3 at 800, 900 or 1000°C for 1—3 hours. During the CO_2 treatment some of the carbon was oxidized, as was evident from the weight loss of powder samples and decrease of particle diameters by cca 20 microns. For comparison, some HCl pretreated carbon powder was heated only in NH_3 at 800, 900 or 1000°C, also 1—3 hours. The real surface area after treatment was determined by the B.E.T. method.

b) *Catalyst impregnation and measuring technique* — Suitably treated carbon powder was impregnated with 40 *mg* Pt/*g* carbon (2 *mg* Pt/cm^2 of the projected electrode surface) by chemical reduction of H_2PtCl_6 in the same manner as described earlier[1].

The consequences of the carbon treatment on the electrochemical behavior of the carbon powder in hydrogen or oxygen fuel cell electrode

were followed by taking the corresponding anodic or cathodic polarization curves in 6N KOH or 5N H_2SO_4 at 40°C, using the same technique measurement as described in ref.[1]. The hydrogen and oxygen were of technical grade. The polarization curves obtained are not corrected for the ohmic drop in the sintered gas sealing disc.

RESULTS AND DISCUSSION

Neither the impregnated commercial active carbon with a surface area of 700 m^2/g nor the carbon pretreated in HCl gave any reasonable activity when tested as oxygen electrodes in H_2SO_4 or KOH. The same was found before for the hydrogen electrode reaction[1]. However, heating of such carbon in CO_2 or NH_3 increased the activity of the powder. This can be seen from Fig. 1 which gives polarization curves for oxygen electrode in 6N KOH for non-treated carbon (curve 1), carbon treated in CO_2 at different temperatures for optimum heating time (curves 2, 3, 4), carbon treated in NH_3 (curve 5), and carbon succesively treated in CO_2 and NH_3 (curve 6). Similar behavior was obtained for oxygen electrode in 5N H_2SO_4. In Fig. 2 potentials of oxygen electrode at 100 mA/cm^2 in 5N H_2SO_4 and 6N KOH and real surface area of the carbon are presented as functions of heating time in CO_2 only.

As is seen, the activity of the electrodes is highest when the surface area of the carbon is a maximum, indicating that for oxygen electrode reaction, as was the case with hydrogen electrode reaction[1], the real surface area plays a very important role. Heating in CO_2 definitely produced a pronounced increase of the real surface area by its slow oxidizing action, as is evident from the weight loss of carbon samples during the heating and the change of surface area during treatment, with a final decrease of surface area when the oxidation was prolonged (cf. Fig. 2).

Further evidence that CO_2 treatment is practically only slow oxidation of carbon was obtained when instead of CO_2 a mixture of argon and oxygen (1 or 2% O_2) was used. After heating at 950°C for 1 or 2 hours in such mixtures polarization curves for hydrogen electrode in acid solution (curves 1 and 2 in Fig. 3) were taken. On the same graph polarization curves for CO_2-treated carbon (curve 3) and carbon heated in pure argon (curve 4) are presented. When more oxygen was present in the argon-oxygen mixture (e.g. 5%) more than half of the carbon sample was burnt up, and the resulting carbon was much less active (curve 5), like in the case of prolonged CO_2 treatment. Between CO_2 and the corresponding argon-oxygen mixture there is practically no difference.

However, the activity of the electrode is not dependent only on the magnitude of the real surface area. During the oxidation of carbon in CO_2 or argon-oxygen mixture a surface layer of a certain type of carbon oxide is formed. According to Smith[2], carbon in contact with oxygen can make two types of oxide called the acid type and alkaline type. They can be distinguished experimentally by the change in pH of neutral KCl solution when the oxidized active carbon is brought in contact with it, giving an acid or alkaline reaction, respectively. Alkaline oxides are obtained when carbon is degassed in vacuum at 1000°C, cooled, and allowed to come in contact with O_2 at temperatures below 300°C or above 700°C, while acid

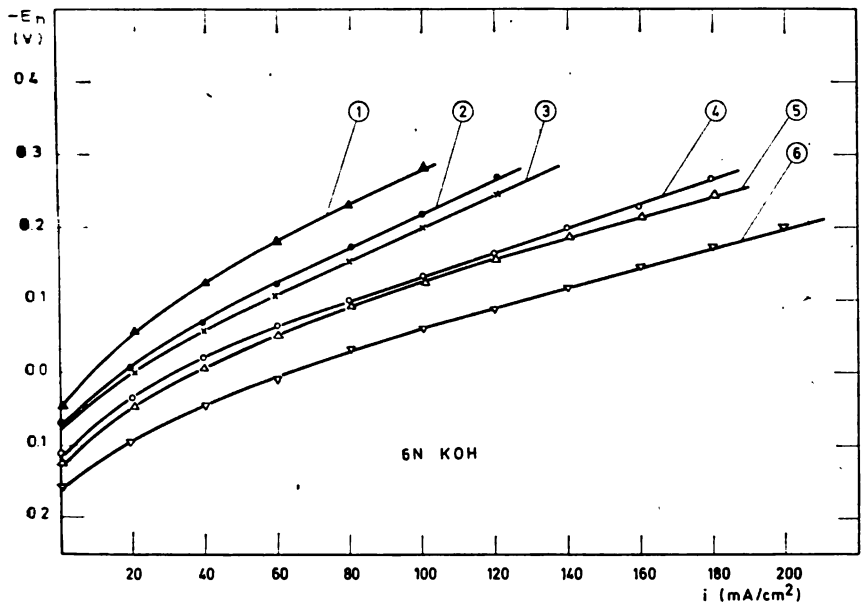

Figure 1

Effect of carbon treatment on oxygen electrode activity in 6N KOH at 40°C:

1. — nontreated carbon
2. — CO_2, 4*h*, 500°C
3. — CO_2, 3*h*, 800°C
4. — CO_2, 2*h*, 950°C
5. — NH_3, 2*h*, 1000°C
6. — CO_2, 2*h*, 950°C + NH_3 3*h* 1000°C

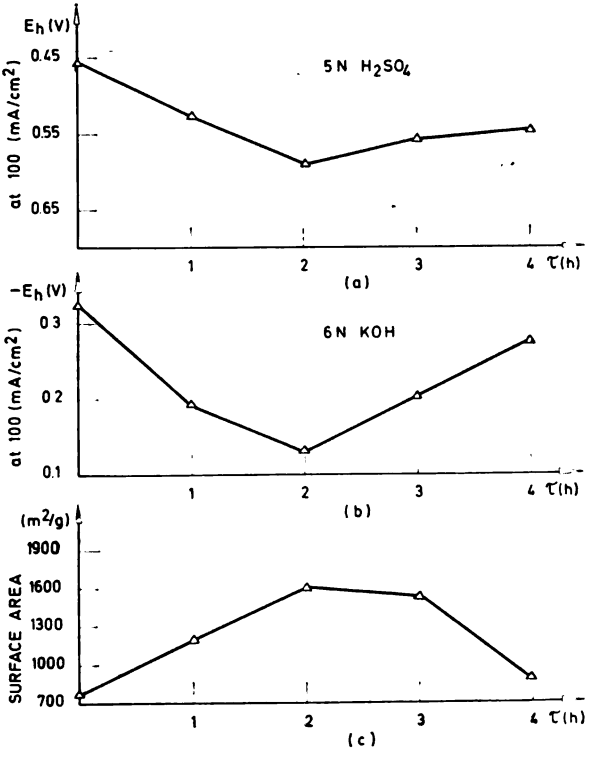

Figure 2

Effect of the time of CO_2 treatment at 950°C:

a) on overpotential at 100 *mA/cm²* in 5N H_2SO_4 at 40°C
b) on overpotential at 100 *mA/cm²* in 6N KOH at 40°C
c) on surface area of carbon

oxides are formed when this contact is made in the 300—700°C range. With this in view, the CO_2-treated carbon (to obtain 1500 m^2/g) was degassed and acid oxide was formed according to the described procedure at 450°C for 1/2 hour.

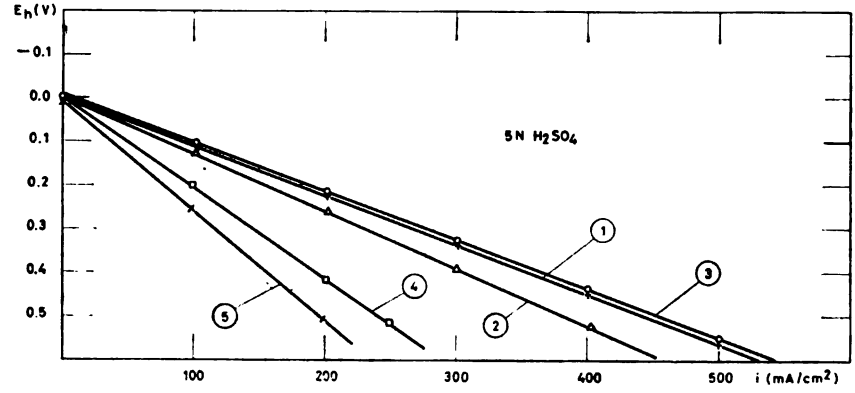

Figure 3

Effect of carbon treatment with various oxidizing media on hydrogen electrode activity in 5N H_2SO_4 at 40°C:

1. — Ar+1% O_2, 1*h*, 950°C
2. — Ar+2% O_2, 2*h*, 950°C
3. — CO_2, 2*h*, 950°C
4. — Ar, 2*h*, 950°C
5. — Ar+5% O_2, 2*h*, 950°C

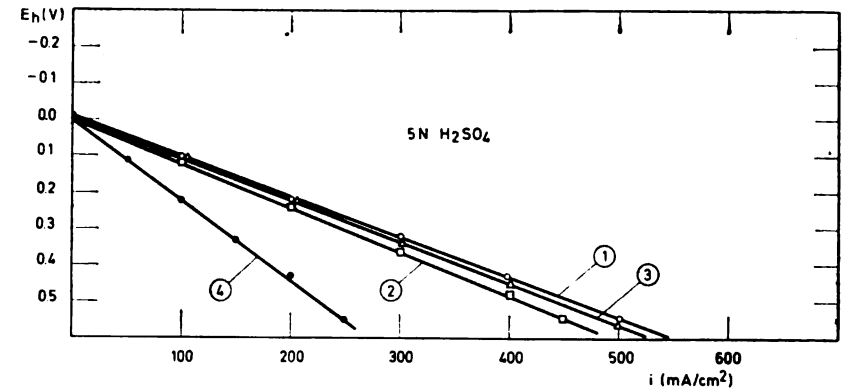

Figure 4

Effect of surface state of carbon, with the same real surface area, on hydrogen electrode activity:

1. — CO_2, 2*h*, 950°C
2. — NH_3, 2*h*, 1000°C
3. — CO_2, 2*h*, 950°C + NH_3, 3*h*, 1000°C
4. — Acid oxides

Polarization curves for hydrogen electrode made from CO_2, CO_2 + + NH_3 and NH_3 treated carbon and carbon with acid oxides are given in Fig. 4. Results from this graph, and results obtained for oxygen electrode in acid and alkaline electrolyte tabulated in Table 1 show the effect of sur-

TABLE 1

Characteristics of Hydrogen and Oxygen Electrodes in Acid and Alkaline Electrolyte at 40°C with Variously Treated Active Carbon

Treatment of carbon	Oxygen electrode Current (mA/cm^2) at 500 mV in 5N H_2SO_4	Oxygen electrode Current (mA/cm^2) at −200 mV in 6 N KOH	Hydrogen electrode Current (mA/cm^2) at 500 mV in 5N H_2SO_4	Hydrogen electrode Current (mA/cm^2) at −500 mV in 6 N KOH	Surface area of carbon (m^2/g) *(approx.)*
CO_2 (2 *h*, 950°C)	100	155	460	270	1500
$Ar + O_2$ (1%) (1 *h*, 950°C)	90	165	445	225	1500
NH_3 (3h, 1000°C)	120	160	380	225	1500
"acid oxide"	40	10	200	90	1500
CO_2(2*h*, 950°C) + NH_3 (3*h*, 1000°C)	220	192	445	275	1900

face state for the same real surface area carbon, being the most effective for CO_2-treated carbon.

Mrha[3] reports that heating in NH_3 can also activate carbon for oxygen electrode, explaining this by formation of surface nitrogen complexes. According to our experience, heating in NH_3 in the 800—1000°C range considerably change the surface area (e.g. 2 hours heating at 1000°C changed the area from 850 to 1300 m^2/g). At the same time, heating in NH_3 has a considerable effect on the activity of the carbon, particularly for oxygen electrode.

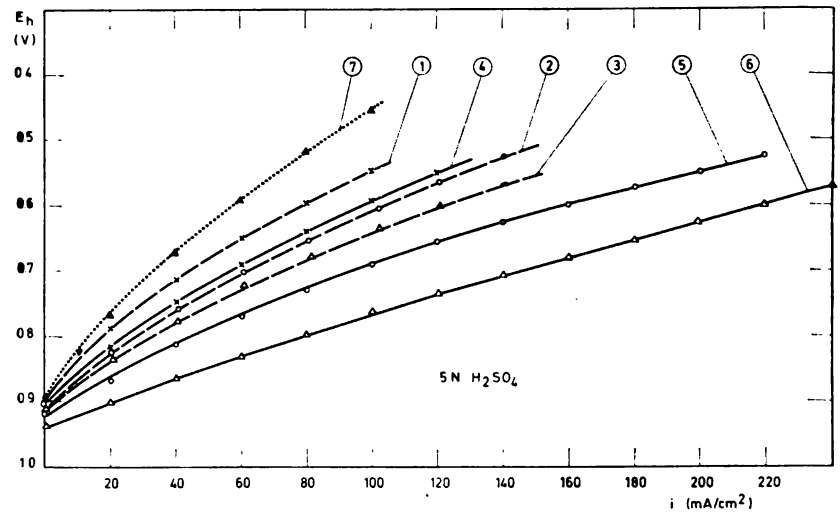

Figure 5

Effect of surface state of carbon, and magnitude of the real surface area on oxygen electrode activity in 5N H_2SO_4 at 40°C:

1. — NH_3, 3*h*, 850°C
2. — NH_3, 3*h*, 900°C
3. — NH_3, 3*h*, 1000°C
4. — CO_2, 2*h*, 950°C + NH_3, 3*h*, 850°C
5. — CO_2, 2*h*, 950°C + NH_3, 3*h*, 900°C
6. — CO_2, 2*h*, 950°C + NH_3, 3*h*, 1000°C
7. — nontreated carbon

Figure 5 presents polarization curves for non-treated carbon (dotted line), carbon heated in NH_3 (dashed lines) at 800, 900 and 1000°C for optimum time (curves 1, 2, 3 respectively), and carbon heated in CO_2 for 2 hours (in order to develop the surface to 1500 m^2/g) with subsequent heating in NH_3 at 800, 900 and 1000°C (full lines, curves 4, 5, 6). Due to the reducing action of NH_3 atmosphere at 800—1000°C, the surface oxides formed in the preceding CO_2 treatment were removed and the activity achieved was probably due to formation of certain nitrogen-containing species.

All the results concerning the surface state of the carbon are summarised in Table 1. For the hydrogen reaction CO_2, Ar + O_2 and NH_3 treatments gave the best result, while the presence of acid oxide on the surface was detrimental. For the oxygen reaction CO_2 + NH_3 treatment was somewhat more effective then CO_2 or Ar + O_2, but the surface area is also increased, to 1900 m^2/g, by this procedure.

In our opinion, the activity of the carbon powder depends primarily on the real surface area. The state of the carbon surface is of no less importance, in the sense that the surface compounds formed during NH_3, O_2, or CO_2 treatment, "alkaline oxides", are more suitable for supporting the platinum catalyst than "acid oxides".

Institute of Chemistry,
Technology and Metallurgy,
and
Faculty of Technology
and Metallurgy, Beograd

Received 19 July, 1968.

REFERENCES

1. Dražić, D. M. and R. R. Adžić. (to be published)
2. Smith, N. "The Chemistry of Carbon-Oxygen Surface Compounds" — *Quarterly Review* (London) 13: 287—305, 1959.
3. Mrha, J. "Study of Catalysts for Fuel Cell Electrodes. IV." — *Collection of Czechoslovak Chemical Communications* (Praha) 32: 708—719, 1967.

GLASNIK HEMIJSKOG DRUŠTVA, Vol. 34, No. 2-3-4, 1969, pp. 211—216

GHDB-52 546.135:546.137:541.135.6:542.8:661.851.3.

Original Scientific Paper

POLARIZATION CHARACTERISTICS OF LEAD DIOXIDE ELECTRODE IN ELECTROLYTIC CHLORATE AND PERCHLORATE PRODUCTION*

by

DARINKA J. STOJKOVIĆ, MILAN M. JAKŠIĆ, and BRANISLAV Ž. NIKOLIĆ

Owing to the fact that it has the properties of an electronic conductor of low specific resistance ($40—50 \times 10^{-6} \Omega\ cm$), causes high overvoltage of oxygen and is sufficiently metastable, lead dioxide has long aroused interest and been applied as a very conveninet anodic material in many industrial electrolytic processes.

The most significant use is undoubtedly the application of lead dioxide electrode anode in such electrical oxidation processes as the manufacture of alkaline perhalogenates, above all perchlorates. In these cases a PbO_2 electrode replaces platinum whose application raises not only investments but also production costs because of considerable corrosion of platinum during the process. Recent data[1] show that the application of PbO_2 electrodes reduces the investments for a manufacturing plant capable of turning out 30 tons of perchlorate daily by five times.

Lead dioxide anodes are much less used in the electrolytic production of chlorates, for which, however, a more suitable anodic material than graphite also has long been sought. As graphite wears away gradually in the process, the distance between the electrodes increases causing higher ohmic resistance and higher power consumption. Also the occurrence of graphite slurry in the electrolyte, particularly at higher temperatures, causes decomposition of hydrochlorous acid and thus decreases the current efficiency[2]. The chemical conversion of hypochlorites to chlorates requires temperatures high enough to reduce the hypochlorite-ion content in the cell and to concentration-polarize the electrochemical reaction of anodic oxidation of hypochlorite into chlorate, accompanied by the corresponding current loss. Because of the increasing corrosion of graphite, the cell temperature is confined to about 40°C.

Since the PbO_2 electrode obtained by electrolytic precipitation to a thickness of 2 *mm* on an indifferent graphite carrier has a life of only two

* Communicated at the 1st Yugoslav Symposium on Electrochemistry, Beograd, January 1968;

years, it is economically less justified in spite of the maintenance of constant interelectrode distance and constant energy consumption. According to our findings, its application for electrolytic chlorate production is not yet justified.

LEAD DIOXIDE ELECTRODE

Lead dioxide occurs in two crystal modifications, as tetragonal β-PbO_2 and orthorhombic α-PbO_2, the former being obtained by electrolytic precipitation from strongly acidid solutions, the latter from neutral and alkaline electrolytes. Because of its considerably greater oxygen overpotential, only β-PbO_2 electrodes[7, 8] are used for electrolytic production of chlorates and perchlorates.

Lead dioxide coatings on lead or other metallic carriers do not protect them from further oxidation.

Titanium exhibits sufficient resistance at oxidation potentials in the production of halogenates and perhalogenates, but the oxide film on the surface (which makes it resistant) results in rather high ohmic polarization which renders impossible its use as a carrier of the lead dioxide layer.

Graphite proved to be sufficiently inert as a lead dioxide carrier for making the electrode. Anodes made out of lead dioxide alone are also possible[3].

EXPERIMENTAL

Formation of Lead Dioxide Electrode on Graphite Carrier. — The procedure for electrolytic precipitation of PbO_2 on graphite carriers was developed by combining or improving other standard procedures[3, 4]. The precipitate was obtained by anodic polarization from combined acidic nitrate and perchlorate solutions. To obtain a sufficiently positive potential for electrolytic precipitation of β-PbO_2, and for precipitation to proceed at a potential which is suitable for the electrolytic production of perchlorates, considerable amounts of sodium perchlorate were added to the electrolyte as well as indifferent nitrate ions. To prevent the occurrence of hydrogen-oxygen flame and *pH* changes during the production of the electrodes, the electrolyte contained cupric nitrate thus allowing precipitation of copper on the cathode. Also added to the solution were minor amounts of surface-active Lissapol NK (ninilphenol ethoxylate), in which 9 moles of ethylene oxide are bound to one mole of nonilphenol mole, to raise the oxygen overpotential on the anode by specific adsorption so as to prevent the liberation of gas and to improve the utilization of nitrate electrolyte. By adding nitric acid an initial *p*H of 1.5—2.0 was obtained and maintained in this region.

Schumacher[5] observed that in electrolytic perchlorate production the PbO_2 electrode displays much greater stability and longer life while enabling higher current efficiency in the presence of small amounts of fluoride ions in the electrolyte. For this reason we also introduced fluoride ions into the nitrate bath during the PbO_2 precipitation itself.

A temperature of 65°C proved to be most suitable for obtaining compact precipitates. To obtain 2 *mm* electrolytic PbO_2 required 5.5 h of electrolysis with a changing current density: 10.8 A/dm^2 for the first 60 min, followed by 5.4 A/dm^2 for 90 min, and 2.7 A/dm^2 for the last 180 min. Greater

densities during precipitation caused corrugated precipitates and cavities due to generation of oxygen[4].

To avoid bubbles in the initial PbO_2 layer, before precipitation the graphite was kept fairly long in distilled water (which forced air out of the pores)[4].

Energetic stirring of the electrolyte readily removes oxygen bubbles which, however, cannot be avoided althogether. Hence it is indispensable not only to stir the electrolyte vigorously but also to move the anode at the same time. In our case, the thin cylindrical anode rotated during the PbO_2 precipitation.

The current efficiency was 98—100%.

Electrolyte composition for the precipitation of PbO_2:

$Pb(NO_3)_2$	355 *g/lit*
$NaClO_4$	70 *g/lit*
$Cu(NO_2)_2\ 3H_2O$	52 *g/lit*
NaF	0.5 *g/lit*
Lissapol NK	0.8 *g/lit*

During electrolysis, $Pb(NO_3)_2$ was added in proportion to the PbO_2 precipitated on the anode.

The carrier for PbO_2 precipitation was unimpregnated graphite of standard quality for chloralkaline electrolysis, manufactured by VEB Elektrokohle Lichtenber, East Germany. The cathode was a Cu coil, to get tenfold the current density relative to the anode.

The surface-active substances oxidize on the anode during the precipitation; the degradation products were removed by extraction with amyl alcohol which was regenerated via distillation[4].

For comparison of electrode characteristics, the stationary method was used to obtain polarization curves for anodes of graphite, platinum, and lead dioxide precipitated on graphite carrier, in solutions for the electrolytic production of chlorates (300—305.0 *g* $NaCl/lit$ 4—5.0 *g* $Na_2Cr_2O_7/lit$) and perchlorates (600.0 *g* $NaClO_3/lit$ 4—5.0 *g* $Na_2Cr_2O_7/lit$).

RESULTS AND DISCUSSION

Figure 1 presents the anodic polarization curves obtained under chlorate production conditions at current densities of practical industrial importance (0—100 mA/cm^2). Throughout the whole measurement range, the PbO_2 electrode exhibits more marked polarization than graphite or platinum. This fact is another argument in favor of our point that PbO_2 electrode certainly cannot be used for electrolytic chlorate production.

The current densities most often used in industrial chlorate production in monopolar cells are 30—60 mA/dm^2. Measurements show that within this region graphite comes sufficiently close to the anodic polarization properties of platinum (Fig. 1), which justifies its industrial application. Thus a method for adjusting the distance between the electrodes as the graphite wears away would further justify the use of graphite in the bipolar chlorate cells and it would not be necessary to seek any more suitable anodic material.

Polarization features of PbO_2 electrode and platinum in electrolytic perchlorate production are shown in Fig. 2. In this case the anodic polari-

zation curve for graphite is left out because of its low oxygen overvoltage oxygen evolves and oxidizes it up to carbon dioxide at a considerably more negative potential.

Anodic polarization curves for platinum and PbO_2 electrode coincide with one another within a fairly broad range of current densities of practical interest.

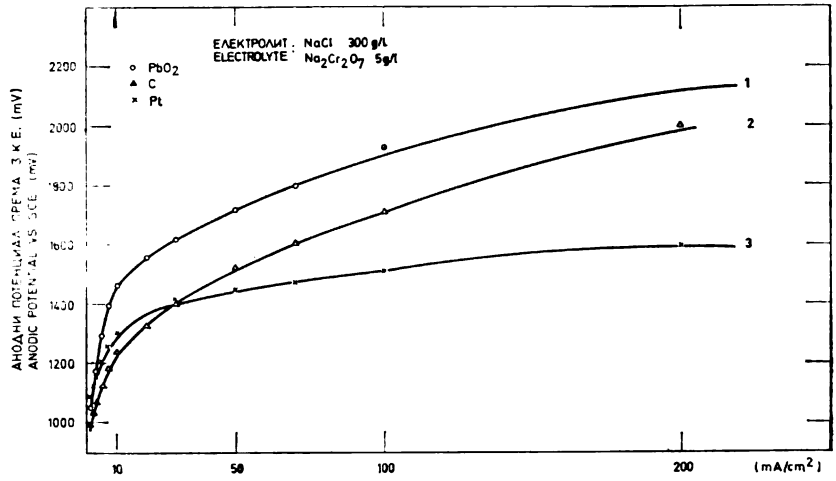

Figure 1

Polarization characteristics of PbO_2, graphite and platinum electrodes in solutions for electrolytic chlorate production

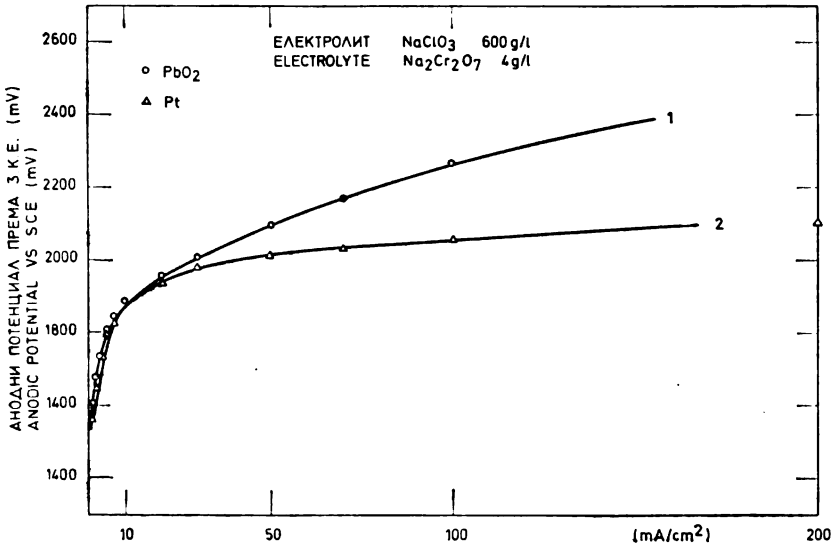

Figure 2

Polarization characteristics of PbO_2 and platinum electrodes in solutions for electrolytic perchlorate production

The equilibrium potential of PbO_2 electrode in acidic solutions[6] corresponds to the reversible potential of chlorate oxidation to perchlorate. Apart from this, PbO_2 electrode is electrolytically precipitated in the presence of a high perchlorate concentration and at the potential which these ions establish in contact with an indifferent graphite electrode. For the production of perchlorate, the platinum anode must yield virtually the same polarization values. It has been established[5] that electrochemically the PbO_2 electrode behaves as a metal. Thus the nearly the same anodic behavior of PbO_2 electrode and platinum during electrolytic perchlorate production justifies replacing platinum by lead dioxide anode, and this brings manifold advantages regarding production costs and investments. Moreover, platinum corrodes during the process while PbO_2 is relatively stable. The shortcoming of PbO_2 electrode is its great brittleness, so that the anode cracks or crumbles after a time. These anodes at present have a life of two years, and their substitution for platinum pays of several times over, particularly considering the identical polarization characteristics and the possibility of precipitate regeneration.

Institute of Chemistry, Technology
and Metallurgy
Department for Electrochemistry
Belgrade

and

School of Technology
Institute for Physical Chemistry
and Electrochemistry
Belgrade University

Received 18 June, 1968

REFERENCES

1. Anon. "New Anodes Chow off for Chemical Procedures" — *Chemical Engineering* July 19: 82—83, 1965; reprint from *Industry Economic News.*
2. Ksenzhek, O. S. and Z. V. Solovei. "Kinetika okisleniia grafita gipokhloritom i khlornovatoi kislotoi" (The Kinetics of Graphite Acidification with Hypochlorite and Chlorous Acid" — *Zhurnal prikladnoi khimii SSSR* 33: 279—283, 1960.
3. Sugino, K. "Preparation, Properties and Application of Lead Peroxide Electrode Manufactured by a New Method" — *Bulletin of the Chemical Society of Japan* (Tokyo) 23: 115—120, 1950.
4. Gibson, F. D. Jr. *Inert Lead Dioxide Anode and Process of Production* — U. S. Patent 2945791 (July 19, 1960).
5. Schumacher, J. C., D. R. Stern, and P. R. Graham. "Electrolytic Production of Sodium Perchlorate Using Lead Dioxide Anodes" — *Journal of the Electrochemical Society* 105: 151—155, 1958.
6. Rüetschi, P. and R. T. Angstadt. "Anodic Oxidation of Lead at Constant Potential" — *Journal of the Electrochemical Society* 111: 1323—1330, 1964.
7. Angstadt, R. T., C. J. Venuto, and P. Rüetschi. "Electrode Potentials and Thermal Decomposition of Alpha-Beta PbO_2" — *Journal of the Electrochemical Society* 109: 177—184, 1962.
8. Rüetschi, P. and B. D. Cahan. "Electrochemical Properties of PbO_2 and the Anodic Corrosion of Lead Alloys" — *Journal of the Electrochemical Society* 105: 369—377, 1958.

GLASNIK HEMIJSKOG DRUŠTVA, Vol. 34, No. 2-3-4, 1969, pp. 217—221

GHDB-53

546.621'161:541.183.12

Original Scientific Paper

INVESTIGATION OF THE SOLUTION OF ALUMINUM-III-FLUORIDE*

by

SLOBODAN D. RADOSAVLJEVIĆ, VERA Č. ŠĆEPANOVIĆ, and MILENA M. JOVANOVIĆ

INTRODUCTION

Anhydrous AlF_3 is practically water insoluble. The crystalline hydrate $AlF_3 \cdot 3H_2O$ is likewise very weakly soluble: in 100 *g* of saturated solution at 25°C there is only 0.41 *g* of $AlF_3 \cdot 3H_2O$[1]. In spite of these facts, when aluminum-III-fluoride is obtained by a wet procedure, e.g. by reaction between HF or H_2SiF_6 and $Al(OH)_3$, it remains in the solution from which solid $AlF_3 \cdot 3H_2O$ is only obtained after crystallization[2, 3].

Two different forms of $AlF_3 \cdot 3H_2O$ are described in the literature: the β-form which is practically insoluble and stable, and the α-form which is soluble and tends to build metastable supersaturated solution. On crystallization the soluble α-form irreversibly changes to the insoluble β-form[1, 3].

In studying some properties of the aluminum-III-fluoride solution obtained by reaction between H_2SiF_6 and $Al(OH)_3$ according to the equation

$$H_2SiF_6 + 2Al(OH)_3 \rightarrow 2AlF_3 + SiO_2 + 4H_2O. \ldots . I \qquad (1)$$

we found indications that what is involved here is not a "metastable supersaturated solution" of aluminum-III-fluoride but soluble autocomplexes of aluminum and fluorine.

Our first hypothesis was that the solution contains the autocomplex Al/AlF_6) or, more precisely, the ions $(Al(H_2O)_6)^{3+}$ and $(AlF_6)^{3-}$. There was, however, reason to believe that also present in the solution were the autocomplexes $AlF(AlF_5)$ or the ions $(AlF(H_2O)_5^{2+}$ and $(AlF_5(H_2O))^{2-}$, and $AlF_2(AlF_4)$, or the ions $(AlF_2(H_2O)_4)^+$ and $(AlF_4(H_2O)_2)^-$.

According to this hypothesis of the structure of aluminum-III-fluoride solution, in all the above cases aluminum would be distributed 50% in the cationic part and 50% in the anionic part of the solution. The distribution of fluorine differs for the three possible cases. If only the autocomplex $Al(AlF_6)$ is present in the solution, all fluorine is bound only in the anionic part. In case of the existence of the autocomplex $AlF(AlF_5)$, about 16.7% F is contained in the cationic part and 83.3% F in the anionic part. With the

* Communicated in part at the 12th Symposium of Chemists of the SR of Serbia, Belgrade, January, 1967.

$AlF_2(AlF_4)$ 33.3% F is bound in the cationic and 66.6% F in the anionic part of the solution

The present study was aimed at experimental verifying the above hypothesis about the composition of the aluminum-III-fluoride solution. To do this we ran aluminum-III-fluoride solution through a Wolfatit KPS cation exchanger and then determined Al and F in the cationic and anionic parts of the solution.

EXPERIMENTAL

Through the reaction of 18% technical grade H_2SiF_6 solution and hydrated alumina (about 40% H_2O) in stoichiometrically ratio according to Eq. (1), an aluminum-III-fluoride solution was obtained containing 122 *g* AlF_3/*lit* instead of the stoichiometrically expected 126 *g* AlF_3/*lit*. The difference of 3—5% AlF_3 results from the adsorption of aluminum-III-fluoride solution on the SiO_2 precipitate in spite of washing. Water used to wash the precipitate was added to the test solution so that its original volume was doubled.

The theoretical capacity of the Wolfatit KPS resin in the Na state is 4.5 *mEq*/*g*. Before using this resin as an exchanger we converted it to the H state and experimentally found that its exchange capacity was now 3.88 *mEq*/*g*. For safety we counted on a capacity of only 2 *mEq*/*g*.

This capacity allows 8 *ml* solution containing up to 125 *g* AlF_3/*lit* to be run on 10 *g* resin. Thus on a column of 10 *g* Wolfatit KPS in the H state, 8 *ml* aluminum-III-fluoride solution diluted with 200 *ml* H_2O was run. The cationic part of the solution, which bound to the resin, was eluted by 200 ml 3% HCl.

Total amounts of Al and F in the test solution containing 122 *g* AlF_3/*lit* were

39.21 *g* Al/*lit* or 0.0392 *g* Al/*ml*
82.78 *g* F/*lit* or 0.0827 *g* F/*ml*

TABLE 1

Amounts of Al and F in Cationic and Anionic Parts of the of AlF_3 Solution

In the solution with 122 *g* AlF_3/*lit*	Cationic part		Anionic part		Total *g*/*ml*	
	g/*ml*	%	*g*/*ml*	%	Found	calculated
Al	0.0194	50	0.0197	50	0.0391	0.0392
F	0.0267	32.8	0.0547	67.2	0.0814	0.0828
F	0.0262	32.1	0.0556	67.9	0.0818	0.0828
F	0.0256	31.2	0.0566	68.8	0.0822	0.0828
F	0.0252	30.3	0.0581	69.7	0.0833	0.0828

By determination of Al and F in the cationic and anionic parts of the solution we invariably found a ratio of 50 : 50% for aluminum, and a cationic-anionic ratio a varying from 30 : 70 to 33 : 67% for fluorine.

Aluminum was determined spectrophotometrically by a slightly modified method after Suresh *et al.*[6], fluorine by Seel's method[7].

Some of the determinations are presented in Table 1.

Since any lengthy keeping of the alumnum-III-fluoride solution could change its composition with possible establishment of new equilibriums, we applied the same investigation procedure to both fresh solutions and those kept at room temperature for 24 h. The results were the same.

DISCUSSION AND CONCLUSION

If aluminum-III-fluoride solution were a "metastable supersaturated solution" of AlF_3, all aluminum in the solution would be present as cations and all fluorine as anions. Our investigations showed that half the total aluminum is bound in the cationic part and the other half in the anionic part. Fluorine too was found in both the cationic and anionic parts of the solution, approximately 1/3 in the cationic and 2/3 in the anionic.

According to the distribution of aluminum in the solution, which amounts to 50% Al in the cationic and 50% Al in the anionic part, the existence of several autocomplexes can be suggested, viz.: $Al/AlF_6/$, $AlF(AlF_5)$, $AlF_2(AlF_4)$. According to the distribution of fluorine, which is mostly near 33% F in the cationic and 67% F in the anionic part, it can be concluded that $AlF_2(AkF_4)$ is the dominant autocomplex. Exclusive existence of the autocomplex $Al(AlF_6)$ is out of the question, since in this case all the fluorine would be in the anionic part. Minor deviations in the distribution of fluorine may indicate some participation of the autocomplexes $AlF(AlF_5)$ and $Al(AlF_6)$ but in small amounts.

Brosset's works[4] show that aluminum and fluorine build numerous complex ions in solutions, 1—5 fluorine ions gradually binding with 1 aluminum ion. According to Brosset[4] the stability of these complexes increases with the number of F-ions. However, the $(AlF_6)^{3-}$ ion was not demonstrated in solutions, and its stability constant (according to which it would be the most stable) was obtained by extrapolation[4]. We hold that this fact indicates that the $(AlF_6)^{3-}$ ion does not exist in solutions but only in the solid, crystalline state. Crystallization of aluminum-III-fluoride solution undoubtedly takes place when conditions are created for the formation of $(AlF_6)^{3-}$ octahedrons which are the basic structural unit in solid AlF_3[5].

Our results show that in aluminum-III-fluoride solutions obtained by wet procedures, most frequently having a pH of about 2.5 and also containing considerable water, the ions AlF^{2+} and AlF_4^- dominate. These ions are probably hydrated, water molecules completing the coordination spheres of aluminum up to its characteristic coordination number 6.

During the crystallization of aluminum-III-fluorid solution, which is most rapd at boiling point and combined with inoculation, what most likely takes place is a mutual exchange of water molecules and fluorine ions and

the formation of $(AlF_6)^{3-}$-octahedrons. Consequently, the crystallization of aluminum-III-fluoride may be represented by the changes

$$(AlF_2 \cdot 4\,H_2O)(AlF_4 \cdot 2\,H_2O) \xrightarrow{t^\circ} (AlF \cdot 5\,H_2O)(AlF_5 \cdot H_2O) \xrightarrow{t^\circ}$$

$$\xrightarrow{t^\circ} Al \cdot 6\,H_2O(AlF_6) = 2\,AlF_3 \cdot 3\,H_2O$$

Institute of Chemistry, Technology
and Metallurgy
and
School of Technology
Institute of Inorganic Chemistry
Belgrade University

Received 3 December, 1968

REFERENCES

1. Ehret, W. F. and F. Y. Frere. "Dimorphism in Aluminum Fluoride Trihydrate" — *Journal of the American Chemical Society* 67: 64—68, January—June 1945.
2. Weinrotter, F. "Aluminum Fluoride Synthesis from Superphosphate Byproduct" — *Chemical Engineering* 132—134, April, 27, 1964.
3. Šćepanović, V. Č. and S. D. Radosavljević.* (Some Factors Influencing the Crystallization Rate of Aluminum-III-Fluoride from Supersaturated Solutions) (In Serbo-Croatian)* — *Glasnik Hemijskog društva* (Beograd) 32 (5—6—7),** 1968.
4. Brosset, C. (Electrochemical and X-Ray Crystallographic Investigation of the Complex Aluminum Fluorides) (In Swedish)* — Stockholm, 1942, pp. 122 (Thesis).
5. Hanc, F., K. Matiaševsky, D. Štempelova, and M. Malinovsky. "Über die Kristallstruktur von AlF_3" — *Acta Chimica Academiae Scientiarum Hungaricae* (Budapest) 32: 309—313, 1962.
6. Suresh, G. G., N. S. Surendra, and A. K. Dey. "Composition and Stability of the Chelate between Aluminium (III) and Sulfo-Dichloro-Hydroxy-Dimethyl-Fuchsone-Dicarboxylic Acid and Analytical Applications of the Reaction" — *Journal für praktische Chemie* (Leipzig) 20: 70—80, 1963.
7. Seel, F. "Neue Methode zur Bestimmung des Fluors" — *Angewandte Chemie* 76: 532—533, 1964.

* Original title not given.
** Available in English translation from Clearinghouse for Federal Scientific and Technical Information, Springfield, Virginia, 22151.

GLASNIK HEMIJSKOG DRUŠTVA, Vol. 34, No. 2-3-4, 1969, pp. 223—232

GHDB-54 546.98:547.421:543.257.1:543:257.5

Original Scientific Paper

STUDY OF THE COMPOSITION OF THE PALLADOUS THIOGLYCOLATE COMPLEX AND THE DETERMINATION OF PALLADIUM WITH THIOGLYCOLIC ACID BY POTENTIOMETRIC AND AMPEROMETRIC TITRATION

by

VILIM J. VAJGAND and MILETA D. JAREDIĆ

In the last ten years or so, thio-compounds have been increasingly used for the quantitative determination of a number of cations. Most of these analyses are done by amperometric titration at the anodically polarized platinum electrode.

For the determination of palladium by this method Songina[1] recommends mercaptobenzothiazole, hexamethylenedithiocarbamate, thionallyde and thiooxime.

Although the reaction of palladous ions with thioglycolic acid was discovered as long ago as 1948[2], it has not been extensively studied yet. We investigated this reaction by spectrophotometry and found that palladous chloride reacts with thioglycolic acid in a molar ratio of 1 : 2, while the absorption maximum appears at 330 $m\mu$. These results were presented in a previous paper[3].

In determining palladium in a mixture of a large number of cations, Widtman[4] found the absorption maximum of the palladous thioglycolate complex at 370 mμ and established a 2 : 3 metal to ligand ratio in the complex. We could not confirm these data by subsequent checks, while Pilipenko and Moslei[5], in a study published after our report, give the stoichiometric ratio as 1 : 2 and the absorption maximum as 332 mμ, which agrees with our findings.

The conflicting data prompted us to examine the palladous thioglycolate complex more closely by other methods as well. We isolated the complex, analyzed it for % elemental composition, recorded its IR (infrared) spectra comparing them with those of its components, determined its stability constant, and, from these data and from the electrochemical behavior of the complex, we worked out procedures for the determination of palladium by potentiometric and amperometric titration.

The results of these investigations agree with those we obtained by spectrophotometry and confirm the previously reported metal-ligand ratio in the complex.

EXPERIMENTAL

Reagents and Apparatus — A 0.02283 M solution of palladous chloride was made by dissolving 1 *g* of palladous chloride (Riedel-de Haen) in 250 *ml* and was standardized with dimethylglyoxyme[6].

A 0.0495 M thioglycolic acid solution was prepared by taking 1.5 *g* 80% thioglycolic acid (Merck) dissolved in 250 *ml* water. The solution was standardized with iodine in acidic medium by potentiometric titration at platinum electrode, analogous to the determination of thiosulfate with iodine.

Potentiometric measurements were made with a Radiometer 22 pH--meter, while for amperometric and biamperometric measurements a Lange MG 1 multiflex galvanometer (sensitive 10^{-9} A/div.) was used. IR spectra were recorded on a Perkin-Elmer Infracord 237 spectrometer.

(1) *Isolation of Palladous Thioglycolate Complex and Investigation of Its Composition*

300 *mg* palladous chloride was dissolved in 20 *ml* water. The solution was heated and 1 : 1 hydrochloric acid added dropwise until full dissolution of the palladous chloride. Then 400 *ml* ethanol and 1.5 *g* 80% thioglycolic acid dissolved in 30 *ml* ethanol were added. The solution was neutralized with a 1 : 1 solution of ammonium hydroxide which brought the *p*H to around 5. A yellow voluminous precipitate was separated by centrifugation. The isolated complex contained coprecipitated chlorides and so was dissolved in water and reprecipitated with ethanol. After repeated precipitation the complex did not contain chlorides. Finally it was washed in ether and dried in a drying chamber at 40°C and then in an exsiccator with calcium chloride.

The percentage ratio of carbon, hydrogen and nitrogen in the complex was established by organic microanalytical methods. For the determination of palladium and sulfur, 152 *mg* complex was dissolved in concentrated nitric acid and was destroyed by electrooxidation after Gasparini. Palladium was determined with dimethylglyoxyme[6], sulfur as barium sulfate. The elemental analysis is given in Table 1. It corresponds to an approximate formula for the complex of $NH_4OOC—CH_2—S—Pd—S—CH_2—$ —COOH

TABLE 1

Elemental Analysis of the Isolated Complex

Element	Found %	Calculated for $Pd/SCH_2COO/_2HNH_4$ %	Difference %
Pd	34.50	34.75	—0.25
S	20.96	20.95	0.01
N	3.80	4.58	—0.78
H	3.14	2.95	0.19
C	15.62	15.75	—0.11

Figure 1 shows IR spectra of thioglycolic acid, ammonium thioglycolate and the palladous thioglycolate complex. The spectra show the absorption band of the carboxyl group with ammonium thioglycolate shifted toward a greater wavelength because of binding with NH_4^+ ion. The spectrum of the complex reveals two carboxyl group bands: one exactly in the same place as with thioglycolic acid, and the other as with ammonium thioglycolate. The presence of the —COOH group absorption band in the spectrum of the complex confirms that palladium is not bound to the carboxyl group.

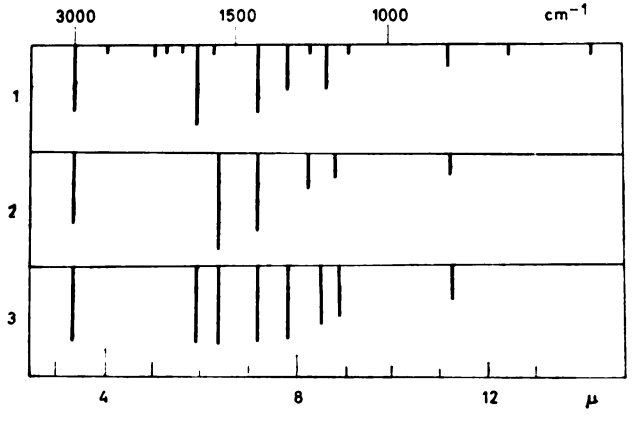

Figure 1

IR spectra of thioglycolic acid (1), ammonium thioglycolate (2) and the isolated complex of palladous thioglycolate (3).

It was proved by electrophoresis that the palladous thioglycolate complex exists in the form of an anion, for moving toward the anode in an electric field. On an 18 *cm* paper strip under a potential difference of 100 V the complex moves 1 *cm* in 3 h 20 min. Electrophoresis was conducted in an ammonia-ammonium chloride medium at *p*H 10.

These data tend to support the formula suggested on the basis of previous results.

To test the stability of the palladous thioglycolate complex several reactions were conducted. The action of hydrogen sulfide on the palladous tetraamine complex, whose stability constant is 10^{30}, yielded brownish black palladous sulfide. Hydrogen sulfide and palladous thioglycolate do not react either in acid or in alkaline media. We did not observe any changes in the palladous thioglycolate solution after several hours of bubbling through hydrogen sulfide. When the alkaline palladous thioglycolate solution was treated with surplus calcium cyanide, the yellow color of palladous thioglycolate gradually disappeared. The solution became entirely colorless after 2 h, the palladous thioglycolate changing into palladous cyanide whose stability constant is 10^{51}.

From these reactions it may be inferred that the stability constant of the palladous thioglycolate complex lies between the constants for the palla-

dous tetraamine and palladous tetracyanide complexes. Its magnitude was found using a palladium electrode prepared according to a procedure described in the literature[7].

The palladous chloride solution was mixed with a great excess of thioglycolic acid so that its concentration after reaction virtually did not change. Pre-reaction concentrations in the solution were: 10^{-4} *g*-ions/*lit* of palladous chloride, and $2 \cdot 10^{-2}$ moles/*lit* of thioglycolic acid. Potentials were measured after driving out air oxygen with a carbon dioxide current in an airtight vessel. A saturated calomel electrode was used for reference. After 2 h the EMF of this galvanic element was steady, remaining constant for one day. The mean potential value from 4 tests with the above concentrations was 0.157 V/NHE.

In an acidic medium the palladous thioglycolate complex dissociates thus

$$Pd(SCH_2COOH)_2 \rightleftarrows Pd^{2+} + 2\,HOOCCH_2S^-$$

The concentration of $HOOCCH_2S$ ions, or briefly RS^-, depends oe the solution *p*H and can be calculated from the dissociation constant of ths thiol group in thioglycolic acid, whose value[8] is $7 \cdot 10^{-12}$. The palladoun ion concentration was computed from the electrode potential, while the conf centration of palladous thioglycolate complex is practically equal that on palladous chloride before reaction.

Substituting the palladous ion concentration ($10^{-28.6}$ *g* ions/*lit*), RS^- concentration ($5.6 \cdot 10^{-11}$ *g*-ions/*l* at *p*H 2.60) and thioglycolate complex concentration (10^{-4} *g*-ions/*l*) into the stability constant equation

$$K_s = \frac{[Pd\,(RS)_2]}{[Pd^{2+}] \cdot [RS^-]^2}$$

gives $pK_s = 45.1$ at 20°C. In a solution with half the initial concentration of thioglycolic acid ($1 \cdot 10^{-2}$ moles/*lit*) but the same concentration of palladous ions ($1 \cdot 10^{-4}$ *g*-ions/*lit*), the value of pK obtained was 45.06.

(2) *Determination of Palladium with Thioglycolic Acid by Potentiometric and Amperometric Titrations*

(A) *Potentiometric Titration* — We tried to use the property of thioglycolic acid to change the oxidation-reduction potential during the formation of stable complexes of some metals for the determination of palladium by potentiometric titration. Titration was done in the presence of a smooth platinum electrode connected to a saturated calomel electrode.

Direct titration of palladous chloride with thioglycolic acid yielded 10% lower than theoretical results. The phenomenom is attributable to palladous ion adsorption on the precipitate that appears toward the end of titration. This is also confirmed by titration in 0.1 N H_2SO_4 where precipitate appears earlier and the errors are greater. If, however, titration is done in a mixture of 75 *ml* ethanol and 25 *ml* 0.1 N HCl, in which precipitate does not form, then a potential jump takes place at a 1 : 2 concentration ratio of palladous chloride and thioglycolic acid, but the reaction is so slow that up to 10 min must be allowed between successive additions of the titrant as the equivalence point is approached. The potentiometric titration curve for palladous chloride is shown in Fig. 2.

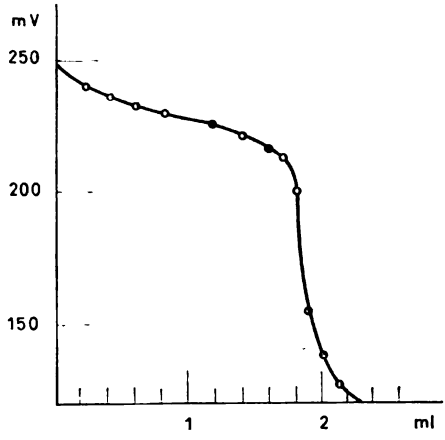

Figure 2

Potentiometric titration curve of 2 *ml* 0.02283 M palladous chloride in 100 *ml* mixture of 0.1 N HCl and ethanol (1 : 4), with 0.0495 M thioglycolic acid

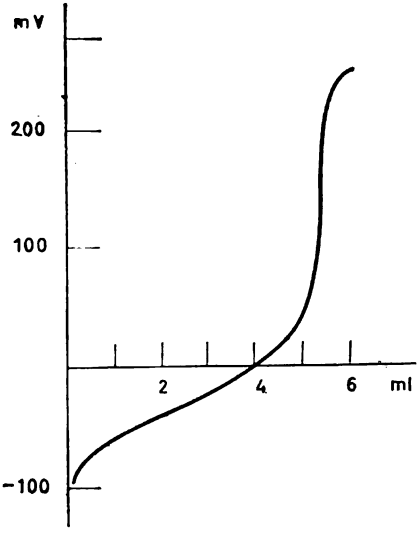

Figure 3

Potentiometric titration curve of 5 *ml* 0.0495 M thioglycolic acid in 100 *ml* 0.1 N HCl with 0.02283 M palladous chloride

Inverse titration, i.e. titration of thioglycolic acid with palladous chloride, proceeds much faster. The potential is established quickly and a jump occurs at the equivalence point. The titration curve is presented in Fig. 3 and the results in Table 2.

In both direct and inverse titration the metal to ligand ratio at the equivalence point is 1 : 2. The slow establishment of the potential near the equivalence point is attributed to the formation of polynuclear palladium complexes with the reagent, which also takes place when copper reacts with thioglycolic acid[9].

(B) *Amperometric Titration* — To determine palladium by amperometric titration we first recorded the polarization curve of $2 \cdot 10^{-4}$ M thio-

TABLE 2

Results of Invers Titration of Palladous Chloride with Thioglycolic Acid

ml of 0.0495 M thioglyc. acid taken	*mg* of Pd used	Calculated amount of Pd (*mg*)	Calcul. amount of Pd (%)
8.00	21.20	21.07	99.4
5.00	13.19	13.17	99.9
4.00	10.55	10.53	99.8
2.00	5.22	5.27	100.7
1.15	3.05	3.03	99.0
1.00	2.61	2.63	100.8
0.80	2.12	2.11	99.3
0.60	1.57	1.58	100.8
0.50	1.31	1.32	100.5
		Mean value:	100.0±0.6

glycolic acid in 0.1 N H_2SO_4 on an anodically polarized rotating platinum microelectrode (600 rpm). The curve is presented in Figure 4. When the potential is going from negative to positive the curve has a broad maximum around 1 V. When it changes in the opposite direction, the maximum occurs at 0.9 V. Between the curves there is considerable hysteresis.

Amperometric titration was performed in 0.1 N HCl. Direct titration of palladous chloride with thioglycolic acid yielded 10% lower than theoretical results, as with potentiometry. Titration was done at +0.9 V, since establishment of constant diffusion current takes a long time at higher potentials.

In invesrse titration, i.e. titration of thioglycolic acid with palladous chloride, the diffusion current decreases in proportion to the decrease of thioglycolic acid concentration. In the vicinity of the equivalence point, the current falls off abruptly down to this point and then levels out (Fig. 5).

Since various substances, including thio-compounds, adsorb on platinum, the change in the slope of the curve before the equivalence point could be ascribed to the adsorption of oxidized products of thioglycolic acid on the electrode. The equivalence point is located at a 2 : 1 ratio between the concentrations of thioglycolic acid and palladous chloride. Titration is easy and quick because the dissolved oxygen does not have to be removed. Titration results are shown in Table 3.

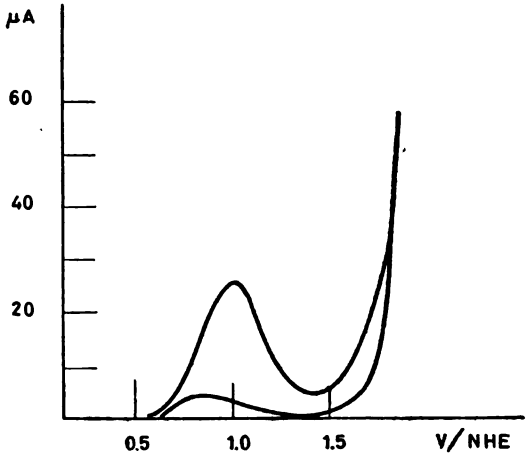

Figure 4

Polarographic curve for $2 \cdot 10^{-4}$ M thioglycolic acid in 0.1 N H_2SO_4, obtained on anodically polarized rotating platinum microelectrode:

(1) potential going from negative to positive

(2) potential going from positive to negative

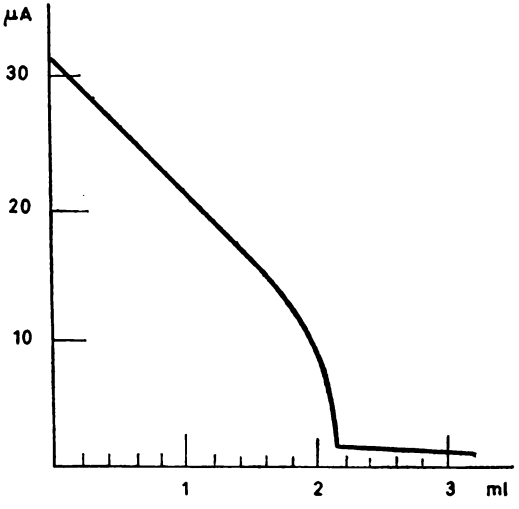

Figure 5

Amperometric titration curve for 2.00 *ml* 0.0495 M thioglycolic acid with 0.02283 M palladous chloride. Supporting electrolyte: 50 *ml* 0.1 N HCl.

$E_a = 0.9$ V/NHE

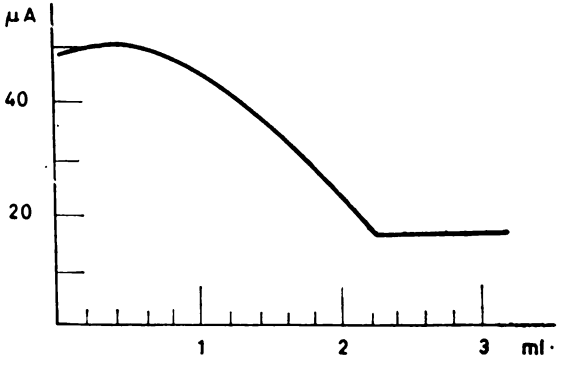

Figure 6

Biamperometric titration curve for 2.00 *ml* 0.0495 M thioglycolic acid with 0.02283 M palladous chloride

Supporting electrolyte 50 *ml* 0.1 N HCl.

$EMF_{pol} = 0.9$ V

TABLE 3

Determination of Palladium by Inverse Amperometric Titration with Thioglycolic Acid

ml of 0.0495 M thioglycolic acid taken	*mg* of palladium used	Calculated amount of Pd (*mg*)	Difference (%)
2.00	5.25	5.27	+0.3
2.00	5.26	5.27	+0.2
2.00	5.25	5.27	+0.3
1.00	2.62	2.63	+0.4
1.00	2.65	2.63	—0.7
1.00	2.65	2.63	—0.7

The determination of palladium using the inverse method was also carried out by biamperometric (dead-stop) titration in the presence of two platinum indicator electrodes polarized with an EMF of 0.9 V. The supporting electrolyte was the same as for amperometric titration. The titration curve is shown in Fig. 6. Palladium in amounts of 0.2—5 *mg* was determined to an accuracy better than 1% (Table 4).

TABLE 4

Determination of Palladium by Inverse Biamperometric Titration (dead-stop method)

ml of 0.0495 M thioglyc. acid taken	*mg* of palladium used	Calculated amount of Pd (*mg*)	Difference (%)
2.00	5.28	5.27	—0.3
2.00	5.28	5.27	—0.3
0.20	0.527	0.526	—0.2
0.10	0.265	0.263	—0.8

School of Sciences
Department of Chemistry
Belgrade University
and
School of Liberal Arts
Priština

Received 8 January, 1969

REFERENCES

1. Songina, O. A. *Amperometricheskoe titrovanie* (Amperometric Titration) — Moskva: Khimiia, 1967, p. 278.
2. König, O. and W. Crowell. "Thioacids as Spot-Test Reagents for Palladium" — *Mikrochemie ver. Mikrochimica Acta* (Wien) 33: 300—302, 1948.
3. Vajgand, V. J. and M. D. Jaredić. * (Spectrophotometric Determination of Palladium with EDTA and Sodium Salt of Thioglycolic Acid) — *Glasnik Hemijskog društva* (Beograd) 31**: 409—417, 1966.
4. Widtman, V. "Colorimetric Determination of Palladium with Thioglycolic Acid" — *Chemicke Listy* (Praha) 58: 211—215, 1964.
5. Pilipenko, A. T. and N. N. Moslei. * (Spectrophotometric Determination of Palladium and Rhodium with Thioglycolic Acid) — *Ukrainskii Khimicheskii Zhurnal* (Kiev) 33: 703—704, 1967.
6. Vogel, A. *Quantitative Inorganic Analysis.* IIIrd *Edition* — London: Longmans and Co., 1961, p. 511.
7. Fasman, A. B., G. G. Kutiukov, and D. V. Sokol'ski. (Reactivity of Palladium II — Complexes in Aqueous Solutions) * (In Russian) — *Zhurnal neorganicheskoi khimii* (Moskva) 10: 1338—1343, 1965.
8. Kolthoff, I. M., W. Stricks, and A. Heydrick. "Formation and Properties of Various Mercuric Mercapto Thioglycolates Formed in Reactions between Mercuric Mercury and Thioglycolic Acid" — *Journal of the American Chemical Society* (Easton) 76: 1515—1519, 1954.
9. Klotz, I. M., G. H. Czeklinski, and H. A. Feiss. "A Mixed-Valence Copper Complex with Thiol Compounds" — *Journal of the American Chemical Society* (Easton) 80: 2920—2923, 1958.

* Original title not given.

** Available in English translation from Clearinghouse for Federal Scientific and Technical Information, Springfield, Virginia, 22151.

GLASNIK HEMIJSKOG DRUŠTVA, Vol. 34, No. 2-3-4, 1969, pp. 233—238

GHDB-55

547.1'13:546.711'131:547.821'131

Original Scientific Paper

MANGANESE CHLORIDE COMPOUNDS WITH ALKYLPYRIDINE HYDROCHLORIDES

by

KOSTA I. NIKOLIĆ, KSENIJA R. VELAŠEVIĆ, and ANĐELIJA B. ĐUKANOVIĆ

In previous studies[1, 2, 3] we investigated the chemical and fluorescent properties of the compounds formed by manganese chloride with certain hydrochlorides of N-heterocyclic bases. It was established that two types of compound are obtained which differ in chemical composition and fluorescence.

In further work in this field we synthesized manganese chloride com.-pounds with the following hydrochlorides of pyridine bases: 2-methylpyridine, 3-methylpyridine, 4-methylpyridine, 2-ethylpyridine, 3-ethylpyridine, 4-ethylpyridine, 2,3-dimethylpyridine, 2,6-dimethylpyridine, 3,4-dimethylpyridine, and 2-methyl,6-ethylpyridine.

EXPERIMENTAL

These compounds are obtained by adding appropriate amounts of ethanol solution of the alkylpyridine bases to an aqueous solution of manganese chloride in the presence of concentrated hydrochloric acid. The solution obtained is slowly evaporated on a water bath. The resulting crystals are treated with chloroform and recrystallized from aqueous solution.

Depending on the molar ratio of the components, two types of compounds are obtained which fluoresce differently. A 1 : 1 molar ratio between the alkylpyridine base hydrochloride and manganese chloride yields red-fluorescing compounds, while a 2 : 1 ratio yields green-fluorescing compounds. The different fluorescence allows quick and easy identification of the two types.

The composition of these compounds was confirmed by analysis for manganese, nitrogen and chlorine. To determine their structure their IR spectra and those of the alkylpyridine bases were recorded. Measurements were made on a Perkin-Elmer, model 237 grating spectrograph lattice. Measurements of absorption spectra were made on a Beckman DU-2 spectrophotometer using 1 *cm* cell. We used water, ethanol and carbon tetrachloride as solvents in spectrophotometry. Figure 1 shows the spectra of ethanol solutions of 3-methylpyridine, 3-methylpyridine hydrochloride and compounds of 3-methylpyridine hydrochloride with manganese chloride.

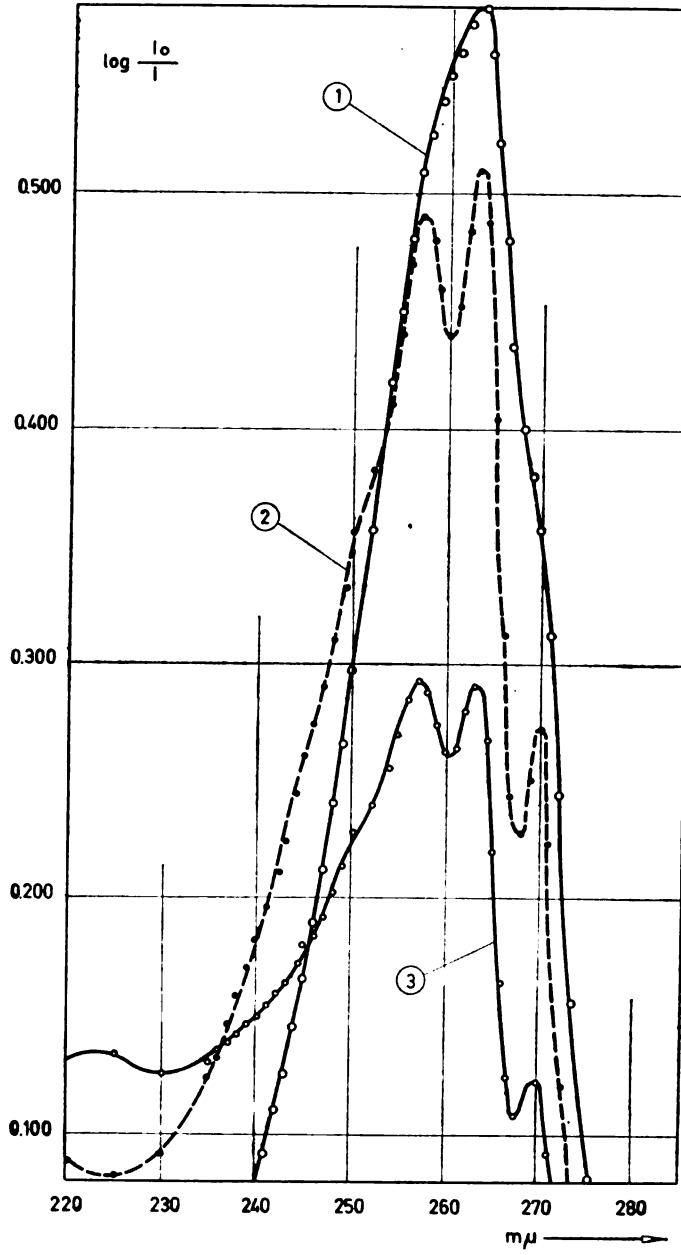

Figure 1

UV absorption spectra of

1. — 3-methylpyridine hydrochloride
2. — 3-methylpyridine
3. — manganese chloride compounds with 3-methylpyridine hydrochloride

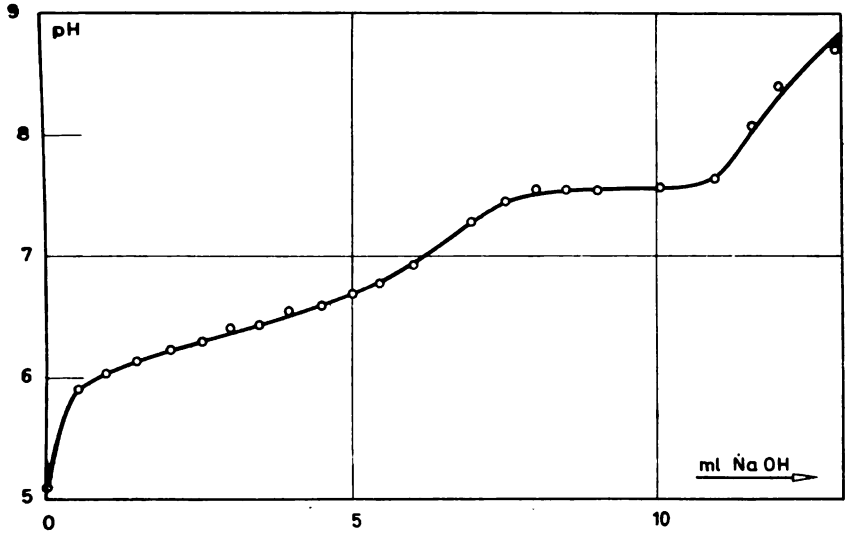

Figure 2
Potentiometric titration curve

TABLE 1

Compound	Ratio (mol)	Color of fluorescence	n m^{max}
2-methylpyridine hydrochloride	1:1	red	640
+ $MnCl_2$	2:1	green	533
3-methylpyridine hydrochloride	1:1	red	634
+ $MnCl_2$	2:1	green	514
4-methylpyridine hydrochloride	1:1	red	634
+ $MnCl_2$	2:1	green	533
2,3-dimethylpyridine hydro-	1:1	red	634
chloride + $MnCl_2$	2:1	green	522
2,6-dimethylpyridine hydro-	1:1	red	640
chloride + $MnCl_2$	2:1	green	540
3,4-dimethylpyridine hydro-	1:1	red	634
chloride + $MnCl_2$	2:1	green	522
2-ethylpyridine hydrochloride	1:1	red	634
+ $MnCl_2$	2:1	green	540
3-ethylpyridine hydrochloride	1:1	red	634
+ $MnCl_2$	2:1	green	515
4-ethylpyridine hydrochloride	1:1	red	634
+ $MnCl_2$	2:1	green	520
2-methyl-5-ethylpyridine hydro-	1:1	red	634
chloride + $MnCl_2$	2:1	green	519

The presence of pyridinium ion was proved by potentiometric titration of aqueous solutions of the compounds with 0.1 N sodium hydroxide. A characteristic titration curve is shown in Figure 2.

By electrolysis of aqueous solutions of the compounds the presence of pyridinium ion was reconfirmed. The reduction of this ion at the cathode yields pyridine.

DISCUSSION

The literature describes two types of compound of pyridine with manganese chloride[4,5,6]. They are distinguished according to color, as it was found that pyridine and manganese chloride in the presence of hydrochloric acid yield green or pinkish crystals. Taylor[4] ascribed the structure $(Py\ H)_2\ MnCl_4$ to the green and $MnCl_2 \cdot Py \cdot HCl \cdot H_2O$ to the pinkish crystals. Fyfe[5], however, gives these compounds the formulas of dibasic complex acids without pyridinium ion, but having pyridine as ligand bound with manganese. He formulates the pink compounds as $H_2MnPyCl_3OH$, the green as $H_2MnPyCl_4$. He established this by molecular weight determination, elemental analysis, potentiometric titration, and by determination of hydrolysis products. He found that these compounds were unstable in solution: dissociation yields first $MnPy_2Cl_4$ whose further decomposition liberates pyridine:

$$MnPyCl_4^{=} = MnCl_4^{=} + 2Py$$

Full hydrolysis of this salt proceeds in two steps:

$$H_2MnPy_2Cl_4 + 2HOH \text{ — } H_2MnPyCl_3(OH)H_2O + PyHCl$$
$$H_2MnPyCl_3(OH)H_2O \text{ — } MnCl_2\ 4H_2O + PyHCl$$

The presence of pyridinium ion resulting from hydrolysis in aqueous solution was proved by potentiometric titration[5].

We tried to synthesize similar compounds using quinoline derivatives according to procedures described by Taylor[4] and Fyfe[5]. We obtained fluorescent compounds only in the presence of concentrated hydrochloric acid[7]. We extended investigations to include alkylpyridine bases and established that they too produce green and red-fluorescing compounds on reacting with manganese chloride in the presence of hydrochloric acid. IR spectra of these compounds in the solid state show the same characteristic maximums due to the pyridine ring. The characteristic pyridinium ion band does not show up in these spectra, which supports the hypothesis of Fyfe[5].

The absorption maximums for the alkylpyridine bases lie at greater wavelengths than those for pyridine. This is due to electron transfer as a result of hyperconjugation of the alkyl groups and the pyridine ring. The absorption spectra of the compounds of manganese with hydrochlorides of alkylpyridine bases in ethanol or carbon tetrachloride solution differ from those in aqueous solution. From Fig. 1 it may be seen that the absorption spectra of ethanol solutions of 3-methylpyridine and of the complex manganese chloride compound with 3-methylpyridine hydrochloride are identical, so it may be inferred that the absorption bands originate from pyridine rather than from pyridinium ion. The absorption spectrum of the compound in aqueous solution coincides with that of methylpyridine in acidic medium and shows the characteristic expansion of the spectrum toward the long

wave end. This is attributed to the addition of protons to the nitrogen atom of the pyridine ring producing pyridinium ion, as has been proved by both potentiometric titration and electrolysis.

Since the presence of pyridinium ion has been proved only in dilute solutions, not in the solid state, we presume that the behavior of manganese chloride compounds with hydrochlorides of alkylpyridine bases can be expressed by Fyfe's structural formula[5]. For the compounds having a 2 : 1 molecular ratio between the respective hydrochloride and manganese chloride, the formula is $H_2Mn\ mPyCl_4$, while for a 1 : 1 ratio it is $H_2Mn\ mPyCl_3OH$, where mPy signifies the corresponding alkylpyridine base. The pressnce of pyridinium ion in aqueous solution is explained by hydrolysis which can also result in the occurrence of complex $MnCl_4$ and $MnCl_3$ ions which then dissociate further. The different behavior of these compounds in the solid state and in solutions gives them different fluorescent properties. The solids fluoresce pure green or red, while the aqueous solutions fluoresce violet-blue due to the pyridinium ion.

Table 1 shows the fluorescent properties of the synthesized compounds.

School of Pharmacology
Department of Physical Chemistry
Belgrade University

Received 13 September, 1968

REFERENCES

1. Nikolić, K. I. "Nove metode dobijanja nekih kompleksa manganohalogenida sa hinolinom" (New Methods for Obtaining Some Complexes of Manganohalides with Quinoline) — *Glasnik Hemijskog društva* (Beograd) 27*: 209—211, 1962.
2. Nikolitch, K., H. Payen, and S. Schlivitch. "Sur la fluorescence de quelques complexes halogenes du manganese et de la pyridine" — *Comptes rendus* (Paris) 250: 4143—4145, 1960.
3. Velaschevitsch, X., S. Schlivitch, and K. Nikolitch. "Sur la fluorescence de quelques complexes du chlorure de manganese et des alcaloides" — *Comptes rendus* (Paris) 257: 3855—3857, 1963.
4. Taylor, S. F. "The Manganohalides of Pyridine and Quinoline" — *Journal of the Chemical Society* (London) 699—701, 1934.
5. Fyfe, W. S. "The Manganohalides of Pyridine" — *Journal of the Chemical Society* (London) 790—793, 1950.
6. Bowman, P. B. and L. B. Rogers. "Effect of Metal Ion and Ligand on Thermal Stability of Metal Amine Complexes" — *Journal of Inorganic and Nuclear Chemistry* (Northern Ireland) 28: 2215—2224, 1966.
7. Nikolić, K., K. Velašević, and A. Đukanović. "Jedinjenja manganohlorida sa raznim metilhinolinhidrohloridima" (Manganese Chloride Compounds with Various Methyl Quinoline Hydrochlorides) — *Glasnik Hemijskog društva** (Beograd) (to be published).

* Available in English translation from Clearinghouse for Federal Scientific and Technical Information, Springfield, Virginia, 22151.

GLASNIK HEMIJSKOG DRUŠTVA, Vol. 34, No. 2-3-4, 1969, pp. 239—244

GHDB-56

547.293:547.293'26:54.07

Original Scientific Paper

SYNTHESIS OF 2-N- AND 2-S-SUBSTITUTED PROPANOIC ACIDS (α-AMINO THIOLACTIC ACIDS) AND THEIR ESTERS*

by

KSENIJA D. SIROTANOVIĆ and ZORICA Ž. NIKIĆ

In a previous paper one of us reported[1] the synthesis of two α-amino thiolactic acid derivatives: S-acetyl-α-acetylamino thiolactic acid (I, R = H) and S-phenyl-α-acetylamino thiolactic acid (II, R = H):

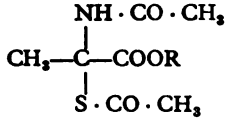

(I)

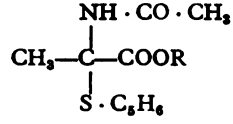

(II)

Both compounds were obtained in two ways: (a) by the condensation of pyruvic acid, acetamide and thioacetic acid or thiophenol, in the presence of concentrated HCl, at room temperature:

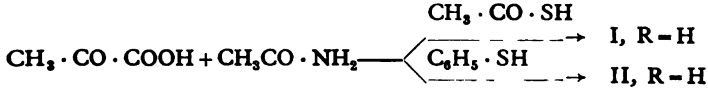

(b) by the action of thioacetic acid or thiophenol on the complex of α-hydroxy-α-acetylamino propionic acid with two moles of acetamide (III):

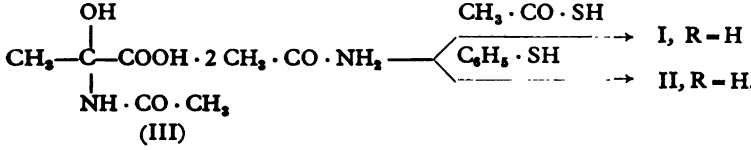

(III)

Compound II (R = H) was also obtained from α-hydroxy-α-phenylthio) propionic acid (IV) by melting it with acetamide:

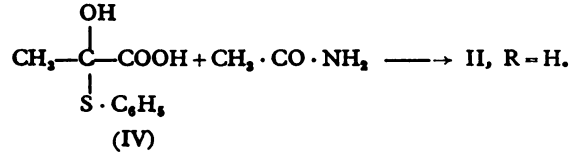

(IV)

* Communicated at the 13th Conference of Chemists of the SR of Serbia, January, 1968.

Continuing our work on the synthesis of substituted α-amino thiolactic acids, we condensed pyruvic acid with other nitrogen and sulfur components. Thus, in addition to acetamide we used urea, urethane and thiourea, and in addition to thioacetic acid and thiophenol, benzyl mercaptan.

The condensations were carried out by the action of concentrated hydrochloric acid, at ordinary temperature, on an equimolecular mixture of pyruvic acid with the nitrogen and sulfur component. In some instances, boron trifluoride was used, while an attempt was also made to carry out the reaction in the absence of a catalyst.

In this way we obtained the following compounds:

1. 2-benzylthio-2-acetamido propanoic acid (VI)
2. 2-acetylthio-2-ureido propanoic acid (VIII, R — H; R′ = $CH_3 \cdot CO$-)
3. 2-phenylthio-2-ureido propanoic acid (VIII, R = H; R′ = = C_6H_5-)
4. 2-benzylthio-2-ureido propanoic acid (VIII, R = H; R′ = = $C_6H_5 \cdot CH_2$).

None of the expected reaction products was obtained with urethane and thiourea in the presence of thioacetic acid, thiophenol or benzyl mercaptan.

The yields of these condensation were better in the presence of hydrochloric acid than in the presence of boron trifluoride or in the absence of a catalyst.

By condensing pyruvic acid with acetamide and benzylmercaptan, instead of the expected 2-benzylthio-2-acetylamido propanoic acid (VI), a complex of 2-hydroxy-2-benzylthiopropanoic acid with two molecules of acetamide (V) was obtained, a compound likewise not reported in the literature so far:

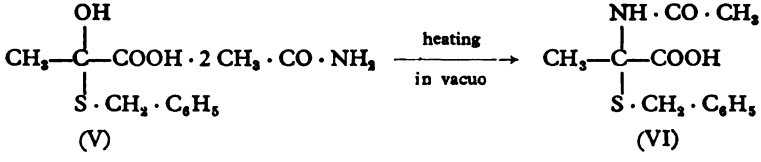

(V) (VI)

The acid VI was obtained in three ways: by heating complex V in vacuo, by melting 2-hydroxy-2-benzylthio propanoic acid (VII) with acetamide:

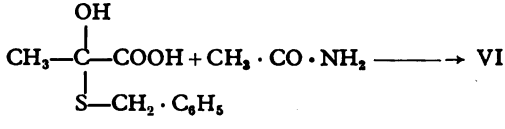

(VII)

and thirdly by passing gaseous hydrogen chloride through a mixture of complex III and benzyl mercaptan:

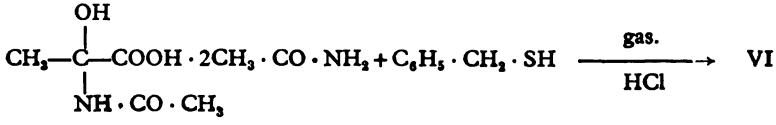

In addition to pyruvic acid, the condensations with the mentioned nitrogen and sulfur components were attempted with ethyl pyruvate, and some with methyl pyruvate as well. However, only one product was obtained, ethyl 2-acetyl-thio-2-ureido propanoate (VIII, $R = C_2H_5^-$, $R' = CH_3 \cdot \cdot CO^-$). Methyl esters of acids I and II were obtained indirectly, by the methylation of free acids with diazomethane.

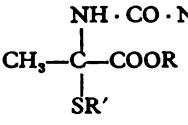

(VIII)

The compounds synthesized are colorless crystalline substances, soluble in ordinary organic solvents. Some of the 2-S-2-ureido propanoic acids (containing the ureido group as the nitrogen component) are insoluble in water and organic solvents. When we tried to crystallize them they gave products melting above 250°C, the structure of which was not determined. No doubt these are polymeric products characteristic for derivatives with urea[2].

EXPERIMENTAL

Melting points are not corrected.

Complex of 2-hydroxy-2-benzylthio propanoic acid with two molecules of acetamide (V)

Pyruvic acid (2.2 *g*, 1/40 M), acetamide (3.0 *g*, 2 × 1/40 M) and benzyl mercaptan (3.1 *g*, 1/40 M) were mixed, The mixture immediately solidified, yielding 96.3% (7.9 *g*) of crude product m.p. 63—4°. Recrystallized from abs. ether it melted at 75—6°.

Analysis:

Calc. for $C_{14}H_{22}O_5N_2S$:	C, 50.90;	H, 6.71;	N, 8.48%
Found:	C, 50.81;	H, 6.49;	N, 8.26%.

2-Benzylthio-2-acetylamido propanoic acid (VI)

A. *Obtained from complex (V) by heating in vacuo.* 3.3 *g* (1/100 M) of complex (V) was heated for 1/2 hour on a water bath in vacuum. The residue washed with ether gave 0.7 *g* (27.67%) of crude product, m.p. 157°. After crystallization from acetone-petroleum ether it melted at 165°.

B. *Obtained from 2-hydroxy-2-benzylthio propanoic acid (VII) by melting it with acetamide.* 2.1 *g* (1/100 M) of VII and 0.74 *g* (1/80 M) of acetamide heated for 1/2 hour in vacuum at 50—60° gave 0.8 *g* (31.6%) of crude product, m.p. 162—3°. Recrystallized from acetone-petroleum ether it melted at 165°.

C. *Obtained from complex III and benzyl mercaptan by blowing through hydrogen chloride gas.* 5.3 *g* (1/50 M) of complex III and 2.5 *g* (1/504) of benzyl mercaptan were dissolved in 10 *ml* absolute ether and gaseous HCl was passed through the mixture for 10 minutes. After filtration and washing

with iced water 1.8 *g* (35.6%) of crude product m.p. 154—5° was obtained, which recrystallized from acetone-petroleum ether melted at 165°.

A mixture of the products obtained under A, B and C above showed no depression.

Analysis:

Calc. for $C_{12}H_{15}O_3NS$:	C, 56.89, H, 5.97; N, 5.53%
Found:	C, 56.91; H, 6.08; N, 5.36%.

2-Acetylthio-2-ureido propanoic acid (VIII, R = H, R′ = $CH_3 \cdot CO^-$)

Pyruvic acid (2.9 *g*, 1/30 M), urea (2.0 *g*, 1/30 M) and thioacetic acid (2.5 *g*, 1/30 M) in the presence of HCl gave 82.97% (5.7 *g*), in the presence of BF_3 42.2% (2.9 *g*), and in the absence of catalyst 11.6% (0.8 *g*) of crude product, m.p. 132—3°. After washing with water, ethanol and ether it melted at 142°.

Analysis:

Calc. for $C_6H_{10}O_4S$:	C, 34.94; H, 4.89; N ,13.59%
Found:	C, 34.73; H, 5.12; N, 13.43%.

2-Phenylthio-2-ureido propanoic acid (VIII, R = H, R′ = $C_6H_5^-$)

Pyruvic acid (2.9 *g*, 1/30 M), urea (2.0 *g*, 1/30 M) and thiophenol (3.7 *g*, 1/30 M) in the presence of HCl gave 79.9% (6.4 *g*) of crude product, while in the absence of catalyst the yield was 68.7%, and in the presence of BF_3 43.5%. Crude product m.p. 141°; recrystallized from EtOH and ether it melted at 144—5°.

Analysis:

Calc. for $C_{10}H_{12}O_3N_2S$:	C, 50.0; H, 5.0; N, 11.67%
Found:	C, 49.54; H, 5.16; N, 12.24%.

2-Benzylthio-2-ureido propanoic acid (VIII), R = H, R′ = $C_6H_5 \cdot CH_2^-$)

Obtained from pyruvic acid (2.2 *g*, 1/40 M), urea (1.5 *g*, 1/40 M) and benzyl mercaptan (3.1 *g*, 1/40 M) in 55.0% yield (3.5 *g*). Crude product m.p. 135—6°; recrystallized from ethanol, m.p. 137°.

Analysis:

Calc. for $C_{11}H_{14}O_3N_2S$:	C, 51.95; H, 5.55; N, 11.02%
Found:	C, 51.58; H, 5.72; N, 11.18%

2-Acetylthio-2-ureido propanoic acid ethyl ester
(VIII, R = C_2H_5 ; R′ = $CH_3 \cdot CO^-$)

Ethyl pyruvate (3.9 *g*, 1/30 M), urea (2.0, 1/30 M) and thioacetic acid (2.5 *g*, 1/30 M) yielded 37.1% (2.9 *g*) of ester which after thorough washing with ethanol and ether melted at 136°.

Analysis:

Calc. for $C_8H_{14}O_4N_2S$:	C, 41.01; H, 6.02; N, 11.97%
Found:	C, 40.92; H, 6.27; N, 12.62%

2-Acetylthio-2-acetylamido propanoic acid methyl ester
(I, R = CH_3^-)

Obtained from 2-acetylthio-2-acetylamido propanoic acid (I, R = H) (4.1 *g*, 1/50 M) and diazomethane (3.0 *g*) in yield of 91.2% (4.0 *g*). Crude product m.p. 158°; recrystallized from abs. ethanol it melted at 165°.

Analysis:

Calc. for $C_8H_{13}O_4NS$:	C, 43.83;	H, 5.98;	N, 6.39;	S, 14.62%
Found:	C, 43.53;	H, 5.97;	N, 6.17;	S, 14.56%

2-Phenylthio-2-acetylamido propanoic acid methyl ester
(II, R = CH_3^-)

Obtained from 2-phenyl-2-acetylamido propanoic acid (II, R = H) (4.8 *g*, 1/50 M) and diazomethane (3.0 *g*) in a 96.7% yield (4.9 *g*). Crude product, m.p. 140°, recrystallized from absolute acetone, melted at 146°.

Analysis:

Calc. for $C_{12}H_{15}O_3NS$:	C, 56.90;	H, 5.97;	N, 5.53;	S, 12.66%
Found:	C, 56.95;	H, 5.93;	N, 5.45;	S, 12.61%.

REFERENCES

1. Sirotanović, K and M Roćen-Bajlon "Sinteze *S*-acetil i *S*-fenil-α-acetilamino-tiomlečne kiseline (α-acetilamino-α-acetil-/fenil/-tiopropionske kiseline)" (Synthesis of *S*-Acetyl and *S*-Phenyl-α-Acetylamino-Thiolactic Acid (α-Acetylamino-α-Acetyl-/Phenyl/-Thiopropionic Acid) — *Glasnik Hemijskog društva* (Beograd) 25—26: 103—108, 1960—1961.
2. Simon, L. J. "Action de l'urea sur l'acide pyruvique (II) Triureide dipyruvique" — *Comptes Rendus des Séances de l'Academie des Sciences* (Paris) 136: 506—508, 1903.

GLASNIK HEMIJSKOG DRUŠTVA, Vol. 34, No. 2-3-4, 1969, pp. 245—250

GHDB-57

547.455.623'226:54.07:55.05

Original Scientific Paper

MONOSACCHARIDE SULPHATES. I.

PREPARATION AND PURIFICATION OF D-GLUCOSE-3-SULPHATE AND D-GLUCOSE-6-SULPHATE.

by

MIRJANA HRANISAVLJEVIĆ-JAKOVLJEVIĆ, RADMILA DIMITRIJEVIĆ and GORDANA MARKOVIĆ

A number of methods have been described for the preparation and purification of monosaccharide sulphates[1, 18]. The main disadvantages of all of them are that they are consuming and yield insufficiently pure products. Direct sulphation[1, 8, 12, 16, 18] represents the least convenient procedure since it is accompanied by polysulphation. Syntheses from different monosaccharide derivatives[3, 8] are better in this respect, although the formation of isometric sulphates cannot be avoided completely. Therefore the main problem in all known synthese is the purification of the reaction products. Various purification techniques based either on chemical or physical properties[14, 18] have been attempted, but none of them was found quite satisfactory.

The present paper describes the synthesis of D-glucose-3-sulphate and D-glucose-6-sulphate and a method for their purification and identification.

Using 1,2 : 5,6-dicyclohexylidene-D-glucofuranose as the starting material, by the action of chlorosulphonic acid in pyridine medium we obtained barium 1,2 : 5,6-dicyclohexylidene-D-glucofuranose-3-sulphate (I) in a very good yield (68.1%). This intermediate was quantitatively hydrolyzed to the corresponding D-glucose-3-sulphate (II). By a similar procedure we synthesized D-glucose-6-sulphate (IV) (yield 82.2%) from 1,2--monocyclohexylidene-D-glucofuranose:

In principle this method of preparation is not much different from Percival's[3] who used diisopropilidene derivatives. However, the results obtained show that cyclohexylidene derivatives are more suitable, since the impurities (some unreacted material) could be easily removed by solvent extraction. Hydrolytic removal of protecting cyclohexylidene groups was easy and quantitative.

The intermediate barium 1,2 : 5,6-dicyclohexylidene-D-glucofuranose--3-sulphate (I) was isolated as a white crystalline product melting at 137°C and having $[\alpha]_D^{20} - 4.65 \pm 1°$ (in ethanol). Elemental analysis corresponded to the molecular formula of I with three molecules of crystalline water. IR spectral analysis proved the presence of sulphate group (ν_{max} 1250 cm^{-1})

and crystalline water (ν_{max} 3500 cm^{-1} and 1640 cm^{-1}). However, TLC on silica gel plates in two different solvent systems showed the presence of two components (R_f 0.56 and 0.76, respectively, solvent *a*). The ratio of components was shown by PLC to be 3 : 1. The major component, with slower chromatographic movement, was designated as I*a* and the other as I*b*. Both components were isolated and their elemental analyses found to correspond to I. On hydrolysis I*a*, I*b* and I all yielded the same product, i.e. barium D-glucose-3-sulphate (II). These facts indicate I*a* and I*b* to be isomers. From scale models and conformations established for the tetrahydrofuran ring[19] it is inferred that isomers I*a* and I*b* differ in the conformation of the five-membrered ring, one having the envelop form (C_s) and the other the half chair form (C_2)[20]. We think that such a deduction is highly probable since IR spectral analysis of I*a* and I*b* revealed differences in the intensity of the bands in the region of 1460—1370 cm^{-1} and 890 and 750 cm^{-1}. Considering the molecular models, such differences could be caused only by the spacial orientation of the substituent in position 4 of the five-membered ring being bisectional or quasi axial. The study of these isomers will be the subject of our further work.

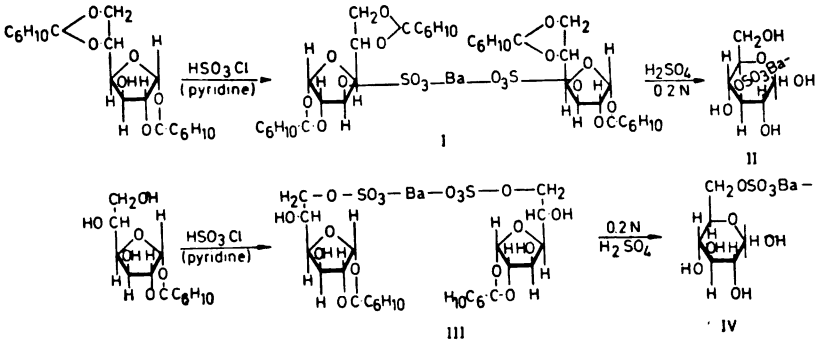

In the synthesis of barium D-glucose-6-sulphate, the intermediate barium 1,2-monocyclohexylidene-D-glucofuranose-6-sulphate (III) was obtained in only one isomeric form.

The purity of all reaction products and of the starting compounds was checked by thin-layer chromatography on silica gel plates. After a series of experiments we found that in solvent systems of benzene-methanol (1 : 1) or butanone saturated with water very good separation of the following glucose derivatives could be achieved in a period of 25—40 minutes: 1,2--monocyclohexylidene-D-glucofuranose, barium 1,2-monocyclohexylidene--D-glucofuranose-6-sulphate, barium D-glucose-6-sulphate, 1,2 : 5,6-dicyclohexylidene-D-glucofuranose, barium 1,2 :5,6-dicyclohexylidene-D-glucofuranose-3-sulphate and barium D-glucose-3-sulphate. Separation of barium D-glucose-3-sulphate from barium D-glucose-6-sulphate, however, was only possible in benzene-methanol mixture. Excellent separation of isomeric barium 1,2 : 5,6-dicyclohexylidene-D-glucofuranose-3-sulphates was achieved in both solvent systems, which enabled us to obtain them in a pure state by preparative thin-layer chromatography (see Table I). The components were detected by spraying with 50% sulphuric acid and subsequent

heating. Zones on PLC were located by the same reagent, applying cellotape strip technique.

The TLC procedure developed is one of the easiest ways for rapid separation and identification of cyclohexylidene derivatives of D-glucofuranose and D-glucofuranose sulphates.

EXPERIMENTAL

TLC was performed on silica gel H (Merck) plates in (a) benzene: methanol (1 : 1), and (b) water-saturated butanon. Paper chromatography was done on Whatman No. 1 filter paper by descending technique in (c) ethylacetate-acetic acid-water (6 : 3 : 2 v/v).[10] The detection reagent was 50% sulphuric acid for TLC and silver nitrate for paper chromatograms. All melting points are uncorrected. IR spectra were recorded on a Perkin-Elmer Model 421 spectrophotometer.

Barium 1,2 : 5,6-dicyclihexylidene-D-glucofuranose-3-sulphate (*I*)

1,2 : 5,6-diciclohexylidene-D-glucofuranose (4 *g*), obtained by Hockett and Miller's procedure[21], was dissolved in dry pyridine (80 *ml*). The solution was cooled to —18° and chlorosulphonic acid in chloroform (4/25 v/v) added dropwise in the course of 2 hours. The reaction mixture was constantly stirred and the temperature kept at about —10°C. After 24 hours standing at room temperature the reaction mixture was treated first with a few milliliters of water and 20 *ml* of pyridine and then diluted with 100 *ml* of water. Sulphate ions were precipitated by the addition of saturated barium hydroxide solution (alkaline reaction to phenolphtalein) and separated by filtration. The excess of barium ions was then removed by passing a stream of carbon dioxide through the solution and adding saturated silver sulphate solution. After filtration silver ions were removed by hydrogen sulphide and the latter by aeration. The deionized solution was concentrated in vacuum at 35° to a volume of about 100 *ml* and the whole procedure with barium hydroxide, silver sulphate and hydrogen sulphide repeated. The residue obtained by evaporation of the solution to dryness (35°, reduced pressure) was first treated with petroleum ether (or *n*-heptane) and then exctracted with hot ethanol. The ethanol extract, after being reduced to a volume of 20 *ml*, was left in the icebox to crystallize. In a few days a white solid separated which after crystallization from ethanol melted at 137°, had $(\alpha)_D^{25°} = -4.65 \pm 1°$ (c = 1.72 in ethanol) and in elemental analysis corresponded to trihydrate of I (Found: C, 41.90; H, 6.55; S, 6.38. $C_{36}H_{58}O_{18}Ba \cdot 3H_2O$ requires C, 41.98; H, 6.22; S, 6.22). Chromatography in solvents (a) and (b) (see section on chromatography) revealed the presence of two components with $R_f = 0.65$ and 0.17 for component Ia and $R_f = 0.76$ and 0.32 for component Ib, respectively.

ν_{max} (KBr) 3460, 1640, 1458, 1250 cm^{-1}

Barium D-glucose-3-sulphate (II)

3 *g* of I, containing components I and II, were dissolved in 100 *ml* of 0.2 N sulphuric acid and kept for 48 hrs at 38°C. After the removal of sulphuric acid by means of solid barium carbonate, the clear filtrate was

evaporated to dryness (35°, reduced pressure). The residue was first extracted several times with hot absolute ethanol, then dissolved in water and precipitated by the addition of absolute ethanol. Giving 1.95 *g* (yield 97%) of white powder having $(\alpha)_D^{25} = +29°$ (c = 2.2, H_2O), $R_f = 0.50$ (solvent b) and an IR spectrum identical with an authentic sample of barium D-glucose-3-sulphate. (Found: C, 20.19; H, 3.12; S, 10.01; Calc. for $C_{12}H_{22}O_{18}$ — Ba: C, 20.45; H, 3.55; S, 9.77).

Barium 1,2-monocyclohexylidene-D-glucofuranose-6-sulphate (III)

1,2-Monocyclohexylidene-D-glucofuranose[21] was dissolved in anhydrous pyridine (3.7/40 wg/v) and treated with chlorosulphonic acid in chloroform (4/24 v/v) at a temperature about —15°. The whole procedure was the same as in the preparation of glucose-3-sulphate. The solution obtained after deionisation was evaporated to dryness and treated with boiling acetone to remove any unreacted starting material. After crystallization from ethanol it melted at 150° and had $(\alpha)_D^{30°} = -3.7° \pm 1°$ (c=5, H_2O), ν_{max} (KBr) 3470, 2940, 1640, 1450, 1250, 1020 and 805 cm^{-1}, R_f = = 0.67 and 0.08 (solvents *a* and *b*, respectively). (Found: C, 35.54; H, 5.24; S, 7.50; Ba, 17.02. $C_{24}H_{38}O_{18}S_2Ba$ requires: C, 35.16; H, 5.12; S, 7.85; Ba, 16.81).

Barium-D-glucose-6-sulphate (IV)

Compound III was dissolved in 0.2 N sulphuric acid and left for 48 hrs at 38°C. After the usual treatment, the product obtained was found to have optical rotation $(\alpha)_D^{25°} = +30°$ (c = 0.9, H_2O), $R_f = 0.33$ (solvent *c*) and $R_f = 0.46$ (solvent *a* TLC). (Found: C, 21.73; H, 3.51; S, 9.90; Ba, 21.00. Calc. for $C_{12}H_{22}O_{18}S_2Ba$: C, 21.98; H, 33.5; S, 9.77; Ba, 20.91.

General procedure for thin-layer chromatography of cyclohexylidene derivatives of glucofuranose and glucofuranose sulphates

Thin-layer chromatography was performed on glass plates (20 × × 13 × 0.5 *cm*) coated with silica gel H (Merck), 0.2 *mm* thick. Development was done in chromatography tanks (24 × 16 × 8 *cm*) previously saturated with the developer, time being 25—40 minutes depending on the developer. After application of sample solutions on the starting line 2 *cm* apart, the chromatoplate was placed in the tank and developed until the solvent front reached a height of about 14 *cm*. Spraying with 50% sulphuric acid followed by air drying and then heating in the oven at about 110° resulted in the formation of dark spots on a white back ground.

The results are given in the Table I.

Preparative thin-layer chromatography of isomeric barium 1,2:5,6-dicyclohexylidene-D-glucofuranose-3-sulphates

Preparative thin-layer chromatography was done on a microscale. Chromatoplates (20 × 13 × 0.5 *cm*) coated with a 0.5 *mm* thick silica gel H layer, and a benzene-methanol (1 : 1) solvent mixture were used. A streak of 10% solution of the mixture was applied along the starting line (about

TABLE 1

Compound	R_f — values	
	MeOH/C_6H_6 (1:1)	Butanone saturated with water
1,2-Monocyclohexylidene-D-glucofuranose	0.79	0.56
1,2:5,6-dicyclohexylidene-D-glucofuranose	0.93	0.84
Barium 1,2-monocyclohexylidene-D-glucofuranose-6-sulphate	0.67	0.08
Barium 1,2:5,6-dicyclohexylidene-D-glucofuranose-3-sulphate		
Isomer Ia	0.56	0.17
Isomer Ib	0.76	0.32
Barium D-glucose-3-sulphate	0.50	—
Barium D-glucose-6-sulphate	0.46	—

30 *mg* on each plate). After two developments, the plates were dried and the zones located by cellotape technique, which consists in applying a narrow strip of cellotape along the edge of the plate. The thin-layer of silica gel stuck to the cellotape is then sprayed with 50% sulphuric acid and gently heated in the oven at 50°C to reveal spots. Zones are located by comparison with cellotape chromatostrips and the marked zones scraped from the plates, extracted with ethanol, evaporated and dried over phosphorous pentoxide in vacuo, weighed. The ratio of the components separated was found to be 3 : 1. Elemental analyses of both components corresponded to trihydrate of I (Isomer Ia. Found: C, 41.93; H, 6.30; S, 6.25; Ba, 13.50. Isomer Ib. Found: C, 41.89; H, 6.50; S, 6.19; Ba, 13.42. $C_{36}H_{58}O_{18}S_2Ba. \cdot 3H_2O$ requires: C, 41.98; H, 6.22; S, 6.22; Ba, 13.31). IR spectral analysis showed differences in the following absorption maxima: Ia, ν_{max} (KBr) 1450 (*m*) 1375 (*m*), 890 (*s*) and 750 (*s*) cm^{-1}; Ib, ν_{max} (KBr) 1450 (*s*), 1370 (*s*) 890 (*vw*) and 745 (*m*) cm^{-1}.

Sulphuric acid hydrolyzes both isomers to the same product, i.e. barium D-glucose-3-sulphate.

ACKNOWLEDGEMENTS

The authors are grateful to the Serbian Research Fund for financial support.

Department of Chemistry
School of Sciences,
Beograd

Received 24 October, 1968

REFERENCES

1. Neuberg, C. and L. Lieberman, "Glucose- and Rohrzuckermonoschwefelsaure. III". — *Biochemische Zeitschrift* 121: 326, 1921.
2 Percival, G. V., and T. H. Soutar, "Carbohydrate Sulphuric Esters. Part I. Glucose and Galactose Sulphates" — *Journal of the Chemical Society*: 1475, 1940.
3 Percival, E. G. V. "Carbohydrate Sulphuric Esters. Part III. The Hydrolysis of iso-Propylidene Glucofuranose Sulphates and Methylglucofuranose Sulphates" — *Journal of the Chemical Society*: 119, 1945.
4. Duff, R. B. "Carbohydrate Sulphuric Esters. Part V. Demonstration of Walden Inversion on Hydrolysis of Barium 1 : 6-Anhydro-β-D-Galactose-2-Sulphate" — *Journal of the Chemical Society* 1597, 1949.
5. Turvey, J. R. and M. J. Clancy, "Some Methods for the Purification of Sugar Sulphates" — *Nature* 183: 537, 1959.
6. Lloyd, A. G. "Chemical Synthesis of Hexose and Hexosamine Sulphates" — *Nature* 183: 109, 1959.
7. Lloyd, A. G "Studies on Sulphatases. 28. Preparation of Sulphates for the Assay of Glycosylsulphatases" — *The Biochemical Journal* 75: 478, 1960
8. Guiseley, K. B. and P. M. Ruoff, "Monosaccharide Sulphates. I. Glucose-6-Sulphate. Preparations, Characterisation of the Crystalline Potassium Salt and Kinetic Studies" — *The Journal of Organic Chemistry* 26: 1248, 1961.
9. Guiseley, K. B. and P. M. Ruoff. "Monosaccharide Sulphates. II. Preparation of Methyl α-D-Glucopyranose-2-Sulphate" — *The Journal of Organic Chemistry* 27: 1479, 1962.
10. Peat, S., J. R. Turvey, M. J. Clancy, and T. P. Williams. "Sulphates of Monosaccharides and Their Derivatives. Part I. Preparation." — *Journal of the Chemical Society* 4761, 1961.
11. Häglund, E., T. Johnson, und H. Urban. "Über den Einfluss von Sulfit- und Bisulfit-Lösungen auf Zucker-Arten bei höherer Temperature (III. Mitteil.)" — *Berichte der Deutschen Chemischen Gesellschaft* 63B: 1387, 1930.
12. Ingles, D. L. "Reaction of Aldoses with Bisulphite and Hydrosulphite. The Formation of Sugar Sulphates" — *Chemistry and Industry* 37: 1159, 1960.
13. Turvey, J. R. *Advances in Carbohydrate Chemistry* 20 — New York and London Academic Press, 1965, p. 183.
14. Whistler, R. L. *Methods in Carbohydrate Chemistry, Vol. II.* — New York: Academic Press, 1963, p. 229.
15. Rees, D. A. "Carbohydrate Sulphates" — *Annual Report of the Chemical Society* 62: 469—487, 1965.
16. Turvey, J. R. and T. P. Williams. "Sulphation of Monosaccharides and Derivatives. Part V. Products of Sulphation of Galactose and Glucose" — *Journal of the Chemical Society* 2242, 1963.
17. Grant, D. and A. Holt. "The Properties of Some Sulphate Derivatives of D-Glucose and D-Galactose" — *Journal of the Chemical Society*: 5026, 1960.
18. Bowker, D. M. and J. R. Turvey. "Thin-Layer Chromatography of Sugar Mercaptals and Sulphates" — *Journal of Chromatography* 22: 486, 1966.
19. Eliel, E.L., N. L. Allinger, S. J. Angyal, and G. A. Morrison. *Conformational Analysis* — New York, London, Sydney: Interscience Publishers, a division of John Wiley and Sons, Inc., 1965, p. 200—206, 278—380, and references cited therein.
20. Kilpatrick, J. E., K. S. Pitzer, and R. Spitzer. "The Thermodynamics and Molecular Structure of Cyclopentane" — *Journal of the American Chemical Society* 69: 2483, 1947.
21. Hockett, R., R. E. Miller, and A. Scattergood. "The Preparation and Proof of Structure of 1,2 : 5,6-Dicyclohexylidene-D-Glucofuranose" — *Journal of the American Chemical Society* 71: 3072, 1949.

GLASNIK HEMIJSKOG DRUŠTVA, Vol. 34, No. 2-3-4, 1969, pp. 251—259

GHDB-58

535.338.4:543.42

Original Scientific Paper

CONDITIONS FOR THE APPLICATION OF ARC-EXCITED SWAN'S BANDS IN QUANTITATIVE SPECTROCHEMICAL ANALYSIS

by

UBAVKA B. MIOČ

In using molecular bands for quantitative spectrochemical analysis several difficulties are encountered. Our interest was centered on the possibility of applying Swan's bands in quantitative analysis using arc and spark excitation. For this purpose we investigated the conditions under which C_2 radical forms and is excited, depending on the excitation source, electrical parameters, atmosphere and pressure which we followed via the C_2 (1.0) band of Swan's system, λ = 4737.1 Å.

Knowledge of the formation and excitation conditions for C_2 radical is of manifold interest. The spectrochemist is interested because C_2 bands appear with carbon electrodes or with carbon-containing materials[1, 2, 3]. The mechanism of C_2 radical formation is interesting for astrophysics, while the manufacturing industry is interested in monitoring it as a soot producing processes.

The mechanism of formation of C_2 radical, which emits Swan's bands, is yet fully understood. From the literature[4, 5, 6], it cannot be concluded that there is only one mechanism of formation and excitation of this radical. It is seen that the mechanism depends on excitation conditions: excitation method, material being excited, and atmoshpere or medium in which excitation takes place[7, 8, 9, 12].

Accordingly, whatever excitation method is selected, it calls for investigations of a host of parameters: electrical parameters, electrode type, choic of atmosphere and pressure.

EXPERIMENTAL

Since arc and spark are standard analytical sources of excitation, the conditions for excitation of Swan's bands with these sources were investigated.

With arc excitation, changes in the intensity of the C_2 (1.0) band head, y = 4737.1 Å as function of current strength were investigated. With spark excitation the changes as a function of induction and capacity were investigated.

The effect of the following atmospheres was studied: air, acetylene, butane, carbon dioxide, argon, and argon-carbon dioxide mixture — at atmospheric and reduced pressures down to 100 *mm* Hg, during which the arc retained its basic discharge characteristics.

All recordings were made on a PGS-2 Karl Zeiss spectrograph, in the 1st spectral order which gives a reciprocal dispersion of about 7 Å/*mm*.

Excitation source were the standard devices for direct and alternating arc and spark.

Ilford N-30 Ordinary plates were used for photography.

For the study of excitation conditions, carbon electrodes (Ringsdorff RW-O) and electrolytic copper electrodes were used.

A controlled atmosphere was obtained using Akimov's mounting[10], or a closed glass chamber made for the experiment[11]. The controlled atmosphere chamber was easily attachable to the part of apparatus for work under reduced pressure. Pressure in the apparatus was read on a closed mercury manometer.

Technical grade gases used for the controlled atmosphere were not purified.

RESULTS AND DISCUSSION

Effect of Electrical Parameters. — For both the DC and the AC arc, the current was changed between 3 and 13 A. Under these conditions the (C_2 (1.0) head band was recorded by microphotometry; the dependence of absorbance on current strength is shown in Figure 1. The shape of the curves of the C_2 (1.0) band head absorbance as function of current is approximately the same for both sources. Emission intensity rises faster at low currents (to 7 A).

These spectra are characterized by considerably lower intensity of emission of the background and rotational band structure with AC arc excitation than DC arc for the same current and other recording conditions.

Spark excitation of carbon electrodes also produced intensive C_2 bands. We studied the emission intensity of the C_2 (1.0) band as a function of the capacity and induction in the spark circuit. Recordings were made in air and argon atmospheres, at atmospheric pressure, using Akimov's mounting. The band head was recorded by microphotometry. Absorbance values for the different capacities and inductions are shown graphically in Fig. 2. Curves 1, 2, 3, and 4 in Figure 2 represent recordings in argon atmosphere, exposure time 6 min; curves 5 and 6 pertain to air atmosphere, exposure time 10 min. It is seen that the emission intensity of the C_2 band head in argon atmosphere considerably exceeds that in air.

As for the effect of capacity and induction, it was observed that change of capacity does not affect the spectral structure but does affect emission intensity, while induction change also changes the spectral appearance. In one series of runs at constant capacity the C_2 (1.0) band was most intensive at the highest induction value ($L = 5$ mH), decreasing with decreasing induction. At the bottom end of the induction range ($L = 0.02$ mH) the spectral structure changes altogether. Emission of molecular bands disappears entirely, and atmosphere lines show up. As induction decreases, the background emission rises sharply, particularly in air. The same was

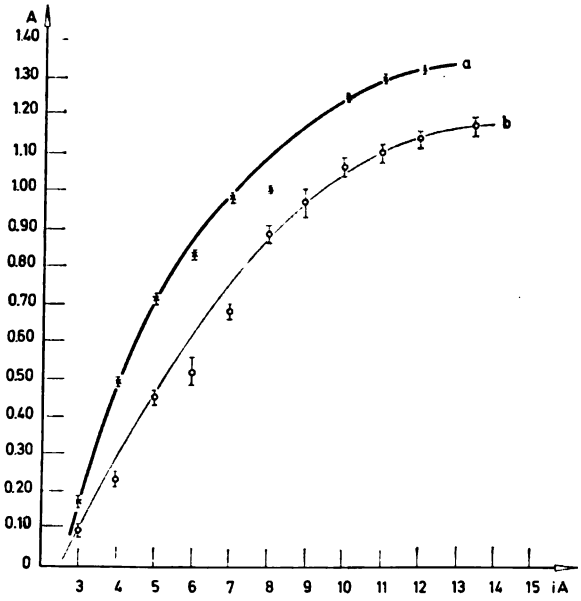

Figure 1

Absorbance of the C_2 (1.0) band head as a function of current for
(a) DC arc
(b) AC arc

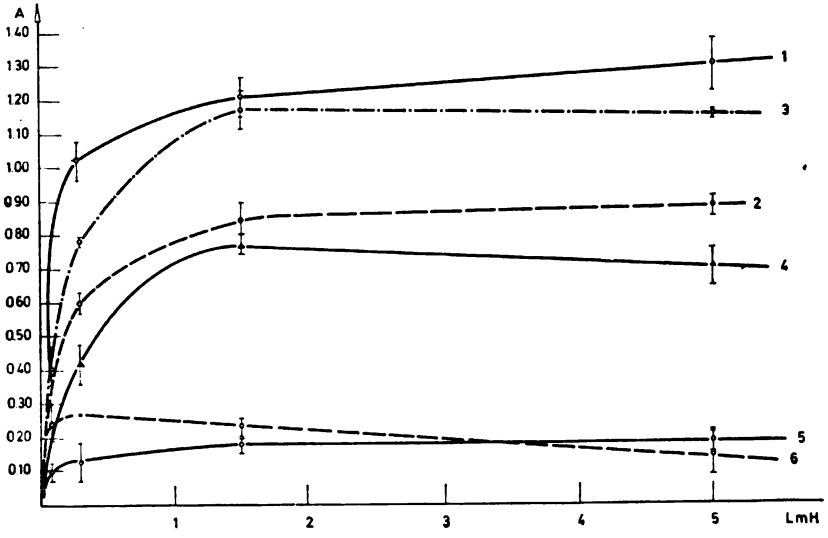

Figure 2

Absorbance of the C_2 (1.0) band head as a function of induction (L) for various capacities in argon atmosphere (1 — $C = 24$ *nF*; 2 — $C = 12$ *nF*; 3 — $C = 6$ *nF*; 4. — $C = 3$ *nF*) and air (5 — $C = 24$ *nF*, 6 — $C = 12$ *nF*)

noted by Kreshkov and Kuchkarev[12] for more restricted induction range (from $L = 0.01$ to $L = 0.45$ mH).

Having studied the effect of electric parameters on the emission intensity of C_2 bands with DC and AC arc and spark, it may be concluded that the AC arc is the most suitable excitation source for quantitative analysis using these molecular bands and a medium-dispersion apparatus. The band heads are sharp, and the background and rotational emission is suppressed, minimizing interference.

For these reasons, the AC arc was given special attention and the effects of atmosphere and pressure on the intensity of C_2 band emission were investigated. Recordings were made in confined or unconfined atmospheres of acetylene, butane, carbon dioxide, air, argon, and a mixture of argon and carbon dioxide.

In working with acetylene and butane at atmospheric and reduced pressures, soot was deposited on the electrodes in large amounts and quite out of control, which hindered quantitative work. Band intensities were not reproducible, and the intensity gain compared with other atmospheres was not significant. Deposition of large amounts of soot was not accompanied by a corresponding increase in the intensity of the C_2 band.

It is particularly notable that we obtained intensive C_2 bands by this excitation in carbon dioxide atmosphere using both carbon and copper electrodes. When other excitation methods were applied in carbon dioxide no emission of C_2 bands was registered[5, 6, 12].

The first recordings in carbon dioxide atmosphere were made at various gas fluxes with carbon electrodes in Akimov's mountaing. The C_2 bands proved to be more intense that in air, but increasing the flow rate did not affect the intensity of the C_2 (1.0) band head.

Preliminary investigations showed that argon at atmospheric pressure intensified the C_2 band emission in spark and AC arc between carbon electrodes. DC arc with carbon electrodes did not give the band, and the atomic emission of the atmosphere prevailed (Fig. 3).

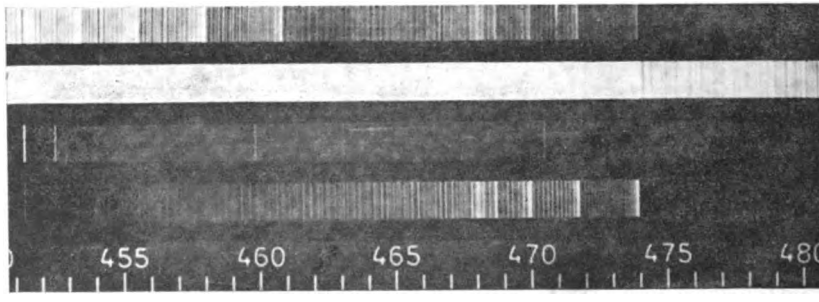

Figure 3

Spectra of carbon electrodes in air (1 — AC arc, 2 — DC arc) and argon atmosphere 3 — AC arc, 4 — DC arc)

In AC arc in argon atmosphere, the rotational structure of the bands is suppressed, the band heads are sharp and well defined, which facilitates quantitative work.

Reduced Pressure Tests — Recordings were made under reduced pressure in different atmospheres. We investigated:

— The effect of reduced pressure of air and argon on the C_2 band emission from carbon electrodes.

— The change in intensity of C_2 band emission with pressure of carbon dioxide atmosphere, using carbon and copper electrodes

— The effect of changing the partial pressure of carbon dioxide mixed with argon on the intensity of C_2 bands from carbon and copper electrodes.

Pressures in all cases lay between 100 and 600 *mm* Hg. The partial pressure of carbon dioxide in argon was varied from 100 to 600 *mm* Hg, while the total pressure in excitation chamber before excitation began was 650 *mm*Hg.

The results show that reducing the pressure of air and argon intensifies the C_2 band emission (Fig. 4). It may be seen that from 400 *mm*Hg down the absorbance increases markedly (by about 100%).

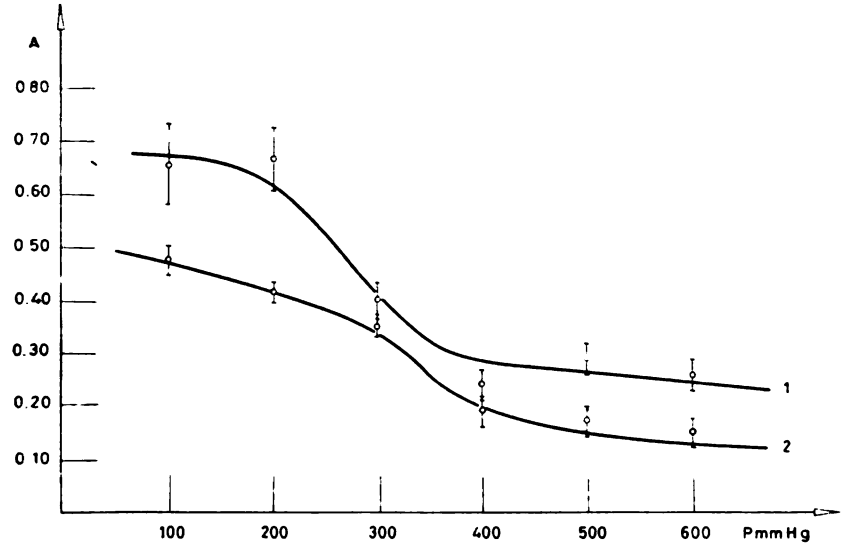

Figure 4

Absorbance of the C_2 (1.0) band head as a function of pressure in air (1) and argon (2)

Absorbance as a function of carbon dioxide pressure, when copper electrodes were used, is a maximum at 300 mmHg, while with carbon electrodes the C_2 emission is much stronger but a minimum appears at a pressure of some 400 mmHg (Fig. 5).

Curve (1) in Fig. 5 represents the function $A = f(p)$ obtained by exposures of 90 sec, while curve (2) was obtained for exposures of 8 sec.

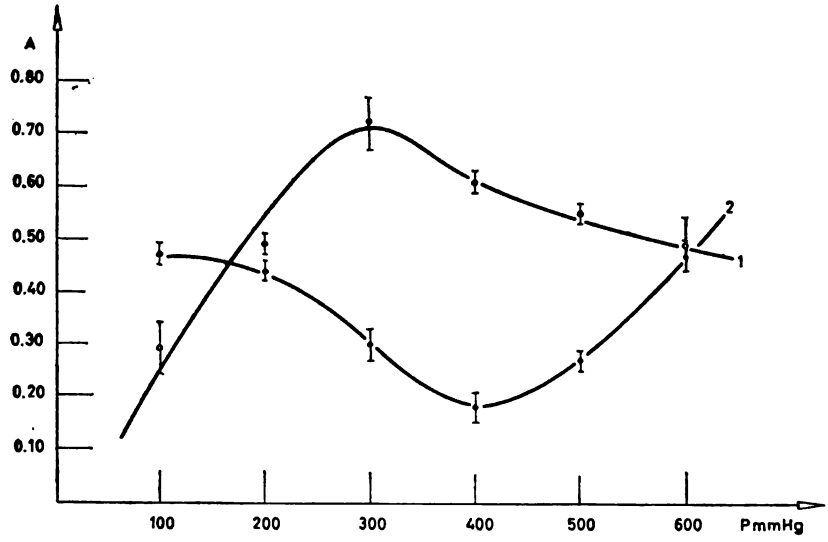

Figure 5

Absorbance of the C_2 (1.0) band head as a function of CO_2 pressure for copper (1) and carbon (2) electrodes

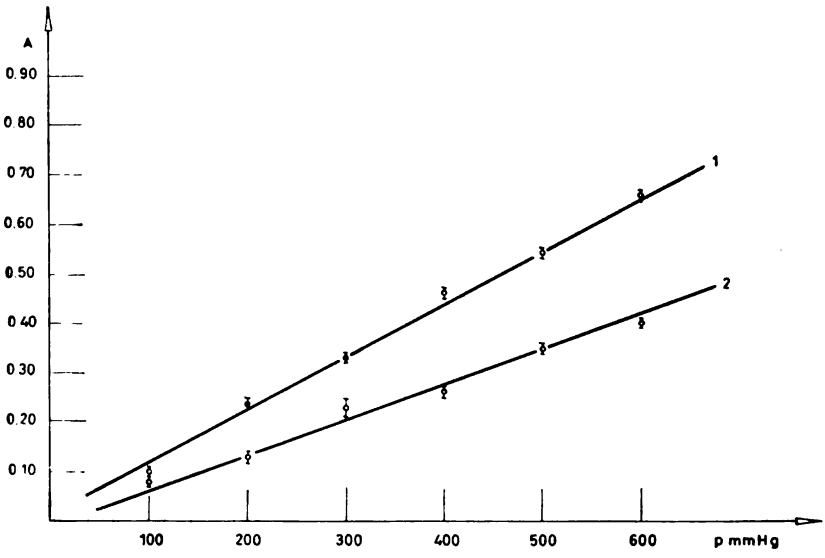

Figure 6

Absorbance of the C_2 (1.0) band head as a function of partial CO_2 pressure for copper (1) and carbon (2) electrodes

The absorbance of the C_2 (1.0) band for carbon and copper electrodes as a function of the partial pressure of carbon dioxide mixed with argon at a total pressure of 650 mmHg is linear (Fig. 6). Under these conditions, and 6 A AC excitation, a linear correlation was found between the intensity of the C_2 (1.0) band head, $\lambda = 4737.1$ Å, and the CO_2 partial pressure, i.e. CO_2 concentration in the sample.

This means that the band head could be used as an analytical band for quantitative determination using arc excitation.

CONCLUSION

The results show that of the excitation sources investigated AC arc is the most suitable for the quantitative determination of carbon via molecular emission. The C_2 (1.0) band head is intense, and interference is low because the background and rotational line radiation is suppressed.

In argon atmosphere the emission of electron-oscillation bands with C_2 bands is stronger and the rotational structure (of higher rotational levels) is suppressed.

The literature on the mechanism of C_2 radical formation[3] shows that this radical is formed already excited at a high rotational level. In an inert gas atmosphere these high levels are deexcitated in collision with the inert gas atoms, resulting in suppression of rotational lines in the band tail.

In air atmosphere the C_2 band emission becomes weak, which may be interpreted by competition from CN radical formation due to the stronger affinity of C for N than of C for C.

In carbon dioxide, acetylene and butane atmospheres, C_2 emissions is stronger but large amounts of soot are deposited which rendered quantitative work under our experimental conditions impossible. The intensity of the C_2 band did not increase commensurately with the amount of soot, which suggests that the two processes though simultaneous are independent.

Reduced pressure facilitates the formation of atomic carbon whose polymerization is the most probable source of C_2 radical. This is borne out by the fact that during excitation with carbon and copper electrodes in different atmospheres in the 3800—5500 Å region we identified only Swan's bands and the bands from the violet system of CN, while CO and CH bands were missing.

School of Sciences
Department of Physics and Chemistry
Belgrade University

Received 10 February, 1969

REFERENCES

1. Burgim, E. D., A. I. Luitii, V. S. Rossikhin, and I. L. Tsikora. "Ob osobennostiakh vozbudhdeniia Swan-ovykh polos C_2 v struiakh parov metalov i organicheskikh soedinenii" (Properties of the Excitation of Swan's C_2 Bands in Currents of Metallic Vapors and Organic Compounds) — *Optika i spektroskopiia* 20: 568, 1966.
2. Rossikhin, V. S. and I. L. Tsikora. "Mekhanizm obrazovaniia nekotorykh radikalov v visokochhastotnom razriade"(Mechanism of the Formation of Some Radicals in High-Frequency Discharge) — *Zhurnal fizicheskoi khimii* 30: 453, 1956.
3. Gaydon, A. G. and H. G. Wolfhard. "IV. Measurements of Light Yield for C_2 Bands" — *Proceedings of the Royal Society* A201: 561, 1950.
4. Marzuvanov, V. L. "Ob osobennostiakh dugovogo razriada v atmosfere nekotorykh gazov" (Properties of Arc Discharge in Atmosphere of Some Gases) — *IAN SSSR Seriia fizicheskaia* 23: 1059, 1959.
5. Mizushima, C., T. Morino, H. Hirao, K. Hirabajachi, K. Kakjehara, and T. Mizushima. "Chemical Reaction in Torch Discharge in Carbon Monoxide and Carbon Dioxide" — *Journal of the American Chemical Society* 72: 5176, 1950.
6. Ostroumenko, P. P, V. S. Rossikhin, and I. L. Tsikora. "Spektroskopicheskoe issledovanie mekhanizma obrazovaniia C_2 v razlichnogo tipa razriadakh v atmosfere uglekislogo gaza" (Spectroscopic Investigation of the Mechanism of C_2 Formation in Different Types of Discharge in Carbon Monoxide Atmosphere) — *Zhurnal prikladnoi spektroskopii* 2: 109, 1965.
7. Jevon, W. *Report on Band Spectra of Diatomic Molecules* — London: The Physical Society, 1932.
8. Rossikhin, V. S. and I. L. Tsikora. "Spektroskopicheskoe izuchenie visokochastotnykh razriadov v gazakh i plameni pri atmosfernom davlenii" (Spectroscopic Study of High-Frequency Discharge in Gases and Flames at Atmospheric Pressure) — *Zhurnal fizicheskoi khimii* 29: 1080, 1955.
9. Mochalov, K. N. "Spektr fakel'nogo razriada" (Spectrum of Torch Discharge) — *Doklady Akademii Nauk SSSR* 67: 241, 1949.
10. Akimov, A. I. "Podavlenie polos tsiana v spektre ugol'noi dugi" (Suppression of Cyanogen Bands in Carbon Arc Spectrum) — *Zhurnal eksperimentalnoi i teoricheskoi fiziki* 33: 434, 1956.
11. Mioč, U. Eksperimentalno istraživanje metode detekcije i određivanja ^{13}C korišćenjem lučne eksitacije C_2 traka (Experimental Investigation of the Detection and Determination of ^{13}C Using Arc Excitation of C_2 Bands) (Thesis) — Beograd, 1968.
12. Kreshkov, A. P. and E. A. Kuchkarev. "O novykh vozmozhnostiakh emissionogo molekularnogo analiza" (New Possibilities of Molecular Emission Analysis) — *Zhurnal prikladnoi spektroskopii* 8: 909, 1968.

GLASNIK HEMIJSKOG DRUŠTVA, Vol. 34, No. 2-3-4, 1969, pp. 261—266

GHDB-59

543.46:547.583.5

Original Scientific Paper

INTERFEROMETRIC PRECIPITATION TITRATIONS

by

VILIM J. VAJGAND and TODOR J. TODOROVSKI

Interferometric precipitation titrations were first described by Berl and Ranis[1] who determined chlorides, sulfates, oxalates and carbonates making use of the formation of hardly soluble compounds during titration. They isolated the precipitate by centrifugation during titration in order to observe the refractive index changes of the solution. They titrated 0.1 N solutions of test substances with standard solution also of 0.1 N.

Marti and Aliod[2] titrated highly dilute (10^{-3} to 10^{-6} N) solutions of iodides and cyanides with silver nitrate. They were able to measure the refractive index changes in the presence of precipitate as well, which considerably simplified the procedure.

More recently, quantitative analysis has been increasingly often using organic reagents which with the tested substance build hardly soluble compounds principally of the chelate type. The great sensitivity of some of these reactions enables the determination of very small amounts of substances in dilute solutions. Determination errors are often less than those when the same ingredients are determined with inorganic reagents.

Presented here are interferometric titrations of some metal ions and anions with organic or inorganic reagents during which hardly soluble complexes form as the reaction product.

EXPERIMENTAL

All readings were made on an ITR-1 interferometer of Soviet make. Depending on the concentration of test substance, titrations were performed in three ways. Solutions of very low concentration (below 10^{-2} N) of a few milliliters volume were titrated directly in the cell of the interferometer, without removal of precipitate. For the titration of 0.014—0.020 N solutions we used a closed vessel (Fig. 1) ovt of which some of the solution could be driven into the interferometer cell (or back to the vessel) by raising or lowering the air pressure. The pipe between the vessel and the cell contained a sintered glass filter to capture precipitate. This apparatus is capable of titrating any volume of the substance being determined. For titrations of highly concentrated solution we took 8-12 samples for each analysis, added different volumes of titrant and after 10 min standing 2 *ml* aliquots were centrifuged at 4000—5000 rpm for 5 min.

The interferometer cell was 10.05 or 20.00 *mm* long depending on the concentration of test substance. Measurements were made in a thermostated cell at 25.0°C. The difference in refractive index was read every 3—4 min after putting the solution into the cell. During this time the temperatures of the reference and test solutions are equalized and the interference fringes settled. The reference solution, water, and the test or titrated-out solution were placed into the left or right cell depending on the change expected in the refractive index.

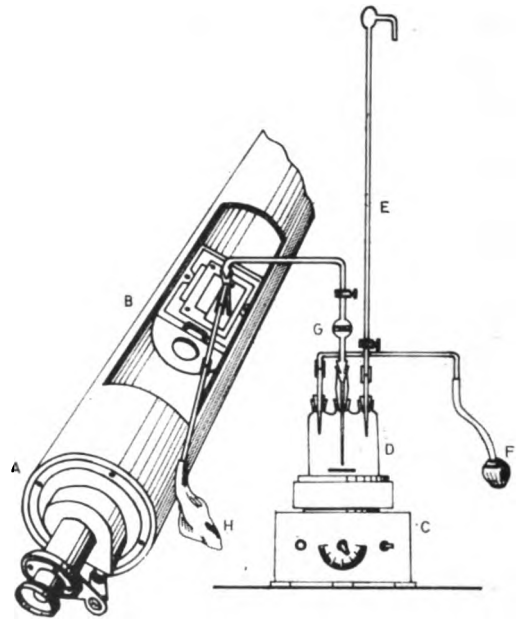

Figure 1

Diagram of the interferometer with the titration vessel:

A — interferometer, B — cell, C — magnetic stirrer, D — titration vessel, E — burette, F — rubber pump, G — sintered glass filter, H — rubber balloon for equalizing the pressure

Solutions for analysis were prepared from chemically pure substances (Merck); standardization was done mainly by gravimetric methods. Concentrations of the titrated substances ranged arround 10^{-2} N, measured out with a 2.000 *ml* microburette. Titrant concentration was usually 6—10 times higher. Analyses involved 0.8 to 5 *mg* of substance.

Standard anthranilic acid solution was prepared by putting 1 *g* chemically pure substance into 7 *ml* 1 N NaOH and diluting the solution to 100 *ml*[3]. Before diluting, acetic acid was added to the solution to make the *p*H 5.5 to 5.6.

The anthranilic acid was standardized with lead or zinc solutions of known concentrations at room temperature according to procedures described in the literature[4, 5].

Copper and nickel solutions were titrated at 70—80°C, because also the gravimetric determination of these metals with anthranilic acid[5] precipitation takes place at elevated temperature. Titrations were done in 8—12 equal aliquots. After addition of different volumes of titrant the aliquots were cooled, centrifuged and the change in refractive index measured.

Lead solution was titrated with a 0.005 M solution of picrolonic acid at room temperature, as is also suggested for the gravimetric determination of lead[6]. Lead was also determined with a 0.01 N solution of $Na_4P_2O_7$ with which it builds a hardly soluble compounds.

Cyanide was determined according to Liebig and Mohr with a 0.05 N $AgNO_3$ solution. A number of metals (Cv^{2+}, Zn^{2+}, Ni^{2+} and Cd^{2+}) in 0.030—0.035 N solutions were successfully titrated with 0.24 N KCN solution and empirical factors for calculating the metals were determined.

In all instances the titration end point was found as the intersection of two straight lines (Fig. 2). The refractive index difference (Δn) slowly decreases down to the equivalence point while once the precipitation is over a small titrant excess causes a jump.

The results of interferometric precipitation titrations of some cations and anions are presented in Table 1.

TABLE 1

Substance titrated	Titrant	No. of determin.	Taken (*mg*)	Found by interf. precip. titr.	Average deviation (%)
Pb^{2+}	Anthranilic acid	6	5.00	4.99 ± 0.01	$\pm 0.2\%$
Cu^{2+}	„	6	1.30	1.32 ± 0.01	$\pm 0.8\%$
Ni^{2+}	„	6	1.60	1.61 ± 0.01	± 0.6
Zn^{2+}	„	6	1.40	$1.40 \pm 0.00_3$	± 0.3
Pb^{2+}	Picrolonic acid	6	0.80	$0.80 \pm 0.00_1$	± 0.1
Pb^{2+}	$Na_4P_2O_7$	6	2.30	2.30 ± 0.01	± 0.4
$Na_4P_2O_7$	$Pb(NO_3)_2$	6	1.00	$0.99 \pm 0.00_3$	± 0.3
CN^-	$AgNO_3$	6	0.80	0.80 ± 0.01	± 1.2

During the titration of cyanide with silver nitrate the refractive index rises at first because of the formation of soluble $(Ag/CN/_2)^-$ ion, and falls off after the end point when $Ag/Ag(CN)_2/$ begins to precipitate (Fig. 3).

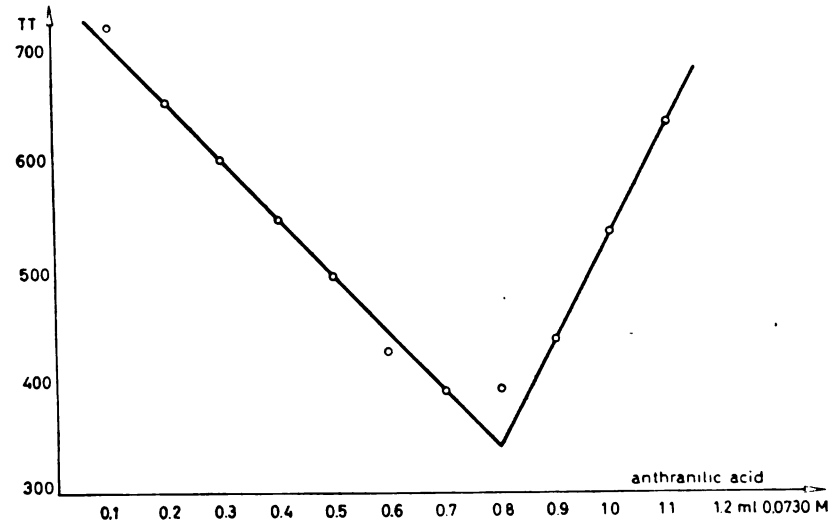

Figure 2

Interferometric titration of 5.00 *ml* 0.00584 *M* solution of $NiCl_2$ with 0.0730 *M* solution of anthranilic acid; echelon cell length 20 *mm*

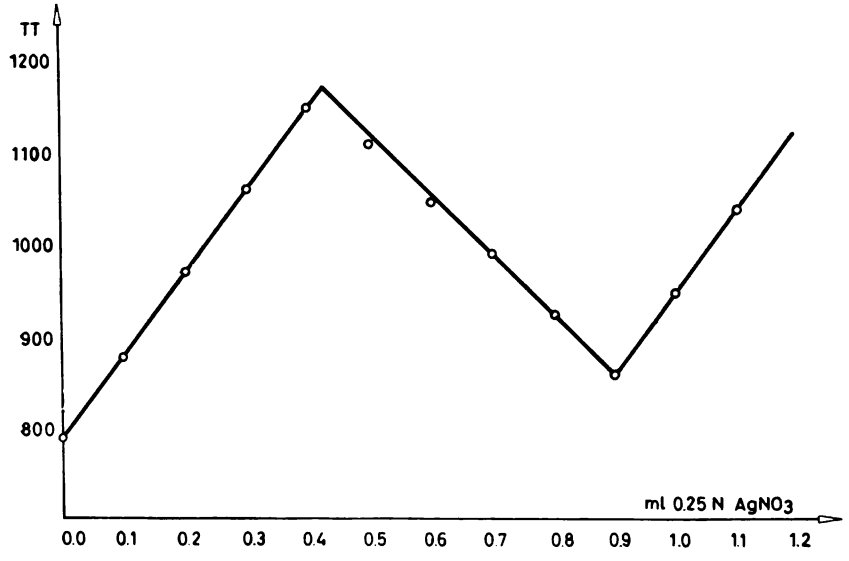

Figure 3

Interferometric titration of 4.50 *ml* 0.0481 *M* solution of KCN with 0.2500 *M* solution of $AgNO_3$; echelon cell length 20 *mm*

The end point can be determined by registering quantitative precipitation of $Ag/Ag(CN)_2/$, but it takes less time to determine cyanide from the reaction $2\ CN^- + Ag^+ = /Ag(CN)_2/^-$.

Gyanide solution can be used as a titrant for metals which form stable complexes. First an inosluble complex is formed and the refractive index falls until the end point, then to rise abruptly because of the dissolution of the precipitate. The two straight lines make an acute angle, so that the end point is established very accurately. The method is reproducible — only it is first necessary to establish the empirical factor for reduction to metal because the composition of the complex also depends on the conditions of precipitation. The determination of some cations by cyanide interferometric precipitation titration is shown in Table 2.

TABLE 2

Substance titrated	No. of determinations	Taken (*mg*)	Found by interf. titration (*mg*)	Average deviat. (%)	Empirical factor
Cu^{2+}	6	0.152	0.152±0.000	±0.0	Cu = 1.131
„	6	1.600	1.566±0.005	±0.3	„
„	6	6.650	6.631±0.057	±0.9	„
Zn^{2+}	6	0.350	0.351±0.002	±0.4	Zn = 1.059
„	6	1.600	1.566±0.005	±0.3	„
„	6	7.100	7.110±0.060	±0.8	„
Cd^{2+}	6	0.250	0.253±0.003	±1.2	Cd = 0.923
„	6	2.500	2.522±0.020	±0.8	„
„	6	25.000	25.230±0.150	±0.6	„
Ni^{2+}	6	0.550	0.552±0.006	±1.0	Ni = 1.064
„	6	1.040	1.040±0.006	±0.6	„
„	6	10.850	10.861±0.087	±0.8	„

The accuracy and reproducibility of the results obtained in all the interferometric precipitation titrations are satisfactory, deviations being with the permissible range. When using organic precipitation reagents the titration of concentrated solutions should be avoided because of large amounts of precipitate being formed.

School of Sciences
Department of Chemistry
Belgrade University

and

School of Technology and Metallurgy
Skopje University

Received 13 September, 1969

REFERENCES

1. Berl, E. and L. Ranis. "Die Anwendung der Interferometrie in Wissenschaft und Technik" — *Fortschritte der Chemie* (Darmstadt) 19: 478—483, 1928.
2. Marti, B. F. and C. M. Aliod. "Sobre les Volumetrias Interferometricas y sus applicaciones" — *I. Inform. de Quimica Analytica* (Madrid) 11: 39—49, 1956.
3. Merck, E. *Organische Reagenzien MERCK für die anorganische Analyse, 2. Auflage* — Weinheim, Bergstrasse: Verlag Chemie G. M. H., 1961.
4. Funk, H. and F. Rämer. "Über die quantitative Bestimmung einiger Metalle mittels Anthranilsäure" — *Zeitschrift für analytische Chemie* (München) 110: 85—88, 1935.
5. Funk, H. and M. Ditt. "Über die quantitative Bestimmung einiger Metalle mittels Anthranilsäure" — *Zeitschrift für analytische Chemie* (München) 91: 332—340, 1933.
6. Hecht, F., W. Reich-Rohrwig, and H. Brantner "Die quantitative Bestimmung des Bleis mit Pikrolonsäure" — *Zeitschrift für analytische Chemie* (München) 95: 152—163, 1933.

GLASNIK HEMIJSKOG DRUŠTVA, Vol. 34, No. 2-3-4, 1969, pp. 267—280

GHDB-60

543.257.1:547.233:547.584

Original Scientific Paper

THE USE OF PHTHALIC ANHYDRIDE IN THE DETERMINATION OF VARIOUS MIXTURES OF PRIMARY, SECONDARY AND TERTIARY AMINES IN ACETIC ACID

by

VILIM VAJGAND and TIBOR PASTOR

The determination of mixtures of primary, secondary and tertiary amines is complicated. A number of papers deal with the properties, behavior and possible use of different reagents and solvents for the separation and determination of individual components of amine mixtures using titration methods, where in the tertiary amines are almost invariably determined in perchloric or hydrochloric acid after acetylation of primary and secondary amines with acetic anhydride. However the determination of mixed primary and secondary amines is much more complex. Usually the sum of total bases in acetic acid or some other solvent is determined in one sample, while in another the primary amine is blocked by adding sallicyl aldehyde[1, 2] which combines with primary amines to form Schiff's base, while the secondary amine, or the sum of the secondary and tertiary amines, is determined in some strong mineral acid.

It has long been the practice to determine acid anhydrides via primary and secondary amines[3-6], but only recently has phthalic anhydride also been used[18] for primary amine determination[7] or for blocking the primary amines in determining mixtures of bases. In this it is of particular significance that amines are titrated in acetic acid (after treating the mixture with phthalic anhydride) because this solvent is practically always used in amine determination. According to this method, suggested by Gal'pern and Bezinger[8] in 1958, under specific conditions primary amines alone react with phthalic anhydride to form phthalimide which does not show basic properties in acetic acid. Emelin and Tsarfin[9] later used the same method to determine primary and secondary amino radicals in polyamines as well. Strepikheev *et al.*[10] and then Hmel'nitskaia and Gribova[11] objected to this method[8] asserting that secondary amines also bind to same extent under the experimental conditions described. In their reply to this remark, Gal'pern and Bezinger[12] stated that good results can only be obtained with the original method[8] in case of appropriate molar ratios between primary and secondary amines. They added that in the meantime they had modified the method so that the accuracy of determination no longer depended on the this factor[13]. In applying Gal'pern and Bezinger's modified method[13], Baibaeva *et al.*[14] found that during the treatment of polyethylene-polyamines with phthalic anhydride in the presence of small

amounts of perchloric acid at room temperature for 1 h only primary amino groups reacted.

There is obviously disagreement about the possible use of phthalic anhydrides in acetic acid for the determination of mixed primary and secondary amines. In extending our research to tertiary amines[15], trying to include their determination in mixtures with primary and secondary amines in glacial acetic acid, we haue encountered the problem of finding conditions under which primary amines will bind with phthalic anhydride. Likewise it had to be found whether the binary compounds of tertiary and primary amines could be titrated under these conditions, and under what conditions was quantitative determination of the three kinds of amine in a mixture possible.

EXPERIMENTAL

All *p.a.* acetic acid available (Kemika, C. Erba, Chemaphol, Feinchemies K-H Kallies KG) contained acetic anhydride, which was removed by heating the acid on an oil bath for 8 h in the presence of 0.3—0.5% sulfuric acid[16], column distilling and taking the fraction distilling over at 118°C. Purity of the fraction was verified by titrating aniline in it with perchloric acid[17].

Amines were purified by distillation column after drying over potassium hydroxide. The purity was checked by refractive index measurements.

0.1 N solution of perchloric acid was prepared by dissolving about 8 *ml* of 70% perchloric acid (Kemika) in pure acetic acid. Water from perchloric acid was bound by adding calculated amounts of acetic anhydride. The solutions were left to stand 24 h before use. Normality of the perchloric acid solution was determined with a standard solution of sodium acetate in acetic acid.

All measurements were by potentiometry on a Radiometer model 22p *p*H-meter, with a Radiometer model G 200 BT glass electrode and a mercurous acetate reference electrode.

For titration of mixtures, first 0.1, 0.15 or 0.3 N solutions of the individual bases were made by weighing out quantities to 0.1 *mg* and dissolving them in acetic acid. The concentration of these solutions was checked by potentiometric titration. Base mixtures for analysis were prepared from these solutions by taking 0.3 meq of each base, which made the total amount of amines approximately 0.6 meq in a binary mixture or 0.9 meq in a ternary mixture.

DETERMINATION OF PRIMARY PLUS TERTIARY AMINE MIXTURE

Technique. — To determine both components two determinations were made:

(1) Determination of the total amount of bases: 0.3 meq of each amine was measured out into a 50 *ml* beaker to which pure acetic acid was added to a total volume 15—20 *ml*. This solution was titrated with 0.1 N solution of perchloric acid in acetic acid in the presence of glass and mercuroacetate electrodes.

(2) Determination of tertiary amine: after measuring out 0.3 meq of each amine solution in a 25 *ml* flask with a ground glass stopper, 1300 *mg*

phthalic anhydride was added and the volume was made up to 7 *ml* with pure acetic acid. Then the flask was placed on an upright condenser and the solution refluxed on a boiling water bath for 40 min for aliphatic amines or for 10 min for N,N-diethylaniline. After this the solution was cooled off by immersing the flask cold water. The condenser walls were washed with acetic acid. Having quantitatively transferred the solution to a 50 *ml* beaker, we titrated it with a perchloric acid solution.

The amounts of tertiary and primary amines found were calculated thus.

$$\text{Tertiary amine } \% = \frac{c \cdot N \cdot M_1 \cdot 100}{1000 \cdot a_1}$$

$$\text{Primary amine } \% = \frac{(b-c) \cdot N \cdot M_2 \cdot 100}{1000 \cdot a_2},$$

where N = normality of the perchloric acid solution

M_1, M_2 = molecular weights of the bases
a_1, a_2 = amounts of bases taken
b = *ml* of perchloric acid used for the titration of the total amines
c = *ml* of perchloric acid used for the titration of tertiary amine

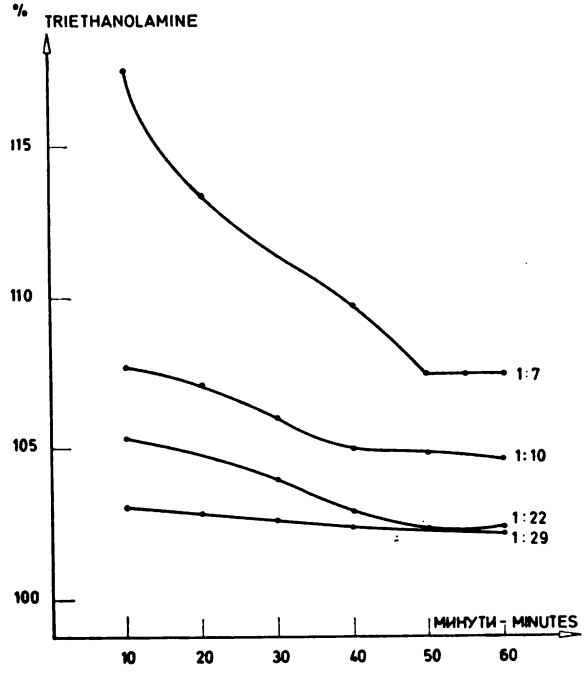

Figure 1

Samples of 0.3 meq of ethanolamine and triethanolamine each in 10.20*ml* of 98% acetic acid in the presence of 0.20 *ml* of 0.1 N perchloric acid were taken for each titration, Molar ratios of ethanolamine to phthalic anhydride were 1:7, 1:16, 1:22 and 1:29.

TABLE 1

Determination of Mixtures of Benzylamine and Triethanolamine

No.	Triethanolamine			Benzylamine		
	Taken *mg*	Found *mg*	Found %	Taken *mg*	Found *mg*	Found %
1.	44.73	44.73	100.00	35.52	35.13	98.90
2.	44.73	44.78	100.11	35.52	35.10	98.82
3.	44.73	44.83	100.22	35.52	35.06	98.70
4.	44.73	44.86	100.29	35.52	35.04	98.65
5.	44.73	44.72	99.98	35.52	35.14	98.93
6.	44.73	44.56	99.62	23.68	23.49	99.20
7.	44.73	44.51	99.51	11.84	11.76	99.32
8.	44.73	44.51	99.51	5.92	5.88	99.34

TABLE 2

Determination of Mixtures of Primary and Tertiary Amines

No.	Prim. amine	Taken *mg*	Found *mg*	Tert. amine	Taken *mg*	Found *mg*	No. of titrns.
1.	Ethanolamine	17.76	17.56±0.06	Triethylamine	31.30	31.41±0,10	5
2.	Benzylamine	35.52	35.24±0.04	Triethylamine	31.30	31.39±0.04	5
3.	Propanolamine	25.09	24.82±0.02	Triethylamine	31.30	31.35±0.02	5
4.	Aniline	28.42	28.19±0.01	Triethylamine	31.30	31.30±0.01	5
5.	n-Propylamine	17.76	13.25±0.04	Triethylamine	31.54	32.36±0.06	5
6.	Aniline	28.42	28.31±0.02	N,N-Diethylaniline	58.74	58.54±0.02	5

To solve the problem of determining ternary basic mixtures, we held it important to find out the conditions for the determination of primary and tertiary amine mixtures in acetic acid by binding the primary amines with phthalic anhydride. To this end we made a systematic study of the influence of the following factors on accuracy: the amounts of phthalic anhydride, water and perchloric acid in the sample solution, the volume of solution and the time of heating. We found that increasing the amount of phthalic anhydride in the solution increased the amount of primary amine reacting, the percentage of the tertiary amine found thus approaching the theoretical value (Fig. 1). The same graph shows incomplete binding of primary aliphatic amines with phthalic anhydride in 98% acetic acid even at a ratio of 1 : 29. Raising the amount of water in the solution also raises the amount of tertiary amine found. This indicates that in the presence of water the product of the reaction between primary amine and phthalic anhydride hydrolyzes. The effect of the perchloric acid present in the solution during heating is similar to that of water but it is less pronounced. The results are also affected by the magnitude of the solution volume during heating of the sample.

On the other hand, with 100% acetic acid and solution volume reduced to 7 *ml*, we obtained good results. Errors of determining components in amine mixtures stated in Tables 1 and 2 do not exceed $\pm 2\%$ relative to the results of potentiometric titration. However, when a mixture of triethylamine and *i*-propylamine was determined under the same experimental

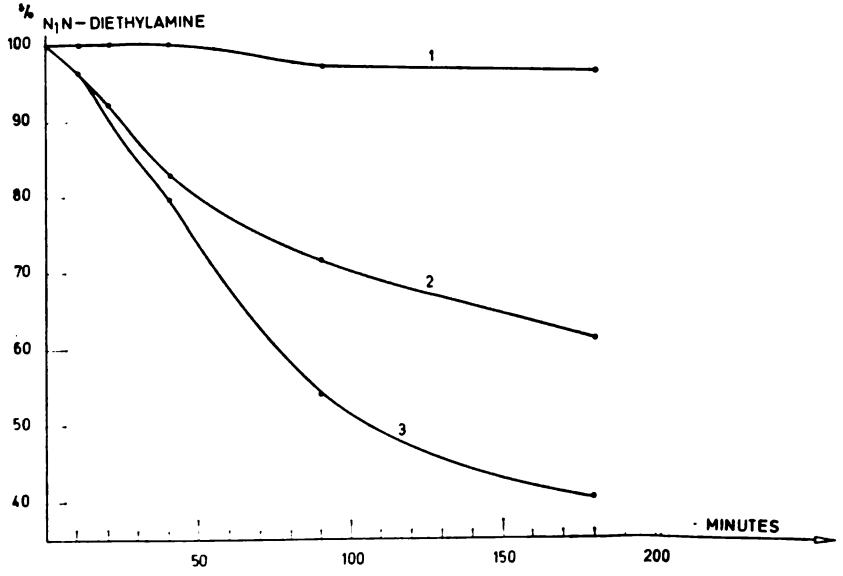

Figure 2

Samples of 44.6 *mg* of N, N-diethylaniline in 7.0 *ml* acetic acid were taken. Titration curves: (1) determination in pure acetic acid, (2) determination in the presence of 1300 *mg* of phthalic anhydride, (3) determination in the presence of 1.0 *ml* of acetic acid.

conditions, about 20% *i*-propylamine did not react. This behavior of *i*-propylamine can be explained by a steric effect.

In the determination of binary mixtures containing a tertiary aromatic amine (N,N-diethylaniline), involving lenghty treatment of the samples with phthalic anhydride on a boiling water bath, we found that the amount of N,N,-diethylaniline was a few percent down on the amount taken. For this reason we examined how the amount of N,N-diethylaniline found depended on the time of heating the solution in pure acetic acid, in the presence of acetic anhydride and phthalic anhydride. The results obtained are presented graphically in Fig. 2. The behavior of N,N,-diethylaniline is explainable by spontaneous autoxidative dealkylation, a process which is catalyzed by both acetic acid and its anhydride[18]. The secondary amine thus obtained inhibits the reaction strongly, but in the presence of acetic anhydride[18] it changes to inactive N-alkylacetanilide. From the decomposition of N,N-dimethylaniline Horner and Knapp[18] also obtained p,p-dimethylamino-diphenylmethane, which agrees with Walter's results[19]. They established that phthalic anhydride does not have a catalytic effect on the autoxidation of aromatic tertiary amines; this does not conform with our findings. In our case, we believe, the autoxidation dealkylation of N,N-diethylaniline takes place first, and then the phthalic anhydride reacts with N-ethylaniline in acetic acid which annuls the inhibitory effect of the secondary amine on the autoxidation of N,N,-diethylaniline.

DETERMINATION OF MIXTURES OF PRIMARY, SECONDARY AND TERTIARY AMINES

Technique. — For the determination of the three components, we determined the following:

(1) In one sample we titrated the total amount of amines in acetic acid.

(2) In a second sample we determined the tertiary amine after acetylation of primary and secondary amines with acetic anhydride as follows:

(a) A mixture of *n*-propylamine, diethylamine and triethylamine, after addition of 6 *ml* acetic anhydride, was kept 45 min at 100°C.

(b) A mixture of ethanolamine, diethanolamine and triethanolamine was worked up for 20 min at 100°C after addition of 3 *ml* acetic anhydride.

(c) A mixture of aniline, N-methylaniline and N,N-dimethylaniline to which 5 *ml* acetic anhydride was added was left 30 min at room temperature before titration.

(3) In a third sample we determined the sum of the secondary and tertiary amine as described below.

Amine solution was measured out into a 25 *ml* flask to which the following was added:

(a) For one mixture — 0.2 *ml* 0.1 N perchloric acid solution, 0.14 *ml* water, 700 *mg* phthalic anhydride, made up to 10.40 *ml* with acetic acid.

(b) For another mixture — 0.2 *ml* 0.1 N perchloric acid, 0.05 *ml* water, 200 *mg* phthalic anhydride, made up to 4.70 *ml* with acetic acid.

Then the procedure for the determination of tertiary amine with phthalic anhydride in a binary mixture was applied.

(c) A procedure for the determination of the sum of tertiary and secondary amines in a third mixture is not given because N,N,-diethylaniline decomposes in the presence of phthalic anhydride in acetic acid.

The amounts of primary, secondary and tertiary amines were computed as follows:

$$\text{Tertiary amine } \% = \frac{c \cdot N \cdot M_1 \cdot 100}{1000 \cdot a_1}$$

$$\text{Secondary amine } \% = \frac{(b-c) \cdot N \cdot M_2 \cdot 100}{1000 \cdot a_2}$$

$$\text{Primary amine } \% = \frac{(d-b) \cdot N \cdot M_3 \cdot 100}{1000 \cdot a_3},$$

where

c = *ml* of perchloric acid used for the titration of the tertiary amine

b = *ml* of perchloric acid used for the titration of tertiary and secondary amines

d = *ml* of perchloric acid used for the titration of the total amines

The other symbols are the same as in the equations for a binary mixture.

The first results immediately indicated the difficulties arising from the use of phthalic anhydrides to separate primary from secondary amines. Figure 3 shows that even under the conditions subsequently given by Gal'-

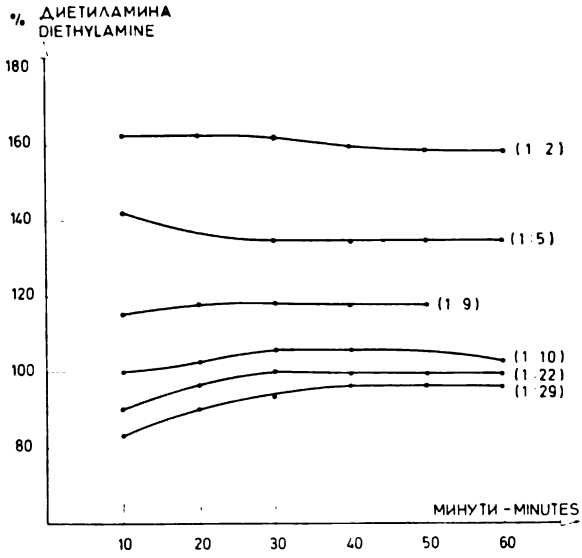

Figure 3

Samples of 0.3 meq of *n*-propylamine, diethylamine and triethylamine each in 10.20 *ml* of 98% acetic acid in the presence of 0.20 *ml* of 0.1 N perchloric acid were taken. Molar ratios of *n*-propylamine to phthalic anhydride were 1:2, 1:5, 1:9, 1:22 and 1:29.

pern and Bezinger, the result for diethylamine was too low in the presence of an increased amount of phthalic anhydride, which indicates that the secondary amine as well as the primary amine reacts with phthalic anhydride. Figure 3 also shows that protracted heating of samples in the presence of small amounts of phthalic anhydride decreased the quantity of diethylamine found but had the converse effect in the presence of a large amount. It must be pointed out, however, that heating longer than 30 min did not substantially affect the results obtained for diethylamine. In investigating the effect of molar ratios and amounts of *n*-propylamine and diethylamine on the results obtained it was found (Fig. 4) that decreasing the amount of *n*-propylamine in the solution also decreased the quantity of diethylamine, and vice versa. The hydrolysis of reaction products depends on the amount of water and perchloric acid present in the solution during the heating of samples, perchloric acid being in this respect much less effective than water (Fig. 5).

Despite the fact that the analysis results are affected by many factors, experimental conditions can be found for certain molar ratios between the bases and under which good and reproducible results are obtainable, as may be seen from Table 3. However, when a binary mixture of diethylamine and triethylamine was determined under the same experimental conditions 25% less diethylamine than taken was found, while an analysis of a mixture

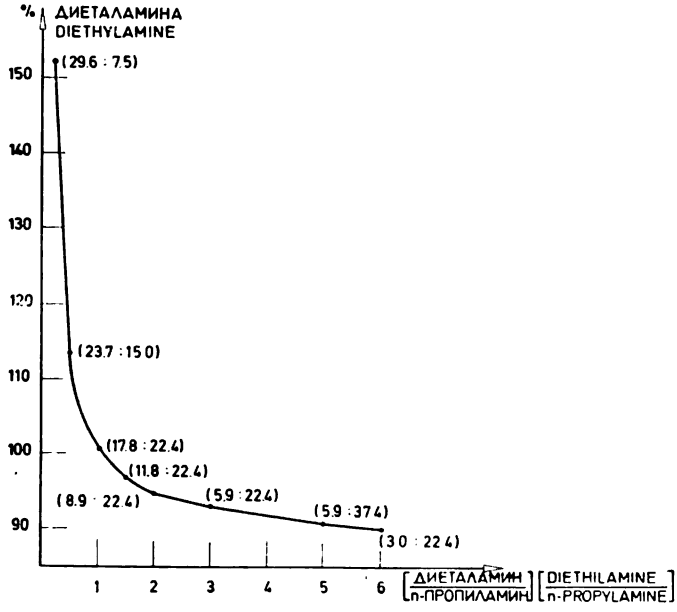

Figure 4

Samples of *n*-propylamine and diethylamine in amounts given at the appropriate points in the graph and 31.6 *mg* of triethylamine in 10.20 *ml* of 98% acetic acid were taken. To each sample 0.20 *ml* 0.1 N perchloric acid and 1000 *mg* of phthalic anhydride were added, and the samples were refluxed 40 min on a water bath.

TABLE 3

Determination of Mixtures of n-Propylamine, Diethylamine and Triethylamine

No.	Triethylamine			Diethylamine			n-Propylamine		
	Taken *mg*	Found *mg*	Found %	Taken *mg*	Found *mg*	Found %	Taken *mg*	Found %	Found %
1.	32.81	32.71	99.7	18.06	18.08	100.1	20.43	20.21	98.9
2.	32.81	32.75	99.8	22.57	22.34	99.0	20.43	20.34	99.6
3.	32.81	32.68	99.6	22.57	22.14	98.1	20.43	20.51	100.4
4.	32.81	32.59	99.3	22.57	22.15	98.1	20.43	20.56	100.6
5.	32.81	32.56	99.2	22.57	22.12	98.0	20.43	20.61	100.9
6.	32.81	32.70	99.7	22.57	22.16	98.2	20.43	20.50	100.3

of *n*-propylamine and triethylamine under the same conditions showed that 16% of the n-propylamine did not react.

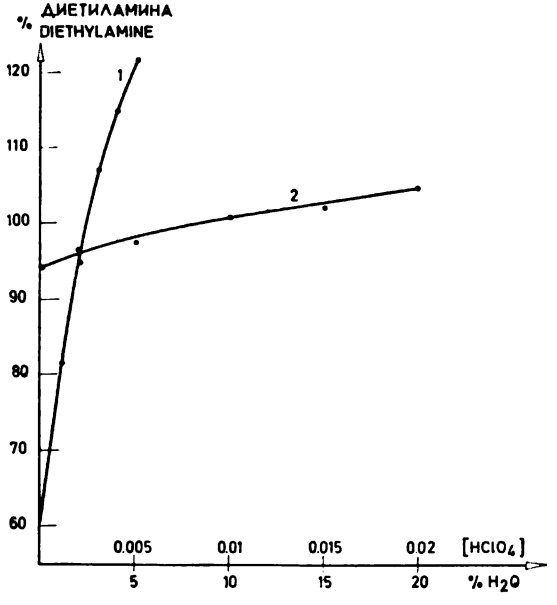

Figure 5

Samples of 0.3 meq of *n*-propylamine, diethylamine and triethylamine each in 10.20 *ml* of acetic acid were taken. The molar ratio of *n*-propylamine to phthalic anhydride in solution was heated for 40 min on a water bath.

Titration curves: (1) effect of different amounts of water on the quantity of diethylamine found in the presence of 0.2 *ml* of 0.1 N perchloric acid, (2) effect of adding different amounts of perchloric acid to the solution in 98% acetic acid.

Similar results were obtained in the determination of ethanolamine mixtures. With this system, taking 0.3 meq of each mixture component (under conditions as specified for this system in the technique explained above), determination errors for individual components did not exceed $\pm 1.5\%$ relative to the mean values obtained by potentiometric titration of the pure bases. However in the titration of a binary mixture, taking the same amounts of amines and under the same conditions, 32% of diethanolamine reacted with phthalic anhydride, while in a mixture of ethanolamine with triethanolamine 15% ethanolamine did not react. It is also noteworthy that when the amount of ethanolamine in solution was varied, the quantity of diethanolamine being kept constant, always the same value for the latter was obtained. This was true provided that the amount of phthalic anhydride in the solution and the solution volume were altered in the same way, i.e. that no changes took place in the molar ratio between ethanolamine and phthalic anhydride, nor in the solution concentration of ethanolamine.

When potentiometrically titrating an atomatic amine mixture (aniline + + N-methylaniline + N,N-diethylaniline) we noted that with samples previously treated with phthalic anhydride the EMF was stable only as long as N,N-diethylaniline was titrated. Afterwards every addition of titrant caused a potential jump but then the EMF gradually descended to its original value. Due to this behavior of the system the sum of N-methylaniline and N,N-diethylaniline could not be determined.

In all determinations the phthalic anhydride combined with primary amines to form phthalamidic acid which at higher temperatures in acetic acid (a hygroscopic substance) changes to phthalimide. In the case of oxyamine compounds (amino alcohols), the hydroxyl radical also reacts with phthalic anhydride yielding the following compound[20]:

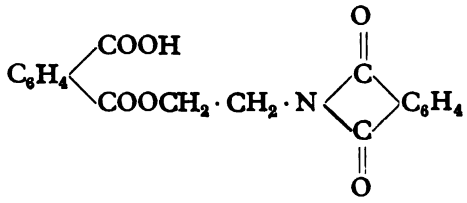

(20)

Secondary amines also react with phthalic anhydride (although at a slower rate) yielding phthalamidic acid.

CONCLUSION

It is inferred from the results that phthalic anhydride can be used for potentiometric determinations of mixtures of aliphatic primary amines or aromatic primary amines with aliphatic tertiary amines in glacial acetic acid. In these determinations the steric effect is considerably more pronounced than in determinations in which acetic anhydride is used to bind primary amines. For analyses of mixtures containing tertiary aromatic amines, phthalic anhydride cannot be used because autoxidative dealkylation of N,N-dialkylaniline occurs when samples are treated with the reagent in acetic acid. For quantitative analyses of mixtures of aliphatic or aromatic primary amines with aliphatic secondary amines, phthalic anhydride can only be used if the approximate ratio of components in the solution is known beforehand. Mixtures of N,N-diethylaniline, N-methylaniline and aniline treated with phthalic anhydride do not show a potential jump at the secondary amine titration end point.

School of Sciences
Department of Chemistry
Belgrade University

Received 10 September, 1968

REFERENCES

1. Wagner, C. D., R. H. Brown, and E. D. Peters. "The Analysis of Aliphatic Amine Mixtures: Determination of Secondary Plus Tertiary Amines by the Azomethine--Acidimetric Method" — *Journal of the American Chemical Society* (Washington) 69 (11): 2611—2614, 1947.
2. Siggia, S., J. G. Hanna, and I. R. Kervenski, "Quantitative Analysis of Mixtures of Primary, Secondary and Tertiary Aromatic Amines" — *Analytical Chemistry* (Washington) 22 (10): 1295—1297, 1950.
3. Johnson, J. B. and G. L. Funk. "Determination of Carboxylic Acid Anhydrides by Reaction with Morpholine" — *Analytical Chemistry* (Washington) 27 (9): 1464—1465, 1955.
4. Siggia, S. and J. G. Hanna "Determination of Carboxylic Acid Anhydrides in the Presence of Their Acids" — *Analytical Chemistry* (Washington) 23 (11): 1717—1718, 1951.
5. Zavarov, G. V. * (Determination of Acetic Anhydride with the Aid of Aniline) — *Zavodskaia Laboratoriia* (Moskva) 21: 791—795, 1955; *Chemical Abstracts* (Columbus, Ohio) 49 (22): 15633, 1955.
6. Kappeier, C. P. A. and W. R. van Goor. "The Anilic Number, an Analytical Index for Testing Dibasic Acid Anhydrides" — *Analytica Chimica Acta* (New York — Amsterdam) 2 (2): 146—149, 1948.
7. Elving, Ph. J. and B. Warshowsky. "Determination of the Alcoholic Hydroxyl Group in Organic Compounds, Phalic Anhydride Method" — *Analytical Chemistry* (Washington) 19 (12): 1006—1010, 1947.
8. Gal'pern, G. D. and N. N. Bezinger. "Opredelenie pervichnykh, vtorichnykh i tretichnykh aminogrupi pri sovmesstnom ikh prisustvii" (Determination of Primary, Secondary and Tertiary Amino Groups in Their Own Mixtures) — *Zhurnal analiticheskoĭ khimii* (Moskva) 13 (5): 603—607, 1958.
9. Emelin, E. A. and Ia. A. Tsarfin. "Opredelenie pervichnykh i vtorichnykh aminogrupi v mnogoiadernykh poliaminakh" (Determination of Primary and Secondary Amino Groups in Multinuclear Polyamines) — *Zhurnal analiticheskoĭ khimii* (Moskva) 17 (6): 759—762, 1962.
10. Strepikheev, Iu. A., A. A. Zalikin, and A. L. Chimishkian. "Opredelenie pervichnykh, vtorichnykh i tretichnykh aminogrupi v mnogoiadernykh poliaminakh" (Determination of Primary, Secondary and Tertiary Amino Groups in Multinuclear Polyamines) — *Zhurnal analiticheskoĭ khimii* (Moskva) 18 (10): 1262—1265, 1963.
11. Khmel'nitskaia, E. Iu. and E. A. Gribova. "Pis'ma v redaktsiiu. Po povodu stat'i G. D. Gal'perna i N. N. Bezinger: Opredelenie pervichnykh, vtorichnykh i tretichnykh aminogrupi pri sovmestnom ikh prisustvii" (Letters to the Editor: On the Article by G. D. Gal'pern and N. N. Bezinger 'Determination of Primary, Secondary and Tertiary Amino Groups in Mixtures') — *Zhurnal analiticheskoĭ khimii* (Moskva) 19 (11): 1417, 1964.
12. Gal'pern, G. D. and N. N. Bezinger. "Otvet na zamechaniia E. Iu. Khmel'nitskoi and E. A. Gribova po povodu stat'i G. D. Gal'perna i N. N. Bezinger" (Reply to Remarks by E. Iu. Khmel'nitskaia and E. A. Gribova to Concerning an Article by G. D. Gal'pern and N. N. Bezinger) — *Zhurnal analiticheskoĭ khimii* (Moskva) 19 (11): 1418, 1964.

13. Kliger, G. A., A. N. Bashkirov, N. N. Bezinger, and Iu. B. Kagan.* (Analysis of the Reaction of Products of Aliphatic Alcohols with Ammonia in the Presence of Hydrogen) — *Neftekhimiia* 1: 397—402, 1961; *Chemical Abstracts* (Columbus, Ohio) 57 (2): 1555, 1962.

14. Baibaeva, S. T., L. P. Krylova, G. I. Shemiakina, and O. I. Podosinovikova. † (Determination of Primary, Secondary and Tertiary Amino Groups in Polyethylenepolyamines) — *Lakokrasochnye materialy i ikh primenenie* 3 (1): 52—54, 1966; *Chemical Abstracts* (Columbus, Ohio) 65 (7): 9734, 1966.

15. Vajgand, V. and T. Pastor. "Derivative Polarographic Titration of Tertiary Amines and Salts of Organic Acids in Acetic Acid in the Presence of Antimony and Quinhydrone Electrodes", "Determination of Tertiary Amines and Salts of Organic Acids, in Glacial Acetic Acid by Dead-Stop Method" — *Journal of Electroanalytical Chemistry* (Amsterdam) 8 (1): 40—48, 49—54, 1964.

16. Novikova, E. N. and L. N. Petrova. "O kolichestvennom opredelenii uksusnogo angidrida" (Quantitative Analysis of Acetic Anhydride) — *Zhurnal analiticheskoĭ khimii* (Moskva) 12 (4): 534—539, 1957.

17. Ellerington, T. and J. J. Nicholls. "Determination of Acetic Anhydride in Mixtures with Acetic Acid" — *The Analyst* (Cambridge) 82 (4): 233—237, 1957.

18. Horner, L. and K. H. Knapp. "Autoxydationsstudien an N, N-dialkilierten Anilinderivaten" — *Die Makromolekulare Chemie* (Basel) 93: 69—108, 1966.

19. Walter, J. "Einige Notizen über Dimethilanilin und dessen Derivate" — *Zeitschrift für Farbenindustrie* 10 (1): 33—35, 17—20, 1911; *Chemisches Zentralblatt* (Berlin) 82 (12): 879, 1911.

20. Wanag, G. and A. Veinbergs. "Kondensation primärer Aminoverbindungen mit Phtalsäureanhydride in Eisessig" — *Berichte Der Deutschen Chemischen Gesellschaft* (Berlin) 75B (12): 1558—1569, 1942.

* Original title not given.

GLASNIK HEMIJSKOG DRUŠTVA, Vol. 34, No. 2-3-4, 1969, pp. 281—290

GHDB-61

547.233:543.257

Original Scientific Paper

DETERMINATION OF PRIMARY, SECONDARY AND TERTIARY AMINE MIXTURES BLOCKING PRIMARY AMINES WITH SALICYLALDEHYDE IN A METHYLETHYLKETONE-ACETIC ACID MIXTURE

by

VILIM J. VAJGAND and TIBOR J. PASTOR

Mixtures of bases can be determined using solvents exhibiting differentiation relative to the bases. The accuracy of determination increases with decreasing value of the titration constant[1, 2] which characterizes titration conditions and is defined by

$$K_T = \frac{K_{b_2} \cdot C_{b_2}}{K_{b_1} \cdot C_{b_1}},$$

where

C_{b_1} and C_{b_2} = base concentrations in solution,
K_{b_1} and K_{b_2} = ionization constants
$K_{b_2} < K_{b_1}$.

For this reason, when determining primary, secondary and tertiary amines in mixtures by titration in nonaqueous solution, the reagents for blocking mixture components should be selected so that the reaction product is the weakest possible base, i.e. that the ratio $\frac{K_{b_2}}{K_{b_1}}$ is as small as possible. In the determination of tertiary amines in base mixtures, the primary and secondary amines are acetylated by acetic acid anhydride. For the titration of the sum of secondary and tertiary amines, benzylaldehyde[3], salicylaldehyde[4-16], phthalic acid anhydride[17, 18] and other substances are used to react with primary amines. The reagent most often used for blocking the primary amines is salicylaldehyde because: (1) amines obtained from other aromatic aldehydes hydrolyze more easily in the presence of water; (2) salicylaldehyde reacts with some secondary amines less strongly than, for example, benzylaldehyde under the same conditions, and (3) salicylaldehyde is very stable towards oxidation by the air[4]. (3) is of major significance, because the buffer effect of the resulting carbonic acid would interfere with the end point determination.

Although the magnitude of $\frac{K_{b_2}}{K_{b_1}}$ depends on the properties of the solvents used, base mixtures are titrated, after treatment with salicylaldehyde, in various solvents: alcohols[4, 6, 11, 12], ketones[9, 11], acetonitrile[10], chloroform[7, 14], acetic acid[13, 15], *i*-propyl alcohol-ethylene glycol mixture[5], and acetic acid-dioxane-nitromethane (acetonitrile) mixture[16]. In some

of these including chloroform, acetonitrile, acetic acid[19] and others, salicylaldehyde amines show basic properties and can be titrated. In such solvents, two titrations are enough to determine the mixture components.

The present paper describes an accurate method for the determination of components in aliphatic or aromatic amine mixtures, using salicylaldehyde to block the primary amines.

EXPERIMENTAL

0.1 N solution of perchloric acid in dioxane was prepared by dissoluting about 8 *ml* 70% perchloric acid, "Kemika", of *p.a.* purity in 1 liter of pure dioxane, to which a calculated amount of acetic acid anhydride to bind the water from the perchloric acid was added. The solution was left at room temperature 24 h before use. Concentration of perchloric acid solutions was determined and checked with a solution of sodium acetate in acetic acid before every use.

Salicylaldehyde "Riedel" was purified through a bisulfite compound after Vogel[20], or simply by distillation under reduced pressure.

Dioxane "C. Erba" and nitromethane "BDH" were purified after Vogel[20], and acetonitrile "Kemika" after Kreshkov[21]. The procedure applied to purify acetic acid and the titration apparatus are described in a previous study[18].

1 *ml* samples of 0.3 N solutions of the bases, or 0.3 meq each, were prepared in acetic acid.

PROCEDURE

To determine all three components of the mixture, two or three titrations were conducted. Total amine during the first run and tertiary amine during the second run were determined as described in a previous study[18]. In the third run, when an aliphatic amine mixture was being titrated, the sum of secondary and tertiary amines was found, and primary amine was determined separately. In the system which contained analine, N-metylaniline, and N,N-diethylaniline, the tertiary and primary amines were determined separately.

Procedure for the Determination of a Mixture of Aniline, N-methylaniline, and N,N-diethylaniline. — 20 *ml* methylethylketone or dioxane and 5 *ml* salicylaldehyde were added to weighed amounts of the bases. After mixing with a magnetic stirrer the solution was left at room temperature for 15 min. Next, 20 *ml* anhydride of acetic acid was added to the solution, which was then mixed and left for 10 min. Then 30—40 *ml* methyl ethylketone was added and the solution was titrated with a 0.1 N solution of perchloric acid in acetic acid or dioxane.

Procedure for the Determination of Aliphatic Amine Mixture — 15—20 *ml* methylethylketone or dioxane and 3—5 *ml* salicylaldehyde were added to a weighed amount of the amine mixture. After mixing, the solution was left at room temperature for 15 min, then 40—50 *ml* methylethylketone was added and the solution titrated in a 0.1 N solution of perchloric acid in dioxane.

The procedure for computing the amounts of different components in the mixture was explained in a previous paper[18].

Since we had failed[18] to determine the components in a mixture of aniline, N-methylaniline and N,N,-diethylaniline in acetic acid by using phthalic acid anhydride, the present study concentrated on this problem. Huber[16] determined aniline mixtures in acetic acid treating the mixture with salicylaldehyde and acetic anhydride, but obtained only one potential jump corresponding to the sum of aniline and N,N-dietylaniline (Fig. 1, curve 1). The accuracy and reproducibility of this method cannot be judged because the author[16] does not mention any results of determinations.

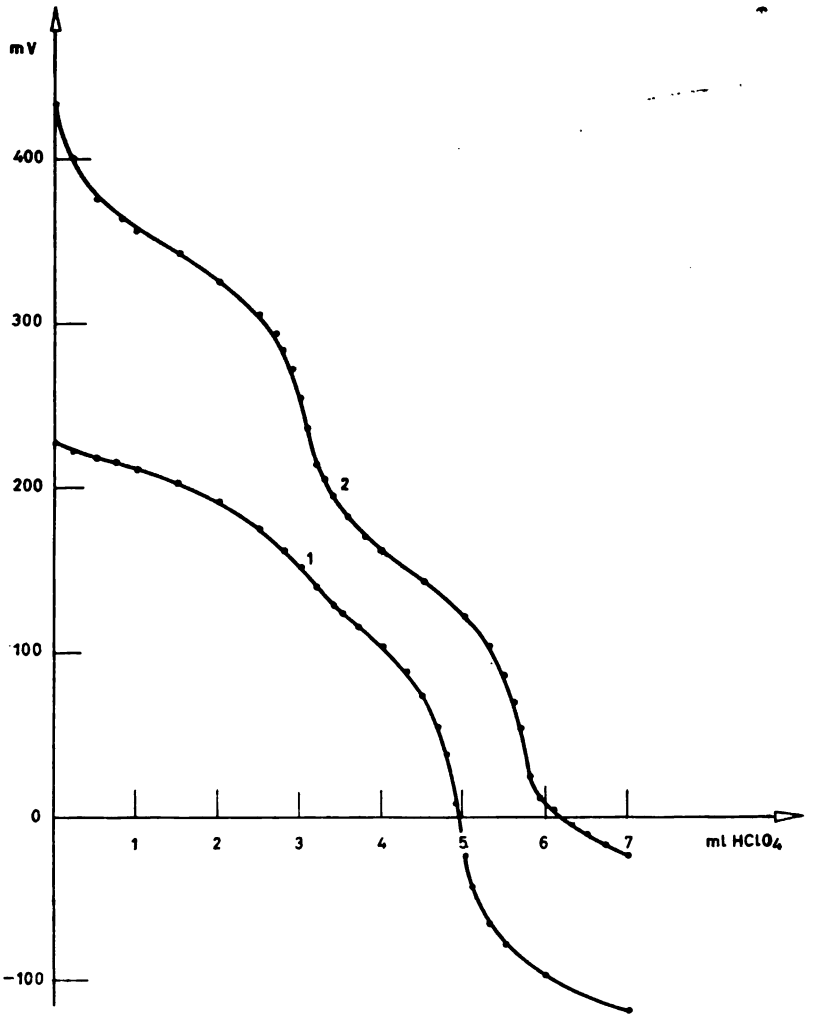

Figure 1

Titration curves of mixtures of aniline, N-methylaniline and N,N-diethylaniline treated with 5 *ml* of salicylaldehyde and 20 *ml* acetic anhydride: 1) in 50 *ml* acetic acid and 2) in a mixture of 3 *ml* acetic acid and 50 *ml* methylethylketone

Using solvents with differentiating properties, such as methylethylketone and dioxane, we succeeded in obtaining two distinct potential jumps after treating the mixture of bases with salicylaldehyde and acetic anhydride (Fig. 1, curve 2). The first potential jump carresponds to N,N-diethylaniline, and the second to the Schiff base obtained from aniline; the acetylated N-methylaniline did not yield any jump. In these determinations, the results

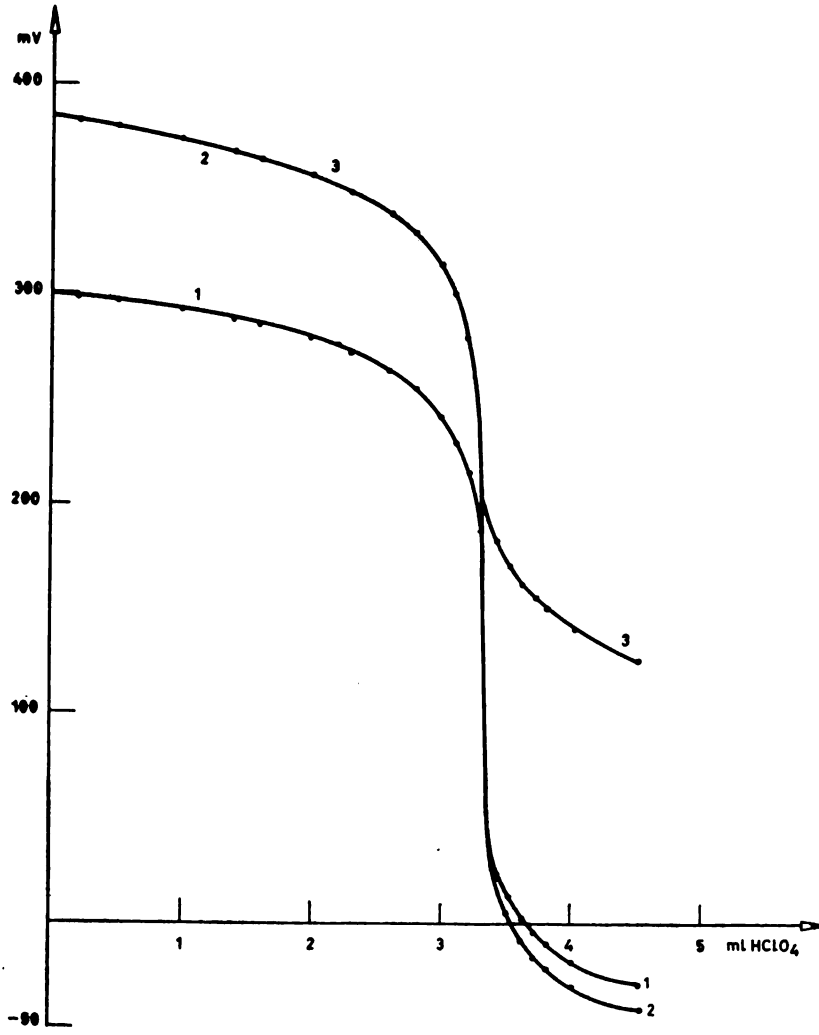

Figure 2

Titration curves of 0.3 meq. of tributhylamine: 1) in 20 *ml* of acetic acid, 2) in a mixture of 15 *ml* acetic acid and 5 *ml* acetic anhydride 3) in the presence of 0.3 meq.; each of benzylamine and dibutylamine in 15 *ml* of acetic acid, after treatment with 5 *ml* of acetic anhydride for 40 minutes on a boiling water bath.

and the shape of the titration curves did not depend on whether a perchloric acid solution in acetic acid or in dioxane was used.

With methylethylketone, better results are obtained not only in the titration of aniline mixtures but also in the determination of aliphatic amine mixtures. When the solution contained large amounts of dioxane, we noticed

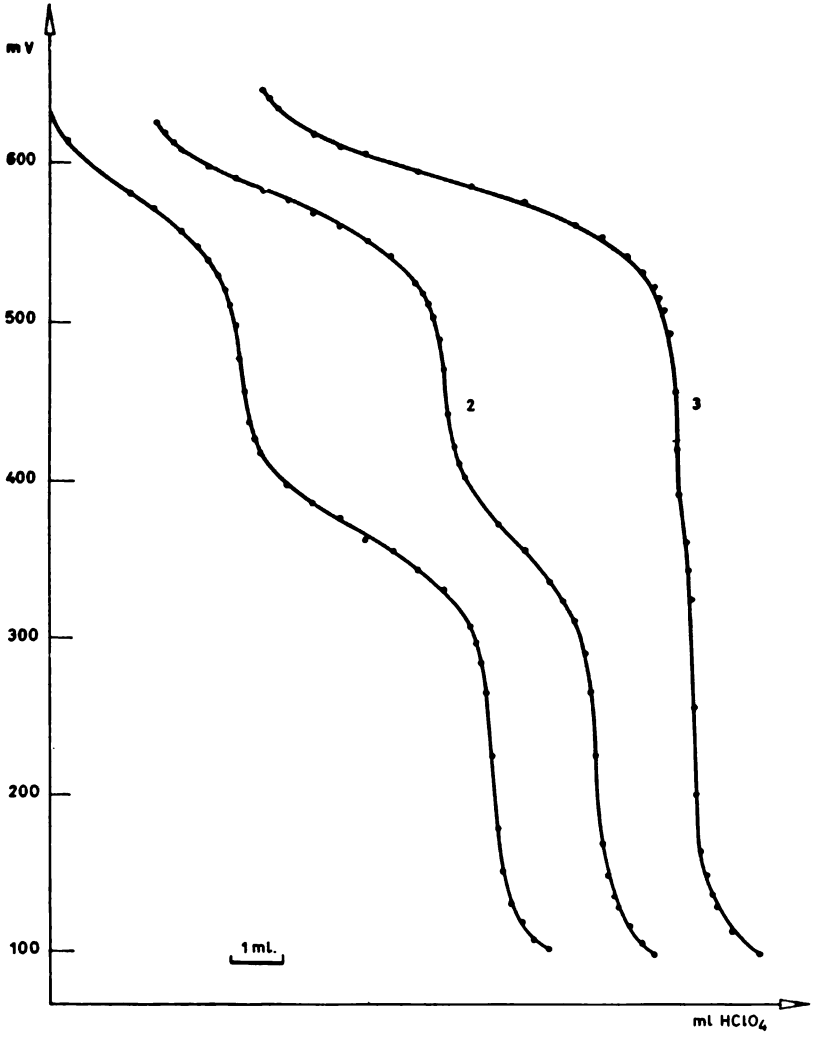

Figure 3

Titration curves of mixtures of tributylamine, diethylamine and benzylamine treated with 5 *ml* of salicylaldehyde in a mixture of 3 *ml* of acetic acid, 20 *ml* dioxane and 50 *ml* methylethylketone. Aamines taken (in *mg*):

1) 55.19 : 11.72 : 55.49
2) 55.19 : 39.06 : 32.64
3) 55.19 : 74.21 : 3.26

TABLE 1

Determination of Mixtures of Analine, N-methylaniline and N, N-diethylaniline

No.	Aniline			N-Methylaniline			N,N-Diethylaniline		
	Taken *mg*	Found *mg*	Found %	Taken *mg*	Found *mg*	Found %	Taken *mg*	Found *mg*	Found %
1.	14.26	14.08	98.7	32.66	32.51	99.5	44.82	45.11	100.6
2.	28.53	28.51	99.9	32.66	32.31	98.9	44.82	44.55	99.4
3.	28.53	28.34	99.3	32.66	33.10	101.4	44.82	44.52	99.3
4.	28.53	27.83	97.6	32.66	32.82	105.5	44.82	45.07	100.6
5.	28.53	28.49	99.9	32.66	32.41	99.2	44.82	44,31	98.9
6.	28.53	28.25	99.0	32.66	32.75	100.3	44.82	44.64	99.6
7.	28.53	28.45	99.7	32.66	32.47	99.4	44.82	44.70	99.7

TABLE 2

Determination of Mixtures of n-Propylamine, Diethylamine and Triethylamine

No.	n-Propylamine			Diethylamine			Triethylamine		
	Taken *mg*	Found *mg*	Found %	Taken *mg*	Found *mg*	Found %	Taken *mg*	Found *mg*	Found %
1.	22.10	22.01	99.6	23.42	23.27	99.4	30.87	30.86	100.0
2.	22.10	22.04	99.7	23.42	23.30	99.5	30.87	30.61	99.2
3.	22.10	22.23	100.5	23.42	23.12	98.7	30.87	30.86	100.0
4.	22.10	22.16	100.3	23.42	23.17	98.9	30.87	30.56	99.0
5.	22.10	21.92	99.2	23.42	23.54	100.5	30.87	30.60	99.1
6.	22.10	22.11	100.0	23.42	23.29	99.4	30.87	30.62	99.2
7.	22.10	21.96	99.4	23.42	23.48	100.3	30.87	30.78	99.7

that the potential jump corresponding to the sum of secondary and tertiary amines appeared somewhat earlier, and thus caused errors in the determination of secondary and primary amines. This behavior of dioxane is explained by its low dielectric constant (E = 2.20): Critchfield and Johnson[7] also found that many secondary amines react with salicylaldehyde in such solvents. Owing to the low dielectric constant, a high resistance appears in the circuit which makes the *p*H-meter oscillate preventing accurate readings of potential after fresh titration substance is added. This difficulty does not arise when methylethylketone, whose dielectric constant is 18.5, is used.

As predicted from the theoretical considerations, the amount of amines in solution and their concentration ratios substantially affect the size of the potential jumps for individual components after the mixture is treated with acetic anhydride or salicylaldehyde. This is obvious from Fig. 2, which gives the titration curve for tributylamine in acetic acid, in a mixture of acetic acid and acetic anhydride, and after the treatment of mixtures of benzylamine, dibuthylamine and tributylamine with acetic anhydride; the concentration of tributylamine in solution was the same. The effect of aniline and N-methylaniline on the potential jump for N,N-diethylaniline, after the aniline mixture has been treated with acetic acid anhydride, is less than in the previous case, which is explained by the differentiating capacity of acetic acid in relation to weak bases. Aside from this, Fig. 3 shows that, in the presence of a small amount of primary amine, and after the mixture is treated with salicylaldehyde, only one potential jump is obtained, or the jumps are so close together that the three components of the mixture cannot all be determined.

The amount of salicylaldehyde in solution (1—5 *ml*) does not affect the accuracy of determination of the mixture components.

The results of determination of two mixtures of bases are given in Tables 1 and 2, from which it can be seen that when the concentrations of individual amines in solution were equal, the errors of determination of the components did not exceed 2% relative to the results obtained by potentiometric determination before mixing.

The mixture of ethanolamines could not be determined using salicylaldehyde, bacause diethanolamine also reacts with salicylaldehyde in all the solvent combinations tried.

School of Sciences
Department of Chemistry
Beograd

Received 16 September, 1968

REFERENCES

1. Roller, P. S. "Theory and Error of Acid-Base Titration" — *Journal of the American Chemical Society* (Washington) 54 (9): 3485—3499, 1932.
2. Izmailov, N. A. "Elektrokhimiia rastvorov" (Electrochemistry of Solutions), in: *Khimiia* (Chemistry) — Moskva, 1966, p. 524.
3. Hawkins, W., D. M. Smith, and J. Mitchel Jr. "Analytical Procedures Employing Karl Fischer Reagent. XII. The Determination of Primary Amines" — *Journal of the American Chemical Society* (Washington) 66 (10): 1662—1663, 1944.
4. Wagner, Ch. D., R. H. Brown, and E. D. Peters. "The Analysis of Aliphatic Amine: Determination of Secondary Plus Tertiary Amines by the Azomethine-Acidimetric Method" — *Journal of the American Chemical Society* (Washington) 69 (11): 2611—2614, 1947.
5. Siggia, S., J. G. Hanna, and I. R. Kervenski. "Quantitative Analysis of Mixtures of Primary, Secondary and Tertiary Aromatic Amines" — *Analytical Chemistry* (Washington) 22 (10): 1295—1297, 1950.
6. Gribova, E. A. and E. Iu. Khmel'nitskaia. "Analiz smesi etanolaminov" (Analysis of Ethanolamine Mixtures) — *Zavodskaia Laboratoriia* (Moskva) 31 (4): 417—419, 1965
7. Critchfield, F. E., and J. B. Johnson. "Determination of Primary, and Secondary Plus Tertiary Amines — A Modified Salicylaldehyde Method" — *Analytical Chemistry* (Washington) 29 (6): 957—959, 1957.
8. Johnson, J. B., and G. L. Funk. "Determination of Primary Aliphatic Amines by an Acidimetric Salicylaldehyde Reaction" — *Analytical Chemistry* (Washington) 28 (12): 1977—1979, 1956.
9. Gribova, E. A., and E. S. Levin. "Titrovanie smesi aminov v nevodnoi srede" (Titration of Amine Mixtures in Nonaqueous Medium) — *Zavodskaia Laboratoriia* (Moskva) 25 (1): 38—41, 1959.
10. Fritz, J. S. "Differential Titration of Amines" — *Analytical Chemistry* (Washington) 25 (3): 407—411, 1953.
11. Kreshkov, A. P., L. N. Bykova, I. D. Pevzner, and L. N. Skripko. "Sintez i analiz vtorichnykh aromaticheskikh diaminov, ispol'zuemykh v kachestve stabilizatorov v proizvodstve polimernykh materialov" (Synthesis and Analysis of Secondary Aromatic Diamines Used as Stabilizers in Production of Polymeric Materials) — *Zhurnal Prikladnoi Khimii* (Moskva-Leningrad) 39 (1): 200—203, 1966.
12. Malone, H. E., and R. E. Barron. "Acid-Base Method for Determining Mixtures of Diethylene Triamine with Hydrazine or Substituted Hydrazines" — *Analytical Chemistry* (Washington) 37 (4): 548—549, 1965.
13. Malone, H. E. "Determination of Mixtures of Hydrazine and 1, 1-Dimethylhydrazine" — *Analytical Chemistry* (Washington) 33 (4): 575—577, 1961.
14. Jackson, J. E. "Determination of Primary Fatty Amines in Amine Mixtures" — *Analytical Chemistry* (Washington) 25 (11): 1764—1765, 1953.
15. Serencha, N. M., J. G. Hanna, and E. J. Kuchar. "Determination of Mixtures of Hydrazine and Monomethylhydrazine by Reaction with Salicylaldehyde" — *Analytical Chemistry* (Washington) 37 (9): 1116—1118, 1965.
16. Huber, W. "Potentiometrische Titration aliphatischer und aromatischer Amine" — *Angewandte Chemie* (Weinheim) 72 (22): 865, 1960.

17. Gal'pern, G. D., and N. N. Goezinger. "Opredelenie pervichnykh, vtorichnykh i tretichnykh aminogrupp pri sovmestnom ikh prisustvii" (Determination of Primary, Secondary and Tertiary Amino Groups in Mixtures) — *Zhurnal Analiticheskoĭ Khimii* (Moskva) 13 (5): 603—607, 1958.

18. Vajgand, V. and T. Pastor. "Primena anhidrida ftalne kiseline pri odredivanju smesa primarnih, sekundarnih i tercijarnih amina u sirćetnoj kiselini" (Application of Phthalic Acid Anhydride in the Determination of Mixtures of Primary, Secondary and Tertiary Amines in Acetic Acid) — *Glasnik Hemijskog društva* (Beograd) (to be published)*.

19. Freeman, S. K. "Determination of Schiff Bases by Titration in Nonaqueous Solution" — *Analytical Chemistry* (Washington) 25 (11): 1750—1751, 1953.

20. Vogel, A. I. *A Text-book of Practical Organic Chemistry Including Qualitative Organic Analysis* — London: Longmans, 1961.

21. Kreshkov, A. P. L. N. Bykova, and N. A. Kazarian. "Kislotnoosnovnoe titrovanie v nevodnykh rastvorakh" (Acid-Base Titration in Nonaqueous Solutions), in: *Khimiia* (Chemistry) — Moskva, 1967, p. 75.

---

* Available in English translation from Clearinghouse for Federal Scientific and Technical Information, Springfield, Virginia. 22151.

GLASNIK HEMIJSKOG DRUŠTVA, Vol. 34, No. 2-3-4, 1969, pp. 291—300

GHDB-62 543.257:546.18:546.268.5.546.72'267

Original Scientific Paper

ARGENTOMETRIC DETERMINATION OF SOME SYSTEMS USING DEPOLARIZATION END POINT

by

MILICA DRAGOJEVIĆ and MOMIR S. JOVANOVIĆ

In previous reports[1, 2] we described a new electrometric method for titration end point determination. The method makes use of the "irreversible potential" after Gaugin[3] who together with his co-workers[4, 5] found that the potential of one inert electrode in an irreversible system solution (for example, sulfite/sulfate) responds only to changes of concentration of the electroactive species (sulfate). This potential does not obey Nernst's equation. As Coursier[6] showed later, this "irreversible potential" remains practically unchanged during the titration of an irreversible system with a reversible titrant until the end point. When the end point is reached, the first traces of both ionic species in the reversible titrant will cause establishment of a "reversible potential" at the indicator electrode (obeying Nernst's equation), this being manifested in a potential jump.

We took as starting points the following hypotheses: if an inert electrode connected to some reference electrode in a balanced circuit is immersed in a solution of certain irreversible system its "irreversible" potential will correspond to the state of polarization of the other electrode. During titration with a reversible titrant, at the end point, and the zero current condition being maintained, this "irreversible" potential will become a Nernst "reversible" potential. This will allow the inert electrode to be effectively depolarized by the electroactive species of the reversible titrant, resulting in a potential jump. The shape of the current-voltage curve of the electrode when it becomes depolarized, i.e. the inflection of the curve, shows that changes take place both in electrode potential and in polarization current. But what is characteristic of the depolarized state of the electrode is a big change in the current caused by a relatively small change in its potential. Thus it is inferred that the beginning of electrode depolarization can be detected far more reliably from a big change in the current than than from the relatively small change in potential. We made use of this for end point determination, terming it the "depolarization end point method".

The depolarization end point method proved to be applicable both for the determination of redox systems[1] and for the determination of precipitation systems after argentometric titrations[2]. In the latter case, platinum can be used instead of silver for the indicator electrode. The fact that pla-

tinum can replace silver for argentometric titrations was discovered by Müller[7] who explained this behavior of platinum by its responsiveness, as a typical redox electrode, to the simultaneous presence of argento and argenti ions in silver nitrate. In precipitation reactions the argento ions alone take part, while the argenti ions (the number of which is far smaller) accumulate in the solutoin. The first traces of excess silver nitrate give rise to the simultaneous presence of lower and higher ionic species of silver in the solution, so that a corresponding Nernst potential is established at the platinum. Many years later, Allen and Hickling[8] presented their version of why platinum works as an indicator electrode in argentometry. They held that platinum previously pretreated in some way (e.g. keeping it in cold concentrated hydrochloric acid for a short time) and then well washed alloys with silver as soon as it is put in a solution which contains a concentration of silver ions of at least 10^{-15} *g*-ions/*l*. Thus the platinum becomes a silver electrode, so its responsiveness to changes in concentrations of the corresponding ions in the solution is clearly explained.

On this occasion we extended our research to include several more systems which are determined by silver nitrate titrations, and to investigate the possible use of unpretreated platinum.

EXPERIMENTAL

Apparatus — The same apparatus as previously described[1] was used (Fig. 1). The measuring instrument was a multiflex galvanometer of sensitivity 10^{-8} A/*mm*. The reference electrode (SCE) was connected to the test solution via an agar-agar/KNO_3 bridge. The microburette used for titrations allowed readings to the third decimal point.

Procedure — Before the beginning of titration the external EMF is balanced off against the EMF of the indicator electrode-test solution-reference electrode system. The EMF applied to compensate the EMF of the cell depends on the titration system but does not have to be known, so that a corresponding instrument does not have to be introduced into the circuit. In the titration of an ideally irreversible system (hydrogen peroxide, for example) the indicator electrode "irreversible potential" remains absolutely unchanged until the end point, so that there is no depolarization of this electrode at all. At the end point, even the least traces of both ionic species of the reversible titrant cause strong depolarization of the indicator electrode, manifested in a sudden current jump. This phenomenon is the consequence of the "reversible potential" being established on the indicator electrode, due to which the previous balance between the two circuits is disturbed.

When titrating systems that are not ideally irreversible, a certain small and increasing depolarization of the electrode is noted immediately after the beginning of titration. However, even though the previous balance of the system is not readjusted the big current jump caused by depolarization due to the presence of a reversible system is registered at the end point.

DETERMINATION OF FERROCYANIDE

Argentometric determination of ferrocyanide using potassium chromate as indicator was described by K. B. Rao[9]. Our object was to determine

the end point by our method while performing titrations after Rao, but this time without an indicator.

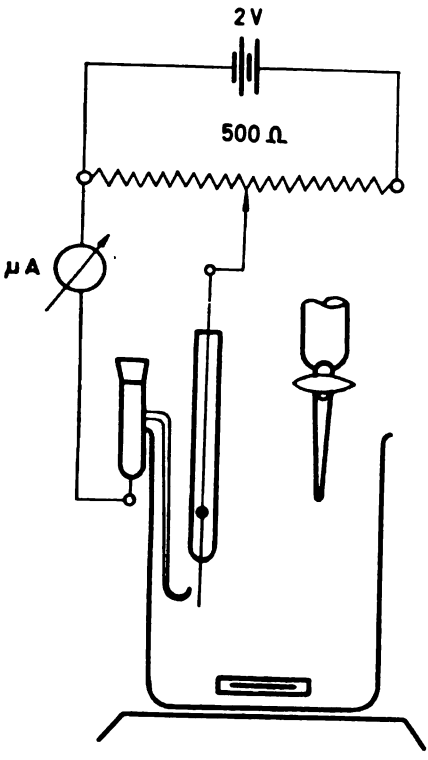

Figure 1

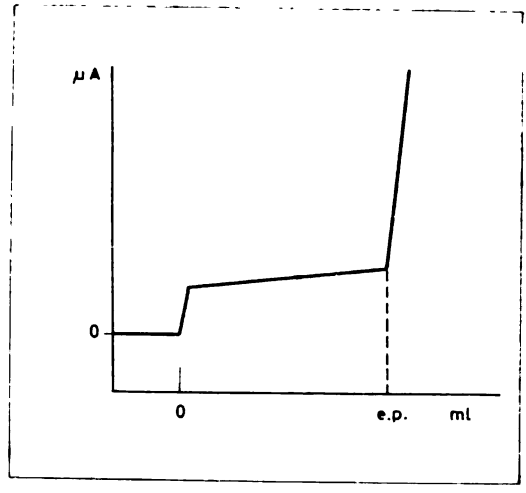

Figure 2

Standardization of Ferrocyanide Solution — D. F. Swinehart[10] has described the determination of ferrocyanide by dead-stop titration using standard zinc sulfate solution. On the other hand, Woodson, Johnson and Cooper[11] describe a simple gravimetric method for the determination of zinc starting from zinc sulfate solution. Having decided to use the methods of these authors we took 5.0287 *g* of Mallinckrodt a.r. metallic zinc and with the aid of platinum dissolved it in dilute sulfuric acid. This solution was then diluted to 1000 *ml*. In several samples a small amount of the solution was evaporated to dryness and weighed. Instead of the expected titer for zinc sulfate of 12.710 *mg/ml*, our solution had

$$T_{ZnSO_4} = 12.381 \ mg/ml$$

After adding 10 *ml* 10% ammonium sulfate and 1 *ml* 6 N sulfuric acid to the ferrocyanide solution, the whole amount was diluted to 50 *ml* and heated to 70—80°C. At a 200 *mV* potential difference between the two platinum electrodes, titration was performed with the zinc sulfate solution until

the current showed an upward trend from its zero initial value. At the end point the traces of excess ferrocyanide were reversibly oxidized at the anode into ferrocyanide, thus enabling the simultaneous depolarization of both electrodes, and consequently giving a current jump.

Five such determinations of ferrocyanide solution with zinc sulfate solution with a titrant consumption of 3.28 ± 0.002 *ml*, according to the reaction scheme

$$2\ K_4/Fe(CN)_6/ + 3\ ZnSO_4 \rightarrow K_2Zn_3/Fe(CN)_6/ + 3\ K_2SO_4$$

gave the following value for the ferrocyanide solution titer:

$$T_{K_4/Fe(CN)_6/} = 17.249\ mg/ml.$$

Determination of Ferrocyanide Using Depolarization End Point — The ferrocyanide solution standardized as above was this time determined using silver nitrate by Rao's method[9], but without an indicator. The taken volumes of ferrocyanide solution were diluted to 50 *ml* and without any addition titrated with the standard silver nitrate. The normality of the ferrocyanide solution ranged between 7.5×10^{-3} and 3.75×10^{-5}, while the titrant concentration varied from 5×10^{-2} to 5×10^{-4} N. Platinum was used as indicator electrode, either platinum pretreated by keeping it in cold concentrated hydrochloric acid for about 10 min, or unpretreated. After the inner circuit had been balanced against the external circuit, the titrant was added dropwise with strong stirring. Whatever indicator electrode was used, an extremely small but rising depolarization was observed from the very beginning of titration. At the end point, however, depolarization occurred suddenly enough for a sharp current jump to be always detectable. The only difference resulting from the kind of platinum used was in the EMF which had to be applied from the external circuit in order to balance the system before the beginning of titration. Table 1 shows only some typical results out of a series of 40 determinations.

TABLE 1

$K_4/Fe(CN)_6/$ Taken *mg*	$K_4/Fe(CN)_6/$ Found, *mg*	Difference *mg*	Error
34.500	34.222	−0.278	−0.81
34.500	34.500	−0.000	0.00
34.500	34.681	+0.181	+0.52
17.250	17.112	−0.138	+0.81
17.250	17.250	0.000	0.00
17.250	17.340	+0.090	+0.52
1.725	1.711	−0.014	+0.52
1.725	1.720	−0.005	−0.81
1.725	1.734	+0.009	+0.52
0.1725	0.1710	−0.0015	−0.81
0.1725	0.1716	−0.0009	−0.52
0.1725	0.1734	+0.0009	+0.52

DETERMINATION OF THIOCYANATES

Volhard's argentometric method for the determination of thiocyanates using ferriammonium sulfate as indicator is inadequate insofar as it is much more convenient to titrate a silver solution with a thiocyanate solution than vice versa. Also, in highly dilute thiocyanate the onset of pinkish clouding of the solution is difficult to detect. Hence the analyst is inclined to establish the end point a little late to be on the safe side.

Our intention was to perform this titration without using an indicator but applying our electrometric method. Also this enables the titration of thiocyanate with silver, which is far more convenient than conversely.

Standardization of Thiocyanate Solution — Solutions of potassium thiocyanate were standardized in two ways: (a) a silver nitrate solution was titrated with the thiocyanate solution using a ferric salt as indicator according to Volhard's method, (b) the thiocyanate solution was titrated with silver nitrate solution applying our balanced circuit technique. At the titration end point a current jump occurs, caused by the depolarization of the indicator electrode (pretreated platinum). In this case 5 *ml* thiocyanate solution was diluted water to 50 *ml* and after the addition of a small amount of dilute nitric acid the liquid was titrated with silver nitrate.

TABLE 2

KCNS Taken *mg*	KCNS found *mg*	
	after Volhard	using depolariz. e.p.
5.000	24.827	24.290
5.000	24.829	24.295
5.000	24,829	24.300
5.000	24.878	24.285
5.000	24.832	24.295

Table 2 shows the results for the standardization of thiocyanate by methods (a) and (b), reduced to a volume of 5 *ml* of the undiluted potassium thiocyanate solution. It may be seen that method (b) yielded several percent lower results. Since with Volhardis method and a rather dilute solution of thiocyanate (around 5×10^{-2} n), the solution might have been somewhat overtitrated to be sure of the and point, we took the results of the electrometric method as valid. According to them, the titer of thiocyanate solution was

$$T_{KCNS} = 4.859\ mg/ml.$$

Determination of Thiocyanate by Depolarization End Point — Thiocyanate solutions whose final concentration before titration were 10^{-4}—10^{-5} n were titrated (after dilute nitric acid was added) with standard silver nitrate solution of appropriate concentration. It is noteworthy that such highly dilute thiocyanate solutions as this cannot be determined by Volhard's technique at all. Analyses were made using either the pretreated or unpreated platinum electrode. No differences were found between the results.

The taken volumes of thiocyanate solution were diluted to 50 *ml*, acidified, and after the circuits had been balanced out were titrated with silver nitrate until the current jump marking the beginning of depolarization of the indicator electrode. Only typical results from the series of 30 determinations are presented in Table 3.

TABLE 3

KCNS Taken *mg*	KCNS Found, *mg*	Difference *mg*	Error %
0.9718	0.9564	−0.0154	−1.5
0.9718	0.9620	−0.0098	−1.0
0.9718	0.9669	−0.0049	−0.50
0.1458	0.1443	−0.0015	−1.0
0.1458	0.1448	−0.0010	−1.68
0.1458	0.1458	0.0000	0.00
0.09718	0.09564	−0.00154	−1.5
0.09718	0.09620	−0.00098	−1.0
0.09718	0.9718	0.00000	0.00

DETERMINATION OF PHOSPHATES

Christian *et al.*[12] recently described a potentiometric method for the determination of phosphates by titration with silver nitrate using a silver indicator electrode. For such titration they suggest 80% ethanol solution of the phosphate buffed with 0.1 *m* sodium acetate solution. We attempted to apply this method determining the end point by depolarization instead of potentiometrically, and using platinum instead of silver indicator electrode.

Standardization of Phosphate Solution — In applying the conditions as suggested[12], a primary sodium phosphate solution was standardized using a silver indicator electrode and performing titration with a standard silver nitrate solution up to the end point calculated in advance, i.e. up to a potential of 297 *mV* relative to SCE. In six analyses the difference in the amount of titrant used did not exceed 0.003 *ml*, giving an average consumption of 0.1000 N silver nitrate of 3.016 *ml* for 1 *ml* phosphate solution. Hence the titer of the phosphate solution was

$$T_{KH_2PO_4} = 13.690\ mg/ml.$$

Determination of Phosphates Using Depolarization End Point — The taken volumes of phosphate solution were diluted with water to 50 *ml* and under the conditions suggested by Christian *et al.*[12] the end point was determined by our method using either pretreated or unpretreated platinum electrode. However, due to the relatively large solubility product of silver phosphate (about 10^{-18}), phosphate solutions whose concentration before determination was below 10^{-3} *m* could not be determined with sufficient accuracy. In such cases a small but rising depolarization of the indicator electrode was observed from the very beginning of titration. As a result the transition of the electrode to the actual depolarized state was not sharp enough, so that the current jump was not well-defined.

This time we also ascertained a very important fact concerning the pretreatment of platinum. It is entirely irrelevant whether the platinum is pretreated or not provided only that it has been previously electrically polarized during use. But if for any reason it is red-heated and not used again it *must be* pretreated.

Table 4 gives only selected characteristic results out of a series of 20 determinations for phosphate concentrations above 10^{-3} *m*.

TABLE 4

KH_2PO_4 Taken *mg*	KH_2PO_4 Found *mg*	Difference *mg*	Error %
27.380	27.222	−0.158	−0.58
27.380	27.380	0.000	0.00
27.380	27.220	−0.160	−0.58
13.690	13.611	−0.079	−0.59
13.690	13.610	−0.080	−0.59
13.690	13.690	0.000	0.00

DETERMINATION OF IODIDE PLUS CHLORIDE MIXTURES

In argentometric determination of cyanide by our method, using platinum instead of silver indicator electrode[2], we got two end points. The first marked the end of silver complexing and the beginning of formation of silver-silver cyanide precipitate, while the second signified the end of this precipitation and the appearence of silver titrant in excess. Encouraged by the possibility of getting two depolarization end points we tried to titrate iodide-chloride mixtures, since the solubility products of the corresponding silver compounds differ considerably.

Standardization of Iodide and Chloride Solutions — These approximately 0.1 *n* solutions were determined with titration using precisely 0.1000 N solution of silver nitrate. The final volume of solutions for determination, which were weakly acidified with nitric acid, was about 50 *ml*. To prevent coprecipitation a small amount of barium nitrate was also added before each determination. Potentiometric titration up to a predetermined end point (at 88 *mV vs* SCE for iodide, and 272 *mV vs* SCE for chloride) was applied, using a sodium nitrate bridge between the titrated solution and the reference electrode and silver as the indicator electrode. It was established that:

2.000 *ml* iodide solution consumed 2.011 *ml* silver solution,
2.000 *ml* chloride solution consumed 2.080 *ml* silver solution.

When titrating the same volumes of these halogenides in a mixture, 2.038 *ml* silver solution was consumed for iodide and 2.040 *ml* for chloride. This change in the consumption of titrant obviously resulted from some coprecipitation of chloride with silver iodide, in spite of the addition of barium nitrate.

Attempted Determination of Halogenide Mixtures Using Depolarization End Point — In titrating a solution of similar composition as above it was again found irrelevant whether the indicator electrode was pretreated or unpretreated platinum. However, a current kick was only observed after the two halogenides had reacted with silver nitrate. The 4.091 *ml* consumption of titrant equalled the sum of titrant consumptions for the individual determinations. Thus, the two end points we expected could not be observed.

The fact that depolarization of the electrode by silver ions does not take place after the end of silver iodide precipitation must be attributed to insufficient concentration of these ions, since silver chloride begins to form immediately. Only after the formation of this precipitate is also completed will the least excess of silver ions be sufficient to cause a sharp and adequate depolarization manifesting as a deflection of the galvanometer.

DISCUSSION

From experience gained so far with the depolarization end point method it is obvious that the method is particularly convenient for the determination of an irreversible system with a reversible system. In view of the confirmed applicability of platinum as a universal redox electrode instead of silver in argentometric titrations, the two end points obtained in the determination of cyanides, and the one end point in the determination of mixed halogenides, the following conclusion may be drawn: at platinum redox electrode it is possible to establish a potential in the presence of the argento/argenti system. The potential established of course depends on the molar ratio between the electroactive species. At a potential within the depolarization range the depolarization of the platinum itself increases with the concentration of argenti ions. Accordingly, a marked depolarization of the platinum will be registered whenever the difference between argenti ion concentrations before and after the end point is big enough, the concentration of argento ions, which do not take part in reaction, changing only very little. The required sufficiently large difference in argenti ion concentrations before and after the end point exists in the case of cyanide titration, but it is insufficient in the titration of mixtures of iodide and chloride. Bearing in mind what has been said and the fact that in this method the platinum either becomes or does not become sufficiently depolarized, unlike silver whose potential is a function of the concentration of the corresponding ions in the solution, Müller's[7] explanation of why platinum can be used instead of silver appears to be more probable. If Allen's and Hickling's[8] hypothesis is applied to explain how platinum can be used in argentometry, it cannot explain why platinum alloyed with silver, thus practically a silver electrode as they themselves say, is incapable of registering a certainly existing difference in silver ion concentration at the moment when iodide precipitation ends and silver chloride formation begins.

School of Technology and Metallurgy
Institute of Analytical Chemistry
Belgrade University

Received 18 October, 1968

REFERENCES

1. Jovanović, M. S. and D. M. Petrović. "Electrometric Titrations with a Single Polarised Electrode" — *Talanta* (Oxford) 13: 815—819, 1966.
2. Jovanović, M. S., F. D. Sigulinsky, and M. Dragojević. "Argentometric Determination of Iodide and Cyanide Using a Depolarisation End-Point" — *Talanta* (Oxford) 13: 1275—1279, 1966.
3. Gaugin, R. "Propriétés réductrices des ions thiocyanique et cyanhydriques. Remarque sur les potentiels d'oxydo-réduction des systemes irréversibles" — *Ananles de Chimie* (Paris) 4: 832—880, 1949.
4. Gaudin, R., G. Charlot, and J. Coursier. "Utilisation des courbes de polarisation dans les dosages électrometrique" — *Analytica Chimica Acta* (Amsterdam) 7: 172—184, 1952.
5. Coursier, J. "Interprétation des mesures potentiométriques au moyen des courbes de polarisation" — *Analytica Chimica Acta* (Amsterdam) 7: 77—94, 1952.
6. Coursier, J. "Prévision des courbes de dosages potentiometriques" — *Analytica Chimica Acta* (Amsterdam) 10: 182—191, 1954.
7. Müller, E. "Zur Elektrometrischen Bestimmung der Chloride" — *Zeitschrift für Electrochemie und Angewandte Physikalische Chemie* (Leipzig—Berlin) 30: 420—423, 1924.
8. Allen, P. L. and A. Hickling. "The Mechanism of the Platinum Indicator Electrode in Argentometry" — *Analytica Chimica Acta* (Amsterdam) 11: 467: 474, 1954.
9. Rao, K. B. "Titration of Ferrocyanide with Silver Nitrate Using Potassium Chromate as Indicator" — *Recueil des travaux chimiques des Pays-Bas* ('s Gravenhage) 84: 69—70, 1965.
10. Swinehart, D. F. "Stannous Chloride-Iodide and Zinc-Ferrocyanide Titrations" — *Analytical Chemistry* (Washington) 23: 380—381, 1951.
11. Woodson, A., B. H. Johnson, and S. R. Cooper. "Amperometric Titration of Zinc with Potassium Ferrocyanide" — *Analytical Chemistry* (Washington) 24: 1198—1199, 1952.
12. Christian, G. D., E. C. Knoblock, and W. C. Purdy. "A Direct Argentometric Titration of Orthophosphate" — *Analytical Chemistry* (Washington) 35: 1869—1871, 1963.

Izdavač:

IZDAVAČKO PREDUZEĆE "NOLIT", BEOGRAD, TERAZIJE 27/II

•

Štampa:

GRAFIČKO PREDUZEĆE "PROSVETA", BEOGRAD
ĐURE ĐAKOVIĆA 21

SRPSKO HEMIJSKO DRUŠTVO (BEOGRAD)

BULLETIN OF THE CHEMICAL SOCIETY Belgrade

(Glasnik Hemijskog društva — Beograd)
Vol. 34, No. 5-6-7, 1969

Published by
SRPSKO HEMIJSKO DRUŠTVO (BEOGRAD)
1970

Translated and published for U.S. Department of Commerce and
the National Science Foundation, Washington, D.C., by
the NOLIT Publishing House, Terazije 27/II, Belgrade, Yugoslavia
1970

Translated by
LAZAR STANOJEVIĆ

Edited by
PAUL PIGNON

Printed in "Prosveta", Beograd

CONTENTS

Page

Jevrem D. Janjić, Dimitrije S. Pešić, and *Dimitrije S. Janković:*
The Ångström Band System of the $C^{12}O^{18}$ Molecule 5

Ubavka B. Mioč:
Spectrographic Determination of ^{13}C by Arc Excitation 9

Boško V. Pavlović, Natalija N. Ikonomov, and *Vladimir M. Vukanović:*
The Radial Temperature Distribution in a DC Arc in Nitrogen Atmosphere under Conditions Used in Spectrochemical Analysis 17

Natalija N. Ikonomov, Vladimir M. Vukanović, and *Boško V. Pavlović:*
Radial Temperature Distribution in a DC Arc in a Mixture of Nitrogen and Water Vapor 29

Vladimir Balek:
The Emanation Method in Studying Solid State Reactions 43

Ladislav J. Horvat:
Conductivity and Dissociation Constant of Liquid Ammonia 53

Dragica N. Đurković and *Rade M. Ćosović:*
Thermal Decomposition of Tungsten Hexachloride 59

Nada P. Vidojević and *Nada M. Novović-Simović:*
Dilatometric Investigation of the Effect of the Heating Rate on the Temperature of the Individual Tempering Stages of Carbon Tool Steels . . 69

Ksenija D. Sirotanović, Milka M. Bajlon-Pastor, Milica M. Obradović, and *Lutvija R. Eminović:*
Reactions of α, β-Unsaturated Aldehydes with Carbamates. I. Action of Ethyl Carbamate on α, β-Unsaturated Aldehydes 77

Miodrag D. Cvetković, Eva J. Levi-Jovanović, Darinka N. Koraćević, and *Gordana M. Bjelaković:*
Action of Colcemide on Growth and Nucleic Acids of *Staphylococcus albus,* Strain 581 85

Sreten N. Mladenović and *Vojislav Filipović:*
Chemical Removal of Oxide from Copper Wires and Electrolytic Regeneration of Cleaning Solution 89

Milan V. Mitrović, Bojan D. Đorđević, Milan K. Bilić, and *Aleksandar Ž. Tasić:*
The Influence of Vibrations on Boiling Heat Transfer 95

Herbert Weisz and *Tibor F. A. Kiss:*
Application of Catalytic Identification Reactions in the Ring Oven Method 103

Tibor A. Kiss, Ferenc F. Gaal, and *Terezia Suranyi:*
Complexometric Determination of Palladium by Back-Titration Using o,o′-Dihydroxy-Substituted Azo Dye Indicators 107

Page

Đorde K. Stefanović, Vilim J. Vajgand, and *Tibor A. Kiss:*
Oscillographic-Chronopotentiometric Titration. V. Acido-Base and Chelatometric Titrations 111

Momir S. Jovanović, Luka J. Bjelica, and *Anka Marinković:*
Neutralization Biamperometric Titrations Using Bismush-Bismuth Pair in Ethanol Solvent 117

Miodrag D. Cvetković:
Quantitative Determination of Deoxyribonucleic Acid with Thyamine as Reference 125

GLASNIK HEMIJSKOG DRUŠTVA, Vol. 34, No. 5-6-7, 1969, pp. 301—304

GHDB-63

535.338.4

Original Scientific Paper

THE ANGSTRÖM BAND SYSTEM OF THE $C^{12}O^{18}$ MOLECULE*

by

JEVREM D. JANJIĆ, DIMITRIJE S. PEŠIĆ, and DIMITRIJE S. JANKOVIĆ

The Angström system emission bands of the $C^{12}O^{16}$ molecule ($B^1\Sigma^+$—$A^1\pi$), easily obtained from a large number of excitation sources, very often occurring as impurities in the spectra of other molecules, have been investigated in great detail[1–3]. McCulloh and Glockler[4] and Douglas and Moller[5] analyzed this system for the $C^{13}O^{16}$ molecule. So far no analysis of the Angström system of the $C^{12}O^{18}$ molecule has been published, although some of its bands have been measured and used for spectroscopic isotope analysis of oxygen[6, 7].

This study was undertaken with a view to supplementing the data and verifying some constants for the CO molecule.

EXPERIMENTAL

The $C^{12}O^{18}$ emission spectrum was excited in a discharge tube with a cylindrical graphite cathode whose design is described by Matić and Pešić[8]. After heating the cathode in a helium stream the tube was filled with oxygen 18 (90.5% $^{18}O_2$). The discharge in the tube, containing a mixture of 9 *mm* Hg He and 6 *mm* Hg $O_2{}^{18}$, was maintained at a current of 35 *mA*. The spectrum was recorded on a 3 *m* Eagle grating diffraction spectrograph ($D = 5.6$ *Å/mm*, first order), and on a medium glass spectrograph ($D = 17$ *Å/mm* at 4800 *Å*). Spectra were registered on Ilford R 40 Panchromatic plates. Iron lines were used to determined wavelengths. Wave numbers are given according to the NBS Tables[9].

RESULTS AND DISCUSSION

The Angström system of the CO molecule comes from the $B^1\Sigma^+$—$A^1\pi$ electronic transition and falls within the range 4100—6700 *Å*. The bands display well-defined heads and shade towards the violet end. At the dispersion used, the bands are partly resolved.

* Communicated in part at the 14th Symposium of Chemists of the S.R. of Serbia, Belgrade, January 1969.

TABLE 1

Wavelengths of Outstanding Bands of $C^{12}O^{18}$

v' v''	λ, Å	ν, cm^{-1}	I
0.4	6034.40	16567.0	8
0.3	5579.95	17916.5	9
0.2	5180.93	19296.2	9
0.1	4828.02	20706.6	10
0.0	4510.84	22162.3	10
1.1	4395.0	22746.7	5

Wavelengths, wave numbers and relative intensities of $C^{12}O^{18}$ band heads are given in Table 1. The general appearance of the spectrum in the region 5100—6200 *Å* in shown in Fig. 1.

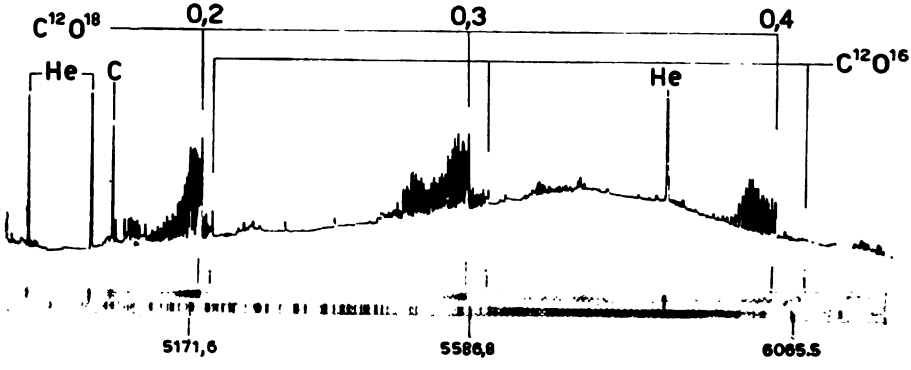

Figure 1

Isotopic shift in the Angström band system of CO

The well developed spectrum free of $C^{12}O^{16}$ bands enabled vibrational constants to be computed for the investigated isotopic molecule. By using the values for the beginning of the system and vibrational frequencies from McCulloh and Glockler[4] and from tables[3] ($w_e' = 2160 \cdot 70$ cm^{-1}; $w_e'' = 1515.61$ cm^{-1}; $w_e'X_e' = 39.30$ cm^{-1}; $w_e''X_e'' = 17.25$ cm^{-1} and $\nu_e = 21852$ cm^{-1}) and the known relationships for isotopic molecules[1], the corresponding constants were computed. From the value of the reduced mass ratio $C^{12}O^{16} : C^{12}O^{18}$ $\rho = \sqrt{\mu/\mu^1} = 0.97584$, the vibrational constants for the beginning of the $C^{12}O^{18}$ bands were obtained (Table 2).

Since the difference between the beginning and the head of the bands ($\nu_o - \nu_h$) in this system is small, the rotatory isotopic effect was of the order of 0.4 cm^{-1} and thus was neglected in computing the total isotopic shift.

TABLE 2

Molecular Constants of $C^{12}O^{18}$

$\nu_e = 21852 \ cm^{-1}$	
$\omega_e' = 2108.5 \ cm^{-1}$	$\omega_e' X_e' = 37.42 \ cm^{-1}$
$\omega_e'' = 1478.99 \ cm^{-1}$	$\omega_e'' X_e'' = 16.43 \ cm^{-1}$

Using the constants for the $C^{12}O^{18}$ molecule from Table 2 to compute ν_0^{18}, and the equation

$$\nu_0^{18} - \nu_h^{18} = \frac{(B_v' + B_v'')^2}{4\,(B_v'' - B_v')}$$

it is possible to calculate the bands heads ($\nu_h^{18}{}_{calc}$) and compare them with the measured $\nu_{2\ meas.}$ Rotational constants were calculated according to the values for the $C^{12}O^{16}$ molecule given in the literature[3]. The results are presented in Table 3, where standard symbols are used.

TABLE 3

Values of ν_0 *and* ν_h *for the Angström system of* $C^{12}O^{18}$

v'	v''	$\nu_0^{18} - \nu_0^{16*}$	ν_0^{18}	$\nu_0^{18} - \nu_h^{18}$	$\nu_h^{18}{}_{calc}$	$\nu_h^{18}{}_{tak.}$	$\nu_h^{18}{}_{calc} - \nu_h^{18}{}_{tak.}$
0	4	122.5	16574.1	4.01	16570.0	16567.0	3.0
0	3	92.4	17921.7	4.7	17917.0	17916.5	0.5
0	2	60.8	19302.1	5.6	19296.5	19296.2	0.3
0	1	27.4	20715.4	6.8	20708.6	20706.6	2.0
0	0	—7.5	22161.5	8.5	22153.0	22158.7	—5.7
1	1	—22.0	22741.9	8.1	22749.0	22746.7	2.3

* Bands from Johnson's data (9)

Agreement between calculated and measured values for band heads are within experimental error except for the (0, 0) band. The measured isotopic shift for the replacement of ordinary oxygen by oxygen 18 unequivocally shows that the CO molecule emits these bands. Good agreement between our measured and calculated values was obtained when the constants for $C^{12}O^{18}$ given by McCulloh and Glocker[4] were used. The analysis also confirmed the accuracy of the Deslandres' scheme given by Johnson[10] for this system of the ordinary CO molecule.

School of Technology
Novi Sad University
Boris Kidrič Institute of Nuclear Sciences
Belgrade

Received 18 June 1969

REFERENCES

1. Herzberg, G. *Spectra of Diatomic Molecules* — New York: D. van Nostrand, 1950.
2. Pearse, R. W. B. and A. G. Gaydon. *The Identification of Molecular Spectra. 3rd Ed.* — London: Chapman and Hall, 1963.
3. *Termodinamicheskie svoistva individual'nykh veschestv. Tom I. Spravochnik. red. V. P. Glushko* (Thermodynamic Properties of Substances. Vol. I. Handbook edited by V. P. Glushko) — Moskva: ANSSSR, 1962, pp. 448.
4. McCulloh, K. E. and G. Glocker. "The Electronic Emission Spectrum of $C^{12}O^{16}$" — *Physical Review* 89: 145—147, 1953.
5. Douglas, A. E. and C. K. Moller. "Predissociations of the $C^{12}O$ and $C^{13}O$ Molecules" — *Canadian Journal of Physics* 33: 125—132, 1955.
6. Rytel, M. "Note on the Angström Bands of the $^{16}C^{18}O$ Molecule" — *Acta Physica Polonica* 34: 953, 1968.
7. L'vov, B. V., V. I. Mosichev, and S. A. Senyuta. "Kolichestvennyi spektralnyi analiz izotopnogo sostava kisloroda" (Quantitative Spectral Analysis of the Isotopic Composition of Oxygen) — *Zavodskaia Laboratoriia* 28: 1322—1324, 1962.
8. Matit', J. S. and D. S. Peshit'. "Spectrographic Analysis of Molybdenum Using a Discharge Tube with Hollow Cathode" — *Revue Roumaine de Chimie* 10: 733—739, 1965.
9. Coleman, C. D., W. R. Bozman, and W. F. Meggers. *Tables of Wavenumbers. Vol. I. NBS Mono.* 3 — Washington, 1960.
10. Johnson, R. C. "A New Band System of Carbon Monoxide (3^1S-2^1P) with Remarks on the Angström Band System" — *Proceedings of the Royal Society* 123: 560—574, 1929.

GLASNIK HEMIJSKOG DRUŠTVA, Vol. 34, No. 5-6-7, 1969, pp. 305—311

GHDB-64

543.42:546.26.02

Original Scientific Paper

SPECTROGRAPHIC DETERMINATION OF ^{13}C BY ARC EXCITATION

by

UBAVKA B. MIOČ

The carbon isotope of mass-13 was discovered by King and Birde[1,2,3] in 1929 analyzing the emission molecular spectrum of carbon from King's vacuum furnace. They identified the band $C_2(1, 0)$, $\lambda = 4737.1$ Å of the Swan system. At 7.4 Å from the $C_2(1, 0)$ band head toward the red end of the spectrum, $\lambda = 4744.5$ Å, they noted an approximately one hundred times weaker band whose structure corresponded to the $C_2(1, 0)$ band. They found that it agreed with the molecular band $C_2(1,0)$ of the radical $^{12}C^{13}C$.

In 1954 Steubing and Günther[4] determined the content of ^{13}C by emission spectrography, using the Swan bands, more precisely the band $C_2(1,0)$. Determinations were done from the mixture Ar + CO or Ar + CH_4 with 1.1—11.9 at% ^{13}C. Excitation was done in 1—5 *mm* capillary tubes, by Tesla coil. Experimental error was 5—9%, and the values obtained were higher than those from mass spectrography.

In 1956 Ferguson and Broida[5] determined the proportion of ^{13}C from C_2H_2 by flame excitation. Spectra were registered photo electrically. The initial concentration was 66 at% ^{12}C while the lowest concentration corresponded to the natural relative abundance of ^{13}C in C_2H_2. Determination error was 4.3%. The disadvantages of the method are the complicated preparation of the specimen as C_2H_2 enriched with ^{13}C, the unknown mechanisms of both C_2H_2 destruction in flame and C_2 radical formation, and possible errors due to ^{12}C in atmospheric CO_2.

Zaĭdel' and Ostrovskaia[6] used the Angström band system, specifically the ^{13}CO band head of wavelength $\lambda = 4131.8$ Å, to determine the ^{13}C content. Isotope shift was 8.2 Å toward longer wavelengths. Determination were made from a mixture of CH_4, air and O_2. Excitation was done by high-frequency discharge without electrodes and the spectra were registered photoelectrically. Errors were 5—7% for 1—5% content of ^{13}C, and 2—3% for 5—60% ^{13}C. The disadvantages of the method are the corrections required because of the overlapping of the observed band head with the $\lambda = 4141.8$ Å of the N_2 radical, and the very strong background emission due to the presence of CH_4, N_2 and O_2 molecules.

EXPERIMENTAL AND APPARATUS

The objective of this study was to work out a practical, sufficiently quick and simple emission spectrographic method for the determination of isotopic rations of the stable carbon isotopes ^{12}C and ^{13}C, using a stan-

dard techniques: arc (*DC* or *AC*) or spark. The $C_2(1, 0)$ band from the Swan system was selected as the analytical band.

The ^{13}C content natural materials is about 1%. The band head of the isotopic radical $^{12}C^{13}C(1,0)$ is found at $\lambda = 4744.5$ *Å*, which means that the isotopic shift relative to the corresponding radical band head is 7.4 *Å* and can be fairly well registered on a moderate dispersion apparatus.

From our earlier studies[7, 8] it may be seen that the quantitative spectrographic analysis of carbon was possible under the following conditions: 6A AC-arc excitation with copper electrodes in CO_2 atmosphere, which at the same time was the investigated specimen.

The specimen enriched with the isotope ^{13}C was in the form of $BaCO_3$ with 54.4 at % of ^{13}C (20th Century Electronics Ltd., England). Standard specimens were prepared by diluting the enriched carbonate with commercial $BaCO_3$ (Merck, Berlin, p. a.).

In a specially designed glass apparatus[8] the specimens were converted by means of 2N HCl into CO_2[9], purified and condensed by liquid nitrogen into gas containers. Some of the standard specimens were taken for mass spectro isotopic analysis. The CO_2 containers were easily connected to the low-pressure apparatus[1, 8].

Since the $^{12}C/^{13}C$ ratio in natural materials is 100 : 1, the $^{12}C^{12}C(1,0)$ band head had to be attenuated for use as an internal standard. For this reason all the specimens were photographed with a six-stage step filter.

A calibration curve was plotted for the photographic emulsion. Since corrections had to be made for the background and since absorbances were often below 0.2, all absorbance values were converted to values of Seidel's function.

The $BaCO_3$ used for making standard specimens itself contained approximately 1.1% ^{13}C, which led us employ the analytical procedure of the addition method[10]. To obtain standard specimens, 1.06 at %, 2.14 at %, 3.21 at % and 5.32 at % ^{13}C were added to the unenriched $BaCO^3$ with unknown content of ^{13}C.

Spectra were recorded as follows:

— Zeiss PGS-2 spectrograph, first order, reciprocal dispersion about 7 *Å/mm*
— slit width: 20 μ
— quantitative illumination with 3 lenses
— six-stage step filter
— controlled atmosphere
— AC-arc excitation, 6 A
— electrodes of electrolytically pure copper, gap 4 *mm*
— exposure 20 min
— Ilford N-30 Ordinary plates, developed in ID-2 1 : 5 at 20°C in a Jarrell-Ash photo processor for 6 min.

The radical bands $^{12}C^{13}C(1,0)$ $\lambda = 4744.4$ *Å* and $^{12}C^{12}C(1,0)$ $\lambda = 4737.1$ *Å* were used for analysis. Microphotometry was performed with a Jarrell-Ash nonregistering microphotometer.

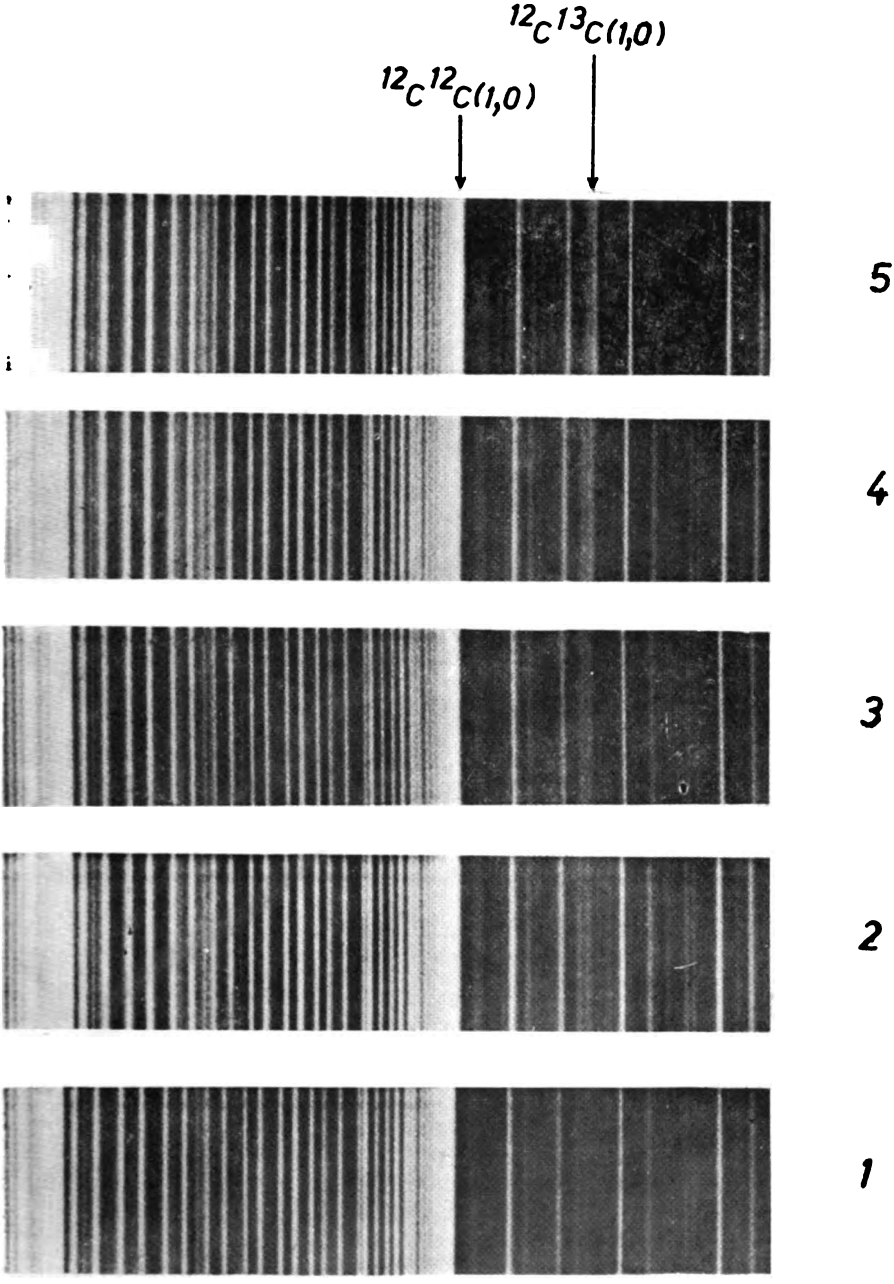

Figure 1

Spectra of standard specimens with different ^{13}C content

1 — Natural content, 2 — 2.20 at%, 3 — 3.28 at%, 4 — 4.35 at%, 5 — 6.46 at%

RESULTS AND DISCUSSION

The spectra are reproduced in Fig. 1. They were scanned by microphotometer and the data processed according to standard procedure. From these data an analytical curve was plotted: $\log (I_{12c\ 13c}/I_{12c\ 13c})$ as a function of log (c) (Fig. 2, a). The plot is not a straight line. By the iterative method we found the comercial $BaCO_3$ used as diluent contained 1.14 at % ^{13}C. This means that the actual ^{13}C concentrations of the standard specimens we prepared were 2.20 at %, 3.28 at %, 4.35 at % and 6.46 at %. Another analytical curve was plotted from these data (Fig. 2, b).

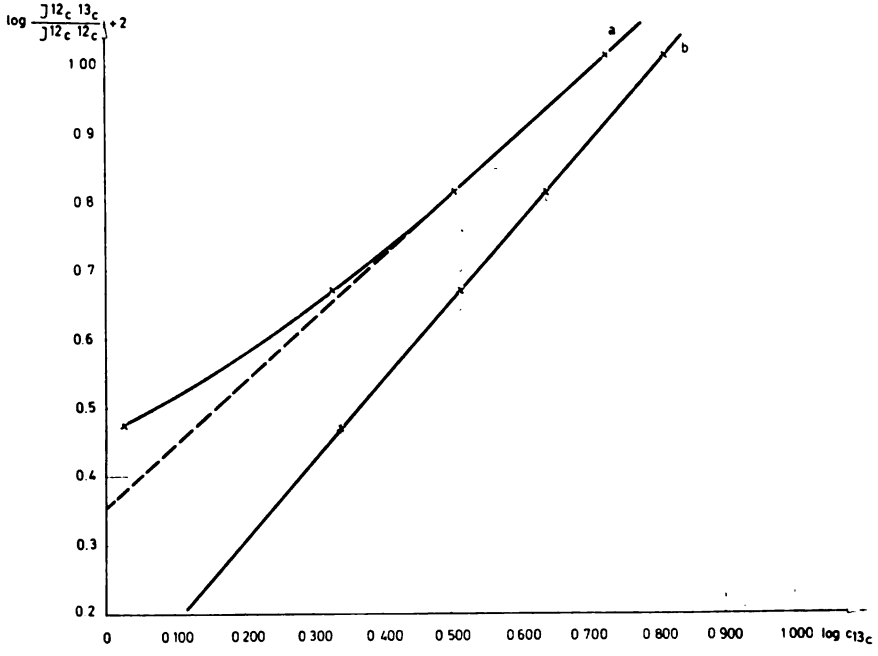

Figure 2

Analytical curve: (a) before iteration
(b) after iteration

The results were statistically processed (Table 1).

The same specimens were analyzed on an SM-521 CSF Paris mass spectrometer ($\alpha = 90°$, $r = 20\ ^0m$) at the Boris Kidrič Institute at Vinča. The results were statistically processed and are given in Table 1.

CONCLUSION

Under the optimum conditions 6A AC-arc excitation with copper electrodes in 300 *mm* Hg CO_2 atmosphere (being at the same time the ana-

TABLE 1

Results of the Analysis of Standard Specimens

Results of emission spectrographic analysis								Results of mass spectrometric analysis				
Addition ^{13}C at %	Determine ^{13}C at %	n	$\bar{v}$	$\sigma_y = \sqrt{\frac{\Sigma(y-\bar{y})^2}{n-1}}$	$\bar{\sigma} = \frac{\sigma_y}{\sqrt{n}}$	$y \pm t\bar{\sigma}_y$	$\frac{\sigma_c}{C} = 2.3\frac{1}{b}\sigma_y \times 100$ %	Determine ^{13}C at %	n	$\sigma_c = \sqrt{\frac{\Sigma(C-\bar{C})^2}{n-1}}$	$\frac{\sigma c}{C} \times 100$ %	$\frac{C_{ES}-C_{MS}}{C_{ES}} \times 100$
1.06	2.20	4	0.470 2	0.031	0.015	(0.470—2) ±0.049	6.2	2.20	7	0.01	0.45	0.0
2.14	3.28	5	0.670 2	0.022	0.010	(0.670—2) ±0.028	4.4	3.02	4	0.01	0.33	7.9
3.21	4.35	5	0.814 2	0.010	0.005	(0.814—2) ±0.013	2.0	4.20	6	0.02	0.47	3.4
5.32	6.46	5	1.013 2	0.017	0.007	(1.013—2) ±0.021	3.4	5.97	7	0.01	0.75	7.5

n — No. of measurements

Y — Logarithm of the ratio of intensities of the analytical bands: $\log \frac{I_{isot}}{I_{stand}}$

t — Constant depending on the degrees of freedom σ^-, tolerance computed for a 95% level of probability

$\frac{\sigma c}{c}$ — Variation coefficient for single determination of ^{13}C concentration

b — Slope of analytical curve. In this case b = 1.15

lyzed specimen), we identified the isotope radical band $^{12}C^{13}C$ (1, 0) $\lambda =$ $= 4744.5$ Å in the specimens with natural ^{13}C isotope ratio as well.

Under these conditions the content of ^{13}C in the enriched specimens was determined quantitatively by the addition method. The ^{13}C content of the commercial $BaCO_3$ used as diluent for making specimens was thereby determined as 1.14 at %.

After all corrections, the data were used to plot an analytical curve. The results were analyzed statistically. The mean variation coefficient for ^{13}C concentrations 10 at % was 5%.

The same specimens were investigated by mass spectrometry and agreement was satisfactory.

The method for the quantitative determination of ^{13}C ratio developed here has particular advantages. Specimens are prepared simply and relatively quickly. The chamber designed for work under reduced pressure proved to be suitable. The relatively small volume (about 200 cm^3) and reduced pressure make large amounts of specimen unnecessary.

This emission spectrographic method for the determination of ^{13}C. can be very successfully applied for concentrations of ^{13}C below 10 at %, with a variation coefficient of 5%, as good as obtained with the other more complex methods of spectro-isotopic analysis.

School of Sciences
Department of Physical Chemistry
Belgrade University

Received 28 February 1969

REFERENCES

1. Birge, R. T. "Further Evidence of the Carbon Isotope Mass-13" — *Nature* 124: 182, 1929.
2. King, A. S. and R. T. Birge. "An Isotope of Carbon, Mass-13" — *Nature* 124: 127, 1929.
3. King, A. S. and R. T. Birge. "Evidence from Band Spectra of the Existence of a Carbon Isotope of Mass-13" — *Astrophysical Journal* 72: 19, 1930.
4 Steubing, W. and R. Günther. "Die Mesgenauigkeit der Spektroskopischen Isotopenbestimmung am Kohlenstoff" — *Osterreichische Chemiker-Zeitung* 55 (76), 1954.
5. Ferguson, R. E. and H. P. Broida. "Stable Carbon Isotope Analysis by Optical Spectroscopy" — *Analytical Chemistry* 28: 1436, 1956.
6. Zaĭdel', A. N. and I. V. Ostrovskaia. "Spektroskopicheskoe opredelenie izotopnogo sostava ugleroda" (Spectroscopic Determination of the Isotopic Composition of Carbon) — *Optika i spektroskopiia* 9: 137, 1960.
7. Mioč, U. "Proučavanje uslova za primenu Swan-ovih traka, dobivenih eksitacijom u luku, u kvantitativnoj spektrohemijskoj analizi" (Conditions for the Application of the Swan Bands from Arc Excitation to the Quantitative Spectrochemical Analysis) — *Glasnik Hemijskog društva* (Beograd) (2—3—4), 1969.
8. Mioč, U. *Eksperimentalno istraživanje metode detekcije i odredivanje ^{13}C korišćenjem lučne eksitacije C_2 traka* (Methods of Detecting and Determining ^{13}C Using Arc Excitation of the C_2 Bands — Experimental Research) (Thesis) — Beograd, 1968.
9. Wickman, F. E., R. Blix, and H. von Ubisch. "On the Variations in the Relative Abundance of the Carbon Isotopes in Carbonate Minerals" — *Journal of Geology* 59: 142, 1951.
10. Ivanov, N. P. "Spektral'noe opredelenie urana metodom izotopnykh dobavok" (Spectral Determination of Uranium by Isotopic Addition Method) — *Izvestiia ANSSSR, seriia fizicheskaia* 23: 1154, 1959.

GLASNIK HEMIJSKOG DRUŠTVA, Vol. 34, No. 5-6-7, 1969, pp. 313—326

GHDB-65

533.92:621.039.617:661.938:66.093.3.

Original Scientific Paper

THE RADIAL TEMPERATURE DISTRIBUTION IN A DC ARC IN NITROGEN ATMOSPHERE UNDER CONDITIONS USED IN SPECTROCHEMICAL ANALYSIS

by

BOŠKO V. PAVLOVIĆ, NATALIJA N. IKONOMOV, and VLADIMIR M. VUKANOVIĆ

The application of emission spectroscopy, which today represents the most widely used procedure in many analytical laboratories, calls for a thorough knowledge of the processes taking place in the source light, i.e. in a plasma. Study of these phenomena also contributes to the new discipline of the physical chemistry of plasma. Three essential approaches to this discipline may be noted concerning the plasma of electric arc. First, with regard to the conditions for excitation and ionization of particles of given elements is it necessary to study the basic parameters of the plasma, such as temperature and electron density, and the spatial distribution of these parameters. Second, the characteristics of the plasma do not depend only on the physical parameters, such as the arc current, but also its chemical composition, particularly on the chemical reactions taking place at high temperatures. Hence the need arises to study the composition of plasma and the processes of dissociation and recombination of atoms, radicals and molecules. Third, the characteristics of the arc plasma, themselves largely conditioned by chemical factors, will govern not only the excitation of particles of the investigated elements but also the mass transport and the time particles stay in the plasma, which all go to determine the intensity of spectral lines.

The present study deals with arc in nitrogen atmosphere. Nitrogen was taken as the simplest atmosphere and the one closest to air. Generally, spectrochemical determinations are made in air at atmospheric pressure.

From the composition of nitrogen plasma at temperatures of arc discharge and the behavior of individual components, general conclusions about nitrogen plasma are drawn. The thermal conductivity of the plasma is considered as an essential factor and an approximate method for its calculation is given. A comparison with literature data fully justifies the procedure applied.

On the basis of the calculated thermal conductivity of the plasma, first the theoretical prediction of the temperature distribution is approached. Central to the theoretical approach is the Elenbaas-Heller energy balance equation for a plasma. Electric power fed to the arc is transported primarily

by thermal conductivity, while other modes of energy transfer, such as by irradiation or magnetic self-compression[1], can be neglected under the given conditions. Here we are not interested in the specially stabilized arc as is used for physical research, but the free-burning arc[2] used in standard spectrochemical practice. The walls of the arc tube, which to a considerable extent define the diameter of the arc model observed, are replaced by an unbounded convective concentric air current. To this arc model we apply Maecker's solution[3] of the Elenbaas-Heller equation, and then introduce the calculated thermal conductivity. Finally the theoretically obtained curve of the radial temperature distribution is compared with the experimental curve.

COMPUTING THE PARAMETERS NEEDED TO SOLVE THE ENERGY BALANCE EQUATION OF THE PLASMA

(a) *Mean Free Path* — For the concentration of particles in nitrogen plasma under a pressure of 1 atm and in the temperature range 1000—10000°K, data from the literature[4, 5] were used: they show some slight differences concerning the electron densities at higher temperatures. The graph in Fig. 1 shows the particle density according to the literature[4]. It may be seen from the graph that N_2 molecules predominate up to 5000°K, and the concentration of other components may be neglected. Above 5000°K the concentration of atomic nitrogen is of the same order of magnitude as that of molecular nitrogen. However, above 7000°K the density of N_2 molecules decreases while that of N^+ ions and electrons is significant, so that the plasma must be treated as a multicomponent system when considering transport phenomena.

Effective velocities (v) of particles in the plasma were calculated from the kinetic theory expression $v = (3kT/m)^{1}/_{2}$. The effe tive velocities of N_2, $N(N^+)$ and e particles in plasmas of different temperature are shown in Fig. 2.

To determine the mean free path it is necessary to know the cross sections for the varied types of elastic collisions .The first group comprises the collisions that may be treated by kinetic theory, collisions between neutral particles, i.e. between nitrogen molecules, nitrogen molecules and atoms, and between nitrogen atoms. The kinetic theory cross sections for these collisions are[6]:

$$Q_{\uparrow N_2}^{N_2} = 8.10^{-16} \ cm^2$$

$$Q_{\uparrow N}^{N_2} = \frac{Q_{\uparrow N_2}^{N_2}}{1.085}$$

$$Q_{\uparrow N}^{N} = \frac{Q_{\uparrow N_2}^{N_2}}{1.18}$$

The temperature dependence of kinetic theory cross sections Q was computed using

$$Q = \left(1 + \frac{C}{T}\right) 8 \cdot 10^{-16} \ cm^2 \qquad (1)$$

where the value of Sutherland's constant used was $C = 113°K$.

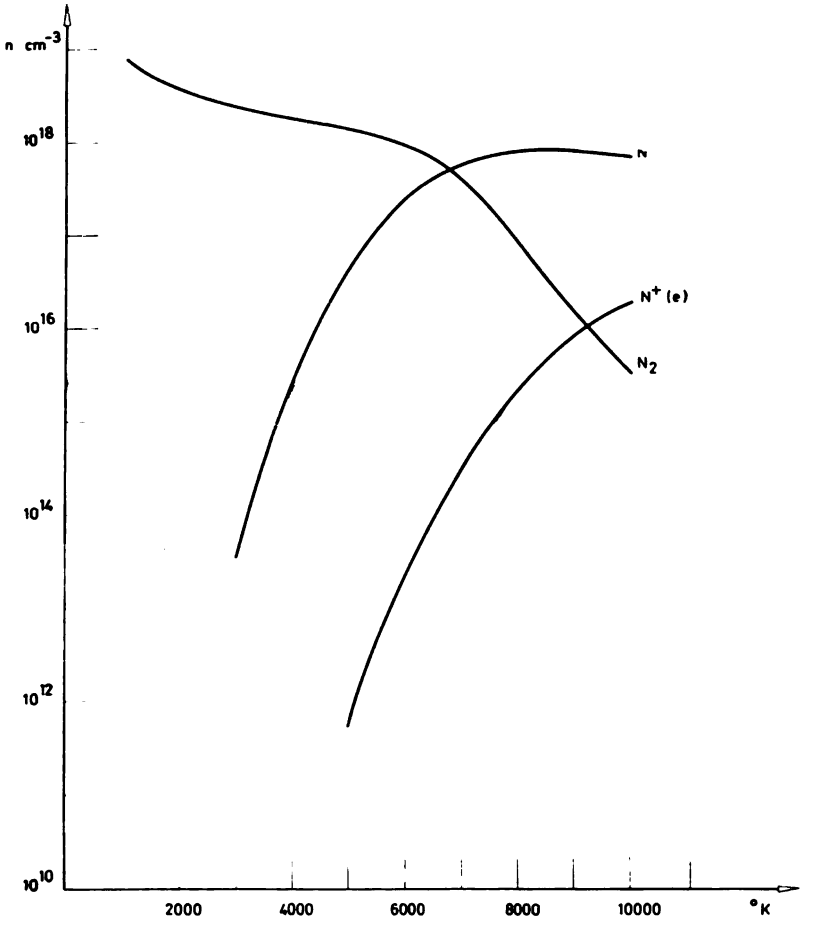

Figure 1
The nitrogen plasma composition after Burhorn and Wienecke [4]

For collisions between neutral particles and electrons the Ramsauer cross sections were used. In the temperature range up to 10000°K[6] they are

$$Q_{e\uparrow}^{N} \simeq Q_{e\uparrow}^{N_2} \simeq 2 \cdot 10^{-15} \ cm^2.$$

For collisions between charged particles we took Gvozdeverov cross sections according to the expression given by Burhorn[6]:

$$Q_G = \frac{e^4}{(kT)^2} \ln \frac{kT}{e^2 n_+^{1/3}} = \frac{6430}{T^2} \cdot 10^{-9} \log \frac{T}{n_+^{1/3}} \qquad (2)$$

where e = electron charge n^+ = density of positive ions

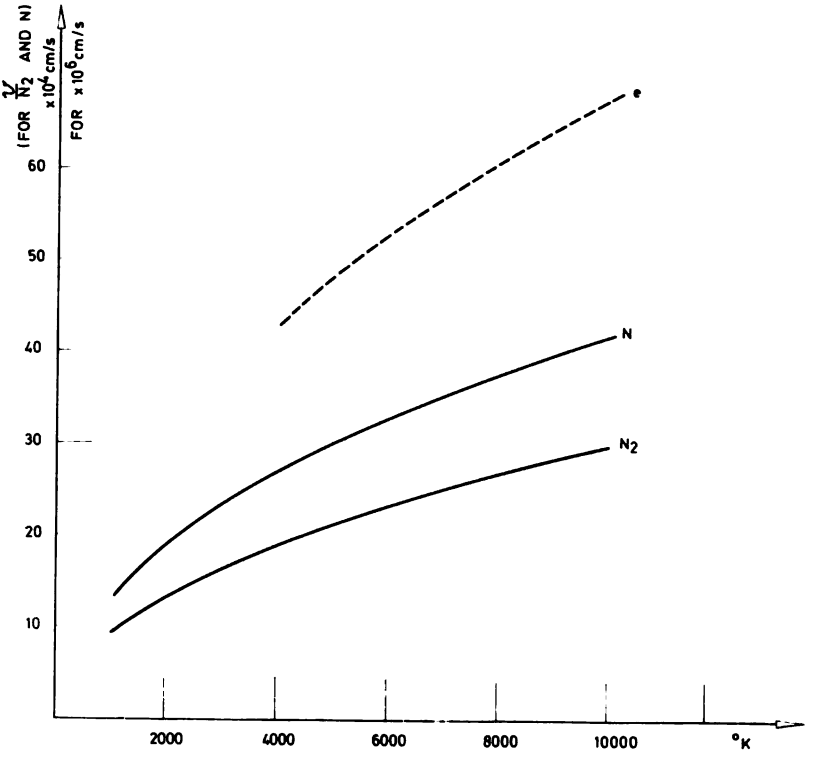

Figure 2
The root mean square velocities

Knowing the cross sections for the collisions of particles in the nitrogen plasma, their concentrations n and masses m, we determined the mean free paths λ. Since the plasma contains several kinds of particle which come into different kinds of collision, the expression used to calculate the mean free path is

$$\lambda_1 = \left[\sum_{i=1}^{k} \left(1 - \frac{1}{2} P_{li}\right) n_i Q_{li} \left(1 + \frac{m_l}{m_i}\right)^{1/2} \right]^{-1} \qquad (3)$$

where λ_l is the mean free path for the particle of species l

n_i = concentration of particles of the i-th species relative to which collisions are observed

Q_{li} = cross section of l for i particles

m_l, m_i = mass of single particles of species l and i

P_{li} is a persistance calculated from the expression

$$P_{li} = \frac{m_l - 0.2\, m_i}{m_l + m_i} \tag{4}$$

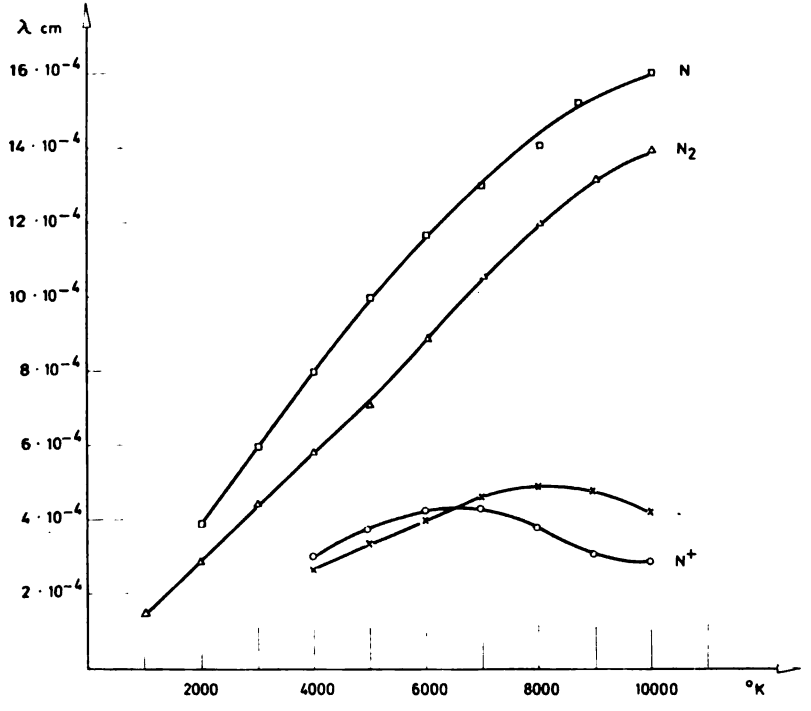

Figure 3

The mean free paths

Figure 3 shows the mean free path for the particles in nitrogen plasma at 1 atm in the temperature range 2000—10000°K.

(b) *Diffusion Coefficients* — Neutral particles (molecules, atoms) and charged particles (ions, electrons) diffuse because of concentration gradients from one zone of the plasma to another. Atoms and ions diffuse from the hotter inner zones out to the cooler zones. This results in recombination, liberating energy. On the other hand, molecules and atoms diffuse the outer,

cooler zones into the hotter inner zones of the plasma in which dissociation and ionization take place. Account must also be taken of the ambipolar diffusion, i.e. of the effect of the electric field in the plasma which originates because of the different mobility of electrons and ions.

Since the nitrogen plasma is a complex system which consists of several components, the treatment of diffusion is also very complex. On the one hand, the literature only gives data for temperatures up to 3000°K[7], where practically speaking only molecules exist, and the concentration of other particles (atoms, ions and electrons) can be neglected. On the other hand, when the problem of transport phenomena in ionized gases is considered, the literature only refers to monoatomic gases[8]. For this reason, to determine the coefficient of diffusion in a multicomponent mixture which contains N_2, N, N^+ and e, we used an approximate method. First we found the binary diffusion coefficients D_{li} of particles of species l in i, applying the relation

$$D_{li} = \frac{1}{3} \frac{n_l \lambda_i v_i + n_i \lambda_l v_l}{n_l + n_i} \tag{5}$$

If diffusion involves charged particles, then the coefficient of ambipolar diffusion is employed:

$$D_{amb(li)} = 2 D_{li}$$

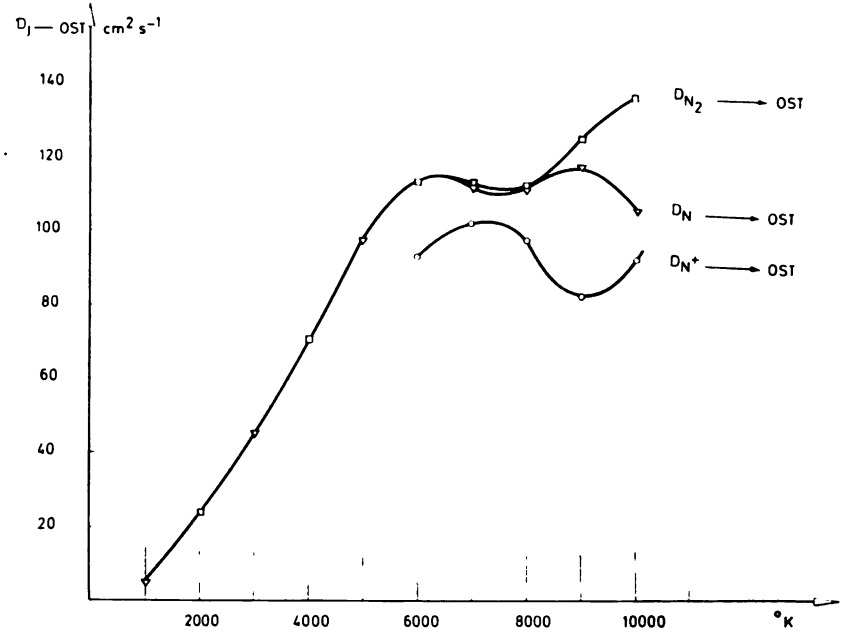

Figure 4

Diffusion coefficients in the nitrogen plasma

Using the graphical data shown in Figs. 1, 2 and 3, the binary diffusion coefficients were calculated according to the two expressions stated above.

All components of the plasma diffuse one into another, so that only the proportion of diffusion of particles of species j into the others need be considered. These diffusion coefficients $D_{j\longrightarrow rest}$, which are shown in Fig. 4, were calculated as

$$D_{j\to rest} = \sum_{\substack{i=1\\ i\neq j}}^{k} \frac{n_i m_i}{\sum n_i m_i} D_{j\to i} \tag{6}$$

(c) *Thermal Conductivity* — Since all particles in the plasma take part in the overall transport of thermal energy, to determine the thermal conductivity by the formula used in our approximate procedure

$$\varkappa = c_p \rho D \tag{7}$$

where c is specific heat, ρ density of plasma particles and D diffusion coefficient, it is necessary to find a diffusion coefficient D which must contain

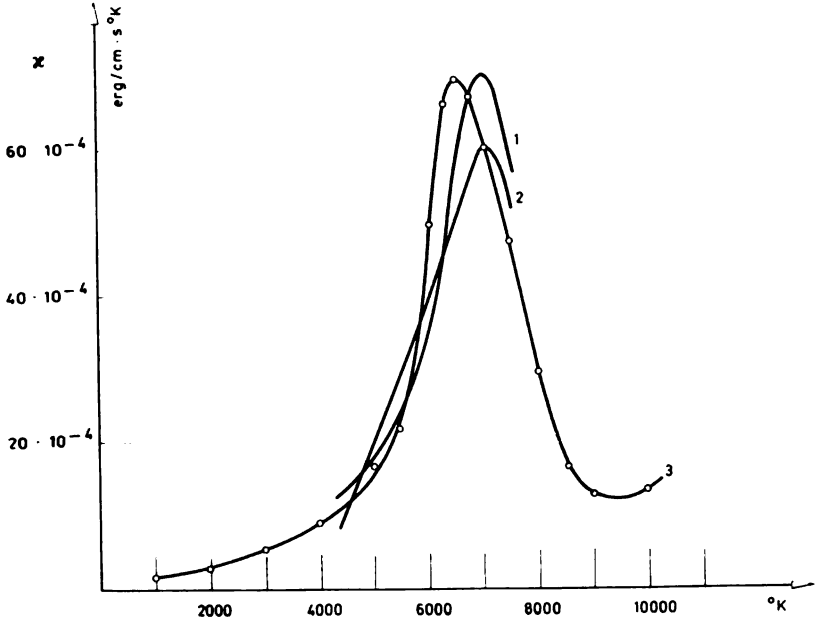

Figure 5

The nitrogen plasma heat conductivity

1. Wienecke [9];
2. Finkelnburg and Macker [10];
3. own data

in itself all the diffusion coefficients for the component particles contained of the plasma. We calculated D by weighing each diffusion coefficient $D_{j \longrightarrow rest}$ and summing.

As the values for c_p and ρ were known from the literature[4], we able to calculated the thermal conductivity within the temperature range 2000——10000°K. Figure 5 shows the values for $\varkappa$ compared with the results of other authors[9, 10]. We took into consideration the contribution of electrons to thermal conductivity, which only becomes significant at temperatures above 8000°K, using the expression[11]

$$\varkappa_e = \frac{2}{3} n_e \lambda_e v_e k(1+x) \tag{8}$$

where k = Boltzmann constant

x = degree of ionization

(e) *Electrical Conductivity* — Here we used the formula

$$\sigma = \frac{n_e e^2 \lambda_e}{m_e v_e} \tag{9}$$

where e = electron charge

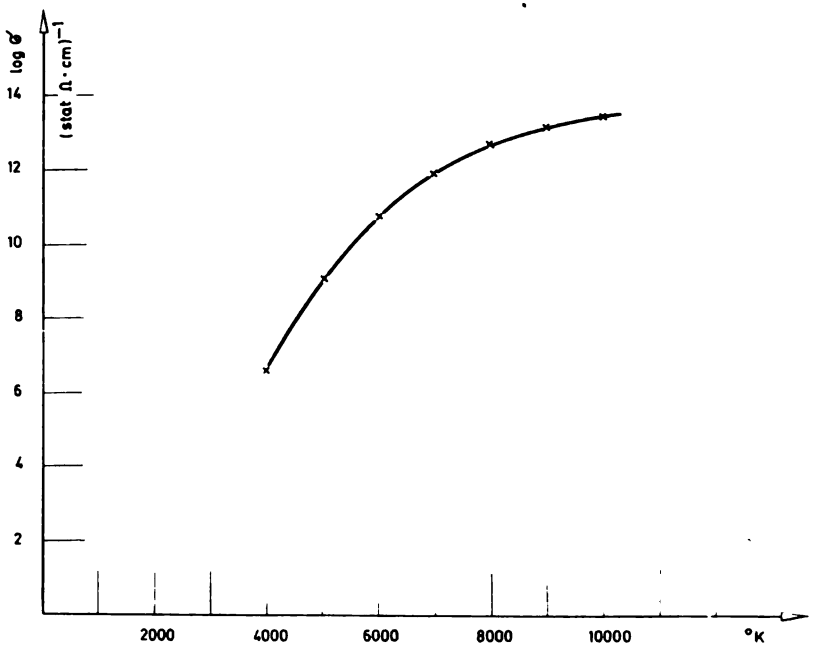

Figure 6

The nitrogen plasma electric conductivity

Data for the electrical conductivity of the nitrogen plasma are given graphically in Fig. 6.

ENERGY BALANCE OF THE PLASMA AND COMPUTING THE RADIAL TEMPERATURE DISTRIBUTION

The energy balance of the plasma of an electric arc is expressed by the Elenbaas-Heller equation which equates electric power per unit volume fed to the system and the heat conducted out of the system:

$$\sigma(T)E^2 = -\frac{1}{r}\frac{d}{dr}\left(r\varkappa\frac{dT}{dr}\right) \tag{10}$$

where $\delta(T)$ = electrical conductivity
E = electric field
r = distance from the arc axis

This equation can only be solved after introducing the variable S (T) which is related to the thermal conductivity as follows:

$$\text{grad } T = \text{grad } S \tag{11}$$

so that the equation above may be written

$$\sigma E^2 = -\frac{1}{r}\frac{d}{dr}\left(r\frac{dS}{dr}\right). \tag{12}$$

For a free-burning arc, Maecker's method for solving this equation is applied. The central zone of the arc is characterized by the existence of electrical conductivity; in the peripheral zone, in which the temperature falls off to room temperature, the concentration of electrons is so small that it can be neglected. Thus the environment of the plasma, down to room temperature, is also effectively included into consideration.

The function S for the central zone has the form

$$S = S_0 - 3f_1S_0[1 - I_1(x)] \tag{13}$$

and for the peripheral zone

$$S = -3zf_1S_0 \ln\rho \tag{14}$$

S_0 = value of S on the axis of the plasma

$$f_1 = \frac{\int_0^{S_0}\int_0^{S}\sigma\,dS\,dS}{\int_0^{S_0}\int_0^{S}\sigma\,dS}\quad;\quad Z = 1.2484;\quad \rho = \frac{r}{R};$$

$I_0(x)$ is the first order Bessel function
R = radius of the plasma

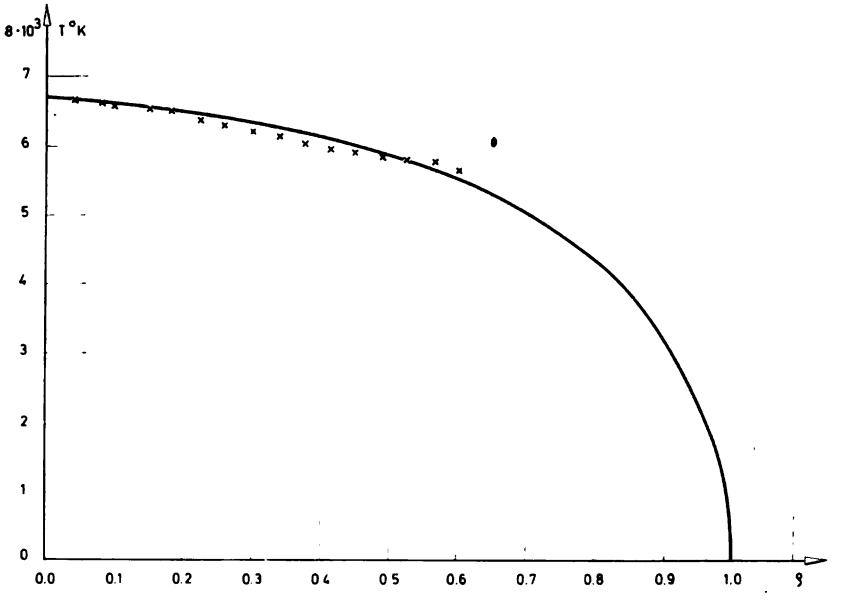

Figure 7

The radial distribution of temperature in the electric arc plasma in nitrogen
——— — theoretical; xxxxx — experimental

Knowing the S function it is possible to get the radial temperature distribution of the free-burning arc. We calculated it using the calculated values for the thermal and electrical conductivity (Fig. 7).

EXPERIMENTAL

A grating spectrograph (Zeiss PGS-2) with a 40 μ × 14 mm slit and Ilford N 30 plates were used. The arc burned in a closed vessel with quartz windows. Purified nitrogen flowed slowly through this apparatus (10 lit/h). The spectrophotography setup was the same as in an earlier study[12]. Since a Dove prism was used the projection of the arc on the slit was turned through 90°. The slit width determined the cross section of the arc observed. It was centered on the middle of the interelectrode space.

The lower electrode, the anode, contained 10 *mg* of carbon powder with traces of ZnO and MgO. The lines ZnI 3072 *Å* and ZnI 3076 *Å* were used to determine the temperature of the arc. Transition probabilities were taken from the literature[13]. These zinc lines were traced by photometer along their whole length and absorbances were converted into intensities. From the intensity distribution obtained in this way the radial distribution of radiation density was computed according to the Abel integral, which was solved using tables[14] on an Eliot 703 electronic computer. From the

calculated radiation densities of the zinc lines the radial temperature distribution in zones of 0.025 *mm* was obtained. The distribution is plotted in Fig. 7.

DISCUSSION

It may be seen that one of the main factors governing the radial temperature distribution is the thermal conductivity, while a major role is played by the energy of reactions which take place in the arc. The marked thermal conductivity maximum (between 6000 and 7000°K) is due to the energy dissociation of N_2 molecules (9.9 eV). Solving the Elenbaas-Heller equation for higher temperatures gives a higher thermal conductivity and a smaller radial temperature gradient.

This radial distribution is highly significant for spectrochemical determinations, as will be shown in a future study[15]. If the reaction energy were much less, the region with lower temperature gradient would be found at considerably lower temperatures, as are only found in the neighborhood of the electrically conducting zone (often referred to as the electric arc plasma). Because of the lower temperature the broad region of temperature gradient would not be useful for excitation of most elements. Furthermore, in this case the electrically conducting zone would be more restricted which would mean a briefer sojourn of particles in the plasma, lower radiation density and lower spectrochemical sensitivity. It also follows from our considerations that a plasma in which chemical reactions do not take place (the case with the noble gases) cannot have any broad low temperature gradient region. Generally in this case the distribution temperature is steep, which again means a shorter time spent by the particles in the plasma and hence a lower spectrochemical sensitivity.

On the other hand, the recombination energy of nitrogen is relatively great, while the broad region of low radial temperature gradient covers temperatures suitable for the excitation of most elements.

It may be seen from Fig. 7 that the shape of the experimental radial temperature distribution in the free-burning arc agrees very well with the theoretical distribution. This confirms not only the correctness of the described solution of the Elenbaas-Heller equation for the energy balance of the plasma but also the accuracy of the procedure for calculating the thermal conductivity as a function temperature, and hence also justifies the procedure for calculating the diffusion coefficient. The approximate method for calculating the thermal conductivity applied here enables an easy approach to the theoretical consideration of the energy balance of the plasma, while the agreement between theory and experiment indicates that it may be applied to other systems as well. In this way theoretical information may be obtained concerning the usefulness of using a particular atmosphere in arc spectral analytical determinations (of course, an account must also be taken of other parameters as well as energy, e.g. molecular emission spectra in the observed spectral region).

Institute of Chemistry, Technology
and Metallurgy
Belgrade

Received 18 December 1968

REFERENCES

1. Maecker, H. "Zur Prüfung der Bogentheorie. Der Wirkungsquerschnitt der Luft bei höheren Temperaturen" — *Zeitschrift für Physik* 128: 289—294, 1950.
2. Sperling, J. "Das Temperaturfeld im freien Kohlebogen" — *Zeitschrift für Physik* 128: 269—278, 1950.
3. Maecker, H. "Über die Charakteristiken zylindrischer Bögen" — *Zeitschrift für Physik* 157: 1—29, 1959.
4. Burhorn, F. and R. Wienecke. "Plasmazusammensetzung, Plasmadichte, Entalpie und specifische Wärme von Stickstoff, Stickstoffmonoxyd und Luft bei 1, 3, 10 und 30 Atm im Temperaturbereich zwischen 1000 und 30000°K" — *Zeitschrift für physikalische Chemie* 215: 269—284, 1960.
5. Irmer, J. and M. Worm. "Die Zusammensetzung eines Stickstoffplasmas im Temperaturbereich von 1000—12000°K bei Drucken von 1 . . . 50 Atm" — *Zeitschrift für physikalische Chemie* 231: 215—227, 1966.
6. Burhorn, F. "Berechnung und Messung der Wärmeleitfähigkeit von Stickstoff bis 1300°K" — *Zeitschrift für Physik* 155: 42—58, 1959.
7. Walker, R. and A. Westenberg. "Molecular Diffusion Studies in Gases at High Temperature. IV. Results and Interpretation of CO_2-O_2, CH_4-O_2, H_2-O_2, CO-O_2 and H_2O-O_2 Systems" — *Journal of Chemical Physics* 32: 436—442, 1960.
8. Devoto, R. "Transport Coefficients of Partially Ionized Argon" — *Physics of Fluids* 9: 354—363, 1966.
9. Wienecke, R. "Experimentelle und Theoretische Bestimmung der Wärmeleitfähigkeit des Plasmas" — *Zeitschrift für Physik* 146: 39—58, 1956.
10. Finkelnburg, W. and H. Maecker. *Handbuch der Physik XXII* — Berling: Spinger-Verlag, 1956, pp. 254—444.
11. Waldmann, L. "The Theory of Lorenz Gas Mixtures" — *Zeitschrift für Naturforschung* (5a): 322—327, 1955.
12. Vukanović, D. "Entmischungseffekt im Plasma des Gleichstrombogens" — *Spectrochimica Acta* 22: 815—824, 1966.
13. Boumans, P. W. J. M. Enkele fundamentele aspecten van de spectrochemische analyse met de gelijkstroomboog — *Diss.* Univ. Amsterdam 1961, pp. 75—76.
14. *Tabellen für Lösung der Abelschen Integralgleizung* — Berlin: Physikalisch-Technisches Institut, Akademie-Verlag, 1960.

GLASNIK HEMIJSKOG DRUŠTVA, Vol. 34, No. 5-6-7, 1969, pp. 327—344

GHDB-66

533.92:621.039.617:661.938

Original Scientific Paper

RADIAL TEMPERATURE DISTRIBUTION IN A DC ARC IN A MIXTURE OF NITROGEN AND WATER VAPOR

by

NATALIJA N. IKONOMOV, VLADIMIR M. VUKANOVIĆ, and BOŠKO V. PAVLOVIĆ

The effect of water vapor on the plasma of an arc burning in a nitrogen atmosphere will be described. First the question arises as to the principle causes of the changes in the features of the plasma induced by water vapor.

The effect of water cooling on the environment of an arc plasma is well known. However, keeping this influence in mind, we seek the causes of changes in the plasma characteristics above all in the plasma itself. The composition of nitrogen plasma[1] is compared with that of a plasma of water vapor components in Fig. 1. The nitrogen plasma at arc temperatures mainly consists of N_2 molecules and N atoms, while the water vapor plasma contains H and O atoms and OH radicals. What is changed if some of the nitrogen atoms and molecules are replaced by H and O atoms and OH radicals, the total pressure remaining constant at 1 atmosphere so that the total number of particles depends only on temperature.

The ionization energies E_I for N_2 and N and those for H, O and OH do not greatly differ: $E_{I\,(N_2)} = 14.5$ eV, $E_{I\,(N)} = 15.6$ eV, $E_{I\,(H)} = 13.6$ eV, $E_{I\,(O)} = 13.6$ eV, and $E_{I\,(OH)} = 13.2$ eV. However, the dissociation energies E_D of the nitrogen molecule $E_{D(N_2)} = 9.9$ eV) and of H_2O, O_2, H_2 and OH (5.2, 5.2, 4.6, and 4.5 eV, respectively), show that the plasmas substantially differ in reaction energies. Along with such other factors as the differences in mass, diffusion constants, etc., the differences in reaction energies will essentially affect the thermal conductivity of the plasma.

Because of their influence on thermal conductivity the differences in reaction energies must also affect the radial temperature distribution in the plasma. This is concluded from the energy balance of the plasma, the balance between the electric power fed in and the energy loss due to thermal conductivity[2].

These considerations also suggest the opposite possibility: from the radial temperature distribution of the plasma conclusions may be drawn about the energies of reactions taking place at high temperatures (at this point we only point out this possibility).

Interest in the investigation of processes governing the influence of chemical reactions on plasma is not confined only to the possibility of theoretical prediction of plasma parameters, nor to the study chemical reactions in the plasma — it is also significant for spectrochemical determinations. For example, in the present case of the plasma of an arc burning in nitrogen atmosphere, the intensities of the spectral lines of elements which reach the plasma by evaporation of a sample from the electrodes will certainly be changed by the addition of water vapor because of the changed temperature distribution. The intensity of spectral lines will change not only because ionization and excitation depend on the temperature and electron density of the plasma, but also because the transport of particles, which determines the time during they stay in the plasma[3], will also change.

Before considering the case of added water vapor, first the theoretically ideal case of a plasma composed of water vapor alone must be examined. Here we must know the composition of the plasma at high temperatures, the mean free path, diffusion constants and specific heats to be able to calculate the thermal conductivity of the plasma in the way described earlier[1]. To solve the energy balance equation we must also know the electrical conductivity of the plasma as a function of temperature.

CALCULATION OF THERMAL AND ELECTRICAL CONDUCTIVITY OF WATER VAPOR AT TEMPERATURES OF 2000—10000°K

(1) *Components of Water Vapor Plasma; Root Mean Square Velocities; Collision Cross Sections in Plasma* — The particle density of water vapor components as a function of temperature from the literature data[4] is shown in Fig. 1. Our calculations are based on this distribution.

The RMS velocities v of particles in the plasma were calculated from the standard kinetic theory expressions given in the graph of Fig. 2.

We used the following values for the cross sections of neutral particle collisions[5]:

$$Q^{H_2}_{\uparrow H_2} = 4.8 \cdot 10^{-16}\ cm^2; \qquad Q^{O_2}_{\uparrow O_2} = 7 \cdot 10^{-16}\ cm^2; \qquad Q^{H_2O}_{\uparrow H_2O} = 1 \cdot 10^{-15}\ cm^2;$$

$$Q^{H_2}_{\uparrow H_2} \approx Q^{O}_{\uparrow O} \approx Q^{O}_{\uparrow H} \approx 1.56 \cdot 10^{-15}\ cm^2.$$

To compute the collision cross sections for other neutral particles the formula $Q = \left[\frac{1}{2}(d_1 + d_2)\right]^2 \pi$ was used, where d_1 and d_2 at the observed temperature are kinetic theory diameters of the colliding particles.

The cross section for collisions of OH radicals was taken as equal to that for water molecules.

The dependence of collision cross sections on temperature was determined according to the relationship

$$\frac{Q_1}{Q_2} = \frac{1 + \frac{C}{T_1}}{1 + \frac{C}{T_2}} \qquad (1)$$

where C is Sutherland's constant: $C = 80°K$ for hydrogen, 130°K for oxygen and 650°K for water.

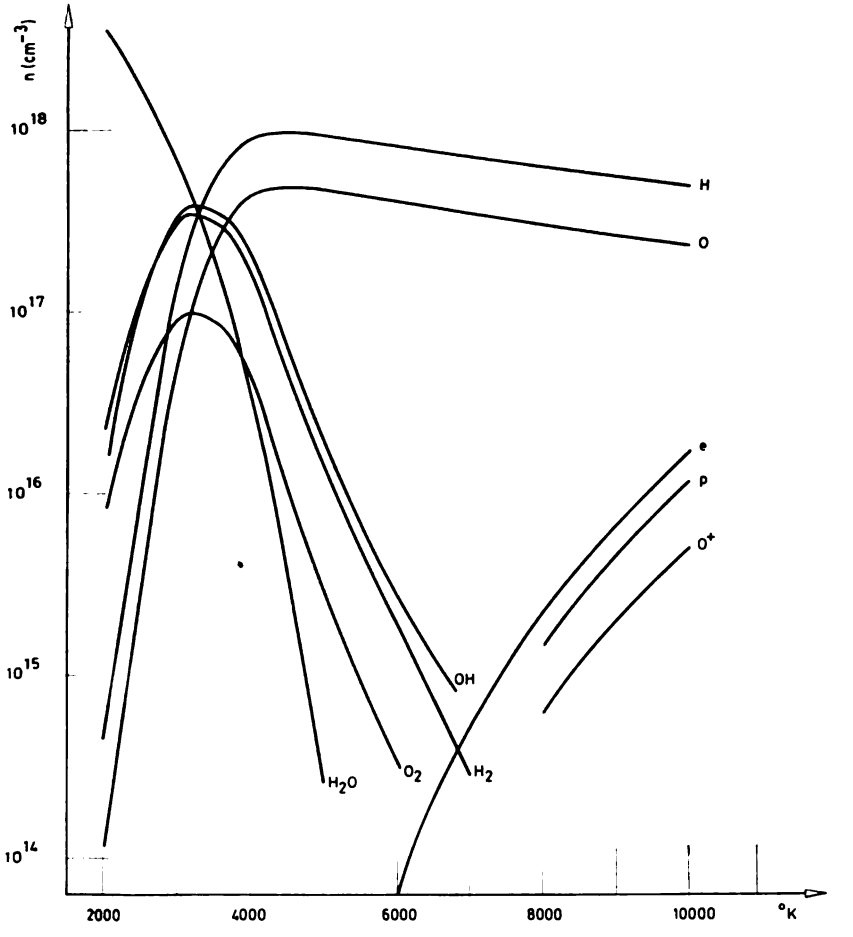

Figure 1

Composition of water vapor plasma at the atmospheric pressure, according to Burhorn and Wienecke [4]

For collisions of atoms and molecules with electrons or ions, these values of Ramsauer's cross sections were used:

$$Q^{i}_{\uparrow H} \approx Q^{e}_{\uparrow H} = 1.3 \cdot 10^{-14}\ cm^2; \qquad Q^{i}_{\uparrow O} \simeq Q^{e}_{\uparrow O} = 2 \cdot 10^{-15}\ cm^2;$$

$$Q^{i}_{\uparrow OH} \simeq Q^{e}_{\uparrow OH} = 2 \cdot 10^{-15}\ cm^2; \qquad Q^{i}_{\uparrow H_2} \simeq Q^{e}_{\uparrow H_2} = 1.2 \cdot 10^{-15}\ cm^2;$$

$$Q^{i}_{\uparrow O_2} \simeq Q^{e}_{\uparrow O_2} = 2 \cdot 10^{-15} cm^2; \qquad Q^{i}_{\uparrow H_2O} \simeq Q^{e}_{\uparrow H_2O} = 2 \cdot 10^{-15}\ cm^2.$$

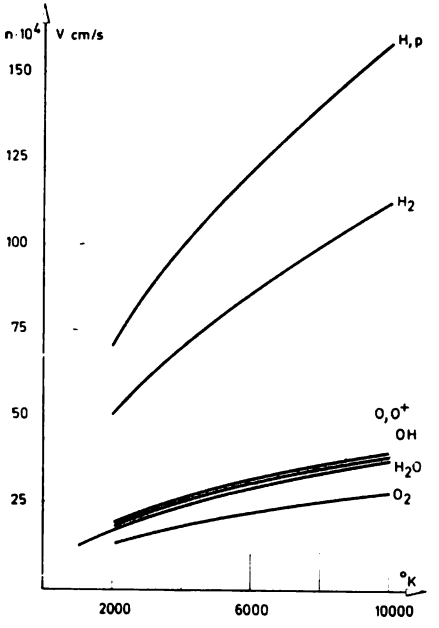

Figure 2
Root mean square velocities

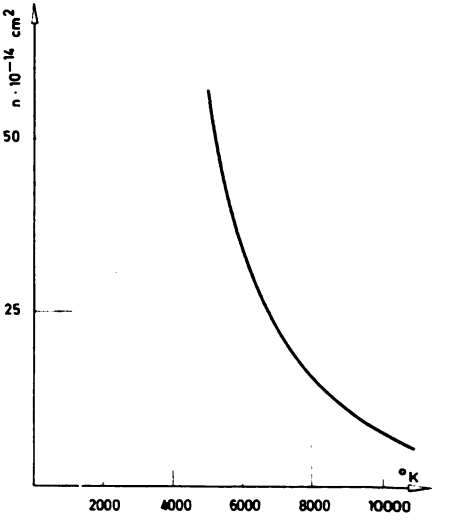

Figure 3
Gvozdover's collision cross sections in water vapor plasma

For collisions between charged particles, Gvozdover's cross sections were used. The graph in Fig. 3 shows the temperature dependence of these cross sections for water vapor plasma.

(2) *Mean Free Path of Particles and Diffusion Coefficients* — Knowing the cross sections for the collisions of particles of water vapor plasma, their concentrations and masses, we can determine the mean free paths using the formula given in our previous paper[1]. Graphs 4a and 4b show the mean free paths for the particles of water vapor plasma at a pressure of $1 \cdot 10^6$ dyn/cm² in the temperature range 2000—10000°K. The mean free path of

the particles in a multicomponent mixture greatly depends on temperature and also on the total number of particles per unit volume of gas at the given moment, on the ratios between particles and on the collision cross sections.

The λ values were calculated only for those particles which occur in sufficient concentrations at the given temperatures (compare graphs 4a, b and 1). Hence λ is not given for H_2O, OH, O_2 and H_2 at temperatures above 7000°K, nor for p and 0^+ at temperatures below 6000°K and 8000°K respectively.

For the determination of diffusion coefficients in a mixture containing H_2O, H_2, O_2, OH, H, O, p, O^+ and e, the method described previously[1] was employed. First the binary diffusion coefficients were calculated and then the diffusion coefficients $D_{j \longrightarrow rest}$. The diffusion coefficients are

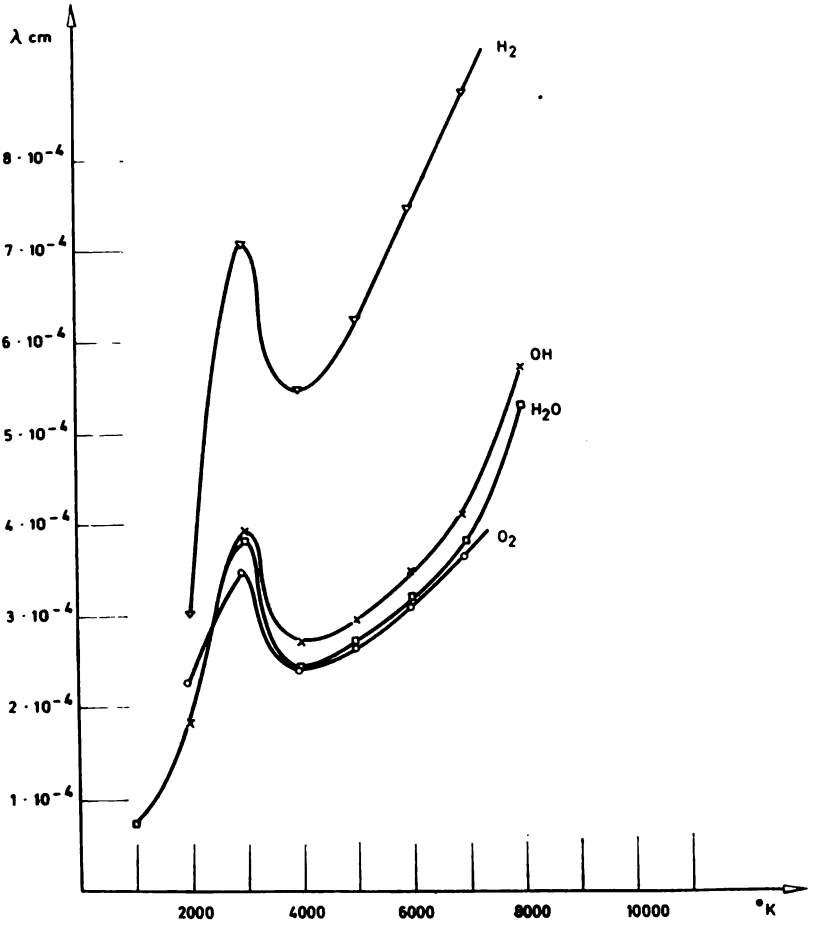

Figure 4

Mean free paths of particles in water vapor plasma

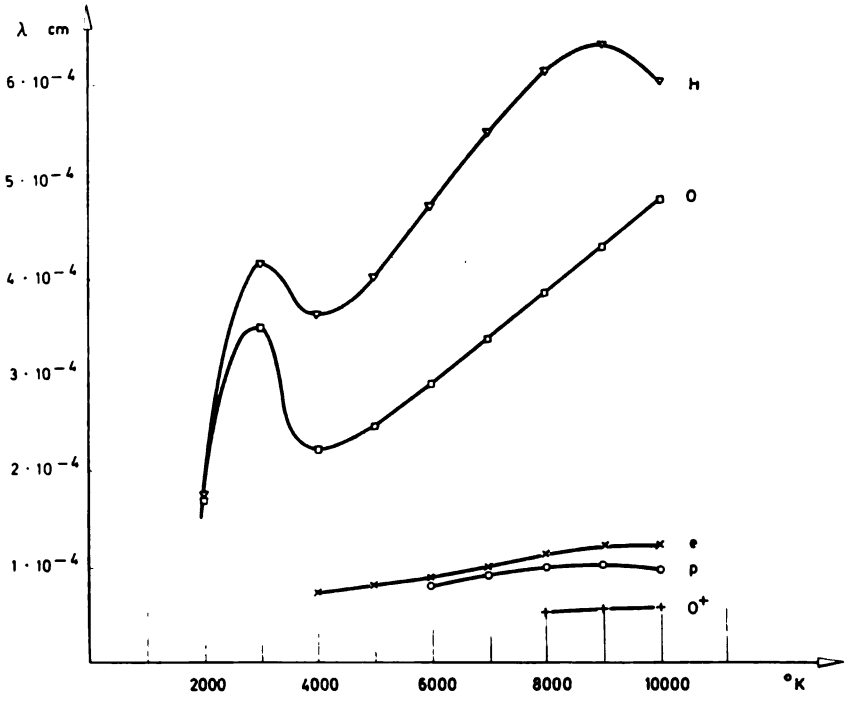

Figure 4b

shown in the graph of Fig. 5. Taking the weighted mean of all the $D_{j \longrightarrow rest}$ the total diffusion coefficient D was obtained:

$T°K$	$D\ cm^2/s$	$T°K$	$D\ cm^2/s$
2000	13.54	7000	93.30
3000	29.99	8000	96.08
4000	33.15	9000	68.87
5000	50.26	10000	42.19
6000	79.76		

(3) *Thermal and Electrical Conductivity of Plasma* — Using the procedure described previously[1] the thermal conductivity of the plasma was computed, from

$$\varkappa = c_p \rho D \qquad (2)$$

where c_p = specific heat at constant pressure
ρ = density of plasma particles
D = diffusion coefficient

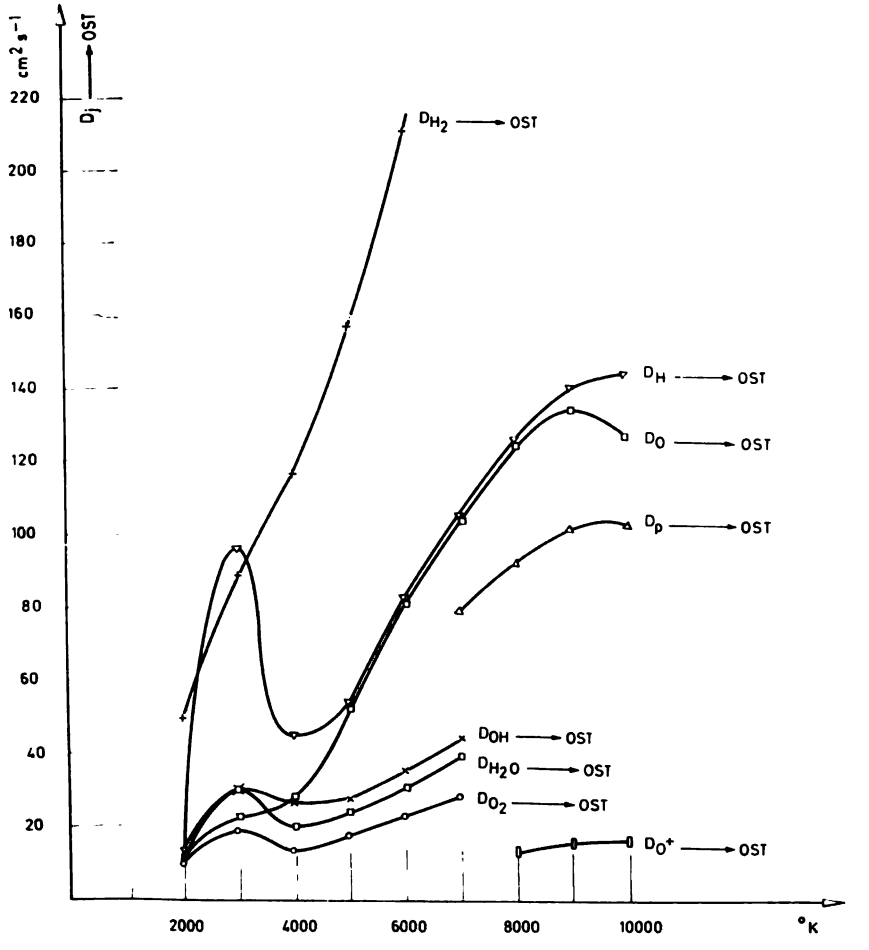

Figure 5

Diffusion coefficients $D_{j \longrightarrow rest}$ in water vapor plasma

The contribution of electrons to the thermal conductivity is very small. It was computed according to the expression

$$\varkappa_e = \frac{2}{3} n_e \lambda_e v_e k (1 + x) \tag{3}$$

where k = Boltzmann's constant
x = degree of ionization

The graph in Fig. 6 shows the values calculated for $\varkappa$. It shows that the thermal conductivity of water vapor is a maximum in the region 3000—

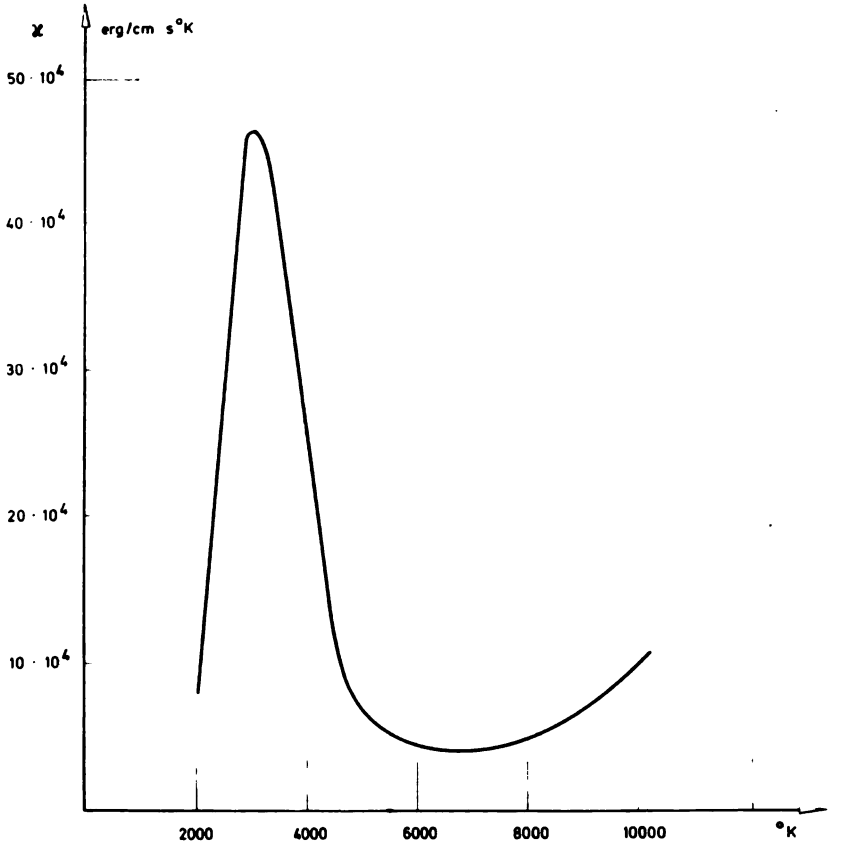

Figure 6
Thermal conductivity of water vapor plasma

—4000°K. The maximum corresponds to the reaction energies of H and O atoms and OH radical recombination.

Electrical conductivity was computed from

$$\sigma = \frac{n_e e_2 \lambda_e}{m_e v_e} \tag{4}$$

Graph 7 shows the calculated electrical conductivity as a function of temperature.

ENERGY BALANCE OF WATER VAPOR PLASMA

The balance between the electric power fed to the arc and the energy given off due to thermal conductivity is expressed by Elenbaas-Heller's equation

$$\sigma(T)E^2 = -\frac{1}{r}\frac{d}{dr}\left(r\varkappa\frac{dT}{dr}\right) \tag{5}$$

where $\sigma(T)$ = electrical conductivity
E = strength of the electric field
r = distance from the arc axis
T = temperature
$\varkappa$ = thermal conductivity

In a previous work[1] we described a solution of this equation for a freely burning arc. Applying Maecker's procedure[2], first we introduce the function S(T), where

$$\varkappa \text{ grad } T = \text{grad } S \tag{6}$$

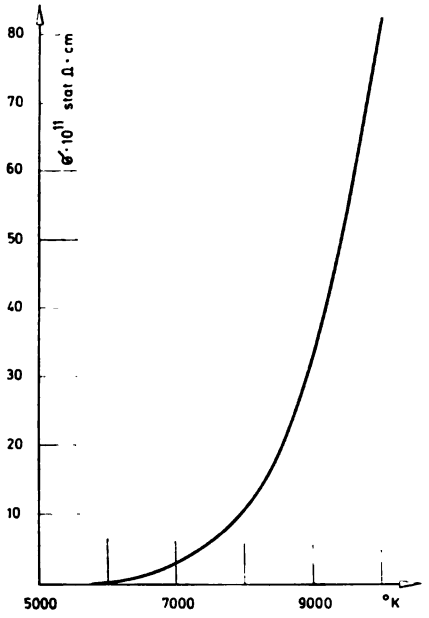

Figure 7

Electrical conductivity of the water vapor plasma

S is given differently for the central zone electrically conducting zone) and the peripheral zone (with negligible concentration of electrons), according to the equations in our earlier paper[1]. The radial temperature distribution in the plasma is calculated according to Eq. (6) from the values obtained for $S(T)$.

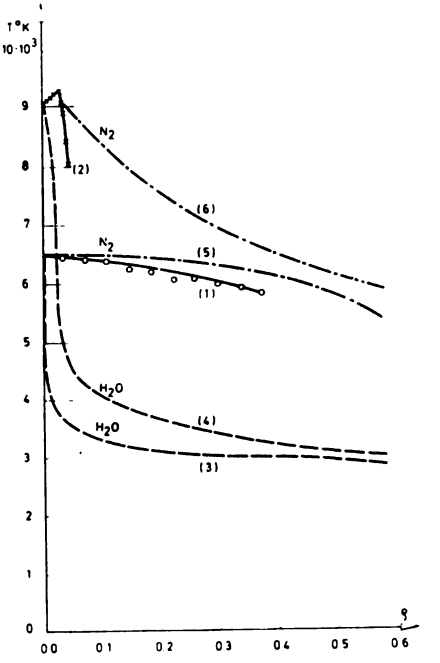

Figure 8

Radial temperature distribution in DC arc in atmospheres of nitrogen, nitrogen and water vapor, and water vapor, as a function of $\rho = r/R$:

Curve 1 Experimentally determined distribution in "nitrogen-like plasma"
Curve 2 Experimentally determined distribution in "water vapor-like plasma"
Curve 3 Theoretical distribution in pure water vapor plasma at an arc-axis temperature of 6500°K
Curve 4 Theoretical distribution in pure water vapor plasma at an arc-axis temperature of 9300°K
Curve 5 Theoretical distribution in pure nitrogen plasma at an arc-axis temperature of 6500°K
Curve 6 Theoretical distribution in pure nitrogen plasma at an arc-axis temperature of 9300°K

Curves 3 and 4 in Fig. 8 show temperature distributions obtained in this way. Curve 3 pertains to a temperature on the arc axis of 6500°K, Curve 4 to 9300°K. The parameter $\rho = r/R$ is plotted on the abscissa, where R is the radius at which the temperature drops to room temperature.

EXPERIMENTAL

To facilitate comparison with the previous results obtained from an arc plasma in pure nitrogen[1], the experimental conditions were kept as close as possible to those in the earlier work. Spectra were recorded on the

same spectrograph (Zeiss PGS-2), with the same slit width (40 μ) and height (14 mm), the same position of the Dove prism to obtain transverse spectrograms, the same electrode shape, and the same 9 A DC arc.

The apparatus in which the arc burned in a slow stream of nitrogen was also similar. However, now a ring electrical heater was placed concentrically below the lower electrode. A groove in this ring contained 1 *ml* distilled water. The time from when the water started boiling to the excitation of the arc was 60 sec; pre-exposure time 3 sec, exposure 1 sec.

The radial distribution of the radiation density was computed from the transverse spectrograms by Abel's integral equation. The temperature was determined from ratio of radiation densities of the lines ZnI 3076 and ZnI 3072 *Å*.

When adding water vapor to the nitrogen atmosphere it was noted that only above a certain amount of vapor resulted in any sudden modification of the arc, with considerably constriction of the plasma. This constriction is illustrated in Figs. 9a and 9b. Figure 9a shows the arc in nitrogen atmosphere, while Fig. 9b shows the constricted arc when water vapor was added to the nitrogen.

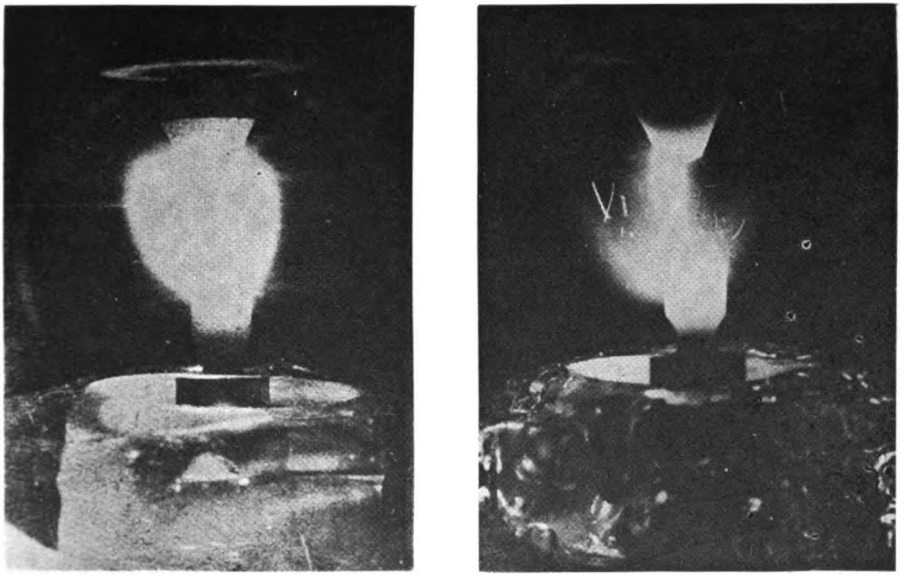

a *b*

Figure 9

Photograph of the arc burning in (a) nitrogen, (b) mixed nitrogen and water vapor

This constriction may also be noted from the transverse spectrograms. Figure 10a shows the spectrogram taken in pure nitrogen, Fig. 10b one in a mixed nitrogen and water vapor atmosphere.

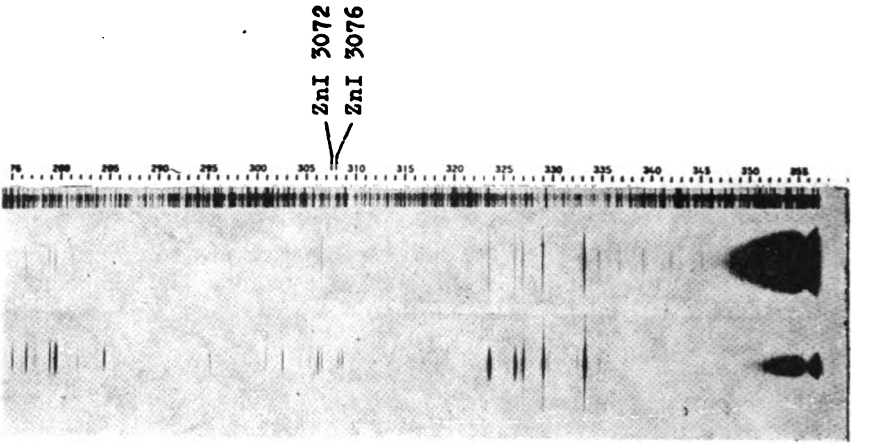

Figure 10

Electric arc spectrograms in (a) nitrogen, (b) mixed nitrogen and water vapor

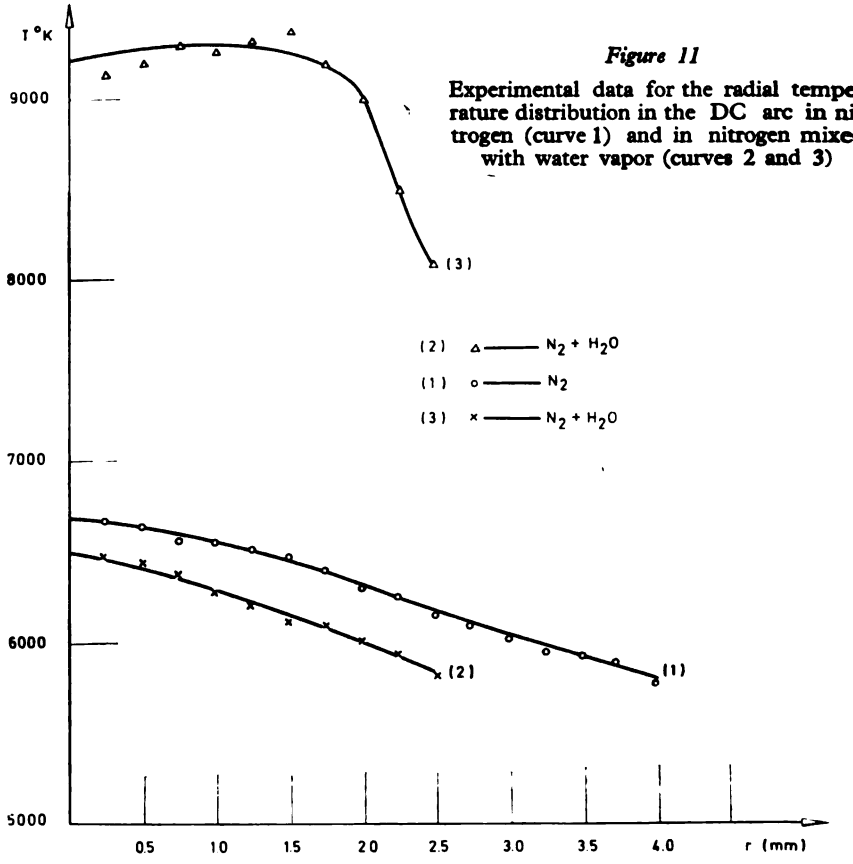

Figure 11

Experimental data for the radial temperature distribution in the DC arc in nitrogen (curve 1) and in nitrogen mixed with water vapor (curves 2 and 3)

It is readily noted from the spectrograms in Fig. 10 that with a sufficient amount of water vapor in the atmosphere the arc plasma temperature rose. In pure nitrogen plasma the ZnI 3072A line, with an excitation potential of 8 eV, was obviously weaker than the ZnI 3076 A line with an excitation potential of 4 eV. However, with water vapor added, the ratio of their intensities was changed in favor of the line with the higher excitation potential.

Radial temperature distributions of the arc plasma in nitrogen atmosphere with water vapor are presented in Fig. 11. For comparison with the earlier results[1], the distribution obtained experimentally in pure nitrogen is also given. Curve 1 is for pure nitrogen, curve 2 for nitrogen plus water vapor but before the constriction of the plasma. After the abrupt transition to this modification, the radial distribution shown by curve 3 was obtained.

The nitrogen atmosphere containing an amount of water vapor not sufficient to cause marked constriction will be called a "nitrogen-like plasma", that after constriction and with the higher temperature a "water-vapor-like plasma".

DISCUSSION

First a comparison will be made between the experimentally found radial temperature distributions in a nitrogen-water vapor mixture and the two theoretically discussed ideal cases for pure water vapor and pure nitrogen. Previously[1] it was shown that there is very good agreement between calculated and measured values for an arc burning in pure nitrogen atmosphere.

Figure 8 presents six curves for the radial temperature distributions as a function of the parameter $\rho = r/R$. Curve 1 is the experimental distribution for a nitrogen-like plasma, curve 2 that for a water-vapor-like plasma. The other four curves are theoretical. As has been stated, curves 3 and 4 are for pure water vapor at temperatures on the arc axis of 6500°K and 9300°K (these were the temperatures measured in nitrogen-like and water--vapor-like plasmas). Curves 5 and 6 are for pure nitrogen at the same temperatures on the arc axis.

It is seen from the graph that the experimental curve for the nitrogen--like plasma, with an axial temperature of 6500°K, does not differ much from the theoretical curve for pure nitrogen, but it is very unlike the theoretical curve for pure water vapor. However, the experimental curve for the water-vapor-like plasma at 9300°K axial temperature differs rather widely from the theoretical curve for pure nitrogen but approximates to that for pure water vapor. It appears the terms we chose to describe the two plasmas are appropriate. The deviation of the experimental curve for the water--vapor-like plasma from the theoretical one for water vapor is explained by the fact that a mixture with nitrogen rather than pure water vapor is involved.

Examining the curve of the radial temperature distribution for water vapor (Fig. 8) and that for the thermal conductivity as a function of temperature (Fig. 6), it may be observed that in the temperature range in which the thermal conductivity is a maximum the radial temperature gradient is conspicuously lower. The same conclusion was drawn for the case of pure nitrogen[1].

The region of high thermal conductivity is actually the zone in which chemical reactions take place; it is determined by reaction energies. Thus, in addition to electrical parameters, the chemical reactions occurring in the plasma essentially govern its characteristics. Conversely, the radial temperature distribution might be employed in principle to get information about the reactions taking place in the plasma.

Constriction of the plasma and rising temperature on the arc axis after addition of water vapor can also be discussed in the context of the thermal conductivity curves. A temperature on the arc axis of 6700°K was experimentally found for pure nitrogen[1]. It corresponds to the maximum of the thermal conductivity as a function of temperature for nitrogen. However, in this domain, raising the concentration of water vapor in the plasma reduces thermal conductivity and the maximum moves down to a lower temperature (Fig. 6). The reduced thermal conductivity raises the temperature gradient and the axial temperature of the arc. The extensive radial zone of the arc with a lower temperature gradient, theoretically predicted, only exists at lower temperatures around the narrow core high temperature. This core here appears as a restricted plasma (Fig. 9b). This interpretation does not rule out the possible action of some other mechanism constricting the plasma and raising the axial temperatures in a given case (e.g. cooling the environment of the plasma).

It may be seen from this discussion that when reacting substances are introduced into the plasma it is possible to theoretically predict the effects of the chemical reactions on plasma parameters. This means that the convenience or inconvenience of a particular effect with regard to sensitivity of spectrochemical analysis may be decided in advance.

Institute of Chemistry, Technology
and Metallurgy
Belgrade
School of Sciences
and
School of Technology and Metallurgy
Belgrade University

Received 11 March 1969

REFERENCES

1. Vukanović, V., N. Ikonomov, and B. Pavlović. "The Radial Temperature Distribution in a DC Arc in Nitrogen Atmosphere under Conditions Used in the Spectrochemical Analysis" — *Glasnik Hemijskog društva* (Beograd) (this number).
2. Maecker, H. "Uber die Charakteristiken zylindrischer Bögen" — *Zeitschrift für Physik* 157: 1—29, 1959.
3. Vukanović, V. "Erfahrungen über den Einfluss der Vorgänge im Plasma bei Spurenanalysen im Lichtbögen" — *Akademie-Verlag* (Berlin) 9—20, 1964.
4. Burhorn, F. and R. Wienecke. "Plasmazusammensetzung, Plasmadichte, Entalpie und spezifische Wärme von Wasserstoff und Wasser bei 1, 3, 10 und 30 atm im Temperaturbereich zwischen 1000 und 30000°K" — *Zeitschrift für physikalische Chemie* 215: 285—292, 1960.
5. Lochte-Holtgreven, W. "Production and Measurement of High Temperatures" — *Reports on the Progress of Physics* 21: 312—313, 1958.
6. Rybakov, V. V. and M. P. Burgasov. *Termodinamicheskii raschët vysokotemperaturnogo gaza* (Thermodynamic Calculations for High-Temperature Gases) — Moskva: Izdatel'stvo "Mashinostroenie", 1968.

GLASNIK HEMIJSKOG DRUŠTVA, Vol. 34, No. 5-6-7, 1969, pp. 345—358

GHDB-67

541.1-16
Original Scientific Paper

THE EMANATION METHOD IN STUDYING SOLID STATE REACTIONS*

by

VLADIMIR BALEK

Present-day study of processes occuring in solids requires the application of various sensitive methods. Radiochemical techniques as well as physical methods are of interest, since they permit different kinds of alterations occuring during phase and chemical transformations and other processes taking place in the solid state to be registered by the liberation of inert radioactive gases.

Inert radioactive gases forming as the result of radioactive decay are often called emanations, and this term is also given to methods of investigation where they are used. The emanation method[1, 2] is based on the introduction of inert radioactive gases into a solid and measurement of their subsequent liberation from the substance (known as the emanating power).

THE INTRODUCTION OF GASES INTO A SUBSTANCE

Labelling can be done in various ways: 1. The classical techniques as suggested by Hahn[1], when trace amounts of the inert gas parent isotope (10^{-11} *g* Th per *g* of solid) are co-precipitated with the solid while it is being prepared. Radioactive gas forms inside the solid as a result of the solid

$$228_{Th} \xrightarrow{\alpha} 224_{Ra} \xrightarrow{\alpha} 220_{Rn} \xrightarrow{\alpha}$$

The inert radioactive gas can also be introduced into a solid by utilising other nuclear reactions or by ion bombardment. In the latter method the radioactive gases radon, krypton, xenon etc. can be introduced directly into the solid. Č. Jech[3] has developed a simple method for introducing inert gases into a substance in a high frequency arc from a Tesla coil for vacuum testing. Ion energy reaches one kev and the penetration depth is 10—30 *Å*, which means that with this method only the surface layers of the solid are labelled.

* Communicated at the 3rd Conference on Ceramics in Electronics, Czechoslovakia, 1968.

2. EMANATION OF GASES FROM THE SOLIDS

A solid body containing atoms of inert radioactive gas is processed in the experimental apparatus of Fig. 1. Its main component is an electric heater with a thermographic unit, heated at a given rate. An activated sample is placed in one aperture of the vessel, while the two others contain an inactive sample for dilatometric analysis and an Al_2O_3 standard for thermography.

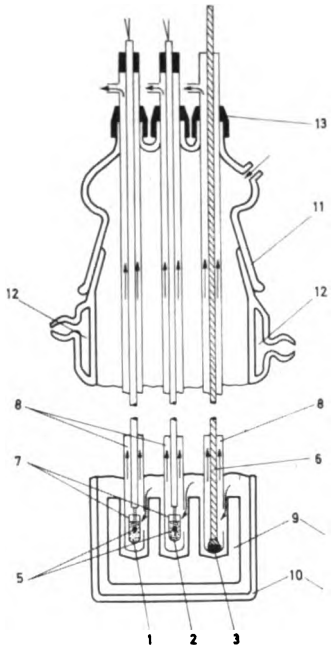

Figure 1

Reaction vessel for emanation measurements 1. Activated sample; 2. DTA standard; 3. dilatometer sample; 5. composite thermocouple; 6. quartz dilatometer rod; 7. quartz vessels; 8. supporting pipes; 9. metal block; 10. quartz outer vessel; 11. ground glass joint; 12. coolant tube.

Emanation, DTA and dilatometry can thus be used simultaneously under identical conditions. The temperature is measured by thermocouples embedded directed into the samples.

Radioactive gases emanating from the activated sample are piped away continuously into the radioactivity measuring chamber (Fig. 3). The apparatus simultaneously registers α activity of radon and the β activity of xenon introduced by ion bombardment. The emanation curve was registered together with the thermograms on a multiple-point electronic potentiometer.

Before giving the results of the experiments, some theoretical relationships describing emanation should be discussed.

The number of atoms emanated from a small crystallite can be written as the sum of two terms[5]:

$$E = \frac{R_0}{4} \cdot \frac{S}{m} \cdot \rho + \sqrt{\frac{D_o}{\lambda}} \cdot \frac{S}{m} \cdot \rho \cdot e^{-\frac{Q^{(1)}}{2RT}} \qquad (1)$$

where Ro is the distance of atomic recoil, ρ is the density of the solid, S is the surface area, Do the coefficient of emanation diffusion, λ is the decay constant of the emanation, m is the mass of the granule, Q is the activation energy of emanation diffusion, R is the gas content, and T is the absolute temperature.

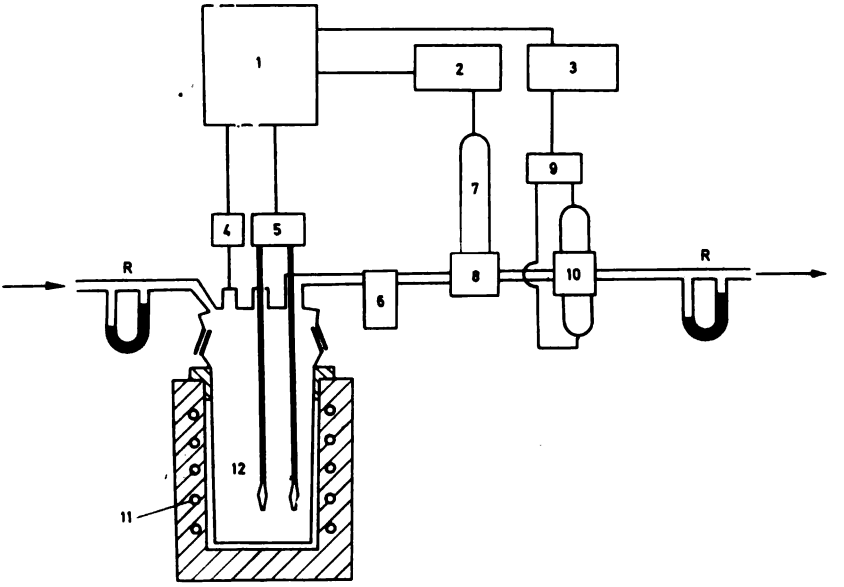

Figure 2

Overall diagram of emanation setup 1. electronic potentiometer; 2. alpha count integrator; 3. beta count integrator; 4. dilatometer pickup; 5. thermocouple; 6. gas dryer; 7. photomultiplier; 8. scintillation chamber; 9. cathode repeater; 10. β emission measurement chamber; 11. electric heater; 12. quartz reaction vessel; R. rheometer.

Figure 3 shows the form of the curve of emanation rate against temperature for a solid which undergoes no chemical or physical change during heating (Al_2O_3 annealed to a high temperature). In this case the curve is exponential, particularly clearly seen on a plot of $\log E = H\left(\frac{1}{T}\right)$. Two segments are obtained: a low temperature segment with a low value of $\frac{\sigma \log E}{\sigma T}$ and a high temperature segment with a high value of $\frac{\log E}{T}$. The knee occurs

at temperatures between 0.4 and 0.52 of the absolute temperatures of fusion, i.e. Tamman temperature. The slopes of the segments can be used to calculate the activation energy of emanation in the given temperature range.

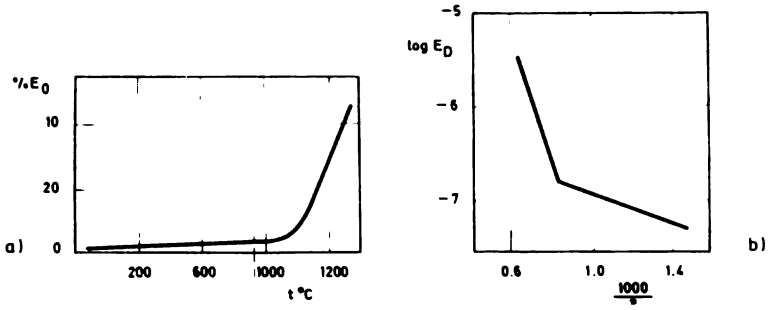

Figure 3

Dependence of emanation capacity on temperature for aluminum oxide annealed to 1350°C
a) in coordinates $E = f(T)$ b) in coordinates $\log E = f(1/T)$

It should be mentioned that if the chemical or physical nature of the solid is altered a deviation from the exponential curve is observed.

3. RESULTS AND DISCUSSION

It follows from equation 1 that the emanating power is $E = K \cdot S$. A number of authors have provided experimental confirmation of this relationship during studies of inorganic oxides (ThO_2, ZrO_2, MgO) (See Fig. 4)[6] has been proposed and a method of determining the absolute value

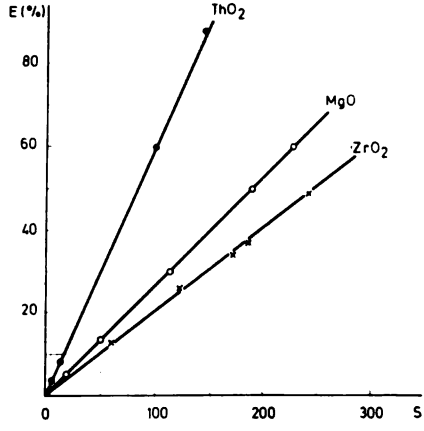

Figure 4

Dependence of emanation capacity on specific surface area for Thorium, Magnesium and Zirconium Oxides

of the specific surface on the basis of the emanation capacity[7]. However it has not been widely utilised, because other methods (BET for example) have proved simpler. On the other hand the emanation method can be used to obtain a qualitative graphical characteristic of the change in surface area while the solid is being heated. It was successfully used in this way to study the sintering of iron oxide[4] and nickel oxide[8] under dynamic conditions (Fig. 5).

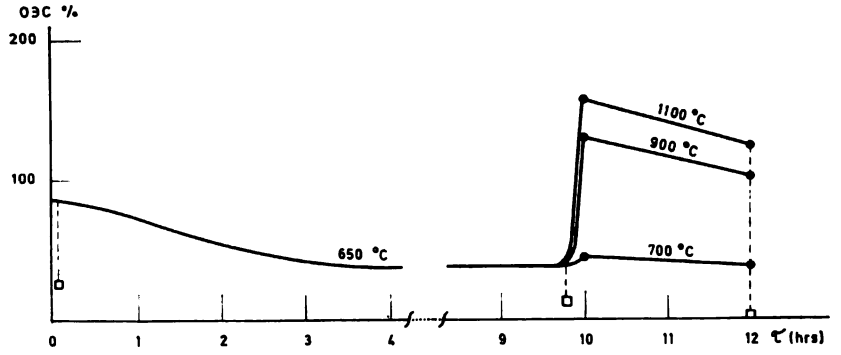

Figure 5

Variation of emanation capacity with time during the isothermic annealing of iron at different temperatures. Room temperature values are indicated by squares.

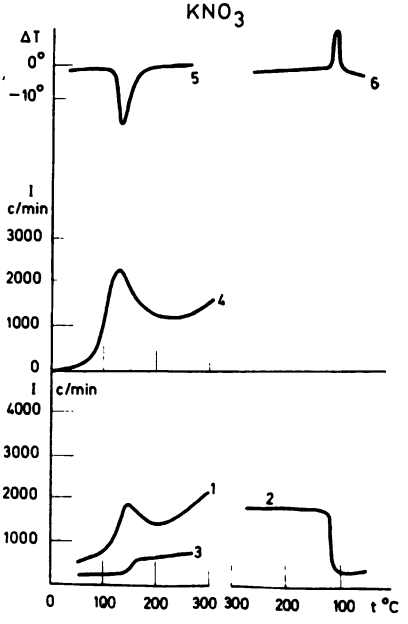

Figure 6

Emanation curves and thermograms of KNO_3. 1. heating emanation curve; 2. cooling emanation curve; 3. repeat heating emanation curve; 4. emanation curve of xenon introduced by ion bombardment; 5. heating thermogram; 6. cooling thermogram.

The emanation method has been used by a number of authors for studying the ageing of hydroxide sediments, polymorphic transformations, hydration and dehydration, and solid state reactions[1, 2].

If during heating the solid undergoes a polymorphic transformation, the emanation capacity changes sharply in the given temperature range. Figure 6 shows the results of some emanation measurements. At a temperature of 128 to 130° C the orthorhombic form of KNO_3 changes to rhombohedric. At this temperature the thermogram shows an endothermic effect; the emanation curve and the thermogram are in good agreement. Moreover the emanation method can be used to detect the initial stage in the formation of a new crystalline phase (which begins here at a temperature of 110° C).

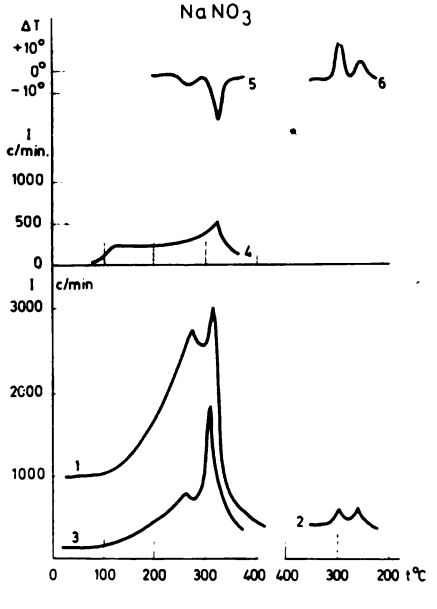

Figure 7

Emanation curves and thermograms of $NaNO_3$. 1. heating emanation curve; 2. cooling emanation curve; 3. repeat heating emanation curve; 4. emanation curve of xenon introduced by ion bombardment; 5. heating thermograms; 6. cooling thermogram.

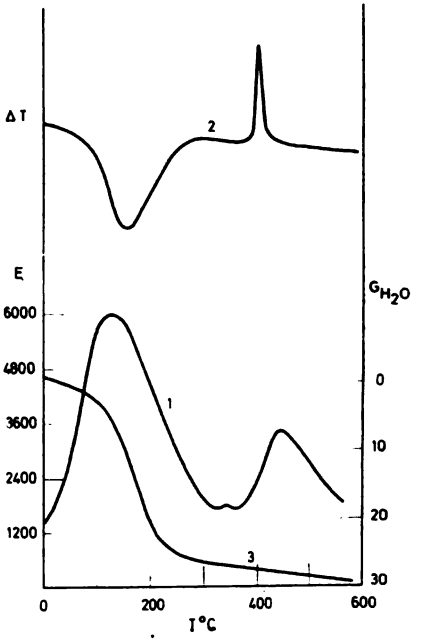

Figure 8

Emanation curve (1) thermogram (2) and thermogravimetric curve (3) of Zirconium Hydroxide

Whereas for potassium nitrate the emanation method only confirms the thermograph measurements, it is particularly valuable in those cases where the transformation does not involve a thermal effect (for example with second order phase transitions). Sodium nitrate is an example[9] (See Fig. 7). The emanation curve has a distinct maximum at a temperature of 275° C, corresponding to a phase transition the maximum at 306° corresponds to

the melting point. In this case the thermogram also shows an effect due to the change in thermal capacity involved in the phase transition[10].

Zirconium hydroxide $Zr(OH)_4$ is an example of a solid undergoing hydration during heating[11]. Results of emanation measurements are given in Fig. 8 together with DTA and TGA curves. Between 60 and 300° C emanation increases due to water being given off. It reaches a peak at 400° C, corresponding to the exothermic effect on the thermogram, associated with the crystallisation of earlier formed zirconium dioxide.

The emanation method provides a valuable means of studying the interaction of solids. We may cite our own study of the formation of zinc ferrite from oxides as an example of solid state reaction. One of the components is labelled, in this case the activated zinc oxide, by coprecipitation of traces of the 228 Th isotope. Figure 9 gives emanation, DTA and dilatometry curves for the mixture. X-ray phase and chemical analyses of intermediate products were also made.

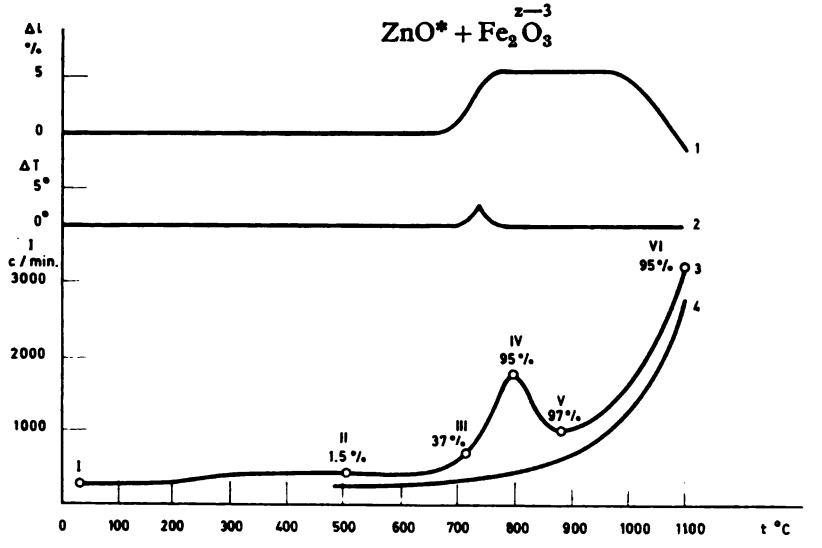

Figure 9

Emanation study of a ZnO + Fe_2O_3 mixture 1. dilatometric curve; 2. thermogram; 3. emanation curve; 4. emanation of $ZnFe_2O_4$ formed by reaction. Percentages of ZnO reacted shown by the figures

The emanation curve (Curve 3) shows an increase at an early stage of the reaction when 1.5% of the zinc oxide at a temperature of 650° C having reacted. The maximum at 790° C corresponds to some 95 % of the oxide having reacted. The curve for a second heating confirmed that the reaction had been complete the first time. The repeat heating curve is determined practically only by the diffusion of the inert gas from the ferrite, and a semi-logarithmic plot of this can provide valuable information regarding difects in the materials, its previous history and other properties important for the

electromagnetic behaviour of ferrites[12]. The study of ceramic sintering under dynamic conditions[4] also has good prospects.

The reaction of Barium Carbonate and Titanium dioxide, which was also studied by emanation method[13, 14] is another example of a solid state reaction. Figure 10 shows the emanation curve of pure TiO_2 and a mixture of ^{222}Th labelled TiO_2. The maximum on the emanation curve of the mixture corresponds to the reaction yielding barium metatitanate. The curve of emanation from $BaTiO_3$ formed during the solid state reaction is given in

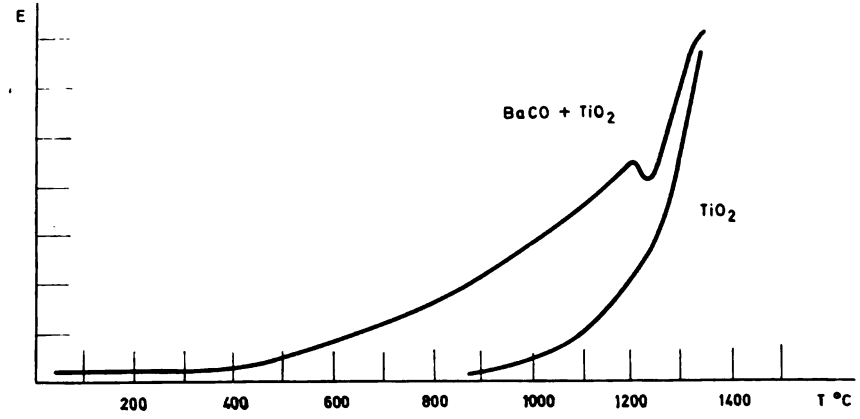

Figure 10

Emanation curves of TiO_2 and a mixture of $TiO_2 + BaCO_3$

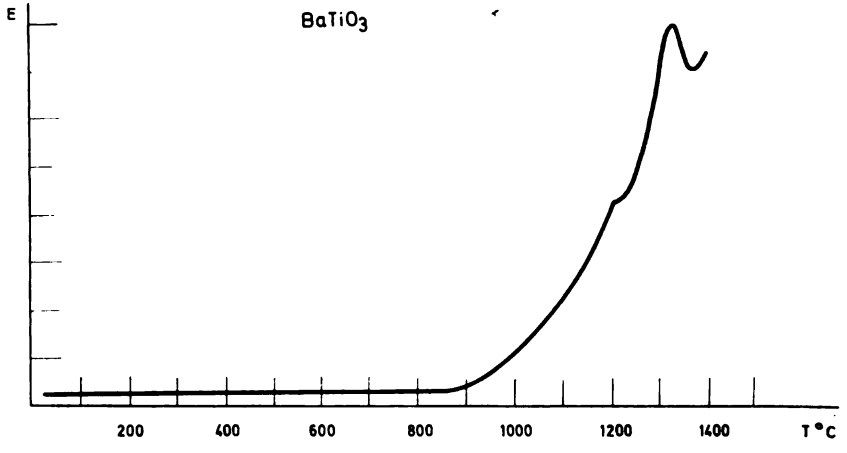

Figure 11

Emanation curve of $BaTiO_3$ formed in solid state reaction

Figure 11. A maximum is clearly visible on the curve and corresponds to a reversible second order or phase transition at 1320° C. An interesting feature is that at a temperature of 120° C, i.e. the magnetic transition temperature, no change in emanating power is observed as was to be expected. The emanation method is sensitive to diffusion changes, while the Curie transition involves only a change in atomic structure.

4. CONCLUSIONS

A change in emanating power indirectly reflects all processes taking place in the solid and involving a change in the specific surface area or the conditions of difussion. Among the latter are: the liberation of absorbed water, chemical transformations, transformations from metastable amorphic to crystalline structures, polymorphic transitions, melting, solid state reactions, ceramic sintering and so on. Supplementary methods such as DTA, dilatometry, thermogravimetry, X-ray phase analysis, can all be used for a fuller interpretation of emanation data.

However the emanation method has a number of specific advantages; it enables structural or surface changes to be registered under dynamic conditions of heating even when the latter does involve a thermal effect. In a number of cases, in the formation of fine crystal lines or amorphous phases for example, it is more sensitive than X-ray phase analysis.

ACKNOWLEDGEMENTS

The author would like to express his gratitude to Prof. K. V. Zaborenko of Moscow State University, under whose supervision some investigations were conducted, and Dr. Č. Jech, Institute of Physical Chemistry of the Czechoslovak Academy of Sciences, Prague, for his interest and valuable remarks.

REFERENCES

1. Hahn, O. J. — *Chem Soc.* 2: 259, 1949.
2. Balek, V. — *Chem. listy* 58: 1261, 1964.
3. Jech, Č. — *Int. J. Rad. and Isotopes* 8: 179, 1960.
4. Balek, V. Doct. Thesis — Moskva, 1967.
5. Balek, V., and K. B. Zaborenko — *Radiokhimiia* 10: 450, 1968.
6. Zhabrova, G. and M. and M. D. Shibanova —*Kin. i Kataliz.* 2: 668, 1961.
7. Heckter, M. — *Glastechnik Ber.* 12: 156, 1934.
8. Gourdier, F., P. Bussiere, B. C. Imelik — *C. R. Acd. Sci.* 264: 1625, 1967.
9. Zaborenko, K. B. and V. Balek — *Zh. Neorg. Khimii* rec'd for publ.
10. Jech, Č., G. M. Zhabrova, S. Z. Roginskii and M. D. Shibanova — *Radiokhimia* 5: 355, 1952.
11. Balek, V., — *J. Inorg. Nucl. Chem.* rec'd for publ.
12. Zabarenko, K. B., A. M. Babeshkin and L. L. Melikhov — *Izv. VUZ ser Khimiia i Khim. Tekhnol.*, 3: 288, 1960.

GLASNIK HEMIJSKOG DRUŠTVA, Vol. 34, No. 5-6-7, 1969, pp. 359—365

GHDB-68

541.132:661.518

Original Scientific Paper

CONDUCTIVITY AND DISSOCIATION CONSTANT OF LIQUID AMMONIA

by

LADISLAV J. HORVAT

Various liquid substances are used as solvents in which chemical reactions take place. Their dissociation can be expected, similarly as with water, to proceed according to the scheme

$$2\,NH_3 \rightleftarrows NH_4^+ + NH_2^-$$

while the ions obtained through dissociation take part in reactions.

Liquefied gases may also be of interest as solvents. Our objective was to study certain properties of liquid ammonia within a broad temperature range, from melting point to the critical temperature. Table 1 shows previously measured values for the conductivity of ammonia.

TABLE 1

Review of Literature Data on the Conductivity of Ammonia

Author	Temperature °C	Conductivity $\Omega^{-1}\ cm^{-1}$
Franklin & Cady[3]	—33.5	$1 \cdot 10^{-7}$
Franklin & Kraus[3]	—73.5	$1.6 \cdot 10^{-8}$
Fredenhagen [4]	—59	2.10^{-8}
	—43	$2.4 \cdot 10^{-8}$
	—37	3.10^{-8}
Monosson & Pleskow [5]	—40	10^{-7}
Hnizda & Kraus [7]	—34	1.10^{-11}
Cueillerou	—71.5	$1.2 \cdot 10^{-7}$
Charret [6]	—67.9	$1.3 \cdot 10^{-7}$
	—61	$1.495 \cdot 10^{-7}$
	—54.9	$1.59 \cdot 10^{-7}$
	—46.5	$1.825 \cdot 10^{-7}$
	—41.3	$1.9 \cdot 10^{-7}$
	—38.9	$1.97 \cdot 10^{-7}$

EXPERIMENTAL

We obtained gaseous ammonia using methods described in the literature[4, 8, 12], from ammonium chloride and sodium hydroxide. A drying system filled with potassium hydroxide, sodium amide and calcium oxide was used. The apparatus was made of Pyrex glass. Measuring cells were also Pyrex, 75 *mm* long tubes with an external diameter of 8 *mm* and with the upper end drawn out into a thick-walled capillary with a 0.3 *mm* platinum wire electrode. The constant of the measuring cells was determined at a temperature of 25° C both before and after measurements of ammonia conductivity.

Liquefaction was achieved by cooling with liquid oxygen. The test substance was distilled in vacuum four successive times before filling the measuring cell which was also filled and sealed in vacuum.

Temperature was measured by a constantan-copper thermocouple[9]. Continuous temperature rise from —80° C to room temperature took place in Dewar's vessel cooled inside liquid oxygen. A double-walled glass device, whose interior was heated by a resistance wire fed from a 12 V battery, was built into the upper part of the vessel. Heating from room temperature to 150° C was done on an oil bath.

An Iskra Ma 5960 electronic instrument was used to measure the electrolytic resistance of the cell, at a frequency of 10^3 Hz. The estimated error of the specific conductivity values was less than 10%.

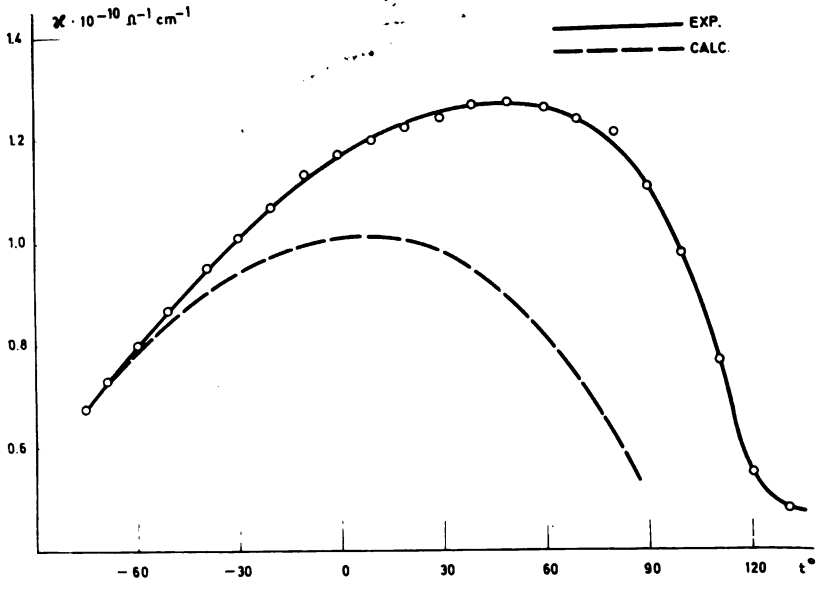

Figure 1

Conductivity of liquid ammonia

RESULTS

All measurements were made in the cells with the meniscus in approximately the same position during the heating. Measurements were made on three cells: mean values are presented in Table 2 and Fig. 1 (experimental curve).

The curve may divided into four ranges of different shape.

TABLE 2

Measured Values for the Conductivity of Ammonia

Temperature °C	Conductivity $\varkappa \cdot 10^{10}$ $\Omega^{-1}\ cm^{-1}$	Temperature °C	Conductivity $\varkappa \cdot 10^{10}$ $\Omega^{-1}\ cm^{-1}$
—77	0.67	40	1.27
—70	0.73	50	1.27
—60	0.80	60	1.26
—50	0.86	70	1.24
—40	0.95	80	1.21
—30	1.01	90	1.10
—20	1.07	100	0.97
—10	1.13	110	0.76
0	1.17	120	0.54
10	1.19	130	0.47
20	1.22	132	0.47
30	1.24		

The first range is from the freezing (—77.7° C) to the boiling (—33.3°C) point, showing a nearly linear change of conductivity with temperature with a gradient of about $0.7 \cdot 10^{-12}\ \Omega^{-1}\ cm^{-1}/°C$. This range may be described by

$$\varkappa_T = A \cdot \rho/\rho_0 \cdot e^{-E/RT},$$

as suggested in the literature[10] for some liquids.

In the temperature range of around 100° C above the boiling point, the temperature coefficient changes sign. The maximum conductivity is at about 50° C. It can also be located by means of the reduced temperature $\tau_m = T_m/T_k$; in this case $\tau_m \sim 0.8$.

The third part of the curve represents a temperature range which shows an again nearly linear fall of conductivity, only with slightly higher temperature coefficient than in the first range.

The last segment of the curve is the range close to the critical temperature. Here the specific conductivity continues to fall, but levels out near the critical temperature. The transition from the liquid to the gaseous state is continuous and the critical temperature was not registered by measuring specific conductance.

DISCUSSION

The conductivity of a substance depends on the velocity and number of charged particles conveying electricity. The shape of the curve is the resultant of the superposition of different temperature-dependent factors directly or indirectly influencing number or velocity of ions.

The specific conductivity as a function of temperature may be written

$$\varkappa_T = A \cdot e^{-E/RT}$$

where

A = constant, the conductivity at infinite temperature
E = activation energy
R = gas constant

According to this equation, $\varkappa$ rises with temperature and tends asymptotically to the value A, approximating a straight line over small intervals (at lower temperatures). The coefficient A is constant only over relatively small changes of temperature. However its variation with temperature is insignificant relative to the exponential term, particularly if when the variation of other factors discussed below is taken into consideration. This means that the variation in A can be disregarded in the first approximation. The constants A and E can be derived from the measurements.

As the temperature rises, other influences must be considered too. The density of the liquid decreases, which means that the volume increases constantly so that the same number of ions is dispersed in an increasing volume, because of which the conductivity falls. The volume and conductivity are hence in the ratio

$$\varkappa_1 : \varkappa_2 = V_2 : V_1$$

or

$$\varkappa_1 : \varkappa_2 = \rho_1 : \rho_2$$

It follows that

$$\varkappa_2 = \varkappa_1 \cdot \rho_2/\rho_1$$

In the equations above V = volume

ρ = density

while subscripts 1 or 2 designate lower and higher temperatures respectively. Denoting the density at the melting point ρ_0 and using the equation for the change of conductivity with temperature, we obtain

$$\varkappa_T = Ao \cdot \rho/\rho_0 \cdot e^{-E/RT}$$

where ρ = density at temperature T.

The dielectric constant is a measure of the insulating properties of the medium and when it decreases the possibility of ions existing also decreases. This fact could be employed to introduce another correction into the original equation and interpret the curve obtained. A liquid has its highest dielectric constant at the melting point, and as the temperature rises the dielectric constant falls. Because of the decreasing ionic stability the number of ions decreases, which reduces the conductivity. This may be expressed

$$\varkappa_1 : \varkappa_2 = \varepsilon_1 : \varepsilon_2$$

or

$$\varkappa_2 : \varkappa_1 = \varepsilon_2 / \varepsilon_1$$

Denoting the dielectric constant at the melting point with Σ_0 and using the previous equation, we obtain

$$\varkappa_T = A \cdot \rho/\rho_0 \cdot \varepsilon/\varepsilon_0 \cdot e^{-E/RT}$$

The equation above does not fully account for the temperature dependence of specific conductivity, but to a first approximation it does fit the experimental curve. It could be further improved by taking other variable factors (viscosity, activation energy, pressure, etc.) into account.

From the experimental results for conductivity we can determine the values of A and E for initial temperatures. For A we obtain $9.15 \cdot 10^{-10}$ $\Omega^{-1}cm^{-1}$, and for the activation energy 1014 *cal/mol.*

Using the equations above, the temperature dependence of the conductivity within the interval for which density and dielectric constant values[10] are known can be computed. The calculation based on the equation

$$\varkappa_T = A \cdot \rho/\rho_0 \cdot \varepsilon/\varepsilon_0 \, e^{-E/RT}.$$

is presented in Fig. 1 ("calc." curve).

DISSOCIATION CONSTANT OF LIQUID AMMONIA

Determinations of the dissociation constant of liquid ammonia have given very different results. Fredenhagen[4] found a value of 10^{-22} at a temperature of —70°C. Cueillerou and Charrst[8] obtained 10^{-29} at —50°C.

Liquid amonia dissociates according to the equation

$$2\,NH_3 \rightleftarrows NH_4^+ + NH_2^-$$

so that the dissociation constant is defined by

$$K = \frac{f_{NH_4^+} \cdot c_{NH_4^+} \cdot f_{NH_2^-} \cdot c_{NH_2^-}}{f_{NH_3} \cdot c_{NH_3}}$$

where $f_{NH_4^+}$, $f_{NH_2^-}$ and f_{NH_3} are corrresponding ionic activity coefficients, and $c_{NH_4^+}$, $c_{NH_2^-}$ and c_{NH_3} are the concentrations of the ions ammonia molecules. For the given case the activity coefficients are very close to one, while $c_{NH_4^+}$ and $c_{NH_2^-}$ are equal so that we may write

$$K = \frac{c^2}{c_{NH_3}}$$

c_{NH_3} designates ammonia concentration, or the number of moles per liter, since the concentrations of NH_4^+ and NH_2^- are negligible. The volume of a mole of ammonia is $V_m = M \cdot V_s$ or $c_{NH_3} = 10^3/V_m$, or $c_{NH_3} = 10^3/M \cdot V_s$. V_m and V_s are molar and specific volume (in cm^3), and M is the molar mass of ammonia. The specific volume can be replaced by the density, to obtain

$c_{NH_3} = 10^3 \cdot \rho/M$. The equivalent conductance, conductivity and ionic concentration (gramequivalents per liter) are combined in the term $\Lambda^\circ = = 10^3 \cdot \varkappa/c$. where Λ° is the equivalent conductance at infinite dilution (as is the case with the ionic concetration in liquid ammonia). Substituting for c and c_{NH_3} from the above expressions in epxression for the dissociation constant we obtain

$$K = \left(\frac{10^3 \cdot \varkappa}{\Lambda^0}\right)^2 \cdot \frac{M}{10^3 \cdot \rho} = \frac{10^3 \cdot \varkappa^2 \cdot M}{\Lambda^{02} \cdot \rho}.$$

Λ° can be obtained from the publications of Franklin, Cady and Kraus[2,3]; its value is 262 $\Omega^{-1} \cdot cm^2$ at a temperature of —33.5°C. The conductivity at this temperature, according to our measurements, is $0.99 \cdot 10^{-10}$ $\Omega^{-1}cm^{-1}$, and the density[10] 0.68 g/cm^3, so that $K = 3.6 \cdot 10^{-21}$ and $P = 14.3 \cdot 10^{-20}$ for the ionic product. Using the more measurements of equivalent conductance at infinite dilution of Hawes[6], Monosson and Pleskov[5] and Gurianova and Pleskov[11], the calculation can also be made for —40°C. The density at this temperature is 0.69 g/cm^3, giving $K = 3.0 \cdot 10^{-21}$ and $P = = 12.1 \cdot 10^{-20}$.

High School of Engineering
Department of Physics
Subotica

Received 24 September 1968

REFERENCES

1. Walden, P. *Das Leitvermögen der Lösungen* — Leipzig: Akademische Verlagsgesellschaft m. b. H., 1924.
2. Franklin, E. C. and J. Cady. — *Journal of the American Chemical Society* 26: 499, 1904 (Walden, II Teils, 279).
3. Franklin, E. C. and K. C. Kraus. — *Journal of the American Chemical Society* 27: 191, 1905 (Walden, II Teils, 279).
4. Fredenhagen, K. "Löslichkeitsprodukte anorganischer Salze im flüssigen Ammoniak" — *Zeitschrift für anorganische und allgemeine Chemie* 186: 1—37, 1930.
5. Monosson, A. and W. Pleskow. "Leitfähigkeit der Alkalinitrate im flüssigen Ammoniak" — *Zeitschrift für physikalischen Chemie* 156: 179—194, 1931.
6. Hawes, W. "The Conductance of Bases in Liquid Ammonia" — *Journal of the American Chemical Society* 55: 4422—4430, 1933.
7. Hnizda, F. V. and K. C. Kraus. "Conductance of Several Salts in Ammonia at —34°C by a Precision Method" — *Journal of the American Chemical Society* 71: 1565—1575, 1949.
8. Cueillerous, J. and M. Charret. "Ouelques proprietes physico-chimiquess de l'ammoniac liquide. I. Conductibilitè specifique de l'ammoniac. II. Produit ionique de l'amoniac" — *Bulletin de la Societè Chimique de France* (Paris) 5:798—802, 1956.
9. Kohlrausch, F. *Praktische Physik* — Stuttgart: Teubner Verlagsgesellschaft, 1955.
10. Landold, Böornstein, and Roth. *Physikalisch-Chemische Tabellen* — Berlin: Springer Verlag, 1959.
11. Gurianova, E. N. and W. A. Pleskov. — *Acta Physico. chim. URSS* 5: 509, 1936 (Landolt-Börnstein, 1960 Band II. 7 Teil, pp. 303—313).
12. Klemenc, A. *Die Behandlung und Reindarstellung von Gasen* — Leipzig: Akademische Verlagsgesellschaft m. b. H., 1936.

GLASNIK HEMIJSKOG DRUŠTVA, Vol. 34, No. 2-3-4, 1969, pp. 367—376

GHDB-69

541.124.7:546.78'16

Original Scientific Paper

THERMAL DECOMPOSITION OF TUNGSTEN HEXACHLORIDE

by

DRAGICA N. ĐURKOVIĆ and RADE M. ĆOSOVIĆ

Some metallic compounds decompose into a metal and a volatile product at temperatures below the metal's melting points. Many methods for obtaining high-purity metals are based on this principle, using various reactions in the vapor phase. The following types of reaction are noteworthy: thermal decomposition, reduction in the vapor phase with hydrogen or gaseous metallic vapors, hydrolysis of metallic vapors, disproportion reactions, pressing out reactions, etc. Through these reactions in the vapor phase, many metals are obtained in various forms: ductile, wire, granulated, powder, etc.[1]

In the technology of obtaining pure metals the thermal decomposition processes are the most significant of all those listed above. Many metallic compounds, such as hydrides, carbonyls, haloids, sulfides, etc., decompose thermally. Thermal decomposition of volatile compounds and deposition of the metal is possible under these conditions[2]:

— The temperature of decomposition or dissociation of the volatile compounds must be below the melting point of the metal being precipitated.
— At the dissociation temperature, the deposited metal should have a low vapor pressure.
— Gasseous reaction products given off (hydrogen, carbonyl, haloid) should be conducted out of the reaction space by recombining into a volatile compound or by degassing.

These conditions indicate that the thermal decomposition method is particularly suitable for metals of high melting point and low volatility. By an analysis of the volatility and dissociation pressure of the compounds of these metals it was established that the haloids of a series of hardly fusible metals are suitable for decomposition, because of their high volatility and dissociation at temperatures below those at which the metals melt.

Of all the haloids, iodides are the most widely used in thermal decomposition, by the method known as the iodide process developed by Van Arkel and de Boer[3]. This process is today employed in industry for refining Group IV metals, particularly titanium, zirconium, hafnium and thorium. Large-scale research is in progress concerning the refining of other metals of high melting points (vanadium, niobium, tantalum, etc) using this method.

Compared with the iodide process, the chloride and bromide thermal decomposition processes are less significant, while the literature does not give data on the use of fluorides[4].

As early as 1923 Van Arkel succeeded in decomposing tungsten hexachloride on tungsten wire heated to 1400°C[5]. Since then very few studies have dealt with the separation of tungsten from the gaseous phase by the thermal decomposition method[6, 7]. Many more treat the reduction of tungsten hexachloride vapor with gaseous hydrogen[8, 9, 10]. The present study concerns the rate of thermal decomposition of tungsten hexachloride on an incandescent wire by the dynamic method, i.e. by the continuous removal of the gaseous chlorine by degassing.

Tungsten hexachloride was decomposed on a tungsten wire in an evacuated glass laboratory apparatus.

APPARATUS AND METHOD

Tungsten hexachloride obtained by chlorination of the metal powder with gaseous chlorine was thermally decomposed. Chlorination tests were made in a quartz laboratory apparatus. The temperature of chlorination was 800°C, that of chloride condensation 150—200°C.

Thermal decomposition tests were carried out in the apparatus shown schematically in Fig. 1. The apparatus consists of:

— System for evacuation and taking off gaseous products
— Reaction vessel for chloride decomposition
— System for heating the wire
— System for thermostating the reaction vessel.

The pumping system allows evacuation of the reaction vessel to between $1 \cdot 10^{-4}$ and $1 \cdot 10^{-5}$ torr, and consists of (Fig. 1): (1) rotary pump, (2) diffusion pump, connected via (3) valve system and (4) cold trap (containing liquid nitrogen) to the reaction vessel. The vacuum in the system is measured with (5) Pirany and (6) Penning vacuum meters.

The second and most important part of the device is the decomposition vessel (7) in which the thermal dissociation takes place. This is a Pyrex glass cylinder with a specially designed head (8) made of brass, while the core of the internal surface are teflon. Teflon conveniently eliminates the problems of corrosion and of sealing and insulating the electrodes.

The electrodes to which the resistance-heated tungsten wire is fastened consists of two parts. The lower part, situated in the interior of the reaction vessel, is of molybdenum, the upper part is copper (water-cooled).

The system for heating the tungsten wire comprises: an autotransformer (9), regulation transformer (10), and current (11) and voltage (12) meters.

The reaction vessel is heated by an insulated Kantal-wire winding on a copper cyllinder (13). The temperature of the reaction vessel is registered and kept constant with a mercury contact thermometer (14) connected via a switch (15) to the heater.

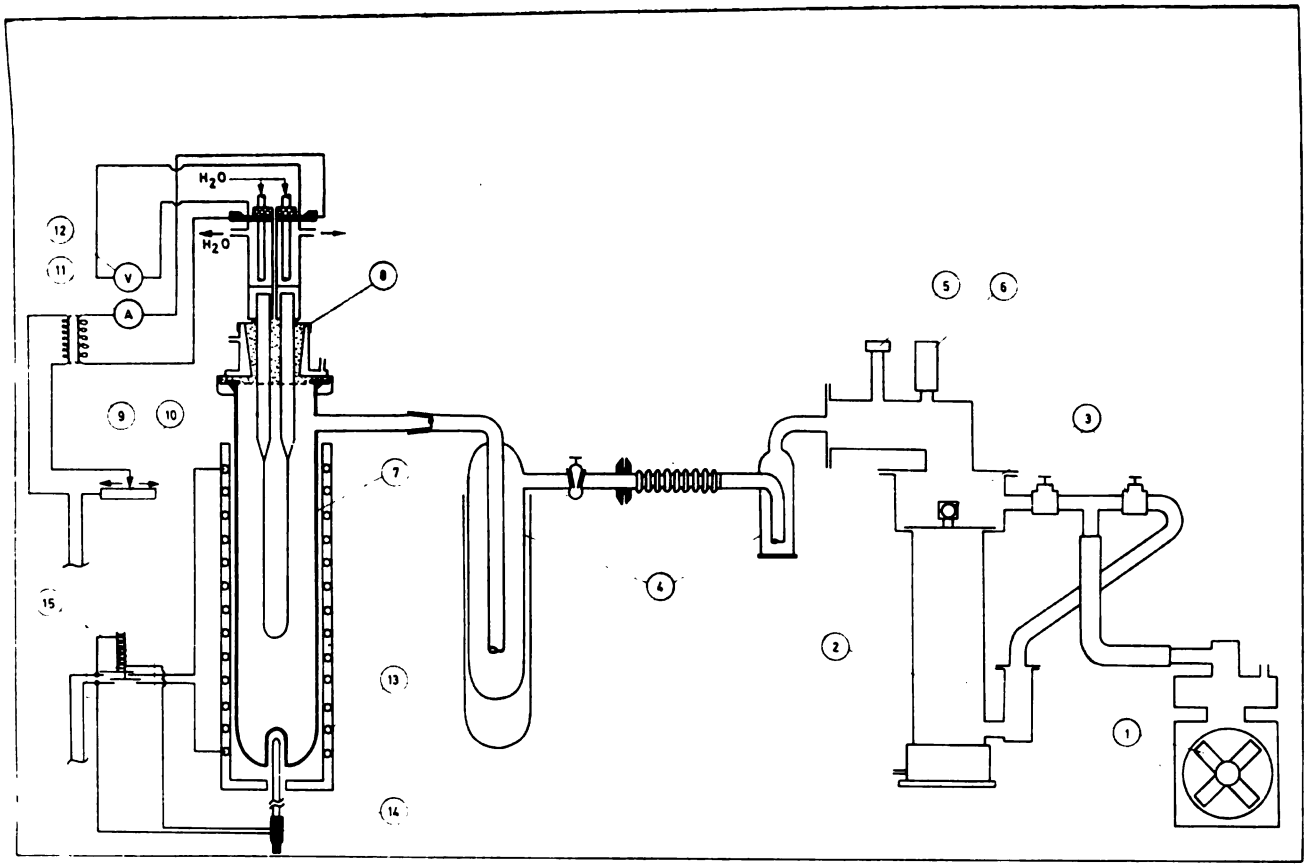

Figure 1

Apparatus for thermal decomposition

(1) Rotary vacuum pump
(2) Diffusion pump
(3) Valves
(4) Cold trap
(5) Pirany vacuum meter
(6) Penning vacuum meter
(7) Decomposition vessel
(8) Metal head
(9) Autotransformer
(10) Regulation transformer
(11) Amperometer
(12) Voltmeter
(13) Heater
(14) Mercury contact thermometer
15) Switch

In decomposition tests a constant amount of hexachloride (50 *g*) was introduced into the reaction vessel which was evacuated to 1×10^{-4} torr and degassed 2 h at room temperature. After degassing the constant dimensioned tungsten wire (0.2 *mm* diameter, 300 *mm* long) was heated to the decomposition temperature by feeding current to the molybdenum electrodes, and then the reaction vessel was heated to the desired working temperature. During the test the following were maintained constant:

— Vacuum, by continuous pumping
— Wire temperature
— Temperature of the reaction vessel
— Surface area of evaporation

The temperature of the tungsten wire was kept constant by regulating the current and voltage according to the principle described in our previous paper[11]. The current-voltage curves for temperature regulation were calculated for different temperatures from literature data on the temperature dependence of the specific electrical resistance and radiation energy loss of tungsten[12].

EXPERIMENTAL RESULTS AND THEIR ANALYSIS

The methods allows continuous registration of the rate of the process because the deposition of the metal on the wire changes its diameter and hence its conductivity. Assuming that the metal is deposited uniformly over the whole wire (justified for small changes of diameter) and that the new cross-sections are concentric circles relative to the original wire, the weight of the deposited metal is proportional to the conductivity increase. The weight of metal at any moment can be calculated from the conductivity on the basis of the law for computing the temperature of the wire[11] and the equation

$$g = \gamma\, l^2 \rho \frac{J}{U} \tag{1}$$

Since for a constant temperature of the wire

$$\gamma\, l^2 \rho = K, \tag{2}$$

it follows that

$$g = K \frac{J}{U} \tag{3}$$

where g = weight of metal, g

γ = density g/cm^3
l = length of wire, cm
ρ = specific electrical resistance, Ωcm
J = current, A
U = voltage drop in wire, V

Differentiating the above equation with respect to time

$$\frac{dg}{dt} = K \frac{d\frac{J}{U}}{dt} \tag{4}$$

we obtain the rate of decomposition, or of deposition on the wire.

The change in weight as a function of conductivity for a tungsten wire 30 *cm* long and the working temperature is shown graphically in Fig. 2.

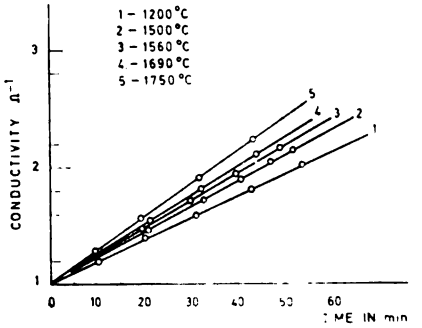

Figure 2

Conductivity increase as a function of time for different wire temperatures

From the values in the graph, the rate of thermal decomposition of tungsten was calculated and the results are shown in the tables.

The rate of thermal decomposition of tungsten hexachloride under constant removal of chlorine depends on two principal factors:

— Temperature of decomposition, i.e. of the wire
— Pressure of the chloride vapor, i.e. temperature of the reaction vessel.

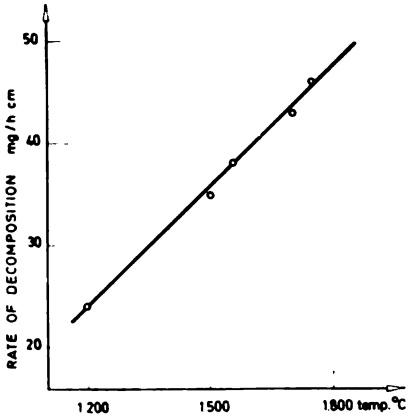

Figure 3

Rate of decomposition as a function of wire temperature

The temperature of decomposition was changed within the range 1200—1750°C, while that of the reaction vessel was kept at 100°C. The change in conductivity of the tungsten wire as a function of time for different decomposition temperatures is shown graphically in Fig. 3. From the data given in the graph the decomposition rates were computed and are numerically presented in Table 1.

TABLE 1

Test No.	Wire temperature °C	Coefficient of straight line $\Omega^{-1}\ h^{-1}$	Constant	Rate of decomposition $mg \cdot cm^{-1} \cdot h^{-1}$
1	1200	1.08	0.678	24
2	1500	1.25	0.842	35
3	1560	1.31	0.857	38
4	1700	1.38	0.942	43
5	1750	1.43	0.954	46

The plot of the velocity as a function of temperature is a straight line (Fig. 4). The coefficient of this line represents the change in the decomposition rate for a given temperature change. It is 3.82 *mg*/100°. At the chloride temperature of 100°C, which corresponds to a WCl_6 vapor pressure of $2.83 \cdot 10^{-3/4}$ *mm* Hg, the decomposition rate rises with temperature only slowly. At pressures below 0.1 *mm* Hg, the decomposition rate is governed by the number of gaseous collisions with the wire. As the temperature rises the probability of dissociation rises too, because the additional energy received by the molecules during collision increases. This explains the very slow increase in the decomposition rate with the rising temperature of the wire.

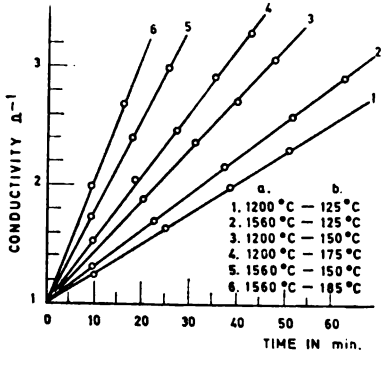

Figure 4

Conductivity increase as a function of time for different wire temperature and WCl_6.

a. Wire temperature
b. Temperature of the vessel.

TABLE 2

Test No.	Temperature of WCl_6 °C	Pressure of WCl_6 *mm Hg*	Temperature of wire °C	Coefficient of straight line $\Omega^{-1}\ h^{-1}$	Constant	Rate of decomposition $mg \cdot cm^{-1} \cdot h^{-1}$
1	100	0.028	1200	1.08	0.678	24
2	125	0.160	1200	1.56	0.678	35
3	150	0.795	1200	2.64	0.678	60
4	175	3.200	1200	3.36	0.678	76
5	100	0.028	1560	1.31	0.857	38
6	125	0.166	1560	1.80	0.857	52
7	155	1.062	1560	4.50	0.857	129
8	185	5.350	1560	6.00	0.857	172

At higher temperatures of the reaction vessel, or greater WCl_6 vapor pressure, the effect of wire temperature on the decomposition rate should be greater. This is confirmed by the tests conducted with reaction vessel temperatures of 125, 150 and 175°C and decomposition temperatures of 1200 and 1560°C.

The effect of the reaction vessel temperature, or of the vapor pressure of WCl_6 on the rate of decomposition was investigated in the range 100—185°C, during which the temperature of decomposition was 1200 or 1560°C. The literature gives very divergent data on the WCl_6 vapor pressure in this temperature range. The pressures given in Table 2 and in the graph were calculated according to Rossini's equation[13]:

$$\log p = 10.732 - \frac{4582}{T}.$$

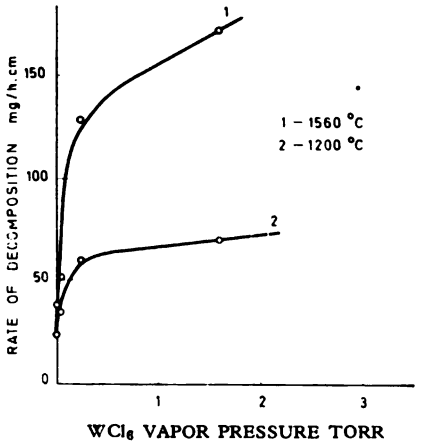

Figure 5

Rate of decomposition as a function WCl_6 pressure

The time dependence of the conductivity of the tungsten wire for different temperatures of the reaction vessel is shown in the graph of Fig. 5. The experimental conditions and rate of decomposition are given in Table 2. This table also presents the WCl_6 vapor pressure for the corresponding temperatures of the reaction vessel. The rate of decomposition as a function of WCl_6 vapor pressure is shown graphically in Fig. 6.

An analysis of the data in the tables and graphs reveals that the rate of decomposition increases with increasing pressure of chloride vapor at both decomposition temperatures. This results from the increased concentration of WCl_6 in the vapor phase, and hence the increased number of chloride molecules which collide with the wire and decompose in unit time. The curves of the rate plotted against chloride vapor pressure have a characteristic parabolic shape which means that as the temperature, or the chloride vapor pressure increases more and more molecules recoil undecomposed and the rate of decomposition asymptotically approaches a finite value which corresponds to the given temperature of decomposition for a given pressure in the reaction vessel.

Generally speaking, the rates of decomposition of tungsten hexachloride per unit length of wire, obtained in this study are considerably higher that in other similar processes. For example, the literature gives the rate of thermal decomposition of titanium tetraiodide as 18 $mg/cm \cdot h$[14], the process being employed in industrial refining of titanium. Considering this and the fact that the deposited metal is ductile, finely crystalline and very pure, the method described here may be regarded as highly promising for obtaining pure tungsten and for coating this metal on other materials.

CONCLUSION

The rate of thermal decomposition of tungsten hexachloride on incandescent wire with continuous removal of chlorine by degassing was investigated as a function of:

— Temperature of the wire, i.e. the temperature of decomposition
— Temperature of the reaction vessel, i.e. the tungsten chloride vapor pressure.

The rate of thermal decomposition of WCl_6 varies within the range 25—170 $mg/h \cdot cm$ and increases with the temperature of decomposition and the chloride vapor pressure.

Institute for the Technology of
Nuclear and Other Mineral
Raw Materials
Belgrade

Received 10 September 1968

REFERENCES

1. Sherwood, E. M. and J. M. Blocher. "Vapor Deposition: The First Hundred Years" — *Journal of Metals* 17 (6): 594—599, 1965.
2. Van Arkel, A. E. "Gewihnung Hochschmelzende Metalle mit thermische Zersetzung" — *Metall Wirtschaft Wissenschaft Technik* 13 (23): 405—408, 1934.
3. Rolsten, F. R. *Iodide Metals and Metal Iodides* — New York: J. Wiley, 1961.
4. Gillardeau, J. *Groissance des cristaux metalliques par decomposition themique des halogenures en phase gazeuse* — CEA-Bibliography No. 93.
5. Van Arkel, A. E. "Einkrystallwolfram" — *Physica* 3: 76, 1923.
6. Van Limpt, A. V. — *Rec. tran. chim. Pays-Bas* 51: 114, 1932.
7. Smithells, C. J. *Tungsten* — London: Charman Mall, 1952.
8. Koref, F. "Versuche über das weiterwachsen von Metallkristallen durch Abscheidung aus der Gasphase" — *Zeitschrift für Electrochemie* 28: 511, 1922.
9. Fischwolgt, H. and F. Koref. "Weiterwachsen von Metallkrystallen durch Abscheidung aus der Gasphase — *Zeitschrift für Technische Physik* 6: 298, 1925.
10. Owen, L. W. "Deposition of Metallic Coating by Chemical Reaction in the Vapour Phase" — *Electroplating and Metal Finishing* 17 (9): 296, 1964.
11. Ćosović, R. and D. Đurković. "Rafinacija titana termičkim razlaganjem jodida" (Refining Titanium by Thermal Decomposition of Iodide) — *Tehnika* 12: 280—283, 1967.
12. Agte, K. N. and I. Vatsesk *Volfram i Molibden* (Tungsten and Molybdenum) — Moskva: Energiia, 1964.
13. Rossini, F. D. and D. D. Wagman. *Selected Values of Physical and Thermodynamic Properties* — N. B. S., 1952, 500, I, II,
14. Runalls, O. J. S. and L. M. Pidgeon. "Observation on the Preparation of Iodide Titanium" — *Journal of Metals* 4 (843), 1952.

GLASNIK HEMIJSKOG DRUŠTVA, Vol. 34, No. 5-6-7, 1969, pp. 377—385

GHDB-70

620.172.22:669.14:66.04

Original Scientific Paper

DILATOMETRIC INVESTIGATION OF THE EFFECT OF THE HEATING RATE ON THE TEMPERATURE OF THE INDIVIDUAL TEMPERING STAGES OF CARBON TOOL STEELS

by

NADA P. VIDOJEVIĆ and NADA M. NOVOVIĆ-SIMOVIĆ

Since the transformations taking place during the tempering of steel are of a diffusive nature, the heating rate may be expected to have a definite influence on the position of the temperature intervals of individual stages of tempering, i.e. on the completeness of the various phases.

In a study of the influence of heating rate on the tempering of carbon steels containing 0.45 and 1.2% C by dilatometry method, Guliaev and Taratorina[1] found that the temperature interval of the first stage of tempering does not depend on the heating rate for rates between 3 and 30000° C/min. For example, under the given conditions the decomposition of martensite, characteristic for the first stage of tempering, takes place in the interval between 80 and 250°C. However, in spite of the above observation, it has been found by X-ray analysis that the amount of carbon precipitating from the supersaturated solid solution at a given temperature is higher the lower the heating rate.

At the higher heating rates attainable by induction heating, e.g. 45000 and 54000°C/min the starting point of martensite decomposition is shifted to 300—350°C and 430—450°C, respectively.

Gridnev[2] has proved that the shift of the temperature interval of the first and third tempering stages of carbon steels with 0.4, 0.8 and 1.2% C is considerable expressed up to heating rates of 6000—9000°C/min.

With increasing heating rate the temperature interval of austenite decomposition shifts toward higher temperatures[1]. At a heating rate of 1.6°C/*min* the decomposition of residual austenite in carbon steel takes place in the interval 230—280°C, at 20°C/*min* in the interval 240—330°C. It has also been noticed that the temperature interval of the second tempering stage expands with increase of the heating rate; this is explained by a decrease in the rate of decomposition of residual austenite under these conditions.

At heating rates above 29000°C/*min* the second tempering stage can no longer be distinguished on the dilatometric curve. The amount of austenite measured after tempering of steel at different rates proves that the trans-

formation of residual austenite still takes place under all circumstances, but whether the austenite is transformed during heating up or cooling down is still an open question.

The absence of a well-defined second stage on the dilatometric curve of steel tempered at high heating rates certain authors[3] explain by a cancelling effect of the volumetric changes resulting from the decomposition of martensite and austenite. This means that at higher heating rates the first and second stages overlap.

On the basis of the above cited data from the literature, it may be concluded that there is no unified opinion about the influence of the heating rate on the temperature intervals of the tempering stages of carbon steels. The influence of carbon content on the temperature intervals of tempering stages of a number of carbon steels was studied in a previous work[1]. In the present work the influence of the heating rate on the position of the first, second and third stages of tempering in carbon tool steels was investigated by the dilatometric method.

Standard specimens of the steels Č. 1840, Č. 1940 and Č. 1943 were tested on a Leitz dilatometer. The data on thermal treatment and the mode of determination of temperature intervals and volumetric changes were described in ref. [4]. During the experiment four different heating rates were used: 5.5, 10.5, 2.3.3 and 44°C/*min*.

RESULTS AND DISCUSSION

From the results shown in Table 1 and the graphs in Figs. 1—4 it may be concluded that increasing the heating rate of tempering had definite effects. The temperature intervals of the first, second and third stages were shifted up in temperature. This is particularly obvious if the results obtained at the lowest and the highest heating rates are compared. Thus in steel Č. 1840 at a rate of ~5.3°C/*min* the first tempering stage began at 78°C and ended at 179°C, while at rate ~45.4°C/*min* it was in the interval 115 to 215°C.

It is noteworthy what with increase of heating rate the beginnings of the first and the third stages were shifted up more than in the case of the second stage. For example, with an increase of heating rate from ~5.6 to ~42.0°C/*min* the beginning of the first and the third stages in steel Č1943 was shifted by 42 and 45°C, respectively, and that of the second stage by only 25°C (see graphs in Figs 1—4). An explanation of the influence of heating rate on the temperature intervals of tempering stages must be sought in different stabilities of martensite and austenite lattices against superheating[5].

Considering the width of the temperature intervals, it may be generally said that with increasing heating rate, even at these relative low rates, a certain tendency toward narrowing of the third stage and widening of the second is detectable, while the width of the first interval remains practically unchanged. E.g., for steel Č 1940, the interval of the third stage at a heating rate of ~44.5°C/*min* was 21°C narrower than at ~5.6° C/*min*, the second stage was wider by 14°C, the first remaining the same.

TABLE 1

Influence of Heating Rate on the Temperatures of Tempering Stages

Steel quality (JUS)	Average heating rate, °/*min*	Temperature interval* °C		
		stage I	stage II	stage III
Č.1840	5.3	78—179	230—277	277—407
	23.2	97—200	245—308	308—426
	45.4	115—215	251—322	322—425
Č.1940	5.6	77—181	231—274	274—393
	10.6	85—189	235—286	286—400
	23.7	100—193	243—300	300—406
	44.5	115—215	262—319	319—417
Č.1943	5.6	74—181	232—279	279—399
	10.4	85—193	242—293	293—414
	23.0	104—200	252—314	314—418
	42,0	116—220	257—324	324—432

* Average value of 2-3 determinations

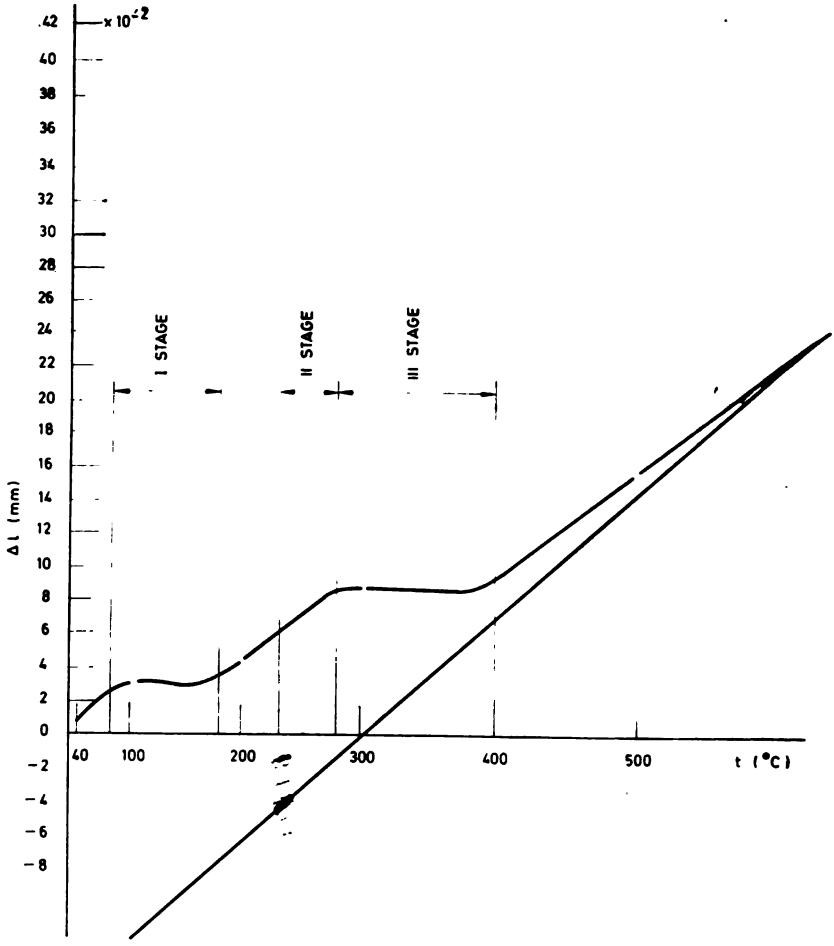

Figure 1

Dilatometric curve of tempering of steel Č. 1943; heating rate — 5.8°/*min*

The phenomenon that the transformation of the third stage should occur more rapidly with the increasing heating rate is in conformity with the influence of temperature (at increased heating rate the transformation occurs at higher temperatures) on the rate of diffusion of carbon and steel atoms relative to the influence of time.

As the decomposition of martensite in the first stage occurs at much lower temperatures, and considering the exponential dependence of the diffusion of C and Fe atoms on temperature, it may be supposed that at the given heating rates the influence of the shifting of the stage to higher

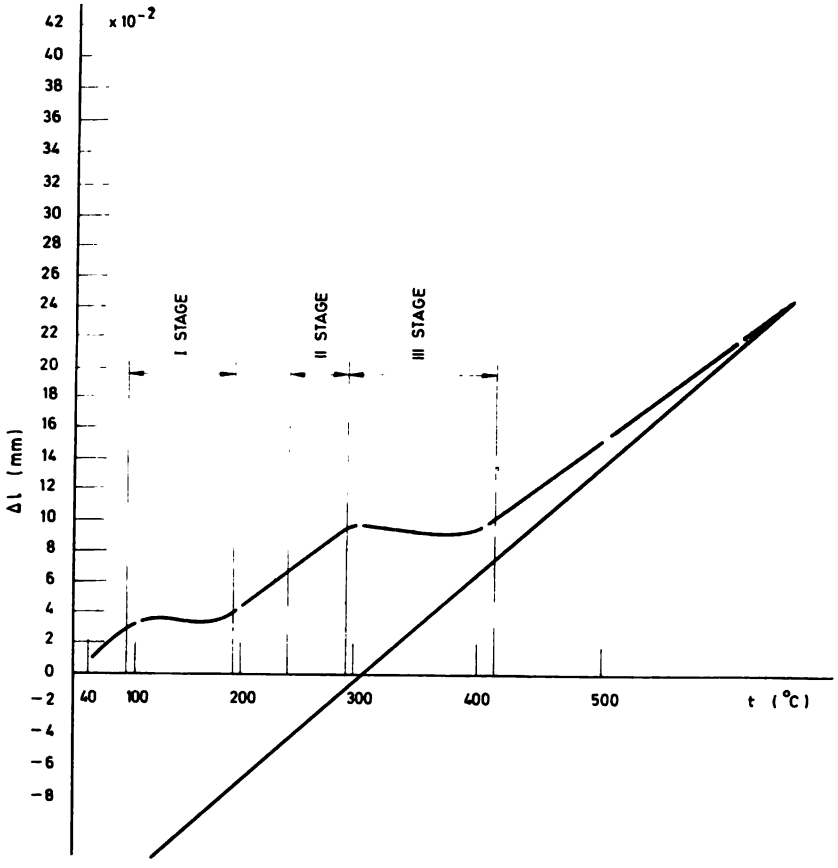

Figure 2

Dilatometric curve of tempering of steel Č. 1943; the heating rate — 10.4°/*min*

temperatures is compensated by a shorter time being available so that the width of the temperature interval of the transformation remains unchanged.

The widening of the temperature interval of the second tempering stage confirms the conclusion of Guliaev and Taratorina that the rate of decomposition of residual austenite decreases with increasing heating rates. However, the interpretation of the phenomenon requires further analysis.

By comparing the dilatometric curves it may be seen that with increasing heating rate (in spite of certain deviations) the contractions accompanying the first and the third stages get less, while the dilatation resulting from decomposition of residual austenite in the second stage increases. This can be explained by the fact that at higher heating rate, i.e. because of the higher temperatures at which the transformations take place, the thermal expansion of the specimen is also greater, this leading to less and

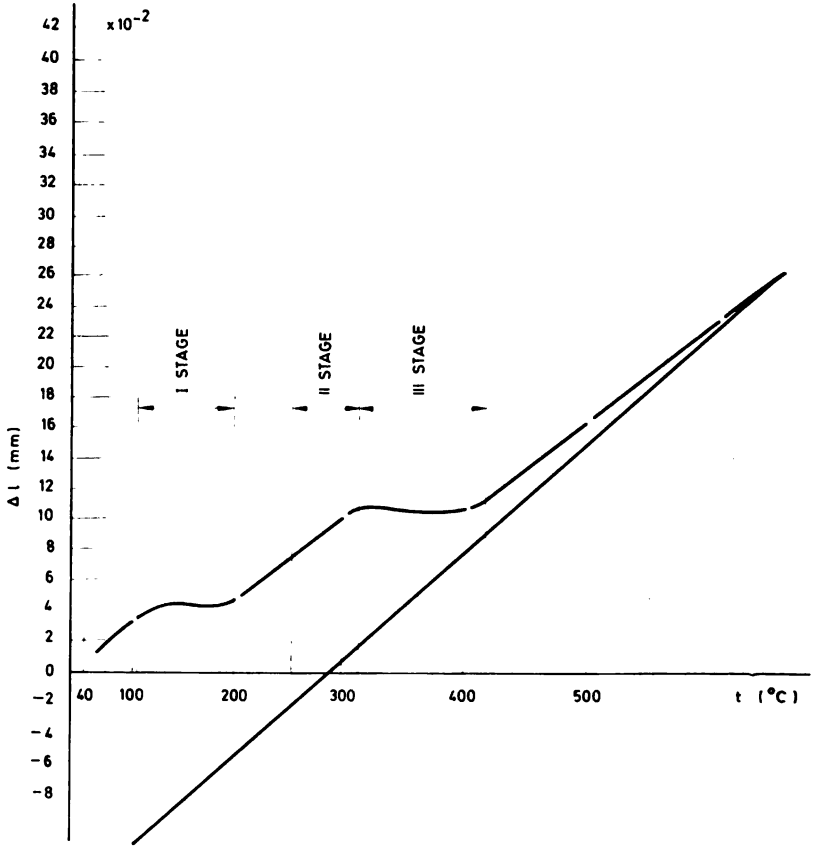

Figure 3

Dilatometric curve of tempering of steel Č. 1943; heating rate — 23.2°/*min*

less contraction associated with the transformations in the first and the third stages and to an intensification of the dilatometry effect of the second stage by superimposition on the elongation due to austenite decomposition. Some overlapping of the stages may also contribute to the reduced volumetric effects of the first and third stages at higher heating rates.

It must be pointed out that since the austenite content of the solid solution at hardening temperature was approximately the same, no difference in the position of the individual tempering stages was noticed between the steels studied at the same heating rate. This was also established in ref. 4 which preceeded the present study.

To sum up, it may be said that the results confirm the conclusions drawn by Gridnev[2] that the influence of heating rate is manifested by a change in position of the temperature intervals of the tempering stages: with increasing heating rate the temperature intervals of the first, second

Figure 4

Dilatometric curve of tempering of steel Č. 1943; heating rate — 42°/*min*

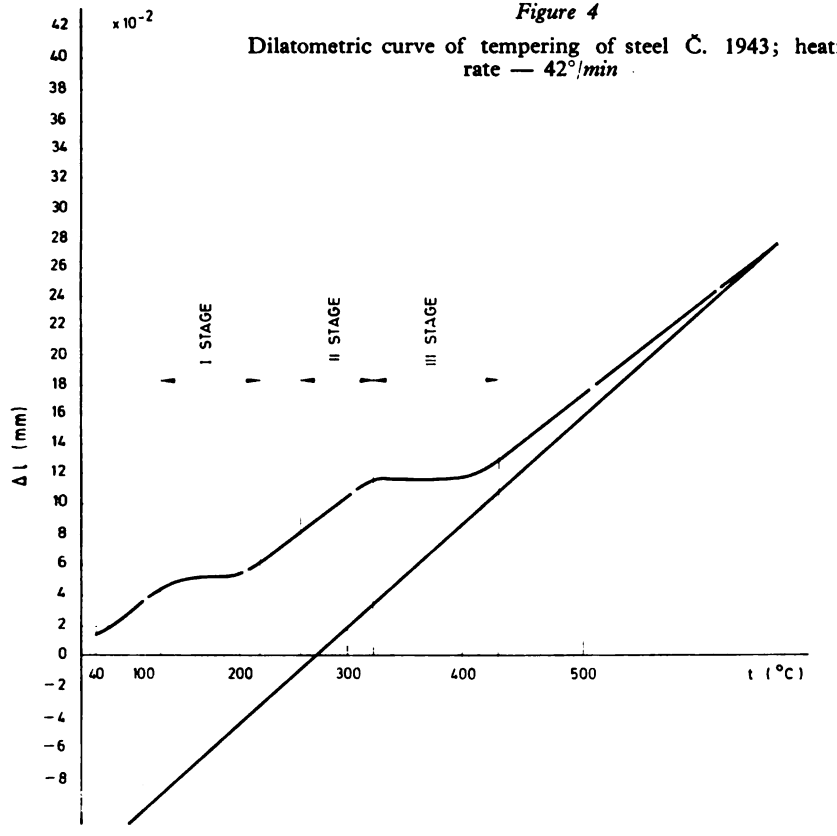

TABLE 2

Influence of Heating Rate on Length Changes of Dilatometric Specimen in the Different Stages

Steel quality (JUS)	Average heating rate °/*min*	Change of length*, $\Delta l \times 100$, *mm*		
		stage I	stage II	stage III
Č.1840	5.3	1.3	2.5	0.9
	45.4	2.3	3.8	0.8
Č.1940	5.6	0.8	2.3	0.8
	44.5	2.3	3.2	1.3
Č.1943	5.6	0.9	2.7	0.4
	42	1.7	3.9	1.2

* Average value of 2-3 determinations

and third stages of the steels shifted to higher temperatures, so that the measured dilatations increased. Also, certain differences in the influence of heating rate on the behavior of martensite and residual austenite were observed.

Faculty of Technology and Metallurgy,
Department of Physical Metallurgy, Belgrade

REFERENCES

1. Guliaev, A. P. and M. V. Taratorina — *Fizika metallov i metallovedenie* 7: 544, 1959.
2. Gridnev, V. N. — *Les Mémoires Scientifiques de la Revue de Metallurgie* 58: 317, 1961.
3. Guliaev, A. P. *Termicheskaia obrabotka stali* (Heat Treatment of Steels) — Moskva: Mashgiz, 1960.
4. Vidojević, P. N. and M. N. Simović-Novović — *Glasnik hemijskog društva* (Beograd) (rec'd. for publication).
5. Lysak, I. L. and G. A. Drachinskaia — *Fizika metallov i metallovedenie* 25: 341, 1968.

GLASNIK HEMIJSKOG DRUŠTVA, Vol. 34, No. 5-6-7, 1969, pp. 387—394

GHDB-71

547.38:547.495

Original Scientific Paper

REACTIONS OF α,β-UNSATURATED ALDEHYDES WITH CARBAMATES. I.

ACTION OF ETHYL CARBAMATE OF α, β-UNSATURATED ALDEHYDES

by

KSENIJA D. SIROTANOVIĆ, MILKA M. BAJLON-PASTOR, MILICA M. OBRADOVIĆ and LUTVIJA R. EMINOVIĆ

In the literature only a few data [1–5] are found concerning the reaction of carbamates with α,β-unsaturated aldehydes, either aliphatic or aromatic. Aliphatic α,β-unsaturated aldehydes have been found to react with carbamates in two ways:

1. Aldehyde (α-bromocrotonaldehyde[1], 2-ethyl-2-hexenal[2]) reacts with three molecules of carbamate (ethyl, 1-ethylpropyl or isopropyl carbamate) yielding the corresponding tricarbamate (I), the reaction involving both the carbonyl group and the ethylenic linkage:

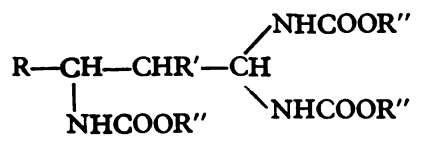

a) $R = CH_3$, $R' = H$, $R'' = C_2H_5$

b) $R = C_3H_7$, $R' = H$, $R'' = (CH_3)_2CH$

c) $R = C_3H_7$, $R' = H$, $R'' = (C_2H_5)_2CH$

I

2. Aldehyde (crotonaldehyde[3]) reacts with two molecules of carbamate (isopropyl or benzyl carbamate). Only the carbonyl group takes part in the reaction and biscarbamates (II) are obtained:

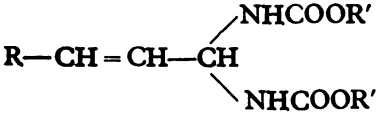

a) $R = CH_3$, $R' = (CH_3)_2CH$

b) $R = CH_3$, $R' = C_6H_5CH_2$

II

As for aromatic α,β-unsaturated aldehydes, the reactions of only two have been reported: cinnamaldehyde and α-ethylcinnamaldehyde. According to Bischoff[4], Kraft[3] and Lewis and co-workers[5] cinnamaldehyde reacts with carbamates (ethyl, isopropyl or benzyl carbamate) yielding only the corresponding biscarbamates (III):

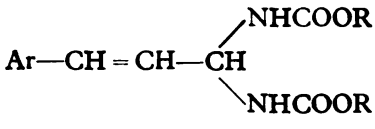

a) Ar = C_6H_5, R = C_2H_5

b) Ar = C_6H_5 R = $(CH_3)_2CH$

c) Ar = C_6H_5, R = $C_6H_5CH_2$

III

However, when reacting carbamates (isopropyl and benzyl carbamates) with α-ethylcinnamaldehyde, Kraft[3] obtained indene derivatives (V). He assumed that the compounds were formed via the addition products (IV) of one molecule of carbamate to a molecule of aldehyde:

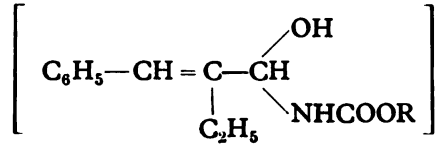

IV

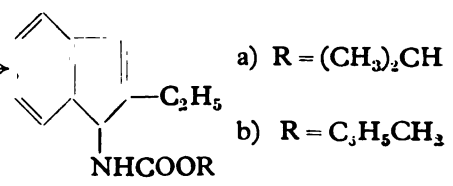

a) R = $(CH_3)_2CH$

b) R = $C_6H_5CH_2$

V

Catch and co-workers[6] treated cinnamaldehyde cyanohydrin with ethyl carbamate and isolated a compound, whose analysis showed it to be the product of reaction of one molecule of cinnamaldehyde with two molecules of ethyl carbamate. They suggested two possible structures for the compound: either that of biscarbamate (IIIa), or that of iminourethane of β-carbethoxyamino-hydrocinnamaldehyde (VI, R = C_6H_5, R′ = H)

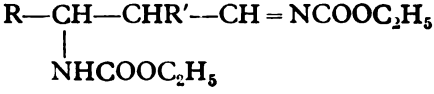

VI

Since the products obtained by Bischoff[4] and Cath and co-workers[6] differ considerably in their melting points (143° and 181° resp.) it is obvious that two different compounds are in question.

We have studied the reaction of ethyl carbamate with the following α,β-unsaturated aromatic aldehydes: cinnamaldehyde, o-, m- and p-nitrocinnamaldehydes, *o*-, *m*- and *p*-chlorocinnamaldehydes and *o*-, *m*- and *p*-methoxycinnamaldehydes, and also with aliphatic α,β-unsaturated aldehydes: crotonaldehyde, 2-hexenal and 2-methyl-2-pentenal. Reactions were carried out in the presence of concentrated hydrochloric acid, gaseous hydrogen chloride or boron fluoride-etherate, either at room or at slightly elevated temperature.

Either dicarbamates or tricarbamates were obtained, depending both on the aldehyde used and the experimental conditions. For example, when ethyl carbamate reacted with cinnamaldehyde, two products were isolated: one that melted at 158° and was shown by elemental analysis to be a tricarbamate, i.e. the product of condensation of one molecule of aldehyde with three molecules of ethyl carbamate, and the other the dicarbamate, melting point 181°.

By hydrolysis of the tricarbamate in the presence of 2,4-dinitrophenylhydrazine the 2,4-dinitrophenylhydrazone of β-carbethoxyamino-hydrocinnamaldehyde (VIIa, $R = C_6H_5$, $R' = H$) was obtained:

$$R—\underset{\displaystyle NHCOOC_2H_5}{\underset{|}{CH}}—CHR'—CH = NNHC_6H_3(NO_2)_2 \qquad \text{VII}$$

On the basis of this evidence we concluded that the product with melting point (158°) near the melting point of Bischoff's product (143°) was 1,1,3-tris(carbethoxyamino)-3-phenylpropane, that is the biscarbamate of β-carbethoxyamino-hydrocinnamaldehyde (Id, $R = C_6H_5$, $R' = H$, $R'' = C_2H_5$) and not the biscarbamate of cinnamaldehyde (IIIa) as Bischoff reported.

By hydrolysis of the dicarbamate (m.p. 181°) in the presence of 2,4-dinitrophenylhydrazine, the 2,4-dinitrophenylhydrazone of cinnamaldehyde was obtained. As the dicarbamate easily decolorizes bromine water and shows intense absorption at 970 cm^{-1} in the IR spectrum (corresponding to the out of plane vibration of H's on a trans-substituted ethylene linkage) we concluded that the dicarbamate ought to be the biscarbamate of cinnamaldehyde (IIIa). If the structure of the compound were that of iminourethane (VI) then the product of hydrolysis would have been identical with product obtained from tricarbamate, but that was not the case.

With nitro-cinnamaldehydes only dicarbamates were obtained. As all the products obtained show characteristic absorption at 960—970 cm^{-1} in the IR spectrum we can assign structure III ($Ar = NO_2C_6H_4$, $R' = H$, $R'' = C_2H_5$) to these compounds as well.

Chloro-cinnamaldehydes react similarly to cinnamaldehyde, yielding both biscarbamates and tricarbamates. The structure biscarbamate (III, $Ar = ClC_6H_4$, $R' = H$, $R'' = C_2H_5$) was assigned to the products obtained, on the basis of: 1. — elemental analysis, 2. — preparation of 2,4-dinitrophenylhydrazones of corresponding unsaturated aldehydes, and 3. — appearance of absorption bands at 960—970 cm^{-1}. Tricarbamates yielded on hydrolysis β-carbethoxy-*o*, *m*- and *p*-chlorohydrocinnamaldehydes, isolated as 2,4-dinitrophenylhydrazones (VII, $R = ClC_6H_4$, $R' = H$).

Of the three methoxy-cinnamaldehydes used, *o*- and *p*- isomers yielded only tricarbamates, while *m*- isomer yielded only resinous products.

If an aldehyde yields both dicarbamate and tricarbamate, the dicarbamate is produced more rapidly. Upon standing in acidic media dicarbamates are converted into the more stable tricarbamates. Aldehydes with a negative substituent in the nuclei (nitro-group) yield only dicarbamates, cinnamaldehyde and chloro-cinnamaldehydes yield both dicarbamates and tricarbamates, while methoxy-cinnamaldehydes, having a substituent which repels electrons, yield only tricarbamates.

With all the aliphatic aldehydes used (crotonaldehyde, 2-methyl-2-pentenal*, 2-hexenal) tricarbamates (I) were obtained, as confirmed by hydrolysis in the presence of 2,4-dinitrophenylhydrazine.

* Kraft reported that no product is yielded by action of isopropyl or benzyl carbamate on 2-methyl-2-pentenal

TABLE 1

Unsaturated aldehyde	Dicarbamate		Tricarbamate	
	Yield %	M. p. °C	Yield %	M. p. °C
Cinnamaldehyde	65	181	80	158
o-Methoxy-cinnamaldehyde	—	—	32	160
p-Methoxy-cinnamaldehyde	—	—	15	136
o-Chloro-cinnamaldehyde	60	184	52	189
m-Chloro-cinnamaldehyde	73	165	41	162
p-Chloro-cinnamaldehyde	37	192	60	158
o-Nitro-cinnamaldehyde	74	178	—	—
m-Nitro-cinnamaldehyde	73	202	—	—
p-Nitro-cinnamaldehyde	80	188	—	—
Crotonaldehyde	—	—	43	105
2-Hexenal	—	—	30	128
2-Methyl-2-pentenal	—	—	16	107

EXPERIMENTAL

Dicarbamates

1. *Dicarbamate of cinnamaldehyde*

A) *Obtained in the presence of hydrochloric acid.* To a solution of 2.7 *g* (0.02 *mole*) of cinnamaldehyde and 7.2 *g* (0.08 *mole*) of ethyl carbamate in absolute ether a drop of concentrated hydrochloric acid was added. A crystalline product precipitated immediately and was washed with ether after 5 minutes. The yield of colorless needles, m.p. 179°, was 3.3 *g* (57%). Recrystallized from absolute ethanol the product melted at 181°.

B) *Obtained in the presence of BF_3 — etherate.* To a solution of 2.7 *g* (0.02 mole) of cinnamaldehyde and 7.2 *g* (0.08 mole) of ethyl carbamate in 10 *ml* abs. ether a drop of $BF_3 \cdot (C_2H_5)_2O$ was added and the mixture was allowed to stand overnight at room temperature. 3.6 *g* (66%) of crude product, m.p. 179°, was obtained. After recrystallization from abs. ethanol the product melted at 181°.

A mixture of the products obtained under A and B above showed no depression.

Analysis:

Calculated for $C_{15}H_{21}N_2O_4$ C 61.64%, H 6.84%, N 9.58%;
Found C 62.23%, H 6.91%, N 9.71%.

Hydrolysis of dicarbamate of cinnamaldehyde. To a solution of 0.3 *g* (1 mole) of dicarbamate in warm ethanol 4 *ml* of 0.25 M solution of 2,4-dinitrophenylhydrazine in mixture of phosphoric acid and ethanol were added[7]. Red crystals, m.p. 252, precipitated immediately.

When mixed with a sample of 2,4-dinitrophenylhydrazone of cinnamaldehyde the product showed no depression.

2. *Dicarbamates obtained from o-, m- and p-chloro-cinnamaldehydes and from o-, m- and p-nitro-cinnamaldehydes* have been reported in earlier papers of K. Sirotanović and co-workers[8, 9].

Tricarbamates

1. *1,1,3-Tris (carbethoxyamino)-3-phenylpropane*

A. *Obtained from cinnamaldehyde.* A mixture of 1.35 *g* (0.01 mole) of cinnamaldehyde and 2.7 *g* (0.03 mole) of ethyl carbamate was melted by mild heating on a water bath, cooled to room temperature, and a drop of concentrated hydrochloric acid was added. The mixture was allowed to stand at room temperature overnight, then ether was added and the mixture left to stand for several hours. 3.1 *g* (80%) of colorless plates, m.p. 156°, precipitated which when recrystallized from ethanol melted at 158°.

B) *Obtained from dicarbamate of cinnamaldehyde.* 2.9 *g* of the dicarbamate was suspended in 15 *ml* of ether, 2 drops of concentrated hydrochloric acid were added and the mixture left to stand overnight. 1.5 *g* (57%) of crude product, m.p. 146—8°, was obtained. Recrystallized from ethanol it melted at 158°.

The melting point of a mixture of the products obtained under *A* and B did not show any depression.

Analysis:

Calculated for $C_{18}H_{27}N_3O_6 \cdot \frac{1}{2}H_2O$ C 55.38%, H 7.18%, N 10.77%;
Found C 55.42%, H 7.21%, N 11.03%.

2. *1,1,3-Tris|carbethoxyamino|-3-|chlorophenyl|-propanes*

A. *Obtained from o-, m- and p-chloro-cinnamaldehydes* as under 1 A. Yields and melting points are given in Table 1. Melting points of products obtained from *o-* and *p*-chloro-cinnamaldehydes in mixture with samples obtained previously[10] did not show any depression.

Analysis for 1,1,3-tris(carbethoxyamino)-3-(3-chlorophenyl)-propane:

Calculated for $C_{18}H_{26}ClN_3O_6$ C 51.98%, H 6.25%, N 10.10%;
Found C 51.82%, H 6.41%, N 10.38%.

B. *Obtained from corresponding dicarbamates* as under 1B. Melting points of mixtures with the respective products obtained under 2A did not show any depression.

3. *1,1,3-Tris|carbethoxyamino|-3-|2-methoxyphenyl|-propane* was obtained from *o*-methoxycinnamaldehyde as under 1A. 1.3 *g* (32%) of crude product,

m.p. 157° was obtained. Recrystallized from acetone-petroleum ether, it melted at 160—161°.

Analysis:

Calulated for $C_{18}H_{29}N_3O_7$	C 55.45%,	H 7.05%,	N 10.22%;
Found	C 54.92%,	H 7.28%,	N 10.39%.

4. *1,1,3-This[carbethoxyamino]-3-[4-methoxyphenyl]-propane.* Through a solution of 1.62 *g* (0.01 mole) of *p*-methoxy-cinnamaldehyde and 3.6 *g* (0.04 mole) of ethyl carbamate in absolute ether (10 *ml*) gaseous hydrogen chloride was bubbled for one minute and the mixture allowed to stand for 7 days at room temperature. Ether was removed in vacuum and the syrupy residue treated first with water and then with ether until it solidified. Yield of the crude product, m.p. 133—4°, was 0.65 *g* (16%); recrystallized from acetone-petroleum ether it melted at 136°.

Analysis:

Calculated for $C_{19}H_{29}N_3O_7$	C 55.45%,	H 7.05%,	N 10.22%;
Found	C 55.05%,	H 7.45%,	N 10.23%.

5. *1,1,3-Tris(carbethoxyamino)-butane.* To a solution of 4.6 *g* (0.05 mole) of crotonaldehyde and 18 *g* (0.2 mol) of ethyl carbamate in 20 *ml* of absolute ether 2 drops of concentrated hydrochloric acid were added and the mixture allowed to stand overnight. The solution was washed with water, ether was removed and the syrupy residue treated with petroleum ether until it solidified. 6.9 *g* (43%) of crude product, m.p. 94—97°, was obtained. Recrystallized from ether-petroleum ether it melted at 105°.

Analysis:

Calculated for $C_{13}H_{25}N_3O_6$	C 48.90%,	H 7.83%,	N 13.16%;
Found	C 48.66%,	H 7.80%,	N 13.09%.

6. *1,1,3-Tris(carbethoxyamino)-hexane.* To a mixture of 2 *g* (0.02 mole) of 2-hexenal and 3.6 *g* (0.04 mole) of ethyl carbamate a drop of concentrated hydrochloric acid was added and the mixture was allowed to stand overnight. The hardened mass was washed with ether and the residue (1.4 *g*, 30%), m.p. 119°, recrystallized from ethanol-water. It melted at 128°.

The melting point of a mixture with a sample obtained previously[11] did not show any depression.

7. *1,1,3-Tris(carbethoxyamino)-2-methylpentane.* A solution of 5 *g* (0.05 mole) of 2-methyl-2-pentenal and 18 *g* (0.02 mole) of ethyl carbamate in 25 *ml* of ether was allowed to stand 4 hours at 30°. After cooling to room temperature 3 drops of concentrated hydrochloric acid were added and the solution allowed to stand overnight at room temperature. The ethereal solution was then washed with water and sodium carbonate and again with water. Ether was removed in vacuum and the syrupy residue treated with water and petroleum ether until it hardened and then washed with a small quantity of tetrahydrofurane. There was 2.7 *g* (16%) of crude crystalline product, m.p. 102°. Recrystallized from an ethanol-water mixture it melted at 106°.

Analysis:

Calculated for $C_{15}H_{29}N_3O_6$ C 51.86%, H 8.29%, N 12.10%;
Found C 51.41%, H 8.45%, N 12.43%.

Hydrolysis of tricarbamates was carried out in the same way as the hydrolysis of the dicarbamates. Melting points and elemental analyses of the resulting 2,4-dinitrophenylhydrazones of β-carbethoxyamino-aldehydes are given in Table 2.

TABLE 2

2,4-Dinitrophenylhydrazones: $R—CH(NHCOOC_2H_5)—CHR'—CH=NNHC_6H_3(NO_2)_2$

R	R′	M. p. °C	Formula	Analysis					
				Calc. C%	Found C%	Calc. H%	Found H%	Calc. N%	Found N%
C_6H_5	H	182	$C_{18}H_{19}N_5O_6$	53.86	54.12	4.73	4.99	17.45	17.44
o-$CH_3C_6H_4$	H	188	$C_{19}H_{21}N_5O_6$	52.90	52.49	4.87	4.66	16.24	15.84
p-$CH_3C_6H_4$	H	173	$C_{19}H_{21}N_5O_6$	52.90	52.78	4.87	4.80	16.24	16.03
o-ClC_6H_4	H	193	$C_{18}H_{18}ClN_5O_6$					16.07	16.31
m-ClC_6H_4	H	181	$C_{18}H_{18}ClN_5O_6$					16.07	16.16
p-ClC_6H_4	H	192	$C_{18}H_{18}ClN_5O_6$					16.07	15.85
CH_3	H	181	$C_{13}H_{17}N_5O_6$	46.01	46.58	5.01	5.35	20.64	20.98
C_3H_7	H	163*							
C_3H_7	CH_3	172	$C_{15}H_{21}N_5O_6$	49.00	49.04	5.69	5.83	19.07	19.52

We are indebted to Ruža Tasovac for the microanalyses.

Department of Chemistry
School of Sciences
Belgrade University
and
Institute of Chemistry, Technology
and Metallurgy
Belgrade

Received 28 February, 1969

* Analytical data reported in a previous paper[11]

REFERENCES

1. Viguier, P. L. "Sur l'aldehyde α-bromocrotonique" — *Comptes Rendus des séances de L'Academie des Sciences* (Paris) 152: 268—271, 1911.
2. Kraft, W. M. and R. M. Herbst. "The Condensation of Carbonyl Compounds with Amides. Aliphatic Aldehydes and Pyruvic Acid with Aliphatic Carbamates" — *Journal of Organic Chemistry* (Baltimore) 10: 483—492, 1945.
3. Kraft, W. M. "The Preparation of Indanone Derivatives by a Carbamate-Aldehyde Reaction" — *Journal of the American Chemical Society* (Easton, Pa.) 70: 3569—3571, 1948.
4. Bischoff, C. "Ueber die Verbindungen des Urethane mit den Aldehyden" — *Berichte der Deutschen Chemischen Gesellschaft* (Berlin) 7: 1074—1084, 1874.
5. Lewis Jr., T. R., F. R. Butler, and A. E. Martell. "Condensation of Amides with Carbonyl Compounds: Benzyl Carbamate with Aromatic Aldehydes" — *Journal of Organic Chemistry* (Baltimore) 10: 145—148, 1945.
6. *The Chemistry of Penicillin* — Princeton, N. J., 1949, pp. 837.
7. Houben-Weyl. *Methoden der organischen Chemie, Band II* — Stuttgart: Verlag Georg Thieme, 1953, pp. 448.
8. Sirotanović, K., M. Bajlon-Roćen, and D. Galović. "Adicija merkaptana na nezasićene aldehide, I. Adicija tiofenola na nezasićene aromatične aldehide" (Addition of Mercaptans to Unsaturated Aldehydes, I. Addition of Thiophenol to Unsaturated Aromatic Aldehydes) — *Glasnik Hemijskog društva* (Beograd) 25—26: 509—518, 1960—1961.
9. Sirotanović, K. and Z. Nikić. "Photochemical Reactions I. Addition of Thiophenol to Bisamides and Bisurethanes of Unsaturated Aromatic and Heterocyclic Aldehydes" — *Tetrahedron* 22: 1561—1564, 1966.
10. Sirotanović, K. and M. Bajlon-Pastor. "Addition of Mercaptans to Unsaturated Aldehydes, II. Addition of Ethyl Mercaptan, Amyl Mercaptan and Benzyl Mercaptan to Unsaturated Aromatic Aldehydes" — *Glasnik Hemijskog društva* (Beograd)* 31: 329—337, 1966.
11. Sirotanović, K. and M. Bajlon-Pastor. "Adicija merkaptana na nezasićene aldehide III. Dobijanje bisuretana i bisamida β-alkilmerkapto-aldehida" (Addition of Mercaptans to Unsaturated Aldehydes. III. Preparation of Bisurethanes and Bisamides of β-Alkylmercapto-Aldehydes) — *Glasnik Hemijskog društva* (Beograd)* 31: 339—349, 1966.

* Available in English translation from National Technical Information Service, Springfield, Virginia, 22151.

GLASNIK HEMIJSKOG DRUŠTVA, Vol. 34, No. 5-6-7, 1969, pp. 395—399

GHDB-72

577.1.547.963.32:576.851.252

Original Scientific Paper

ACTION OF COLCEMIDE ON GROWTH AND NUCLEIC ACIDS OF *STAPHYLOCOCCUS ALBUS*, STRAIN 581*

by

MIODRAG D. CVETKOVIĆ, EVA J. LEVI-JOVANOVIĆ, DARINKA N. KORAĆEVIĆ, and GORDANA M. BJELAKOVIĆ

The antimitotic properties of colchicine[1] have prompted many researchers to investigate the inhibitory effect of this alkaloid on the growth of various tumors. To this end, the action of colchicine was investigated both clinically and in the laboratory. Some research pertains to the effect of colchicine and its derivatives on the synthesis of nucleic acids and proteins in various tissues and organisms. Hell and Cox[2] studied the influence of colchicine and its derivative colcemide (2-demethylcolchicine) on DNA synthesis in the skin of guinea-pig ear using thymidine tritium. They found that synthesis was depressed, more markedly by colchicine. However, Chakraborty and Biswas[3] found much quicker incorporation of thymine (^{14}C-thymine) and uracil (^{14}C-uracil) into DNA and RNA. They also used solchicine to induce tumors, and considered it a cancerogenic substance.

Discrepancies between results from animal and plant tissues led us to examine the influence of colchicine on bacteria. We studied the effect of its less toxic derivative colcemide (Colcemide, Ciba) both on the growth of bacteria[4] and on their DNA and RNA content.

MATERIAL AND METHOD

The nonpathogenic Strain 581 of *Staphylococcus albus* was cultivated in 1% glucose broth to which colcemide (Ciba) was added in amounts of 300, 200, 100 and 50 *mcg/ml*. The control test tubes had corresponding amounts of sterile physiological salt solution instead of colcemide solution. The growth of bacteria in cultures was estimated with a nephelometer.

Nucleic acids were prepared by a combined method after Schmidt-Thannhauser[5] and Schneider[6]. Quantitative determination of RNA and DNA was performed via pentose and phosphorus, ribose after Mejbaum[7], deoxyribose after Burton[8], and phosphorus after Chen[9] with certain modifications[10].

Readings were taken on a Unicam spectrophotometer SP 600.

* Financed by the Association of Medical Research Institutions under contract No. 188/I.

TABLE 1

Number of Bacteria per ml Culture (in millions)

Concentration of colcemide *mcg/ml*	Number of exp.	$\bar{X}$	Sd	$S\bar{x}$	T-test	P
300	30	95.83	101.10	41.26	26.74	<0.01
Control for 300 *mcg/ml*	30	1330.0	50.20	20.48		
200	30	410.0	468.83	191.36	5.05	<0.01
Control for 200 *mcg/ml*	30	1380.0	17.89	7.30		
100	30	1196.6	186.50	76.12	4.03	<0.01
Control for 100 *mcg/ml*	30	1520.0	59.33	24.21		
50	30	1495.0	41.83	17.07	1.76	>0.10
Control for 50 *mcg/ml*	30	1540.0	46.48	18.97		

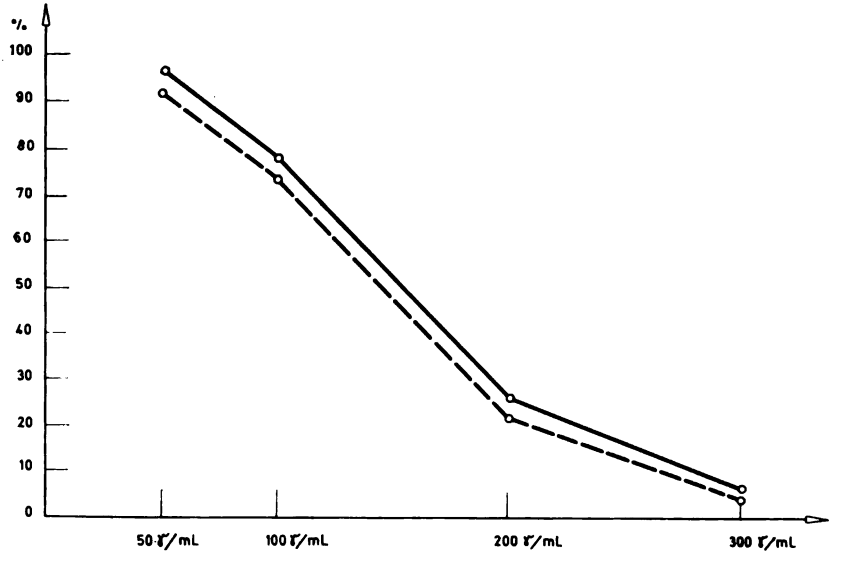

Figure 1

The growth of *Staphylococcus albus*, strain 581 in the presence of different concentrations of colcemide

——— Percentage growth in relation to control with physiological solution

- - - - - Percentage growth in relation to control without physiological solution

RESULTS AND DISCUSSION

Colcemide in concentrations of 300, 200 and 100 *mcg/ml* had a pronounced bacteriostatic action (Table 1 and Fig. 1). Some inhibition of growth was noted even with the 50 *mcg/ml* concentration, but the difference was not statistically significant. Hence the inhibitory effect of colcemide directly depends on its concentration. Changes in concentration of nucleic acids were also noted. With the colcemide concentration of 300 *mcg/ml* the amount of RNA was reduced by 95.6%, with 200 *mcg/ml* the reduction was 74% (both decreases statistically highly significant). At concentrations of 100 and 50 *mcg/ml*, the changes in RNA content were not statistically significant (Table 2).

TABLE 2

Quantity of RNA Expressed as mcg P/100 mg of Lipid-Free Residue

Concentration of colcemide *mcg/ml*	Number of exp.	$\bar{X}$	Sd	$S_{\bar{g}}$	T-test	P
300	6	12.17	5.28	2.15	6.93	<0.01
200	6	76.33	24.61	10.04	4.86	<0.01
100	6	238.38	12.81	5.22	1.20	>0.05
50	6	334.79	35.04	14.30	0.81	>0.05
Control	15	294.84	30.88	7.95		

The DNA content of cultures with the highest colcemide concentration (300 *mcg/ml*) was reduced by 59.5%, while with lower concentrations no significant differences were noted (Table 3).

TABLE 3

Quantity of DNA Expressed as mcg P/100 mg of Lipid-Free Residue

Concentration of colcemide *mcg/ml*	Number of exp.	$\bar{X}$	Sd	Sg	T-test	P
300	6	40.48	22.95	9.37	8.36	<0.01
200	6	76.66	42.38	17.30	0.61	>0.05
100	6	94.12	14.21	5.80	0.14	>0.05
50	6	105.49	24.10	9.83	0.14	>0.05
Control	15	99.46	14.92	3.84		

The ratio between total RNA and total DNA per unit weight of dry residue shows that the changes in the RNA and DNA contents were not parallel: for the stronger concentrations of colcemide the RNA: DNA ratio

was markedly reduced, while it was slightly augmented for the 50 *mcg/ml* concentration (Table 4).

TABLE 4

Ratio Between the Quantity of RNA and DNA

Concentration of colcemide	300 *mcg/ml*	200 *mcg/ml*	100 *mcg/ml*	50 *mcg/ml*	Control
RNA/DNA	0.30	0.99	2.53	3.17	2.96

These data show that colcemide has a more marked influence on RNA than DNA in this bacteria.

It is known from the literature that when colcemide acts on rat liver cells it arrests mitosis in metaphase, prevents the synthesis of cytoplasmatic RNA and causes a reduction of this acid of up to 30%[11]. On the other hand, in plant material increased RNA and DNA synthesis under the effect of colchicine was found[3]. Our results show that colcemide considerably inhibits the growth and reduces the RNA and DNA contents of *Staphylococcus albus*. Since the investigations are still in progress nothing final can be said about the mechanism of the changes observed.

CONCLUSION

The effect of colcemide on *Staphylococcus albus*, strain 581 was investigated. In concentrations of 300, 200 and 100 *mcg/ml* it inhibited the growth of the bacteria. In concentrations of 300 and 200 *mcg/ml* it also reduces their content of nucleic acids, affecting RNA much more than DNA. In a 50 *mcg/ml* concentration it had no substantial effect either on growth or on the amounts of nucleic acids.

School of Medicine
Biochemistry Department
Microbiology Department
Niš

Received 11 December 1967

REFERENCES

1. Taylor, E. W. — *The Journal of the Cell Biology* 19: 1—18, 1963.
2. Hell, E. and D. G. Cox. — *Nature* 197: 287—288, 1963.
3. Chakraborty, A. and B. B. Biswas. — *Experimental Cell Research* 38: 57—65, 1965.
4. Krebs, D. and H. Bloss — *Zentral Blatt für Bakteriologie, Parasitenkund, Infektionskrankheiten und Hygiene* 200: 468—479, 1966.
5. Schmidt, G. and S. J. Thannhauser. — *Journal of Biological Chemistry* 161: 83—89, 1945.
6. Schneider, W. — *The Journal of Biological Chemistry* 161: 293—303, 1945.
7. Mejbaum, W. — *Zeitschrift für Physiologische Chemie* 258: 117—123, 1939.
8. Burton, K. — *The Biochemical Journal* 62: 315—323, 1956.
9. Chen, P. S., T. Y. Toribara, and H. Warner — *Analytical Chemistry* 28: 1956—1958.
10. Chambon, P. *Contribution a l'etude de l'effet des rayons x sur les nucleotides acidosolubles de tissu splenique chez le rat blanc* (Thèse) — Strasbourg, 1958.
11. Kleinfeld, R. G. and J. E. Sisken. — *The Journal of Cell Biology* 31: 369—379, 1966.

GLASNIK HEMIJSKOG DRUŠTVA, Vol. 34, No. 5-6-7, 1969, pp. 401—407

GHDB-73 669.3:62-426:54-31:66.094.1:541.8.004.86

Original Scientific Paper

CHEMICAL REMOVAL OF OXIDE FROM COPPER WIRES AND ELECTROLYTIC REGENERATION OF CLEANING SOLUTION*

by

SRETEN N. MLADENOVIĆ and VOJISLAV FILIPOVIĆ

The drawing of copper wire to a finer gauge wire is only possible when oxide is absent from the surface of the wire. Removal of oxide from copper wires is usually done in sulfuric acid solutions, and the completion of the process is in most cases judged by eye[1].

After the removal of oxide the Cu-enriched sulfuric acid solution is electrolysed, using an insoluble anode, for regeneration of the sulfuric acid and precipitation of the valuable copper, according to the reaction

$$2CuSO_4 + 2H_2O = 2Cu + 2H_2SO_4 + O_2$$

This regeneration is conducted not only for economic reasons — sulfuric acid solutions and copper compounds are strong poisons for flora and fauna and the safety regulations require that the harmful effects of these substances be neutralized. By eletrolytic regeneration of the sulfuric acid and copper sulfate solutions the maximum economic efficiency is obtained while avoiding the discharge of poisonous waste. The profitability of removing oxide from copper wires increases the shorter time this process takes, or the higher the quality of the copper and the current efficiency of the eletrolytic regeneration.

EXPERIMENTAL

Our tests showed that the time taken to remove oxide from the surface of a copper wire depends on the concentration of the sulfuric acid and copper sulfate, solution temperature, and to some extent on stirring. To determine the time required, oxide coated sample wires 100 *mm* long and 6 *mm* dia, drawn at the Moša Pijade factory in Svetozarevo were subjected to the action of a solution of sulfuric acid and copper sulfate. Copper oxide dissolves entirely in this solution, while metallic copper dissolves negligibly.

* Communicated at the 13th Symposium of Chemists of the S. R. of Serbia, Belgrade, 22—24 January 1968.

Cleaning and electrolysis of the used cleaning solution were conducted in a 240 × 145 × 150 *mm* glass bath with 5 lit solution. The time of oxide removal and the current efficiency were investigated using 6% to 16% sulfuric acid solutions. The results are shown in Table 1 and Fig. 1.

TABLE 1

Effect of Sulfuric Acid Concentration on the Duration of Cleaning and Current Efficiency

Solution components		Temperature of solution °C	Cleaning time *min*	Current efficiency %
Copper *g/lit*	Sulfuric acid %			
19.9	5.9	55.0	26	94.0
20.0	7.8	55.0	15	98.9
20.0	10.4	55.0	9.0	94.0
19.9	11.9	55.0	8.0	91.0
19.8	14.0	55.0	7.0	90.8
19.9	16.2	55.0	6.0	89.9
Cathode current density: 150 A/m^2				
Anode current density: 230 A/m^2				

From the data in Table 1 it may be seen that the oxide removal time decreases as the concentration of sulfuric acid increases. Figure 1 shows that with increasing sulfuric acid concentration the cleaning time decreases faster at first, but from 10% concentration upward it falls much more slowly.

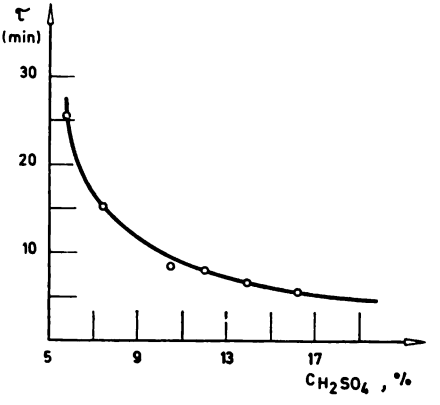

Figure 1

Dependence of cleaning time on sulfuric acid concentration

With the increasing sulfuric acid concentration the current efficiency of electrolytic copper regeneration with lead anodes and copper cathodes shows a downward trend.

The effect of copper concentration in the solution on cleaning time was investigated with sulfuric acid solutions containing 17 to 30 *g/lit* copper. The results are presented in Table 2 and Fig. 2. From Table 2 it may be concluded that this time increases with increasing copper concentration in solution. The rate of decomposition of oxide in these solutions agrees with the theoretical predictions.

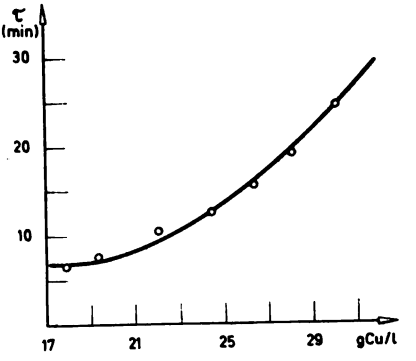

Figure 2

Dependence of cleaning time on copper content

TABLE 2

Effect of the Concentration of Copper in Solution on the Duration of Cleaning and Current Efficiency

Solution components		Temperature of solution °C	Cleaning time *min*	Current eff.ciency %
Copper *g/lit*	Sulfuric acid %			
17.8	10.7	55	7.0	95.8
19.3	10.4	55	8.5	95.3
22.0	10.7	55	11	95.7
24.4	10.6	55	13	95.8
26.4	10.5	55	16	95.1
27.9	10.6	55	20	96.0
30.0	10.7	55	25	95.9

Cathode current density: 150 A/m^2

Anode current density: 230 A/m^2

The coefficient of current efficiency of copper in electrolytic regeneration of these solutions remains virtually constant.

According to the results of our tests (Table 3, Figs. 3 and 4), the temperature of the solution affects not only the cleaning time but also the current efficiency. The results in Table 3 show that the higher the temperature of the solution the shorter the cleaning time, while the current efficiency rises at first and then falls off. With rising temperature up to about 55°C the cleaning time falls off faster than it does above this temperature.

TABLE 3

Effect of Temperature on the Duration of Cleaning and Current Utilization Efficiency

Solution components		Temperature of solution °C	Cleaning time *min*	Current efficiency %
Copper *g/lit*	Sulfuric acid %			
20.7	10.3	40	21	86.4
20.7	10.4	45	15	91.3
20.5	10.3	50	12	95.2
20.5	10.3	55	9.0	95.4
20.6	10.4	60	8.0	94.2
20.5	10.3	70	6.0	87.5
20.6	10.2	75	5.0	87.0

Cathode current density: 150 A/m^2
Anode current density: 230 A/m^2

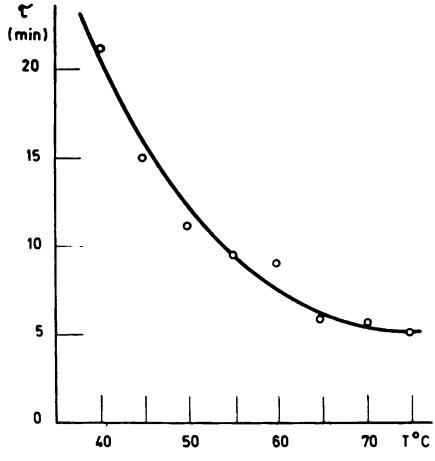

Figure 3

Dependence of cleaning time on temperature

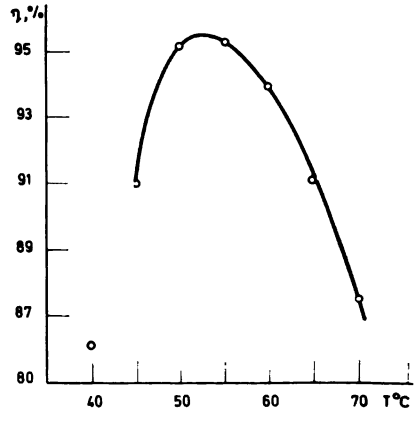

Figure 4

Dependence of current efficiency on temperature

TABLE 4

Change in Potential of Copper Wire during Cleaning

Cleaning time *min*	Potential *V*
0.5	0.361
3.0	0.341
5.0	0.334
7.0	0.331
9.0	0.329
11.0	0.329
13.0	0.329
15.0	0.329
20.0	0.329

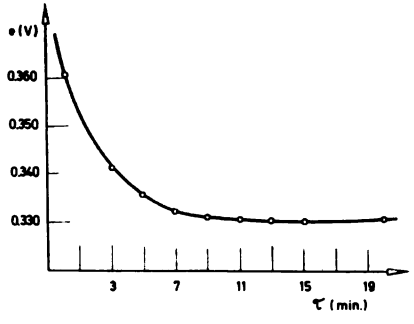

Figure 5

Change in the potential of the copper during cleaning

It may be inferred from Fig. 4 that the maximum current efficiency of electrolytic regeneration of these solutions is obtained within the temperature range 50—60°C. At cathode current densities of 130 to 230 A/m^2 the efficiency varied between 90% and 95% without any apparent regularity.

During the cleaning of oxide from wire surface it was established that the potential of the wires became more negative, to become constant at the end of cleaning. Changes in the electrochemicalpotential of the copper wire during cleaning in a solution of sulfuric acid (10.2%) and copper sulfate (19.7 *g* Cu/lit) at 55°C are shown in Table 4 and Fig. 5. The potential ceases to change after 9 min of cleaning. This time also corresponds to the time of cleaning. From these results it may concluded that measuring the electrochemical potential of the copper wire in the cleaning solution can be employed for determination of the end of cleaning, and could be utilized in automation of the process.

School of Technology and Metallurgy
Department of Physical
Chemistry and Electrochemistry
Belgrade University

Received 17 June 1969

REFERENCES

1. Smiriagin, A. P., N. Z. Dnestrovskii, A. D. Landikhov, N. N. Kreindlin, G. N. Krucher V. A. Golovin, B. L. Urin, and V. N. Gol'dreer. *Obrabotka tsvetnykh metallov i splavov* (Treatment of Nonferrous Metals and Alloys) — Moskva: Gosudarstvennoe nauchno-tekhnicheskoe izdatel'stvo literatury po chernoi i tsvetnoi metallurgii, 1961.

GLASNIK HEMIJSKOG DRUŠTVA, Vol. 34, No. 5-6-7, 1969, pp. 409—417

GHDB-74

536.24:534

Original Scientific Paper

THE INFLUENCE OF VIBRATIONS ON BOILING HEAT TRANSFER

by

MILAN V. MITROVIĆ, BOJAN D. ĐORĐEVIĆ, MILAN K. BILIĆ, and ALEKSANDAR Ž. TASIĆ

Vibrations of a solid surface in contact with a fluid disturb the boundary layer and the secondary steady flow in the fluid, thereby influencing the process at phase boundaries.

For process engineering the influence of heat and mass transfer between the solid body and the fluid, whether in a biphasic system or in a third phase occurring at the boundary surface, are of particular interest. The boiling of a liquid at a heated solid surface is one of the technically and theoretically most important cases of heat transfer between two phases with the generation of a third phase.

The objective of this study was to examine heat transfer and the kinetics of boiling from a heated horizontal disk vibrating at right angles to its plane in a stationary liquid. We wanted to extend our research to include the transfer of heat from vibrating elements to polyphasic systems. We believed that influences of the vibrations on the fluid other than those mentioned above would also appear. They would be related to the creation and break-away of vapor bubbles from the solid surface, because of which additional effects would be obtained involving the hydrodynamics of the system and the conditions of heat transfer.

REVIEW OF THE LITERATURE

The effect of different modes mechanical and acoustic vibration on heat transfer under natural or forced convection has been investigated most for monophasic systems. The vibrating elements most often used to investigate heat transfer were cylinder, channel or tube[1–4], wire[5–7], or plate[8–12].

The effect of vibration on heat transfer in a boiling single-component liquid system and in solutions has only been studied on a very small scale. Kovalenko[13] investigated the effect of vibration on heat transfer to boiling water at low and moderate specific heat fluxes. The frequency range investigated was 700—3000 Hz at specific heat fluxes of 4000—25000 $kcal/m^2h$. The amplitude was changed between 0.15 and 0.35 *mm*. The results show that vibration intensified heat transfer at low heat fluxes. Nangia and Chon[14]

carried out experiments to determine the effect of vibration on heat transfer to water boiling at atmospheric pressure. Wires of 0.254 *mm* diameter were heated electrically and vibrated electromagnetically at frequencies from 20 to 115 *c/s* and amplitudes of 0.03—0.178 *mm*. Heat flux from the wire was increased by as much as 200%. The effect of supersonic vibration on boiling in the critical zone was investigated by Ornatskii and Shcherbakoov[15]. They used 0.4 *mm* nickel-chromium wire, 45—55 *mm* long. The critical heat flux was increased 60%. The effect of vibration on the heat transfer coefficient in boiling liquid under forced convection was researched by Bergles[16]. He found that increasing the water flow speed reduced the influence of vibration on heat transfer.

EXPERIMENTAL

Apparatus — To facilitate the comparison of the present results with those from earlier work[11] we used a vibrating body of the same dimensions and shape as before. This body, on which the liquid was made to boil, was

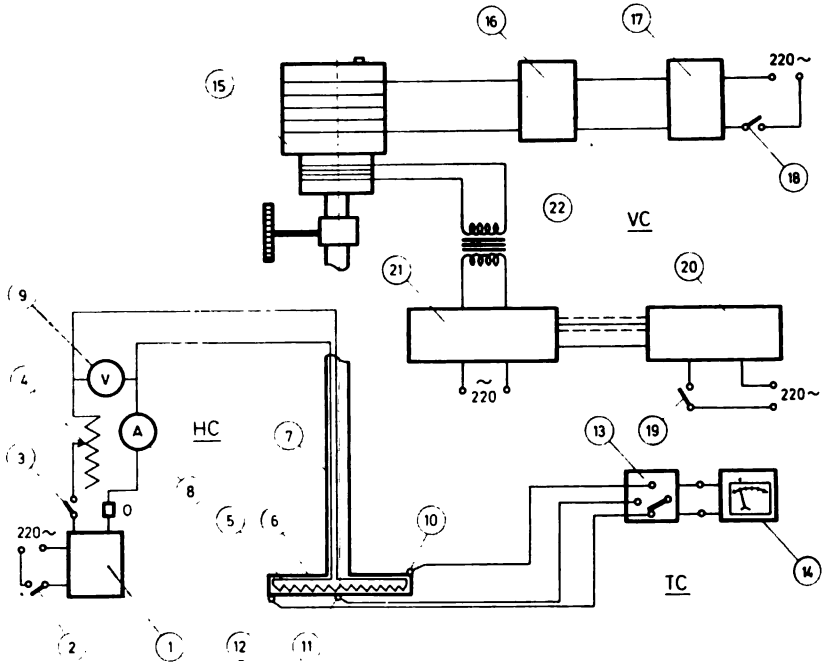

Figure 3.1
Circuit diagrams

KG — heater circuit
1 — stabilizer; 2, 3 — switches; 4, 5 — rheostats; 6 — disk;
7 — hollow ceramic rod; 8 — amperometer; 9 — voltmeter
KT — Thermocouple circuit
10, 11 12 — thermocouples; 13 — multipole switch; 14 — millivoltmeter;
KV — Vibrator circuit
15 — vibrator; 16 — rectifier; 17 — stabilizer; 18, 19 — switches;
20 — RC generator; 21 — low-frequency amplifier; 22 — transformer.

a disk 50 *mm* in diameter and 4 *mm* thick, attached to a 200 *mm* long ceramic rod 8 *mm* in diameter. The disk was placed in the middle of a 1 lit glass beaker. The ceramic rod was connected to an electromechanical vibrator, and via the rod and flexible conductors the disk electrically heated and connected to instruments for measuring its surface temperature. A picture of the disk, the apparatus and the circuit diagram are presented in Fig. 3. 1.

The disk consists of two copper plates 1 *mm* thick, one flat and one with a 1 *mm* flange. The two plates were hard soldered together with silver, with an electric heater in the space between them, made of ⌀ 0.3 *mm* Kantal resistance wire of 48.2 Ω/m. The resistance wire is coiled into a ⌀ 1.6 *mm* spiral and placed in the hollow between the plates in the form of a bifilar flat spiral with the two ends in the center of the disk. The spiral is insulated from plates by mica, while coils are insulated from one another with a ceramic cement which fills in the whole remaining space between the plates. This cement also keeps the heater coils in position. The heater terminals are connected to copper wires passing through 2 of the 4 channels in the ceramic rod. Three thermocouples (copper-constant, ⌀ 0.2 *mm*) were soldered on the external surface of the disk. The position of the thermocouples and the cross section of the disk are shown in Fig. 3. 1.

The vibrator works on the principle of a dynamic loudspeaker. The amplitude and frequency were changed by altering the voltage and frequency of the current driving the moving coil of the vibrator, derived from an audio generator and a 50 W LF amplifier. The frequency range employed was 18—50 Hz, at amplitudes of 0—2.7 *mm*. Amplitudes were measured optically by a calibrated microscope.

METHOD

All measurements were made in double-distilled deaerated water at atmospheric pressure. To achieve steady conditions and desired differences in temperature between the disk and the water, the latter was heated with an external heater which kept the vessel at the desired constant temperature. The time to achieve steady state, i.e. steady temperetures of the water and the surface of the disk, was to 2—3 *h* depending on the water temperature. Because of the relatively low power of the heater in the disk, the maximum temperature difference between the disk surface and the boiling water was 14° C when the disk was stationary. At the same heat flux but with vibrations the difference in temperature was still less, which confined our measurements to a relatively narrow range of boiling, far from the range of the occurrence of a vapor film on the disk. The difference in temperature was reduced by reducing water power and hence the heat flux from the disk. The maximum flux achieved was $6.55 \cdot 10^4$ *kcal*/m^2h. The maximum flux was limited because of the design difficulties involved in fitting a more powerful heater into the cavity of the disk. The heat flux was measured with an ampermeter and a woltmeter connected to the heater terminals. The heater power was changed with an adjustable transformer connected via a magnetic stabilizer to the mains.

In the first series of tests, the difference between the disk surface temperature and the saturation temperature with the disk stationary,

i.e. under conditions of boiling with natural convection, was recorded as a function of the heat flux from the disk surface.

In the second series of measurements, the disk was vibrated during measurement, at different amplitudes and frequencies. Heat flux, amplitude and frequency were kept constant during one run, and readings were taken when the steady state had been achieved.

DISCUSSION

Heat transfer from the stationary disk is presented in Fig. 3. 2 (curve 1). This graph and the others which show the effect of vibration, plot the difference between the temperature of the disk surface and the saturation temperature as a function of the heat flux from the disk. The curves show two clearly defined zones of heat transfer when the disk is stationary, one in which the temperature difference rises steeply with increasing heat flux, which can be explained by natural convection without boiling, or with boiling from a small number of centers of nucleation, and the other corresponding saturated boiling with separate bubbles, in which considerable heat fluxes are obtained at small differences in temperature. This zone must extend still more, because the range of film boiling, according to the theory of boiling, occurs at considerably greater heat fluxes than those we achieved.

The existence of the two zones was confirmed by the observation of bubbles which formed and broke off from the disk surface. In the former range, a limited number of small bubbles formed on the disk, probably due to the liberation of residual dissolved gases. In the transitional region between the two zones the number of centers of nucleation increases, some of the bubbles grow and break away from the surface. In the latter zone there is ebullition. It is to be noted that the upper and lower surfaces of the disk are not the same because of its horizontal position. Considerably better defined phenomena take place on the upper surface, while rather large bubbles appear on the lower surface and remain around the disk center. This restricts the possibility of a full interpretation of heat transfer to the boiling liquid from the stationary disk since the proportions of the heat transferred from the upper and lower faces cannot be determined.

Figures 3.2, 3.3 and 3.4 show the effect of vibrations of different amplitudes and frequencies on heat transfer during boiling under the same conditions as those for the stationary disk. All graphs compare the curves with vibration and those for the non-vibrating disk. Thay show that an increase in frequency or in amplitude intensifies heat transfer both in the boiling range and below boiling. The effect of vibration is manifested in two ways:

1) Increased heat transfer without boiling
(2) Lowering of the transitional region in temperature

The increase in heat transfer in the first zone is approximately linear and does not depend on the temperature difference between the disk surface and the fluid, which is in agreement with earlier results[11]. The increase in the heat transfer coefficient can be ascribed to the development of secondary steady currents generated by the vibrations and superimposed on the natural convection. It may also be attributed to the effect of vibration on the thermal boundary layer. The second phenomenon can be attributed to several factors.

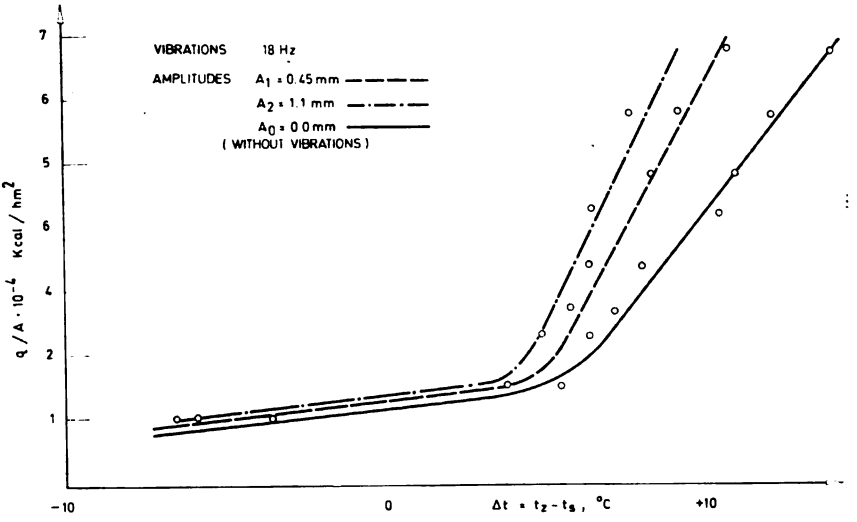

Figure 3.2

Dependence of heat flux on the difference between the temperature of the disk surface and that of the boiling water, for stationary disk and at a frequency of 18 Hz with different amplitudes

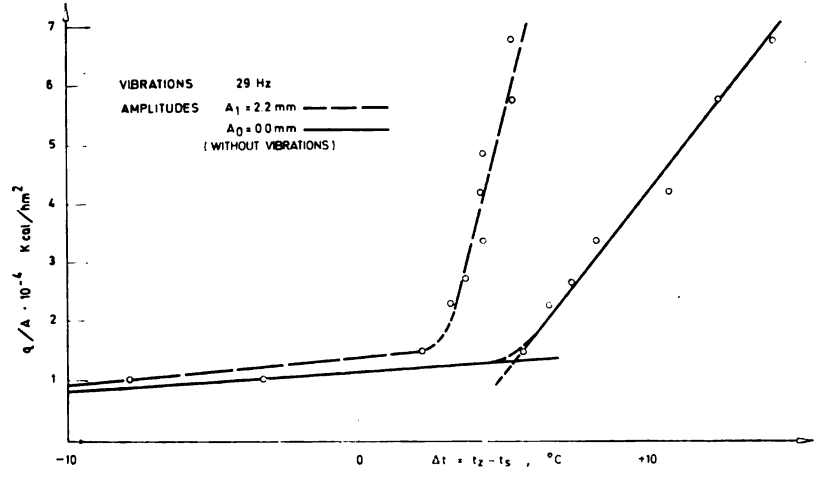

Figure 3.3

Dependence of heat flux on the difference between the temperature of the disk surface and that of the boiling water, for stationary disk and at a frequency of 29 Hz and amplitude 2.2 *mm*

Apart from the effect of vibrations already mentioned, in this case the bubbles break off earlier under the influence of vibration; centers of nucleation are formed at the wave nodes in the boundary layer, and the surface is sooner freed for another nucleation. Vibrations obviously considerably augment the phenomena which otherwise appear during boiling. Because of the superposition of these phenomena, the effect of vibrations in the boiling zone is considerably greater than in the zone without boiling.

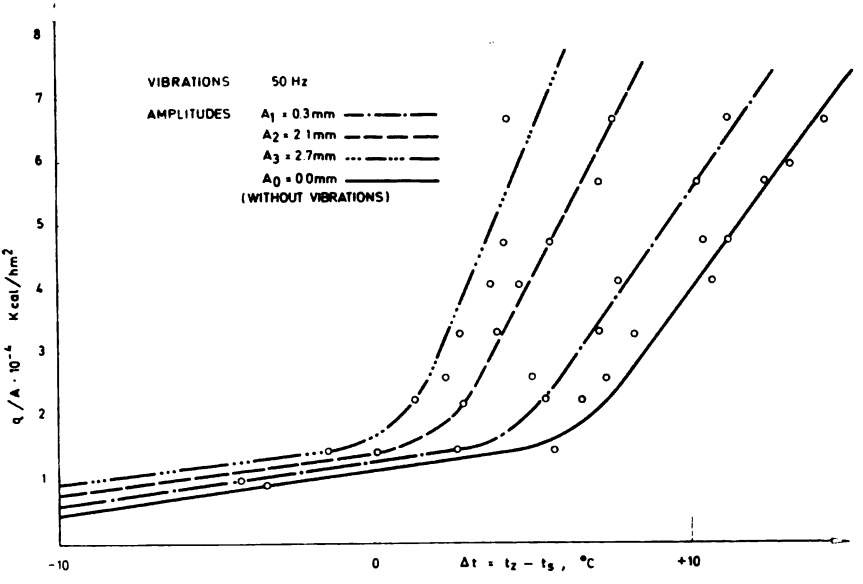

Figure 3.4

Dependence of heat flux on the difference between the temperature of the disk surface and that of the boiling water, for stationary disk and at a frequency of 50 Hz with different amplitudes

With vibrations, the mode of boiling on the upper and lower faces of the disk becomes much more symmetrical, that is the influence of natural convection decreases with increasing amplitude and frequency.

CONCLUSION

No quantitative conclusions on the effects of amplitude and frequency of vibration on heat transfer in the boiling zone can be drawn from the results of this study. The superposition of the factors mentioned and those of the shape and size of the heated object and the vessel, possible resonance at certain frequencies, and of the free surface in the vessel, all make for such complex relationships that they cannot yet be covered comprehensively. They will be the subject of future study.

However, the qualitative picture obtained from the graphs clearly demonstrates the basic phenomena. Practically speaking, it may be seen that vibrations can intensify heat transfer during boiling by as much as 450%, at the maximum amplitude and frequency used (Fig. 3, 4). This increase is very significant given that the heat transfer coefficient is anyway relatively high during ebullition. Another significant fact is that vibrations can lower the beginning of steady boiling so that overheating of liquid on heated surfaces can be avoided, a fact which may be of technical importance.

All this indicates the significance of investigating the effect of vibrations on boiling from both the theoretical and practical engineering aspects.

School of Technology
Department of Chemical and Metallurgical Engineering
Belgrade University

Received 30 May, 1968

REFERENCES

1. Martinelli, R. S. and L. M. Boelter. "The Effect of Vibration on Heat transfer by Free Convection from a Horizontal Cylinder", in: *Proceedings of the Fifth International Congress of Applied Mechanics,* Cambridge, Mass., 1938— New York: Willey, 1939.
2. Kalashnikov, N. V. and V. I. Chernikin. "Teplootdacha vibriruiushchikh podogrevatelei" (Heat Transfer of Vibrating Heaters) — *Teploenergetika* (10): 78—80, 1958.
3. Fand, R. M. and E. M. Peebles. "A Comparison of the Influence of Mechanical and Acoustical Vibrations on Free Convections from a Horizontal Cylinder" — *Journal of Heat Transfer, Transactions of the American Society of Mechanical Engineers, series C* (hereafter to be called *J. H. T.*) 84: 268, 1962.
4. Bergles, A. E. and P. H. Newell. "The Influence of Ultrasonic Vibrations on Heat Transfer to Water Flowing in Annuli" — *Journal of Heat Mass Transfer* 8 (10): 1273—1280, 1965.
5. Lemlich, R. "Effect of Vibrations on Natural Convective Heat Transfer" — *Industrial and Engineering Chemistry* 47 (6): 1175—1180, 1955.
6. Deaver, F. K., W. R. Penney, and T. B. Jefferson. "Heat Transfer from an Oscillating Horizontal Wire to Water" — *J. H. T.* 84: 251—254, 1962.
7. Anantanarayanan, R. and A. Ramachandran. "Effect of Vibration on Heat Transfer from a Wire to Air in Parallel Flow" — *J. H. T.* 80: 1426, 1958.
8. June R. R. and M. J. Baker. "The Effect of Sound on Free Convection Heat Transfer from a Vertical Flat Plate" — *J. H. T.* 85: 279, 1963.
9. Schoenhals, R. J. and J. A. Clark. "Laminar Free Convection Boundary-Layer Perturbations due to Transverse Wall" — *J. H. T.* 84: 225—232, 1926.
10. Scanlan, J. A. "Effect of Normal Surface Vibrations on Laminar Forced Convective Heat Transfer" — *Industrial and Engineering Chemistry* 50 (10): 1565—1568, 1958.
11. Mitrović, M. *Doktorska disertacija br. 4524* (Doctoral Thesis No. 4524) — Beograd: Tehnološko-metalurški fakultet, 1965.
12. Fand, R. M. and J. Kaue. "The Influence of Sound on Free Convection from a Horizontal Cylinder" — *J. H. T.* 83: 133—148, 1961.
13. Kovalenko, V. F. "Opytnoe issledovanie vlianila vibratsii na teplootdachu pri kipenii" (Experiments on the Influence of Vibrations on Boiling Heat Tranfer) — *Teploenergetika* (2): 76—77, 1958.
14. Nangia, K. K. and W. Y. Chon. "Some Observations on the Effect of Interfacial Vibration on Saturated Boiling Heat Transfer" — *Journal of American Institute of Chemical Engineers* 13: 872—883, 1967.
15. Ornatskii, A. P. and V. K. Shcherbakov. "Intensifikatsiia teploobmena v oblasti krizisa s pomoshch'iu ultrazvuka" (Ultrasonic Augmentation of Heat Transfer in Critical Zone) — *Teploenergetika* (1): 84, 1959.
16. Bergles, A. E. "The Influence of Flow Vibrations on Forced-Convection Heat Transfer" — *J. H. T.* 86: 559—560, 1964.

GLASNIK HEMIJSKOG DRUŠTVA, Vol. 34, No. 5-6-7, 1969, pp. 419—421

GHDB-75

541.128:543.061

Original Scientific Paper

APPLICATION OF CATALYTIC IDENTIFICATION REACTIONS IN THE RING OVEN METHOD

by

HERBERT WEISZ and TIBOR F. A. KISS*

The ring oven method can be regarded as a special spot-test analysis technique on filter paper, in which, however, the substances to be identified do not react with the reagent in the form of spots, but react in much higher concentration as sharply defined circular lines (22 *mm* in diameter) [1].

Identification reactions based on the catalytic effect are most often very sensitive, because the reaction product to be observed is not formed by stoichiometric reaction between the reagent and the substance to be identified, but the latter is a catalyst for a reaction in which most often a considerable conversion of reaction material takes place. It is to be expected that such catalytic identification reactions will be more sensitive if the substance acting as the catalyst and which is to be identified, is further concentrated in a sharply defined line, as is possible in the ring oven method.

The substance to be identified is washed out with an appropriate washing solution in the ring zone of a round filter paper, as is usually done in the ring oven method, and than sprayed with or dipped in the reagent solution.

In the sharply defined ring zone, a fast coloration (or decoloration) resulting from the catalytic effect of the substance to be identified is observed. Blank tests must always be carried out too.

Several examples of such reactions, already mentioned in the first edition of the monograph on ring oven technique[1], will be described here. Detailed procedures and detection limits will be presented. To obtain high sensitivity, very identification conditions must be strictly adhered to.

All the reactions described here were carried out on ⌀ 55 *mm* MN 2260 filter paper (Machery, Nagel und Co., Düren).

Identification of Copper (II) by Catalytic Acceleration of the Iron (III) — Thiosulphate Reaction[2,3]

A drop of the test solution (1 μl) is placed by capillary pipette in the center of a round filter paper, washed out on the ring oven (ROFA, Vienna)

Adress: Department of Chemistry, University of Novi Sad, Yugoslavia

three times with 10 μl at a time of 0.1% KNO_3 solution, and then dried in a stream of warm air. A blank test is carried out in the same way. If the rings (or sectors of them) are sprayed with 0.05 M sodium thiosulphate solution and immediately after that with iron (III) thiocyanate solution (aqueous solution of 2 *g* KCNS is added to a solution of 1.5 *g* $FeCl_3 \cdot 6H_2O$ in 5 *ml* 2 N HCl + 10 *ml* H_2O and diluted with H_2O to 100 *ml*) then the test ring is decolored faster than the blank. The decoloration is considerably faster down to about 10^{-4} μg (= 0.1 *ng*) of Cu in the whole ring. Because of the filter paper always contains traces of copper, the blank test ring will also be decolored.

Identification of Bismuth (III) with Alkaline Stannite Solution[3,4]

A drop of the test solution is washed out into the ring with 0.1 N HCl and dried. After that the filter paper (or a sector of it) is dipped in 10 *ml* of stannite solution (equal parts of 20% NaOH solution and of a solution of 5 *g* $CnCl_2 \cdot 2\,H_2O$ + 5 *ml* conc. HCl + 95 *ml* H_2O are mixed directly before use) to which 3 drops of 3% lead acetate solution is added. After some time, which depends on the quantity of bismuth, in the ring zone a sharply defined greyish brown-black line of metallic lead appears. This well-known reaction is based on the inductive effect of bismuth reduction on lead reduction. With a bismuth content of 10^{-2} μg in the ring a black color appears after about 10 *min*, and with 10^{-3} μg after 25 *min*. If the run is continued to 45 *min* it is possible to identify even 10^{-7} μg (= 0.1 *pg*) of bismuth with some certainty.

Here, as in other catalytic identification reactions, the detection limits cannot be determined with any accurcy, because the uncatalysed reactions in the blank test also proceed to some extent. Here, the ring oven method has an advantage because the site of the reaction is precisely defined.

Identification of Phosphate with Molybdate-Ascorbic Acid[3, 5, 6]

A drop of the test solution (1 μl) is placed on a filter paper wetted with 6 μl of double-distilled water. About 4 μl of 0.25 M sodium molybdate solution is added dropwise and then washed out into the ring zone on the ring oven with water and 2 N HNO_3, alternately. Immediately after that, the filter paper is dipped in 0.05 M ascorbic acid solution for 1—2 *min* and thoroughly washed under tap water. A bright blue ring remains considerably different from the corresponding ring zone of the blank test.

About 10^{-4} μg of phosphate can be identified in this way. If coloring of the blank test is minimized by special precautions (storing solutions in polyethylene bottls, thoroughly cleaning the pipettes with chrome-sulphuric acid), still smaller amounts. As low as 10^{-6} μg or even 10^{-8} μg, can be identified with some certainty.

Identification of Sulphide, Thiosulphate, Thiocarbamide and Cystein with the Iodine-Azide Reaction[3,7]

A drop of the test solution (1 μl) is washed out into the ring zone with distilled water, dried in a stream of warm air and sprayed with an iodine-azide solution (3 *g* NaN_3 is dissolved in 100 *ml* of 0.1 N iodine solution). After

only a few seconds the ring zone has already become colorless. The color contrast becomes more explicit if the filter paper additionally is sprayed with starch solution. A blank test is carried out!

Between 10^{-2} — 10^{-3} μg of the mentioned substances can be identified reliably.

We would note that the same catalytic reactions have also been studied for application to semi-quantitative ring-ovem-spot-colorimetry[1]. The results were not satisfactory because the colorations and decolorations were not reliably reproducible.

SUMMARY

The application of catalytic identification reactions in the ring oven method is discussed. The substance to be identified and which is a catalyst is concentrated on a filter paper in a sharply defined circular line and sprayed with or dipped in a reagent solution.

The method is illustrated by means of four known catalytic identification reactions.

ACKNOWLEDGEMENT

We would like to thank the Alexander von Humboldt Foundation which made this work possible through a fellowship (T. K.).

Department of Analytical Chemistry
Institute of Chemistry
University of Freiburg in Breisgau
Federal Republic of Germany

Received 13 May, 1969

REFERENCES

1. Weisz, H. *Microanalysis by the Ring Oven Technique* — Oxford: Pergamon Press, 1961.
2. Feigl, F. *Tüpfelanalyse, Band I,* — Frankfurt/Main: Akademische Verlagsgesellschaft, 1960.
3. Hahn, F. L. and G. Leimbach "Eine eigenartige katalystische Reaktion als Nach weis und Bestimmungsverfahren für kleine Kupfer-mengen" — *Berichte der deutschen chemischen Gesellschaft* (Berlin) 55: 3070—3074, 1922.
4. Feigl, F. and P. Krumholz. "Beiträge zur analytischen Auswertung komplexchemischer und induzierter Reaktionen" — *Berichte der deutschen chemischen Gesellschaft* (Berlin) 62: 1138—1142, 1929.
5. Crouch, S. R. and H. V. Malmstadt. "Mechanistic Investigation of Molybdenum Blue Method for Determination of Phosphate" — *Anallytical Chemistry* (Washington) 39: 1084—1089, 1967.
6. Bognar, J. and J. Czekkel. "Ultramikrobestimmung von Phosphat auf katalytischer Grundlage mit Hilfe der Simultankomparation methode" — *Mikrochimica Acta* (Wien): 1014—1024, 1965.
7. Feigl, F. "Uber einen neuen empfindlichen Nachweis von Sulfiden und Thiosulfaten" — *Zeitschrift für analytische Chemie* (München) 74: 369—376, 1928.

GLASNIK HEMIJSKOG DRUŠTVA, Vol. 34, No. 5-6-7, 1969, pp. 423—426

GHDB-76

543.244.6:546.98

Original Scientific Paper

COMPLEXOMETRIC DETERMINATION OF PALLADIUM BY BACK-TITRATION USING O,O'-DIHYDROXY-SUBSTITUTED AZO DYE INDICATORS

by

TIBOR A. KISS, FERENC F. GAÀL and TERÈZIA SURÀNYI

In complexometric determination of palladium (II) by back-titration using Eriochrome Black T[1, 2] or some other o,o'-dihydroxy-substituted azo dye as indicator, an irreversible color change and the blocking of indicator at higher concentrations of palladium (II) ion were found to occur (Table 1).

We have found[4–6] that the values for log K_{MY}* are several units higher in 70% ethanol than in water, as Schwarzenbach and Ackerman[3] have shown. This has been employed to avoid the blocking of Eriochrome Black T in the EDTA titration of scandium[7], copper[8], nickel[9], aluminum[10–12] and iron[12, 13].

We succeeded in avoiding the blocking of o,o'-dihydroxy-substituted azo dye indicators in determination of palladium (II) by back-titration using 70% ethanol as the solvent. Thus a method has been worked out which can further be used for the determination of great concentrations of palladium (II) by a reversible color change.

EXPERIMENTAL

Reagents

Standard solution of 0.05 M EDTA[14], zinc nitrate, magnesium sulphate and manganese (II) sulphate were used. Molarities of the metal salt solutions were determined by inverse titration with EDTA as the primary standard substance using Eriochrome Black T as indicator.

The molarity of a 0.025 M palladium (II) chloride solution was determined by back-titration with zinc nitrate solution using Xylenol orange is indicator[15].

The indicator mixture was obtained by grinding Eriochrome Black T, Erio B, Erio SE, Erio R, Eriochrome Red B or Cal-Red with potassium nitrate in the ratio 1 : 100 to a very fine powder.

* K = stability constant

Other reagents and solvents: 96 % ethanol, methanol, acetone, 1 N sodium hydroxide and ascorbic acid (A. R.).

PROCEDURE

2—4 *ml* of 0.025 M weakly acidic palladium (II) chloride solution and 2—4 *ml* of 0.05 M standard EDTA solution were placed in a 50 *ml* beaker. Ethanol was added with constant stirring to 70 % of the total volume. The pH was adjusted to 10 ± 1 using 1 N sodium hydroxide. After additon of about 50 *ml* indicator powder the excess of EDTA was titrated with 0.05 M solution of zinc nitrate, manganese (II) sulphate or magnesium sulphate until a sharp color change indicated the end point. If manganese sulphate was used as back-titrant it was necessary to add 0.1 g of ascorbic acid or hydroxylamine hydrochloride.

RESULTS

The results are summarized in Table 1. As can be seen they are within the range generally achieved in complexometric back-titrations.

TABLE 1

Complexometric Determination of Palladium (II) by Back-titration with Zinc Nitrate, Magnesium Sulphate or Manganese (II) Sulphate as Standard Solutions in Presence of Eriochrome Black T in Water or 70% Ethanol as Solvent.

mg Palladium taken	Back-titrated with standard solution of:							
	Zinc				Magnesium		Manganese	
	in water		in 70 % ethanol					
	R %*	σ**	R %*	σ**	R%*	σ**	R %*	σ**
1.021	+2.4	0.08	—	—	—	—	—	—
3.402	+5.3	0.42	—	—	—	—	—	—
5.256	***	—	+0.11	0.025	—0.24	0.030	+0.15	0.018
8.409	***	—	+0.09	0.027	+0.12	0.025	—0.10	0.025
10.51	***	—	+0.41	0.027	+0.48	0.032	+0.51	0.020

* Relative error in percent. Mean value of nine determinations.

** Standard deviation in mg of palladium. Calculated from 9 determinations.

*** Indicator blocked right at the beginning of the titration.

DISCUSSION

The presence of ethanol obviates blocking of the indicator so that the titration can be performed slowly near the end point and a reversible color change is obtained. Due to the low solubility of metal salts in ethanol, its concentration should not exceed 70 %.

Instead of ethanol, methanol, 2-propanol, acetone or other organic solvents[12, 13] can be used. The effect of these solvents was explained in one of our previous papers[12].

Due to the great stability of the palladium (II)-ammonia complex, the usual ammonium hydroxide — ammonium chloride buffer cannot be applied.

As platinum(II) and platinum (IV) form stable chloro-complexes, these ions do not interfere. Ruthenium (III) and iridium (IV) do not interfere either, while rhodium (III) and osmium (IV) do.

SUMMARY

A method for the determination of palladium (II) by back-titration of the added excess of standard EDTA solution has been developed. The back--titration is performed at pH 10 ± 1 with zinc nitrate, magnesium sulphate or manganese (II) sulphate as standard solutions using an o,o'-dihydroxy--substituted azo dye indicator (Eriochome Black T, Erio B, Erio SE, Eriochrome Red B or Cal-Red). The blocking of the indicator is avoided by using 70 % ethanol as solvent. Quantities of 1—11 *mg* of palladium were determined in 20 *ml* of titrated solution. Platinum (II), platinum (IV), ruthenium (III) and iridium (IV) do not interfere, while rhodium (III) and osmium (IV) do.

University of Novi Sad,
Department of Chemistry

Received 9 April, 1969.

REFERENCES

1. Kinnunen, J. and B. Wennerstand. "EDTA Titration of Palladium" — *Chemist-Analyst* (Phillipsburg, N. J.) 47: 11, 1958.
2. McNevin, W. M. and O. H. Kriege. "Chelation of Platinum Group Metals. Complexometric Titration of Palladium" — *Analytical Chemistry* (Easton, Pa.) 27: 535—536, 1955.
3. Schwarzenbach, G. and H. Ackerman. "Komplexone XII. Die Homologen der Äthilendiamintetraessigsäure und ihre Erdalkalikomplexe" — *Helvetica Chimica Acta* (Basel) 31: 1029—1048, 1948.
4. Kiss, T. and T. Surànji. "Titrimetrische Bestimmung von Magnesium mit ÄDTA in äthanolhaltiger Lösung" — *Mikrochimica Acta* (Wien)9: 1102—1105, 1968.
5. Kiss, T. and O. Knežević. "Complexometric Determination of Magnesium in Magnesium Stearate" — *Microchemical Journal* (Easton, Pa.) 13: 459—462, 1968.
6. Kiss, T., F. Gaàl, T. Surànji, and I. Zs'grai. "Folgetitrimetrische Bestimmung von Calcium und Magnesium mit ÄDTA in äthanolhaltiger Lösung" — *Analytica Chimica Acta* (Amsterdam) 43: 340, 1968.
7. Wünsch, L. "Komplexometrische Titrationen (Chelatometrie) XIII. Bestimmung des Scandiums" — *Chemicke Listy* (Praha) 49: 843—847, 1955; *Collection of Czechoslovac Chemical Communications* (Praha) 20: 1007—1112, 1955.
8. Kiss, T., Gy Ràdy, and L. Erdey. "Komplexometrische Bestimmung von Kupfer mit ÄDTA durch Rücktitrationen gegen Eriochromschwarz T" — *Periodica Polytechnica* (Budapest) 10: 303—307, 1966.
9. Canić, V. and T. Kiss. "Addition of Ethanol in the EDTA Titration of Nickel" — *Chemist-Analyst* (Phillipsburg, N. J.) 52: 111, 1963.
10. Canić, V. and T. Kiss. "Prilog kompleksometrijskom određivanju metala IV. Određivanje aluminijuma" ("Complexometric Determination of Metals, IV. Determination of Aluminum") — *Glasnik hemijskog društva* (Beograd) 28*: 143—147, 1963.
11. Canić, V., and T. Kiss. "Određivanje alumin'juma t'trac'jom sa EDTA" (Complexometric Determination of Aluminum") — *Hemijska industrija* (Beograd) 18: 5—7, 1964.
12. Kiss T. "Deblokierung von Eriochromschwarz T bei Rücktitrationen von Kobalt, Eisen, Kupfer, Nickel und Aluminium unter Verwendung von organischen Lösungsmitteln" — *Zeitschrift für Analytische Chemie* (Wiesbaden) 208: 334—336, 1965.
13. Kiss, T. "Deblokiranje eriohromcrnog T" (Deblocking of Eriochrome Black T) — *Hemijska industrija* (Beograd) 19: 243—247, 1965.
14. Blaedel, W. J., and T. H. Knight. "Purification and Properities of Disodium Salt of Ethilenediaminetetraacetic Acid as a Primary Standard" — *Analytical Chemistry* (Easton, Pa.) 26: 741—743, 1954.
15. Iurist, I. M., and Z. V. Tiukova. "Kompleksometricheskoe opredelenie palladiia" (Complexometric Determination of Palladium) — *Zavodskaia laboratoriia* (Moskva) 28: 798—799, 1962.

* Available in English translation from National Technical Information Service, Virginia, Springfield, 22151.

GLASNIK HEMIJSKOG DRUŠTVA, Vol. 34, No. 5-6-7, 1969, pp. 427—434

GHDB-77

543.257.1:621.317.75:543.244.6

Original Scientific Paper

OSCILLOGRAPHIC-CHRONOPOTENTIOMETRIC TITRATION. V.* ACIDO-BASE AND CHELATOMETRIC TITRATIONS**

by

ĐORĐE K. STEFANOVIĆ, VILIM J. VAJGAND, and TIBOR A. KISS

In the previous parts of this study[1–4] we described the principles of a new procedure for end-point determination. On the example of the titration of arsenic (III) with potassium bromate the influence of various factors on the accuracy of this oscillographic-chronopotentiometric method were studied and the techniques for redox and precipitation titrations of some compounds were worked out.

This paper presents the results of our further research which show that this method of end-point determination can be successfully applied to acido-base and chelatometric titrations as well.

Acido-base titrations were conducted in the presence of a quinhydrone electrode. Using 1 N sodium hydroxide the changes in the DC potential of the indicator electrode were sufficiently great to cause marked distortions of the oscillograms, allowing determination of the end-point.

In potentiometric titrations with ethylenediaminetetraacetic acid (EDTA), for which macro indicator electrodes are used as a rule, sufficiently great changes in potential at the equivalence point are obtained. For the oscillographic-chronopotentiometric titrations we had to use a micro indicator electrode at which the DC potential changes were much too small to lead to any detectable distortion of the oscillogram. For this reason we first had to modify the potentiometric methods so as to achieve a big enough potential change with a microelectrode. To this end we had to augment the pMe*** changes at the end-point in the fol'owing ways[5]: (a) titrating more concentrated (0.1 N) solutions, (b) using chelating agents which build more labile secondary chelates, and (c) reducing the concentration of these agents. The last was achieved in two ways: either the metal was titrated with EDTA in an acidic solution up to near the end-point, and only then a minimum amount of chelating agent was added, or it was determined

* Parts I—IV published in earlier numbers of this journal.

** Communicated at the International Symposium on Instrumental Analytical Chemistry, Budapest, 1966.

*** pMe = negative logarithm of the ionic concentration of the metal being titrated.

by inverse titration without chelating agent. Using these modifications, iron (III) was directly potentiometrically titrated at a platinum electrode at pH 3 in the presence of nitrate as a labile chelating agent[6], copper at pH 7.5 in the presence of pyridine[7], a pH 5—6 in the presence of a mixture of ammonia and amonium acetate [8] and a mixture of ammonia, ammonium acetate and ammonium thiocyanate[9]. Using a rotary mercury indicator microelectrode we titrated nickel, zinc, magnesium and manganese at pH 7.5 in the presence of pyridine as chelating agent[7]. In all these determination we achieved considerable potential changes, 100—150 *mV*, at the end-point. Under the given working conditions this enabled oscillographic-chronopotentiometric determination of these end-points.

EXPERIMENTAL

Reagents

Preparation of 0.1 Standard Solutions — Merck p.a. chemicals were purified, their purity checked and solutions prepared according to standard procedures: 1 N hydrochloric acid[10a], 1 N sodium hydroxide[10b], disodium ethylenediaminetetraacetate dihydrate[11], zinc chloride[12], ferric chloride[13], magnesium chloride[13], copper nitrate[13], and nickel nitrate[13].

Standardization of Solutions. — The normality of the hydrochloric acid was checked by potentiometry with sodium carbonate[10c], that of sodium hydroxide with potassium biphthalate[14] in the presence of a quinhydrone electrode, that of ferric chloride[6], copper nitrate[7] nickel nitrate[7] and magnesium chloride[7] with an EDTA SOLUTION.

Apparatus

For the potentiometric titrations we used a pH-meter (PHM 22p), a TTA 1 titration set, a K 100 calomel electrode, a K 601 mercurous sulfate electrode, and a P 101 platinum electrode (produced by Radiometer).

For the oscillographic-chronopotentiometric titrations the apparatus described in a previous paper[1] was used.

METHOD

Titration of Hydrochloric Acid with Sodium Hydroxide — This titration was done in the presence of quinhydrone electrode, with an AC source of 20 *V*, a 100 *KΩ* resistor and a 0.33 *μF* condenser, vertical preamplification and different electrodes (Table 1). Corresponding distortions of oscillograms are shown in Fig. 1, and the results obtained in Tables 1 and 2.

Titrations with EDTA solution

General Procedure. — 5—15 *ml* 0.1 M solution of the metal is measured into a 50 *ml* beaker with a burette, the pH is adjusted with a corresponding

TABLE I

Survey of Conditions in Oscillographic-Chronopotentiometric Titrations of Hydrochloric Acid with Sodium Hydroxide by the Use of Quinhydrone Electrode

No. of experiment	Electrodes		Operating conditions of the current circuit (1)			Oscillogram Figure No.	Relative error in %	Average deviation in %
	Phase	Ground	$V \sim$	$k\Omega$	μF			
1	A	A	20	100	0.33	2a*	0.7	0.5
2	A	B	„	„	„	2a**	0.4	0.4
3	A	C	„	„	„	2a***	—0.2	0.3
4	A	SCE	„	200	„	2b+	0.4	0.4
5	B	A	40	„	0.22	2b+	0.5	0.4
6	C	A	„	100	0.33	2b++	—	—

Notes:

1) See figure 1 of the previous paper (1)
* small oscillogram distortions
** greater oscillogram distortions
*** greatest oscillogram distortions
A platinum wire electrode of 0.5 *cm* length
B platinum electrode "Radiometer" P 101
C platinum foil, 20 cm^2
D saturated calomel electrode
\+ medium oscillogram distortions
\+ + without oscillogram distortion

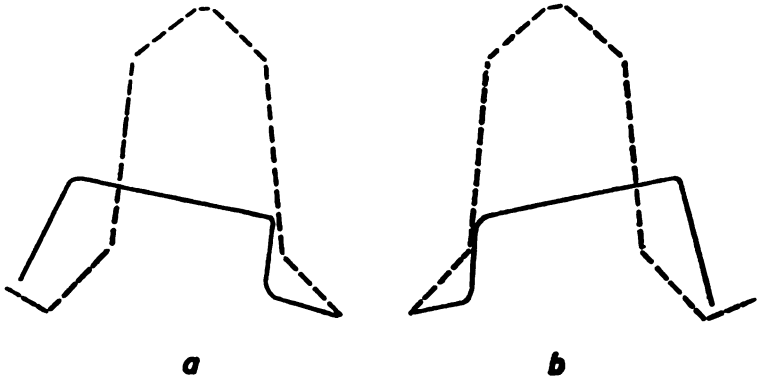

Figure 1.

Oscillogram distorsions during oscillographic-chronopotentiometric titrations of hydrochloric acid with 1 N natrium hydroxide under conditions presented in table I.

By determination No. : a = 1—3 b = 4,5

The form of oscillogram: – – – – – before the end-point
——————— at the end-point

buffer solution, the platinum microelectrode (0.5 *cm* thin U-shaped wire) is immersed in the solution which is then connected via an electrolytic bridge with a saturated calomel electrode with a large mercury surface area (10 cm^2). This galvanic cell is connected into the circuit for oscillographic-chronopotentiometric titration (Fig. 1 in the previous work[1]). The AC source voltage was 260 *V*, the resistor 200 $K\Omega$, the condenser 0.22 μF, and the KO4701 an oscillograph Avala. With constant magnetic stirring, the solution was titrated with the standard EDTA solution until abrupt distortion of the oscillogram. The results are given in Table 2.

TABLE 2

Results of Various Oscillographic-Chronopotentiometric Titrations

Substance titrated	Titrant	Relative error in %	Average deviation in %
Hydrochloric acid	Sodium hydroxide	0.1	0.3
Ferric chloride	EDTA	0.6	1.2
Cupric nitrate	EDTA	0.0	1.0
Manganous nitrate	EDTA	1.0	1.0
Magnesium chloride	EDTA	0.6	1.1
EDTA	Ferric chloride	—0.7	1.0
EDTA	Cupric nitrate	0.3	0.9
EDTA	Nickel nitrate	1.0	1.1
EDTA	Manganous nitrate	0.9	0.9
EDTA	Magnesium chloride	—0.3	1.0
Nickel nitrate	EDTA	—0.8	0.9

REMARK: The results are mean values of 8 determinations of 10—100 *mg* of titrated substance in 100 *ml* solution.

Ferric Chloride was titrated at pH 2 at 80°C in a solution containing ammonium acetate pH 5 as buffer[6]. Distortions of the oscilogram are shown in Fig. 2a.

Cupric nitrate was titrated in the presence of pyridine[7]. The oscillogram was distorted somewhat differently and less markedly when a 260 *V* AC source was used (Fig. 2b) instead of 40 *V* (Fig. 2c). It was also titrated by the addition of 1 *ml* 10% solution of ammonium acetate and 1—2 drops of 1 : 1 ammonia and 1 *ml* 5% solution of ammonium rhodanide at 40°C with a 260 *V* AC source[9]. Oscillogram distortions from these determinations are presented in Fig. 2d. The same distortions were obtained when the titration was done without ammonium rhodanide[6]. The results from determinations of copper are stated in Table 2.

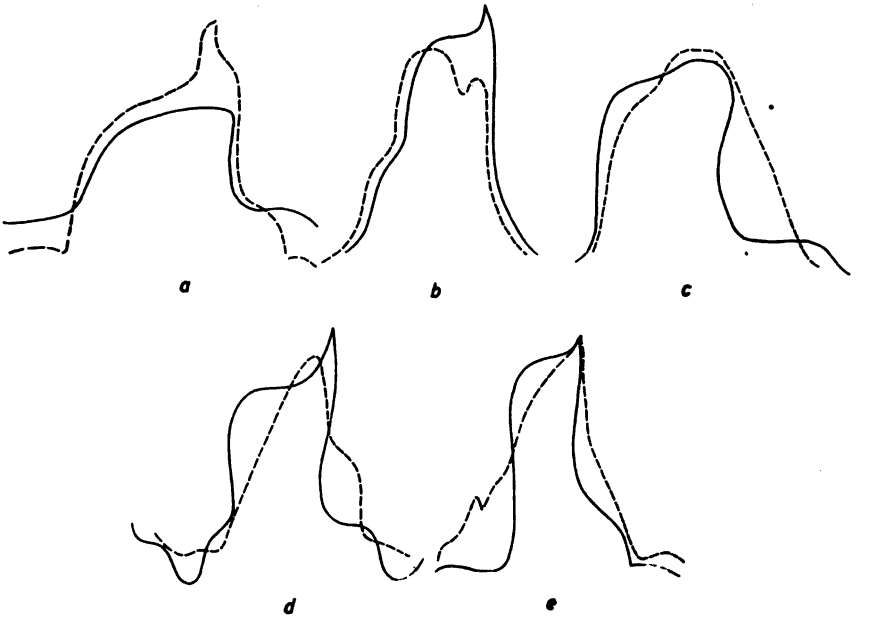

Figure 2

Oscillogram distortions during oscillographic-chronopotentiometric titrations with 0.1 M EDTA using platinum wire indicator micro electrode (thin wire, 0.5 *cm* long, *V*-shaped), SCE large surface 200 *K*Ω resistor and 0.22 μF condensator.*

Determination of 0.1 M:

a = ferric chloride (6) on 260 *V* ~
b = copper nitrate in the presence of pyridine (7) on 260 *V* ~
c = copper nitrate in the presence of pyridine (7) on 40 *V* ~
d = copper nitrate in the presence of ammonium acetate (6,9) on 260 *V* ~ nickel and manganese nitrate in pyridine (7) on 120 *V* ~
e = magnesium chloride in pyridine (7) on 120 *V* ~

The form of oscillogram: — — — before the end-point
——— at the end-point

Nickel Nitrate, Manganese Nitrate and Magnesium Chloride were titrated in 50% pyridine[7] using a 120 *V* AC source. Distortions of the oscillogram are shown in Fig. 2d. For the titration of magnesium, the pH was adjusted to 10 with 2 N sodium hydroxide (Fig. 2e). The results are in Table 2.

CONCLUSION

We have shown that the oscillographic-chronopotentiometric method can be successfully applied for end-point determination of acido-base and chelatometric titrations. In addition, procedures have been developed for the titration of hydrochloric acid with sodium hydroxide, and of iron (II) chloride, copper (II) nitrate, nickel nitrate, manganese (II) nitrate and magnesium chloride with EDTA, plus all the inverse titrations.

* See figure 1 in the previous paper (1)

Different working conditions and the effect of factors on the accuracy of these determinations have been investigated. Relative errors and standard deviations of the results are on the whole within the limits of the corresponding simple potentiometric titrations. Satisfactory results were achieved in titration of 10^{-1} to 10^{-3} N solution with 1 to 10^{-1} standard solutions.

School of Sciences
Department of Chemistry
Belgrade University
Department of Chemistry
Novi Sad University

Received 28 February 1969

REFERENCES

1. Stefanović, Đ. K., V. J. Vajgand, and T. A. Kiss. † (Oscillographic-Chronopotentiometric Titration. I. Principle of the Method) — *Glasnik Hemijskog društva* (Beograd) 33* (2-3-4), 1968.
2. Stefanović, Đ. K., V. J. Vajgand, and T. A. Kiss. "Oscillographic-Chronopotentiometric Titration. II. The Influence of Direct Current Flow and the Composition of the Solution Titrated on the Accuracy of the Determination" — *Glasnik Hemijskog društva* (Beograd).
3. Stefanović, Đ. K., V. J. Vajgand, and T. A. Kiss. "Oscillographic-Chronopotentiometric Titration. III. The Influence of the Elements of the Alternating Circuit and the Electrodes on the Accuracy of the Determinations" — *Glasnik Hemijskog društva* (Beograd).
4. Stefanović, Đ. K., V. J. Vajgand, and T. A. Kiss. "Oscillographic-Chronopotentiometric Titration. IV. Redox and Precipitate Forming Titrations" — *Glasnik Hemijskog društva* (Beograd).
5. Kiss, T. A. † (A Method of End-Point Determination in Chelatometry and Development of a New Method for Metal Estimations with Ethylenediaminetetraacetic Acid) (thesis) — Beograd: Prirodno-matematički fakultet, 1965.
6. Přibil, R., Z. Koudela, and B. Matyska. "Use of Complexons in Chemical Analysis. XIII. Potentiometric Determination of Certain Cations by Means of Complexon III Solution" — *Collection of Czechoslovak Chemical Communications* (Praha) 16: 80—85, 1951.
7. Siggia, S., D. W. Eichlen, and R. C. Reinhart. "Potentiometric Titrations Involving Chelating Agents, Metal Ions and Metal Chelates" — *Analytical Chemistry* (Easton, Pa.) 27: 1745—1749, 1955.
8. Belcher, R., D. Gibbons, and T. S. West. "The Determination of Copper by Complexometric Titration with Ethylenediaminetetraacetic Acid" — *Analytica Chemica Acta* (Amsterdam) 13: 226—229, 1955. See also: Belcher, R., D. Gibbons, and T. S. West. "Effect of Ethylenediaminetetraacetic Acid on the Ferrous (Ferric and Cuprous) Cupric Oxidation-Reduction Systems" — *Analytica Chimica Acta* (Amsterdam) 12: 107—114, 1955.
9. Přibil, R. "Potentiometric Titration of Copper with Ethylenediaminetetraacetic Acid" — *Himija* (Praha) 2: 185—188, 1952.
10. Kolthoff, I. M. and E. B. Sandell. *Anorganska kvantitativna analiza* (Inorganic Quantitative Analysis) — Zagreb: Školska knjiga, 1951, (a) p. 496, (b) p. 501, (c) p. 496.
11. Blaedel, W. J. and H. T. Knight. "Purification and Properties of the Disodium Salt of EDTA as a Primary Standard" — *Analytical Chemistry* (Easton, Pa.) 26: 741—743, 1954.
12. Flaschka, H. A. *EDTA Titrations* — New York: Pergamon Press, 1959, p. 63.
13. Sajó, I. *Komplexometria* — Budapest: Müszaki Könyvkiadó, 1962, p. 120.
14. Kolthoff, I. M. and E. B. Sandell. "Direct and Reverse Titration of Sulfuric Acid with Barium Hydroxide" — *Industrial and Engineering Chemistry, Analytical Edition* (Penna) 3: 115—117, 1931.

† Original title not given.

* Available in English translation from National Technical Information Service, Springfield, Virginia, 22151.

GLASNIK HEMIJSKOG DRUŠTVA, Vol. 34, No. 5-6-7, 1969, pp. 435—443

GHDB-78

543.257.5:541.135.5:546.87

Original Scientific Paper

NEUTRALIZATION BIAMPEROMETRIC TITRATIONS USING BISMUTH-BISMUTH PAIR IN ETHANOL SOLVENT

by

MOMIR S. JOVANOVIĆ, LUKA J. BJELICA and ANKA MARINKOVIĆ

With a view to possible application of the simple and inexpensive biamperometric method, particularly for routine neutralization titrations, the use of bismuth electrodes in the neutralization of strong acids with strong bases in aqueous solutions was described in an earlier work[1]. One of the electrode behaves like an indicator electrode and the other like a reference electrode until the end point, and then they exchange functions. Titration curves are V-shaped because the cathode (anode) current falls from the start to the end point, and with further addition of the titrant the anode (cathode) current increases. In a second paper we presented the results of determinations of mixtures of strong and weak acids, also aqueous solution[2].

The present work is concerned with the application of a pair of bismuth electrodes for the titration of mixtures of weak acids of sufficiently distant pK values. With this in view, ethanol-water, i.e. dilute ethanol, was used as the solvent, with a lower DK value and therefore a somewhat more marked differentiating effect. Mixtures of picric (pK 0.80 and acetic (pK 4.76) acid, and picric and benzoic (pK 5.20) acid in differing molar ratios were determined.

EXPERIMENTAL

Apparatus — For all determinations the apparatus shown in Fig. 1 was used. The alkaline titrant was kept in polyethylene bottles and carefully protected from the action of atmospheric CO_2. The bismuth electrodes in the biamperometric circuit for the end point determination were made from pure metallic powdered bismuth (Mallinckrodt, a.r.) melted in a glass tube in a bunsen flame. The tube was crushed and the ⌀ 5 *mm* metal rod was drawn into a tight rubber sheath from which it protruded only very little. The detecting instrument was a Lange light-spot galvanometer of sensitivity 1×10^{-8} *A/mm* scale. A double Ni-Cd cell was used as the source of polarization voltage on the electrodes.

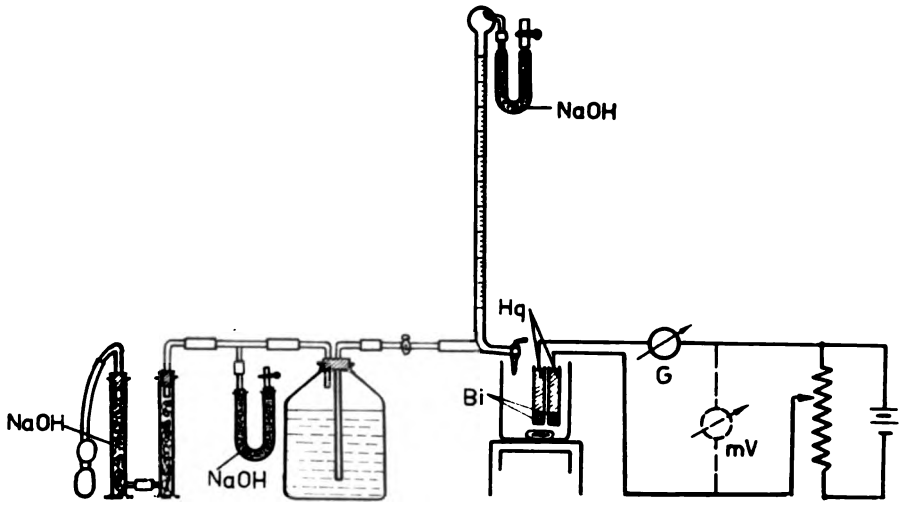

Figure 1

(A) *Titration in 50% Ethanol*

Solution. — An approximately 0.1 n aqueous solution of *sodium hydroxide* (Chemapol, Prague, p.a.) was standardized with an aqueous solution of hydrazine sulfate (BDH, p.a.), earlier suggested as the primary standard[3], by means of potentiometric titration at a glass electrode pH-meter Radiometer PHM 22r).

Approximately 0.05 n alcoholic solutions of *picric acid* (Kemika, Zagreb, p.a.), *acetic acid* (C. Erba, Milan, p.a.) and *benzoic acid* (Reanal, Budapest, p.a.) were standardized with the same titrant by potentiometric titration and by the biamperometric method using a bismuth pair. The results agree fully, as may be seen from the graphs in Figs. 2, 3 and 4.

Procedure. — Mixtures of picric and acetic and picric and benzoic acid were determined in molar ratios 1 : 1, 1 : 10 and 10 : 1. About 50 *ml* 1 : 1 ethanol-water solvent was added to the taken volume of the corresponding acids. Before every determination the bismuth electrodes had to be cleaned with the finest emery paper. A polarization of about 300 *mV* from an external current source had to be put on the electrodes to achieve a change of about 30 divisions on the meter scale in one direction during titration. The indicator (cathode) current stabilizes almost completely soon after the electrodes are submerged and titration must be begun immediately, because the indicator electrode does get depolarized although the currents involved are small. Particularly towards the end of titration and for a little after the end point, it is recommended that the titrant should be added in equal small increments. The end point corresponds to minimum indicator current.

Titration curves for all combinations of the two acid mixtures are presented in Figs. 5 and 6.

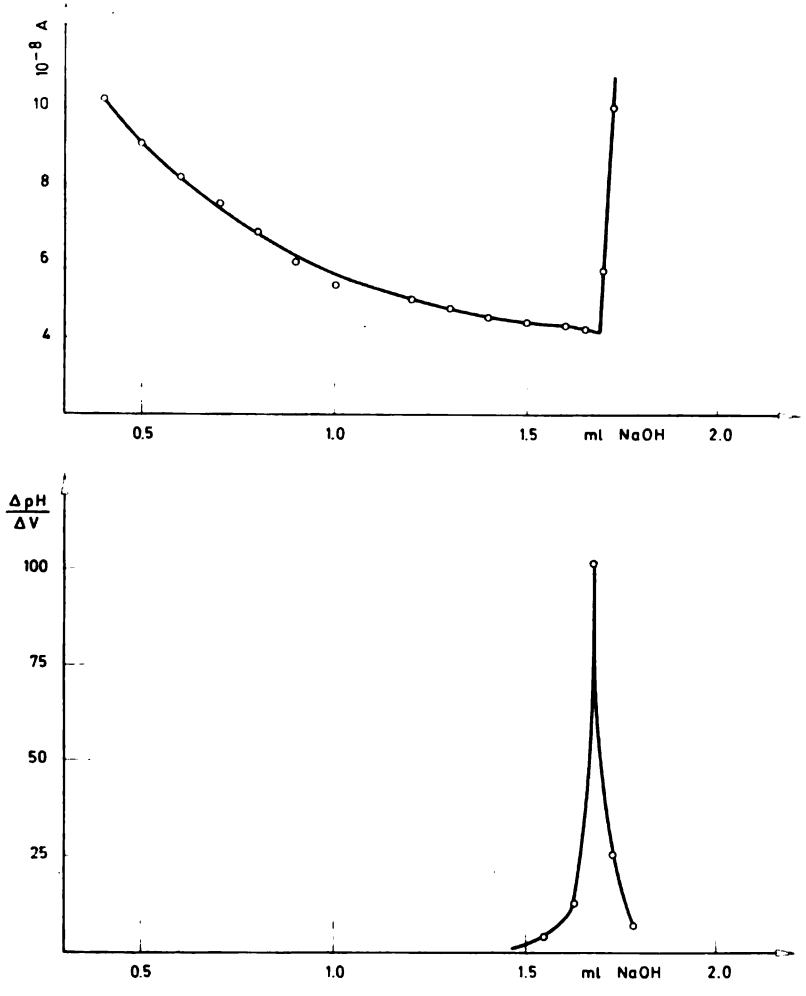

Figure 2

Picric acid

(B) *Titrations in Undiluted Ethanol*

Solutions. — Approximately 0.04 n alcoholic solution of *sodium hydroxide* (Chemapol, Prague, p.a.) was standardized with an aqueous solution of hydrazine sulfate by potentiometric titration. The already used alcoholic solutions of *picric*, *acetic* and *benzoic* acids were restandardized, this time in undiluted ethanol solvent. A slight difference was found between these and the previous values when pure water was used as the solvent.

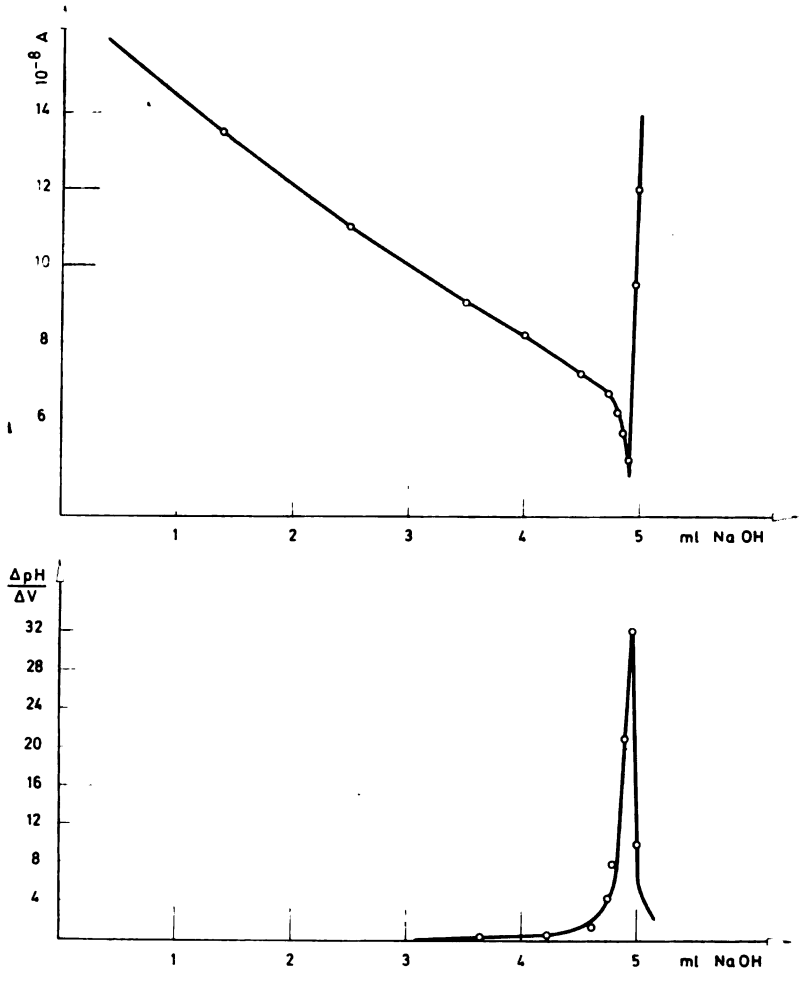

Figure 3

Acetic acid

Procedure. — This time too, mixtures of picric and acetic and picric and benzoic acid molar ratios 1 : 1, 1 : 10 and 10 : 1 were investigated. Employing the same technique as described above, the titration curves shown in Figs. 7 and 8 were obtained.

RESULTS AND DISCUSSION

Irrespective of whether titration was done in 50% or in undilute ethanol solution, the results were virtually identical. For this reason they are present undifferentiated in Tables 1 and 2.

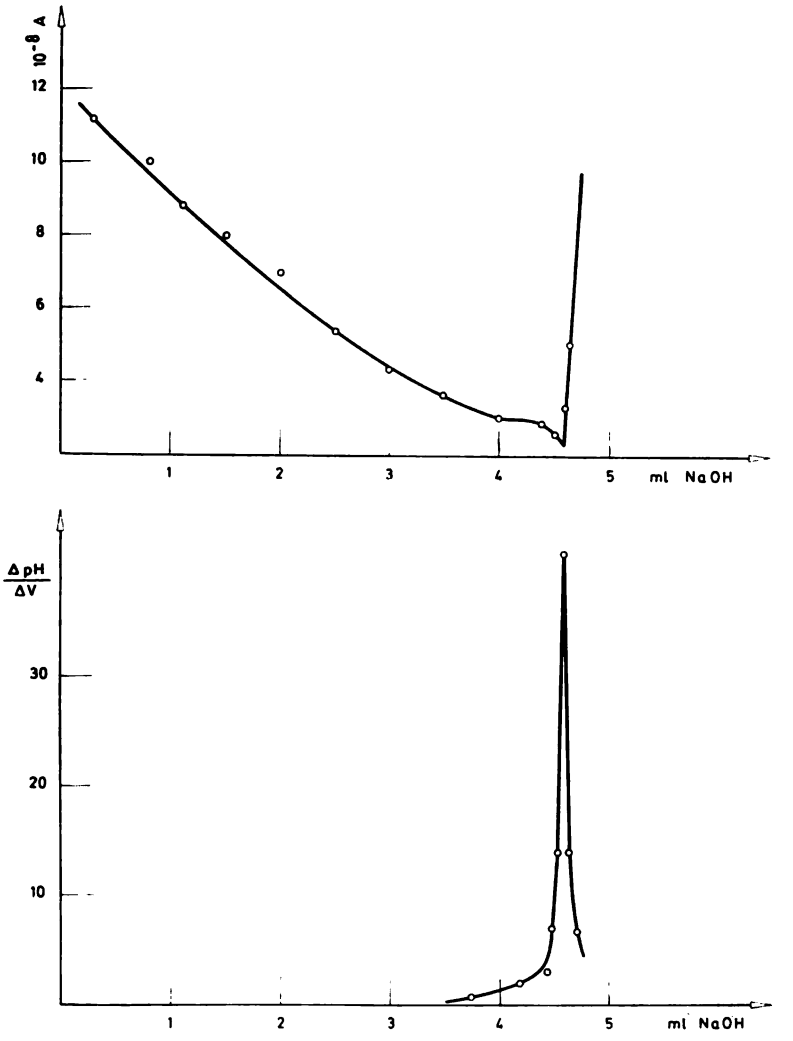

Figure 4

Benzoic acid

It may be seen that better results were obtained the wider the interval between the pK values of the mixture components, which is as was expected. The greater the pK value of the weaker component, the larger the error in determining small quantities of this acid. Some of the weaker acid is always titrated before the end point for the stronger acid is reached, the more the greater the pK value of the former.

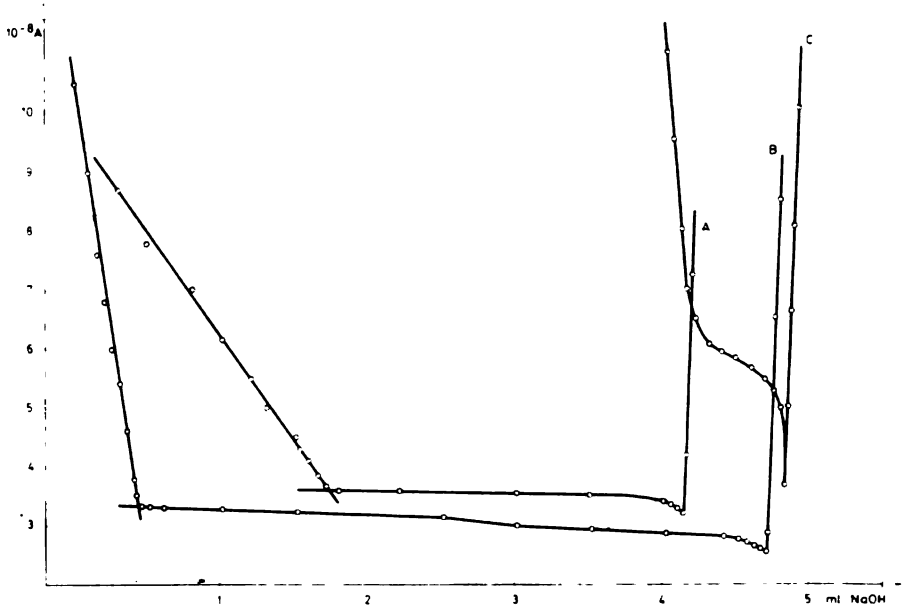

Figure 5

Picric/acetic acid mixture molar ratio:
(a) 1 : 1, (b) 1 : 10, (c) 10 : 1

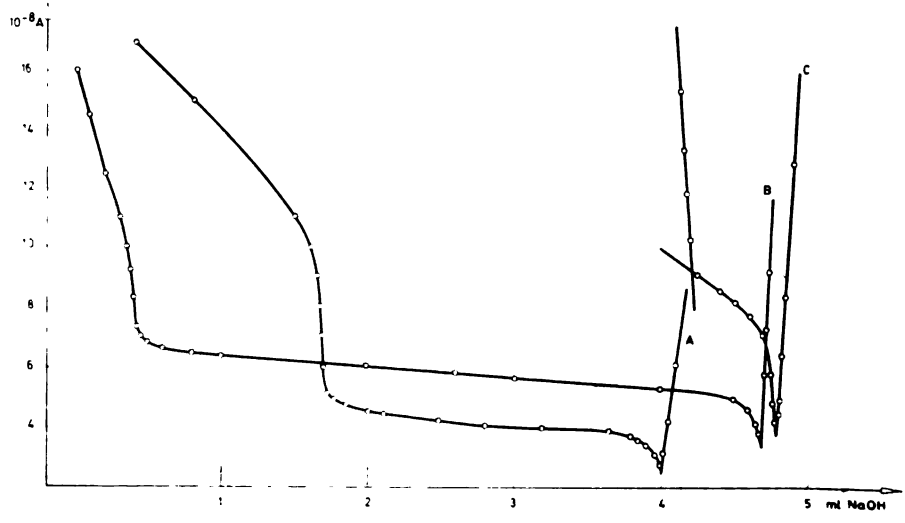

Figure 6

Picric/benzoic acid mixture molar ratio:
(a) 1 : 1, (b) 1 : 10, (c) 10 : 1

TABLE 1

Determination of Picric/Acetic Acid Mixture

No. of titrs.	Picric acid				Acetic acid			
	Taken *mg*	Found *mg*	σ_m *mg*	Error %	Taken *mg*	Found *mg*	σ_m *mg*	Error %
11	34.12	34.34	0.130	0.68	13.40	13.32	0.045	0.59
11	8.53	8.64	0.041	1.55	23.40	23.22	0.025	0.76
11	84.80	85.06	0.123	0.29	3.35	3.30	0.038	1.40

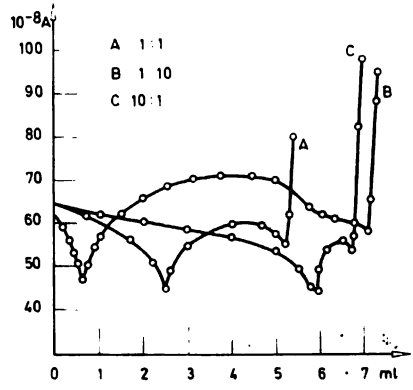

Figure 7

Picric/acetic acid mixture molar ratio: (a) 1 : 1, (b) 1 : 10, (c) 10 : 1

TABLE 2

Determination of Picric/Benzoic Acid Mixture

No. of titrs.	Picric acid				Benzoic acid			
	Taken *mg*	Found *mg*	σ_m *mg*	Error %	Taken *mg*	Found *mg*	σ_m *mg*	Error %
11	34.92	35.05	0.105	0.36	25.32	25.36	0.071	0.14
11	8.73	8.79	0.084	0.75	47.48	47.22	0.113	0.58
11	85.30	85.48	0.114	0.19	6.02	5.80	0.054	3.74

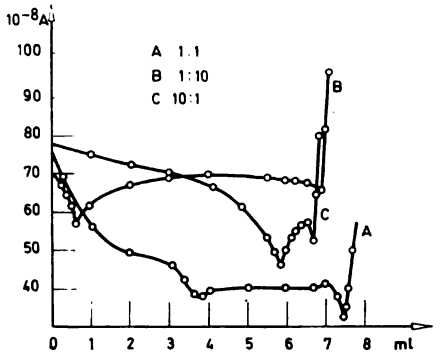

Figure 8

Picric/benzoic acid mixture molar ratio: (a) 1 : 1, (b) 1 : 10, (c) 10 : 1

CONCLUSION

Mixtures of picric and acetic and picric and benzoic acid in molar ratios 1 : 1, 1 : 10 and 10 : 1 were determined in 50% ethanol and in undilute ethanol as solvent. The results agree with those obtained by potentiometry. However, the biamperometric method using bismuth electrodes is more convenient for routine analyses because of its simplicity and the mechanical robustness of the electrodes.

Department of Chemistry
Novi Sad University
School of Technology and Metallurgy
Belgrade University

Received 9 April 1969

REFERENCES

1. Jovanović, M. S. and R. B. Babić. "Amperometrijsko određivanje hlorovodonične kiseline primenom bimetalnog sistema bizmut-bizmut" (Amperometric Determination of Hydrochloric Acid Using the Bismuth-Bismuth Bimetallic Pair" — *Glasnik Hemijskog društva* (Beograd) 29*: 11—15, 1964.
2. Jovanović, M. S. and D. Bakale. "Biamperometric Neutralization Titrations Using the Bismuth-Bismuth Pair of Electrodes" — *Zeitschrift für Analytische Chemie* (Wiesbaden) 244: 101—102, 1969.
3. Kolthoff, I. M. "The Volumetric Analysis of Hydrazine by the Iodine, Bromate, Iodate and Permanganate Methods" — *Journal of the American Chemical Society* (Easton, Pa.) 46 (2): 2009, 1924.

* Available in English translation from National Technical Information Service, Springfield, Virginia, 22151.

GLASNIK HEMIJSKOG DRUŠTVA, Vol. 34, No. 5-6-7, 1969, pp. 445—450

GHDB-79

547.963.32:535.243

Original Scientific Paper

QUANTITATIVE DETERMINATION OF DEOXYRIBONUCLEIC ACID WITH THYMINE AS REFERENCE

by

MIODRAG D. CVETKOVIĆ

In standard laboratory practice the quantitative determination of RNA and DNA is carried out by determining one of the basic components of their nucleotide composition: pentose, phosphorus, or purine and pyrimidine bases. Very often the corresponding pentoses are taken as the reference, the results being expressed in terms of phosphorus. Mejbaum's ribose method[1] with the orcinol indicator reaction is widely used for determining RNA, while the diphenylamine method after Dische[2] modified by Burton[3] is often used for DNA. These colorimetric methods are not specific, and there is the possibility of interference in heterogeneous material such as extracts of animal and particularly plant tissues.

Even the determination of phosphorus is not specific. It is done after mineralization and hydrolysis, and the most widely used methods are those based on the appearance of a blue color during the reduction of phosphomolybdic acid. For this reduction, hydroquinone is commonly used, as in the methods of Bell and Doisy[4], Fiske and Subbarow[5] and Macheboeuf and Delsal[6], or ascorbic acid, as in the methods of Marinetti[7] and Chen[8]. With phosphorus there is always the hazard of contamination by the non-nucleic phosphorus fraction, even if the acid-soluble phosphorus, phospholipids and phosphoproteids are carefully removed. With the much used Schmidt-Thannhauser method[9], according to Davidson and Smellie[10] ribonucleotides alone account for about 75% of the total phosphorus in the acid-soluble fraction ribonucleotide. By ionophoresis these authors found at least six non-nucleotide phosphate derivatives in addition to four ribonucleotides.

Spectrophotometric determination of bases, because of their property of absorption in the UV spectrum, is recommended by many authors as an accurate and simple method. But here again contamination difficulties are encountered. With the Schmidt-Thannhauser method, considerable amounts of proteins also get into the ribonucleotide fraction, interfering with the UV absorption. To avoid this, Fleck and Munro[11] put forward a modification in which the time of digestion is shortened, the concentration of the base reduced and delipidation left out. To remove the interference by protein decomposition products, following the Schmidt-Thannhauser procedure, Tsanev and Markov[12] made measurements at two wavelengths.

The preparatory technique with hot acid extraction after Schneider[13] also is used often for the UV spectrophotometrical determination

of nucleic acids. With this procedure too it is possible for non-nucleins with absorption properties similar to those of nucleic acid to interfere. To remove the effects of these impurities, Spirin[14] suggests such modifications as reduced temperature and shorter time of heating.

All this indicates the great difficulties involved in selecting the reference for quantitative determination of nucleic acids.

Thymine is a specific component of the base system of DNA. It is a compound only encountered in this system so that the quantitative determination of DNA in terms of thymine would rule out any interference, which is not so with the methods based on the determination of phosphorus and pentose in DNA.

CHOICE OF METHOD

Quantitative determination of thymine is possible by chemical, fluorometric and chromatographic or UV spectrophotometric methods.

Woodhouse[15] and Pircio and Cerecedo [16] determined thymine chemically applying Hunter's test[17] with a diazo reagent (p.-diazobenzene sulfonic acid) modified by Koestler and Hanke[18]. Woodhouse[15] determined DNA in terms of thymine, but the procedure is intricate and much more complex than the corresponding chemical methods for pentoses and phosphorus, so that it is not convenient for practical determinations of DNA.

The fluorometric method used by Roberts and Friekdin[19] is fairly specific and very sensitive, but it requires a special device (fluorometer) which many laboratories do not have.

Quantitative determination of thymine by UV spectrophotometry after its chromatographic separation from an acidic hydrolyzate of DNA is done according to Wyatt's procedure[20]. This technique appeared to us the most convenient for the quantitative determination of thymine as the reference for DNA, and we made us of it in this stage of our research.

MATERIAL AND METHOD

Pure preparations of commercial highly polymeric calf thymus DNA (BDH) were used for the tests. In addition to DNA, pure thymine (BDH) was used. Fresh calf thymus, transported chilled from the slaughterhouse, was used to check the efficiency of the procedure.

DNA was hydrolyzed in concentrated 72% $HClO_4$ in fused test tubes on a boiling water bath for 1 h. Hydrolyzate aliquots were put on Arches 301 filter paper and the bases were separated by chromatography. Measurements were made on a Beckman DU sepctrophotometer. To verify the efficiency of hydrolysis, phosphorus was quantitatively determined in the hydrolyzate by Chen's method[8].

For the quantitative determination of thymine in the preparations the identical procedure was applied using pure thymine.

To establish the efficiency of the procedure, calf thymus was investigated according to Schmidt-Tannhauser[9] and Schneider[13] replacing trichloracetic with perchloric acid as suggested by Ogur and Rosen[22]. Then the P-DNA content was determined by Burton's method using di-

phenylamine and at the same time DNA was determined by measuring thymine as explained above.

The optical density factor of pure thymine solution at a wavelength of 263 $m\mu$ was found to be 9.7 per microgram of thymine. We used this value for the quantitative determination of thymine in DNA hydrolyzates from which thymine was separated by paper chromatography, eluted and determined by spectrophotometry at the same wavelength as for pure thymine. To calculate the DNA concentration in the sample we applied the following formula:

$$C_{DNA} = \frac{E_{t\,263} - E_{t\,290}}{9.7} \cdot \frac{100}{\%\ \text{thymine}}$$

For the determination of DNA via thymine one may use the dry powder obtained after delipidation, without separating DNA from RNA and without deproteinization of the DNA.

RESULTS AND DISCUSSION

Table 1 compares amounts (absolute) and concentrations of DNA obtained by the diphenylamine method and in terms of thymine. It may be seen that the values are nearly identical, those obtained via thymine being only slightly lower. This small difference might result from some small amounts of substances present in the hydrolyzate and extract of the Schmidt-Thannhauser procedure which cause dyeing with diphenylamine.

TABLE 1

A Comparison of the Diphenylamine and Thymine UV Absorption Methods Mean values and standard deviation

	No. of analyses	Absolute DNA content (*mg*)	DNA per 100 *g* of fresh thymus (*mg*)
Diphenylamine method	8	82.52 ±0.61	236.47 ±1.78
Thymine UV absorption method	7	81.99 ±2.28	236.21 ±6.42

In Wyatt's procedure[20] thymine is located rather near the solvent front. Since impurities pile up at the front itself, the thymine spots might get contaminated. Simply by observing the paper in transmitted light, thymine spots can be seen sharply separated from the impurities at the solvent front. Moreover, to be able to establish the purity of the thymine fraction with greater precision, we calculated the ratios between bases and the ratios between purines and pyrimidines. All ratios were approximately 1,

as is shown in Table 2, which ruled out the possibility of contamination of the chromatogram.

TABLE 2

Molar Ratio of DNA Bases Extracted from Calf Thymus

A = Adenine, T = Thymine, G = Guanine, C = Cytosine

No. of detns.	A/T	$\frac{A+G}{C+T}$	$\frac{A+T}{G+C}$
7	0.955	0.988	1.025
	±0.033	±0.029	±0.032

Thymine is a specific component of the DNA molecule and can be used as a reliable reference for the absolute amount and concentration of DNA. In view of its specificity, as a reference thymine undoubtedly has the advantage over the other components, e.g. phosphorus and pentoses. Also the procedure does not call for separation of DNA from RNA before the quantitative determination of thymine and thus simplifies the technique making it as a whole just as simple as the methods using pentose or phosphorus. Neither is any special extraction of DNA from its compounds with proteins necessary. Amino acids and other impurities present in the acid hydrolyzate of DNA prepared for chromatography are far enough away from where the thymine is localized. With the procedure described thymine can be separated from all the other components of the DNA molecule for separate quantitative determination. Thereby the DNA itself is determined, which excludes any possibility of contamination or interference.

However, apart from the obvious advantages there are certain limitations on the application of this method. Above all, the content of purine and pyrimidine bases, and thymine itself, differs from species to species and even from tissue to tissue, so that the thymine content of the DNA samples must be determined previously for each tissue

In addition to this, the base ratios in DNA molecules are affected by other factors. Hudnik-Plevnik and Simić[23] established that the base ratios change in irradiated bacteria, thymine being reduced. Even the preparation procedure may induce changes in the base composition of the DNA. We have found[24] that preparing DNA according to a modification of Orlov's method[25] brings about considerable changes in base ratios with great reduction of thymine.

CONCLUSION

Thymine can be used as the reference for the quantitative determination of DNA in tissues. It is determined by UV spectrophotometry after chromatographic separation from tissue hydrolyzate.

When thymine is used as the reference for the determination of DNA it must be taken into consideration that DNA's is from different tissues have different thymine contents, and that the base composition of DNA and the thymine content itself may be changed by various factors.

ACKNOWLEDGMENT

Our thanks are due to N. Đorđević and R. Spasenović for assistance in this work.

The research was financed by the Association of Medical Research Institution, under contract No. 5106.

School of Medicine
Department of Biochemistry
Belgrade University

Received 11 December 1967

REFERENCES

1. Mejbaum, W. — *Zeitschrift für Physiologische Chemie* 258: 117—123, 1939.
2. Dische, Z. — *Mikrochemie* 8: 4—9, 1930.
3. Burton, K. — *The Biochemical Journal* 62: 315—323, 1956.
4. Bell, R. D. and E. A. Doisy. — *The Journal of Biological Chemistry* 44: 55—67, 1920.
5. Fiske, C. H. and Y. Subbarow. — *The Journal of Biological Chemistry* 66: 375—400, 1925.
6. Macheboeuf, M. and J. Delasal. — *Bulletin de la Societe de Chimie Biologique* 25: 116—120, 1943.
7. Marinetti, G., J. Erbland, M. Albrecht, and E. Stolz. — *Biochimica et Biophysica Acta* 30: 543—548, 1958.
8. Chen, P. S., T. Y., and Huber Warner. — *Analytical Chemistry* 28: 1956—1958, 1956
9. Schmidt, G. and S. J. Thannhauser. — *The Journal of Biological Chemistry* 161: 83—89, 1945.
10. Davidson, J. N. and R. M. S. Smellie. — *The Biochemical Journal* 52: 599—606, 1952
11. Fleck, A. and H. Munro. — *Biochimica et Biophysica Acta* 55: 571—583, 1962.
12. Tsanev, R. and G. G. Markov. — *Biochimica et Biophysica Acta* 42: 442—452, 1960.
13. Schneider, W. C. — *The Journal of Biological Chemistry* 161: 293—303, 1945.
14. Spirin, A. S. — *Biokhimiia* 23: 656—662, 1958.
15. Woodhouse, D. L. — *The Biochemical Journal* 44: 185—187, 1949.
16. Pircio, A. and L. R. Ceresedo. — *Archives of Biochemistry* 26: 209—213, 1950.
17. Hunter, G. — *The Biochemical Journal* 30: 745—747, 1936.
18. Koessler, K. K. and M. T. Hanke. — *The Journal of Biological Chemistry* 39: 497—519, 1919.
19. Roberts, D. and M. Friedkin. — *The Journal of Biological Chemistry* 233: 483—487, 1958.
20. Wyatt, C. R. — *The Biochemical Journal* 48: 584—590, 1951.
21. Chargaff, E. *The Nucleic Acids*, Vol. I. — New York: Academic Press Inc.: 1955, pp. 308.
22. Ogur, M. and G. Rosen. — *Archives of Biochemistry* 25: 262—276, 1950.
23. Hudnik-Plevnik, T. and M. M. Simić. — *Bulletin of the Boris Kidrič Institute of Nuclear Sciences* (Belgrade) 11: 231—233, 1961.
24. Cvetković, M. D., in: *Symposium on the Methods of Estimation, Isolation and Fractionation of Nucleic Acids, Varna, October 1965.*
25. Orlov, A. S. and E. M. — *Biokhimiia* 26: 934—939, 1961.
26. Cvetković, M. D. and P. P. Milošević. — *Glasnik hemijskog Društva* (Beograd) 30*: 17—28, 1965.

* Available in English translation from National Technical Informations Service, Springfield Virginia, 22151.

Izdavač

IZDAVAČKO PREDUZEĆE "NOLIT", BEOGRAD, TERAZIJE 27/II

*

Štampa

GRAFIČKO PREDUZEĆE "PROSVETA", BEOGRAD,
ĐURE ĐAKOVIĆA 21

TT 69-51006/8-9-10

SRPSKO HEMIJSKO DRUŠTVO (BEOGRAD)
THE SERBIAN CHEMICAL SOCIETY (BELGRADE)

BULLETIN OF THE CHEMICAL SOCIETY Belgrade

(Glasnik Hemijskog društva — Beograd)

Vol. 34, No. 8-9-10, 1969

Translated from Serbo-Croatian

Translated and published for U.S. Department of Commerce and the National Science Foundation, Washington, D.C., by the NOLIT Publishing House, Belgrade, Terazije 27/II, Yugoslavia
1971

Translated and published for U.S. Department of Commerce and
the National Science Foundation, Washington, D.C., by
the NOLIT Publishing House, Terazije 27/II, Belgrade, Yugoslavia
1971

Translated by
PAVEL ČMELIK

Edited by
PAUL PIGNON

Printed in "Prosveta", Beograd

CONTENTS

Page

Svetomir D. Cvijović and Milan V. Mitrović:
Presentation and Verification of a Modification of the Adsorption Method for Mass Flux Measurement 5

Milenko V. Šušić, Dušan R. Vučelić, Stevan V. Paušek, and Dragan B. Karaulić:
Sorption of Gases and Vapors on Synthetic Zeolite 17

Slobodan Končar-Djurdjević and Ivanka Petković:
Dynamic Adsorption of Organic Vapors on Blocked Silica Gel. II . . . 25

Milenko V. Šušić and Ahmed Kh. Ghonaim:
Polarographic Behavior of Titanium IV in the Presence of Diethylenetriaminepentaacetic Acid (DTPA) 31

Milutin Stefanović, Ratko Jankov and Miroslav Gašić:
The Reduction of Δ^4-Androstene-3,17-dione-11β-ol by Metal Hydrides 37

Milutin Stefanović, Aleksandar Jokić and Dušan Mi'jković:
Intramolecular Cyclization of 16-Furfurylidene-17β-Hydroxy-steroids by Catalytic Hydrogenation 45

Vladimir Leskovac:
Purification of Malic Dehydrogenase from Pig Heart and Reactivity of Its Sulphohydride Groups 57

Jelena J. Bojanović, Milanka O. Čorbić, Anka D. Jevtović, and Rajko V. Živković:
Metabolic Relations of Proteins, Lipids and Glucides. XIII. The Electrophoretic Patterns of Lipoproteins in Dog Blood Serum During the Slow Infusion of Glucose in Fasting and in Alimentary Hyperlipemia . 67

Zagorka J. Filipović and Miroslav M. Bresjanac:
Phosphorous in Plants and the Substitutive OH^- Ions of Soil 77

Velimir D. Canić and Nada U. Perišić-Janjić:
Separation of Cations by Circular Thin-layer Chromatography on Starch 83

Dušan M. Vučurović and Miodrag A. Spasić:
Chlorination of Yugoslav Nickel-bearing Iron Ores. I. Chlorination of Natural Ores 87

Miodrag A. Spasić, and Dušan M. Vučurović:
Chlorination of Yugoslav Nickel-bearing Iron Ores. II. Chlorination of Reduced Ores. 93

Dušan M. Vučurović and Miodrag A. Spasić:
Chlorination of Yugoslav Nickel-bearing Iron Ores. III. Simultaneous Reduction and Chlorination 99

GLASNIK HEMIJSKOG DRUŠTVA, Vol. 34, No. 8-9-10, 1969, pp. 453—464

GHDB-80

541.183.55:661.183.7:547.869

Original Scientific Paper

PRESENTATION AND VERIFICATION OF A MODIFICATION OF THE ADSORPTION METHOD FOR MASS FLUX MEASUREMENT

by

SVETOMIR D. CVIJOVIĆ and MILAN V. MITROVIĆ

INTRODUCTION

The existing experimental facilities for tracking changes in the diffusion boundary layer are restricted to only a few techniques[1,2], each having its advantages and disadvantages. For the study of mass transfer in liquids these are even fewer, and the adsorption method appears to have a number of advantages here. However, this method has also certain disadvantages, among which the most severe in the case of adsorption on a silica gel film[3] are unsatisfactory homogeneity and inadequately defined roughness of the adsorptive surface, instability at higher temperatures, and mechanical instability. Hence this method excludes not only the study of mass transfer under different temperature conditions, but also the measurement of the small-scale local mass transfer coefficients because of the surface inhomogeneity. The main disadvantage of the modification of the adsorption method using oxidixed aluminum as adsorbent[4] is the fact that even at a relatively small mass flux the mass transfer kinetics becomes heterogeneous, this making study of higher mass transfer rates practically impossible. Still another disadvantage of this method is the adsorption of a chemically indefined substance, because the dyes for dyeing aluminium oxide are usually of the dispersion type having a wide particle size range in the colloidal region.

Our aim in this study was to make use of the specific advantages of the above mentioned modification of the adsorption method and to eliminate the disadvantages at the same time. Naimely, if porous aluminum oxide is used as the adsorption surface and methylene blue is adsorbed on silica gel impregnated into the pores of this surface, then the reaction surface and the adsorption should have considerably better characteristic, viz:

— well-defined silica gel — methylene blue adsorption system,
— well-defined, reproducible and homogeneous surface,
— thermally stable surface (0°C — 80°C),
— equal facilities for measuring both low and higher mass flux,
— Possibility for simultaneous study of mass and heat transfer at elevated temperatures.

PREPARATION AND EXAMINATION OF ADSORPTION SURFACE

One of the prerequisites for successful application of the adsorption method is knowledge of the relationship between the quantity of adsorpbent on the reactive surface and the relative intensity of the light reflected from it before and after adsorption. For this purpose 2 cm square plates made of 0.5 cm thick 99.6% pure aluminum were examined. The plates were sand-blasted in order to make the surface homogeneous, this enabling better diffusion of light. Oxidation was done in the same way as for the corresponding modification of the adsorption method[4]. The pores produced are approximately 1 μ in diameter and 20 μ deep. The number of pores per square cm was approximately $20 \cdot 10^6$. The pores are funnel--shaped, with the tops towards the surface. They are almost regularly distributed in the centers of hexagons with a certain deformation in shape and arrangement showing the direction of rolling of the aluminum sheet. The size of the silica-gel treated pores could not be determined, but they must certainly have been considerably smaller then the original ones in the oxidized layer.

The plates prepared in this way were then immersed in a solution made by mixing together equal parts of 1.12 density water-glass and water and kept there as long as necessary for diffusion of the solution into the pores of the aluminum oxide. The solution was gelled by the addition of a 1% sulphuric acid solution in 3 : 1 volume ratio. Gellification took 3 to 4 hours. The gel was scraped off and then the plates washed with a jet of water and dried. The time the plates were left in the water-glass was not observed to have an essential influence on later adsorption of methylene blue, i.e. no difference in the color intensity was found between surfaces kept in the solution for 2 to 24 hours. The adsorptive characteristics of the surface were not changing during handling provided the physical structure of the oxidized surface was not disturbed. The oxidized surface was photographed under an electron microscope before and after applying silica gel (Figs. 1 and 2). However, it must be mentioned that the adsorptivity of porous aluminum treated in this way is somewhat reduced. The methylene blue is then only adsorbed on silica gel in the pores, because this dye cannot be adsorbed on the layer of aluminum oxide produced by electrolysis.

Figure 1

Aluminum oxide surface, magnification × 4000

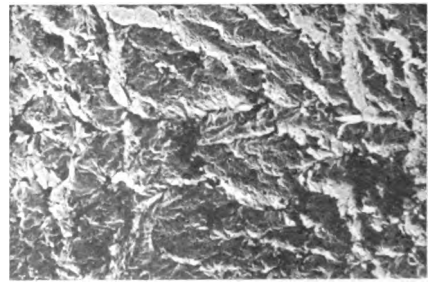

Figure 2

Adsorption surface, magnification × 4000.

TABLE 1

Reflection properties of the adsorption surface

$R_0 = 100$ $\Delta R/R_1 = 71.3$

R_1	A	98.4	100.0	101.0	100.0	100.4
	B	98.0	98.6	100.8	100.4	98.8
R_2	A	30.4	29.0	28.0	28.0	28.0
	B	29.6	28.8	27.4	28.0	28.4
$\frac{\Delta R}{R_1}$	A	69.1	71.0	72.3	72.0	72.0
	B	69.7	70.7	72.8	72.0	71.3

In carlier studies relationships between color intensity and the duration of adsorption or solution concentration were found, and good homogeneity of the colored and uncolored surface was verified. The color intensity was determined as the relative difference in the reflection of light before and after the adsorption. In these measurements a special plate was used as the blank standard, the intensity of light refleceted from it being taken as unity. The intensity of light was measured with a photocell mounted on the photographic eyepiece of the microscope and feeding a galvanometer.

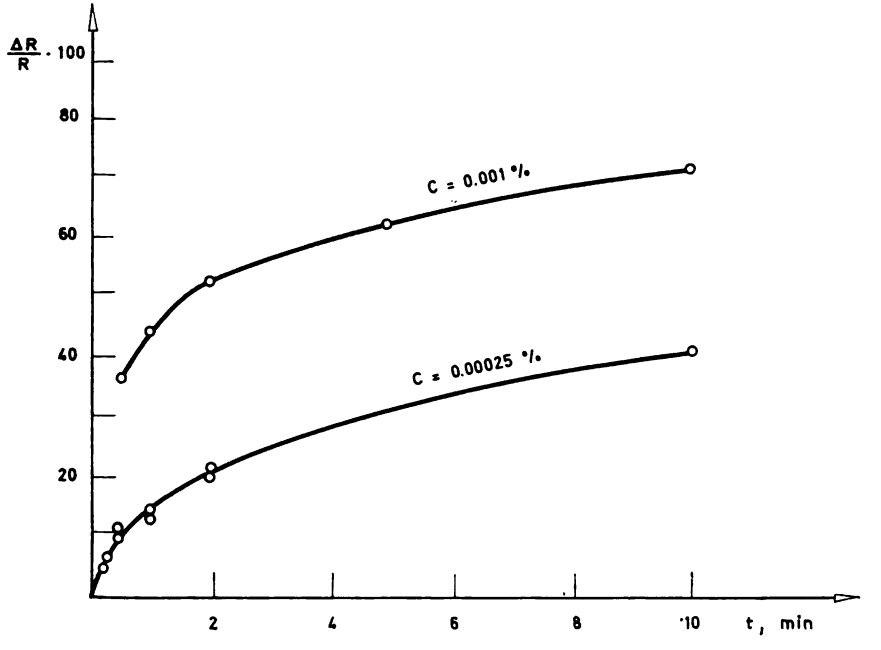

Fig. 3

Relative change of reflected light as a function of adsorption time

A special diaphragm was placed under the cell to enable meassurement of reflected light from 1 mm² of the examined surface on the microscope stage. The objective used had a magnification of × 40. A typical optical homogeneity of the surface is shown in Table 1, where measurements of the color intensity are given for one (A) and the other (B) side of the plate before (R_1) and after (R_2) the adsorption. The dependence of the percentage change in the intensity of reflected light on the duration of adsorption of methylene blue from 0.001% and 0.00025% aqueous solutions (Fig. 3) was measured in order to check the method under natural convection of color cn the surface and to determine a suitable adsorption time. The results indicate the existence of a definite and continuous relationship between the amount of methylene blue adsorbed on the surface, i.e. the surface concentration of the adsorbate, and the intensity of reflected light.

THE CALIBRATION CURVE

To get the relationship between the relative reflection and the concentration of methylene blue on the adsorption surface the amount of the substance adsorbed must be determined. This may be achieved either by a convenient dissclving of methylene blue and its subsequent determination from the solution or by applying a definite small amount of dilute dye solution to a restricted surface, a know surface concentration being obtained after adsorption and the evaporation of water. Satisfactory agreement was obtained between measurements made according to both procedures.

If methylene blue is dissolved out after the adsorption very dilute solutions are obtained, and these can only be determined by colorimetry. After a number of experiments with different concentrations of various acid and base solutions, a 5% solution of hydrochloric acid was chosen

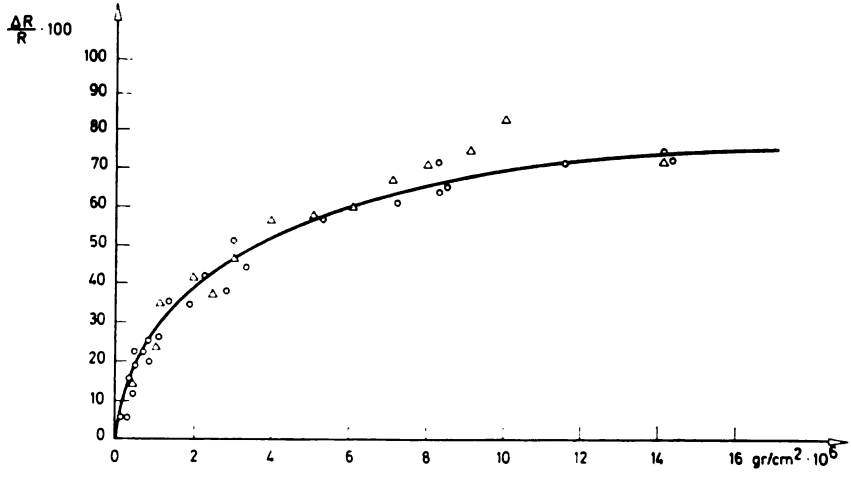

Fig. 4

Relative reflection of light as a function of surface concentration of methylene blue

as the solvent and this fulfilled all necessary colorimetric conditions, viz., stable and clear solutions of methylene blue, differing in shade from the corresponding aqueous solutions. The measurements were made on a Lange universal colorimeter calibrated with the same solution used as the solvent. The results are shown in Fig. 4. The adsorption time for all points was 5 minutes. The concentration of the solution in which the adsorption was performed was changed. The reproducibility of the results was satisfactory.

Analogous results were obtained by applying a definite amount of methylene blue solution of known concentration from a microburette to a 2 cm^2 circular surface. After evaporation of the solution the homogeneously colored circular surface was measured colorimetrically. The results are also displayed in Fig. 4. In spite of the fact that both the adsorption time and the concentration of the solution were changed, agreement with the results obtained by dissolving methylene blue was satisfactory.

A characteristic feature is the non-linearity of the calibration curve. This indicates considerable deviations from the Lambert-Beer law and may be ascribed both to the character of light transmission through the layer of adsorbent and reflection at the adsorbent and metal surfaces, and to the high concentrations of dye on a thin layer of adsorbent. If the dye is assumed to be adsorbed uniformly throughout the whole layer of the adsorbent approximately 25 μ thick, a maximum dye concentration was 10^{-2} g per cm^3 oxide. Further, if the facts that the dye is adsorbed only on silica gel in the pores and that the concentration of dye in the adsorbent decreases with depth are considered, the concentrations must be much higher and for these even with the ideal transmission of light through the adsorbent the Lambert-Beer law does not apply.

VERIFICATION OF THE METHOD

For verifying the proposed modifications of the adsorption method experimental local coefficients of mass transfer were determined theoretically and by other methods. For this purpose systems in which quantitative data could be easily obtained experimentally and compared with analytical expressions were used.

DIFFUSION FLUX ON ROTATING DISC

The mass flux on a rotating disc under laminar flow conditions ($Re = 10^4$—10^5) is given by the expression[5]

$$j = 0.62\, D^{2/3} \nu^{-1/6}\, \omega^{1/2}\, C_0. \qquad (1)$$

This expression assumes zero concentration on the reactive surface. If the equilibrium concentration of active substance on the surface can be neglected then the coeficient of adsorptive mass transfer is

$$k_0 = 0.62\, D^{2/3}\, \nu^{-1/6}\, \omega^{1/2}. \qquad (2)$$

The disc was 10 *cm* in diameter and 0.8 *cm* thick, rotating in a vessel of 60 *cm* diameter and 125 *lit* volume. The solution concentration was between 0.00025 and 0.0009% methylene blue in water. The diffusion coefficient of methylene blue in water at 20°C is $4.75 \cdot 10^{-6}$ cm^2/sec. The adsorption time was 5 minutes. Under these conditions the mass transfer coefficient is given by

$$k = \frac{c_s/t}{c_0}. \tag{3}$$

The surface concentration c_s was measured both via the intensity of reflected light and by dissolving out the methylene blue and subsequent colorimetry measurement of the obtained solution. The results are shown

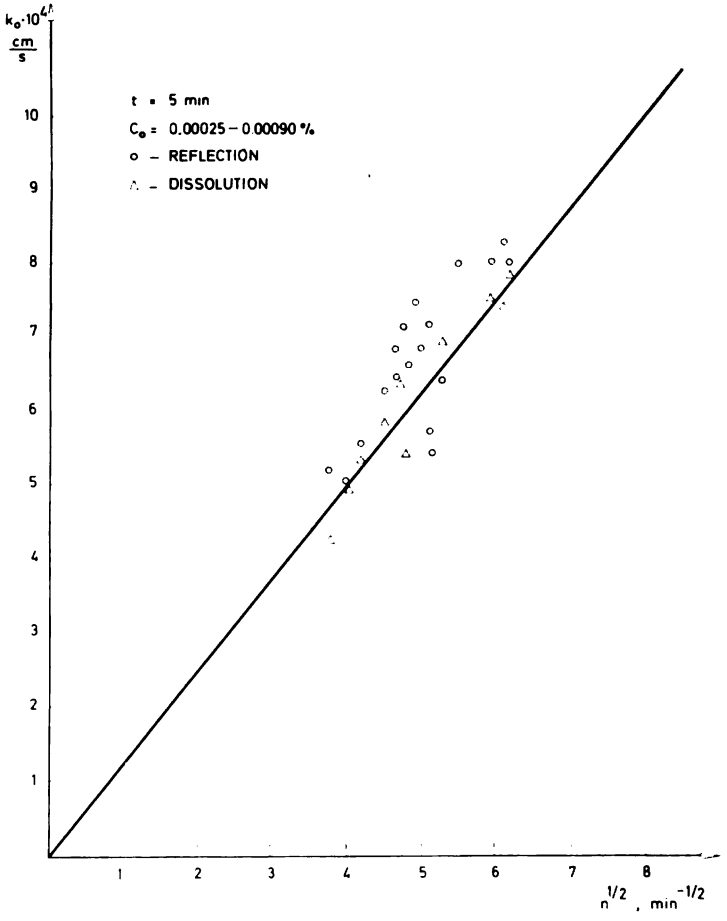

Fig. 5

Dependence of mass transfer coefficient on angular velocity, laminar flow

graphically in Fig. 5. They are in good agreement with the theoretical equation. The scattering of the points may be explained by differences in roughness of the discs, this strongly influencing the reflection of light. Hence it may be concluded that, in principle, the reflection measurement of mass transfered is applicable when local mass transfer is measured and compared on the same object, and measurement by dissolving when the average value mass transfer is measured on a whole surface being colored either uniformly or nonuniformly. However, the results show a satisfactory agreement for both methods and all dye concentrations used.

For transitional or turbulent flow the coefficient of mass transfer is given by the expression[4]

$$k_t = \frac{0.01}{\alpha}\left(\frac{D}{\nu}\right)^{-3/4} \cdot \left(R \cdot \omega\right)\left(\frac{\nu}{R^2\,\omega}\right)^{1/10}, \qquad (4)$$

where α is a coefficient depending on the experimental conditions. The mass flux was measured at a distance of 1 *cm* from the disc edge, only via the intensity of reflected light because dissolving out the methylene blue was difficult owing to a relatively high surface concentration. Due to vibrations of the disc, a transition flow regime appeared at low Reynolds numbers (about 10^4). The results of investigations in this region are given on the graph in Fig. 6.

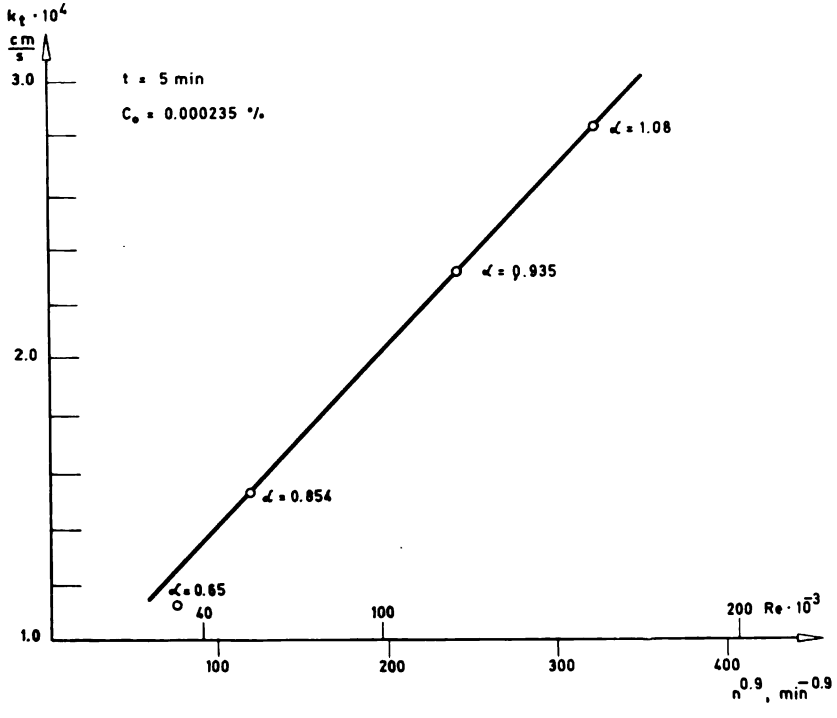

Fig. 6

Dependence of mass transfer coefficient on angular velocity (Re), transitional flow

The linear relation indicates the reliability of the results obtained and also the applicability of the method under turbulent flow conditions, i.e. for $Re = 10^5$.

The studies of mass transfer from a turbulent flow indicate that the method is also applicable for greater Reynold numbers (up to $3 \cdot 10^5$), but with a further increase of turbulence saturation of the adsorptive surface appears, i.e. a mixed mass transfer kinetics, which can be only partly obviated by the corresponding decrease of concentration in the solution. The results are given in Fig. 7.

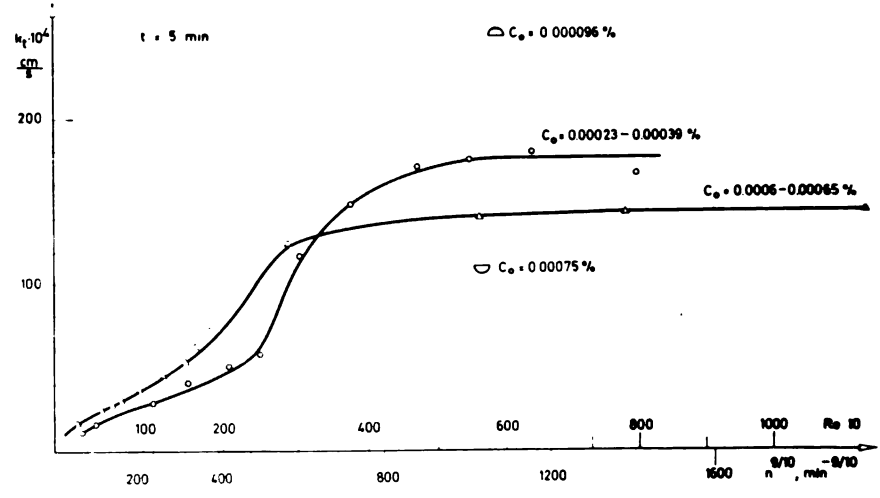

Fig. 7

Dependence of mass transfer coefficient on angular velocity, turbulent flow

In further investigations the applicability of this method for 10 to 1000 times lower dye concentrations should be examined.

RELAXATION OF DIFFUSION FLUX ON ROTATING DISC AND FLAT PLATE

The proposed method and the influence of the adsorption time were studied relative to relaxation of the diffusion flux on rotating disc in the laminar flow region. The results show lower values than the theory (Fig. 8). These are shown in terms of the local coefficients of mass transfer for surfaces of 1 mm^2. With adsorption times of 15, 10 and 7.5 minutes good agreement with theory was obtained, the scattering of results about the theoretical curve being about $\pm 10\%$.

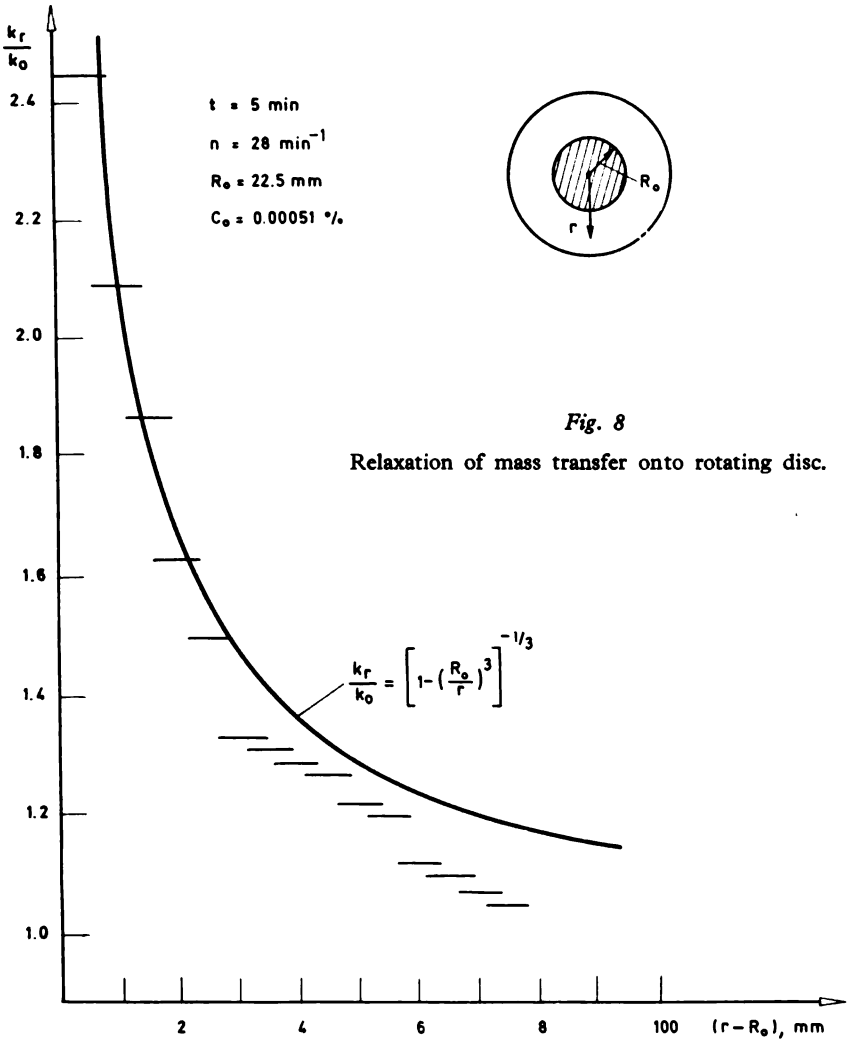

Fig. 8

Relaxation of mass transfer onto rotating disc.

Similar results were obtained in measurements of relaxation on a flat plate. (Fig. 9).

On the basis of these results it may be concluded that the proposed modification of the adsorption method has certain advantages over the earlier ones[6, 7], especially in that it allows measurements of small-scale local mass transfer coefficients over a wide range of mass flux, or Reynolds numbers, and the potential possibility for simultaneous measurement of mass and heat transfer. The method covers all ranges of laminar and transitional flow and of turbulent flow up to $Re \simeq 3 \cdot 10^5$; the latter limit can possibly be extended still further. The objects may be any shape and roughness up to an average peak height of $\sim 2\,\mu$. There is also no restriction

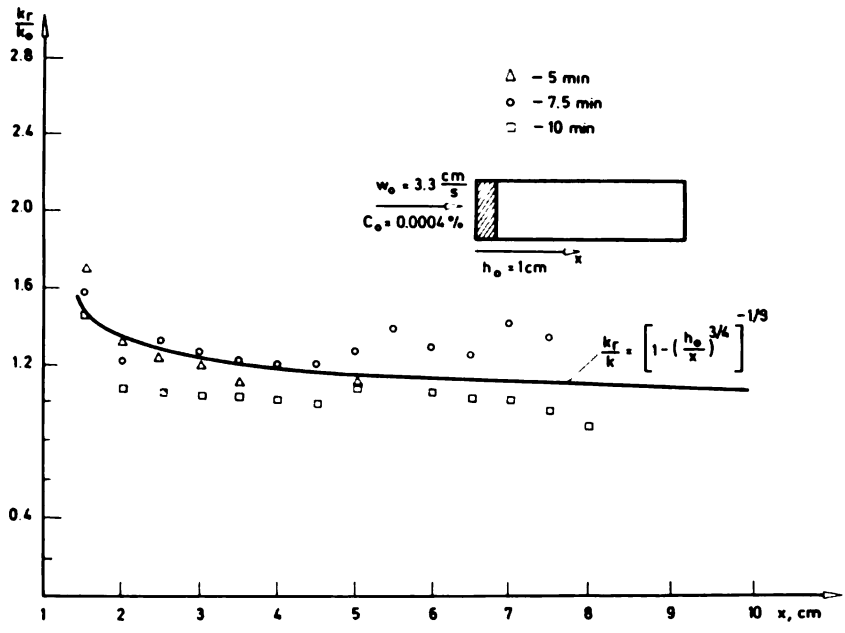

Fig. 9
Relaxation of mass transfer onto flat plate

as to the object dimensions, and thanks to the low concentration, non-toxicity and non-corrosiveness of the dye studies may be made in any system with circulating water. Quantitative measurements of the average and local mass transfer may be made down to a surface area of 1 mm^2, but with the use of a special photometric microscope (Reichert) this may probably be extended down to $10 \times 10\,\mu$, this being the lower limit considering the size and distribution of pores, considerably less roughness being assumed, of course. The method was found to be applicable at all temperatures of water from 0°C up to approximately 80°C, when the oxide pores begin to close. Aqueous solutions of glycol, glycerine or sucrose may also be used as the primary fluid, this enabling variation of the viscosity and the Schmidt number over wide ranges. The mechanical characteristics of the surface make the application of this method possible even under extreme conditions (high pressures, high flow velocities, water with a solid suspended in it, flow in porous medium).

Consequently the proposed method may be widely used for the study of mass transfer and analogously also of heat and momentum transfer in chemical engineering, hydraulics and mechanical engineering, providing quantitative data both on the local and the total coefficient of friction and heat and mass transfer.

School of Technology and Metallurgy,
Belgrade Univ,. and Institute of Chemistry,
Technology and Metallurgy, Center for
Process Engineering, Belgrade

Received 1 October, 1969

REFERENCES

1. Končar-Djurdjević, S. "Adsorpcija po hidrodinamički određenim uslovima" (Adsorption under Defined Hydrodynamic Conditions) — *Glasnik hemijskog društva* (Beograd) 14(14): 233—249, 1949.
2. Sogin, H. H. "Laminar Transfer from Isothermal Spanwise Strips on a Flat Plate" — *Journal of Heat Transfer* 82: 53—63, 1960.
3. Končar-Djurdjević, S. "Analogija izmedu dinamičke adsorpcije i konvektivnog prenošenja toplote" (Analogy between Dynamic Adsorption and Convective Heat Transfer) — *PhD Thesis, University, of Belgrade, 1967.*
4. Mitrović, M. "Prenos mase na anodno oksidisani aluminijum pod uslovima prirodne konvekcije" (Mass Transfer onto Anodized Aluminum under Natural Convection) — *Glasnik hemijskog društva* (Beograd) 27 (2—3):* 77—84, 1962.
5. Levich, V. T. *Fiziko-khimicheskaia gidrodinamika* (Physical Chemistry in Hydrodynamics) — Moskva: Gos. Izd. fiz. mat literatury, 1959.
6. Mitrović, M. and S. Končar-Djurdjević. "Ispitivanje adsorpcije iz rastvora na rotirajuće diskove" (Study of Adsorption from Solution on Rotating Discs) — *Glasnik hemijskog društva* (Beograd) 28(7):* 45—58, 1963.
7. Mitrović, M. and S. Cvijović. "Prenos mase na rotirajuće diskove" (Mass Transfer onto Rotating Discs) — *Zbornik prvog Jugoslovenskog simpozijuma o hemijskom inženjerštvu, Beograd, 1967* (Proceedings of the First Yugoslav Symposium on Chemical Engineering, Belgrade, 1967) — pp. 34—40.

* Available in English translation from National Technical Information Service, Springfield, Virginia, 22151.

GLASNIK HEMIJSKOG DRUŠTVA, Vol. 34, No. 8-9-10, 1969, pp. 465—472

GHDB-81

541.183.56:661.183.6
Original Scientific Paper

SORPTION OF GASES AND VAPORS ON SYNTHETIC ZEOLITE

by

M. V. ŠUŠIĆ, D. R. VUČELIĆ, S. V. PAUŠEK and D. B. KARAULIĆ

Molecular sieves, i.e. synthetic zeolites, are alumino-silicates which, owing to their crystalline structure, behave specifically as sorbents of gases and vapors[1, 2, 3, 4]. The CaA sieve has a cubic lattice, $a = 12.32$ Å, $O_h^1 = Pm3m$, with cavities 11.4 Å in diameter and channels connecting these 4.7—4.9 Å.

The sieves show a high affinity towards polar and nonsaturated compounds because of the close surface potential fields. The adsorption of gases from mixtures is usually selective, both because of the adsorbent structure and because of the nature of the molecules being adsorbed.

The influence of the presorption of polar molecules (water, ammonia and certain alcohols) on the sorption of nitrogen and oxygen[3], methane, carbon monoxide and hydrogen[10] has been investigated. It has been shown that it leads to a considerable and permanent change of the sorption of these gases. The phenomenon has been explained by the occupation of the sieve ducts and cavities by polar molecules, this at the same time leading to a decrease in the free diameter of channels and cavities for the passage of gases.

EXPERIMENTAL

(*Equipment and Measuring Techniques*)

The investigations were made by means of gas chromatography, NMR and conventional sorption measuring technique.

Gas chromatography. The gas chromatography was done on a Perkin-Elmer 154-D chromatograph. A mixture of alcohols, nitrogen and oxygen prepared in a microliter syringe was injected into the high-temperature evaporator of the chromatograph. Columns of standard metal or glass U-tubes packed with the Linde zeolite 5A (CaA), this being previously heated in a stream of dry argon at 350°C for 25 hours.

Adsorption and desorption of alcohols. Two techniques were combined i.e. the volumetric (where allowed by the vapor pressure) and a gravimetric one similar to Bark's method. At the same time measurements were also made with the NMR spectrometer. The cell with the sample was placed

between the poles of the spectrometer electromagnet, and the temperature was monitored to ± 0.5°C by a termocouple built inside the cell in direct contact with the adsorbent. The pressure was measured by an open mercury manometer. In all experiments the samples were previously degassed at 450°C and 10^{-5} *mm*Hg pressure during 4 hours.

NMR measurements. These were made on a broad-line spectrometer, made by Jožef Štefan, Ljubljana, having a constant frequency of 30 Mc/s and a variable magnetic field of 7500 Gauss.

Standard gases of 99% purity additionally purified in the usual way were employed. Alcohols were of p. a. purity BDH. The zeolite Linde 5A was prepared in powder form by grinding the granulated BDH zeolite.

RESULTS

Gas chromatography was used to investigate the effect of the presorption of aliphatic alcohols (from C_1 to C_4) on the adsorption of nitrogen and oxygen. A mixture of 0.8 molar fraction nitrogen and 0.2 molar fraction oxygen is completely separated at 100 °C (Fig. 1, curve No 1). However, in the case of a mixture of 0.63 molar fraction nitrogen, 0.17 molar fraction oxygen and 0.2 molar fraction methyl or ethyl alcohol with a total of about $1 \cdot 10^{-5}$ mole/g zeolite, the retension times for nitrogen and oxygen become so close

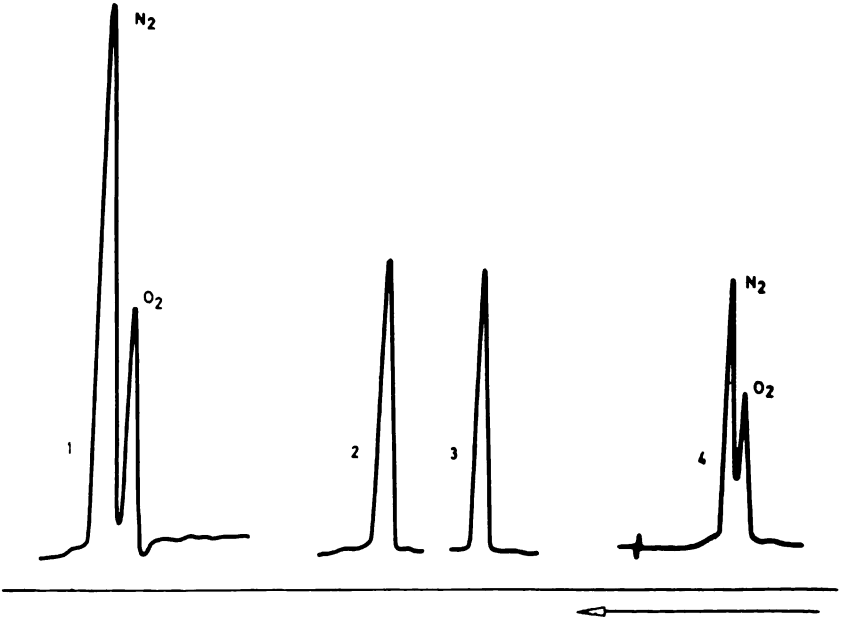

Fig. 1

Influence of alcohols on the retention time of oxygen and nitrogen at 100°C. Curve: 1 — mixture of O_2 and N_2; 2 — mixture of O_2, N_2 and ethyl alcohol; 3 — mixture of O_2, N_2 and methyl alcohol; 4 — mixture of O_2, N_2 and propyl alcohol

that no separation occurs and the two gases produce a common signal (Fig. 1, curves No. 2 and 3). Propyl alcohol and isopropyl alcohol behave in the similar way, although less effective (Fig. 1, curve No. 4, and Fig. 2). However, the presorption of more than 0.63 molar fraction of isopropyl alcohol in an absolute amount of 0.36 mole/g zeolite produces a new effect. There is a reduction in the carrier-gas flow and the operating conditions of the chromatograph get completely deranged. The column becomes practically impermeable to the gas.

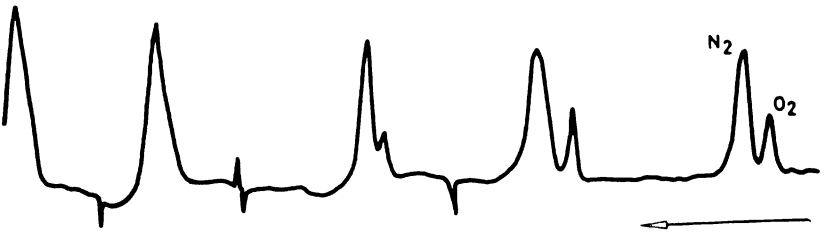

Fig. 2

Influence of increasing quantity of isopropyl alcohol in mixture with O_2 and N_2 on the retention time of O_2 and N_2

The presorption of *n*-butyl alcohol changes the retension times of oxygen and nitrogen in such way that at the outlet of the column nitrogen appears first instead of oxygen (Fig. 3). It must be pointed out that the descri-

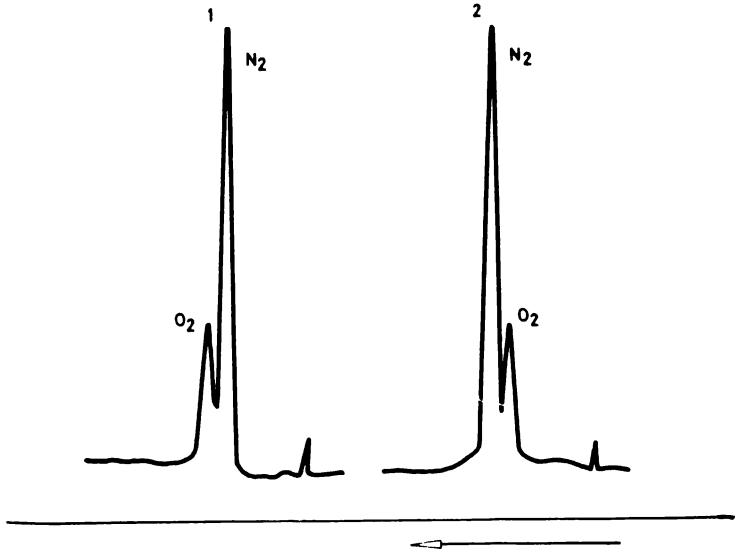

Fig. 3

Influence of n-butyl alcohol on retention time of O_2 and N_2; 1 — with alcohol; 2 — without alcohol

bed action of the alcohols was observed to be temporary with quantities up to 1 $\cdot 10^{-5}$ mole/g zeolite, i.e. it was observed only with simultaneous presence of alcohol vapor and the gases in the column, contrary to the results in ref. 10 obtained by the presorption of greater quantities of alcohol and water. If alcohol is introduced into the column first and only then the mixture of oxygen and nitrogen, the system behaves almost the same as if no alcohol had been present.

The branched butyl alcohol isomers cause instantaneous blockage of the column.

Absorption measurements were carried out by desorption of methyl alcohol from the zeolite in the temperature interval between 296 and 389 °K. The zeolite surface area, determined by the BET method from the low-temperature adsorption of nitrogen, was about 750 m^2/g, this being within the usual limits, i.e. 500—800 m^2/g (according to references 3, 4 and 6). From the isostere of desorption (Fig. 4), showing a knee at 315 °K, the differential

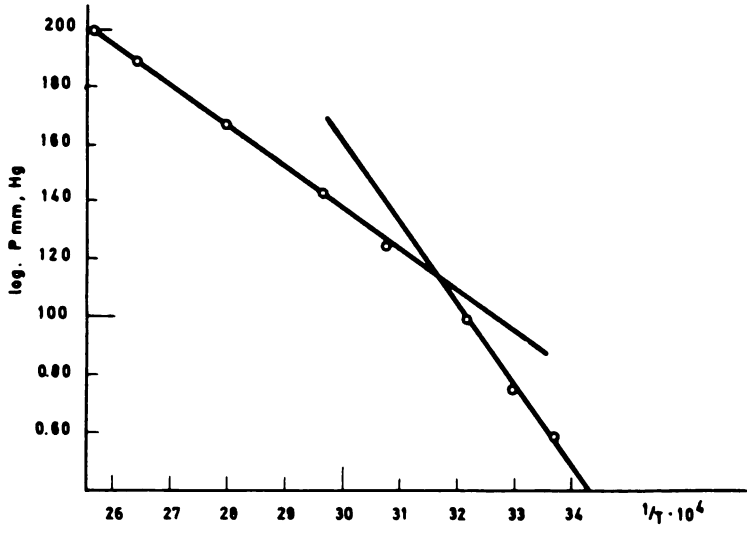

Fig. 4

The desorption isostere of methyl alcohol

heats of desorption (for a degree of surface covering $\theta = 0.7$, at a specific area of 750 m^2/g) were determined for two temperature ranges:

$Q_1 = 10.2$ kcal.mole^{-1} for the interval between 296 and 315 °K;
$Q_2 = 6.2$ kcal.mole^{-1} for the interval between 315 and 389 °K.

The calculated entropy for the first interval is 34.4 and 32.0 e.u., and for the second 20.8 and 17.0 e.u.

Analysis of the results shows that the volume (V) of methyl alcohol vapor adsorbed per g adsorbent depends on the temperature (T) and the equilibrium pressure (P) (Fig. 5) according to equation

$$V = A - B\left(\frac{P}{T}\right).$$

The coefficients A and B for the interval between 296 and 389 °K were determined by the least squares method, this giving

$$V = 284.1 - 50.0\left(\frac{P}{T}\right).$$

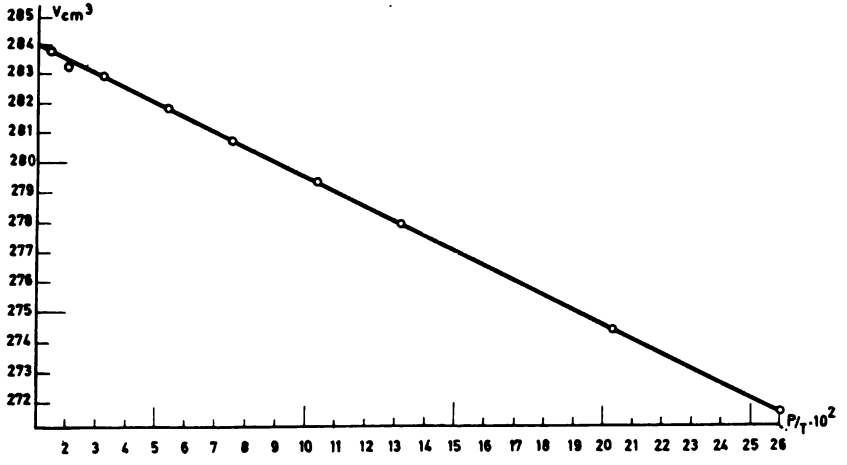

Fig. 5
Desorption of methyl alcohol

The width of the NMR output signal changed during desorption (Fig. 6) and showed a knee at 313 °K, this corresponding to the knee on the desorption isostere. On the basis of these data the activation energy for surface mobility was determined to be 3.9 kcal · mole^{-1} for the interval between 296 and 313 °K, and 1.8 kcal · mole^{-1} for that between 313—389 °K.

According to the results, desorption of methyl alcohol occurs in two stages, the first being with the higher and the second with the lower heat of desorption. In the temperature interval between 296 and 315 °K (heat of desorption 10.2 kcal · mole^{-1}) this process is taking place in the kinetic region, and the heat and entropy of desorption are, as expected, higher than for condensation. The activation energy of surface mobility for the same temperature interval is considerably lower than the heat of desorption, this also being correct. Above 315 °K (heat of desorption 6.6 kcal · mole^{-1}) the majority of the alcohol molecules in the zeolite lattice are already desorbed, but desorption is slowed down by diffusion of vapor through the zeolite chan-

nels and the mechanism enters the transitional diffusion-kinetic region. Here the heat and entropy of desorption are considerably lower than the corresponding values for the conversion of pure liquid into gas, this proving that

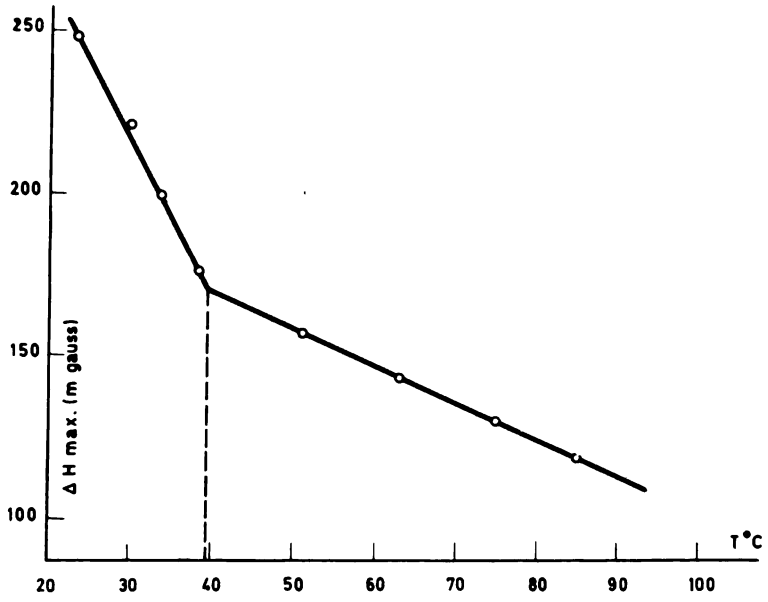

Fig. 6

Dispersion signal width variation of adsorbed methyl alcohol with temperature

desorbed molecules are trapped inside the lattice at that temperature. Hence the activation energy of surface mobility decreases to a value close to the activation energy of diffusion. A considerable influence of diffusion, manifested in a similar way, was also observed by the authors of references 6—9 for desorption of water on zeolite 4A. The short-lived action of presorbed alcohols can hardly be explained only by the hindrance effect, which should be permanent[10] because alcohol remains adsorbed on zeolite.

CONCLUSION

The adsorption of oxygen and nitrogen in a mixture with vapors of aliphatic alcohols (from C_1 to C_4) on the synthetic zeolite Linde 5A (CaA) has been studied. Particular attention was paid to the adsorption of methyl alcohol. The presence of alcohol vapors was found to change the adsorptive properties of the zeolite, and hence also the retention times of oxygen and nitrogen. In the case of methyl alcohol two isosteric heats of desorption, 10.2

and 6.6 kcal · mole^{-1}, were found for two temperature regions with corresponding activation energies of surface mobility determined by NMR 3.9 and 1.8 kcal · mole^{-1}, respectively. The volume of adsorbed methyl alcohol vapor per g zeolite was found to depend on the temperature (T) and the equilibrium pressure (P) according to the equation $V = A - B\left(\frac{P}{T}\right)$, where A and B are constants. The influence of alcohols adsorbed in a total quantity up to 10^{-5} mole/g zeolite on the retention times of nitrogen and oxygen was found to be temporary, i.e. was only observed when the alcohols were adsorbed simultaneously in a mixture with these gases.

Dept. of Physical Chemistry,
School of Sciences, Belgrade University
Institute for the Application of Nuclear
Energy in Agriculture, Forestry and Veterniary Science, Zemun
Institute of Chemistry, Technology and Metallurgy, Belgrade

Received 15 May, 1968

REFERENCES

1. Barrer, R. M. and E. A. D. White. "The Hydrothermal Chemistry of Silicates. Part II. Synthetic Crystalline Sodium Aluminosilicates" — *J. Chem. Soc.*: 1561—1572, 1952.
   "The Hydrothermal Chemistry of Silicates. Part I. Synthetic Lithium Aluminosilicates" — *J. Chem. Soc.*: 1267—1279, 1951.
   "Synthesis of a Zeolitic Mineral with Chabazite-like Sorptive Properties" — *J. Chem. Soc.*: 127—143, 1948.
2. Barrer, R. M. and N. McCallum. "Hydrothermal Chemistry of Silicates. Part IV. Rubidium and Caesium Aluminosilicates" — *J. Chem. Soc.*: 4029—4035, 1953.
3. Breck, D. W., W. G. Eversole, R. M. Milfon, T. B. Reed and T. L. Thomas, "Crystalline Zeolites. I. The Properties of a New Synthetic Zeolite, Type A" — *J. Chem. Soc.* 78: 5963—5972, 1956.
   "Crystalline Zeolites. II. Crystal Structure of Synthetic Zeolite, Type A" — *J. Chem. Soc.* 78: 5972—5977, 1956.
4. Barrer, R. M. and A. B. Robins. "Sorption of Mixture. Part II. Equilibria between Binary Gas-Mixture and Some Zeolites" — *Trans. Faraday Soc.* 49: 929—936, 1953.
5. Šušić, M., V. Vučelić, S. Paušak, D. Karaulić and V. Milaković-Vučelić. † (Nuclear Magnetic Resonance Method for the Determination of Specific Surface Area. Study of the State of Adsorbed Polar Vapors on Zeolite Linde 5 A) — *Glasnik hemijskog društva* 73:* 1975—1984, 1969.
6. Dubinin, M. M., E. G. Zhukovskaia and K. O. Murdmaa. † (Study of Adsorption Properties and the Secondary Porous Structure of Adsorbents Having Molecular-Sieve Action) — *Izvestiia Akademii Nauk SSSR* 12: 2113—2121, 1962.
7. Lezin, I. S. and M. M. Dubinin. † (On the Kinetics of Water Sorption on Zeolites) — *Doklady Akademii Nauk SSSR* 171: 382, 1966.
8. Dubinin, M. M. † (The Modern State of the Theory of Volume Filling of Microporous Adsorbents at Adsorption of Gases and Vapors on Charcoal Adsorbents) — *Zhunral fizicheskoi khimii* 39: 1305—1317, 1965.
9. Kabanova, O. N. and D. P. Timofeev. † (Determination of Water Vapor Diffusion Coefficient in Granulated Zeolites by the Method of Sorption from a Carrier Gas Stream) — *Izvestiia Akademii Nauk SSSR* (*Otd. Khim.*) (1): 176, 1963.
10. Neimark, I. E., M. A. Pointkovskaia, A. E. Lukash and R. S. Tiutiunik. † (Exchange of the Selective Properties of the Synthetic Zeolites) — Moskva: Izdatel'stvo Akademii Nauk SSSR, 1962.

† Original title not given.

* Available in English translation from National Technical Information Service, Springfield, Virginia, 22151.

GLASNIK HEMIJSKOG DRUŠTVA, Vol. 34, No. 8-9-10, 1969, pp. 473—479

GHDB-82

541.183.56:547.53:661.183.7

Original Scientific Paper

DYNAMIC ADSORPTION OF ORGANIC VAPORS ON BLOCKED SILICA GEL. II.

by

SLOBODAN KONČAR-DJURDJEVIĆ and IVANKA PETKOVIĆ

The same system as described in ref. 1 was used, i.e. silica gel blocked with methylene blue and the vapors of organic solvents in air, except for benzene vapor concentrations somewhat lower than the saturation concentration at the working temperature.

Our aim was to investigate the influence of different concentrations of the solvent vapors on dynamic adsorption on the blocked adsorbent. Papers of a similar nature have already been published in this Bulletin[1, 2].

EXPERIMENTAL

The apparatus used was mainly the same as in ref. 1. However, the following minor alterations were made: The air was sucked into the system via a sulphuric acid wash-bottle and a water-free calcium chloride-packed U-tube and then led into the copper tube thermostat where its temperature was made 15 °C. The dried and temperature controlled air was divided into two streams passing through separate differential manometers for measurement of volume.

The first stream passed through a bubbler filled with organic solvent in order to saturate it. The other stream was later mixed with the first in a mixing vessel to get the desired concentration of the organic solvent vapor. The mixture so obtained was passed through a thermostat to bring it up to 25 °C and then through the adsorbent in a U-tube inside the same thermostat, so that adsorption took place at 25 °C. At this point the air was sucked out of the system by a water pump.

The U-tube with the adsorbent was first weighed every 5 minutes and then every 15 minutes until constant weight.

The adsorbent was silica gel prepared by the sulphuric acid and water-glass method as in ref. 3. It was blocked at room temperature from the aqueous solutions of methylene blue, the concentrations being the same as in the previous work: 0.03, 0.1, 0.2, 0.3 and 0.5%. To 100 *ml* of solution about 3 *g* of degassed silica gel was added.

The same technique was used both with regard to the static adsorption of methylene blue on the gel and the dynamic adsorption of the organic solvent vapor on the blocked adsorbent.

In this paper we report only on the adsorption of benzene vapor from the air. The benzene was of *pro analysi* quality.

The air carrying benzene vapor will be termed "primary" and the pure air used for diluting "secondary". The total flow rate of primary plus secondary air mixture was kept constant, i.e. 2.30 lit/min. During the experiment only the ratios between the primary and secondary air were changed.

The partial pressure of benzene vapor in the air saturated at 15 °C was 58.8 *mm* Hg, this being equal to the vapor pressure of benzene at this temperature. The above value was obtained grafically and by computation.

In order to obtain different concentrations of benzene vapor the primary and secondary air were mixed together in the ratios given in Table 1.

TABLE 1

Mixture	Primary air saturated with vapor *l/min*	Secondary air *l/min*
I	2.30	—
II	2.07	0.23
III	1.10	1.20
IV	0.77	1.53
V	0.23	2.07

RESULTS

Curve 1 in Fig. 1 shows the dynamic adsorption of benzene vapor from the air saturated at 15 °C on the unblocked silica gel. Curves 2, 3, 4 and 5 show adsorption from the mixtures indicated in the table by II, III, IV and V. Here the concentrations of benzene vapor were lower than in the first mixture.

From the graph, it is apparent that the reduction of the benzene partial pressure in the mixture led to a reduction of the quantity of benzene adsorbed on the unblocked adsorbent.

Figures 2, 3, 4 and 5 show the dynamic adsorption of diluted benzene vapor (see the table) on gel blocked with different quantities of methylene blue. Here, just as with the unblocked gel, reduction of the concentration of benzene vapor in the mixture also led to a reduction of the quantity of benzene adsorbed.

The broken line I in Fig. 6 shows the dependence of the quantity of benzene adsorbed in the equilibrium state (g/g) on the previously adsorbed quantity of methylene blue (g/g). In this case the partial pressure of benzene in the mixture was 58.8 *mm* Hg, i.e. equal to the vapor pressure of benzene at 15 °C.

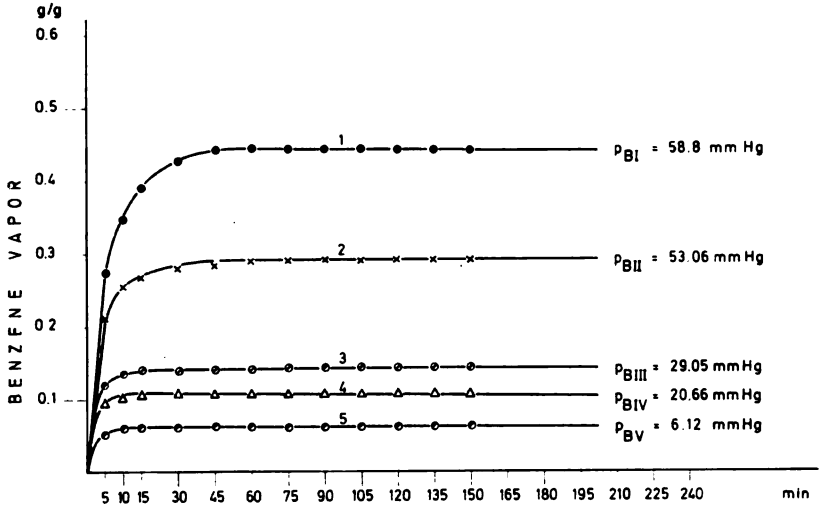

Fig. 1

Dynamic adsorption of different concentrations of benzene vapor in air on unblocked silica gel

o unblocked gel,

× blocked gel 0.0101 *g/g* methylene blue;

● " " 0.0340 " " "

⊘ " " 0.0690 " " "

● " " 0.101 " " "

△ " " 0.164 " " "

The broken lines II, III, IV and V in the same figure show the adsorption at benzene partial pressures 53.11 *mm* Hg, 29.16 *mm* Hg, 20.65 *mm* Hg and 6.16 *mm* Hg.

It may be seen that all points for the blocked adsorbent lie on a straight line, while the point corresponding to the unblocked adsorbent lies above it. The higher the concentration of benzene vapor in the mixture the greater the deviation of this point.

CONCLUSION

The dynamic adsorption of benzene at different mean partial vapor pressures (p_{BI} = 58.8 *mm* Hg; p_{BII} = 53.11 *mm* Hg; p_{BIII} = 29.16 *mm* Hg; p_{BIV} = 20.65 *mm* Hg; p_{BV} = 6.16 *mm* Hg) in a mixture with dry air on un-

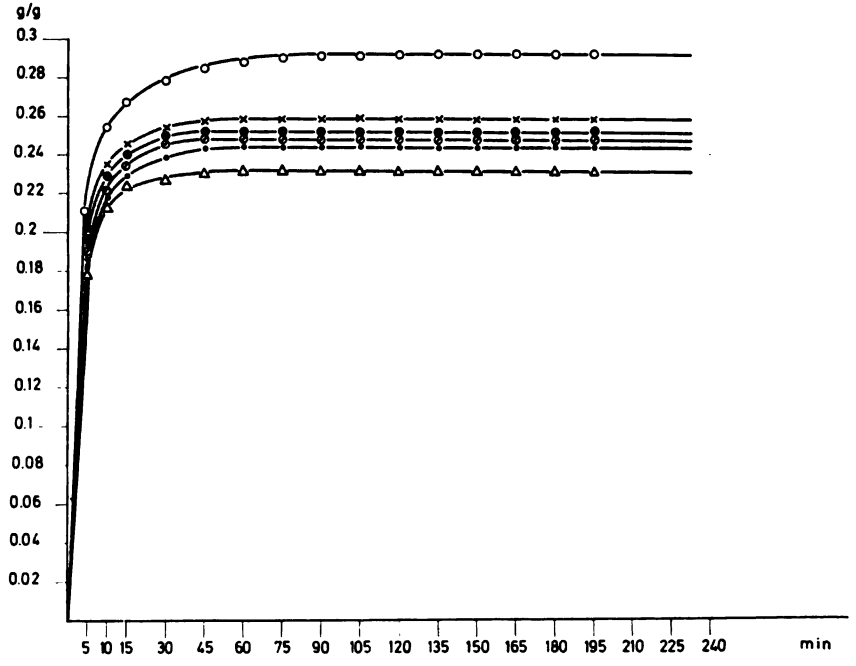

Fig. 2

Dynamic adsorption of benzene vapor of mean partial pressure 53.11 mm Hg on silica gel blocked with different quantities of methlylene blue

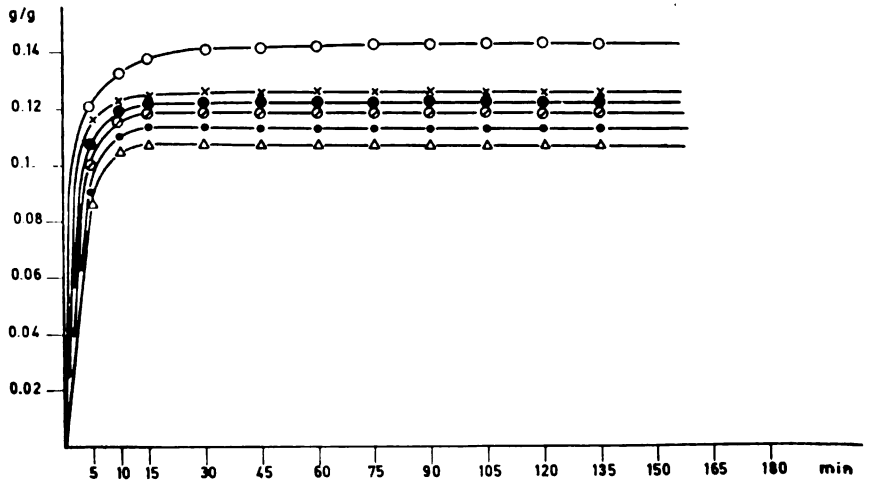

Fig. 3

Dynamic adsorption of benzene vapor of mean partial pressure of 29.16 mm Hg, on silica gel blocked with different quantities of methylene blue

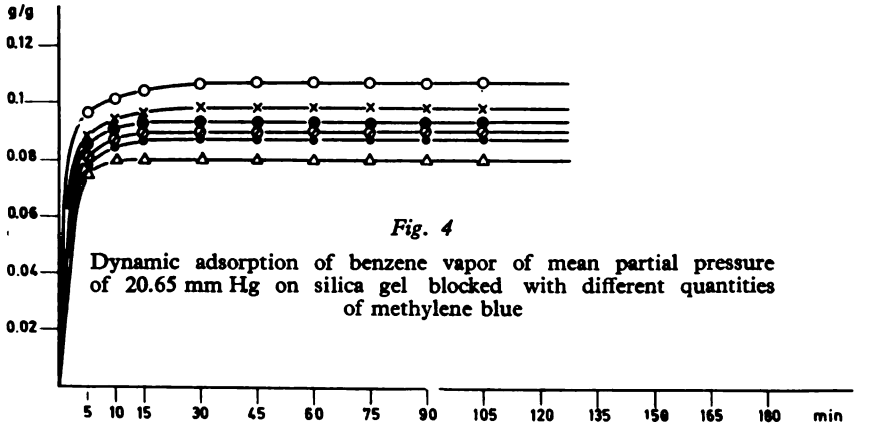

Fig. 4

Dynamic adsorption of benzene vapor of mean partial pressure of 20.65 mm Hg on silica gel blocked with different quantities of methylene blue

○ unblocked gel;

× blocked gel 0.0101 *g/g* methylene blue;

● „ 0.0340 „

⊘ „ 0.0690 „

• „ 0.101 „

△ „ 0.164 „

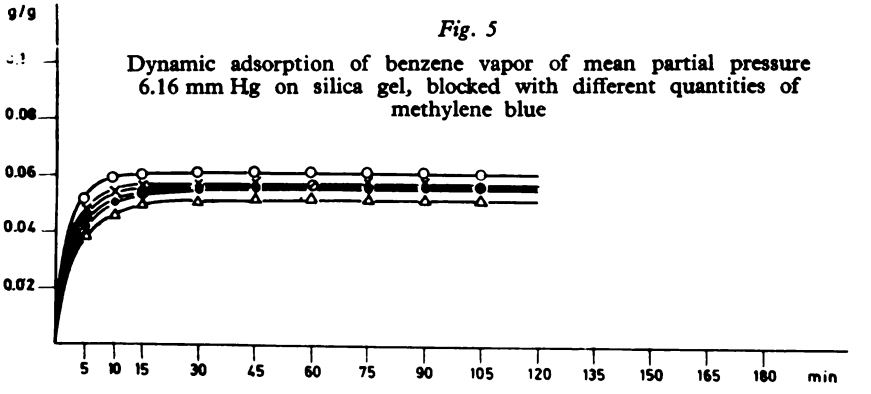

Fig. 5

Dynamic adsorption of benzene vapor of mean partial pressure 6.16 mm Hg on silica gel, blocked with different quantities of methylene blue

○ unb . d gel;

× blocked gel 0.0101 *g/g* methylene blue;

● „ 0.0340 „

⊘ „ 0.0690 „

• „ 0.101 „

△ „ 0.164 „

blocked silica gel and on gel previously blocked with different quantities of methylene blue from aqueous solutions (0.0101 *g/g*; 0.0340 *g/g*; 0.069 *g/g*; 0.101 *g/g* and 0.164 *g/g*) has been studied.

The air was saturated with benzene vapor at 15 °C, while the dynamic adsorption took place at 25 °C.

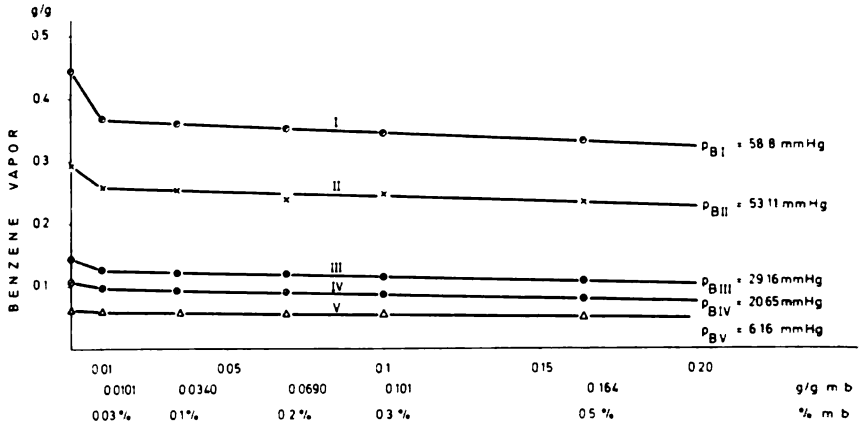

Fig. 6

Dependence of the quantity of benzene vapor adsorbed (g/g) an the previously adsorbed quantity of methylene blue (g/g) for different benzene vapor partial pressures

From Figs. 1, 2, 3, 4 and 5 it may be seen that the higher the benzene partial pressure in the mixture the more was adsorbed on the unblocked gel. On the other hand, the bigger the quantity of methylene blue used to block the gel, the smaller the quantities of vapor adsorbed.

The dependence of the quantity of vapor adsorbed in the equilibrium state (*g/g*) on the previously adsorbed quantity of methylene blue (*g/g*) is shown in Fig. 6. For constant benzene partial pressure a linear dependence was obtained, except for the point corresponding to the unblocked adsorbent.

Here to the decrease in the quantity of vapor adsorbed was greatest between the unblocked gel and that blocked with the smallest quantity of methylene blue.

School of Technology and Metallurgy,
Belgrade Univ.

Received 3 March, 1969

REFERENCES

1. Končar-Djurdjević, S. and I. Petković. — *Glasnik hemijskog društva* (Beograd) **30**:* 245—260, 1965.
2. Končar-Djurdjević, S. and I. Petković. — *Glasnik hemijskog društva* (Beograd) (to be published).
3. Boreskov, G. and co-workers. — *Zhurnal fizicheskoi khimii* **22**: 603—617, 1948.

* Available in English translation from National Technical Information Service, Springfield, Virginia, 22151.

GLASNIK HEMIJSKOG DRUŠTVA, Vol. 34, No. 8-9-10, 1969, pp. 481—487

GHDB-83

543.253:546.821:547.2

Original Scientific Paper

POLAROGRAPHIC BEHAVIOR OF TITANIUM IV IN THE PRESENCE OF DIETHYLENETRIAMINEPENTAACETIC ACID (DTPA)

by

MILENKO V. ŠUŠIĆ and AHMED KH. GHONAIM

The work of many investigators has shown that titanium can be determined polarographically. Zeltzer[1], and Lingane and Kennedy[2] investigated the polarography of titanium in solutions of mineral acids. Vendenbosch[3] states that titanium is reduced from a solution of 0.1 M potassium oxalate and 1.0 M sulphuric acid containing 0.005 percent gelatine, and also from solutions of tartarate and citrate as supporting electrolytes. Some analytical methods using these supporting electrolytes have been developed as well[4, 5, 6, 7]. Pecsok *et al.*[8, 9, 10] reinvestigated the polarography of titanium in the presence of organic acids and also proved that the Ti(IV)-EDTA system is suitable for the determination of titanium; they showed that the half-wave potential is dependent on pH in the region from 3 to 8.7, and independent below pH 2. According to Pršibil and Malat[11], Ti(IV) gives one wave in 0.4 M acetic acid solution in the presence of 10^{-2} M complexon I ($E_1/_2 = -0.33$ *V*) and in the presence of 10^{-2} M complexon III ($E_1/_2 = -0.12$ *V* vs SCE). Van Dalen and Graham[12] used *m*-nitrophenylarsenic acid. Our preliminary work[13] showed that Ti(IV) in the presence of DTPA is reduced at dropping mercury electrode. The aim of the present paper is to evaluate the polarographic behavior of the Ti(IV)-DTPA system.

EXPERIMENTAL

Apparatus. A Radiometer Type PO3h recording polarograph was used and all pH measurements were made with a Beckman pH-meter.

Reagents. Aqueous solutions of titanium were prepared by precipitating titanium hydroxide from the solution of potassium titanium oxalate in HCl and by dissolving the precipitate in the least possible amount of HCl. The solutions were then standardized gravimetrically. Slightly alkaline DTPA solutions were prepared by dissolving the appropriate amounts in NaOH and diluting with distilled water to the desired volume.

RESULTS

In very dilute HCl solution titanium gave an irreversible polarographic wave as reported in the literature[14]. By the addition of DTPA to such a solution one or two waves appeared at more positive potentials than in HCl

depending on the pH and the concentration of complexon, indicating the formation of different Ti(IV)-DTPA complexes which are reduced at different potentials.

In HCl solutions of pH < 3 containing a very small concentration of DTPA one wave was obtained at —0.6 *V* (SCE). By increasing the concentration of DTPA another wave appeared at —0.27 *V* (SCE), and the diffusion current was divided between these two waves. On further increase of the complexon concentration, the first, more positive, wave increased while the second one decreased. At complexon concentrations higher than 10^{-3} M and constant Ti(IV) concentration of 10^{-3} M, the wave at —0.27 *V* (SCE) predominated. During these changes the total diffusion current was approximately constant (Fig. 1) and the half-wave potential was independent of the DTPA concentration, indicating that the Ti(IV)-DTPA and Ti(III)-DTPA complexes have the same number of ligands, namely one.

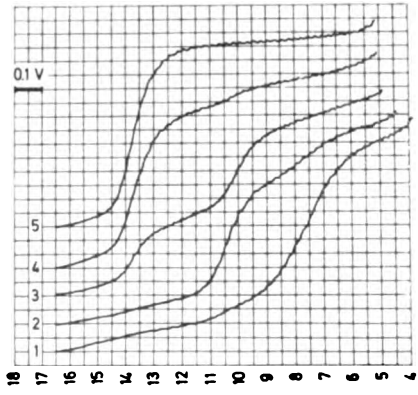

Fig. 1

Polarographic waves of Ti(IV) in HCl solutions containing different concentration of DTPA at pH = 2, and 1.10^{-3} M Ti(IV); curve: 1 — without DTPA, 2. — 1.10^{-4}, 3.—5.10^{-4}, 4. — 1.10^{-3} and 5. — 2.10^{-3} M DTPA, starting from zero potential (SCE)

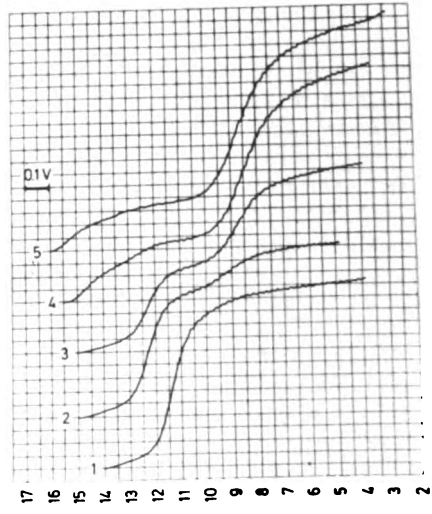

Fig. 2

Influence of pH on the polarographic wave of Ti(IV)-DTPA complexes; curve: 1. — pH = 2, 2. — pH = 2.75, 3. — pH = 3.25, 4. — pH = 4.15, 5. — pH = 4.5, starting from zero potential (SCE)

By increasing the pH of the solution, starting from the condition where only one wave existed at —0.27 *V*, the second wave began to develop again at the expense of the first one. At pH higher than 4.5, only the second wave was present (Fig. 2). The half-wave potential of the first wave was found to be independent of pH while that of the second one became more negative with increasing pH (Table I). The slope $\Delta E_{1/2}/\Delta$ pH taken from the table

is 0.13, indicating that one hydrogen ion is consumed in the electrode reaction.

TABLE I

pH	—2.05	2.55	2.80	3.25	3.73	4.25
$E_{i/2}$	—0.280	0.275	0.272	0.272	0.275	0.280
$-E''_{i/2}$	—	—	very small	0.580	0.642	0.710

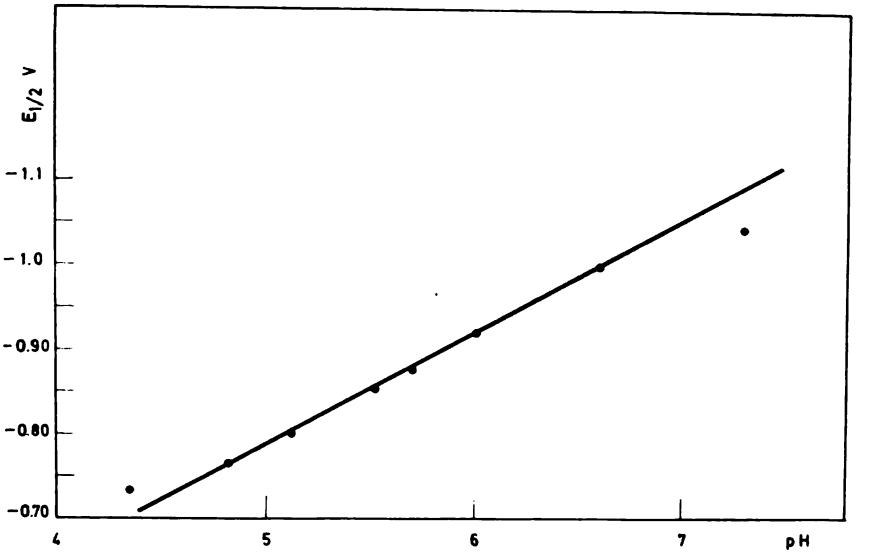

Fig. 3

Change of the half-wave potential of the second wave with pH; 1.10^{-3} M Ti(IV), 0.1 M DTPA and acetate buffer 0.2 M

At pH > 4.5, where only the second wave existed, at constant concentration of titanium and DTPA the half-wave potential was a linear function of pH (Fig. 3). From the slope $\Delta E_{1/2}/\Delta$ pH, which is 0.132, it follows that one hydrogen ion takes part in the electrode reaction, as is also the case at pH < 4.5.

With increasing DTPA concentration at constant pH and constant concentration of Ti(IV) the half-wave potential of this wave becomes more negative (Fig. 4).

In the pH range from 2 to 4, the reversibility of the electrode reaction for the first wave was studied by ploting $\log \frac{i_d - i}{i}$ against E_{de} and by apply-

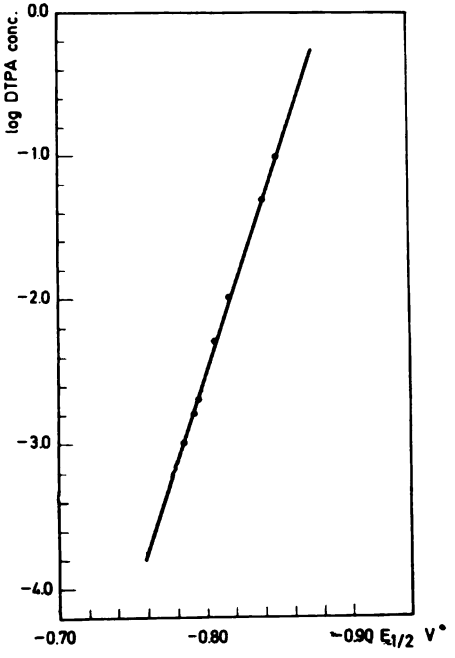

Fig. 4

Dependence of the half-wave potential of the second wave on DTPA concentration; pH = 5.5 and 1.10^{-3} M Ti(IV)

ing Tomes's equation (15). The results indicate an almost reversible electrode reaction involving one electron (Fig. 5).

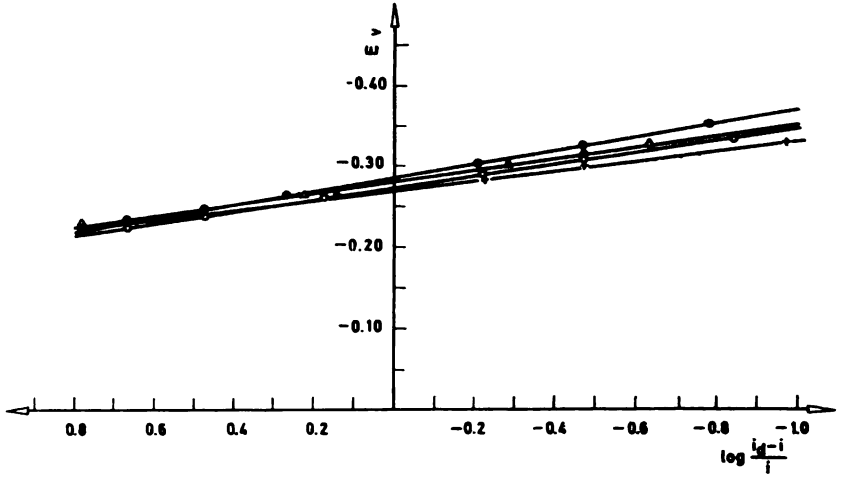

Fig. 5

Plots of $\log \frac{i_d - i}{i}$ against E_{de} for the first wave at different pH: ● —2.07, △ — 2.55, o — 2.80, x — 3.25

The second wave was found to be irreversible and the value of αn was calculated from the maximum diffusion current by plotting $\log \frac{i_d' - i'}{i'}$ against E_{de} according to the method given by Meites[16] and checked by Koutecky's method[17]. The calculated values of αn by these methods are in good agreement, as seen from Table II, showing that the polarographic wave is due to an irreversible one-electron reduction process.

TABLE 2

pH	Ref. 16 $\Delta E/\Delta \log \frac{i_d' - i'}{i'}$	αn	Ref. 16 $E_{3/4} - E_{1/4}$	αn	Ref. 17 $\Delta \log \mu/\Delta E$	αn
4.35	0.119	0.456	0.115	0.449	7.57	0.448
4.82	0.106	0.510	0.110	0.470	7.57	0.448
5.12	0.140	0.387	0.140	0.370	7.14	0.423
5.52	0.119	0.460	0.130	0.460	5.56	0.329
5.70	0.120	0.470	0.120	0.430	6.55	0.387
6.00	0.119	0.456	0.115	0.450	6.45	0.382
6.60	0.109	0.500	0.110	0.470	7.58	0.448
7.30	0.113	0.480	0.109	0.490	6.25	0.370

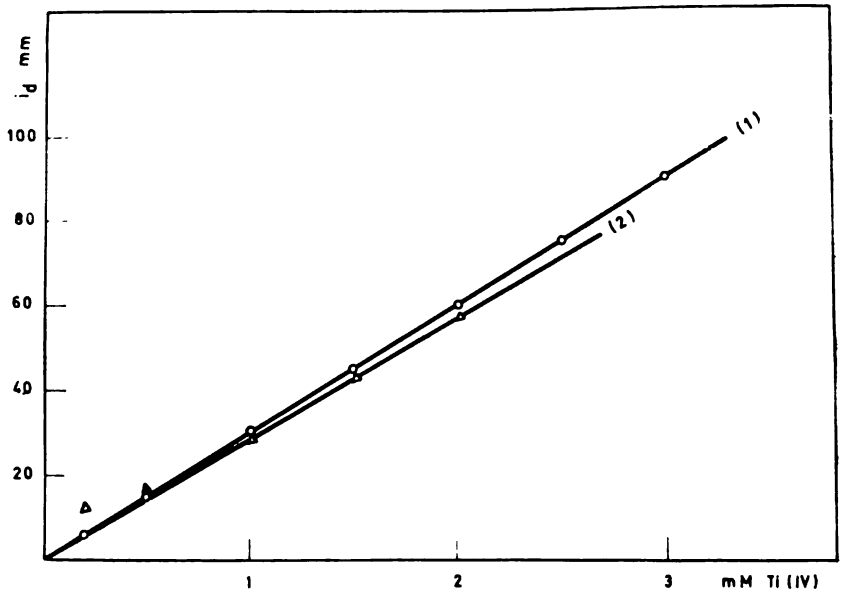

Fig. 6

Dependence of the diffusion current on Ti(IV) concentration; curve: 1. — first wave at pH = 2 and 0.05 M DTPA, 2 — second wave at pH = 5.58 and 0.1 M DTPA

At constant DTPA concentration and constant pH the diffusion current of both waves was found to be proportional to the Ti(IV) concentration (Fig. 6).

SUMMARY

The polarography of the Ti(IV)-DTPA system has been studied. Ti(IV) gives one or two waves, depending on the pH and DTPA concentration. The half-wave potential of the more positive wave is independent of pH and DTPA concentration and that of the second (more negative) dependent on pH and DTPA concentration; one hydrogen ion takes part in the corresponding electrode reaction which is irreversible. The diffusion current was found to be a linear function of titanium concentration at constant pH and constant DTPA concentration.

School of Sciences,
Institute of Physical Chemistry, Belgrade Univ.
Institute of Chemistry, Technology
and Metallurgy, Belgrade

Received 15 May, 1968

REFERENCES

1. Zeltzer, S. — *Collection Czechoslov. Chem. Communications* 4: 319, 1932.
2. Lingane, J. J. and J. H. Kennedy. — *Anal. Chim. Acta* 15: 294, 1956.
3. Vandenbosch, V. — *Bull. Soc. Chim. Belg.* 58: 532, 1949.
4. Adams, D. F. — *Anal. Chem.* 20: 891, 1948.
5. Graham, R. P. and A. Hitchen. — *Analyst* 77: 533, 1952.
6. Graham, R. P. and J. A. Maxwell. — *Anal. Chem.* 23: 1123, 1951.
7. Graham, R. P. and A. Hitchen. — *Can J. Chem.* 30: 661, 1952.
8. Pecsok, R. L. — *J. Am. Chem. Soc.* 73: 1304, 1951.
9. Pecsok, R. L. — *J. Chem. Educ.* 29: 597, 1952.
10. Pecsok, R. L. and E. F. Maverick. — *J. Am. Chem. Sci.* 76: 358, 1954.
11. Pršibil, R. (Complexones in Analytical Chemistry) (in Russian) — Moskva: Inostrannaia literatura, 1960, pp. 59, 73.
12. Van Dalen, E. and R. P. Graham. — *Annal. Chim. Acta* 12: 489, 1955.
13. Ghoniam, A. Kh. and M. V. Šušić. — *Glasnik hemijskog društva* (Beograd) 33* 39, 1968.
14. Strubl, R. — *Collection Czechoslov. Chem. Communications* 10: 475, 1938.
15. Tomeš, I. — *Collection Czechoslov. Chem. Communications* 9: 12, 81, 150, 1937.
16. Meites, L. and J. Israel. — *J. Am. Chem. Soc.* 83: 4903, 1961.
17. Koutecký, J. — *Chemické listy* 47: 323, 1953.; *Collection Czechoslov. Chem. Communications* 18: 597, 1953.

* Available in English translation from National Technical Information Service, Springfield, Virginia, 22151.

HLASNIK HEMIJSKOG DHUŠTVA, Vol. 34, No. 8-9-10, 1969, pp. 489—495

GHDB-84

612.616.3:66.094.1
Original Scientific Paper

THE REDUCTION OF Δ^4-ANDROSTENE-3,17-DIONE-11β-OL BY METAL HYDRIDES

by

MILUTIN STEFANOVIĆ, RATKO JANKOV AND MIROSLAV GAŠIĆ

The reduction of steroidal ketones by means of metal hydrides is a very thoroughly investigated reaction. The influence of various substituents and functional groups including both conjugated and isolated double bonds has also been studied and it was found that, in general, the presence of an α, β-double bond has no effect on the course of this reduction[1]. However, in the case of a Δ^4-3-ketone, the reported data are often contradictory with regard to the ratio of the two possible epimeric allylic alcohols formed[2]. The different degrees of stereospecificity have been discussed in terms of steric hindrance to the approach of the reagent and the relative thermodynamic stabilities of the possible transition states leading to the products[3]. Most of these arguments are summarized in Barton's rule[4], according to which a Δ^4-3-ketone, being relatively unhindered, should be reduced mainly to the equatorial (i.e. pseudoequatorial) alcohol.

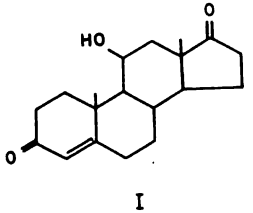

I

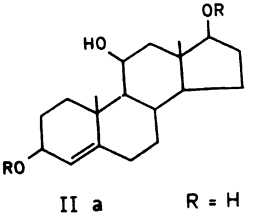

II a R = H
b R = Ac

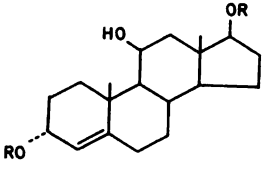

III a R H
b R Ac

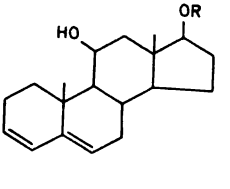

IVa R H
b R Ac

Fig. 1

During a current investigation designed to parallel earlier work on the synthesis and microbiological transformation of 5,10-seco-steroids[5, 6], it was necessary to convert Δ^4-androstene-3,17-dione-11β-ol (I) to Δ^4-androstene-3β, 11β, 17β-triol (II). The obvious choice to effect this conversion was the reduction of (I) by metal hydrides. The reduction of I by means of lithium aluminium hydride and sodium borohydride has already been described[7, 8]. Although the two reduction methods were not studied in great detail, the results indicated a high degree of stereospecificity, i.e. the formation of only the pseudoequatorial alcohol in these reactions. However, the reported analytical data for the obtained allylic alcohol (IIa) were different. In repeating those experiments we found that the reduction of (I) with both metal hydrides is not as stereospecific as described and that both epimeric alcohols (IIa) and (IIIa) are formed, although in slightly different ratio. It could also be concluded that the previously reported analytical data actually relate to mixtures of epimers (IIa) and (IIIa). These results prompted us to investigate the reduction of I by various reducing agents and the thermodynamic stabilities of both the epimeric alcohols in more detail; our results are summarized in the following table:

TABLE 1

Metal hydride	Solvent	T°	Equatorial isomer %*	Overall recovery %
LAH_4	Et_2O	reflux	65	95
„	Et_2O/THF 1:1	„	65	95
„	THF	„	65	95
$NaBH_4$	MeOH	„	75	95
„	„	25	75	95
„	iPrOH	25	75	95
„	„	reflux	75	80
B_2H_6	THF	25	70	60
$Al(iOPr)_3$	iPrOH	reflux	60	80

* % calculated relative to total ammount of isolated IIa and IIIa.

In order to obtain more information about the relative thermodynamic stability of alcohols (IIa) and (IIIa), both epimers were separately equilibrated by means of aluminum isopropylate in isopropanol in the presence of catalytic amounts of acetone. The experiments lasted 48 hrs at reflux temperature giving rise to a 60 : 40% ratio of epimers (IIa) and (IIIa), with an overall recovery of cca. 80%.

The separation of epimers (IIa) and (IIIa) was achieved by repeated column chromatography; the optical rotation data for crude products of experiments 1—6 also confirm the relative ratio found by quantitative

separation. The proof of the structure for (IIa) and (IIIa) was obtained by elemental microanalysis, IR and NMR spectra, and by chemical means. Thus, upon oxidation by chromic acid, both epimers yielded adrenosterone (Δ^4-androstene-3,11,17,-trione), identical with an authentic sample. Upon dehydration, both epimers afforded the same heteroannular diene (IVa). The rates of dehydration were not measured but qualitative data indicated that the pseudoaxial epimer (IIIa) eliminated water at a slightly faster rate. Rigorous proof of the stereochemistry at C-3 for both epimers could not be obtained. However, the nuclear magnetic resonance spectra strongly support configurations as shown in Fig. II. The angular methyl group signals appear exactly at the calculated positions for both epimeric alcohols and the corresponding 3, 17-diacetates[9]. The overall features of the NMR-spectra of both epimers are very alike. In the region of τ 4.7—5.8* there are two sets of signals, each corresponding to two hydrogen atoms; the C-17α- and C-11α- hydrogen pattern appears as a practically identical multiplet in the region of τ 5.3—5.8. The vinyl group resonances show some interesting features of olefinic proton signals. For example, the vinylic hydrogen in IIb appears as a broad singlet at 4.9 and the axial 3α-hydrogen at 4.85 (broad). In IIIb, however, the pattern corresponding to the vinylic and the equatorial 3β-hydrogen appears as an AB system in which part A (3β-H) is further split by hydrogen atoms at C-2, τ_A being at $\sim$4.85 and τ_B at $\sim$4.65. The vicinal coupling between the vinylic and the 3β-hydrogen in IIIa and IIIb is 5 cps, also indicating a substantial dihedral angle deviation and distorsion of ring A in IIIa (IIIb), as compared with its epimer IIa (IIb), respectively. The NMR spectral data are also in agreement with the following two chair-like conformations of ring A for IIa and IIIa, respectively:

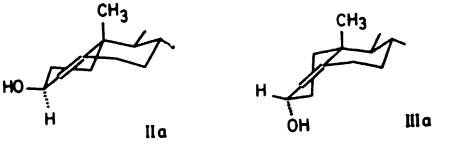

Fig. 2

It seams reasonable to assume that the introduction of a substituent in the allylic position in the six-membered ring containing unsaturation causes a change in conformation by which the substituents in both cases become pseudoequatorial. This assumption is in agreement with the relatively small differences in the thermodynamic stabilities of the two reduction products.

The results of our experiments regarding the stereochemistry of the reduction of the conjugated ketone (I) can be explained by assuming that

* The discussion of spectra refers to the diacetates IIb and IIIb, taken in $CDCl_3$; the spectra of the epimeric alcohols, due to their low solubility, were taken in deuterated pyridine and showed the same characteristics.

the presence of an α, β-double bond at the bridgehead position leads to the flattening of the lower portion of ring A and eliminates steric hindrance coused by the 5α-hydrogen, thus making the carbonyl group accessible from both sides of the molecule. Since the difference in the thermodynamic stabilities of the two epimers is quite small, a rather nonstereospecific reduction by metal hydride occurs. The slightly higher yield of the pseudoequatorial isomer (IIa) in experiments 3—6 can be explained by the greater stability of the solvated reducing species in pseudoequatorial position[10].

EXPERIMENTAL

Melting points were taken on a Kofler hot-stage apparatus. Infra-red spectra were recorded (in KBr pellets) on a Perkin-Elmer Model 337 spectrophotometer. UV spectra were recorded on an Perkin-Elmer Model 137UV. Ultraviolet-Visible spectro-photometer. Unless otherwise noted, NMR spectra were determined on a Varian A-60-A spectrometer in deuterochloroform solution, using TMS as the internal reference standard. The optical rotations were measured on 1% solutions in ethanol. Column chromatography was performed on Merck Silicagel 0.05—0.2 *mm*, thin-layer chromatography on Merck Kiesel-gel G.

Reduction of Δ⁴*-androstene-3,17-diene-11*β*-ol* (*I*).

(*A*). *Reduction with lithium aluminum hydride.* A solution of $LiAlH_4$ (0.5 *g*) in dry ether (50 *ml*) was added to a solution of I (1.0 *g*) in dry ether (250 *ml*) and the mixture stirred at reflux temperature for 4 hours. Excess hydride was decomposed with water and the organic layer separated, washed with water, dried and evaporation to dryness. Thin-layer chromatography (Et_2O/EtOAc 1 : 1) detected the presence of two products with R_f values 0.30 and 0.22 for IIa and IIIa, respectively. The solid residue was suspended in benzene, 10 *g* of silica-gel was added and the mixture evaporated to dryness. The residue was suspended in benzene and chromatographed on a 100 *g* silica-gel column. Elution with benzene-ether (7 : 3) afforded 0.45 *g* of pure Δ⁴-androstene-3β,11β, 17β-triol (IIa). A sample recrystalized from EtOAc had the following characteristics: m.p. 226—230°C; $(\alpha)_D^{23°} = + + 75° \pm 3°$; IR ν_{max} 3430 (broad, -OH), 1650 (weak, > C=C <) *cm*$^{-1}$; NMR (in deuterated pyridine) τ 4.44, 4.50, 5.22, 5.50, 6.15, 8.44, 8.59. NMR (in $CDCl_3$) 81 cps 3 H singlet (C-19) and 61 cps 3 H singlet (C-18).

Calculated for $C_{19}H_{30}O_3$	C 74.47	H 9.87
Found	H 74.19	H 9.74

Further elution with benzene ether (6 : 4 and 1 : 1) afforded 0.2 *g* of pure Δ⁴-androstene-3α,11β,17β-triol (IIIa). A sample recrystalized from EtOAc had the following characteristics: m.p. 178—182°; $(\alpha)_D^{23°} = +145° \pm \pm 5°$. IR ν_{max} 3380 (broad). 1680, 1600 (weak, > C=C <). NMR (in deu-

terated pyridine) τ 4.37 (doublet $J_{H_3H_4}$ 5 cps), 4.55, 5.20, 5.58, 6.20, 8.47, 8.62, NMR (in $CDCl_3$) 77 cps 3 H singlet (C-19) and 61 cps 3 H singlet (C-18).

Calculated for $C_{19}H_{30}O_3$	C 74.47	H 9.87
Found	C 74.71	H 10.01

The intermediate fractions representing a mixture of IIa and IIIa (350 *mg*) were rechromatographed affording an additional 165 *mg* of pure IIa and 135 *mg* of pure IIIa, increasing the overall yield of IIa to 0.615 *g* (65%) and the yield of IIIa to 0.335 *g* (35%); total recovery 950 *mg* (95%).

The acetates IIb and IIIb were prepared in the usual way (Ac_2O/pyridine) affording samples which recrystalized from MoOH showed the following characteristics:

IIb: m.p. 153—154°; $(\alpha)_D^{23°} = +30° \pm 3°$, lit. (11): m.p. 152—154° and $(\alpha)_D^{23°} = +26°$. IR ν_{max} 3470 (sharp), 1735, 1715, 1650 (weak) and 1250 (broad) *cm*$^{-1}$. NMR τ 4.80 (2 H broad singlet), 5.26—5.80 (2 H multiplet centered at 5.50), 7.98 (6 H singlet), 8.65 (3 H C-19 singlet) and 8.94 (3 H C-18 singlet).

Calculated for $C_{23}H_{34}O_5$	C 70.74	H 8.78
Found	C 70.64	H 8.74

IIIb: m.p. 161-163°C; $(\alpha)_D^{23°} + 210° \pm 5°$. IR ν_{max} 3530, 3470, 1715, 1705, 1650 and 1250 (broad) *cm*$^{-1}$. NMR τ 4.51—4.72 (1 H doublet centered at 4.60, $J_{H_3H_4}$ 5 cps), 4.80, 5.23—5.72 (2 H multiplet centered at 5.50), 7.98 (6 H singlet) 8.72 (3 H C-19 singlet) and 8.94 (3 H C-18 singlet).

Calculated for $C_{23}H_{34}O_5$	C 70.74	H 8.78
Found	C 70.70	H 8.80

The reduction of Δ^4-androstene-3,17-dione-11β-ol (I) in a mixture of THF and other or in pure THF at reflux temperature (4 hours) gave exactly the same results.

(*B*). *Reduction with sodium borohydride.*

(*a*) *IN METHANOL:* To a solution of I (1.0 *g*) in MeOh (100 *ml*) $NaBH_4$ (1.0 *g*) was added and the mixture stirred at 25°C for 48 hours. It was then diluted with water and extracted with ether: the organic layer was washed with water, dried and evaporated to dryness. The solid residue was applied to a silica-gel column in the same way as in (A). After chromatography, 0.710 *g* (75%) of IIa and 0.240 *g* (25%) of IIIa was obtained (total recovery 95%). When the reduction was carried out at reflux temperature (6 hours), practically the same results were obtained.

(b) IN ISOPROPANOL: To a solution of I (1.0 *g*) in isopropanol (120 *ml*) $NaBH_4$ (1.0 *g*) was added and the mixture stirred for 48 hours; same work up as in (a) yield 75% of IIa and 25% of IIIa (overall recovery 95%). The same amounts of reagent and solvent were used to investigate the reduction of 1.0 *g* of I at reflux temperature (6 hours); although the

ratio of epimeric alcohols obtained was essentially the same (75 and 25%), the overall recovery of alcoholic fraction was only cca 80%.

(*C*). *Reduction with diborane.* B_2H_6 was passed through a solution of 1.0 *g* of I in 100 *ml* of THF; the reaction was followed by TLC. After one hour, no appreciable amounts of starting material were present. The reaction was continued for 1 hour longer and quenched with ice. The mixture was extracted with ether and worked up in the usual manner. After chromatography, 0.410 *g* of IIfa and 0.195 *g* of IIIa were isolated. Some 210 *mg* of unidentified (olefinic) material was also isolated.

(*D*). *The Meerwein — Ponndorf reduction.* To a solution of I (1.0 *g*) in isopropanol (100 *ml*) a solution of $Al(iOPr)_3$ (1.5 *g*) in isopropanol (100 *ml*) was added, and the mixture stirred at reflux temperature for 6 hours. The solution was cooled diluted with water and extracted with ether; the ethereal layer washed till neutral, dried and evaporated to dryness. The solid residue was applied to a chromatography column as in (A), yielding 0.480 *g* (60%) of IIa epimer and 0.320 *g* (40%) of IIIa epimer (overall recovery 80% of alcoholic compounds). Another 150 *mg* of unidentified (olefinic) material was obtained.

The equilibration of IIa and IIIa.

To a solution of IIa (1.0 *g*) in isopropanol (120 *ml*) a solution of $Al(iOPr)_3$ (1.5 *g*) in isopropanol and 1 *ml* of absolute acetone were added, and the nixture stirred at reflux temperature for 100 hours. The same work up as in (D) yielded 0.510 *g* of IIa (60%) and 0.340 *g* (40%) of IIIa, with a total recovery of 85%. Nearly the same ratio of products (59% and 41%) was obtained when epimeric IIIa was used as starting material, the total recovery being 80% (a slight increase in olefinic material).

Preparation of $\Delta^{3,5}$*-androstadiene-11*β*,17*β*-diol (IVa).*

To a solution of IIa (100 *mg*) in acetone (6 *ml*) 2 N HCl (2 *ml*) was added and the mixture left at 40°C for 20 minutes. The solution was diluted with water, extracted with ether, washed till neutral and dried. The crude product crystalized from MeOH yielding the diene (IVa), m.p. 132°C; $(\alpha)_D^{23°} = -99° \pm 5°$. UV ν_{max} 227, 235 and 243 *mμ* (E = 15,500). IR ν_{max} 3420 (broad), 1650 *cm*$^{-1}$. This compound crystalized only with difficulty, the results of elemental microanalysis being unsatisfactory. However, perfect analytical data were obtained for the corresponding 17β-acetate (IVb), which was prepared in the usual manner (Ac_2O/pyridine): m.p. 124°—126°C; $(\alpha)_D^{23°} = -117° \pm 5°$. UV ν_{max} 227, 235 and 243 *mμ* (E = 16,000). IR ν_{max} 3540, 3460, 1735, 1655 and 1250 *cm*$^{-1}$. NMR τ 4.05, 4.30, 4.70, 5.22—5.72 (2 H multiplet centered at 5.47), 7.98 (6 H singlet), 8.79 (3 H C-19 singlet) and 8.94 (3 H C.18 singlet).

Calculated for $C_{21}H_{30}O_3$	C 76.32	H 9.15
Found	C 76.14	H 9.06

SUMMARY

The stereochemistry of the reduction of Δ^4-androstene-3,17-dione-11β-ol by various reducing agents was investigated. Contrary to earlier results, it was found that both epimeric Δ^4-androstene-3β,11β,17β-triol (IIa) and Δ^4-androstene-3α,11β,17β-triol (IIIa) were formed, the ratio depending upon the reducing agent applied. The thermodynamic stability of epimers (IIa) and (IIIa) was investigated.

Department of Chemistry,
School of Sciences,
Belgrade University;
Institute of Chemistry,
Technology and Metallurgy,
Belgrade

Received 8 October, 1969

REFERENCES

1. Fieser, L. and M. Fieser. *Steroids* — New York: Reinhold Publishing Company, 1959 Ch. 7.5 and references therein.
2. a) Nace, H. R. and G. L. O'Conor. "The Reduction of Cholestanone by Lithium Aluminium Hydride and Aluminium Alkoxides" — *The Journal of the American Chemical Society* (Washington) 73: 5824—5826, 1951.
   b) Dauben, W. G., R. A. Micheli and J. F. Eastham. "The Reduction of Steroidal, Enol Acetates with Lithium Aluminium Hydride and Sodium Borohydride" — *The Journal of the American Chemical Society* (Washington) 74: 3852—3855, 1952.
   c) Norymberski, J. K. and G. F. Woods. "Partial Reduction of Steroid Hormones and Related Substances" — *Journal of the Chemical Society* (London): 3426—3430, 1955.
   d) Zorbach, W. W. "The Reduction of Methyl-3-oxo-Δ^4-etiocholenate with Sodium Borohydride" — *The Journal of the American Chemical Society* (Washington) 75: 6344—6346, 1953.
   e) McKennis, H. and G. W. Gaffney. "Synthesis of Allocholesterol and Epiallocholesterol" — *The Journal of Biological Chemistry* (Baltimore) 175: 217—220, 1948.
   f) Pelc, B. "Reduktion des Methyltestosterons mittels komplexer Hydride und Aluminiumisopropylat" — *Collection of Czechoslovak Chemical Communications* (Praha) 25: 309—312, 1960.
   g) Shopee, C. W. and G. H. R. Summers. "Reduction of Cholest-5-en-3-one with Lithium Aluminium Hydride" — *Journal of the Chemical Society* (London): 687—689, 1950.
   h) Wheeler, O. H. and J. L. Mateos. "Rates of Borohydride Reduction of Some Ring A and B Steroid Ketones" — *Canadian Journal of Chemistry* (Ottawa) 36: 1049—1052, 1958. Wheeler, O. H. and J. L. Mateos. "Stereochemistry of Reduction of Ketones by Complex Metal Hydrides" — *Canadian Journal of Chemistry* (Ottawa) 36: 1431—1435, 1958.
3. a) Loewenthal, H. J. E. "Selective Reactions and Modification of Functional Groups in Steroid Chemistry" — *Tetrahedron* (Oxford) 6: 269—303, 1959.
   b) Gaylord, N. G. *Reduction with Complex Metal Hydrides* — New York: Interscience Publishers, 1956, Chapters 7.2.1. and 7.2.4.
   c) Eliel, E. L. *Stereochemistry of Carbon Compounds* — New York: McGraw-Hill Book Comp., Inc., 1962, Ch. 8.7.
   d) Eliel, E. L., N. L. Allinger, J. J. Angyal and G. A. Morrison. *Comformational Analysis* — New York: Interscience Publishers, 1956, Ch. 5.
4. Barton, D. R. "The Stereochemistry of Cyclohexane Derivatives" — *Journal of the Chemical Society* (London): 1027—1040, 1953.

5. a) Mihailović, M. Lj., M. Stefanović, Lj. Lorenc and M. Gašić. "5,10-Seco-Steroids a New Type of Steroid Derivatives Containing a Ten-Membered Ring" — *Tetrahedron Letters* (Oxford) 28: 1867—1870, 1964.

b) Mihailović, M. Lj., Lj. Lorenc, M. Gašić, M. Rogić, A. Melera and M. Stefanović. "Configuration and Reactivity of Ten-Membered 5,10-Seco-Compounds Obtained by Fragmentation of 5-Hydroxy-Steroids" — *Tetrahedron* (Oxford) 22: 2345—2358, 1966.

6. Stefanović, M. M., M. Hranisavljević-Jakovljević, I. Pejković-Tadić and M. Marić. "Microbiological Transformation of 5,10-Seco-Steroids. I." — *Glasnik hemijskog društva* (Beograd) 33*: 239—244, 1968.

7. Caspi, E., P. K. Grover, N. Grover, E. J. Lynde and Th. Nussbaumer. "The Dienol-Benzene Rearrangement in C_{19} Series" — *Journal of the Chemical Society* (London): 1710—1716, 1962.

8. Chang, E. and N. Kenny. "Preparation and Purification of 1,2-^{3}H-11 β-Hydroxy-Testosterone" — *Steroids* (San Francisco) 1: 325—330, 1963.

9. Schaltegger, H. and F. X. Müllner. "Über die epimeren 7-Brom-Cholesterylester und die Konfiguration der C-7-Substituented in der Colesterinreihe" — *Helvetica Chimica Acta* (Basel) 34: 1096—1110, 1951.

10. a) Bhacca, N. C. and D. H. Williams. *Application of NMR Spectroscopy in Organic Chemistry* — Holden-Day, Inc., 1964.

b) Karplus, M. "Contact Electron-Spin Coupling of Nuclear Magnetic Moments" — *The Journal of Chemical Physics* (New York) 30: 11—15, 1959.

11. Bird, C. W. and R. C. Cookson. "Control of Basic Strength by Steric Hindrance to Solvation of Ammonium Ions" — *Chemistry & Industry* (London): 1479—1480, 1955.

12. Searle, G. D. & Co. "Trioxygenated Androstane Derivatives, Brit. Pat. 1,004,029" — *Chemical Abstracts* 63: 16424b.

* Available in English translation from National Technical Information Service, Springfield, Virginia, 22151.

GLASNIK HEMIJSKOG DRUŠTVA, Vol. 34, No. 8-9-10, 1969, pp. 497—507

GHDB-85

66.095.252:66.092.57:547.92

Original Scientific Paper

INTRAMOLECULAR CYCLIZATION OF 16-FURFURYLIDENE-17 β-HYDROXY-STEROIDS BY CATALYTIC HYDROGENATION

by

MILUTIN STEFANOVIĆ, ALEKSANDAR JOKIĆ and DUŠAN MILJKOVIĆ

The formation of 1,6-dioxa-(4.4)-spiro-nonane (IV) by catalytic reduction of β-furylacrolein (I) was observed by Burdick and Adkins in 1934 (1,2). The spiro-compound (IV) was obtained in maximum yield of 33% using finely powdered nickel on kieselguhr as catalyst, at 160° and 100—200 atm of hydrogen pressure. However, using Adams' platinum catalyst the bicyclic spiro-compound (IV) was not isolated[3]. 3-(2'-furyl)-propanol-1 (II) was proved to be an intermediate in the reductive cyclization of β-furylacrolein[4, 5]. Starting from II and using Burdick and Adkins experimental conditions, IV was obtained in a yield of 38%. Further, 3[2'-(3',4'-dihydro)--furyl]-propanol^{-1} (III) was assumed to be also an intermediate, addition of a hydroxy group to the double bond of the vinyl-ether function being the next step:

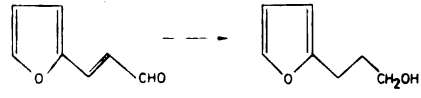

I II

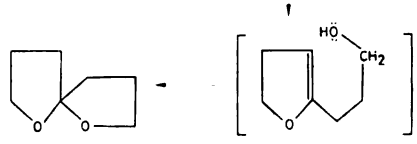

IV III

We attempted to study the reductive cyclization reaction in more detail, taking steroids as substrates, for the following reasons:

a) Steroidal sapogenins have biological activity, so we thought that synthetic steroidal spiro-ketals might be of interest in this respect too.

b) Steroidal spiro-ketals having the hydroxymethyl group next to the oxygen in ring F would represent interesting model substances for studying the "cholegenin-isocholegenin" rearrangement[6].

c) Different platinum and palladium catalysts have never been tested for their effectivness in reactions of reductive cyclization.

We carried out the following sequence of reactions:

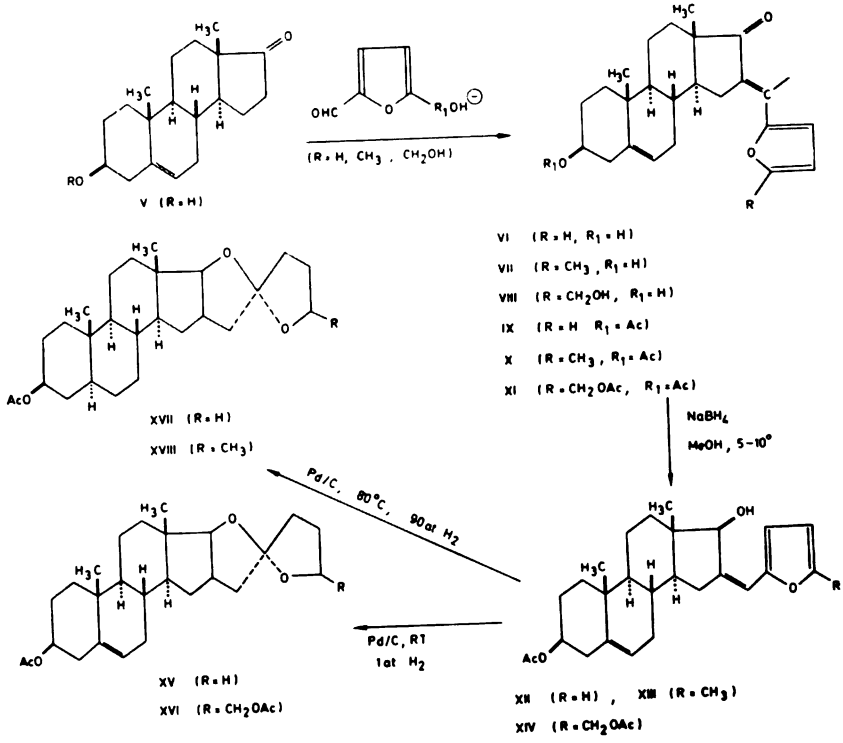

The compounds VI, VII and VIII were prepared by condensing 3 β--hydroxy-5-androsten-17-one (V) with furfural ,5-methylfurfural and 5-hydroxymethylfurfural, respectively, in the presence of alkali. The corresponding 16-furfurylidene derivatives were obtained in almost quantitative yield, with high stereospecificity (7). They are all *trans*, i.e. the vinyl hydrogen of the furfurylidene rest is closer to the carbonyl function than to the furan ring. This was deduced on the basis of NMR spectra; the signal at 7.2 ppm for this vinyl proton represents an appreciable downfield shift which could be explained by its proximity to the carbonyl group.

The compounds VI, VII and VIII were converted to the corresponding acetates (IX, X and XI) by means of acetic anhydride either upon heating, or at room temperature in the presence of pyridine.

Sodium borohydride reduction of IX, X and XI in methanol at 5—10° proceeded stereospecifically giving quantitativelly yields of the corresponding 17 β-hydroxy-compounds (XII, XIII and XIV).

Product XII was hydrogenated over Adams' platinum catalyst in ethyl acetate under normal conditions, whereupon 3 β-acetoxy-16 β (3)-17 β (2')--1',6'-dioxa-(4.4)-nonano-5-androstene (XV) was formed in a small yield[8]. Among eight different products formed during this catalytic hydrogenation (separated in two zones of four on TLC), two were isolated, namely 3 β-ace-

toxy-16 β-tetrahydrofurfuryl-17 β-hydroxy-5-androstene (XIX) in a 40 % yield, and its 16 α-tetrahydrofurfuryl isomer (XX) in a small yield:

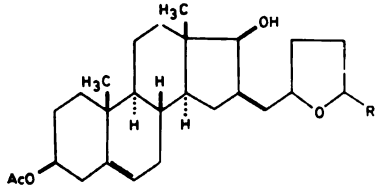

XIX (R = H)
XXIV (R = CH_2OAc)
XXVII (R = CH_3)

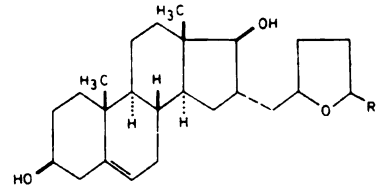

XX (R = H)

The catalytic hydrogenation of XII in ethyl alcohol under normal conditions using 10% palladium on charcoal gave the internal spiro-ketal (XV) in a yield of 20%. The other main product was 3 β-acetoxy-16 β-furfuryl-17 β-hydroxy-5-androstene (XXI), obtained in 75% yield:

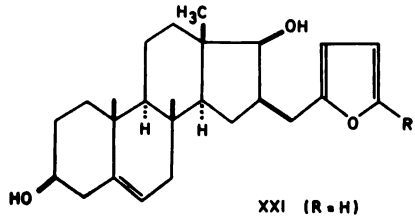

XXI (R = H)
XXII (R = CH_3)

This experiment proved palladium to be more a effective catalyst than platinum for the reductive cyclization reactions, leaving the C-5 double bond unchanged and thus permitting the formation of the 4-en-3-one system.

We found that the best condition for the reductive cyclization were: 5% palladium on charcoal as catalyst, 95% ethanol as solvent, temperature 80°, and a hydrogen pressure of 90 atm over a period of 7 hrs. However, under these conditions the C-5 double bond is also hydrogenated, so that XII gave 3 β-acetoxy-16 β-(3')-17 β (2')-1',6'-dioxa-(4.4)-nonano-5 α-andorstane (XVII) in a yield of 50%. The other product was 3 β-acetoxy-16 β-tetrahydrofurfuryl-17 β-hydroxy-5 α-andiostane (XXII) in a yield of 30%:

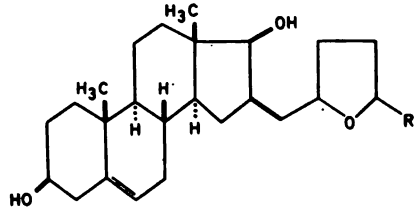

XXII (R = H)
XXV (R = CH_3)

The structure of 3 β-acetoxy-16 β (3')-17 β (2')-1',6'-dioxa-(4.4)-nonano-5-androstene (XV) was deduced from the IR and NMR spectra. The characteristic sharp maxima for XV at 1722, 1233, 1096, 1080, 1064, 1017, 990, 975, 920 and 903 cm^{-1} correspond well to the IR spectra of steroid sapogenins whose bicyclic side chain shows maxima in the 1350—870 cm^{-1} region[9]. In the NMR spectrum the signal at $\delta = 5.36$ (*d*) (J = 4.6) corresponds to the vinyl proton at C-6, proving that in this case the C-5 double bond remains unchanged during catalytic hydrogenation. Signals at $\delta = 4.05$ (*d*) (J = 9.8) and $\delta = 3.9$ (*m*) correspond to the ether protons of the spiro--ketal side chain. The doublet at 4.05 ppm is due to coupling with the proton at C-16 ($\delta = 2.9$ *m*). The interaction of the protons at C-16 and C-17 was proved by decoupling experiments (irradiation in the region of cca. 2.9 ppm converted the doublet at 4.05 ppm into a singlet). The position of the NMR signal for the proton at C-16 represents a downfield shift of more than 1 ppm. This could be explained by the proximity of the proton at C-16 to the oxygen atom in ring F, i.e. the orientation of this oxygen atom might be α (formulae XV, XVI, XII and XVIII illustrate this hypothesis).

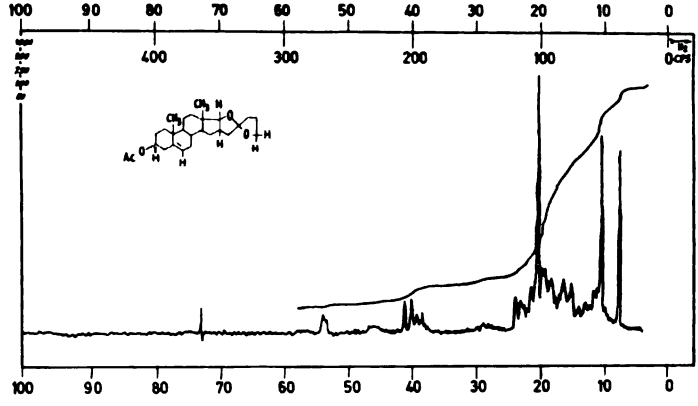

IR spectrum of 3 β-acetoxy-16 β (3')-17 β (2')-1',6'-dioxa-[4.4]-nonano-5-androstene (XV)

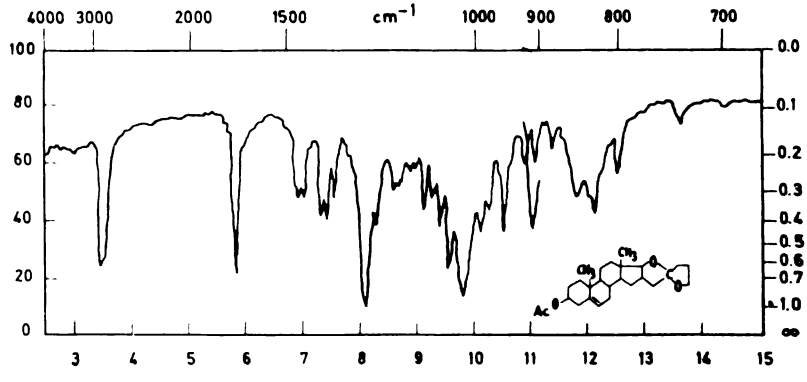

NMR spectrum of 3 β-acetoxy-16 β (3')-17 β (2')-1',6'-dioxa-[4.4]-nonano-5-androstene (XV)

Our attempts to prepare a spiro-ketal having the hydroxymethyl group next to the oxygen atom in ring F, in order to bring about the "cholegenin--isocholegenin" rearrangement, were not succesful. Starting from XIV and using ethanol as solvent, 5% palladium on charcoal as catalyst, under a hydrogen pressure of 90 atm at 80°C, 3 λ-acetoxy-16 β (3')-17 β (2')-1',6'-dioxa--(4.4)-(5'-(methyl)nonano-5 α-androstane (XVIII) was obtained in a yield of cca. 50%. When the hydrogenation was carried out under normal conditions the expected spiro-diacetate (XVI) was isolated only in traces. The structure of spiro-ketal XVIII was deduced on the basis of elemental analysis, IR and NMR spectra; in addition, XVIII was proved to be identical with the spiro-compound obtained from dehydroepiandrosterone and 5--methylfurfural according to the reaction scheme shown on page 2.

The formation of 5'-methyl- and 5'-acetoxymethyl-spiro-ketals was also accompanied by the following reduction products: 3 β-acetoxy-16 β--(5'-methyl) furfuryl-17 β-hydroxy-5-androstene (XXIII), 3 β-acetoxy-16 β-(5'-acetoxymethyl) tetrahydrofurfuryl-17 β-hydroxy-5-androstene (XXIV) and 3 β-acetoxy-16 β-(5'-methyl)-tetrahydrofurfuryl-17 β-hydroxy-5 α-androstene (XXV).

Direct catalytic hydrogenation of 3 β-acetoxy-16-furfuryl-idene-5-androsten-17-one (IX) was carried out in the presence of Adams' platinum catalyst or Raney nickel under normal conditions. The spiro-ketals XV or XVII were not obtained, thus showing that the presence of the 17 β-hydroxy group is essential for the reductive cyclization. The isolated products in these reductions were: 3 β-acetoxy-16 β-tetrahydrofurfuryl-5-androsten-17-one (XXVI), 3 β-acetoxy-16 β-tetrahydrofurfuryl-17 β-hydroxy-5-androstene (XIX) and 3 β-acetoxy-16 α-tetrahydrofurfuryl-17 β-hydroxy-5-androstene (XX).

From experimental results we can propose the following mechanism:

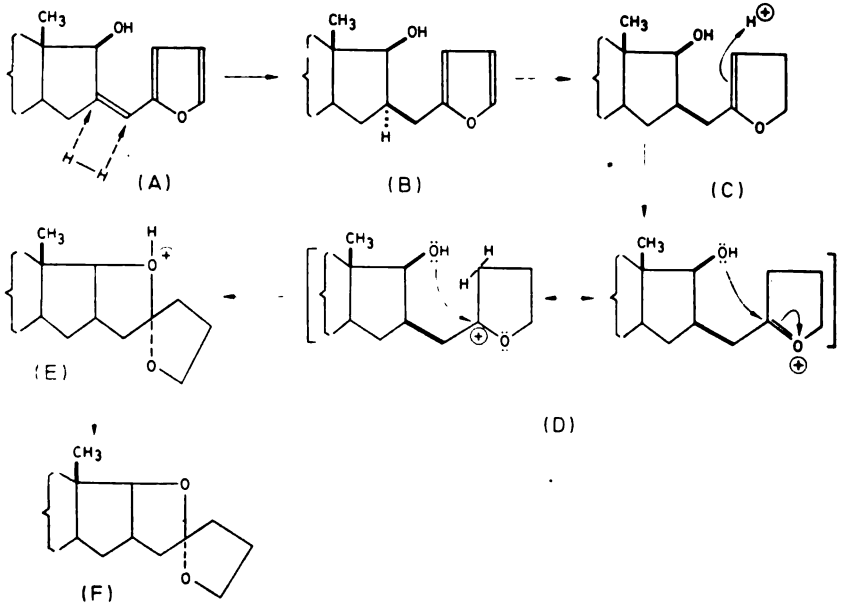

The first step involves the catalytic hydrogenation of the 16-(3',4')--exocyclic double bond of A, which proceeds stereospecifically, thus giving the 16 β-furfuryl derivative (B), the first intermediate we succeeded in isolating. Catalytic hydrogenation may proceed further, without isolating B, to the dihydro-furan intermediate C, which was not isolated. The stable carbonium ion D is formed on protonation of C, its rearrangement by nucleophilic attack of the 1'-OH group at position 5' being the next step. Spirane F is finally obtained by deprotonating E.

EXPERIMENTAL

Melting points (uncorrected) were taken on a Kofler hot-stage apparatus. Infrared spectra were recorded (in KBr pellets) on a Perkin-Elmer Model 337 spectrophotometer (UV spectra: Perkin-Elmer Model 137). NMR--spectra were taken on a Varian 60 A-60 Spectrometer in $CDCl_3$ using TMS as internal standard (chemical shifts are given in ppm and coupling constants in cps; symbols *d*, *t*, *q* and *m* indicate doublet, triplet, quartet and multiplet, respectively; the numbers in parentheses represent the number of protons of the corresponding peak. Thin-layer chromatography was performed on Silica-gel G (according to Stahl) with benzene-ethyl acetate (7: 3). Specific rotations were determined in $CHCl_3$ solution unless otherwise stated.

3β-hydroxy-16-furfurylidene-5-androstene-17-one (*VI*)

Five grams of 3β-hydroxy-5-androstene-17-one (V) was dissolved in 150 *ml* of methanol and then 30 *ml* of 30% NaOH and 5 *ml* of freshly distilled furfural were successively added. The reaction mixture was left at room temperature under nitrogen for two hours, during which time bright yellow crystals formed. After standing at 0° for an additional 6 hrs, the crystals were filtered with suction and washed with dilute methanol. The product obtained weighed 6.4 *g* after drying in vacuo at 60° overnight. M.p. 190° (from methanol) $(\alpha)_D^{20} = -107°$ (c = 0.57); UV spectrum: $\lambda_{max} = 327\,m\mu$ ($\varepsilon = 26000$); IR-spectrum: 3509, 1640, 1563, 1026, 1010, 892, 752 cm^{-1}.

Calculated for $C_{24}H_{30}O_3$	C 78.65	H 8.25
Found	C 78.27	H 8.34

3β-hydroxy-16-(5'-methyl)-furtfurylidene-5-androsten-17-one (*VII*)

M.p. 133—134° (from acetone), $(\alpha)_D^{20°} = -80°$ (c = 0.82).

Calculated for $C_{25}H_{32}O_3$	C 78.91	H 8.48
Found	C 78.33	H 8.88

3β-hydroxy-16-(5'-hydroxymethyl)-furfurylidene-5-androstene-17-one (*VIII*):

M.p. 250° (from acetone — methanol), $(\alpha)_D^{20} = -105°$ (c = 0.92).

Calculated for $C_{25}H_{32}O_4$	C 75.72	H 8.13
Found	C 75.32	H 8.25

(The compounds VII and VIII were prepared in a manner similar to that described for VI the reaction mixture was diluted with an equal volume of water before filtering crude VII and VIII).

3 β-acetoxy-16-furfurylidene-5-androsten-17-one (IX)

a) Six grams of 3β-hydroxy-16-furfurylidene-5-androstene-17-one (VI) was dissolved in 100 *ml* of dry pyridine, 20 *ml* of acetic anhydride was added and the reaction mixture was left at room temperature for 24 hours. Two liters of cold water were then added to the reaction mixture and the product was extracted with ether. The ether layer was successively washed with dil. aq. HCl, 5% aq. $NaHCO_3$ and water. The ether extract was dried over anh. Na_2SO_4 and after filtering off the drying agent, ether was removed in vacuo. 6.2 *g* (92%) of pure IX was obtained.

b) Eight grams of VI was heated with 200 *ml* of acetic anhydride on a water bath, over a period of 3 hours. The cold reaction mixture was then poured into two liters of ice-water, where a slightly yellow oil separated, which solidified on standing. The product was filtered with suction and dried in vacuo at 60° overnight. The yield of crystalized IX (from methanol) was almost quantitative.

M.p. 196°; $(\alpha)_D^{20} = -165°$ (c = 0.58); UV-spectrum: $\lambda_{max} = 325\ m\mu$ ($\varepsilon = 27600$); IR-spectrum: $\nu_{max} = 1724, 1626, 1550, 1250, 1026, 1010, 885, 746\ cm^{-1}$; NMR-spectrum: $\delta = 7.60$ (d) (J = 1.8) (1); cca. 7.2 (*m*) (1); 6.64 (d) (J = 6.3) (1); 6.52 (q) (J = 3.6 and 1.8) (1); 5.44 (d) (J = 4.0) (1); cca. 4.6 (m) (1); 2.02 (*s*) (3); 1.09 (*s*) (3); 0.96 (*s*) (3).

Calculated for $C_{26}H_{32}O_4$	C 76.44	H 7.90
Found	C 76.30	H 7.99

3β-acetoxy-16-(5'-methyl)-furfurylidene-5-androstene-17-one (X)

M.p. 182° (from methanol): $(\alpha)_D^{20} = -235°$ (c = 1.28)

Calculated for $C_{27}H_{34}O_4$	C 76.74	H 8.11
Found	C 76.65	H 8.25

3β-acetoxy-16-(5'-acetoxymethyl)-furfurylidene-5-androsten-17-one (XI)

M.p. 146° (from methanol)

Calculated for $C_{29}H_{34}O_6$	C 72.47	H 7.55
Found	C 72.17	H 7.24

(The compounds X and XI were prepared from VII and VIII using the acetylation procedure described for IX by route *b*).

3β-acetoxy-16-furfurylidene-17β-hydroxy-5-androstene (XII)

Five grams of 3β-acetoxy-16-furfurylidene-5-androsten-17-one (IX) was dissolved in 600 *ml* of methanol and 400 *ml* of isopropanol. Two grams of sodium borohydride was added in portions to this solution, during two hours. The reaction mixture was then poured into two liters of ice-water

and acidified with 2N acetic acid to pH 6. After standing overnight, the white crystals were filtered with suction and washed thoroughly with water. The yield of 3β-acetoxy-16-furfurylidene-17β-hydroxy-5-androstene (dried in vacuo at 60° overnight) was 5 *g* (99%).

M.p. 214—215° (from methanol); $(\alpha)_D^2 = -160°$ (c = 0.64); UV-spectrum: $\lambda_{max} = 271$ *mμ* (ε = 24700); IR-spectrum: $\nu_{max} = 3425$, 1724, 1626, 1550, 1258, 1026, 1010, 879, 742 *cm*$^{-1}$; NMR-spectrum: δ = 7.39 (d) (J = 1.75) (1); cca. 6.4 (*m*) (2); 6.2 (*d*) (J = 3.0) (1); 5.40 (*d*) (J = 4.0) (1); cca. 4.6 (*m*) (1); 4.0 (*s*) (1); 2.02 (*s*) (3); 1.06 (*s*) (3); 0.70 (*s*) (3).

Calculated for $C_{26}H_{34}O_4$	C 76.06	H 8.34
Found	C 75.50	H 8.30

3β-acetoxy-16-(5'-methyl)-furfurylidene-17β-hydroxy-5-androstene (XIII)

M. p. 174° (from acetone); $(\alpha)_D^{20} = -133°$ (c = 1.46)

Calculated for $C_{27}H_{36}O_4$	C 76.38	H 8.55
Found	C 76.05	H 8.60

(Compound XIII was prepared by dissolving 4 *g* of X in 200 *ml* of methanol and then proceeding in the same way as described for XII. The yield of recrystalized material (from acetone) was 4 *g* (99%).

3β-acetoxy-16-(5'-acetoxymethyl)-furfurylidene-17β-hydroxy-5-androstene(XIV)

M. p. 95° (from acetone)

Calculated for $C_{29}H_{38}O_6$	C 72.17	H 7.94
Found	C 72.00	H 8.38

(Compound XIV — prepared in an analogous way to XIII — had to be purified by chromatography on alumina using benzene-ethyl acetate (9 : 1). XIV was obtained in 80% yield, the by-product being 3β-acetoxy--16-(5'-hydroxymethyl)-furfurylidene-17β-hydroxy-5-androstene (m.p. 161°), formed during reduction with sodium borohydride).

Catalytic hydrogenation of 3β-acetoxy-16-furfurylidene-17β-hydroxy-5-androstene (XII)

(a) With *Adams' platinum catalyst*

Five grams of 3β-acetoxy-16-furfurylidene-17β-hydroxy-5-androstene (XII) was dissolved, with slight warming, in 400 *ml* of ethyl acetate, Adams' platinum catalyst (0.5 *g*) was added and hydrogenation was carried out under normal conditions during 4—6 hours. After filtering the catalyst and removing the solvent in vacuo, 30 *ml* of methyl alcohol was added whereupon white crystals of *3β-acetoxy-16β-tetrahydrofurfuryl-17β-hydroxy-5-androstene* (XIX) separated out, in a yield of 30%.

XIX: m.p. 210—212° (from methanol); $(\alpha)_D^{20} = -61°$ (c = 1.00); IR-spectrum: $\nu_{max} = 3356$, 1720, 1235, 1070 *cm*$^{-1}$;

NMR-spectrum: $\delta = 5.40$ (*d*) (J = 4.0) (1); cca. 4.6 (*m*) (1); cca. 3.8 (*m*) (4); 3.3 (*s*) (1); 2.02 (*s*) (3); 1.04 (*s*); 0.78 (*s*) (3).

Calculated for $C_{26}H_{40}O_4$	C 74.96	H 9.68
Found	C 74.80	H 9.61

The mother liquor from XIX, after removing methanol, was dissolved in benzene and chromatographed on silica-gel using benzene-ethylacetate (4 : 1) as eluent. *3β-acetoxy-16β-(3')-17β(2')-1',6'-dioxa-4.4-nonano-5-androstene* (XV) was isolated in a very small yield (cca. 100 *mg*, i.e. 2.5%)

XV: m.p. 170—172° (from methanol); $(\alpha)_D^{20} = 0°$ (c = 1.00);

IR-spectrum: $\nu_{max} = 1722, 1233, 1096, 1080, 1064, 1046, 1017, 990, 975, 920, 903\ cm^{-1}$; NMR-spectrum: $\delta = 5.36$ (*d*) (J = 4.6) (1); cca. 4.6 (*m*, broad) (1); 4.05 (*d*) (J = 9.8) (1); cca. 3.9 (*m*) (2); 2.9 (*m*) (1); 2.02 (*s*) (3); 1.04 (*s*) (3); 0.74 (*s*) (3);

Calculated for $C_{26}H_{38}O_4$	C 75.32	H 9.24
Found	C 75.13	H 9.14

On further chromatography we isolated 3β-acetoxy-16-α-tetrahydrofurfuryl-17 β-hydroxy-5-androstene (XX) in a small yield.

XX: m.p. 145°; $(\alpha)_D^{20} = -53.7°$ (c = 1.0)

Calculated for $C_{26}H_{40}O_4$	C 74.96	H 9.68
Found	C 74.64	H 9.79

The rest of XIX was also isolated in a yield of 10%, the overall yield of XIX being thus 40%. The other reduction products were not isolated in a pure form.

(b) *With 10% palladium on charcoal*

13 grams of 3β-acetoxy-16-furfurylidene-17β-hydroxy-5-androstene XII) was dissolved in 600 *ml* of 95% ethanol, 5 gram of 10% Pd/C was added and hydrogenation was carried out under normal conditions for 6 hours. After removing the catalyst and solvent methanol was added whereupon 6.5 grams of *3β-acetoxy-16β-furfuryl-17β-hydroxy-5-androstene* (*XXI*) crystalized out. XXI had the following characteristics: m.p. 165—166°; $(\alpha)_D^{20} = -35°$ (c = 0.89)

Calculated for $C_{26}H_{36}O_4$	C 75.69	H 8.80
Found	C 75.44	H 8.79

The mother liquor from XXI was chromatographed on silica-gel affording a further 2 grams of XXI (overall yield of XXI 75%). 2.6 *g* of the internal spiro-ketal — XV — was also obtained (20% yield).

(c) *With 5% palladium on charcoal under pressure*

5 grams of XII was dissolved in 400 *ml* of 95% othanol, 3 grams of 5% Pd/C was added and the hydrogenation was carried out under a hydro-

gen pressure of 90 atm at 80°C for 7 hours. After removing the catalyst and solvent, methanol was added and a colorless crystalline product of m.p. 180—182° was obtained in 45% yield. This substance was identified as *3 β-acetoxy-16 β (3')-17β(2')-1',6'-dioxa-(4.4)-nonano-5α-androstene* (*XVII*); $(\alpha)_D^{20} = +66°$ (c = 1.5).

Calculated for $C_{26}H_{40}O_4$	C 74.96	H 9.68
Found	C 75.37	H 9.67

The mother liquor from XVII was chromatographed on alumina whereby *3β-acetoxy-16β-tetraxydrofurfuryl-17β-hydroxy-5α-androstene* (*XXII*) was obtained in 30% yield (m.p. 138—140°)

Calculated for $C_{24}H_{42}O_4$	C 74.60	H 10.11
Found	C 74.83	H 10.06

Catalytic hydrogenation of 3 β-acetoxy-16-(5'-acetoxymethyl)-furfurylidene-17 β-hydroxy-5-androstene (*XIV*)

(a) *With Adams' platinum catalyst*

3.5 *g* of XIV was dissolved in 150 *ml* of ethyl acetate, 0.4 *g* of Adams' catalyst was added and hydrogenation was carried out under normal conditions during 2 hours. Among eight different products only two were isolated and characterised (chromatography on alumina using as cluent different ratios of cyclohexane, benzene and ethyl acetate):

3 β-*acetoxy-16* β-(*5'-methyl*)-*furfuryl-17* β-*hydroxy-5-androstene* (*XXIII*): m. p. 160—162°; $(\alpha)_D^{20} = -27.6°$ (c = 0.75)

Calculated for $C_{27}H_{38}O_4$	C 76.02	H 8.98
Found	C 75.64	H 8.90

3 β-*acetoxy-16* β-(*5'-acetoxymethyl*)-*tetrahydrofurfuryl-17* β-*hydroxy-5-androstene* (*XXIV*): m.p. 200—202°;

Calculated for $C_{29}H_{44}O_6$	C 71.28	H 9.08
Found	C 71.40	H 9.10

(b) *With 10% palladium on charcoal*

5 *g* of XIV was dissolved in 150 *ml* of 95% ethanol, 2.5 *g* of 10% palladium on charcoal was added and hydrogenation was carried out under normal conditions over a period of 6 hours (400 *ml* of hydrogen was absorbed). After removing the catalyst and solvent, 3 β-acetoxy-16 β-(5'-methyl)-furfuryl-17 β-hydroxy-5-androstene (XXIII) crystalized from methanol (1 *g*). The rest was chromatographed on silica-gel using cyclohexane-ethyl acetate (9 : 1) as eluent. Another 3 *g* of XXIII was isolated, the total yield of XXIII being thus 71%. Only a trace of the internal spiro-ketal, namely *3* β-*acetoxy-7'-acetoxymethyl-16* β (*3'*)-*17* β (*2'*)-*1',6'-dioxa-(4.4)-nonano-5-androstene* (*XVI*) was obtained; m.p. 208°;

Calculated for $C_{29}H_{42}O_6$	C 71.57	H 8.70
Found	C 70.57	H 8.85

(c) *With 5% palladium on charcoal under pressure*

2.5 *g* of XIV in 200 *ml* of 95% ethanol with 2.5 *g* of 5% Pd/C, was hydrogenated under a hydrogen pressure of 70—80 atm at 80°C during 8 hours. Usual work-up and crystalization from methanol gave a 50% yield of *3 β-acetoxy-7'-methyl-16β (3')-17 β (2')-1',6'-dioxa-(4.4)-nonano-5 α-androstene (XVIII)*.

XVIII: m.p. 133°;

Calculated for $C_{27}H_{42}O_4$	C 75.31	H 9.83
Found	C 75.59	H 9.95

Chromatography of the mother liquor gave 30% yield of *3 β-acetoxy-16 β-(5'-methyl)-tetrahydrofurfuryl-17 β-hydroxy-5 α-androstene (XXV)*, m.p. 125°.

Calculated for $C_{27}H_{44}O_4$	C 69.72	H 10.60
Found	C 69.61	H 10.57

(Catalytic hydrogenation of 3 β-acetoxy-16-(5'-methyl)-furfurylidene-17 β--hydroxy-5-androstene (XIII) under pressure (the same conditions as described for XIV) gave XVIII and XXV in 50% and 30% yield, respectively.)

Catalytic hydrogenation of 3 β-acetoxy-16-furfurylidene-5-androsten-17-one (IX) in the presence of Raney nickel

2 *g* of IX was dissolved in 100 *ml* of ethyl acetate, 4 *g* of Raney nickel (W_2, Fluka) was added and hydrogenation was carried out under normal conditions for 2 hours. Chromatography on silica-gel gave 3 β-acetoxy-16 β-tetrahydrofurfuryl-5-androsten-17-one (XXVI) in 60% yield.

XXVI: m.p. 176°; $(\alpha)_D^{20} = +25°$ (c = 0.60)

Calculated for $C_{26}H_{38}O_4$	C 74.96	H 9.68
Found	C 74.40	H 9.80

XIX (in 20% yield) and XX (in 5% yield) were isolated too.

ACKNOWLEDGEMENT

The authors are grateful to the Yugoslav Federal Research Fund for financial support.

SUMMARY

Steroidal spiro-ketals "having" similar structure to natural sapogenins were obtained by catalytic hydrogenation of 16-furfurylidene-17 β-hydroxy derivatives of 3 β-acetoxy-5-androstene, in yields up to 50%.

Department of Chemistry
School of Sciences
Belgrade University
and
Institute of Chemistry
Technology and Metallurgy
Belgrade

Received 10 November, 1969

REFERENCES

1. Burdick, H. E. and H. Adkins. — *J. Am. Chem . Soc.* 56: 438, 1934.
2. Farlow, M., H. E. Burdick, and H. Adkins. — *J. Am. Chem. Soc.* 56: 2498, 1934.
3. Bray, R. H. and R. Adams. — *J. Am. Chem. Soc.* 49: 2101, 1927.
4. Alexander, K., L. S. Hafner, G. H. Smith, and L. E. Schniepp. — *J. Am. Chem. Soc.* 72: 5506, 1950.
5. Alexander, K., L. S. Hafner, and L. E. Schniepp. — *J. Am. Chem. Soc.* 73: 2725, 1951.
6. Fieser, L. and M. Fieser. *Steroids* — New York: Reinhold Publishing Company, 1959, Ch. 21 and references therein.
7. Hause, H. O. *Modern Synthetic Reactions* — New York: W. A. Benjamin, 1965, pp. 220—221 and references therein.
8. Stefanović, M., D. Miljković, M. Miljković, A. Jokić and B. Stipanović. — *Tetrahedron Letters:* 3891, 1966.
9. Jones, R. N., E. Katzenelenbogen and K. Dobriner. — *J. Am. Chem. Soc.* 75: 158, 1953.

GLASNIK HEMIJSKOG DRUŠTVA, Vol. 34, No. 8-9-10, 1969, pp. 509—517

GHDB-86

577.158:591.412

Original Scientific Paper

PURIFICATION OF MALIC DEHYDROGENASE FROM PIG HEART AND REACTIVITY OF ITS SULPHOHYDRIDE GROUPS

by

VLADIMIR LESKOVAC

Malic dehydrogenase (L-malate: NAD oxidoreductase, EC 1.1.1.37) occurs in animal organisms in two different forms, one being of predominantly cytoplasmic and the other of mitochondric origin[1]. The elaboration of a method for preparing pure cytoplasmic malic dehydrogenase was found to be indispensable for a study on the structure and mechanism of MDH*[2] because this enzyme cannot be obtained commercially in the pure form. On the other hand, the pure mitochondric form may be obtained commercially (made by Boehringer & Soehne, Mannheim).

In present paper studies on the number and reactivity of MDH SH--groups are described. The role of SH-groups in the catalytic process of MDH was first shown by Pfleiderer and Hohnholz[3] in 1959. During the last four years specific labelling of the cysein residue, this being essential for enzymatic catalysis, has been achieved in a number of NADH-dependent dehydrogenases e.g. lactic dehydrogenase[4, 5], alcohol-dehydrogenase[6] and glyceraldehyde-3-phosphate-dehydrogenase[7] from various species. These papers pointed out the significant role of free SH-groups in the enzymatic catalysis of NADH-dependent dehydrogenases.

1. PREPARATION OF CYTOPLASMIC MDH FROM PIG HEART

Preparation of crude extract. The preparation was done according to the following three methods.

a) A method based on that of Delbrück *et al.*[8] for the extraction of animal tissues and on its application to the extraction of cytoplasmic MDH from bovine heart according to England and Breiger[9]. According to this method, the primary material (pig heart) is macerated and then homogenized in a Starmix homogenizer with four times the amount of ice-cold isotonic sucrose solution (0.25 M) buffered with pH 7.5 0.01 M triethanolamine.

* Abbreviations: m-MDH — mitochondric malic dehydrogenase; c-MDH — cytoplasmic malic dehydrogenase; PCIMB — p-chloro-mercuric-benzoate; DTNB — 5,5'--dithiobis-/2-nitro-benzoic acid/; EDTA — ethylenediamine-tetraacetic acid; K_2 — reaction rate constant of the second order.

Under relatively mild mechanical and osmotic treatment in the isotonic buffer solution the mitochondric form of the enzyme remains to a large extent intact and bound to the undestroyed structure of the mitochondria, while the sucrose extract is only to a small extent contaminated by the mitochondric form. Only the cytoplasmic form of the enzyme from the tissue is dissolved in the sucrose buffer.

b) The second method consists in homogenizing the macerated tissue in four times the amount of ice-cold distilled water. Both forms of the enzyme dissolve (the mitochondric form via plasmolysis of mitochondria) and can be simultaneously isolated from the aqueous solution.

Approximately the same yields are obtained by the two above methods.

c) The third method is based on our observation that in isolating lactic dehydrogenase from pig heart[10], after the adsorption of LDH activity on calcium phosphate gel and centrifuging the gel, there was still a considerable MDH activity in the supernatant. The aqueous extract contained both forms of the enzyme (mitochondric and cytoplasmic) in the ratio 2 : 1. During the treatment of it with calcium phosphate gel some of the MDH activity dissapeared. In this method the yield of cytoplasmic MDH is 40—50% lower than in the first two. However, from the practical side, it has priority because starting with the same primary material three enzymes — LDH, cytoplasmic and mitochondric MDH — can be obtained simultaneously.

Purification of the Enzyme from Crude Extract

Processing of the enzyme was done in a cooling chamber at 2—3°C, the pH of each enzyme solution being maintained at 7.5 by the addition of 2% ammonium hydroxide.

Stage I. Fresh pig hearts were cleaned of fat and blood vessels, chopped and passed through a mincing machine. A quantity of 3 *kg* minced meat was then homogenized in portions in a Starmix homogenizer with the triple amount (9 *lit*) of ice-cold distilled water (2 *min/portion*). The tissue suspension was stirred mechanically and then centrifuged for 30 minutes at 3000 rpm. The supernatant was freed from fat by filtering through glass wool. Electrophoresis on starch gel showed that the supernatant contained both forms of the enzyme (cytoplasmic and mitochondric). Further extraction with water was found to be unnecessary because it resulted in only a 10% increase of MDH activity.

To the enzyme solution 30 to 35 *g* of calcium phosphate gel (3 *g* dry gel per liter of solution) was added with slow stirring. The calcium phosphate suspension was stirred mechanically for 30 minutes and then centrifuged at 3000 rpm. The major part of the LDH activity was adsorbed on the gel. This could be used for preparation of the pure LDH. The MDH activity appeared in the supernatant. The specific activity of the crude extract was 15 to 20 i.u./*mg* protein.

Stage II. The supernatant from the previous stage was brought to 40% saturation by adding solid ammonium sulphate and then stirring for 30 minutes. The suspension was left to stand for 6 hours and then centrifuged at 3000 rpm. The supernatant was then saturated to 90% with ammonium

sulphate, stirred for 30 minutes and left overnight. After this the suspension was centrifuged again at 3000 rpm.

Stage III. The residue from the previous stage was dissolved in 1 liter 0.1 M sodium phosphate buffer pH 7.5 and gradually brought to 40% saturation with ammonium sulphate. After a 3 hours standing the suspension was centrifuged at 16000 rpm. The supernatant was saturated to 90% by adding ammonium sulphate and after standing for 6 hours the suspension was centrifuged for 30 minutes at 16000 rpm. The supernatant was dissolved in the smallest possible volume of 0.1 M sodium phosphate buffer pH 7.5. The specific activity was 36 to 46 i.u./*mg* protein.

Stage IV. The enzyme solution from the previous stage was left to dialyse overnight in two 10-liter portions of 0.01 M sodium phosphate buffer pH 7.5. The dialysate (400 *ml*) was cleared for 30 minutes in the centrifuge at 35000 rpm. One half of the dialysate (200 *ml*) was then run on a Sephadex G-100 column (60 × 7 *cm*) which had been equilibrated with the same buffer solution. During this stage incomplete separation of protein fractions was observed if the loading of the column exceeded 5 *g* protein per liter of the Sephadex packing. The column was then washed with the same buffer. Two distinct protein fractions appeared in the eluate. MDH activity was found only in the first elution peak, while the second had a dark red color and contained blood proteins and other protein fractions of similar molecular weight. The fractions with the highest MDH activity were brought together and saturated to 90% with ammonium sulphate. After standing overnight, the suspension was centrifuged for 30 minutes at 35000 rpm. The residue was dissolved in the smallest possible volume of the buffer solution. The specific activity was 59 to 64 i.u./*mg* protein.

Stage V. The enzyme solution from the previous stage was dialysed overnight in three 10-liter portions of 0.01.M sodium phosphate buffer pH 7.5. The dialysate was cleared by 30 minutes centrifuging at 35000 rpm. It was then run on a 30 × 5 *cm* DEAE-Sephadex-A-50 column (3.5 meq/*g*) which had been treated according to the technique described by Stephenson and Zamečnik[11], and equilibrated with 0.01 M sodium phosphate (pH = = 7.5) as the starting buffer. The column was washed with 1 liter starting buffer. Small fractions of the eluate were collected by means of a fraction collector. The cytoplasmic form of the enzyme was adsorbed in the upper part of the column, while the mitochondric form, carried by the starting buffer, passed freely through (Fig. 1). After this the column was connected to a stirring vessel containing 1 liter starting buffer solution. The stirring vessel was then connected with another one having the same shape and volume but filled with 1 liter of 0.3 M sodium phosphate buffer pH 7.5. A fast-rotating magnetic stick assured the thorough stirring of the buffers. In this way a linear salt gradient was achieved on the inlet end of the column. Small fractions of the eluate were collected with a fraction collector. The fractions with increased MDH activity appeared at buffer concentration 0.15 M. These fractions were then brought together and saturated to 85%. Electrophoresis on starch gel showed that only the mitochondric form on the column contained the unadsorbed MDH activity, while the MDH activity eluted by the salt gradient contained only the cytoplasmic form of the enzyme. The specific activity after separation of the column was 360—460 i.u. /*mg* protein

for cytoplasmic and 270—360 i.u./*mg* protein for mitochondric MDH. The fractions of mitochondric MDH were usable for further preparation of the pure substances.

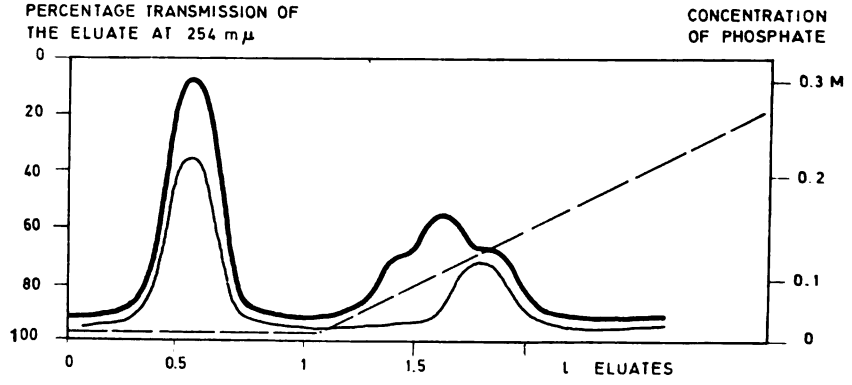

Fig. 1

Separation of cytoplasmic from mitochondric MDH on a DEAE-Sephadex-A-50 chromatographic column. ▬▬▬ Percentage transmission of the eluate at 254 mμ, ———— Relative enzymatic activity, — — — — — — Concentration of phosphate in sodium phosphate buffer pH 7.5.

Stage VI. Cytoplasmic MDH from the previous stage was repurified on a 40 × 3 *cm* DEAE-Sephadex-A-50 column in the same way. The specific activity after the second purification was 450—550 i.u./*mg* protein.

Stage VII. The eluate from previous stage was slowly brought to 70% saturation by the addition of ammonium sulphate and left overnight. The suspension was then centrifuged for 30 minutes at 35000 rpm. The supernatant was saturated to 85% with ammonium sulphate and again left overnight. After this the suspension was centrifuged and recrystallisation of the enzyme repeated. The pure cytoplasmic MDH had a specific activity of 550—640 i.u./*mg* protein, a pale red color and precipitated at 80—85% saturation with ammonium sulphate. In starch gel electrophoresis the enzyme was distinctly resolved.

2. STARCH GEL ELECTROPHORESIS OF THE ENZYME

The migration of MDH on starch gel was examined with the following chemicals: commercial starch gel made by Boehringer, mitochondric MDH from pig heart having a specific activity 460—730 i.u./*mg* and cytoplasmic MDH prepared from pig heart according to the above described technique having specific activity 550—640 i.u./*mg* protein. In electrophoresis both enzymes (cytoplasmic and mitochondric MDH) showed a characteristic microheterogeneity (Fig. 2).

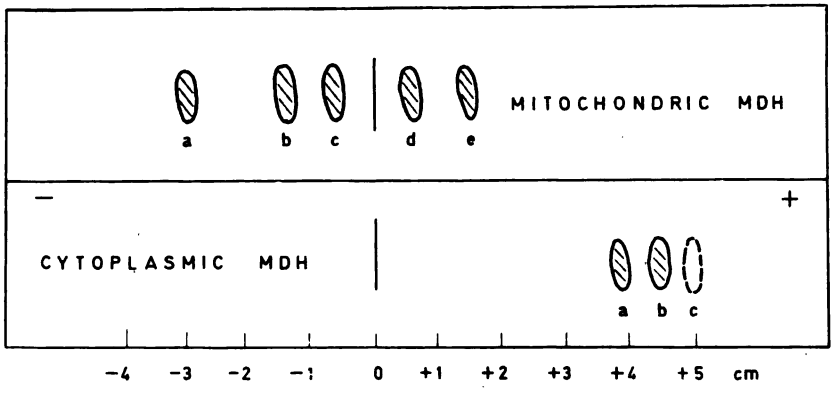

Fig. 2

Electrophoresis of cytoplasmic and mitochondric MDH in 0.15 M sodium borate pH 8.5 buffer at 30 V/cm. Duration of electrophoresis: m-MDH — 7 hours, c-MDH — 4 hours. The enzyme-active and protein bands overlap. Color of microcomponents described in the text.

TABLE I

Preparation of Cytoplasmic MDH from 3 kg of Pig Heart

Stage	Total activity i.u.(x10³)	Protein *mg*	Specific activity i.u./*mg*	Yield %
I. Precipitation after adsorption on calcium phosphate gel	1090	60.00	18.2	100.0
II., III. Fractionation with ammonium sulphate	765	18.700	41	70.0
IV. Filtration on Sephadex G-100	635	10.00	53.5	58.2
V. First chromatographic separation on DEAE-Sephadex (mitochondric MDH)	123 (240)	300 (760)	410 (315)	11.3*) (22.1)
VI. Second chromatographic separation on DEAE-Sephadex	90	180	50	8.3*)
VII. Recrystallization with ammonium sulphate	71	120	590	6.5*)

*) Cytoplasmic MDH only.

At pH 7 the microcomponents of the two enzymes were completely resolved. At pH 8.5 of the 0.15 M sodium borate buffer the mitochondric MDH was resolved into five enzymatically active components of approximately the same intensity. At the same pH the cytoplasmic MDH was resolved into three components, one of lower intensity than the other two (Fig. 2,c). Attempts to resolve the microcomponents of cytoplasmic MDH on an anion exchanger were in vain. The pure cytoplasmic MDH was chromatographed on a DEAE-Sephadex column with a long linearly rising salt gradient, as described under the preparation of the enzyme. Although only the symmetric peak of the MDH activity appeared in the eluate, the fractions at the leading edge of the peak were appreciably richer in *b* component (Fig. 2), those at the trailing edge in *a* component of the enzyme, relative to the whole peak.

3. REACTIVITY OF SH-GROUPS OF MITOCHONDRIC MDH

In order to find out the total number of SH-goups in mitochondric MDH, the method for determination of free SH-groups according to Boyer[12] and Ellman[13] was used. The enzyme was first incubated for 60 minutes in 7.5 M urea and 0.1 M sodium phospahte buffer pH 7.8. The specific activity dropped to below 2% of its initial value. The inactive enzyme was then transferred to a solution of 7.5 M urea with PCIMB or DTNB solution. By the addition of PCIMB the extinction at 255 mμ reached a maximum in the first minute and remained constant for half an hour. By Boyers' method a total of 14 moles of free SH-groups is titrated per mole of enzyme (molecular weight 67000). After the addition of DTNB the extinction at 405 mμ also reached its peak and, stabilized with 0.01 M EDTA, remained constant for a few hours. In Ellman's method a total of 13 moles of free SH-groups is titrated per mole of the enzyme. In 4 M urea the reaction of the enzyme with DTNB was slower. The rise in the extinction at 405 mμ showed that all SH-groups of the enzyme reacted according to a pseudo-first order kinetics with a K_2 1.170 M^{-1} min^{-1}. The difference in reactivity of individual SH-groups could not be determined in 4 M urea.

The difference in reactivity of SH-groups and their participation in catalysis became clear when DTNB reacted with the enzyme in its native state. Figure 3 shows the reaction of DTNB with the native enzyme.

As there was a large excess of the inhibitor (DTNB) the analysis could be done according to Guggenheim's method[14]. From the Guggenheim analysis (the upper curve in Fig. 3) two sorts of SH-group may be distinguished according to their reactivity. The first two groups per enzyme molecule react faster, with a constant K_2 of 5.0 M^{-1} min^{-1}, and next four slower with a K_2 of 1.3 M^{-1} min^{-1}. An exact determination of K_2 was only possible for the first six SH-groups. Turbidity due to denaturing of the enzyme appeared after 4 to 5 SH-groups per enzyme molecule had reacted. By Kohland's kinetic analysis[15] the SH-groups reacting with DTNB were resolved into one fast and one slow reaction (the lower curve in Fig. 3). These reactions were plotted on a graph in terms of their half-periods, these being calculated from K_2. The parallel curves of the retarded enzymic activity as the four "slow" SH-groups react indicates the vital role they play in the enzymatic catalysis.

The two "fast" groups were not essential for the catalysis. The number of four essential SH-groups per enzyme molecule was derived from the graph in Fig. 3. At a retardation of 50% approximately two essential SH-groups reacted with DTNB. The parallel course of the two reactions enabled an extrapolation of the DTNB reaction to four essential SH-groups, i.e. complete retardation of the enzymatic activity.

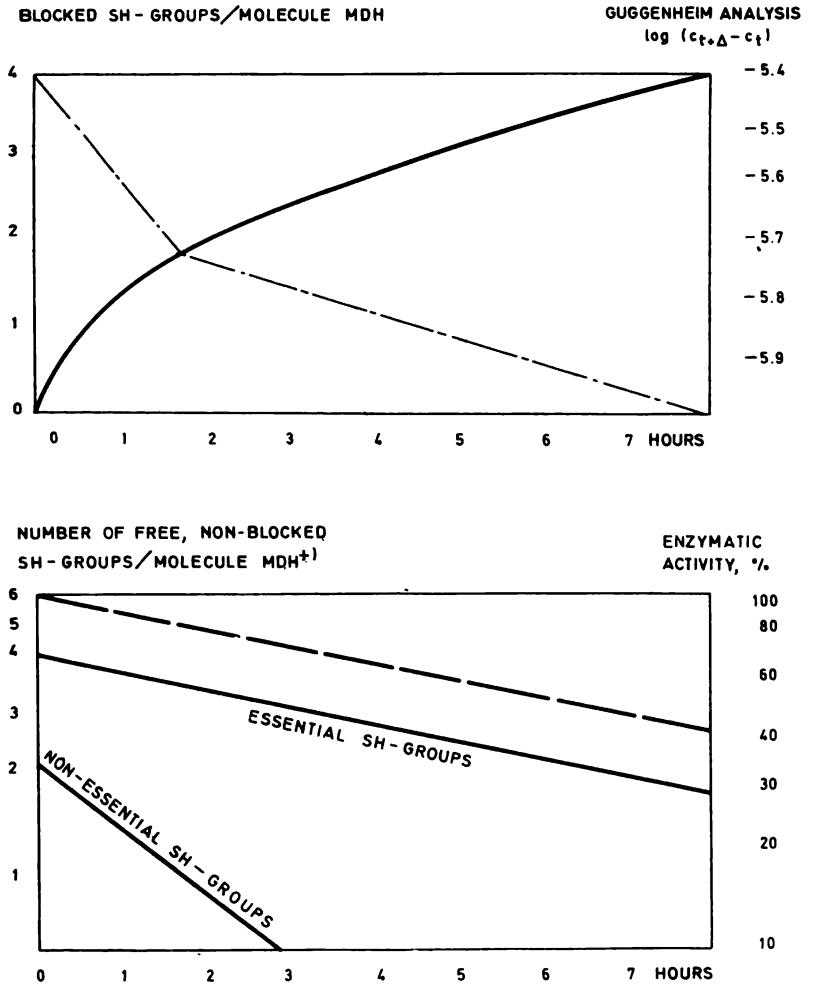

Fig. 3

Reaction of native m-MDH (4.35 μM) with DTNB (1.3 mM) in 0.55 *ml* 0.1 *M* sodiumphosphate pH 7.8 Buffer. ———— Reaction of SH-groups with DTNB, measured at 405 *mμ*. Above: —.—.—.—.— Guggenheim analysis of DTNB reaction. Below: Koshland analysis of the total reaction between SH-groups and DTNB; — — — — — Enzymatic activity.

As already described in a previous work[16], cytoplasmic MDH from pig heart with a total of 6—7 SH-groups per molecule (molecular weight 67000) also has two non-essential and a maximum of approximately four essential SH-groups. Although having different composition and probably different primary structure[17, 18, 2], both forms of the enzyme appear to have the same number of two reactive, non-essential and a maximum of four essential SH-groups in their molecule.

MATERIAL AND METHODS

Preparation of the enzyme. A refrigerating centrifuge made by W. Stock--Maschinenbau, Marburg/L (4.5 *lit* capacity at 3000 rpm) and a high-speed centrifuge made by Measuring & Scientific Equipment Ltd., London (1.5 *lit* capacity at 16000 rpm and 0.45 *lit* at 35000 rpm) were used. Concentrations of protein were determined according to the Biuret method with a conversion factor of 17.0. Enzymic activity was determined according to Boehringer method[19] in international units (one i.u. converts 1 μM of the substrate per minute at 25°C). Starch gel made by Connaught Laboratories, Toronto was employed for electrophoresis. Protein was fixed to the gel with amido--black and its enzymatic activity read under ultraviolet light after spraying with a solution of 2 *mg* oxaloacetate and 5 *mg* HADH in 10 *ml* 0.1 M sodium phosphate buffer pH 7.5. Separation on the chromatographic column was monitored by continual measurement of the UV absorption of the eluate at 254 *mμ* on a Uvicord 4701 A made by LKB, Stockholm. The fractions were collected in a synchronous fraction collector (LKB RadiRac Fraction Collector 3401 B). The high-voltage electrophoresis was carried out on a Pherograph-Original-Frankfurt (L. Hormuth, Inh. E. E. Vetter, Wiesloch/Baden). The Sephadex-G and DEAE column packings wree obtained from Pharmacia, Uppsala.

Reactions with SH-Groups

(a) *Reaction of m-MDH with PCIMB in 7.5 urea* a.— A quantity of 0.1 *ml* enzyme (10 *mg/ml*) and 0.1 *ml* PCIMB (1 *mg/ml*) solutions were mixed together with 2 *ml* 8 M solution of urea. Blank standard; b. — 2 *ml* urea solution and 0.2 *ml* buffer; c. — 0.1 *ml* PCIMB solution, 2 *ml* urea solution and 0.1 *ml* buffer; d. — 0.1 *ml* enzyme solution, 2 *ml* urea solution and 0.1 *ml* buffer. All substances were dissolved in 0.1 M sodium phosphate buffer pH 7.8. The extinction of all solutions was measured against the buffer at 255 *mμ* in a 1 *cm* cell. The extinction of the S-Hg bond was taken to be

$$E_{S-Hg} = E_a - E_d - (E_c - E_b).$$

(b) *Reaction of m-MDH with DTNB in 7.5 M urea.* 0.1 *ml* enzyme (10 *mg/ml*) and 0.2 *ml* DTNB (1 *mg/ml*) solutions were mixed together with 2.9 *ml* 8 M solution of urea. These substances were dissolved in 0.1 M sodium phosphate pH 7.8 buffer (with 0.01 M EDTA). The absorption at 405 *mμ* was measured in a 1 *cm* cell against 0.2 *ml* DTNB solution, 2.9 *ml* urea solution and 0.1 *ml* buffer.

(c) *Reaction of m-MDH with DTNB in 4 M urea.* 0.09 *ml* enzyme (10 *mg/ml*), 0.2 *ml* DTNB (1 *mg/ml*) and 1.55 *ml* 8 M urea, all dissolved in 0.1 M sodium phosphate pH 7.8 buffer (with 0.01 M EDTA), were mixed with 1.26 *ml* of the same buffer solution. The absorption at 405 *mμ* was measured in a cell with a 1 *cm* light path, against 0.2 *ml* DTNB solution, 1.55 *ml* solution urea and 1.35 *ml* buffer as a standard. Duration of the reaction: 1 hour at 25°C.

(d) *Reaction of native m-MDH with DTNB.* 0.05 *ml* enzyme (10 *mg/ml*) and 0.2 *ml* DTNB (1.4 *mg/ml*), dissolved in 0.1 M sodium phosphate buffer pH 7.8 (with 0.01 M EDTA), were mixed with 0.3 *ml* of the same buffer. The absorption at 405 *mμ* was measured in a 2 *mm* light-path cell, against a standard of 0.2 *ml* DTNB solution and 0.35 *ml* buffer. For determination of the enzyme activity 10 *μl* aliquots of the reaction mixture were taken. Duration of the reaction: 7 hours at 25°C.

Institut für Biochemie der
J. W. Goethe-Universität, Frankfurt/M

Received 14 February, 1969

REFERENCES

1. Christie, G. S. and J. D. Judah — *Proc. Roy. Soc.* (London) 141: 420, 1953.
2. Leskovac, V. *Dissertation,* Frankfurt/M (W. Germany), 1968.
3. Pfleiderer, G. and E. Hohnholz — *Bioch. Z.* 331: 245, 1959.
4. Holbrook, J. J., G. Pfleiderer, M. Volz, K. Mella, V. Leskovac and R. Jeckel — *Europ. J. Biochem.* 1: 476, 1967.
5. Fondy, T. P., J. Everse, G. A. Driscoll, F. Castillo, F. E. Stolzenbach and N. O. Kaplan — *J. Biol. Chem.* 240: 4219, 1965.
6. Ting-Kai Li and B. L. Vallee — *Biochem.* 3: 869, 1964.
7. Harris, J., B. P. Meriweather, and J. H. Park — *Nature* (London) 197: 154, 1963.
8. Delbrück, A., E. Zebe, and Th. Bücher. — *Bioch. Z.* 331: 273, 1959.
9. Englard, S. and H. H. Breiger — *Bioch. Bioph. Acta* 56: 571, 1962.
10. Straub, F. B. — *Biochem. J.* 34: 483, 1940.
11. Stephenson, M. L. and P. C. Zamečnik — *Proc. Ntl. Acad. Sci. USA* 47: 1627, 1961.
12. Boyer, P. — *Am. Soc.* 76: 4331, 1954.
13. Ellman, G. L. — *Arch. Bioch. Bioph.* 82: 70, 1959.
14. Guggenheim, E. A. — *Phil. Mag.* 2: 538, 1926.
15. Koshland, D. E. Jr., E. J. Ray and M. J. Erwin— *Feder. Proc.* 17: 1145, 1958.
16. Leskovac, V. and G. Pfleiderer — *Z. physiol. Chemie:* 1969 (in press).
17. Kitto, G. B. and N. O. Kaplan — *Biochem.* 5: 16, 1966.
18. Devenyi, T., S. J. Rogers and R. G. Wolfe — *Nature* (London) 210: 489, 1966.
19. *Boehringer-Informationen* — Mannheim, 1961.

GLASNIK HEMIJSKOG DRUŠTVA, Vol. 34, No. 8-9-10, 1969, pp. 519—527

GHDB-87

547.96 + 547.915.5 + 547.918:591.111.1

Original Scientific Paper

METABOLIC RELATIONS OF PROTEINS, LIPIDS AND GLUCIDES. XIII.

THE ELECTROPHORETIC PATTERNS OF LIPOPROTEINS IN DOG BLOOD SERUM DURING THE SLOW INFUSION OF GLUCOSE IN FASTING AND IN ALIMENTARY HYPERLIPEMIA

by

JELENA J. BOJANOVIĆ, MILANKA O. ČORBIĆ, ANKA D. JEFTOVIĆ and RAJKO V. ŽIVKOVIĆ

The papers dealing with the influence of glucose on clearing the plasma in postprandial hyperlipemia[1, 3, 7, 8] have attracted much interest because of prospects for a new approach to certain unsolved problems in the resorption and transport of fats. According to Albrink and co-workers[1], glucose clears the hyperlipemic plasma because it removes triglycerides from the circulation by activation of the adipose tissue, this eliminating breakdown products and directing them into the fat depots. However, Lossow and co-workers[9] found that glucose decreases the decomposition of triglycerides and the oxidation of fatty acids. On the other hand, Dole[7] holds that the action of glucose on lipids in the postabsorptive state may be compared with that of intravenous insulin, while its clearing effect he ascribes to the endogenous insulin.

During the investigation of the clearing effect of insulin it was found that the rapidly insulin-cleared plasma of dogs with alimentary hyperlipemia was clouded again by intravenously administered glucose [10]. In order to get information about the direct action of glucose on the metabolism of lipids and on other processes accompanying the clearing of the hyperlipemic plasma we investigated the action of glucose injected into fasting[4] and hyperlipemic[5] dogs. The results indicated that immediately after the administration glucose had the opposite effect to that usually ascribed to it. During the first 15 minutes a pronounced increase of turbidity and an increase in the relative content of the large-molecule lipoproteins and chylomicrons occurred, and the serum cleared only after 30 minutes. As we presumed that such an effect was connected with certain reactions during glucose metabolism, whose direct influence on the elimination of alimentary hyperlipemia was rendered disputable by these investigations, our aim was to find out whether the rate of administration of glucose had any influence on the phenomena or whether similar changes also appeared when the blood sugar level was kept high for a longer period of time. For this purpose we investigated the action of slow infusion of glucose on serum lipoproteins in fasting dogs and

in dogs with hyperlipemia induced after fasting. It was also of interest to seek a correlation with the changes in the free and esterified fatty acids found under similar experimental conditions[11].

MATERIAL AND METHOD

The dogs weighed between 19 and 25 *kg* and had all been fed under the same conditions for 7 days. From the first experimental group consisting of 7 dogs (5 male and 2 female) blood was taken for examination after 48--hour fasting, and the infusion of glucose solution (75 *g* glucose dissolved 90 *min.* in 500 *ml* physiological solution) started immediately after this. The other group (7 dogs; 3 male and 4 female) was given a fatty meal consisting of 20 *g* lard per *kg* of body-weight mixed with 400 *g* minced horse-meat, after a 48-hour fasting. Blood samples were first taken 5 hours after the meal, at maximum hyperlipemia, and then during the infusion of glucose (20, 40, 70 and 90 *min.*) and 30 and 90 minutes after it. The separation and determination of the serum lipoproteins was carried out by paper electrophoresis according to the technique described in ref. 4.

RESULTS AND DISCUSSION

The examination of the serum lipoproteins of dogs with exhausted carbohydrate reserves (48-hour fasting) showed that the slow infusion of glucose lead to changes similar to those during the administration of big quantities of glucose in a single injection.

At the beginning of the slow infusion of glucose the α-lipoprotein fraction decreased, normalizing again at 70 and 90 minutes. This reduction in the relative α-lipoprotein level is similar to that during the administration of glucose in a single injection, but unlike the rapid introduction of glucose, when this fraction reaches its lowest level after 15 minutes[4], during infusion the decrease is slower down and reaches its lowest level only after 40 minutes infusion (Fig. 1.A). However, the magnitude of the α-lipoprotein decrease is independent of the mode of introduction of glucose. The changes, although small, are statistically significant. On the cessation of infusion the α--lipoprotein level still increases and after 90 minutes it was somewhat higher than in fasting.

The β-lipoprotein fraction is increased during the first 40 minutes of infusion (Fig. 1, B) and then decreased, so that after 90 minutes it had fallen lower than normal. On cessation of infusion it decreased still further and after 90 minutes was lower than in fasting. The changes in β-lipoproteins are in the same direction as those during the injection of glucose[5], but are less pronounced. The highest β-lipoprotein level was reached after 40 minutes infusion, while in the case of a single glucose injection change was greatest after 15 minutes.

The low level of neutral fats established throughout the entire circulation in fasting increased during the first 40 minutes of infusion (Fig. 1, D) like the β-lipoprotein level. Although the increase is considerable (36% as

against the untreated animals), the level of this fraction was not high enough to cause a change in turbidity. After the 70-minute infusion, when an increase of α-lipoproteins was recorded, the neutral fats and β-lipoproteins were decreasing. While the changes in the β-lipoprotein fraction and chylomicron zone induced by the injection of glucose were in direct correlation with the changes in glycemia[4], and in α-lipoproteins in reciprocal correlation, similar correlations with glycemia were also found during the slow infusion of glucose[11] but they disappeared after only 70 minutes. At the moment of ceasing the infusion the neutral fats had returned to the level before the administration of glucose, and this was practically maintained 90 minutes later.

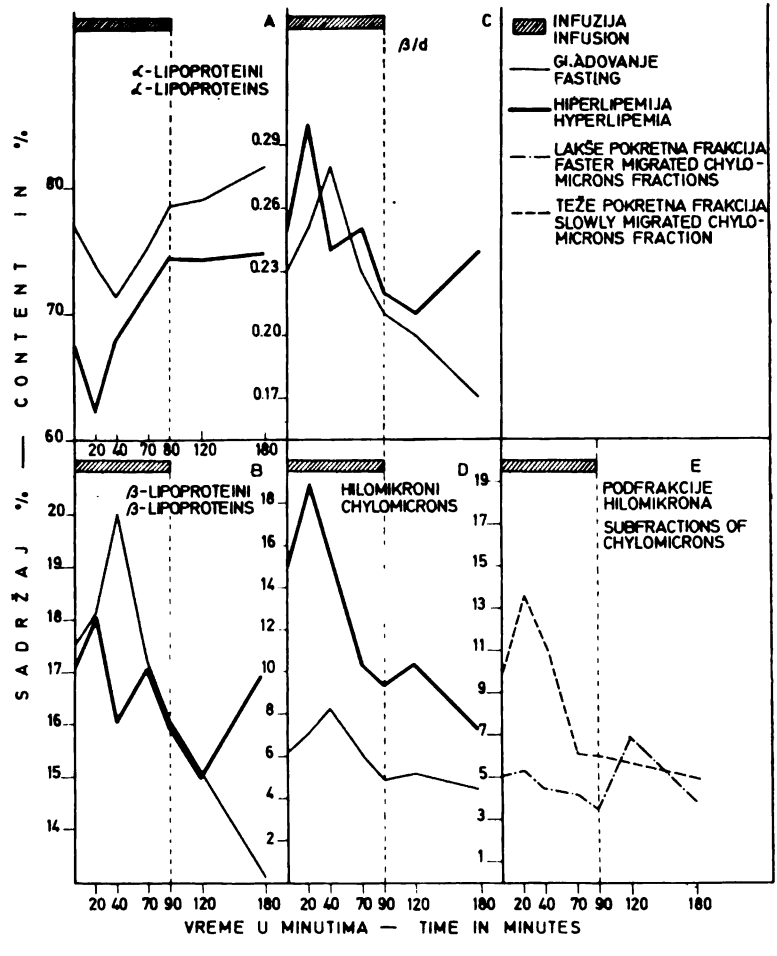

Fig. 1

Lipoprotein fractions in blood serum of dogs in fasting and hyperlipemia during glucose infusion

TABLE I

The Relative Levels of Lipoprotein Fractions in Blood Serum of Fasting Dogs during Glucose Infusion

	α-LIPOPROTEINS							β-LIPOPROTEINS						
	N	20	40	70	90	120	180	N	20	40	70	90	120	180
No.	7	6	6	7	6	6	6	7	6	6	7	6	6	6
R	71.4—80.4	69.8—78.2	65.2—75.3	71.8—81.2	76.9—82.1	69.8—83.5	76.2—86.3	14.5—21.4	15.7—21.9	16.4—25.6	13.6—21.8	12.3—18.7	11.7—22.1	10.7—19.0
M	76.7	73.9	71.3	75.3	78.5	79.0	81.6	17.5	18.9	20.3	17.8	16.3	15.7	13.9
SD	3.20	3.10	3.35	3.37	2.30	5.01	4.48	2.59	2.27	3.31	2.78	4.27	3.58	3.78
SE	1.20	1.26	1.37	1.27	0.95	2.05	1.83	0.98	0.93	1.35	1.14	1.74	1.46	1.54
CV%	4.16	4.19	4.69	4.47	2.93	6.34	5.49	14.80	12.01	16.30	15.64	26.21	22.86	27.19
a		—3.65	—7.03	—1.89	+2.24	+3.00	+6.37		+8.00	+16.06	+1.54	—6.91	—10.51	—20.57
b		p>0.05	p<0.05	p>0.05	p>0.05	p>0.05	p=0.05		p>0.05	p>0.05	p>0.05	p>0.05	p>0.05	p>0.05
	CHYLOMICRONS							β/α						
No.	7	6	6	7	6	6	6	7	6	6	7	6	6	6
R	4.2—8.5	4.6—9.6	6.7—11.5	4.4—8.5	2.8—5.8	3.8—8.1	24—59	0.18—0.30	0.21—0.28	0.23—0.39	0.19—0.30	0.15—0.24	0.14—0.31	0.12—0.25
M	6.1	7.1	8.3	6.1	4.9	5.2	4.5	0.23	0.25	0.28	0.23	0.21	0.20	0.17
SD	1.41	2.20	1.78	1.51	1.17	1.68	1.41	0.04	0.02	0.06	0.04	0.03	0.06	0.06
SE	0.53	0.89	0.72	0.57	0.48	0.68	0.58	0.02	0.01	0.02	0.01	0.01	0.02	0.02
CV%	23.00	30.53	21.37	24.88	23.88	32.31	31.61	17.39	8.00	21.43	17.39	14.28	30.00	35.29
a		+16.48	+35.89	0.00	—20.06	—15.17	—27.24		+8.69	+21.73	0.00	—8.69	—13.04	—26.09
b		p>0.05	p<0.05	—	p>0.05	p>0.05	p≈0.05		p>0.05	p>0.05	—	p>0.05	p>0.05	p>0.05

No — Number of cases
R — Range of value
M — Mean value
SD — Standard deviation
SE — Standard error
CV% — Coefficient of variation
a — % of decrease or increase in relation to the normal value (N)
b — Level of significance of changes

Similar changes in the lipoprotein fractions were obtained by the infusion of glucose in hyperlipemia, only their intensity and time of onset were different.

The α-lipoprotein fraction, whose level in hyperlipemia is lower than in fasting[2, 4, 5, 6], decreased most after the 20-min. infusion (this change being statistically significant) but the magnitude of the changes was similar to that in fasting (Fig. 1, A). However, after longer infusions this fraction abruptly increased, so that at the end of infusion it was higher than before the infusion (this increase being statistically significant). After the interruption of infusion the α-lipoprotein level remained practically unchanged.

The β-lipoprotein fraction, being approximately the same both in fasting and in hyperlipemia, changed very little during the infusion (the changes being statistically insignificant), and at the moment of interruption reached almost the same level as in hyperlipemia before the beginning of infusion.

The neutral fat fraction appeared in the form of two subfractions of which one occupied a wide space between β-lipoproteins and the base line, and the other smaller and less mobile situated quite close to the base line[5]. During slow infusion of glucose these two fractions exhibited changes of different magnitude (Fig. 1, D and E). While the spread out subfraction changed little during the infusion, the *x*-subfraction containing less mobile components showed big, statistically significant changes reciprocally correlating with those of α-lipoproteins. The increase was biggest 20 minutes after the beginning of infusion, when serum turbidity also increased[11]. The most pronounced changes were recorded during the first 70 minutes of infusion, while later during and after infusion the changes were much less. While the changes in α- and β-lipoproteins in hyperlipemia during the infusion of glucose were similar to those after a single injection[4], the changes in the neutral fat subfractions induced by glucose clearly depend on the mode of administration. After the injection of glucose chiefly the more mobile fraction of the chylomicron zone increases, while the increase of the less mobile *x*-subfraction is negligible. Contrary to this, the slow infusion of glucose induced a big increase of the *x*-fraction, but the increase in the chylomicron zone was relatively small, this giving evidence of qualitative differences in the composition of the neutral fats under these experimental conditions and of the endogenous origin of the *x*-subfraction lipids. During the clearing of the serum, regardless of the mode of introduction of glucose, the *x*-subfraction decreases, and usually disappears completely.

The effect of glucose on the neutral fats during infusion agrees completely with the state and changes of the serum free and esterified fatty acids and with serum transparency[11].

The phenomenon of a lag in the glucose-induced changes in fasting (relative to the effect induced in hyperlipemia) could be explained by a higher activity of the lipid and carbohydrate metabolism in hyperlipemia, so that the kinetics of the processes involved are also different.

CONCLUSION

The blood serum lipoproteins of dogs in fasting and in alimentary hyperlipemia during and after the slow infusion of glucose were investigated. The results showed that the effect of glucose on the α- and β-lipoproteins

TABLE 2

The Relative Level of Lipoprotein Fractions in Blood Serum of Dogs in Hyperlipemia during Glucose Infusion

	α-LIPOPROTEINS							β-LIPOPROTEINS						
	N	20	40	70	90	120	180	N	20	40	70	90	120	180
No.	7	5	5	5	4	5	6	7	5	5	5	4	5	6
R	63.8—72.0	55.7—66.1	58.6—76.9	68.8—76.3	70.9—77.5	70.5—78.9	69.6—78.2	13.7—19.4	15.5—23.8	13.2—20.7	11.8—20.7	9.7—22.8	9.9—21.0	14.0—25.0
M	67.8	62.3	68.0	71.9	74.4	74 3	74.8	17.1	18.5	16.2	17 8	16.2	15.3	17.9
SD	3.12	4.33	7.26	2.94	3.00	3.66	3.59	1.92	4.42	2.67	3.73	5.48	5,01	3.74
SE	1.18	1.93	3.25	1.31	1.50	1.63	1.46	0.72	1.97	1.19	1.67	2.74	2.24	1.52
CV%	4.60	6.95	10.68	4.08	4.03	4.93	4.79	11.21	23.84	16.46	21.00	33.83	32.68	20.90
a		—8.04	+0.29	+6.13	+9.75	+9.64	+10.41		+8.29	—5.37	+3.74	—5.37	—10.45	+4.50
b		$p<0.05$	$p>0.05$	$p\approx0.05$	$p<0.05$	$p<0.05$	$p<0.01$		$p>0.05$	$p>0.05$	$p>0.05$	$p>0.05$	$p>0.05$	$p>0.05$
	β/α							CHYLOMICRONS						
No.	7	5	5	5	4	5	6	7	5	5	5	4	5	6
R	0.19—0.29	0.21—0.41	0.17—0.35	0.15—0.30	0.13—0.32	0.13—0.29	0.18—0.36	3.1—5.8	4.4—8.4	3.4—5.0	3.3—5.9	2.7—3.9	4.8—11.2	2.1—54
M	0.25	0.30	0.24	0.25	0.22	0.21	0.24	5.1	5.4	4.5	4.2	3.5	6.9	3.9
SD	0.04	0.09	0.07	0.06	0.88	0.07	0.06	0.98	1.70	0.63	1.09	0.53	2.51	1.38
SE	0.01	0.04	0.03	0.03	0.04	0.03	0.02	0.37	0.76	0.28	0.49	0.27	1.12	0.56
CV%	16.00	30.00	29.17	24.00	36.36	33.33	25.00	19.03	31.65	14.03	26.13	15.32	36.17	34.93
a		+20.00	—4.00	0.00	—12.00	16.00	—4.00		+4.27	—12.81	—19.03	—32.81	+34.76	—23.30
b		$p>0.05$	$p>0.05$	—	$p>0.05$	$p>0.05$	$p>0.05$		$p>0.05$	$p>0.05$	$p>0.05$	$p<0.05$	$p>0.05$	$p>0.05$

	X-FRACTION							CHYLOMICRONS +X						
No.	7	5	5	5	4	5	6	7	5	5	5	4	5	6
R	6.5—13.3	11.2—15.4	5.5—17.2	1.9—7.6	2.4—9.2	3.9—7.1	3.5—7.8	12.1—19.1	16.1—21.4	9.9—21.5	7.8—11.8	6.3—12.8	7.0—12.6	5.3—10.5
M	9.9	13.6	11.3	6.1	6.0	5.7	5.0	15.1	18.9	15.8	10.3	9.4	10.4	7.3
SD	2.41	1.70	5.37	2.45	2.87	1.65	1.98	2.51	2.07	5.16	1.55	2.65	2.08	2.23
SE	0.98	0.76	2.40	1.09	1.43	0.95	0.99	1.03	0.92	4.62	0.68	1.32	0.93	0.91
CV%	24.22	12.51	47.44	40.00	48.07	28.79	39.68	16.61	10.92	32.64	15.03	28.10	20.06	30.63
a		+36.48	+14.14	—38.50	—40.08	—42.41	—49.85		+25.41	+4.63	—31.77	—37.59	—31.37	—51.82
b		p<0.05	p>0.05	p<0.05	p=0.05	p<0.05	p=0.05		p<0.05	p>0.05	p<0.01	p=0.01	p=0.01	p<0.001

No. — Number of cases
R — Range of value
M — Mean value
SD — Standard deviation
SE — Standard error
CV% — Coefficient of variation

a — % of decrease or increase in relation to the normal value (N)

b — Level of significance of changes

during infusion was similar to that observed after a single injection. The changes characteristic for the effect of glucose on lipoproteins in fasting were found to be delayed relative to the state observed on the introduction of glucose in a single injection and during its slow infusion in hyperlipemia.

The biggest changes during infusion in hyperlipemia were found in neutral fats, especially in the x-subfraction, and they were in pronounced reciprocal correlation with those of α-lipoproteins. The changes in the neutral fats (chylomicrons and the x-subfraction lipids) found during and after infusion provided valuable information for understang of the state of lipids, the role of glucose in metabolic processes during hyperlipemia, and glucose elimination.

Department of Chemistry,
School of Medicine, Belgrade University
Department of Biochemistry,
School of Medicine, Belgrade University

Received 10 September, 1968.

REFERENCES

1. Albrink, M. J., J. R. Fitzgerald and E. B. Man. "Reduction of Alimentary Lipemia by Glucose" — *Metabolism, Clinical and Experimental* 7: 162—171, 1958.
2. Albrink, M. J. "Lipoprotein Pattern as a Function of Total Triglyceride Concentration of Serum" — *Journal of Clinical Investigation* 39: 536, 1961.
3. Bierman, E. L., I. L. Schwartz and V. P. Dole. "Action of Insulin on Release of Fatty Acids from Tissue Stores" — *American Journal of Physiology* 191: 359—362, 1957.
4. Bojanović, J., M. Čorbić and P. Milošević. "Odnos metabolizma belančevina, lipida i glicida. XI. Dejstvo intravenski date glukoze na raspodelu lipoproteinskih frakcija seruma pasa u gladovanju" (Metabolic Relations of Proteins, Lipids and Glucides. XI. Effect of Intravenous Injection of Glucose on the Distribution of Serum Lipoprotein Fractions in Fasting Dogs) — *Glasnik hemijskog društva* (Beograd) 32*: 327—334, 1967.
5. Bojanović, J., M. Čorbić and Dj. Panjević. "Odnos metabolizma belančevina, lipida i glicida. XII. Dejstvo intravenski date glukoze na raspodelu lipoproteinskih frakcija seruma pasa u alimentarnoj hiperlipemiji" (Metabolic Relations of Froteins, Lipids and Glucides. XII. Effect of Intravenous Glucose on the Distribution of the Serum Lipoprotein Fractions in Dogs in Alimentary Hyperlipemia) — *Glasnik hemijskog društva* (Beograd) 32*: 335—341, 1967.
6. Cornwell, D. G., F. A. Kruger, G. J. Hamwi and J. B. Brown. "Studies on the Characterization of Human Serum Lipoproteins Separated by Ultracentrifugation in a Density Gradient. II. Serum Lipoproteins in Hyperlipemic Subjects" — *American Journal of Clinical Nutrition* 9: 41, 1961.
7. Dole, V. P. "A Relation between Non-Esterified Fatty Acids in Plasma and The Metabolism of Glucose" — *Journal of Clinical Investigation* 36: 884—885, 1957.
8. Ghata, J., L. Salamin, J. Lewin and E. Azérad. "Action du glucose sur l'hyperlipémie alimentaire chez le sujet normal et le diabetique" — *Nutritio et Dieta* 3: 264—280, 1961.
9. Lossow, W. J. and I. L. Chaikoff. "Carbohydrate Sparing of Fatty Acid Oxidation. I. The Relation of Fatty Acid Chain Length to the Degree of Sparing. II. The Mechanism by which Carbohydrate Spares the Oxidation of Palmitic Acid" — *Archives of Biochemistry and Biophysics* 57: 23—40, 1955.
10. Nešković, M., J. Bojanović, M. Čorbić, Lj. Stefanović, Z. Mladenović-Stojimirović, I. Kulić-Japundžić and D. Kostić. "Effect of Insulin on Metabolism of Proteins, Lipids and Glucides. VI. Action o Glucose on the Insulin Clearing Effect" — *Zbornik radova Medicinskog fakulteta Beograd* 1: 37—45, 1962.
11. Nešković, M., J. Bojanović, Lj. Stefanović, M. Čorbić, Ž. Čupić and R. Živanović. "Odnos metabolizma belančevina, lipida i glicina. V. Dejstvo infuzijom date glukoze na masne kiseline pasa u gladovanju i hiperlipemiji" (Metabolic Relations of Proteins, Lipids and Glucides. V. Effect o Glucose Infusion on the Plasma Fatty Acids of Dogs in Fasting and in Hyperlipemia) — *Acta med. Iug.* 21* 136—147, 1967.

* Available in English translation from National Technical Information Service, Springfield, Virginia, 22151.

GLASNIK HEMIJSKOG DRUŠTVA, Vol. 34, No. 8-9-10, 1969, pp. 519—534

GHDB-88

546.18:581.1

Original Scientific Paper

PHOSPHORUS IN PLANTS AND THE SUBSTITUTIVE OH^- IONS OF SOIL*

by

ZAGORKA J. FILIPOVIĆ and M. M. BRESJANAC

The ions absorbed by plants from the soil are partly found in the soil solution[2], but considerably more adsorbed on the micelles of soil colloids[4] (these two being in a mutual equilibrium). The concentration of ions in the soil solution is usually very low[7] and because of that the ions adsorbed on the soil colloids also take part in plant nutrition[5, 6, 8, 9, 11, 12].

However, regardless of whether the plant absorbs the ions from the solution or from the micelle, any theory of plant nutrition must, according to Overstreet and Jacobson[10], be based on the fact that "the absorption of ions is a substitutive process: during the absorption of cations an equivalent quantity of H^+ ions, and during the absorption of anions an equivalent quantity of OH^- or HCO_3^- ions are emitted from the surface of the plant root". Because the ions emitted from the root surface result from the plant's respiration they represent an inexhaustible source for substitution[11].

If this interpretation of the process is applied to the uptake of phosphorus, then the existence of a certain correlation between the concentration of phosphorus in plants and the concentration of hydroxyl ions in the soil may be expected, because according to the above hypothesis the absorption of phosphorus must take place by negative phosphate ions being absorbed by the root and negative OH^- ions emitted into the soil colloids in exchange.

In order to check this hypothesis we determined both the concentration of phosphorus in a number of plant samples and the concentration of the substitutive OH^- ions in the corresponding soil samples (the OH^- ions adsorbed on the micelles of soil colloids).

MATERIAL AND METHOD

The samples were collected during two vegetation periods. The plants were growing under the most diverse ecological conditions (the samples originated from various parts of Yugoslavia).

Phosphorus was determined in the leaves of the following plants: maize, rye, barley, sunflower, soybean, cabbage, bean, potato, tomato, lavender and foxglove.

* Supported by the Research Fund of the SR of Serbia.

The material was washed in double distilled water, dried at 105°C and phosphorus determined[1], its concentration being expressed as *mg* P per 100 *g* dry vegetable material.

Soil samples were taken from underneath every plant at a depth of 15 and 50 *cm*. The average sample of these two was dried in air and the concentration of the substitutive hydrogen ions[12] determined. The concentration of the substitutive OH^- ions was determined. As the reciprocal value, and expressed in meq per 100 *g* soil.

RESULTS AND DISCUSSION

Phosphorus was found in quantities between 60 and 520 *mg* per 100 *g* of sample, and hydroxyl ions between 3 and 16 meq per 100 *g* soil sample.

By plotting these results, the following figure was obtained:

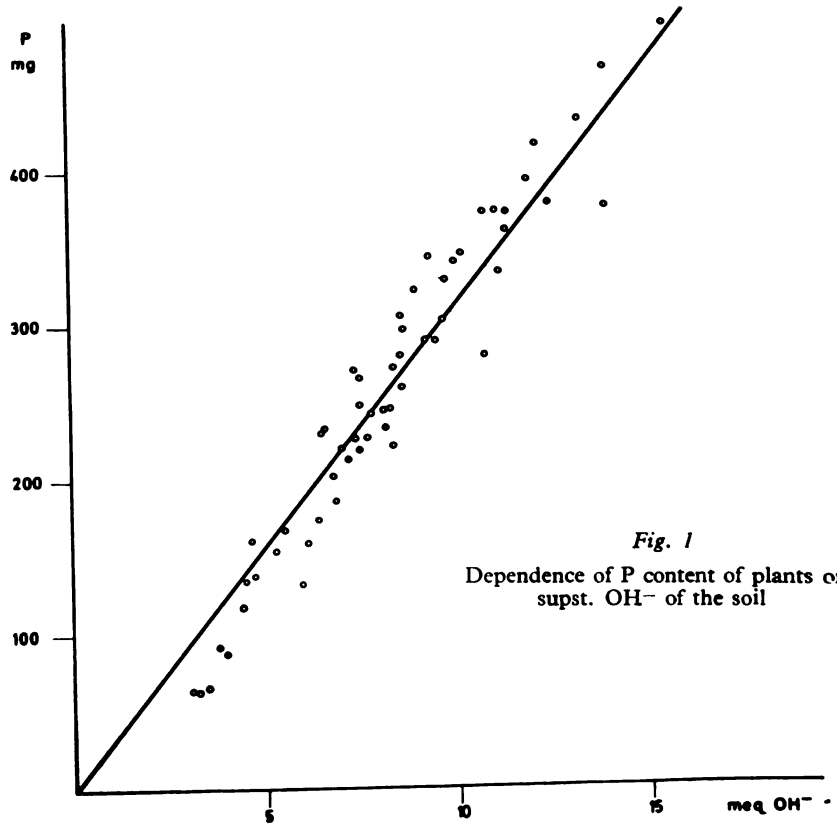

Fig. 1

Dependence of P content of plants on supst. OH^- of the soil

TABLE 1

No.	Plant and location	I P *mg*	II HPO_4^{-2} *meq*	III $H_2PO_4^{-1}$ *meq*	IV OH^-_{supet} *meq*
1	Wheat Valjevo	152	9.8	4.9	5.3
2	Wheat Lajkovac	161	10.4	5.1	4.7
3	Tomato Vinkovci	220	14.3	7.0	7.0
4	Maize Mladenovac	218	14.1	7.0	7.5
5	Soybean Čačak	225	14.5	7.3	7.7
6	Maize Vrnjci	232	15.0	7.5	7.3
7	Wheat Mali M. Lug	244	15.7	7.9	8.2
8	Maize Bled	246	15.9	8.0	8.3
9	Sunflower Sarajevo	249	16.1	8.0	8.8
10	Wheat Ruma	259	16.7	8.3	8.6
11	Tomato Samoš	270	17.4	8.7	8.4
12	Wheat Čačak	296	19.1	9.5	8.7
13	Wheat Plitvice	288	18.6	9.3	9.5
14	Cabbage Alibunar	300	19.4	9.7	9.7
15	Sunflower Osijek	332	21.4	10.7	11.2
16	Maize Kruševac	359	23.1	11.5	11.4
17	Soybean Jajinci	379	23.9	11.9	11.4
18	Maize Novi Sad	371	23.9	11.9	11.1
19	Bean Deliblato	461	29.7	14.8	14.8
20	Cabbage Crepaja	489	31.4	15.7	15.7
	m-eq (ratio) Phosphate: OH^-		2 : 1	1 : 1	

It may be seen that the higher the concentration of hydroxyl ions adsorbed on the soil micelles the higher the concentration of phosphorus in the plants. A direct proportionality between these two quantities supports the above hypothesis about the substitutive interchange of ions between the root and its external surroundings.*

From the practical point of view, the correlation in Fig. 1 provides us with very interesting information: from a known concentration of substitutive OH^- ions in the soil the concentration of phosphorus in plants may be estimated. However, as far as theory is concerned, the fact that a constant corresponding to the atomic weight of phosphorus (P = 31) appears in the equation

$$mg\ P = 31 \times meq\ OH^-,$$

expressing the correlation in Fig. 1 is of no less interest.

According to the substitutive hypothesis the number of ions being substituted must also be equivalent. In order to find out whether the substituted OH^- ions were equivalent to one of the two forms of phosphorus ion, we calculated meq's of $H_2PO_4^{-1}$ and HPO_4^{-2} ions in all the samples on the basis of the known quantity of phosphorus in the plants. Some of the results are given in Table 1.

To check equivalence, let us take for example sample No 16. The foliage of this plant contained 359 *mg* P per 100 *g* sample. Depending on the form in which the ions were taken up by the plant, this phosphorus could build up:

23.1 *meq* HPO_4^{-2} or 11.5 *meq* $H_2PO_4^{-1}$

From the table it may be seen that the soil on which plant No 16 was grown contained 11.4 meq hydroxyl ions. The meq ratios between phosphate and hydroxyl ions are the following:

HPO_4^{-2} : OH^-	$H_2PO_4^{-1}$: OH^-
23.1 : 11.4	11.5 : 11.4
2 : 1	1 : 1

As the equivalents of the substances being substituted must be in a ratio of 1 : 1, it may be concluded that this plant must have absorbed phosphorus in the form of $H_2PO_4^{-1}$ ions. The same conclusion may be easily drawn for all the samples in Table 1 (compare the third and fourth columns). It is further supported by the fact that given two differently charged ions that carrying the lower change is more easily absorbed by the plant.

Hence in over 75% of the samples (see note on page 3) the quantity of phosphorus was equivalent to that of OH^- ions in the colloidal fraction of the soil.

According to the above discussion, our results back up the hypothesis of substitutive interchange of ions between the plant root and its surroundings. However, if another theory could more successfully explain ion uptake by plants, it must, as far as phosphorus is concerned, take into account the following experimental fact (Fig. 1):

* *Note:* A dependence of this type[3] was found in over 75% vegetable samples examined; the type found in the remaining 25% is to be considered in a separate paper.

The quantity of phosphorus absorbed by a plant is in direct proportion to and equivalent to the quantity of OH^- ions adsorbed on the micelle of the soil colloids.

SUMMARY

A quantitative dependence of the concentration of phosphorus in the leaf of various plants on the concentration of substitutive OH^- ions in the soil colloids has been found. It has also been found that the examined plants absorbed phosphorus in the form of $H_2PO_4^{-1}$ ions and in a quantity equivalent to that of OH^- ions in the colloidal fraction of the soil.

Dept. of Inorganic Chemistry,
School of Pharmacy, Belgrade University

Received 3 June, 1968

REFERENCES

1. Dickman, S. R. and R. H. Bray. "Colorimetric Determination of Phosphate" — *Indust. Eng. Chem. Anal. Ed.* 12: 665, 1940.
2. *Encyclopedia of Plant Physiology IV* — Berlin-Göttingen: Springer Verlag, 1958, pp. 248.
3. Filipović, Z. and M. Bresjanac. "Zavisnost sadržaja fosfora u listu biljaka od sadržaja vodonikovih jona zemljišta" (Dependence of Phosphorus in Plant Leaf on Hydrogen Ion Content Soil) — *Glasnik hemijskog društva* (Beograd) 33*: 511—515, 1968.
4. Gedroĭts, K. K. *Pochvennyi pogloshchaĭushchiĭ kompleks, rasteniia i udobreniia* (Soil Absorptive Complex, Plant and Fertilizer) — Moskva: Sel'khozgiz, 1953.
5. Jenny, H. and R. Overstreet. "Cation Interchange between Plant Roots and Soil Colloids" — *Soil Science* 47: 257—272, 1939.
6. Jenny, H. and E. W. Cowan. "The Utilization of Absorbed Ions by Plants" — *Science* 77: 394—396, 1933.
7. Laatsch, W. *Dynamik der mitteleuropäischen Mineralboden* — Dresden: T. Steinkopff, 1954.
8. Mangel, K. *Ernährung und Stoffwechsel der Pflanze* — Jena: G. Fischer Verlag, 1961.
9. Overstreet, R. and H. Jenny. "Studies Pertaining to the Cation Absorption Mechanism of Plant in Soil" — *Soil Sci. Amer. Proc. (1939)* 4: 125—130, 1940.
10. Overstreet, R. and L. Jacobson. "Mechanism of Ion Absorption by Roots" — *Annual Rev. of Plant Physiology* Vol. 3, 1952.
11. Peterburgskii, A. W. *Obmenno pogloshchnie v pochve i usvoenie rasteniiami pitatel'nykh veshchestv* (Interchange Absorption in Soil and Plant Nutrient Uptake) — Moskva: Visshaia shkola, 1959.
12. Peterburgskii, A. W. *Adsorptionprocesse im Boden und Würzelernährung der Pflanze* — *Plant and Soil* 11(2), 1959.
13. Sokolov, A. V. "Opredelenie v pochve podvizhnogo aliuminiia" (Determination of Mobile Aluminum in Soil) — *Khimizatsiia sotsialisticheskogo zemledeliia* 7, 1939.

* Available in English translation from National Technical Information Service, Springfield, Virginia, 22151.

GLASNIK HEMIJSKOG DRUŠTVA, Vol. 34, No. 8-9-10, 1969, pp. 535—539

GHDB-89

543.544:547.458.61:541.183.123.2

Original Scientific Paper

SEPARATION OF CATIONS BY CIRCULAR THIN-LAYER CHROMATOGRAPHY ON STARCH

by

VELIMIR D. CANIĆ and NADA U. PERIŠIĆ-JANJIĆ

The cations divided in five analytical groups according to the classical hydrogen-sulphide scheme have been separated by Seiler and co-workers[1, 2] by ascending a thin-layer chromatography on silica gel. Klamberg[3] has separated the cation analytical groups on a thin layer of cellulose. Hashmi and co-workers[4, 5] have separated the cations and anions by the circular thin-layer chromatography on silica gel and alumina. They have separated 40 cations divided in five groups by extraction with various organic solvents.

Continuing with our previous investigations[6, 9] on the separation of cations by the ascending technique on starch we investigated thin-layer chromatography on maize starch.

EXPERIMENTAL

Cations were previously divided into the analytical groups according to the classical scheme as described in previous paper[6–8].

Preparation of plates. 10 *g* cleaned and dried maize starch was suspended in 20 *ml* water and circular plates sprayed with this suspension from a distance of 20 *cm*. The quantity was sufficient for two plates 20 *cm* in diameter. The plates were air dried.

Test solutions. For the separation of different cation groups the following solutions were used:

0.25 M aqueous solutions of $AgNO_3$, $Hg_2(NO_3)_2$ and $Pb(NO_3)_2$

0.1 M solutions of $Cu(CH_3COO)_2 \cdot H_2O$, $Cd(NO_3)_2 \cdot H_2O$, $Pb(NO_3)_2$, $Hg(NO_3)_2 \cdot H_2O$ and $Bi(NO_3)_3 \cdot 5H_2O$ in 3 N HNO_3

0.1 M solutions of As_2O_3, $SbCl_3$ and $SnCl_2 \cdot H_2O$ in 3 N HCl

0.1 M aqueous solutions of $Fe(NO_3)_3 \cdot 9H_2O$, $CrCl_3 \cdot 6H_2O$, $Al(NO_3)_3 \cdot 9H_2O$, $Co(NO_3)_2 \cdot 6H_2O$, $Ni(NO_3)_2 \cdot 6H_2O$, $Mn(NO_3)_2 \cdot 6H_2O$ and $Zn(NO_3)_2$

0.25 M aqueous solutions of $CaCl_2 \cdot 6H_2O$, $Sr(NO_3)_2 \cdot 6H_2O$, $BaCl_2 \cdot 6H_2O$ and $MgSO_4 \cdot 7H_2O$

0.25 M aqueous solutions of LiCl, NaCl, KCl and NH_4Cl.

Communicated at the XIVth Symposium of Serbian Chemists, Belgrade, January 1969.

The chemical used were p.a. purity. Quantities of 1 μl each solution and 1 μl mixture of cations of the different groups obtained by mixing together equal parts of every solution, were applied to the plates in the form of a circular spot.

Development with the corresponding solvents was performed in a saturated atmosphere at room temperature during about 90 minutes, the solvent front advancing about 10 *cm*. After the development the plates were dried in a stream of warm air and then sprayed with the corresponding reagents for identification. All spots were visible immediately after development. All the more important experimental data are given in Table 1.

Figure 1 shows the division of cations according to analytical groups.

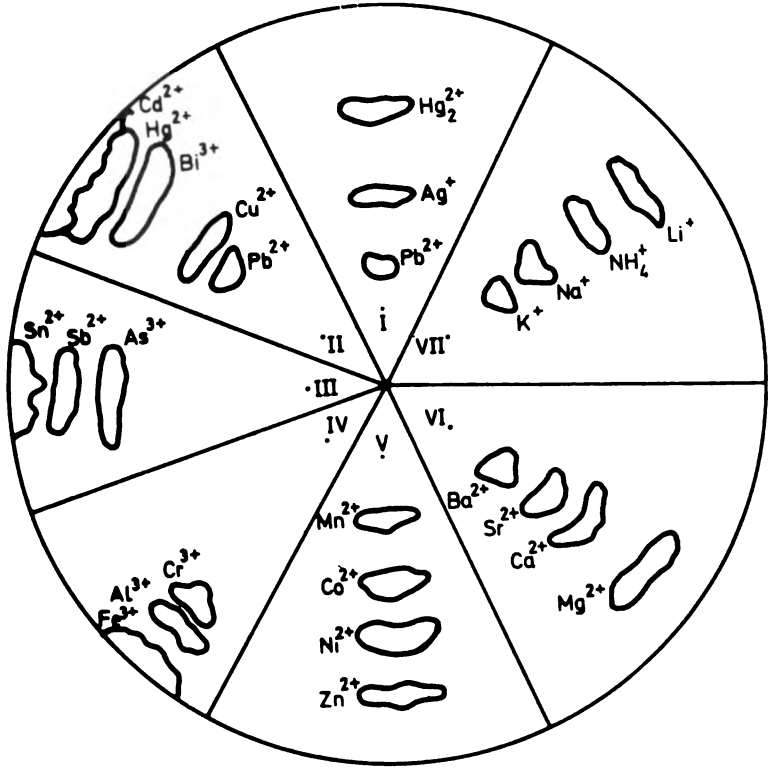

Fig. 1

Separation of analytical groups by circular thin layer chromatography using the corresponding solvents.

RESULTS AND DISCUSSION

From the chromatograms and R_f values obtained, it may be concluded that the cation analytical groups can be separated on a thin layer of maize starch by the circular technique. Seven different solvents were used,

TABLE I

Cation	Solvent	R_f values	Detection reagent	Limit of sensitivity $\mu g/\mu lit$	Color of the spot
Hg_2^{2+}	I	0.65	A	50	black
Ag^+	„	0.37	„	27	brown
Pb^{2+}	„	0.11	„	52	brown
Cd^{2+}	II	0.94	„	11.2	light yellow
Hg^{2+}	„	0.84	„	20.1	black
Bi^{3+}	„	0.72	„	20.9	dark brown
Cu^{2+}	„	0.46	„	6.4	dark brown
Pb^{2+}	„	0.36	„	20.7	brown
Sn^{2+}	III	0.95	B	11.9	pink
Sb^{3+}	„	0.76	„	8.8	pink
As^{3+}	„	0.60	„	7.5	orange
Fe^{3+}	IV	0.95	C	5.6	black
Al^{3+}	„	0.67	„	2.7	light yellow
Cr^{3+}	„	0.55	„	5.2	light grey
Zn^{2+}	V	0.72	„	6.5	yellow
Ni^{2+}	„	0.54	„	5.86	dark red
Co^{2+}	„	0.37	„	5.89	brown
Mn^{2+}	„	0.20	„	5.59	grey violet
Mg^{2+}	VI	0.86	„	6.08	yellow
Ca^{2+}	„	0.60	„	10.00	yellow
Sr^{2+}	„	0.44	„	21.00	yellow
Ba^{2+}	„	0.22	„	34.00	yellow
Li^+	VII	0.75	D	1.75	— white on the dark background
NH_4^+	„	0.44	„	4.25	— white on the dark background
Na^+	„	0.30	„	5.75	— white on the dark background
K^+	„	0.19	„	9.75	— white on the dark background

SOLVENTS:

I Acetone-i propanol-3N HNO_3 (2:6:2)
II Ethanol-i propanol-5N HCl (6:2:2)
III Acetone-ethanol-5N HCl (2:6:2)
IV Acetone-water-conc. HCl (8:1.2:0.8)
V Butanol-pyridine-diethylaniline-5N HCl (5:1:2:2)
VI I-Propanol-water-5N HCl (4:3:3)
VII Methanol-conc. HCl-water (8:1:1)

REAGENTS FOR IDENTIFICATION:

A. 1M $(NH_4)_2S$
B. 0.1% solution of dithizone in chloroform
C. 0.5% solution of 8-hydroxichinoline. After spraying the plates are exposed to ammonia vapor and spots are observed under UV light.
D. Cations of group V are identified by heating the plates to 100°C.

the sequence during separation with these being the following (in order of increasing R_f values):

$$Hg_2^{2+} > Ag^+ > Pb^{2+}$$

$$Cd^{2+} > Hg^{2+} > Bi^{3+} > Cu^{2+} > Pb^{2+}$$

$$Sn^{2+} > Sb^{3+} > As^{3+}$$

$$Fe^{3+} > Al^{3+} > Cr^{3+}$$

$$Zn^{2+} > Ni^{2+} > Co^{2+} > Mn^{2+}$$

Somewhat better separation was achieved with these solvents by the circular technique than by ascending chromatography. The solvents used earlier for the separation of cations by the ascending technique could not be used here. In addition, this procedure has the advantage of needing smaller quantities of solvents. The sensitivity is given in the table; it is relatively high, between $1 \cdot 10^{-6}$ and $2.5 \cdot 10^{-7}$ *g* ions.

CONCLUSION

Cation analytical groups have been separated by circular chromatography using 7 different solvents.

Department of Chemistry,
University of Novi Sad, Yugoslavia

Received 1 September, 1969

REFERENCES

1. Seiler, H. and M. Seiler. "Anorganische Dünnschicht Chromatographie" — *Helvetia Chimica Acta* (Basel) 43: 1939, 1960.
2. Seiler, H. and W. Rothweiler. "Anorganische Dünnschicht Chromatographie — Trennung der Alkali Gruppe" — *Helvetia Chimica Acta* (Basel) 44: 941, 1961.
3. Klamberg, H. and K. Randerath. *Dünnschicht-Chromatographie* — Weinheim Bergstr.: Verlag Chemie GmbH., 1962, p. 221.
4. Hashmi, M. H., A. M. Shahid and A. A. Ayaz. "Application of Circular Thin Layer Chromatography to Inorganic Qualitative Analysis" — *Talanta* (Oxford) 12: 713, 1965.
5. Hashmi, M. H., A. M. Shahid, A. A. Ayaz, F. R. Chughtai, N. Hassan and A. S. Adil. "Identification of Forty Cations and Nineteen Anions by Circular Thin Layer Chromatography" — *Analytical Chemistry* (Washington) 38: 1554, 1966.
6. Canić, V. D. and S. M. Petrović. "Trennung der Kationen mit Hilfe der Dünnschicht--Chromatographie auf Stärke (I. und IV. Gruppe)" — *Zeitschrift für analytische Chemie* (Berlin) 211: 321, 1965.
7. Canić, V. D., S. M. Petrović and A. K. Bem. "Trennung der Kationen mit Hilfe der Dünnschicht-Chromatographie auf Stärke (II. Gruppe)" — *Zeitschrift für analytische Chemie* (Berlin) 213: 251, 1965.
8. Canić, V. D., M. N. Turčić and N. U. Perišić. "Trennung von Kationen mit Hilfe der Dünnschicht-Chromatographie auf Stärke (III. Gruppe)" — *Zeitschrift für analytische Chemie* (Berlin) 228: 258, 1967.
9. Canić, V. D., S. M. Petrović and S. E. Petrović. †(Separation of Alkali Metals on Starch Thin Layer) — *Glasnik Hemijskog Društva* (Beograd), (to be published).

† Original title not given.

GLASNIK HEMIJSKOG DRUŠTVA, Vol. 34, No. 8-9-10, 1969, pp. 541—547

GHDB-90

66.094.403:622.341:546.74

Original Scientific Paper

CHLORINATION OF YUGOSLAV NICKEL-BEARING IRON ORES. I.

CHLORINATION OF NATURAL ORES

by

DUŠAN M. VUČUROVIĆ and MIODRAG A. SPASIĆ

INTRODUCTION

First attempts to use chlorine in the processing of complex ores date from the end of the last and the beginning of this century[1, 2, 3]. Beginning with the second decade of this century the process of chloridising roasting and chlorination have been more and more frequently used in various fields of metallurgy. For chlorination, besides gaseous chlorine, various salts, such as NaCl, $CaCl_2$, iron chloride etc., have been used.

Chlorination is applied to various nickel bearing substances: nickel compounds, ores and minerals, metallic nickel, etc. A number of authors chlorinated oxide ores bearing nickel, cobalt and iron with gaseous chlorine in the presence of coal, thus obtaining chlorides and volatile chlorides, both of natural and previously reduced nickel-bearing iron ore[4, 5, 6], silicate-oxide ore from the USSR[7, 8, 9], partly reduced ores[10], nickel bearing ore from New Caledonia[11, 12] and oxide ore from the USSR[13, 14]. Laterite iron ores have been chlorinated with chlorine and the gas mixtures chlorine-oxygen and chlorine-oxygen-nitrogen-carbon monoxide[15]. Ores of the same type have also been chlorinated selectively with a mixture of 5% Cl_2 and 95% O_2[16], as were ores previously reduced with a mixture of CO + + CO_2[17]. Cu-Ni ores have been chlorinated in the presence of SCl_2 and $SiCl_4$ as activators [18, 19], and so have sulphide Fe-Ni ores[20, 21] and concentrates[22, 23].

Beside ore, natural garnierite was chlorinated after reduction in the presence of coal[7, 24–28], likewise metallic nickel, nickel compounds[29, 30, 31], nickel oxide after reduction[32], nickel minerals[33], etc. Ferric chloride has also been used as the chlorinating agent [34, 35, 36]. Some authors used clorination as the starting point for the speration of iron and nickel from chromium[37] or for the separation of iron and nickel[38].

By leaching chlorinated ores with water, a nickel oxide concentrate 50—60 times richer in nickel than the ore was obtained[28, 29]. Investigations have been made covering reactions between oxides and chlorides[6], reduction of chlorides with hydrogen[6, 39], oxidation of chlorides and reduction of oxides for obtaining nickel and cobalt[35] and the decomposition kinetics of cobalt, nickel and copper chlorides[40, 41]. By thermodynamic and experi-

mental investigations the stability of chlorides was found to increase in the order Co, Ni, Cu, this corresponding to the decrease in chemical affinity of these for oxygen[40, 41]. Among the nickel compounds, the most easily chlorinated is NiS, followed by NiO and metallic nickel, and Ni-silicates and Ni-ferrite the most difficult[39].

Numerous authors have investigated the possibilities of chloridising roasting of nickel-bearing iron ores[42, 43, 44, 45], nickel-bearing serpentines[46, 47], etc.

Chlorination is also more and more used in other fields of non-ferrous metallurgy owing to certain very significant characteristics of chlorides, such as: relatively high volatility, low melting point, good solubility, the differences in volatility between different chlorides, etc. Many such problems as the strong corrosive effect of chlorine on the equipment have successfully been overcome by the use of modern materials.

The thermodynamics and kinetics of chlorination have also been thoroughly studied. The normal affinity of metals (and their compounds) for chlorine is given for 1 gram mole of chlorine, according to the scheme

$$2Me + Cl_2 = 2MeCl$$
$$Me' + Cl_2 = Me'Cl_2$$
$$2/3Me'' + Cl_2 = 2/3Me''Cl_3,$$

and is expressed as the change of the isobaric potential, viz:

$$\Delta Z^\circ = -RT \ln K.$$

The higher the negative ΔZ° accompanying the reaction of a substance with chlorine, the stronger its affinity for the latter. Data on the volatility of certain chlorides are given in Table 1.

TABLE 1

Vapor Pressure of Chlorides in Dependence on Temperature

Chloride	Vapor pressure, mm Hg					
	1	10	100	200	400	760
	Temperature °C					
$AlCl_3$	100	123.8	152	162	172	180
$NiCl_2$	671	759	866	904	945	987
$CoCl_2$	—	—	843	904	974	1050
$FeCl_2$	—	700	842	897	961	1026
$FeCl_3$	194	235.5	272.5	285	298	319
$MnCl_2$	—	778	960	1028	1108	1190
NaCl	865	1017	1220	1296	1375	1465
Cu_2Cl_2	546	702	960	1077	1249	1490

The nickel and divalent iron chlorides formed in low-temperature chlorination remain in the residue, while ferric chloride strongly evaporates (Table 1). In high-temperature chlorination the majority of other chlorides evaporate intensively.

EXPERIMENTAL

Subject and Objective of Investigations

These investigations were concerned with nickel-bearing iron ores with the purpose of examining the possibilities for their complex processing by chlorination.

Yugoslav nickel-bearing iron ores originated from decomposition of ultrabasic rocks. Their deposits stretch from Zagrebačka gora through the middle of the country as far as the Greek and Albanian borders. Their geological, geophysical and stratigraphic characteristics were described in our previous paper[48]. The results of chemical, mineralogical and DTA studies of ore samples were also given therewith. The chemical composition of these ores is given in Table 2. It may be seen that the first two are very poor in nickel. The ore form the Lipovac deposit is more valuable due to a somewhat higher content of iron and about 1% Ni.

TABLE 2

Chemical Analysis of the Ores from Mokra Gora, Goleš and Lipovac

Element or compound	Ores		
	Mokra gora	Goleš	Lipovac
Fe	18.65	12.20	38.70
Fe_2O_3	19.40	17.20	30.70
FeO	6.05	0.20	21.38
SiO_2	39.11	56.63	13.95
Al_2O_3	6.30	2.50	7.22
MnO	0.32	0.20	0.54
Cr_2O_3	2.40	1.70	4.16
NiO	—	1.59	—
Ni	0.602	1.25	1.015
Co	0.04	0.04	0.052
MgO	11.50	5.25	6.16
CaO	0.80	0.25	4.05
TiO_2	0.03	0.03	0.05
S	0.10	0.04	0.025
CO_2	0.10	0.05	1.60
$-H_2O$	4.00	10.18	1.65
$+H_2O$	8.75	3.57	3.40

The low content of useful components, the complex chemical and mineralogical composition, and other properties of these ores rule out existing processing technologies. Because of this, extensive investigations were undertaken to find technically and economicaly acceptable processes for their exploitation[49, 50, 51, 52]. One of these was chlorination for a complex processing. For this purpose numerous experiments on low- and high-temperature chlorination of natural ore and ore previously reduced with hydrogen and of chlorination in the presence of coal were performed.

The ore samples were ground to 100% 200 mesh. Chlorination was performed in the stationary state with gaseous chlorine. The apparatus, similar to that in ref. 49, consisted of an electric furnace provided with a temperature regulator, quartz tube and bath, chlorine cylinder, gas flow gauge, etc.

CHLORINATION OF NATURAL ORES

Experiments in the chlorination of natural, i.e. untreated ores from the Mokra Gora, Goleš and Lipovac deposits were performed at 900°C. The aim was to determine the influence of temperature and duration of chlorination on the volatility of nickel and iron chlorides. The results obtained with the theoretical quantities of chlorine are shown in Figs. 1 and 2.

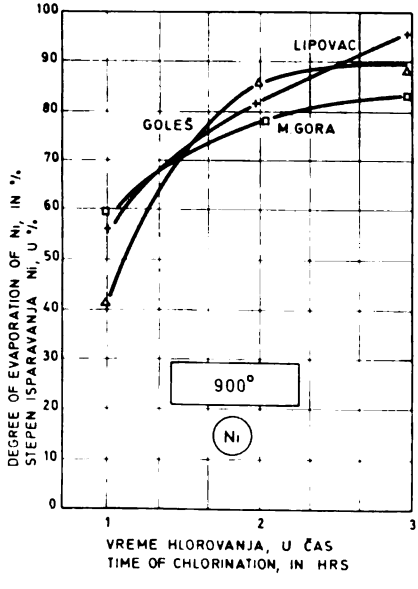

Fig. 1

Kinetics of evaporation of nickel in the form of chlorides

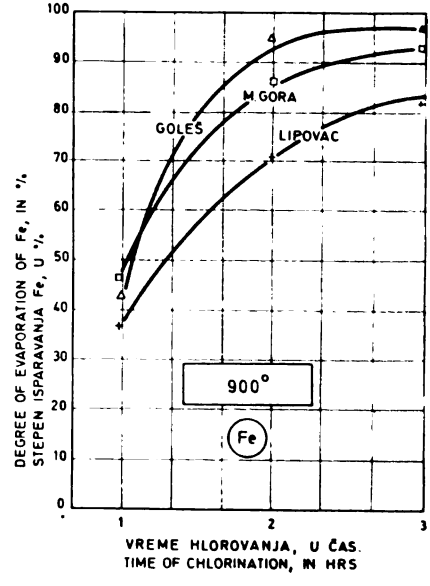

Fig. 2

Kinetics of evaporation of iron in the form of chlorides

From the results it may be seen that the nickel compounds in the ores of Mokra Gora and Goleš chlorinated more intensively at the beginning

of the process than did iron compounds. The iron chlorination rate rose after an hour, and at 2 and 3 hours the intensities of the two were about equal. In the degree of chlorination of nickel there is no essential difference between the ores. The slightly higher chlorination of the Lipovac ore was probably due to the character of the nickel minerals, which are here predominantly sulphides. The reason for the smaller total quantity of iron chlorinated in this ore, apart from the kind of minerals present, may be sought in the considerably higher concentration of this metal than in the other two ores, this making diffusion difficult, and in factors of a kinetic nature.

One of the essential characteristics of the chlorination of natural ores is the fact that: a. — results are poor after short treatment but relatively good after about 3 hours; b. — nickel and iron chlorinate approximately according to their concentration in the ore, i.e. no essential selectivity can be achieved.

SUMMARY

From extensive theoretical and experimental investigations on chlorination of nickal bearing iron ores from three Yugoslav deposits the following conclusions may be drawn:

1. Yugoslav nickel-bearing iron ores are poor. They differ in genetic, chemical and mineralogical characteristics. The nickel content varies from 0.6 to 1.25%, and iron from 12 to 39%.

2. In the chlorination of natural ores with the theoretical quantity of chlorine at 900°C, the degree of chlorination and evaporation of nickel and iron depend on the duration of the process. The evaporation of nickel after 1-hour chlorination was 40 to 60%, after 2 hours 78 to 88.4% and after 3 hours 83 to 95%, depending upon the kind of the ore. With iron the chlorination after 1 hours was 37.5 to 46.5%, after 2 hours 70 to 95% and after 3 hours 82.6 to 96.8%.

3. Nickel and iron chlorinate approximately in direct proportion with their concentration in the ore, i.e. no selective chlorination can be attained.

School of Technology and Metallurgy, Department of Metallurgy of Nonferous Metals, Belgrade University

Received 15 April, 1968

REFERENCES

1. Swinburg, J. — *Trans. Faraday Soc.* 2: 115, 1903.
2. Ashcrobf, F. A. — *Trans. Inst. Min. Met.* 3: 95, 1092.
3. Baker, C. F. — *Trans. Amer. Electrochem. Soc.* 12: 155, 1907.
4. Duval, A. L. and D. Adrian. — *US Patent No. 1,343,485* Nov. 7, 1923.
5. *French Patent No. 711,826* May 31, 1930.
6. Lebedev, P. S. — *Sbornik trudov Moskovskogo Instituta stali* 5, 1935.
7. Bogatskii, D. P. — *Zhurnal prikladnoĭ khimii USSR* 17: 346, 1944.
8. Urazov, G. G. and D. P. Bogatskiĭ. — *Izvestiia AN SSSR OKhN* 8: 194:, 1948.
9. Bogatskiĭ, D. P. and G. G. Urazov. — *Izvestiia AN SSSR OKhN* 8: 898, 1957.

10. Brown, H. and J. Sylwester. — *US Patent No. 2,067,874* Jan. 12, 1938.
11. Gehita, T. and J. Masao. — *Japanese Patent No. 8706* June 26, 1961.
12. Gehita, T. and J. Masao. — *Japanese Patent No. 15510* Sep. 6, 1961.
13. Berdnikov, A. E. — *Tsvetnye metally* 9: 91, 1938.
14. Losev, K. J. — *Tsvetnye metally* 2: 60, 1940.
15. Neimitsu, A. and G. Furum. — *J. Iron and Steel Inst. Japan* 84(4): 432, 1962.
16. Furui, T. and A. Suva. — *J. Min. and Met. Inst. Japan* 19: 319, 1963.
17. Kasibara, K. and S. Tanaka. — *Japanese Patent No. 7855* July 11, 1962.
18. Morozov, I. S. and G. G. Urazov. — *USSR Patent No. 50,479* Feb, 28, 1937.
19. Morozov, I. S. and G. G. Urazov. — *USSR Patent No. 51,631* Aug. 31, 1937.
20. Fink, G. G. and R. E. Vivien. — *Canadian Patent No. 321,511* Apr. 19, 1932.
21. Borchers, H. — *Metall. und Erz.* 33: 435, 1936.
22. Kenworthy, H. and K. Kerschner. *Metalurgical Investigations of Southeastern Missouri Resources. US Bur. Mines Report Invest. 4999* — 1953, p. 37.
23. Shimayama, T. — *Japanese Patent No. 8302* Sep. 17, 1959.
24. Bogatskiĭ, D. P. — *Izvestiia AN SSSR* 45: 67, 1944.
25. Urazov, G. G. and D. P. Bogatskiĭ. — *Izvestiia AN SSSR OKhN* 2: 194, 1948.
26. Urazov, G. G. and D. P. Bogatskiĭ. — *Izvestiia AN SSSR OKhN* 8: 898, 1957.
27. Bogatskiĭ, D. P. and G. G. Urazov. — *Zhurnal prikladnoĭ khimii USSR* 31: 201, 1958.
28. Bogatskiĭ, D. P. and G. G. Urazov. — *Zhurnal prikladnoĭ khimii USSR* 31: 325, 1958.
29. Denisov, S. N. — *Izvestiia VUZ Tsvetnykh metallov* 2: 58, 1959.
30. Zialinski, E. — *Arch. Erzbergbau Erzaufbereitung Metallhütenwesen* 1: 31, 1934.
31. Urazov, G. G. and T. S. Morozov. — *Tsvetnye metally* 10 (6): 109, 1935.
32. Shindo, H., Y. Nigoya and K. Ishii. — *Sugyo Kway Shi* 13: 689, 1959.
33. Tratsevitskaia, V. J. and Iu. R. Ratner. — *Trudy Instituta Metallurgii AN SSSR* 12: 45, 1963.
34. Mayer, R. F. — *US Patent No. 1,870.863* Aug. 9, 1932.
35. Perin, P. — *US Patent No. 2,750,285* June 12, 1956.
36. Daubenspeck, J. M. — *US Patent No. 2,733,983* Feb. 7, 1954.
37. Hart, Ch. — *US Patent No. 2,030,868* Feb. 18, 1936.
38. Hart, Ch. — *US Patent No. 2,030,867* Feb. 18, 1937.
39. Graham, M. E. and E. Beider. — *US Patent No. 2, 677,604* May 4, 1954.
40. Smirnov, V. N. and A. M. Tikhonov. — *Izvestiia AN SSSR OTN* 9: 48, 1956.
41. Tikhonov, A. M. and V. N. Smirnov. — *Uralskiĭ bilten Inst.* 58: 167, 1957.
42. Wescott, E. — *US Patent No. 2,036,664* Apr. 7, 1937.
43. Graham, M. E., W. A. Reed and J. R. Cameron. — *US Patent No. 2,766,115* Oct. 9, 1956.
44. Cornelies, L. — *Dutch Patent No. 89,510* Nov. 15, 1958.
45. Heertjes, P. M. and L. Cornelies. — *Rec. Trav. Chem.* 79: 595, 1960.
46. Müller, R. and W. Hasse. — *Berg. und Hüttenmenn M. m. Hochschule Leiben* 96: 209, 1961.
47. Kitte, E. and J. Kitte. — *Rev. Fac. Ing. Guiw.* 25: 133, 1956.
48. Vučurović, D. — *Tehnika — Rudarstvo, geologija i metalurgija* (2): 241, 1966.
49. Vučurović, D. — *Tehnika — Rudarstvo, geologija i metalurgija* (5): 794, 1966.
50. Vučurović, D. — *Tehnika — Rudarstvo, geologija i metalurgija* (11): 1903, 1966.
51. Vučurović, D. — *Tehnika — Rudarstvo, geologija i metalurgija* (6): 979, 1967.
52. Vučurović, D. — *Tehnika — Rudarstvo, geologija i metalurgija* (5): 785, 1968.

GLASNIK HEMIJSKOG DRUŠTVA, Vol. 34, No. 8-9-10, 1969, pp. 549—554

GHDB-91

66.094.403:622.341:546.74

Original Scientific Paper

CHLORINATION OF YUGOSLAV NICKEL-BEARING IRON ORES. II.

CHLORINATION OF REDUCED ORES

by

MIODRAG A. SPASIĆ and DUŠAN M. VUČUROVIĆ

As described in the first part[1], a number of authors preceded chlorination of nickel ores or compounds with gaseous chlorine by reduction, in order to convert nickel in the lattice of complex compounds into the free metallic state and therefore make its reaction with chlorine easier.

The conditions of preliminary reduction depend on the object of chlorination. Some author[2, 3] have carried out preliminary reduction with hydrogen, the product being then chlorinated with gaseous chlorine in order to obtain volatile nickel and iron chlorides. Partial reduction of ore has also been done with hydrogen at 600°C in order to convert nickel into the metallic state, iron being left mainly in the form of oxide. By subsequent chlorination of the product at 200°C the major part of the nickel but only a small fraction of the iron are converted into chlorides[4]. A number of authors[5–10] have extensively studied the chlorination of garnierite and nickel-bearing ores. After reduction the ores were chlorinated at low temperatures (300—600°C), at which 80.5% of the nickel chlorinates in 2 hours, while at the elevated temperatures (700—900°C) practically 100% nickel and cobalt and 90—96% iron chlorinate. After the separation of the products a nickel oxide concentrate with 32.57—37.19% Ni and 7.14—8.23% Fe was obtained, about 50 to 60 times richer in nickel than the original ore. Nickel oxide and garnierite from New Caledonia were chlorinated after preliminary reduction with hydrogen[11], laterite ore after reduction with a $CO+CO_2$ mixture[12]. Other materials have also been chlorinated after preliminary reduction.

EXPERIMENTAL

Conditions and Aims

The degree of reduction of nickel in the ore depends on a number of factors, among them the kind of ore, the nickel-bearing mineral, conditions of reduction, the kind of reducing agent, etc. The conditions of reduction were determined in preliminary investigation[13] and were such as to enable the conversion of most of the nickel into metalic state. These conditions were:

Ore	*Temperature (°C)*	*Time (min.)*
Mokra Gora	950	45
Goleš	1000	45
Lipovac	1000	60

After reduction the ore was cooled in an inert atmosphere and then chlorinated with chlorine under determined conditions.

The investigations were undertaken in order to determine the optimum conditions for extraction of nickel and other compounds by chlorination.

CHLORINATION AT LOW TEMPERATURES

The reduced ores were chlorinated at temperatures between 100 and 500°C 1 to 2 hours. The product of chlorination was leached with water in order to get nickel and other chlorides into aqueous solution. Leaching was carried out at the boiling point of the pulp for 60 minutes[14]. Under these conditions all chlorinated nickel from the ore went into solution, while the quantity of dissolved iron was less than 1% of its total amount in the ore. The results are shown in Fig. 1.

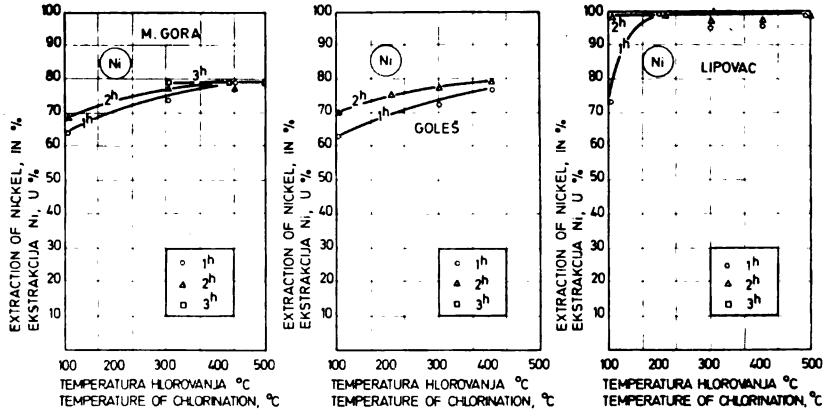

Fig. 1

Dependence of the degree of extraction of nickel on ore chlorination conditions

From the graph a very interesting phenomenon may be noticed, viz. the fact that a high degree of chlorination of nickel was attained at as low a temperature as 100°C, this not being noticed in earlier studies. The phenomenon may be explained by the structure and state of the nickel after reduction. Particular success was achieved in the chlorination of Lipovac ore, where practically all the nickel was chlorinated at very low temperatures (100—200°C) in 1—2 hours.

CHLORINATION AT HIGH TEMPERATURES

The ore for chlorination at high temperatures was treated in the same way as in the previous case. The process was carried out at between 700 and 900°C 0.5—3 hours. The volatile chlorides given off process were collected in a condenser. The results are shown in Fig. 2.

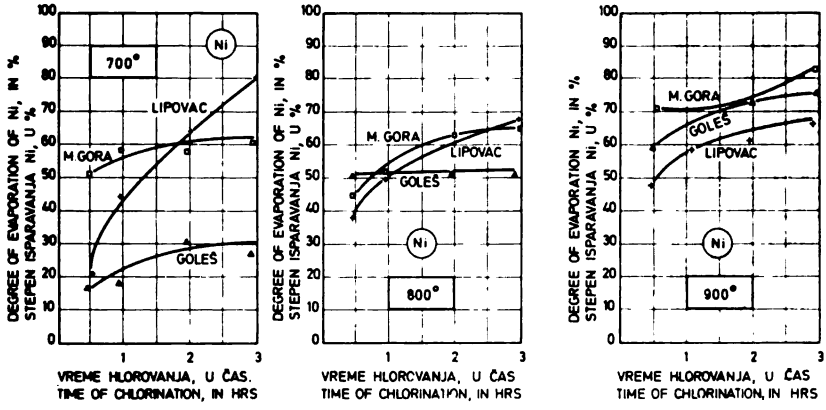

Fig. 2

Kinetics of evaporation of nickel in the form of $NaCl_2$ during chlorination of ores

The rate of conversion of nickel into volatile chloride was found to increase regularly with temperature and time of chlorination. However, the rate of evaporation was lower than anticipated. The total amount of chlorinated nickel was certainly considerably higher than that evaporated, leading to the conclusion that the kinetics of evaporation limits the process.

Comparing the chlorination of natural ore and of previously hydrogen -reduced ore it may be seen that the latter did not give the anticipated effect. Further, from the results of chlorination at low and high temperatures no clearly expressed relationship between the degree of chlorination and evaporation can be observed.

From the results in Fig. 3 the degree of evaporation of iron in the form of chloride may be seen to be higher than in the case of nickel, and to increase more (Goleš, Lipovac) or less (M. Gora) with temperature. The total evaporation of iron was very high and considerably higher than for nickel, this agreeing with the thermodynamic calculations but disagreeing with the results obtained in the case of silicate ores[10].

Comparing the chlorination of natural and reduced ores, the latter may be seen to give the same effects after a considerably shorter reduction time.

CONCLUSION

Investigations have been undertaken to determine the effect of chlorination on Yugoslav nickel-bearing ores from Mokra Gora, Goleš and

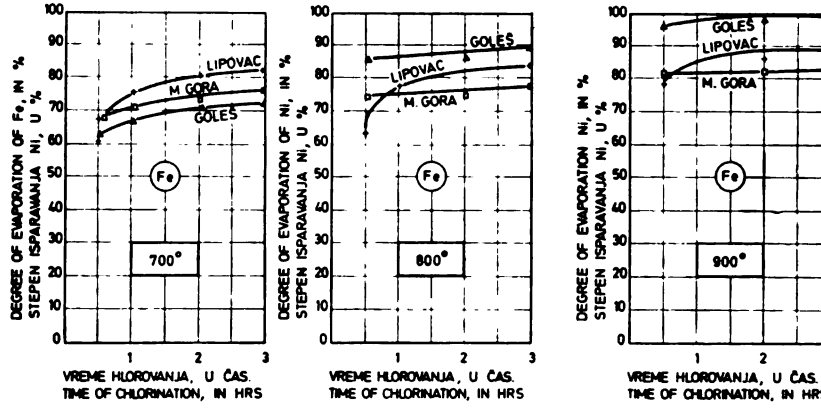

Fig. 3

Kinetics of evaporation of iron in the form of chlorides during chlorination of ores

Lipovac after their reduction with hydrogen. Chlorination was carried out at low and high temperatures.

Chlorination conditions at low temperatures were: temperature 100—500°C, time 1—2 hours. The chlorinated ore was leached with boiling water 60 minutes. From the results the following conclusions may be drawn:

1. A high degree of chlorination was attained at only 100°C: after 1 to 3 hours this was 65—70% in the case of M. Gora and Goleš ores, and 74—100% in the case of the Lipovac ore.

2. The maximum extraction of nickel from M. Gora and Goleš ores was about 80% and from Lipovac practically 100%.

3. The high chlorination of metallic nickel at such low temperatures can be explained by the structure and state of the nickel powder after reduction.

4. The amount of iron which goes into solution amounts less than 1%, this enabling the production of nickel-rich concentrates.

High-temperature chlorination was carried out at between 700 and 900°C 1 to 3 hours. From the results it may be seen that:

1. The maximum degree of evaporation of nickel, 68.5 to 84.7% after 3 hours at 900°C, depending on the kind of the ore, is lower than expected. This indicates that there is no clear relationship between the degree of chlorination and evaporation of nickel.

2. The degree of evaporation of iron in the form of chloride was very high, higher than that of nickel, this being in agreement with the thermodynamic calculations but disagreeing with certain practical results. At a temperature of 900°C and a time between 0.5 and 3 hours it was 82% (M. Gora) 99—100% (Goleš) and 86—88.9% (Lipovac) of nickel.

3. Comparing the chlorination of natural and reduced ores it may be seen that with the latter the same effect was obtained in 4 to 5 times shorter time, this being an essential advantage over the former.

As the obtained results are, generally speaking, somewhat inferior to what was expected, our further investigations are concentrated on chlorination of ores in the presence of coal, i.e. on simultaneous reduction and chlorination.

School of Technology and Metallurgy, Department of Metallurgy of Nonferous Metals, Belgrade University

Received 15 April, 1968

REFERENCES

1. Vučurović, D. and M. Spasić. — *Glasnik hemijskog društva* (Beograd) 34 (8—9—10), 1969 (this number).
2. Baker, C. F. — *Trans. Am. Electrochem. Soc.* 12: 155, 1907.
3. Hart, Ch. — *Us Patent No. 2,030,868* Feb. 7, 1954.
4. Lebedev, P. S. — *Sbornik trudov Moskovskogo Instituta Stali* No. 5, 1935.
5. Bogatskiĭ, D. P. — *Izvestiia AN SSSR* 45: 67, 1944.
6. Bogatskiĭ, D. P. — *Zhurnal prikladnoĭ khimii USSR* 17: 346, 1944.
7. Urazov, G. G. and D. P. Bogatskiĭ. — *Izvestiia AN SSSR OKhN* 2: 194, 1948.
8. Urazov, G. G. and D. P. Bogatskiĭ. — *Izvestiia AN SSSR OKhN* 8: 898, 1957.
9. Bogatskiĭ, D. P. and G. G. Urazov. — *Zhurnal prikladnoi khimiĭ USSR* 31: 201, 1958.
10. Bogatskiĭ, D. P. and G. G. Urazov. — *Zhurnal prikladnoi khimiĭ USSR* 31: 325, 1958.
11. Shindo, H., Y. Nigoya and K. Iskii. — *Sugyo Kway Shi* 13: 689, 1959.
12. Kasibara, K. and S. Tanaka. — *Japanese Patent No. 7855* July 11, 1962.
13. Vučurović, D. — *Tehnika — Rudarstvo, geologija i metalurgija* (5): 794, 1966.
14. Bogatskiĭ, D. P. — *Izvestiia AN SSSR OTN* 8: 895, 1947.

GLASNIK HEMIJSKOG DRUŠTVA, Vol. 34, No. 8-9-10, 1969, pp. 555—561

GHDB-92

66.094.403:622.341:546.74

Original Scientific Paper

CHLORINATION OF YUGOSLAV NICKEL-BEARING IRON ORES. III.

SIMULTANEOUS REDUCTION AND CHLORINATION

by

DUŠAN M. VUČUROVIĆ and MIODRAG A. SPASIĆ

INTRODUCTION

The advantages of simultaneous reduction and chlorination consist in improved conditions for chlorinating metal at the moment of its release from the compound its elimination from the reactive medium in the form of volatile chlorides. A number of authors have carried out chlorination of various materials in the presence of coal as the reducing agent. By chlorinating oxide nickel ores in the presence of 20—25% coal an efficiency of 78—92% Ni was attained[1]. Low-temperature chlorination of nickel-bearing ores from New Caledonia in the presence of 30% coal dust relative to the ore weight[2-3] and separating the chlorinated ore with water gave a 94% Ni yield. The process has also been used for selective chlorination and separation of nickel and iron from chromium[4-5] and for various other purposes and materials.

EXPERIMENTAL

Conditions and Purpose of Investigation

This series of experiments was undertaken in order to investigate the effect of simultaneous reduction and chlorination of ore on the yield of nickel and iron and compare the results, process parameters and other factors with those obtained in chlorination of natural[6] and hydrogen-reduced ores[7].

Chlorination was performed at 800, 900 and 950°C during 0.5—2 hours. The coal used was from Kreka mines, 100% 100 mesh and in quantities considered optimal for reduction and separation with ammonia[8], viz. 10% of the ore weight in the case of M. Gora and Lipovac ores, and 12% in the case of Goleš ore. The quantity of chlorine was theoretical.

The integral effect of chlorination, i.e. the quantities of evaporated chlorides and the fraction remaining in the residue, which was later separated with water, was investigated. These two fractions of chlorinated metal, i.e. evaporated (e) and the residual, later separated with water (r), make up the total chlorinated metal (t) expressed as a percentage of the total metal content of the ore.

Chlorination of nickel. The results obtained under the above mentioned conditions are shown graphically in Figs. 1 and 2.

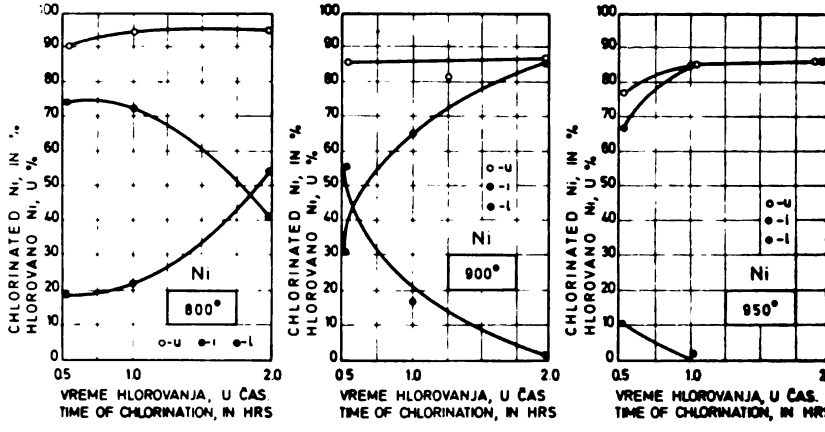

Fig. 1

Kinetics of chlorination of nickel in the Mokra Gora ore in presence of 10% coal

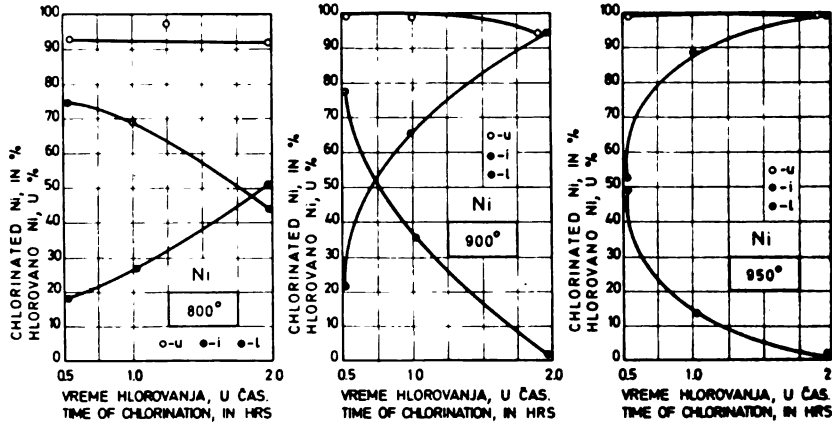

Fig. 2

Kinetics of chlorination of nickel in the Goleš ore in presence of 12% coal

From these graphs it may be seen that the evaporating nickel fraction increases with temperature and time, and under certain conditions constitutes the total chlorinated metal. The conditions for maximum evaporation of nickel in the form of chloride are: for Mokra Gora ore: 900°C for

2 hours, or 950°C 1 hour, in both cases 86% Ni being chlorinated; for Goleš ore: 900 and 950°C 2 hours, 94.1 and 100% Ni being chlorinated. The kinetics of nickel evaporation as affected by chlorination conditions is shown in Fig. 3.

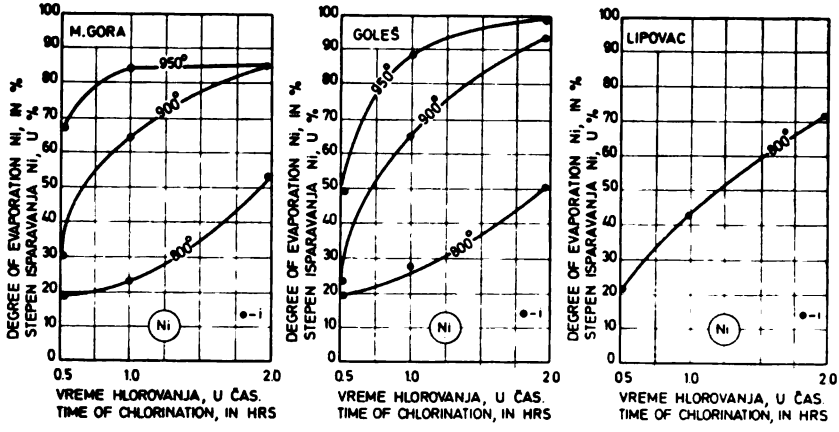

Fig. 3

Kinetics of evaporation of nickel in the form of chlorides during chlorination of ores from Mokra Gora, Goleš and Lipovac in presence of coal

The quantity of nickel remaining in the chlorinated ore in the form of chloride changes with temperature and time inversely to the evaporated fraction.

The total chlorinated nickel from the Mokra Gora ore has a maximum at 800°C. The fall observed at 900 and 950°C is probably due to crystal transformations of minerals in the ore, some of the nickel remaining unreduced and unchlorinated.

By comparing the chlorination of natural and hydrogen-reduced ores and with simultaneous reduction in the presence of coal it may be noticed that the last process is technically and economically most suitable for Mokra Gora ore. In the case of Lipovac ore most of the nickel is chlorinated at low temperatures after preliminary reduction with hydrogen.

Chlorination of iron. The effect of simultaneous reduction of Mokra Gora, Goleš and Lipovac ores with coal and chlorination with the theoretical quantity of gaseous chlorine on the degree of evaporation of iron is shown in Fig. 4. it may be seen that: 1. — iron in these ores, as in the chlorination of the natural and previously reduced ores, is chlorinated faster and in a higher degree than nickel; 2. — simultaneous chlorination and reduction is the most effecient process; 3. — high evaporation of iron is obtained (practically 100%); 4. — no selection of nickel and iron in the evaporating chlorides is achieved: the Ni : Fe ratio in the chlorides is approximately the same as in the ore.

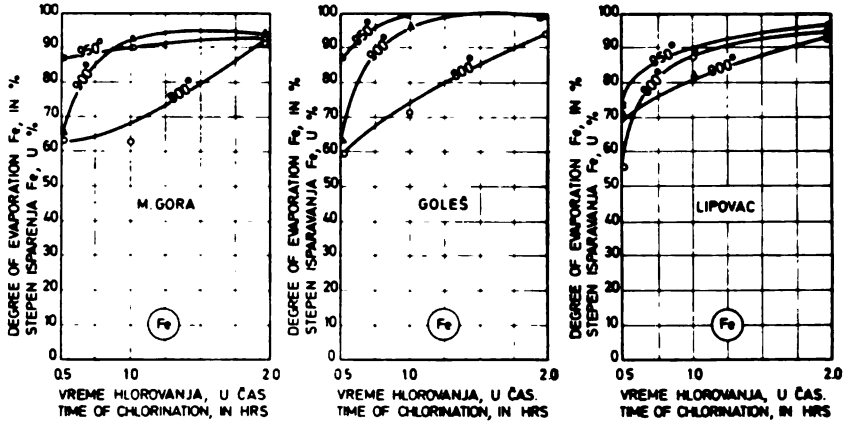

Fig. 4

Kinetics of evaporation of iron in the form of chlorides during chlorination of ores from M. Gora, Goleš and Lipovac in presence of coal

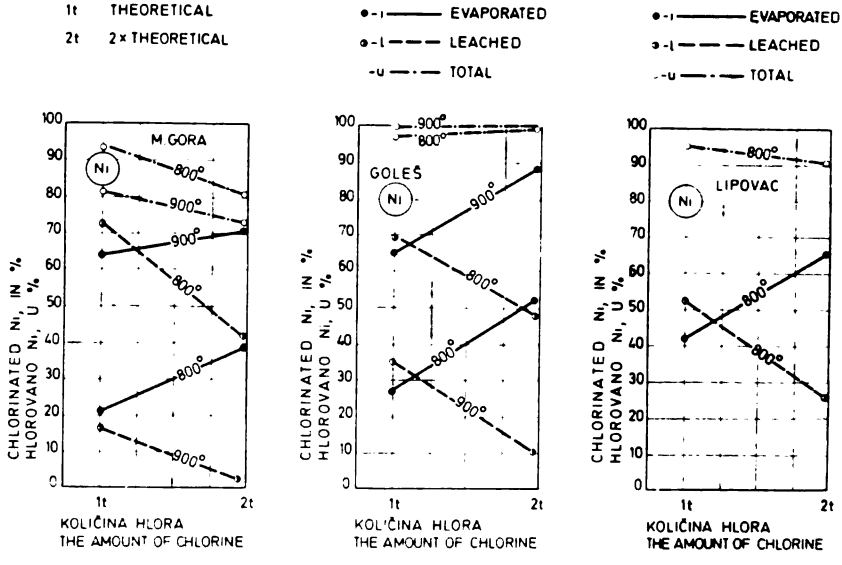

Fig. 5

Dependence of the degree of chlorination of nickel from the ores of Mokra Gora, Goleš and Lipovac on the amount of chlorine

THE INFLUENCE OF CHLORINE ON CHLORINATION AND EVAPORATION OF NICKEL AND IRON FROM ORES

The study of the influence of chlorine quantity on chlorination ores is both of technical and economical interest. The experimental results obtained with chlorination in the presence of coal for 60 minutes are shown in Figs. 5 and 6. It is apparent that the quantity of nickel evaporated considerably increases with increasing quantity of chlorine from 1 *t* (theoretical) to 2. *t*. Therefore it is clear that by using twice the theoretical quantity of chlorine considerably better results would evidently be obtained. Particularly the quantities of chloride evaporated would be greater and the amount in the residue less.

Increasing the quantity of chlorine speeds up the mechanism and kinetics of chlorination and makes the removal of evaporated chlorides from the apparatus easier. The latter effect may probably be achieved by increasing the quantity of gas in the chlorinating system, part of the chlorine being replaced by an inert gas.

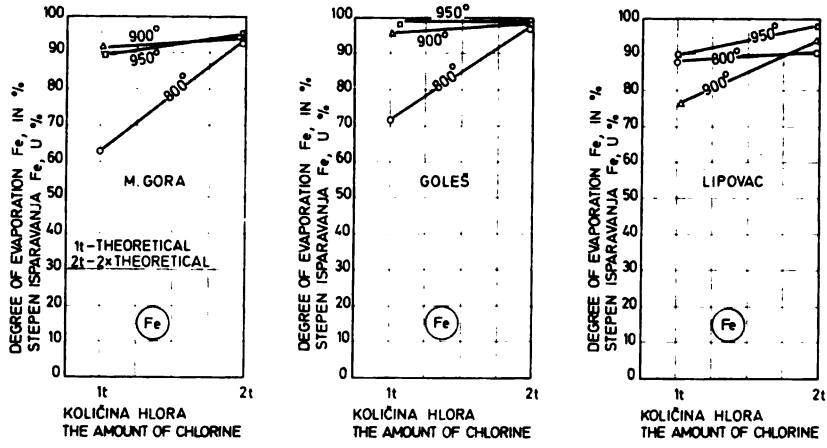

Fig. 6

Dependence of the degree of chlorination of iron from the ores of Mokra Gora, Goleš and Lipovac on the amount of chlorine

The effect of chlorine quantity on the chlorination of iron is similar to that with nickel (Fig. 6).

CONCLUSION

From experiments on the chlorination of M. Gora, Goleš and Lipovac ores with gaseous chlorine in the presence of coal the following conclusions may be drawn:

1. In simultaneous reduction and chlorination more evaporated (in all three ores) and total chlorinated nickel (Mokra Gora and Goleš ores) is obtanied, with Lipovac ore while practically all the nickel chlorinates at low temperatures after preliminary reduction with hydrogen.

2. The quantity of nickel evaporated in the form of chloride increases with temperature and time, and under certain conditions it represents the total quantity of the metal.

3. The conditions for a maximum evaporation of nickel are: for Mokra Gora ore 900°C for 2 hours or 950°C 1 hour, 86% Ni chlorinating in both cases; for Goleš ore 900 and 950°C 2 hours, 94.1 and 100% Ni being chlorinated.

4. A certain decrease of the total quantity of nickel chlorinated at 900 and 950°C relative to that obtained at 800°C from M. Gora ore is due to crystallographic transformations and the character of the ore minerals.

5. The same regularities are also observed with iron. Also, as in previous experiments, iron is chlorinated faster and in a higher degree than nickel (95—100%). Simultaneous reduction and chlorination is found to be more effective than other methods.

6. The Ni : Fe ratio in the evaporated chlorides is approximately the same as in the ore. Hence no selection of these two metals is obtained.

7. Increasing the quantity of chlorine accelerates the mechanism and kinetics of chlorination and evaporation of metal, thus giving better results.

Further investigations are under way of various factors in the reduction and chlorination of ores with the aim of improving the process, increasing the efficiency of chlorination, the selection of nickel and iron, the economics of the process, etc. Particular attention will be paid to the catalytic action of various inorganic salts and minerals.

School of Technology and Metallurgy,
Department of Metallurgy of Nonferous Metals,
Belgrade University

Received 15 April, 1968

REFERENCES

1. Berdnikov, A. E. — *Tsvetnye metally* 9: 91, 1938.
2. Gehita, T. and J. Masao. — *Japanese Patent No. 8706* June 26, 1961.
3. Gehita, T. and J. Masao. — *Japanese Patent No. 15510* Sept. 6, 1961.
4. Lebedev, P. S. — *Sbornik trudov Moskovskogo Instituta Stali* 5, 1935.
5. Hart, Ch. — *US Patent No. 2,030,867* Feb. 18, 1937.
6. Vučurović, D. and M. Spasić. — *Glasnik hemijskog društva* (Beograd) 34 (8—9—10), 1969 (this number).
7. Spasić, M. and D. Vučurović. — *Glasnik hemijskog društva* (Beograd) 34 (8—9—10), 1969 (this number).

Izdavač

IZDAVAČKO PREDUZEĆE "NOLIT", BEOGRAD, TERAZIJE 27/II

*

Štampa

GRAFIČKO PREDUZEĆE "PROSVETA", BEOGRAD,
ĐURE ĐAKOVIĆA 21